LEABHARLANN CHOLÁISTE NA TRÍONÓIDE, BAILE ÁTHA CLIATH | TRINITY COLLEGE LIBRARY DUBLIN
Ollscoil Átha Cliath | The University of Dublin

Terms and Conditions of Use of Digitised Theses from Trinity College Library Dublin

Copyright statement

All material supplied by Trinity College Library is protected by copyright (under the Copyright and Related Rights Act, 2000 as amended) and other relevant Intellectual Property Rights. By accessing and using a Digitised Thesis from Trinity College Library you acknowledge that all Intellectual Property Rights in any Works supplied are the sole and exclusive property of the copyright and/or other IPR holder. Specific copyright holders may not be explicitly identified. Use of materials from other sources within a thesis should not be construed as a claim over them.

A non-exclusive, non-transferable licence is hereby granted to those using or reproducing, in whole or in part, the material for valid purposes, providing the copyright owners are acknowledged using the normal conventions. Where specific permission to use material is required, this is identified and such permission must be sought from the copyright holder or agency cited.

Liability statement

By using a Digitised Thesis, I accept that Trinity College Dublin bears no legal responsibility for the accuracy, legality or comprehensiveness of materials contained within the thesis, and that Trinity College Dublin accepts no liability for indirect, consequential, or incidental, damages or losses arising from use of the thesis for whatever reason. Information located in a thesis may be subject to specific use constraints, details of which may not be explicitly described. It is the responsibility of potential and actual users to be aware of such constraints and to abide by them. By making use of material from a digitised thesis, you accept these copyright and disclaimer provisions. Where it is brought to the attention of Trinity College Library that there may be a breach of copyright or other restraint, it is the policy to withdraw or take down access to a thesis while the issue is being resolved.

Access Agreement

By using a Digitised Thesis from Trinity College Library you are bound by the following Terms & Conditions. Please read them carefully.

I have read and I understand the following statement: All material supplied via a Digitised Thesis from Trinity College Library is protected by copyright and other intellectual property rights, and duplication or sale of all or part of any of a thesis is not permitted, except that material may be duplicated by you for your research use or for educational purposes in electronic or print form providing the copyright owners are acknowledged using the normal conventions. You must obtain permission for any other use. Electronic or print copies may not be offered, whether for sale or otherwise to anyone. This copy has been supplied on the understanding that it is copyright material and that no quotation from the thesis may be published without proper acknowledgement.

MESOZOIC-TERTIARY TECTONICS OF SE IRELAND AND GENETIC LINK TO OFFSHORE EXTENSIONAL BASINS

Volume 2 of 3

By

Michael J. M. Cunningham

Submitted to the University of Dublin for the degree Doctor of Philosophy

November 2000

TRINITY COLLEGE
20 MAR 2001
LIBRARY DUBLIN

THESIS
6320.2

VOLUME 2

Title Page

List of Figures

Chapter 1

Figure 1.1:- Simplified Mesozoic-Tertiary map of Ireland.

Figure 1.2:- Map showing major faults in the north of the Irish landmass.

Figure 1.3:- Map of Kingscourt outlier.

Figure 1.4:- Map of Wexford outlier.

Figure 1.5:- Simplified geology map and topography of Ireland.

Figure 1.6:- Map of Ireland and offshore Mesozoic-Tertiary basins.

Figure 1.7:- Free air gravity map of the Celtic and central-southern Irish Sea regions.

Figure 1.8:- Map of Porcupine basin.

Figure 1.9:- Map of offshore wells.

Figure 1.10:- Bathymetry of the continental shelf and abyssal plain, west of Ireland.

Figure 1.11:- Free air gravity map of NE Atlantic.

Figure 1.12:- Simple diagram of Mohr circle.

Figure 1.13:- Block diagram of transpression.

Figure 1.14:- Conceptual model of strike-slip faults with pronounced curvature.

Figure 1.15:- Bouguer gravity anomaly map of Ireland.

Figure 1.16:- Dextral transform model.

Chapter 2

Figure 2.1:- Map showing towns and lines of communication in the area of study.

Figure 2.2:- Principal of the very low frequency (VLF) method.

Figure 2.3a,b:- Simplified solid geology and structure map of study area.

Figure 2.4:- Map of known faults.

Figure 2.5:- Two maps showing known warm springs in the area of study.

Figure 2.6:- Graphs showing temperature measurements.

Figure 2.7:- Contoured map of elevation of study area.

Figure 2.8:- Map showing borehole database.

Figure 2.9:- Map showing interpolated thickness of overburden in study area.

Figure 2.10:- Thick overburden sections near the town of Kinnegad (Co. Meath).

Figure 2.11:- Map showing bedrock elevation.

Figure 2.12:- Composition of cored overburden material, south of Newcastle (Co. Dublin).

Figure 2.13:- Solid geology map of VLF-R survey area.

Figure 2.14a:- Modelled thicknesses of overburden from VLF-R measurements.

Figure 2.14b:- Modelled resistivity values of the lower layer.

Figure 2.15:- Aeromagnetic map of study area (GSI).

Figure 2.16:- Bouguer anomaly contours.

Figure 2.17:- Map showing occurrence of small Bouguer anomalies in Central Midlands.

Figure 2.18a,b:- Maps of Bouguer gravity and magnetic anomaly.

Chapter 3

Figure 3.1:- Location map of structural areas.

Figure 3.2:- Key structural localities along the northern margin of the Leinster batholith.

Figure 3.3:- Rose diagrams of structural elements.

Figure 3.4:- Location of structures at locality 1.

Figure 3.5:- Map of magmatic foliation.

Figure 3.6:- Location map of thin-section studies.

Figure 3.7:- Summary map of structures at locality 2 (Sandycove).

Figure 3.8:- Summary map of structures at locality 1 (Blackrock-Seapoint).

Figure 3.9:- Summary map of structures at locality 3 (Sorrento-Killiney).

Figure 3.10:- Deformation map of quartz showing strength envelope.

Figure 3.11:- Palaeostress reconstructions .

Figure 3.12:- Regional geology of the Howth peninsula.

Figure 3.13:- Summary of structure at Balscadden bay, Howth.

Figure 3.14:- Extensional jog on Southern Boundary fault.

Chapter 4

Figure 4.1:- Map of the pre-Tertiary geology of the Kish Bank basin.

Figure 4.2:- Map of seismic database.

Figure 4.3:- Principal of CDP stacking.

Figure 4.4:- Principal of diffraction.

Figure 4.5:- The gravity trend in the Kish Bank basin.

Figure 4.6:- Structural interpretation of unmigrated WINCH4A line.

Figure 4.7:- Map showing locations of Mesozoic basins in the Irish Sea region.

Figure 4.8:- Free-air anomaly map of the Irish Sea region.

Figure 4.9:- Well stratigraphy of Kish basin.

Figure 4.10:- Small section of the WNW-ESE trending TRIST-92-14 line.

Figure 4.11:- Map of onshore-offshore pre-Tertiary geology.

Figure 4.12:- Correlation of Kish basin with Kingscourt.

Figure 4.13:- Geoseismic interpretation over Bray Fault zone.

Figure 4.14:- Mesozoic-Tertiary rocks in the Ulster basin.

Figure 4.15:- N-S seismic line interpreted by Corcoran & Clayton (1999).

Figure 4.16:- Small section of the SW-NE trending TRIST-92-21 line.

Figure 4.17:- Contoured bathymetry map over the Kish basin.

Figure 4.18:- Bathymetry of Irish sea.

Figure 4.19:- Three video stills of the Codling fault.

Figure 4.20:- Pre-Tertiary geology map with seismic lines.

Figure 4.21:- Line AIR 78-61, Kish basin.

Figure 4.22:- Line AIR 78-62, Kish basin.

Figure 4.23:- Line AIR 78-63 shows small positive flower structure.

Figure 4.24:- Line AIR 78-64 shows basement offset.

Figure 4.25:- Line AIR 78-66 shows palaeo-channel.

Figure 4.26:- Line AIR 78-53.

Figure 4.27:- Map showing extent of palaeo-channel, based on seismic evidence.

Figure 4.28:- Contour map of magnetic frequency.

Figure 4.29:- Total Magnetic Intensity (Reduced-to-Pole) image for the Kish Bank basin.

Figure 4.30:- RTP image over Kish Basin, created by World Geoscience.

Figure 4.31:- Image is the first horizontal (non-directional) derivative.

Figure 4.32:- Pseudo-depth slice of aeromagnetic anomaly.

Figure 4.33:- Pseudo-depth slice two.

Figure 4.34:- Pseudo-depth slice three.

Figure 4.35:- Principal of log-power spectrum and Fourier analysis.

Figure 4.36:- Pseudo-Depth Slice 4.

Figure 4.37:- Azimuth 4 is a derivative of pseudo-depth slice 4.

Figure 4.38:- NW trending lineament in Kish basin.

Figure 4.39:- Azimuth 3 highlights shallow magnetic lineament.

Figure 4.40:- Azimuth 3 image.

Figure 4.41:- Azimuth 2 image.

Figure 4.42:- Azimuth 2 displays the smallest signal-to-noise ratio.

Figure 4.43:- Location Map of wells showing estimates of exhumation.

Figure 4.44:- Structural Correlation of Lough Neagh and Kish basin.

Figure 4.45:- Modified geological and structural maps of Kish basin.

Chapter 5

Figure 5.1:- Shaded-relief topographic image of SE Ireland.

Figure 5.2:- Location of areas of geomorphic and tectonic interest.

Figure 5.3:- Simple geological map of SE Ireland with topography.

Figure 5.4:- Regional 1milligal Bouguer gravity anomaly map.

Figure 5.5:- Map of plutons and geology of study areas.

Figure 5.6:- Geological map of the Northern and Upper Liffey Valley plutons.

Figure 5.7:- Geological map of the Lugnaquillia pluton.

Figure 5.8:- Geological map of the Tullow pluton.

Figure 5.9:- Geological map of the Blackstairs pluton.

Figure 5.10:- Theoretical slope profiles.

Figure 5.11a:- Elevation histogram for the Leinster Mountain chain.

Figure 5.11b:- Elevation histogram of Wicklow Massif.

Figure 5.12:- Digital elevation model and elevation histogram for the Vartry area.

Figure 5.13:- Bouguer gravity map of Vartry area of study.

Figure 5.14:- Shaded relief topographic image of the Vartry study area.

Figure 5.15a,b,c:- Statistical graphs showing the relationship between elevation and rock.

Figure 5.16:- Solid bedrock geology map of Vartry area.

Figure 5.17:- NW illuminated hillshade looking NNE.

Figure 5.18:- Slope image of Vartry area.

Figure 5.19a,b,c:- Statistical graphs of slope and elevation in the Vartry area.

Figure 5.20:- Graph showing the frequency of slopes in the area.

Figure 5.21a,b:- Histogram of slopes.

Figure 5.22:- Graph showing slope skewness based on lithology.

Figure 5.23a,b:- Graph showing slope characteristics of the main lithological types.

Figure 5.24a,b:- Histogram of slope type on Quartzites.

Figure 5.25a,b:- Histogram and cumulative frequency of slope type on Ribband Group.

Figure 5.26a,b:- Histogram and cumulative frequency of slope type on aureole rocks.

Figure 5.27a,b:- Histogram and cumulative frequency of slope on Northern pluton.

Figure 5.28:- Graph of normalised slope distribution for the main lithologies (Vartry).

Figure 5.29a,b:- Relief images of the Vartry area.

Figure 5.30a,b,c:- Descriptive statistical graphs of rock and relief.

Figure 5.31a,b,c,d,e:- Relief histograms for the main lithologies in the Vartry area.

Figure 5.32:- Image illustrating the main aspect in the Vartry area.

Figure 5.33:- Fluvial geomorphology.

Figure 5.34:- River profiles crossing the Vartry escarpment.

Figure 5.35:- Topographic image of the Vartry area looking west.

Figure 5.36a,b,c:- NW-SE geological, slope and relief profiles of the Vartry area.

Figure 5.37:- Model for Vartry area.

Figure 5.38:- DEM and elevation histogram for the Bunclody area of study.

Figure 5.39:- Shaded relief topographic image of the Bunclody study area.

Figure 5.40:- Solid bedrock geology map.

Figure 5.41:- Bouguer gravity anomaly of the Bunclody area.
Figure 5.42a,b,c:- Statistical graphs of slope and elevation in the Bunclody area.
Figure 5.43:- Slope image of Bunclody area.
Figure 5.44a,b,c:- Statistical graphs showing slopes on main lithological types.
Figure 5.45:- Graph showing the frequency of slopes in the area.
Figure 5.46a,b:- Histogram and cumulative frequency of slope type on Tullow rock.
Figure 5.47a,b:- Statistical graphs of slope and lithology in the Bunclody area.
Figure 5.48a,b:- Histogram and cumulative frequency of slope type for Blackstairs rocks.
Figure 5.49:- Graph showing slope skewness based on lithology.
Figure 5.50a:- Histogram and cumulative frequency of slope type for aureole rocks.
Figure 5.51a,b:- Histogram and cumulative frequency of slope type for aureole.
Figure 5.52a:- Histogram and cumulative frequency of slope type for Ribband Group.
Figure 5.53a,b:- Histogram and cumulative frequency of slope type for all rocks.
Figure 5.54:- Graph of normalised slope distribution for the main lithologies (Bunclody).
Figure 5.55a,b:- Relief images of the Bunclody area.
Figure 5.56a,b,c:- Descriptive statistical graphs between various rock type and relief.
Figure 5.57a,b,c,d,e:- Relief histograms for the main lithologies.
Figure 5.58:- Shaded relief topographic image of the Bunclody area.
Figure 5.59a,b:- Two topographic relief images of the Bunclody area.
Figure 5.60:- Sketch showing extent of Lower Carboniferous unconformity.
Figure 5.61a,b,c:- WNW-ESE geological, slope and relief profiles of the Bunclody area.
Figure 5.62:- Hillshaded image of the Nore and Barrow Rivers.
Figure 5.63:- Model for Bunclody area.
Figure 5.64:- DEM and histogram for the Glen of Imail area of study.
Figure 5.65:- Topographic relief image of the Glen of Imail area looking ~ W.
Figure 5.66:- Solid bedrock geology map.
Figure 5.67:- Bouguer gravity anomaly map of the Glen of Imail area.
Figure 5.68:- Shaded relief topographic image of the Glen of Imail.
Figure 5.69a,b,c:- Statistical graphs between lithology and elevation.
Figure 5.70:- Slope image of Glen of Imail area.

Figure 5.71a,b,c:- Statistical graphs of slope and elevation in the Glen of Imail area.

Figure 5.72a,b,c:- Histogram and cumulative frequencies of the Ribband Group.

Figure 5.73a,b:- Statistical graphs of slope and lithology in the Glen of Imail area.

Figure 5.74:- Graph of skewness for slope distribution of rock type.

Figure 5.75a:- Histogram and cumulative frequencies for Tullow rocks.

Figure 5.76a:- Histogram and cumulative frequencies of rocks of the Kilcullen Group.

Figure 5.77a:- Histogram and cumulative frequencies of the Lugnaquillia plutonic rocks.

Figure 5.78a:- Histogram and cumulative frequencies of the Northern pluton.

Figure 5.79a,b:- Graph of normalised slope distribution for the main lithologies (Glen of Imail).

Figure 5.80a,b:- Relief images of the Glen of Imail area.

Figure 5.81a,b,c:- Descriptive statistical graphs of rock type and relief.

Figure 5.82a,b:- Relief histograms for the Ribband Group and aureole.

Figure 5.83:- Relief histogram of the Tullow pluton.

Figure 5.84:- Relief histograms for the Kilcullen Group.

Figure 5.85:- Relief histograms for the Lugnaquillia pluton.

Figure 5.86:- Relief histograms for the Northern pluton.

Figure 5.87a,b:- Fluvial geomorphology.

Figure 5.88a:- NNE-SSW geological, slope and relief profiles of the Glen of Imail area.

Figure 5.89:- Model for Glen of Imail area.

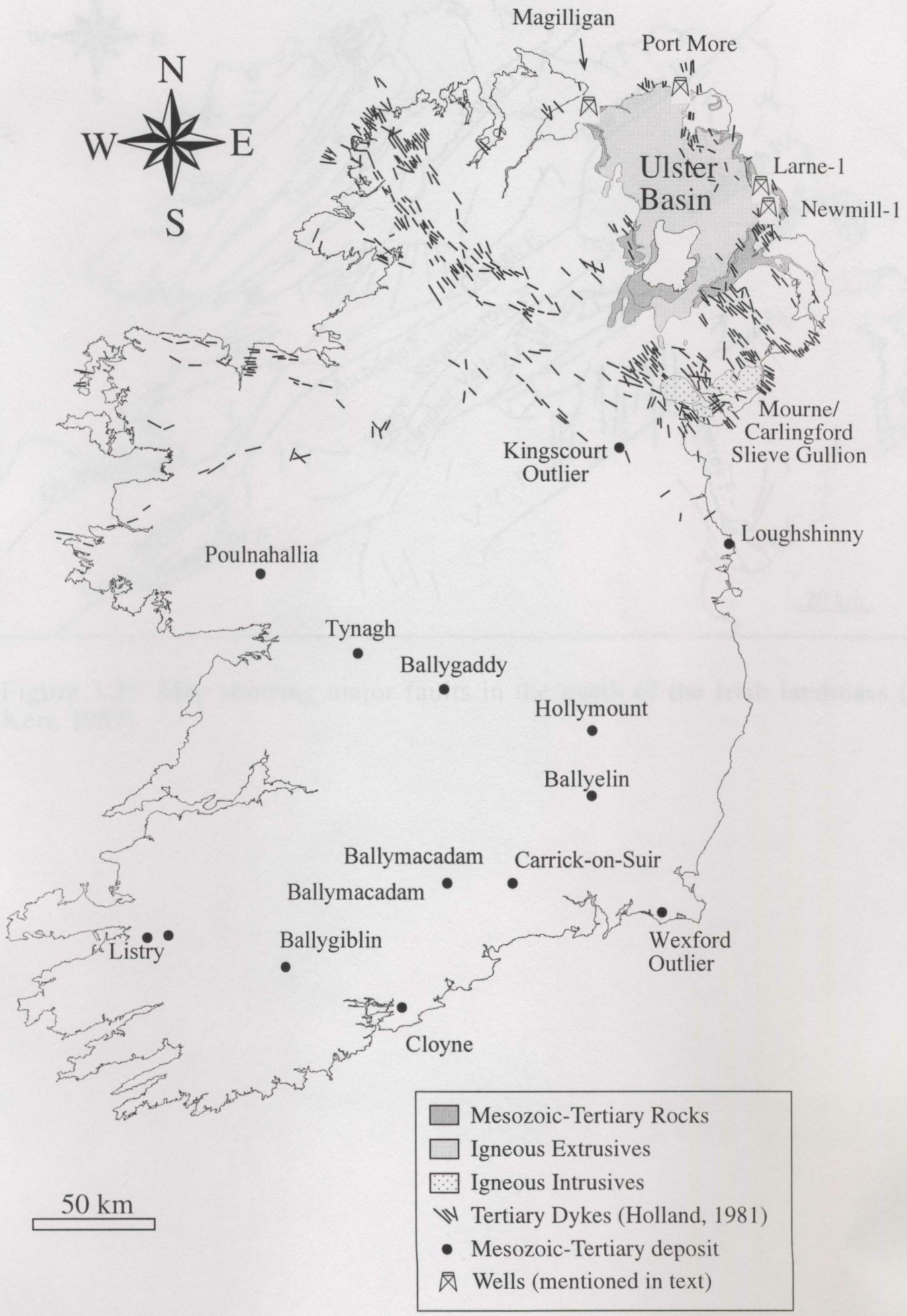

Figure 1.1:- Simplified map of Ireland showing Mesozoic-Tertiary stratigraphy and igneous rocks and other Mesozoic-Tertiary deposits.

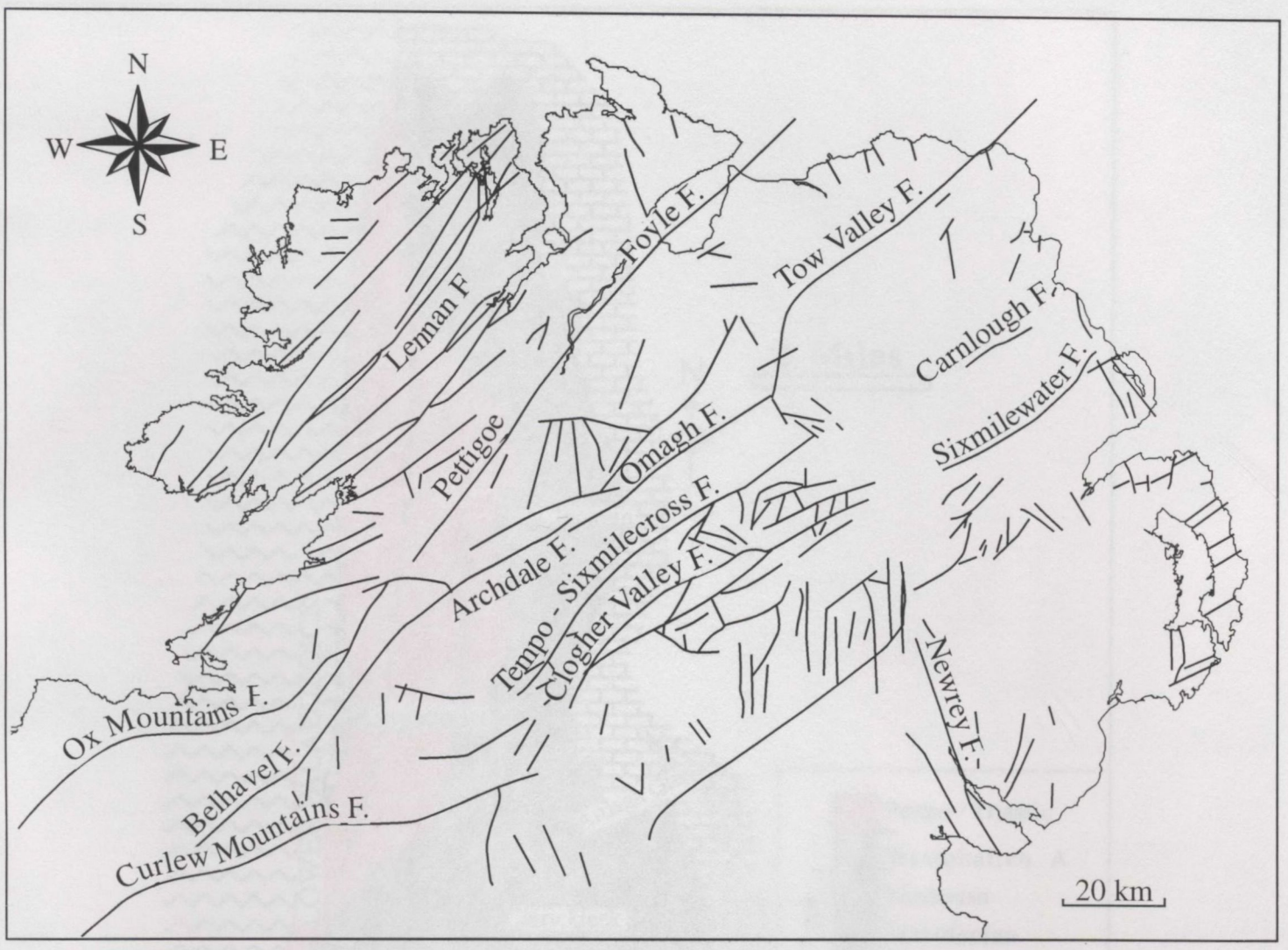

Figure 1.2:- Map showing major faults in the north of the Irish landmass (after Kerr, 1987).

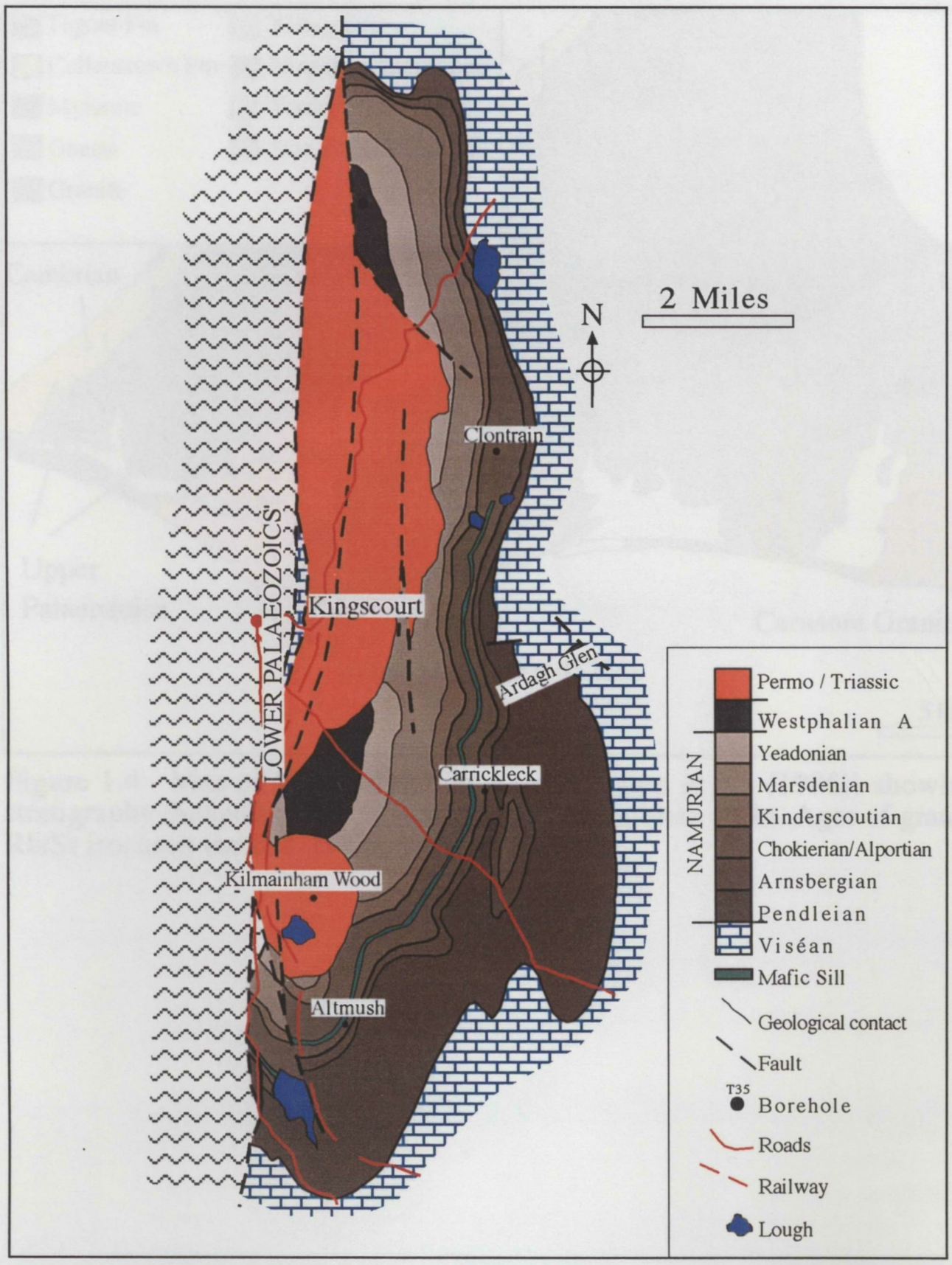

Figure 1.3:- Map of Kingscourt outlier showing Late Carboniferous-Mesozoic stratigraphy preserved in the hanging-wall of ~N-S fault, forming a half grabenal structure.

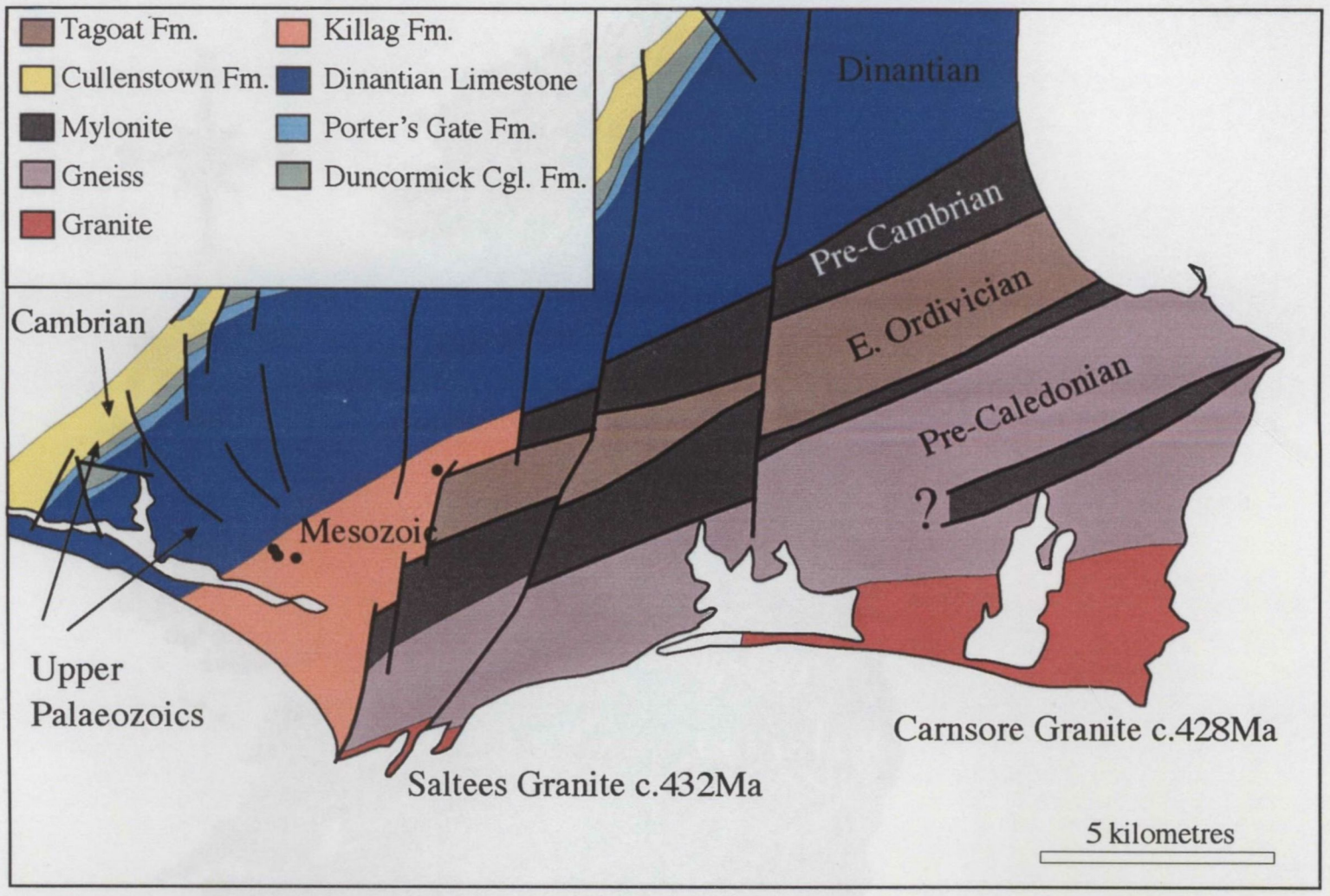

Figure 1.4:- Map of Wexford outlier (after Clayton *et al.*, (1986)) showing Mesozoic stratigraphy faulted against Palaeozoic and Precambrian rocks. Ages of granites based on Rb/Sr isochron method (O'Connor *et al.*, 1988).

- Lough Neagh Clays
- Cretaceous
- Jurassic
- Triassic
- Permian
- Coal measures
- Millstone grit & Sands
- U. Avonian
- U. Carb. limestones
- M. Carb. limestones
- L. Carb. limestones
- L. Avonian
- Kiltorcan beds
- Old Red Sandstone
- Dingle beds
- Silurian quartzite
- Ordovician
- Cambrian quartzite
- Schist/gneiss
- Quartzite
- Limestone
- Tertiary basalt
- Pre-Cenozoic basalts
- Rhyolites
- Diorite gabbro dolerite
- Granite

— Faults

Figure 1.5:- Simplified geology map and topography of Ireland. Areas of highest relief occur on oldest rocks, except the Tertiary aged Mourne granites and the Tertiary basalts in the NE of County Antrim.

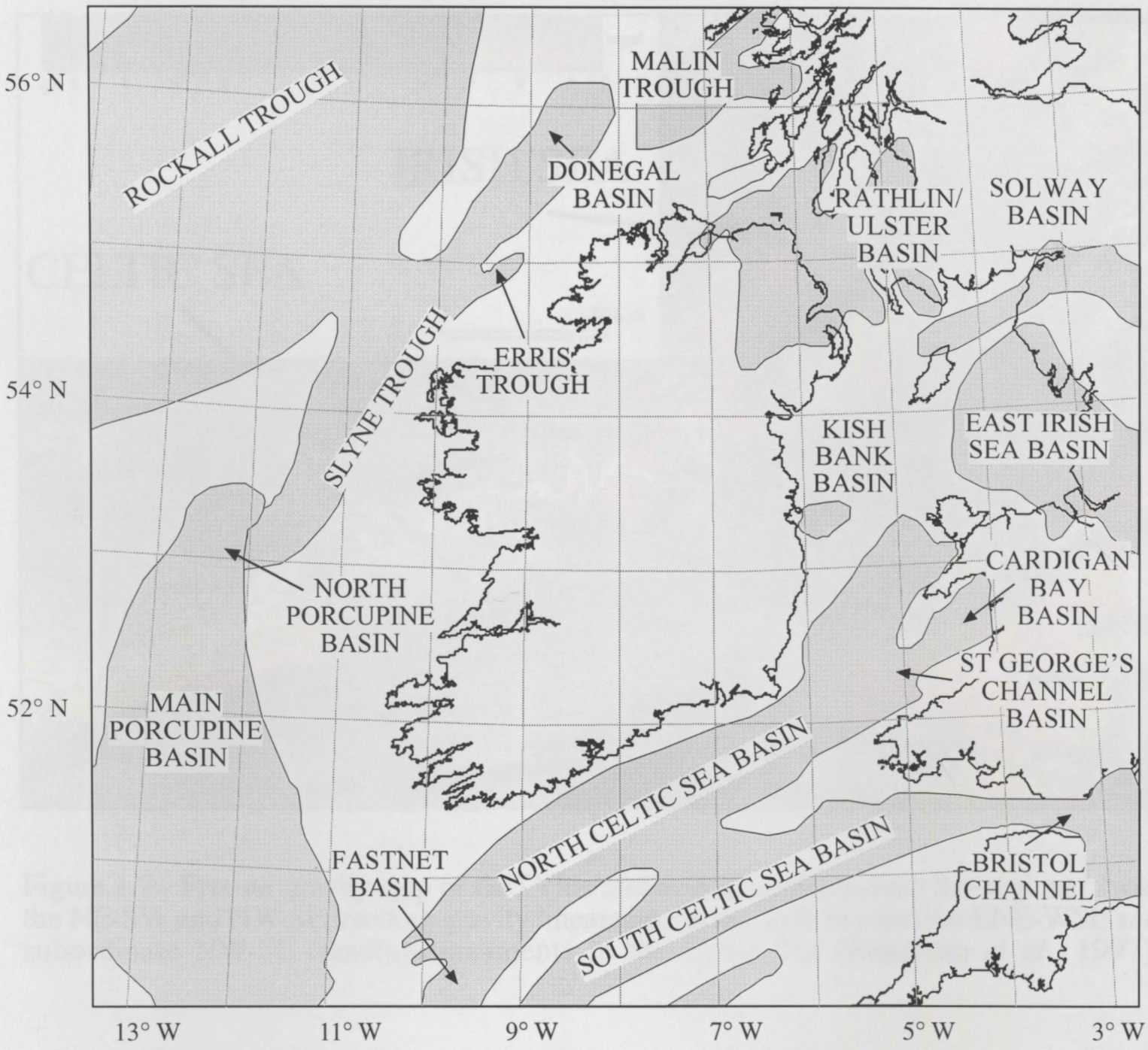

Figure 1.6:- Map of Ireland and offshore Mesozoic-Tertiary basins.

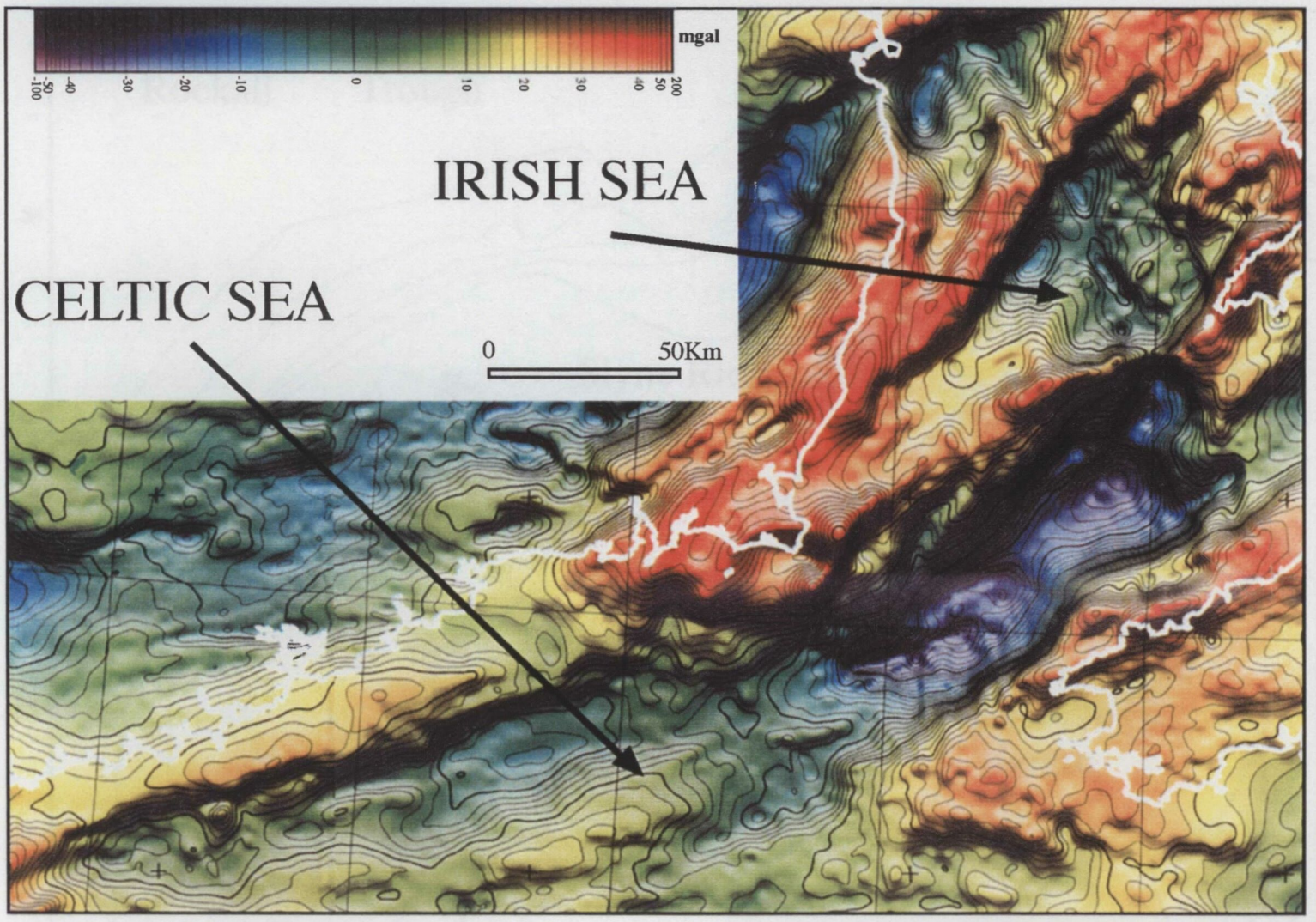

Figure 1.7:- Free air gravity map of the Celtic and central-southern Irish Sea regions. Note the NE-SW and NW-SE trending gravity lineaments in the Irish Sea and the ENE-WSE and subordinate NW-SE trending lineaments in the Celtic Sea (Readman *et al.*, 1997).

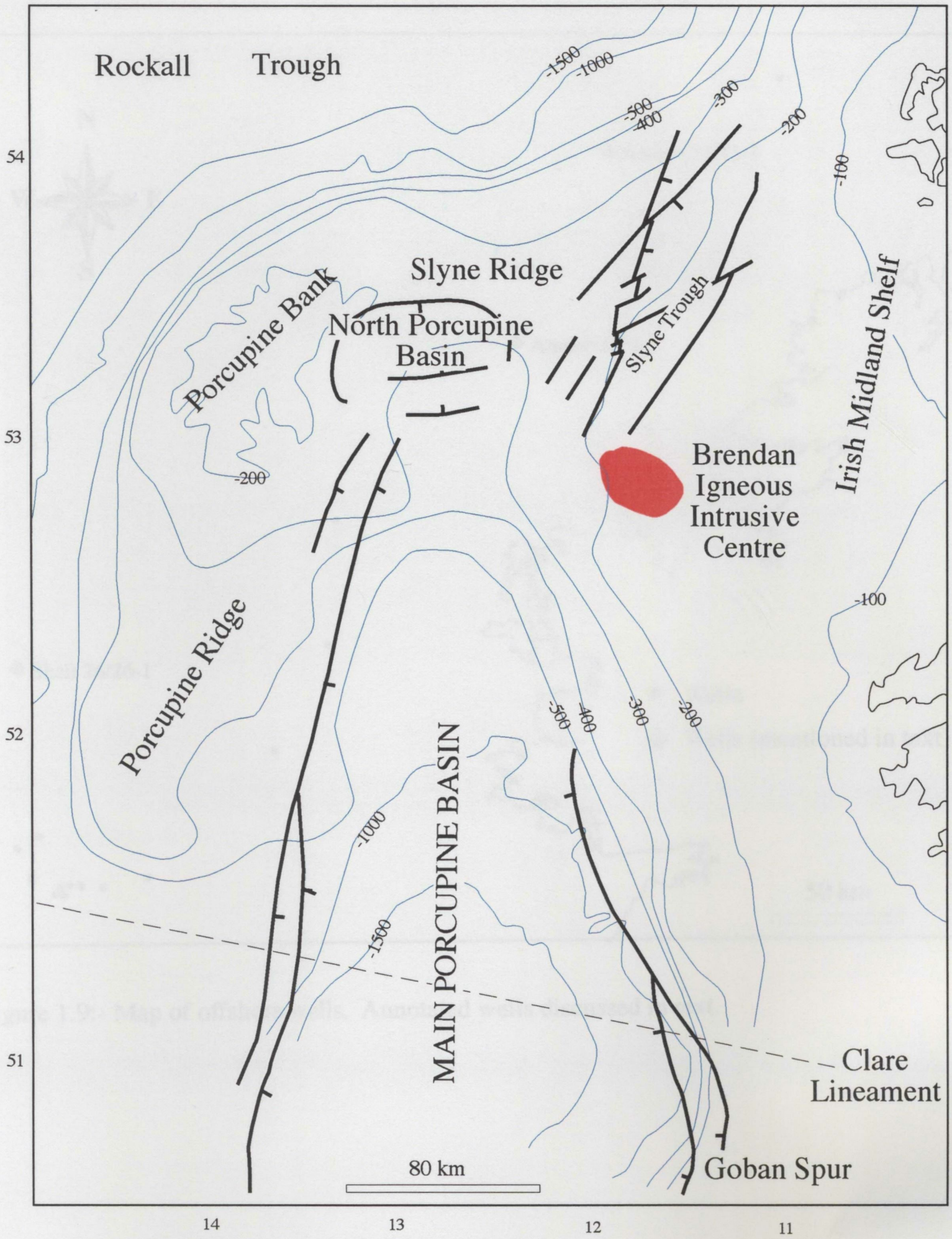

Figure 1.8:- Map of Porcupine Mesozoic-Tertiary basin (Moore & Shannon, 1991) and adjacent bathymetric highs. Note the location of the Clare lineament and compare with Charlie Gibbs Fracture zone on figure 1.11.

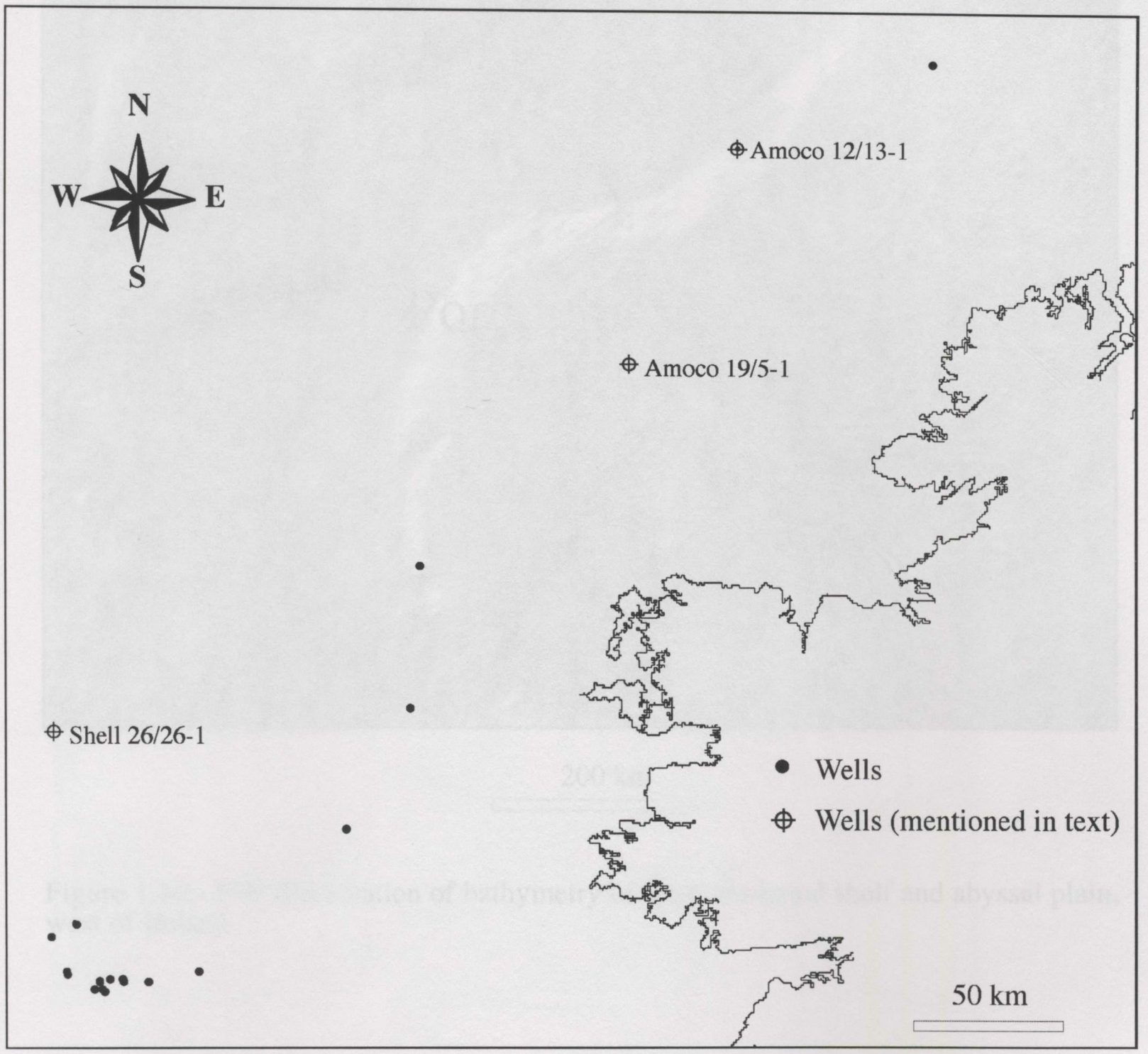

Figure 1.9:- Map of offshore wells. Annotated wells discussed in text.

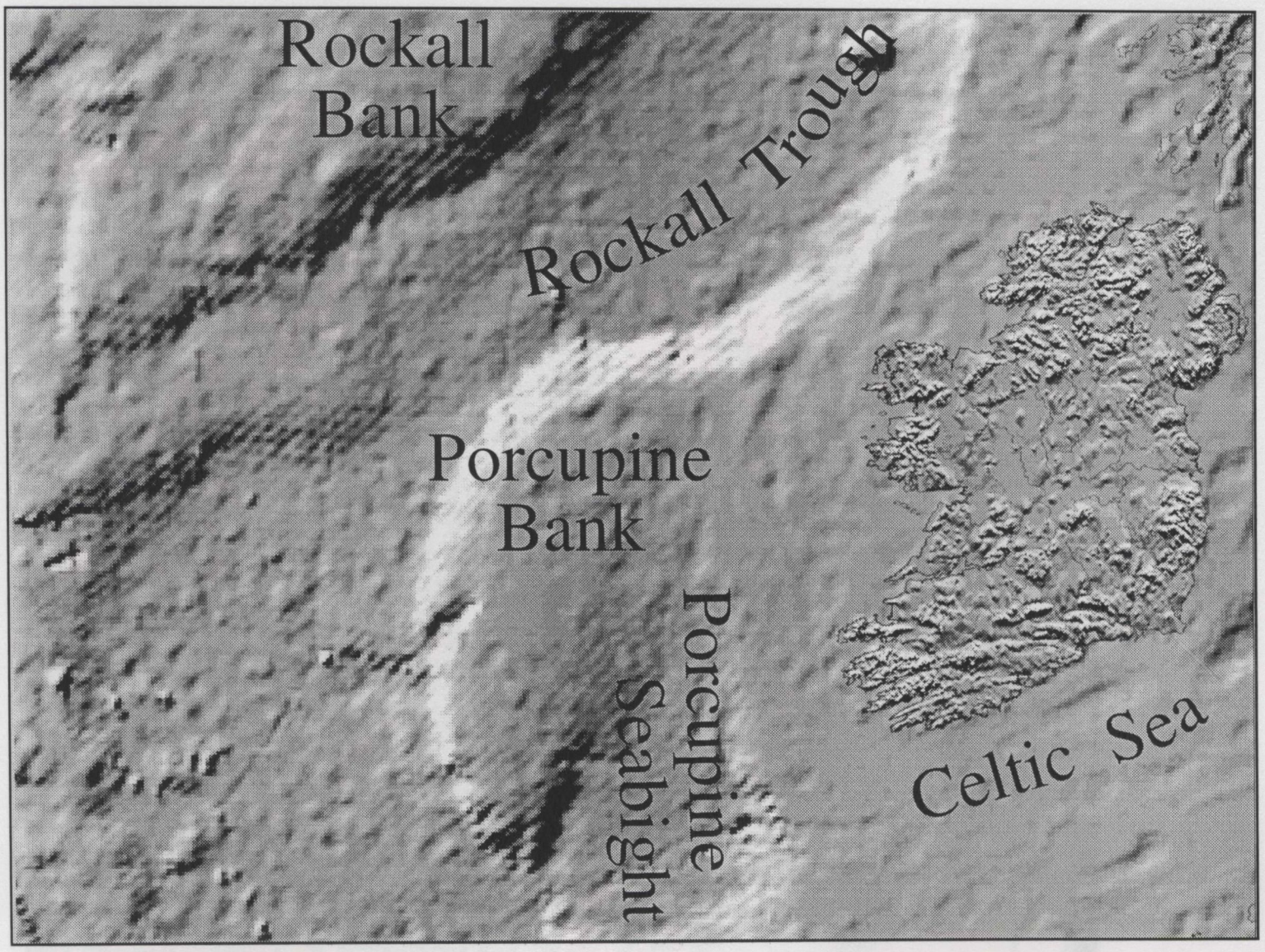

Figure 1.10:- NW illumination of bathymetry of the continental shelf and abyssal plain, west of Ireland.

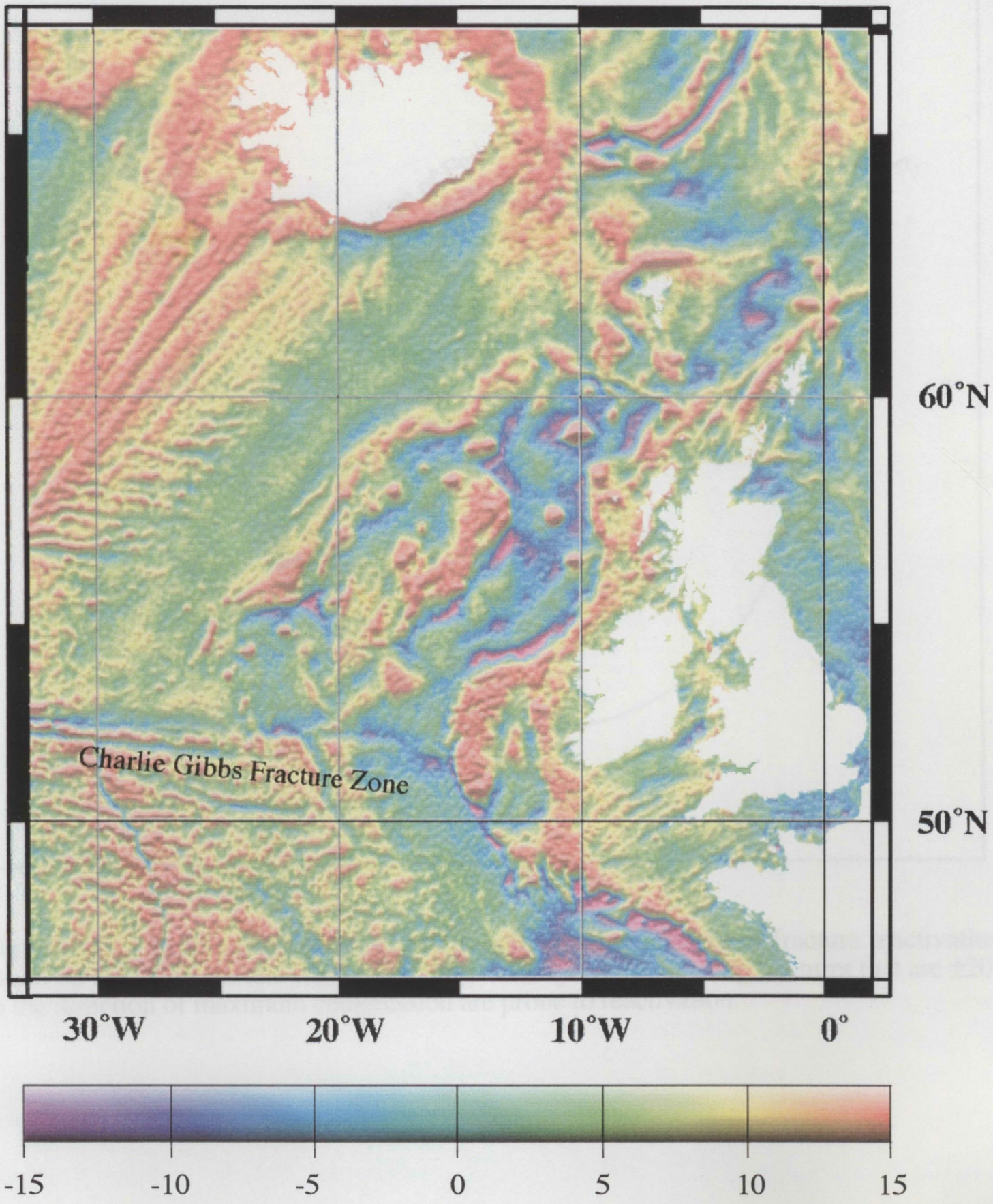

Figure 1.11:- Free air gravity map (after Sandwell & Smith, 1995) of NE Atlantic. Note the ~E-W trend of the Charlie Gibbs Fracture zone, which represents a major transform to the ~N-S Atlantic spreading ridge.

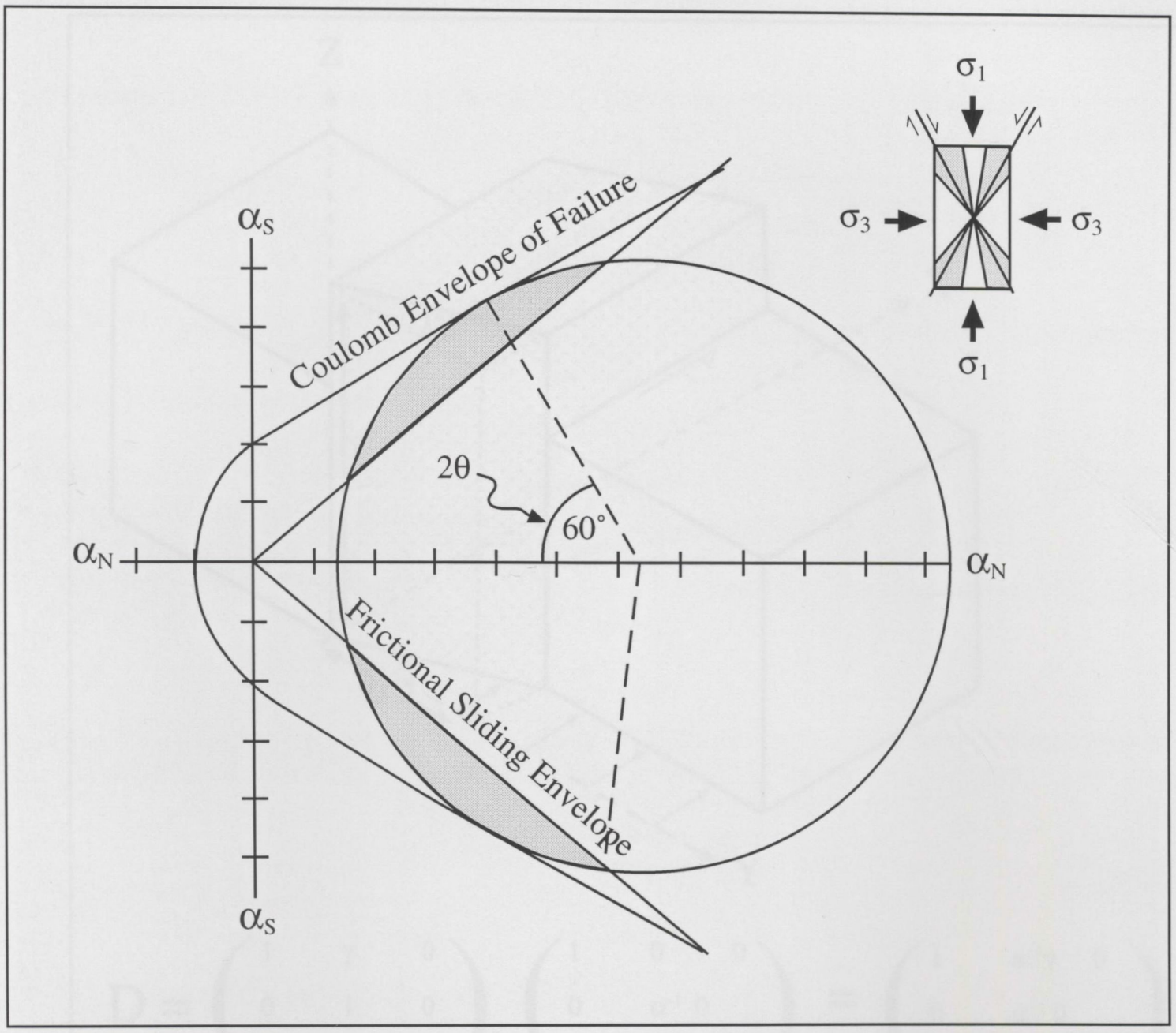

Figure 1.12:- Simple diagram of Mohr circle illustrating concept of fracture reactivation based on the Coulumb and frictional sliding envelopes. Pre-existing fractures that are ±20° to the direction of maximum compression are prone to reactivation.

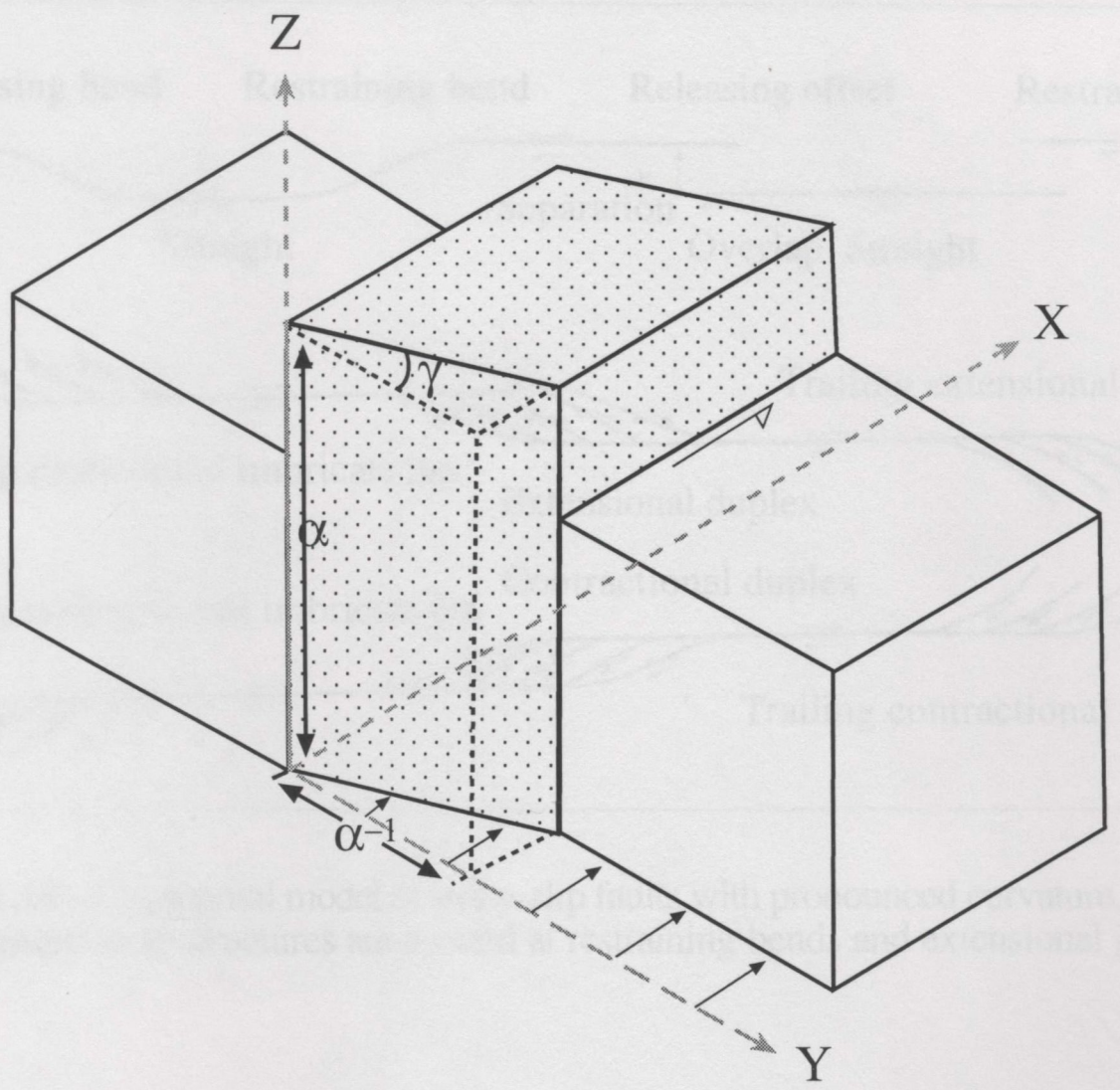

$$D = \begin{pmatrix} 1 & \gamma & 0 \\ 0 & 1 & 0 \\ 0 & 0 & 1 \end{pmatrix} \begin{pmatrix} 1 & 0 & 0 \\ 0 & \alpha^{-1} & 0 \\ 0 & 0 & \alpha \end{pmatrix} = \begin{pmatrix} 1 & \alpha^{-1}\gamma & 0 \\ 0 & \alpha^{-1} & 0 \\ 0 & 0 & \alpha \end{pmatrix}$$

Figure 1.13:- Block diagram of transpression with constant-volume (after Sanderson & Marchini, 1984).

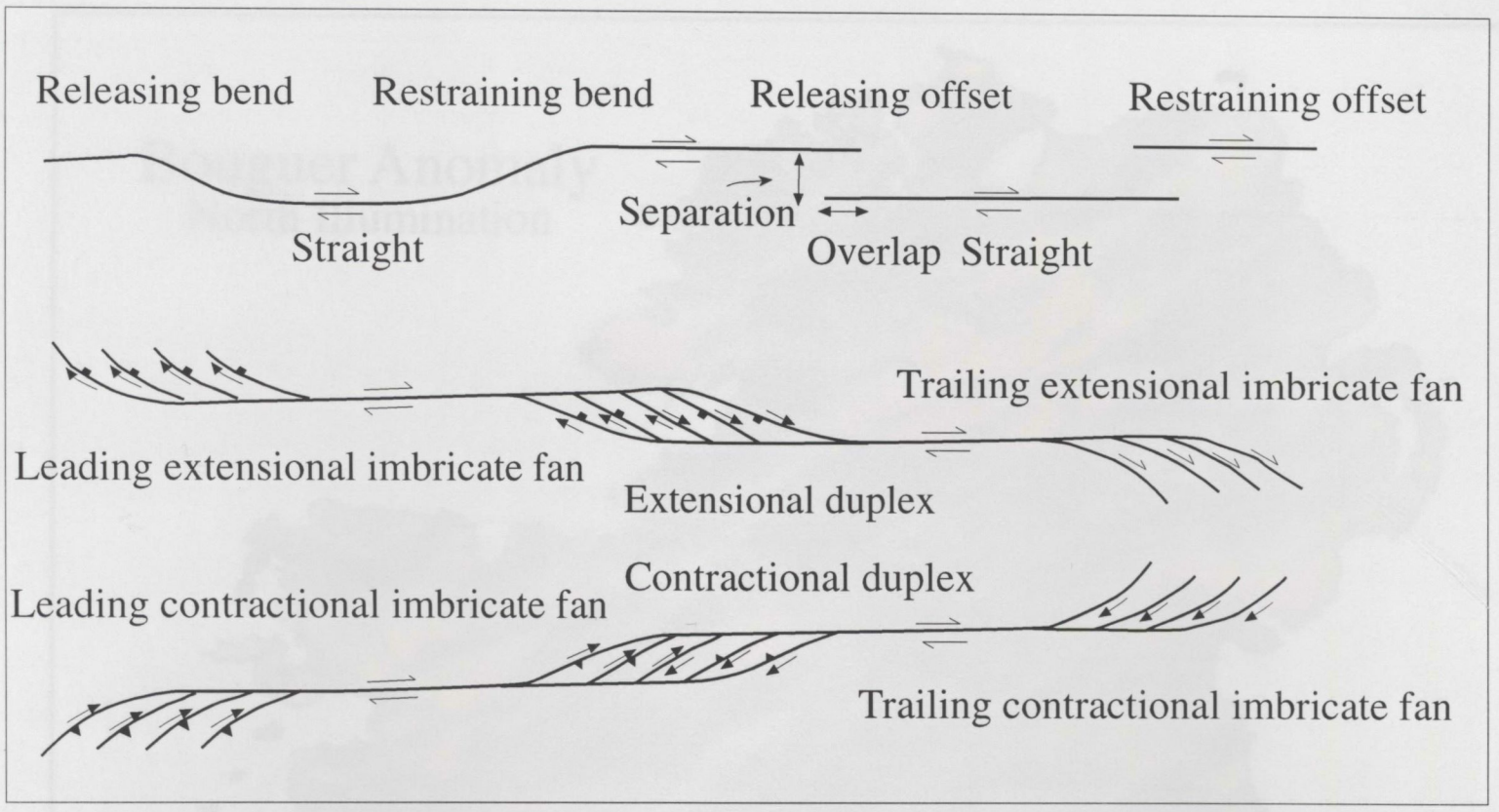

Figure 1.14:- Conceptual model of strike-slip faults with pronounced curvature. Transpressional and transtensional structures are located at restraining bends and extensional jogs respectively.

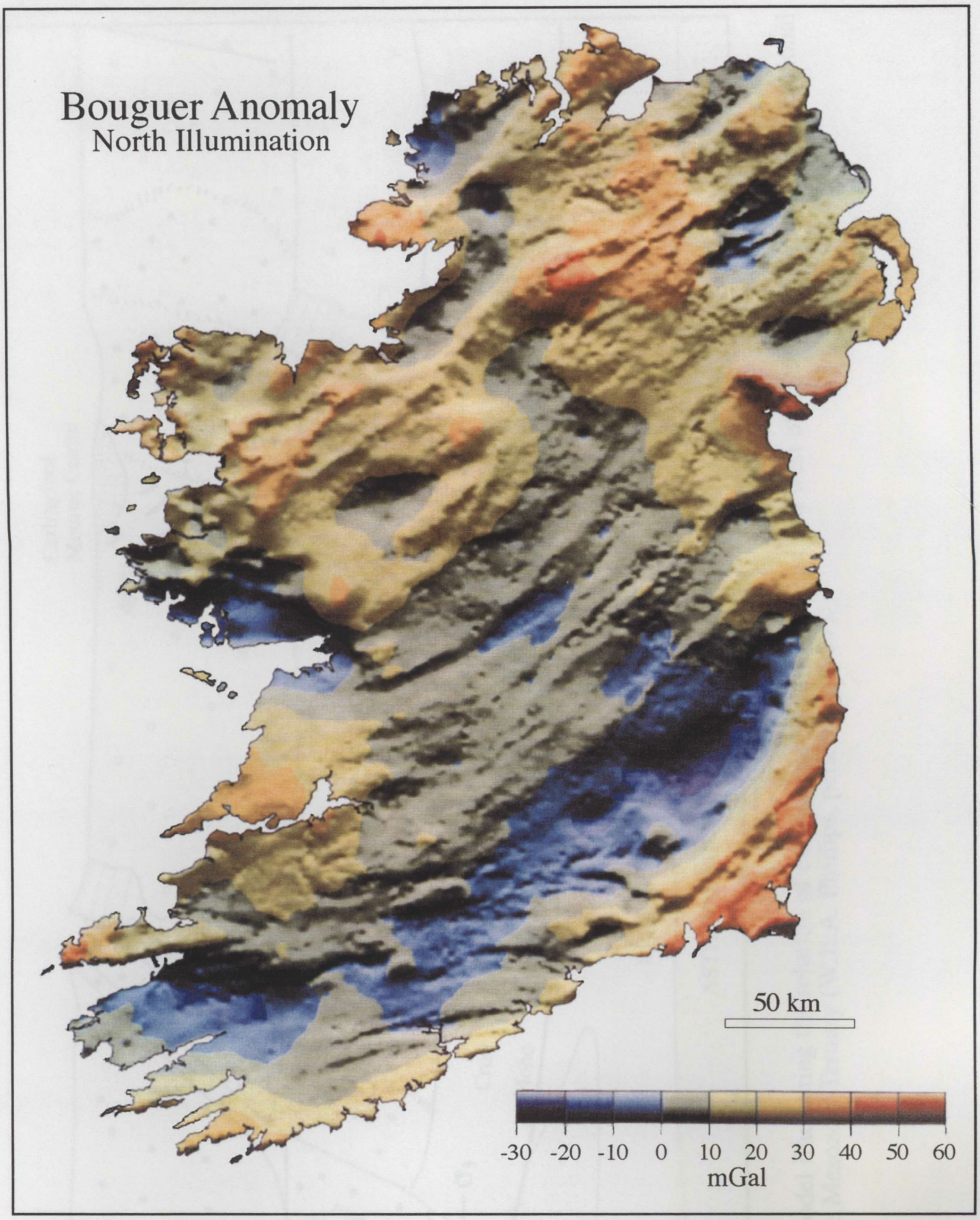

Figure 1.15:- Bouguer gravity anomaly map of Ireland with illumination from the north (Readman *et al.*, 1997). Areas of low and high anomaly are generally associated with granite and crystalline basement rocks respectively (compare with figure 1.5). The gravity shows strong NE-SW and subordinate NW-SE trends. In the south (Munster basin), and on the eastern and western coasts of the country, the gravity trends are ~E-W.

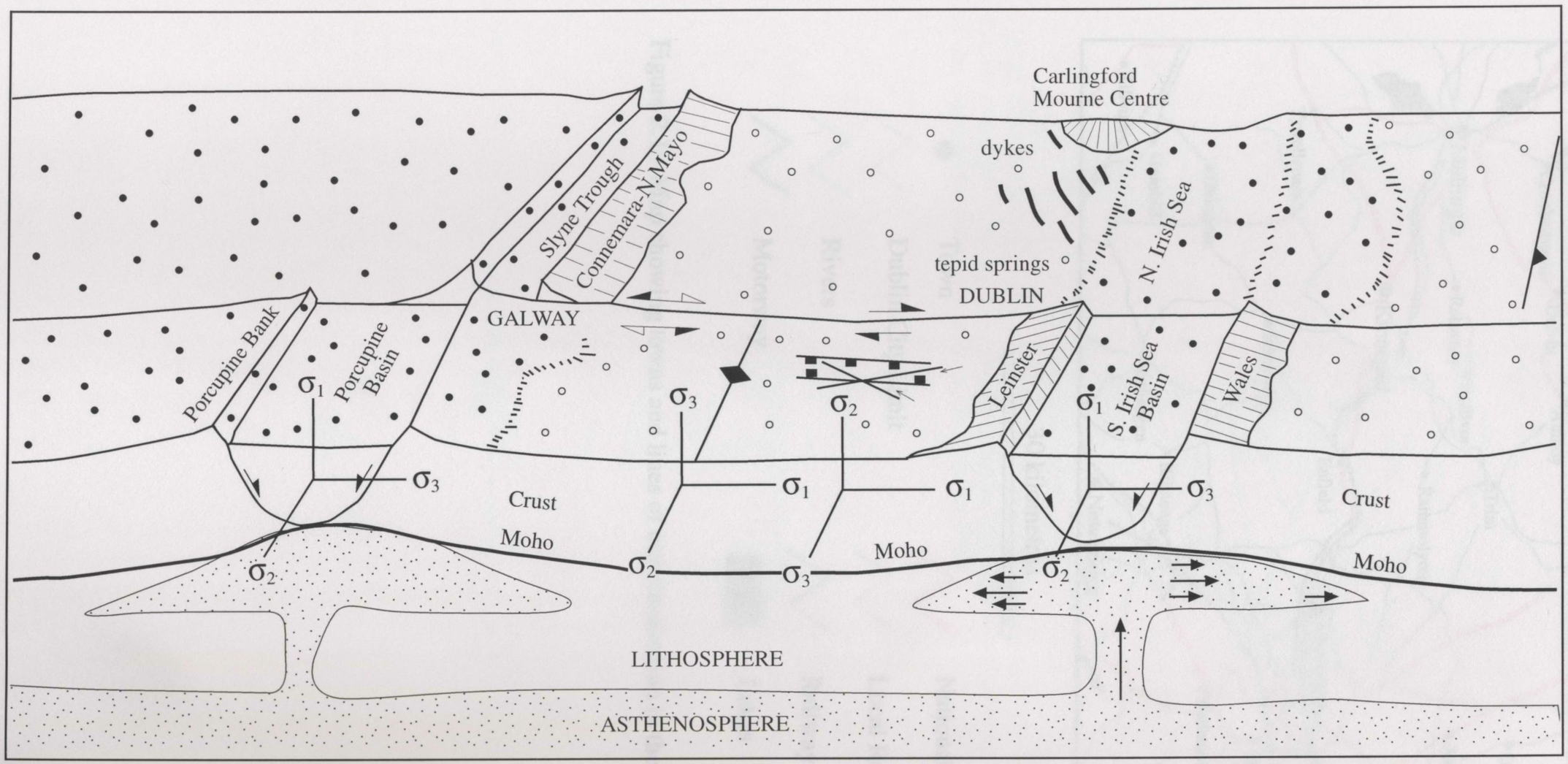

Figure 1.16:- Dextral transform model illustrating the relation of extensional basins to the east and west of Ireland with onshore compressional and transform structures during the Mesozoic-Tertiary (W.E.A. Phillips, pers. com. 1997).

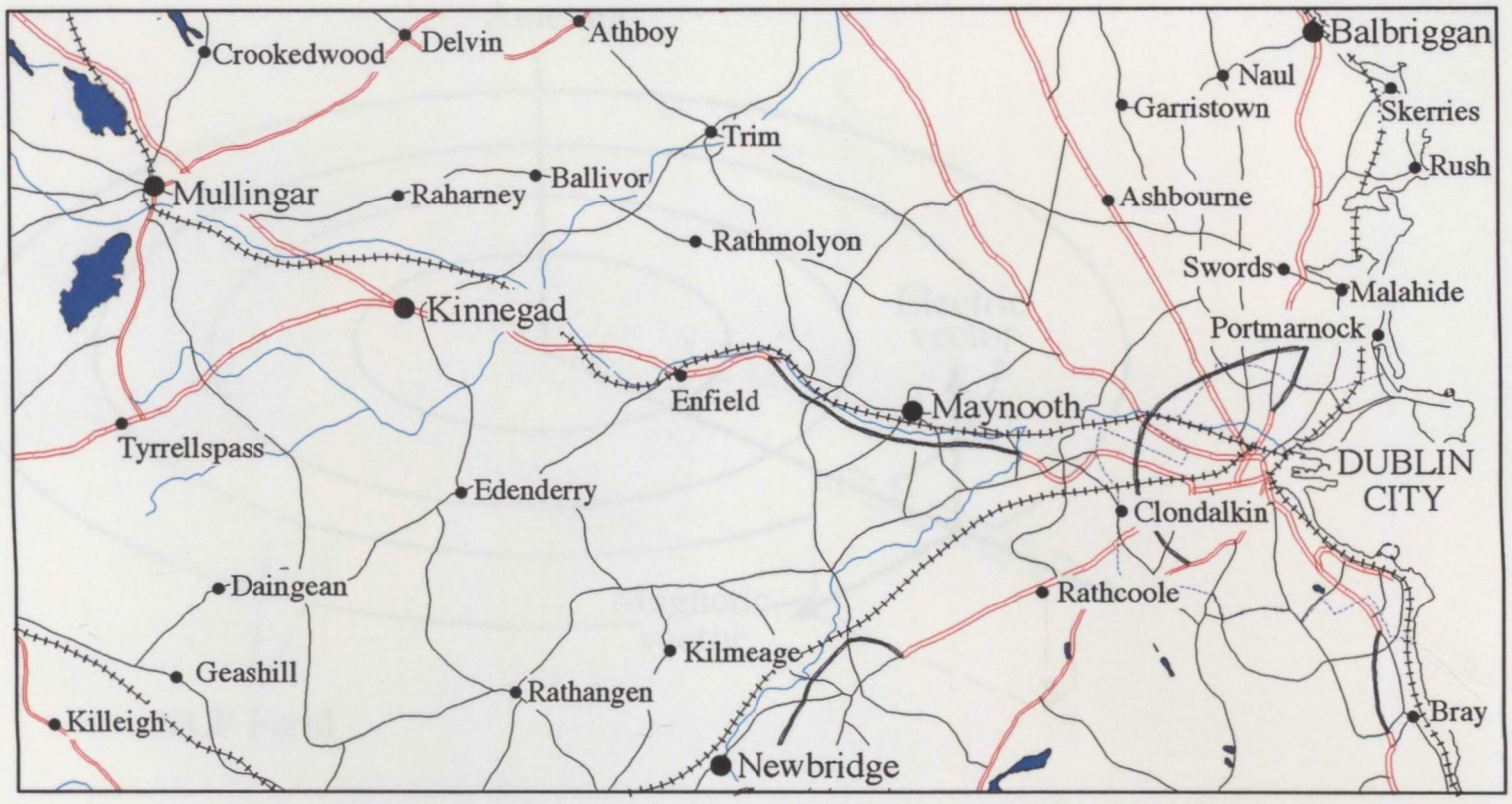

Figure 2.1:- Map showing towns and lines of communication in the area of study.

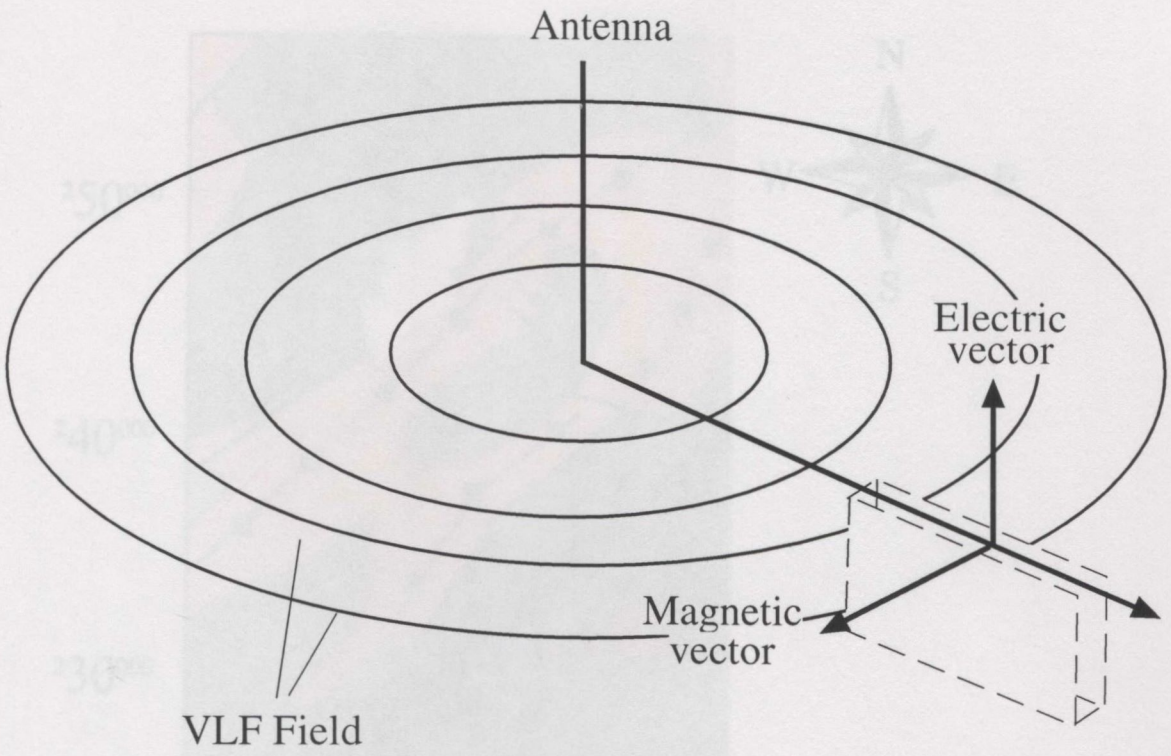

Figure 2.2:- Principal of the very low frequency (VLF) method. The dashed lines show a tabular conductor striking towards the antenna which is intersected by the magnetic vector of the electromagnetic field (Kearey & Brooks, 1984).

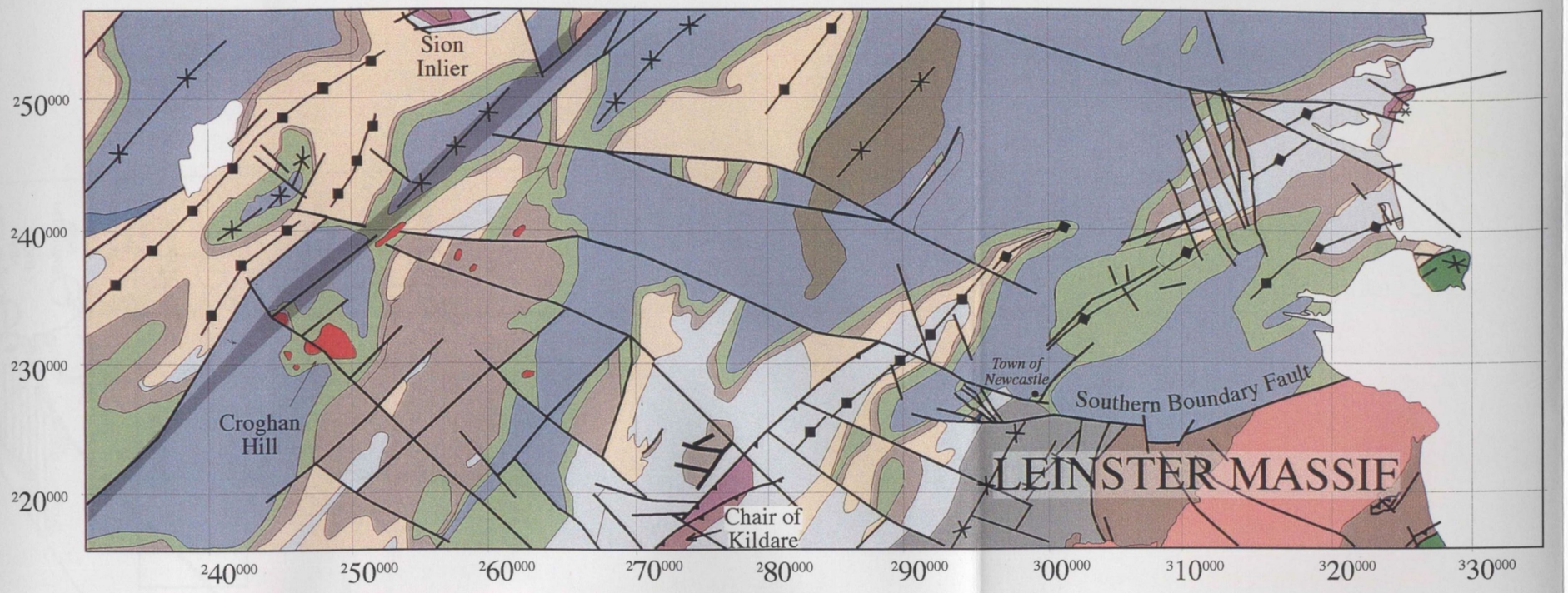

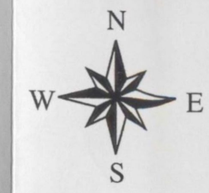

Deltaic and marine sandstones, siltstones and mudstones with minor marl (Namurian).

Basinal limestones. Predominantly dark laminated, argillaceous calcisilitites and calcareous shales with limestone turbidites (Brigantian - Holkerian[Visean]).

Shallow water limestones. Mixture of pale calcarenites with dark grey micrites, olistostromes, and basinal limestones (Holkerian - Chadian[Visean]).

Shallow marine, pale grey massive limestones with shelf margin oolite banks and black mudstone/basinal facies (Chadian - Courcyan [Visean - Tournaisian]).

Waulsortian limestones. Massive, pale grey biomicrites (Courceyan [Tournaisian]).

Basal Carboniferous Transgression Facies. Argillaceous Bioclastic Limestones. Medium to dark grey fossiliferous argillaceous calcarenites and subordinate calcareous shales (Courceyan [Tournaisian]).

Old Red Sandstone. Sandstones, conglomerates and siltstones - alluvial flanglomerates and terrestrial sediments (Devonian to Lower Carboniferous).

Slate, shale and greywacke. Kilcullen Group (Llandovery - Ludlow).

Fine-grained metasedimentary rocks of the Ribband Group (Tremadoc - Llanvirn).

Dark green/gray shale and siltstone (Llanvirn).

Slates, quartzites and graywackes of the Bray Group (Upper Cambrian to Lower Ordovician).

Carboniferous aged volcanics - basaltic rocks (Chadian and Asbian).

Leinster Batholith (see Appendix 3). Northern and Upper Liffey Valley Plutons (c.404Ma). Caledonian.

Normal/Strike-Slip Fault

Thrust or Reverse Fault

Syncline

Anticline

Town of Newcastle (Co. Dublin)

Figure 2.3(a):- Simplifed solid geology map of study area. Note the right step offset of the southern boundary fault near the town of Newcastle (Co. Dublin), and the subsequent 'horsetail' termination of the original fault strand. Darkened area approximates trace of Iapetus suture.

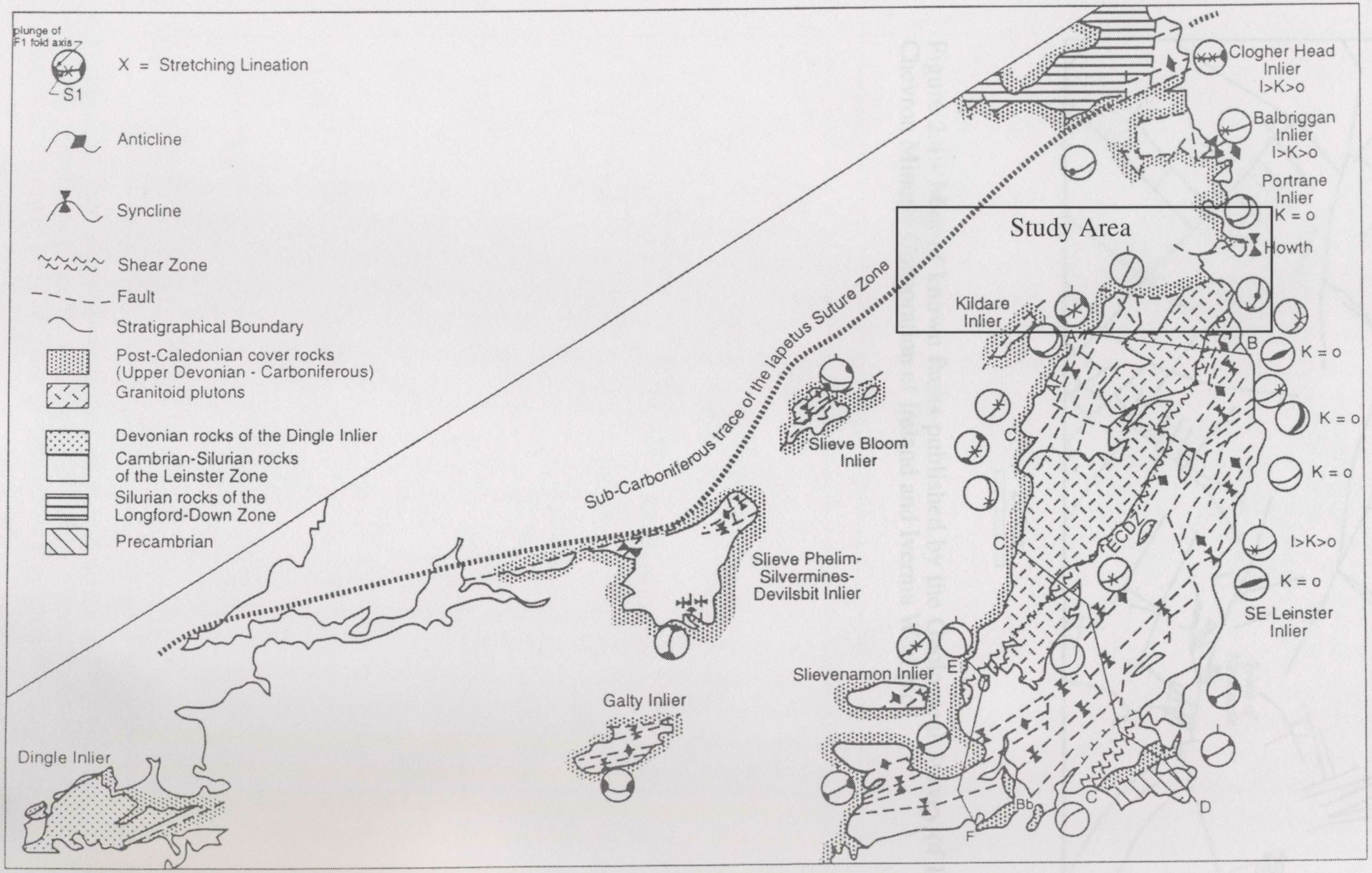

Figure 2.3(b) Summary of structures in Central Ireland (W.E.A. Phillips, pers. comm. 2000).

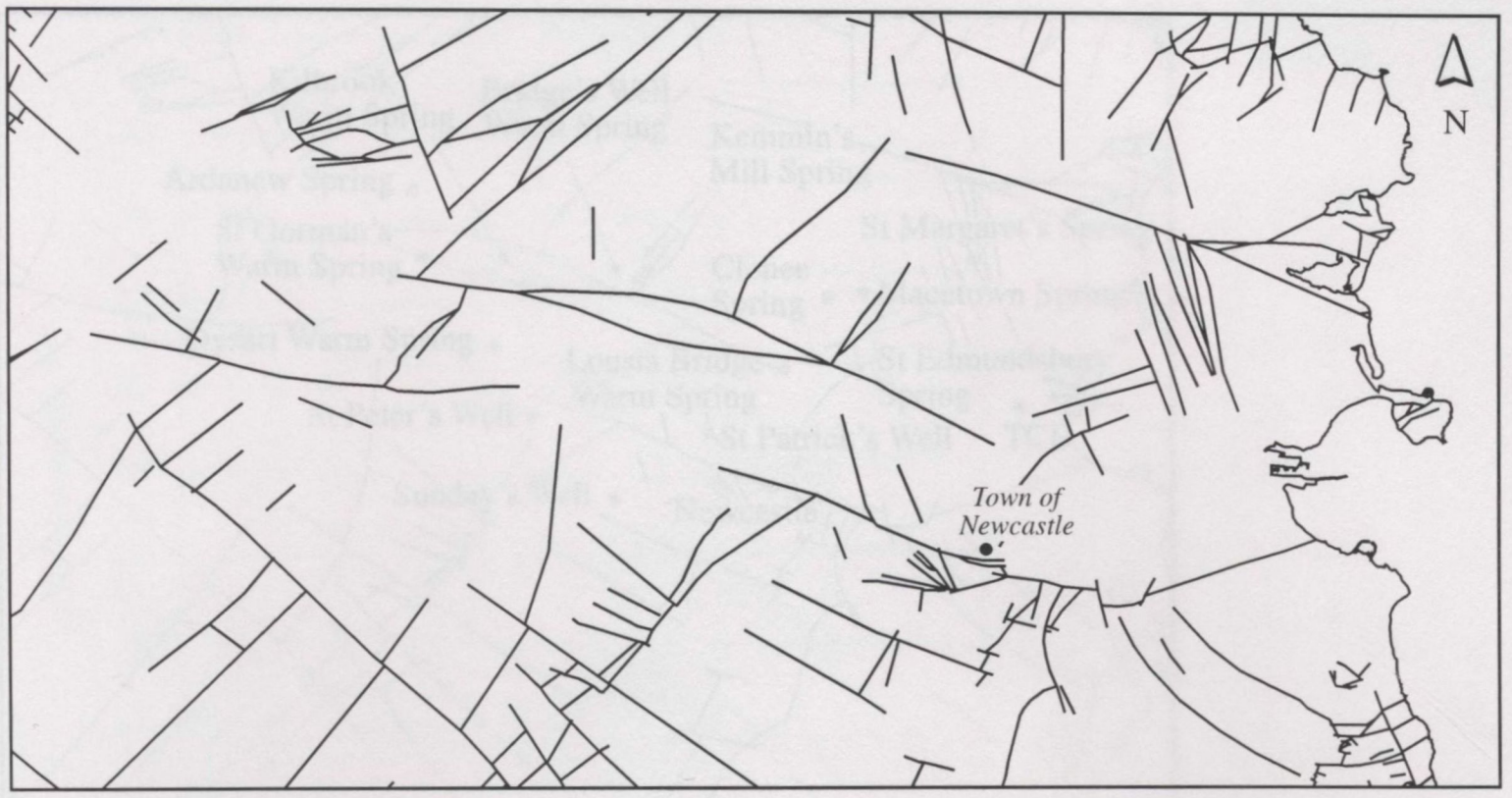

Figure 2.4:- Map of known faults published by the Geological Survey of Ireland, and Chevron Mineral Corporation of Ireland and Ivernia West plc.

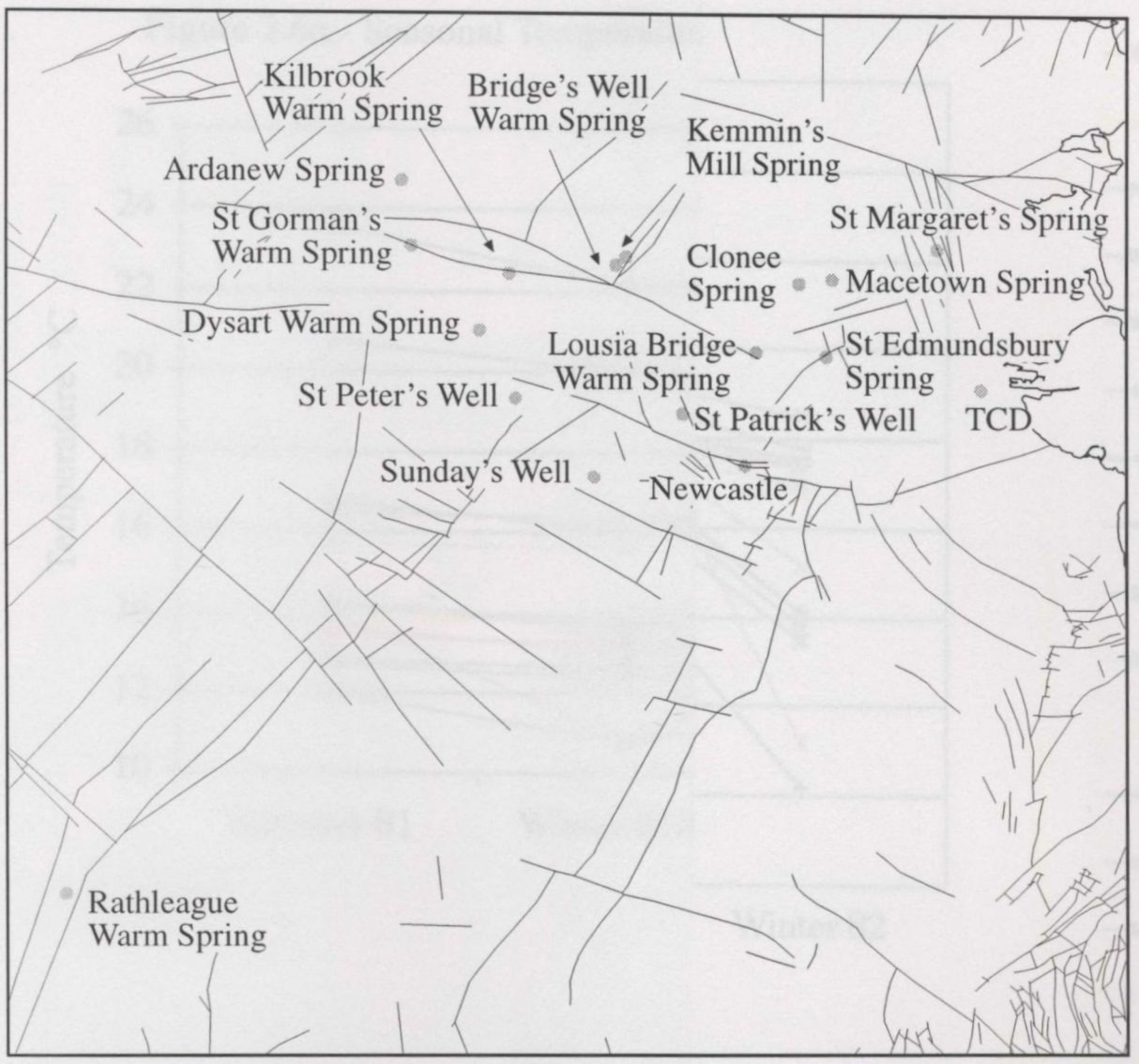

Figure 2.5:- Two maps showing the names and codes of known warm springs in the area of study. An additional well to the south of the study area is also shown; 1017W. Data obtained from Burdon & Burns (1983).

Figure 2.6a:- Seasonal Temperature Variation of Irish Springs

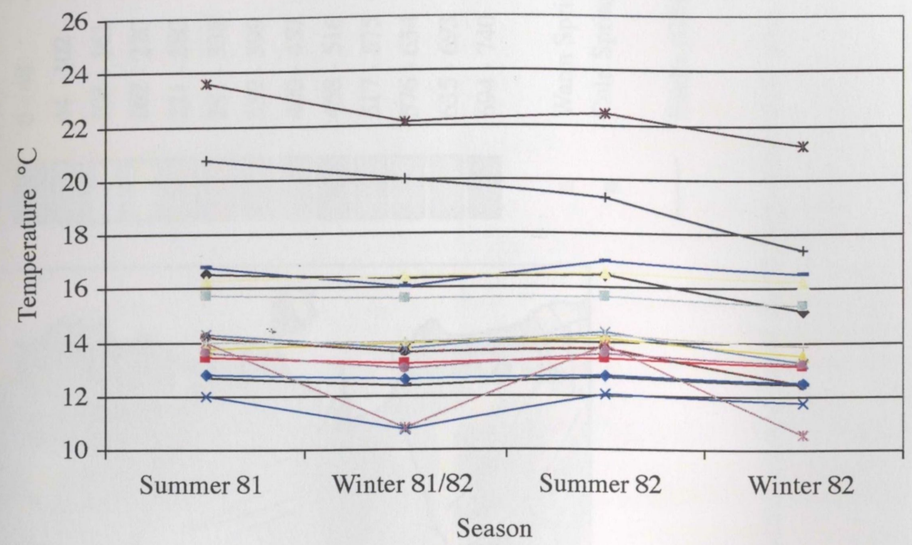

Figure2.6b:- Mean temperature of springs

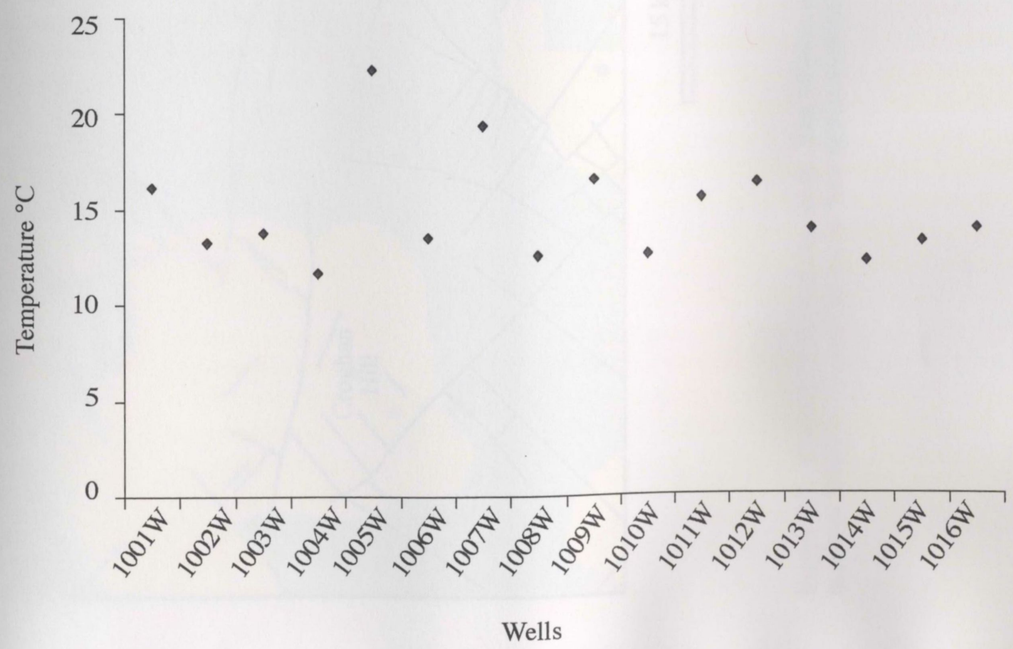

Figure 2.6c:- Deviation from Mean

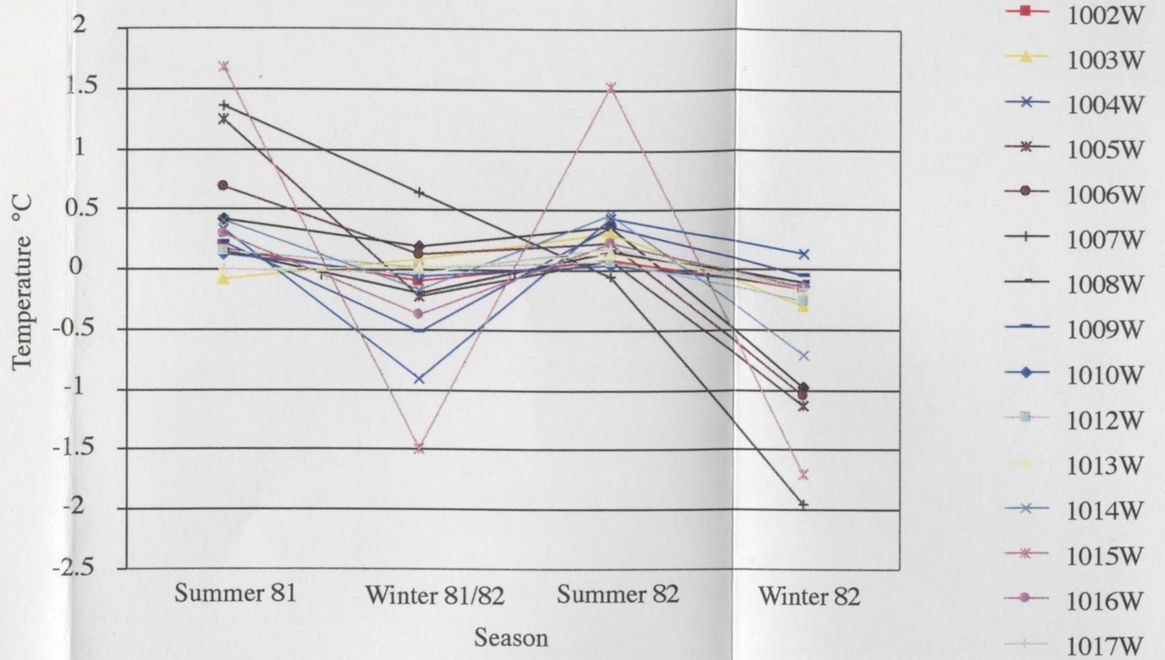

Figure2.6d:- Maximum, minimum and mean temperatures of springs

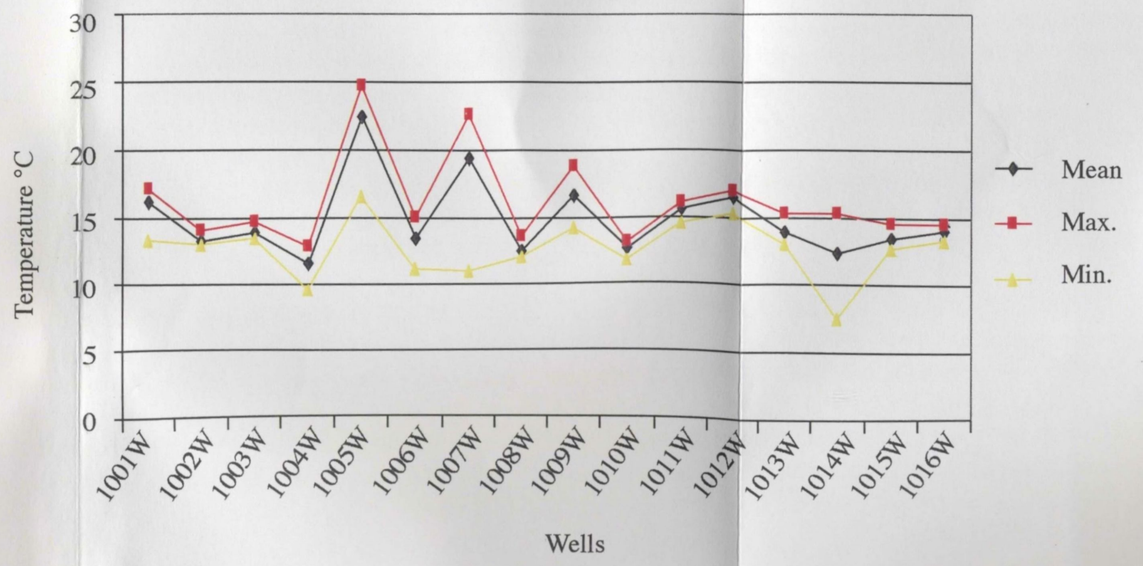

Figure 2.6:- Graphs showing temperature measurements recorded from May 1981 to January 1983 (Minerex Limited).

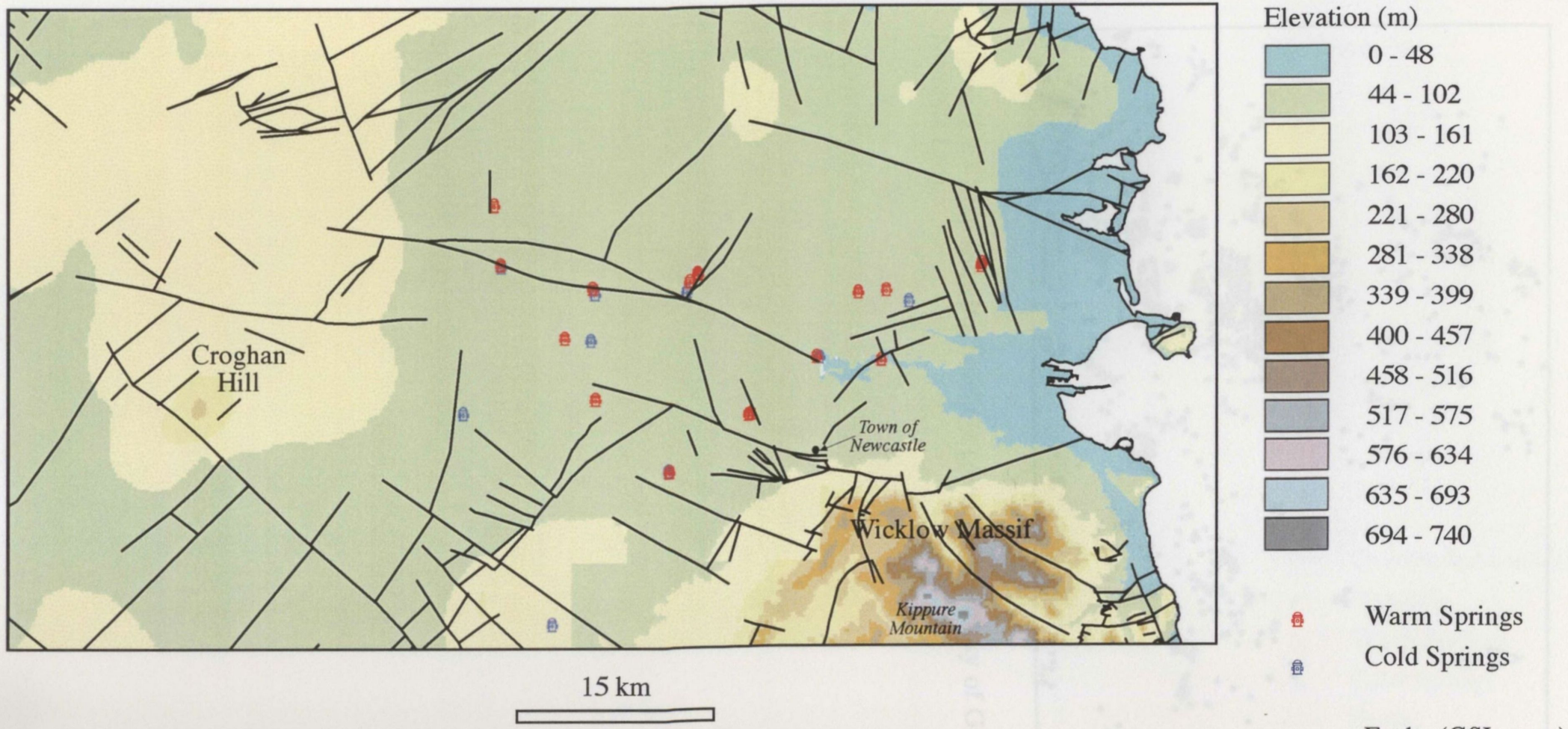

Figure 2.7:- Contoured map of elevation. The DEM is of 200m spatial resolution, with the exception of the SE part of the study area, i.e. the northern Wicklow Mountains are at 50m spatial resolution (chapter 5).

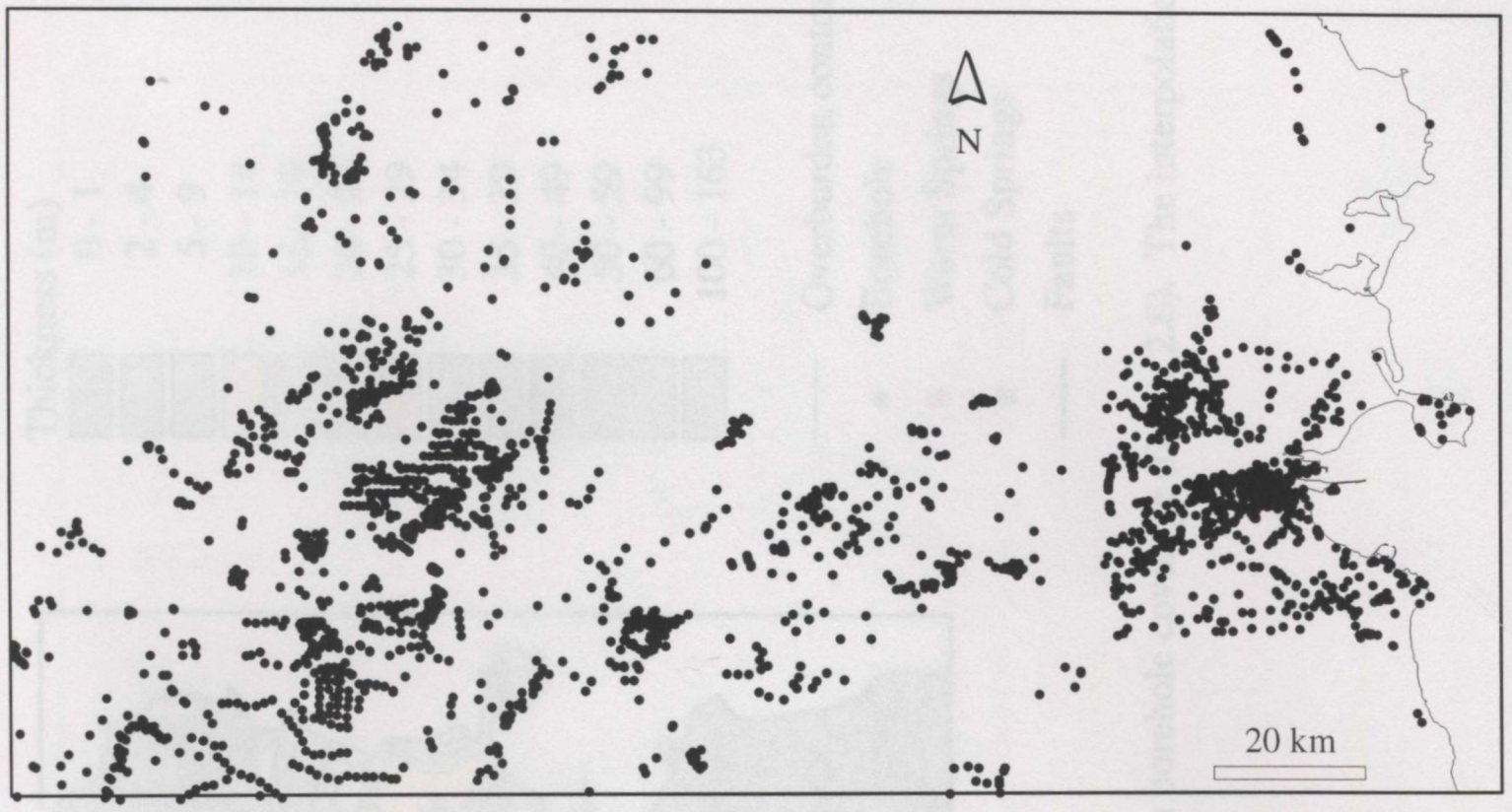

Figure 2.8:- Map showing borehole coverage (courtesy of GSI, Navan Resources and Noranda Ltd).

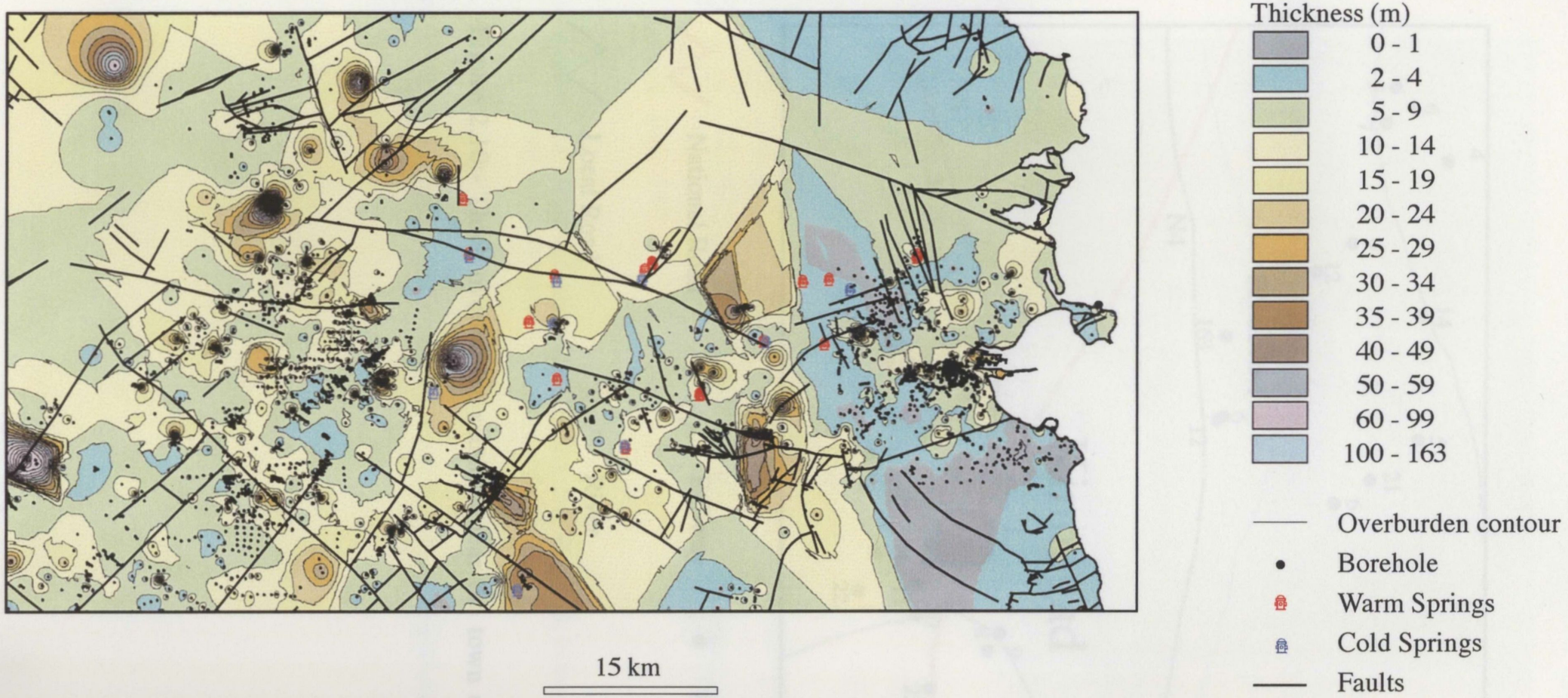

Figure 2.9:- Map showing interpolated thickness of overburden in study area, derived from borehole coverage (figure 2.8). The interpolation was calculated using the 'nearest neighbour' method with ArcView GIS software.

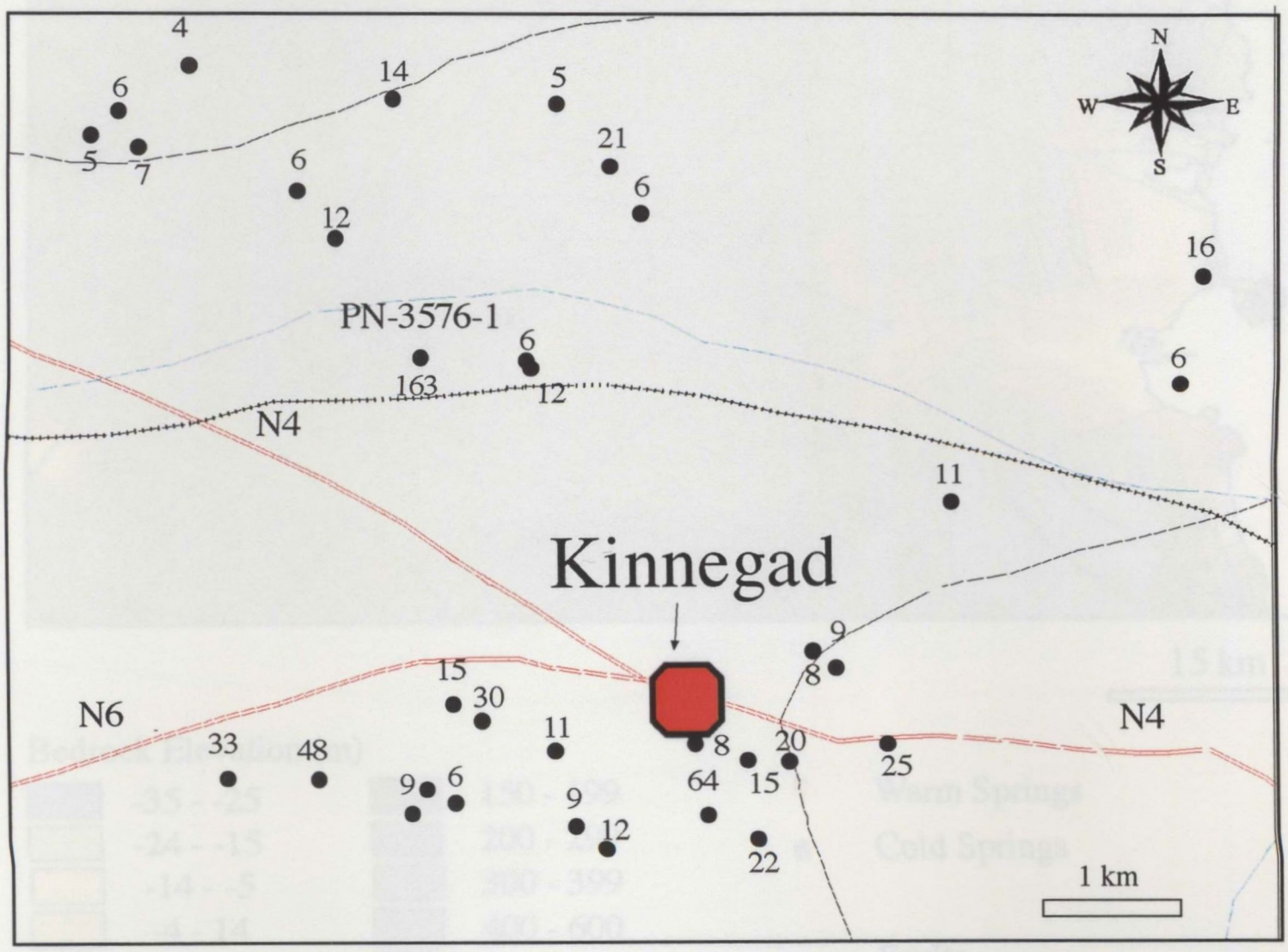

Figure 2.10:- Thick overburden sections near the town of Kinnegad (Co. Meath).

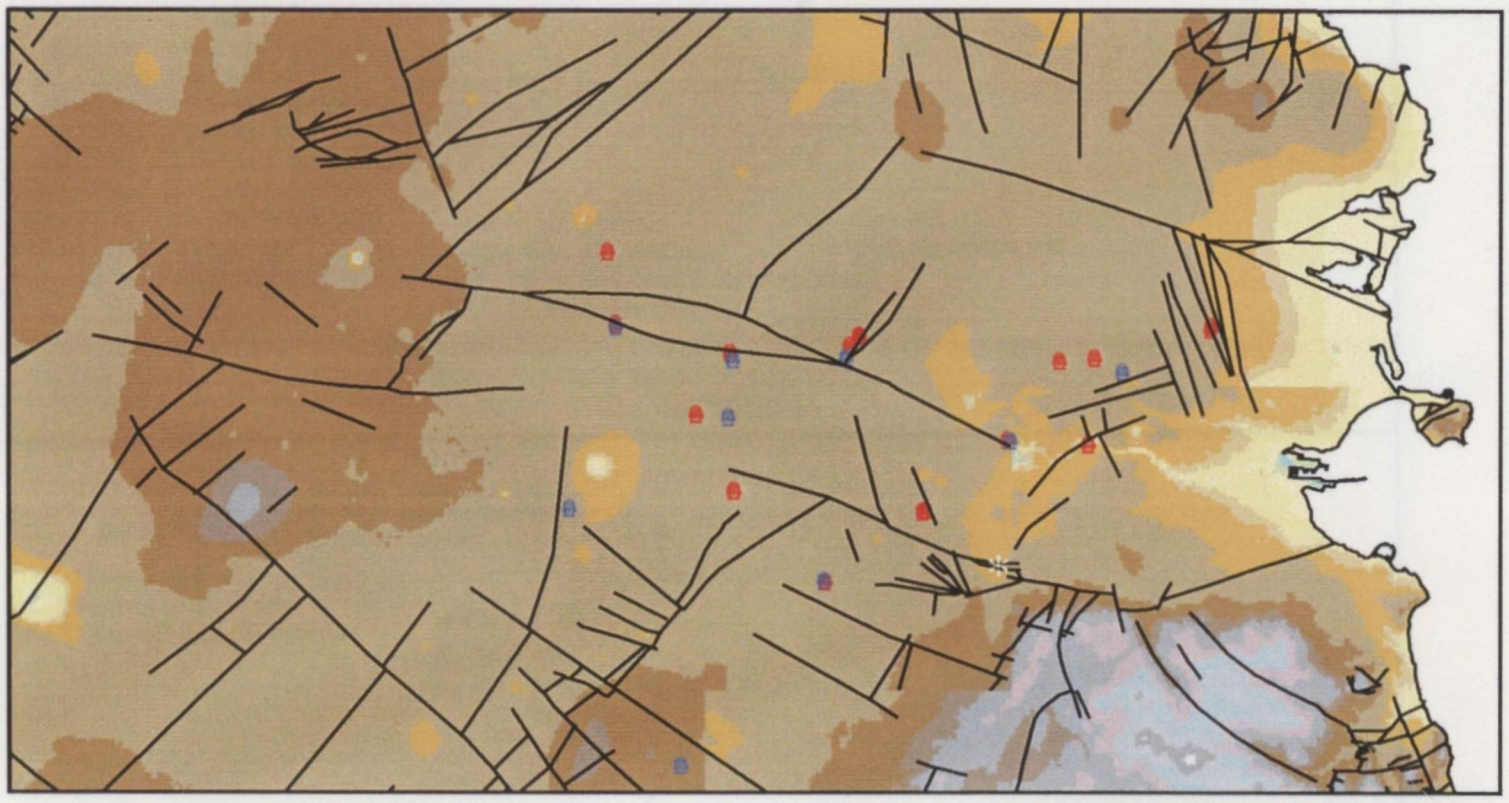

Figure 2.11:- Map showing bedrock elevation. Bedrock in borehole CN-NC-08 (Newcastle, Co. Dublin) is below present-day sea-level.

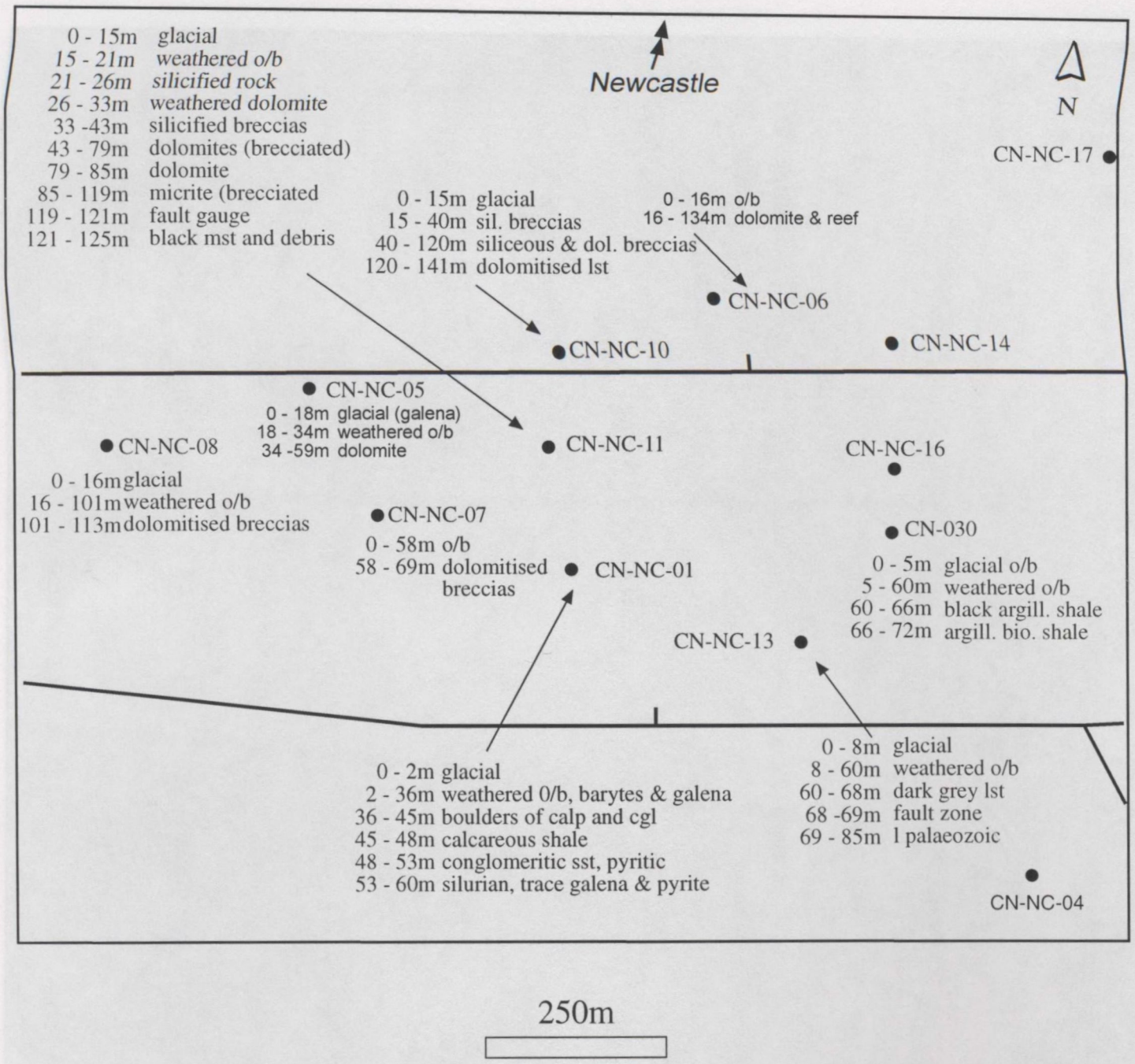

Figure 2.12:- Composition of cored overburden material, south of the town of Newcastle (Co. Dublin).

Basinal limestones (Calp). Predominantly dark laminated, argillaceous calcisilitites and calcareous shales with limestone turbidites (Brigantian - Holkerian).

Shallow water limestones (Ballysteen Formation). Mixture of pale calcarenites with dark grey micrites, olistostromes, and basinal limestones (Holkerian - Chadian).

Slate, shale and graywacke (Carrighill Formation). Kilcullen Group (Llandovery - Ludlow).

◆ Boreholes

250 m

N

Figure 2.13:- Solid geology map of VLF-R survey area. E-W faults downthrow Carboniferous limestones to the north. Silurian rocks occur in the south.

Figure 2.14a:- Modelled thicknesses of overburden (m) from VLF-R measurements. The resistivity of the upper layer is assumed to be 300Ωm.

Basinal limestones (Calp). Predominantly dark laminated, argillaceous calcisilitites and calcareous shales with limestone turbidites (Brigantian - Holkerian).

Shallow water limestones (Ballysteen Formation). Mixture of pale calcarenites with dark grey micrites, olistostromes, and basinal limestones (Holkerian - Chadian).

Slate, shale and graywacke (Carrighill Formation). Kilcullen Group (Llandovery - Ludlow).

◆ Boreholes

● VLF Station

250m

N

Figure 2.14b:- Modelled resistivity values of the lower layer, assuming an upper layer resistivity of 300Ωm.

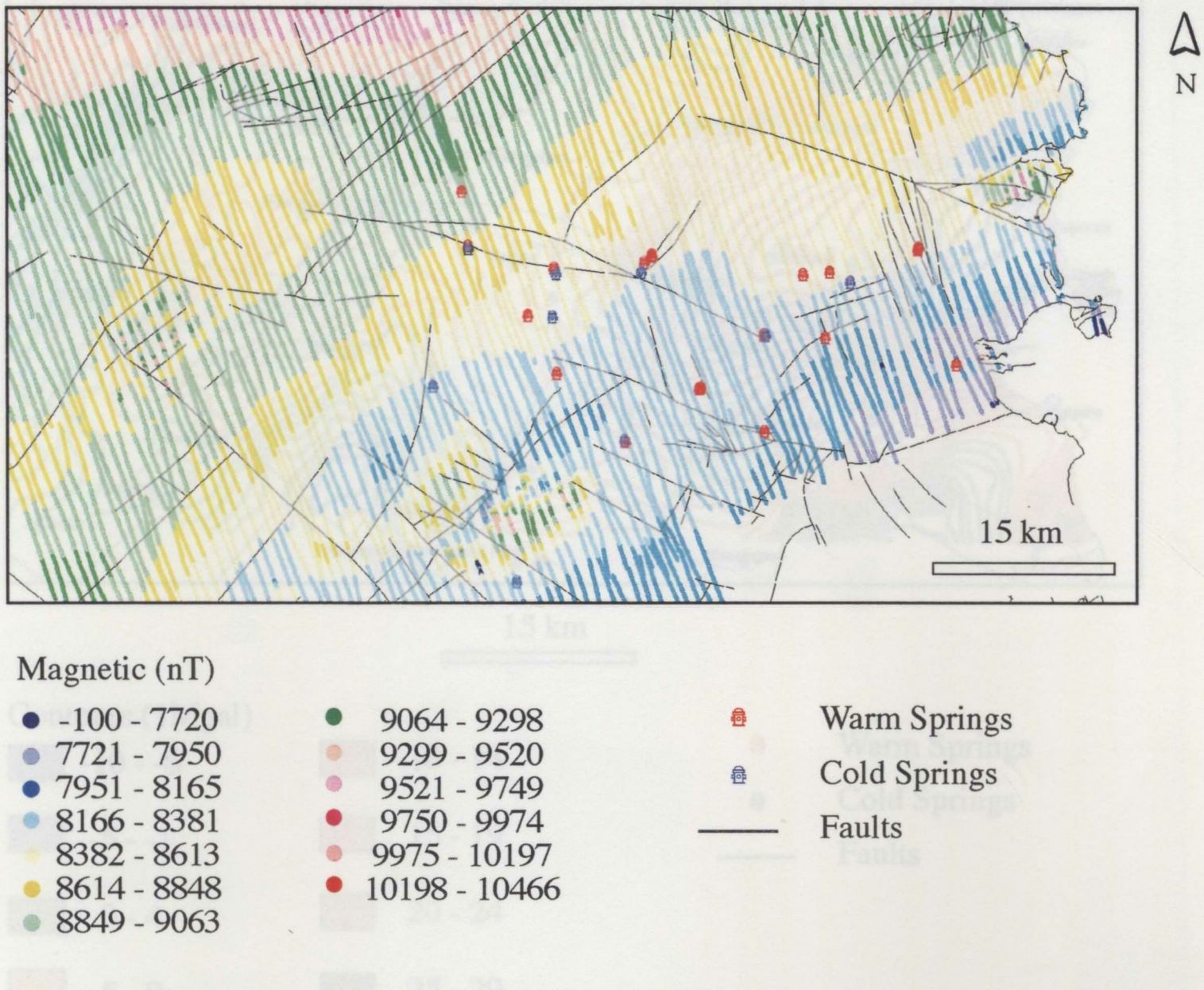

Figure 2.15 :- Total aeromagnetic anomaly map of study area . Faults and warm springs are also shown. nT = nanotesla.

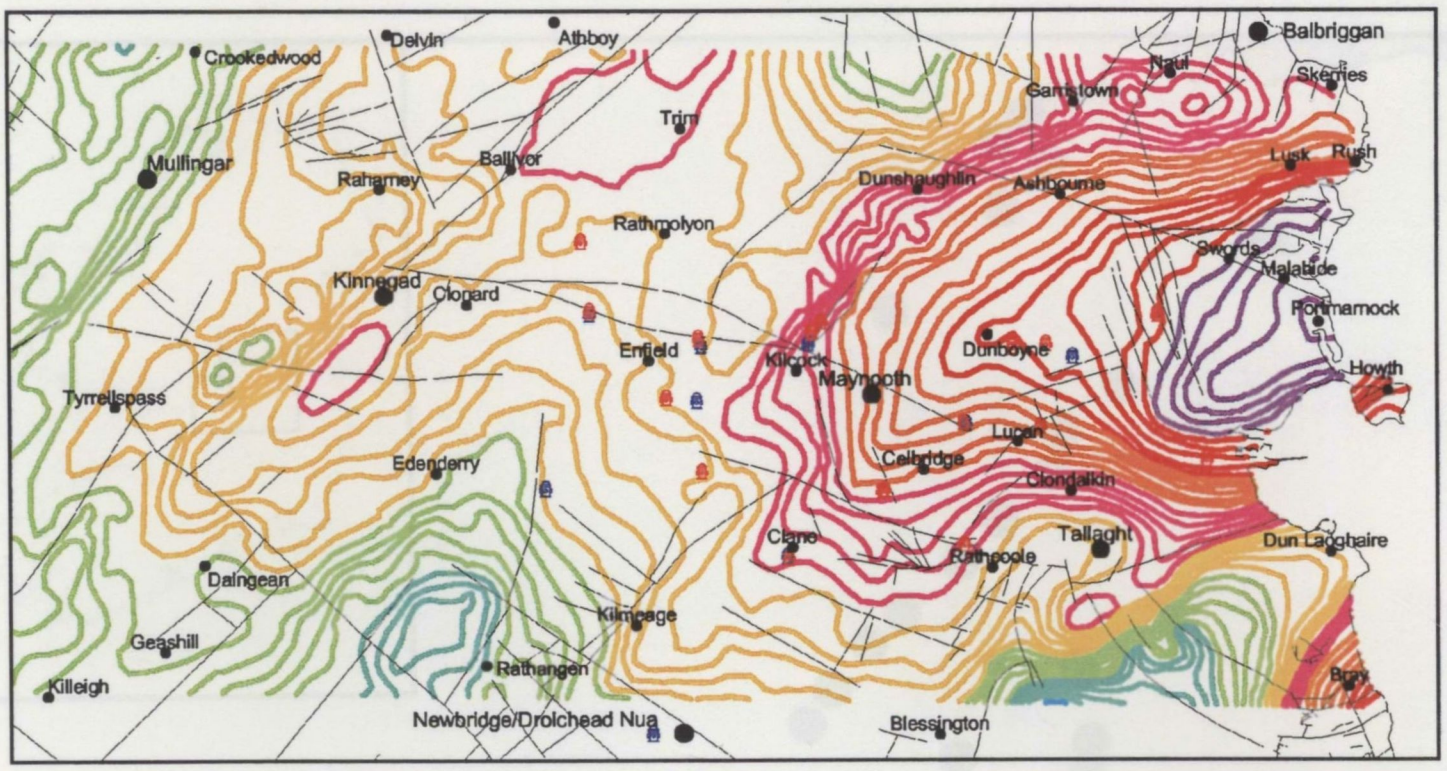

Figure 2.16:- Bouguer gravity anomaly contours (derived from DIAS maps) of 1-milligal spacing. Faults and warm springs are also shown.

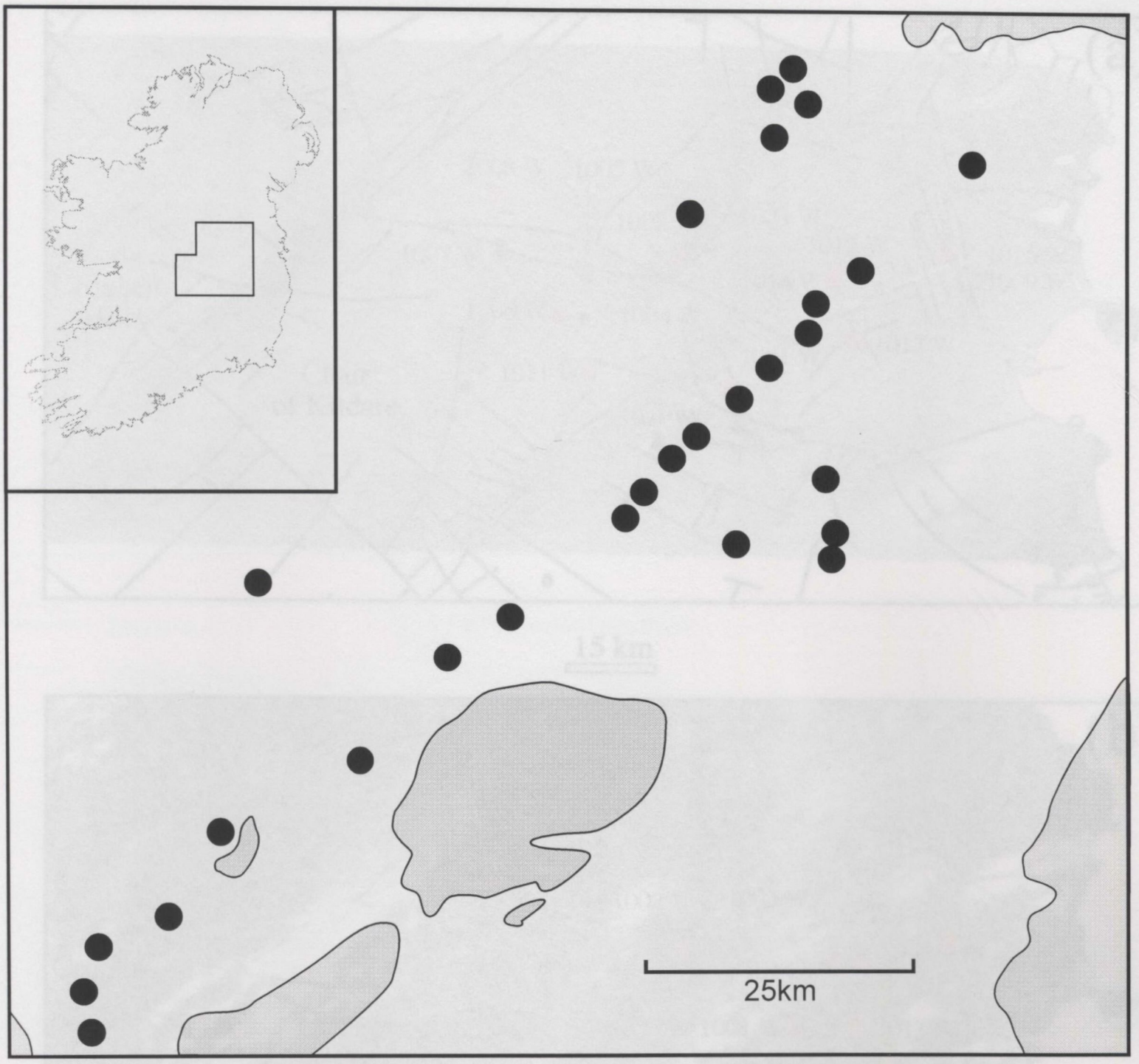

Carboniferous

L. Palaeozoics

Gravity anomalies

Figure 2.17:- Map showing occurrence of small high gradient Bouguer anomalies in the Central Midlands plain (Murphy, 1962).

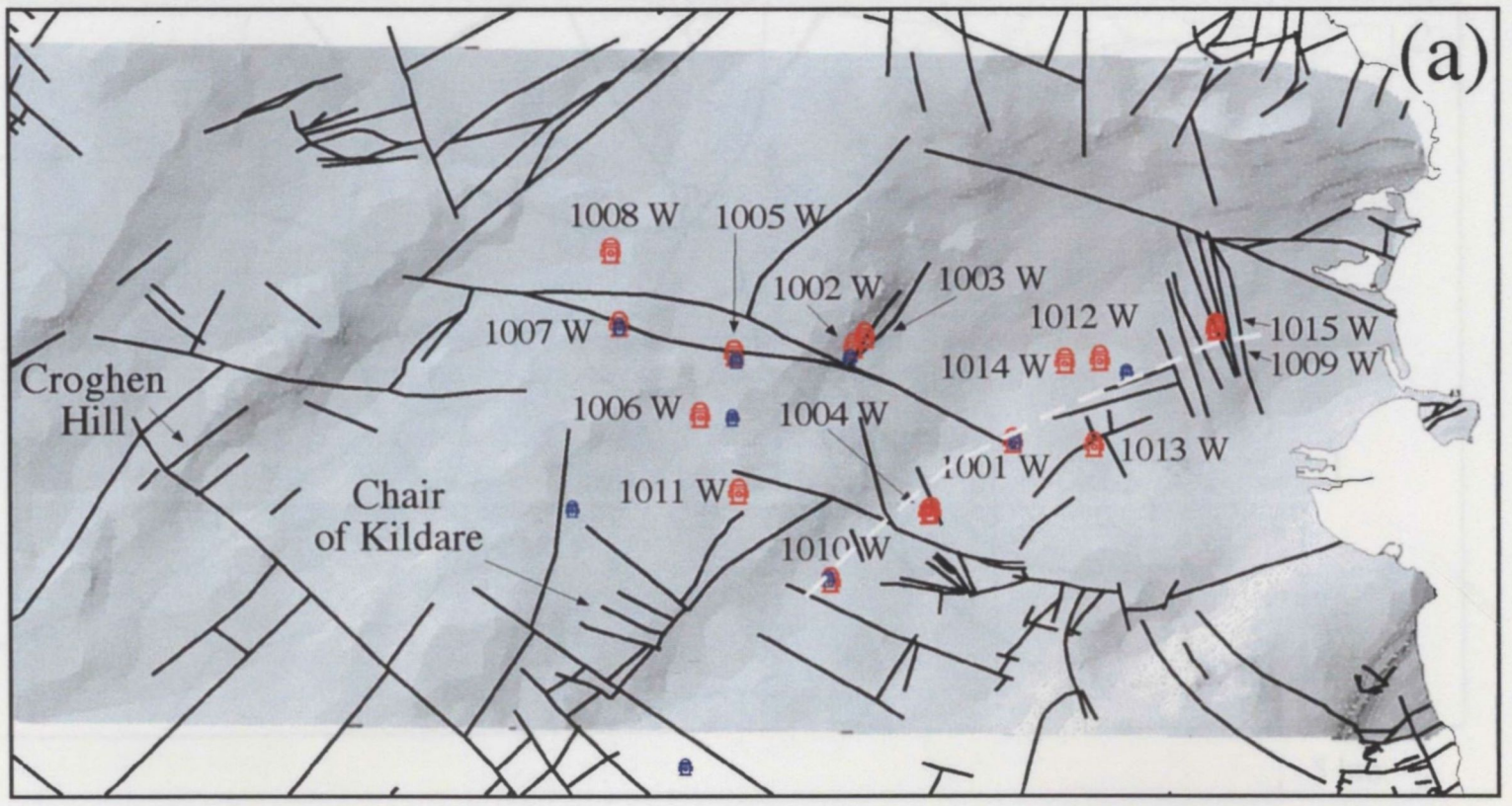

Figure 2.18a,b:- Maps of NW Illumination of the Bouguer gravity and magnetic anomaly, respectively, in the area of study. The association of NE-SW geophysical trends with faults and warms springs is shown.

Figure 3.1:- Location map of structural areas.

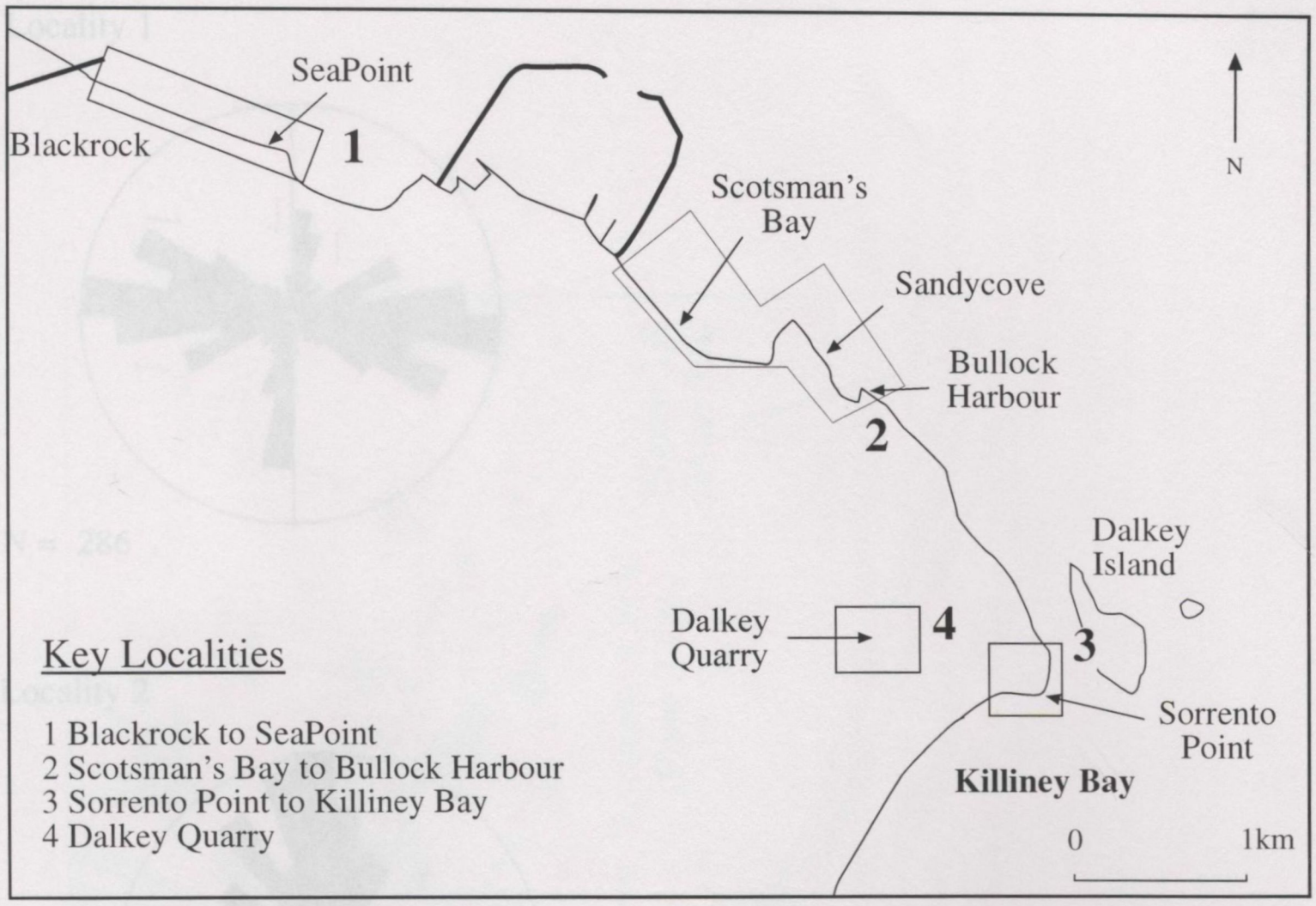

Figure 3.2:- Key structural localities along the northern margin of the Leinster batholith.

Locality 1

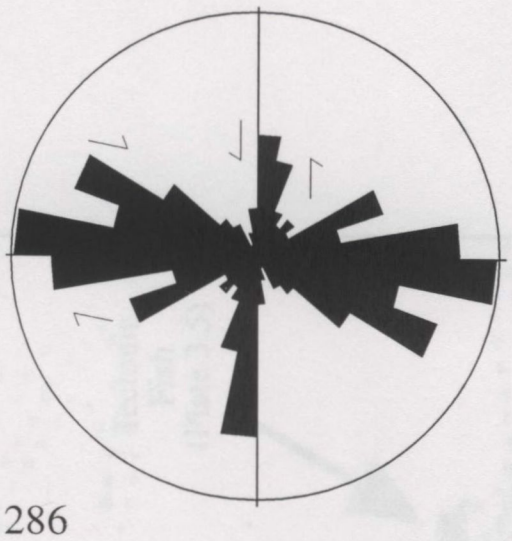

N = 286

Locality 2

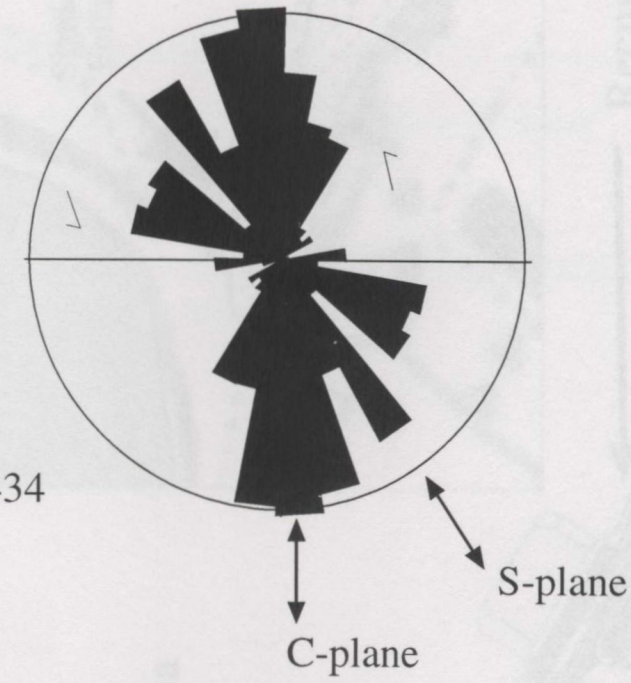

N = 434

Locality 3

N = 177

Figure 3.3:- Rose diagrams of structural elements (i.e. trend of foliation, fish, lineation, shear zone etc) for localities one to three.

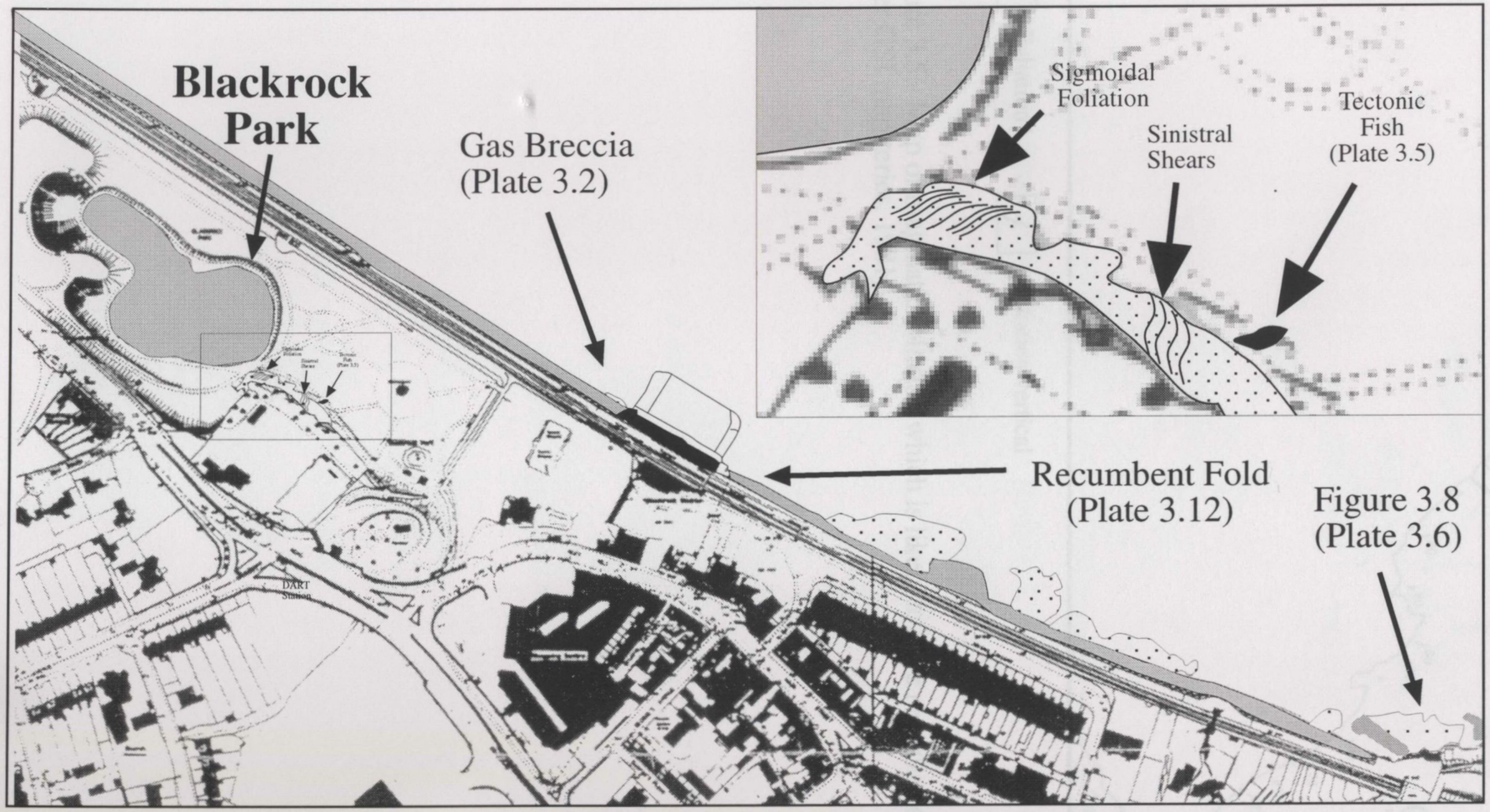

Figure 3.4:- Location of structures at locality 1, Blackrock section.

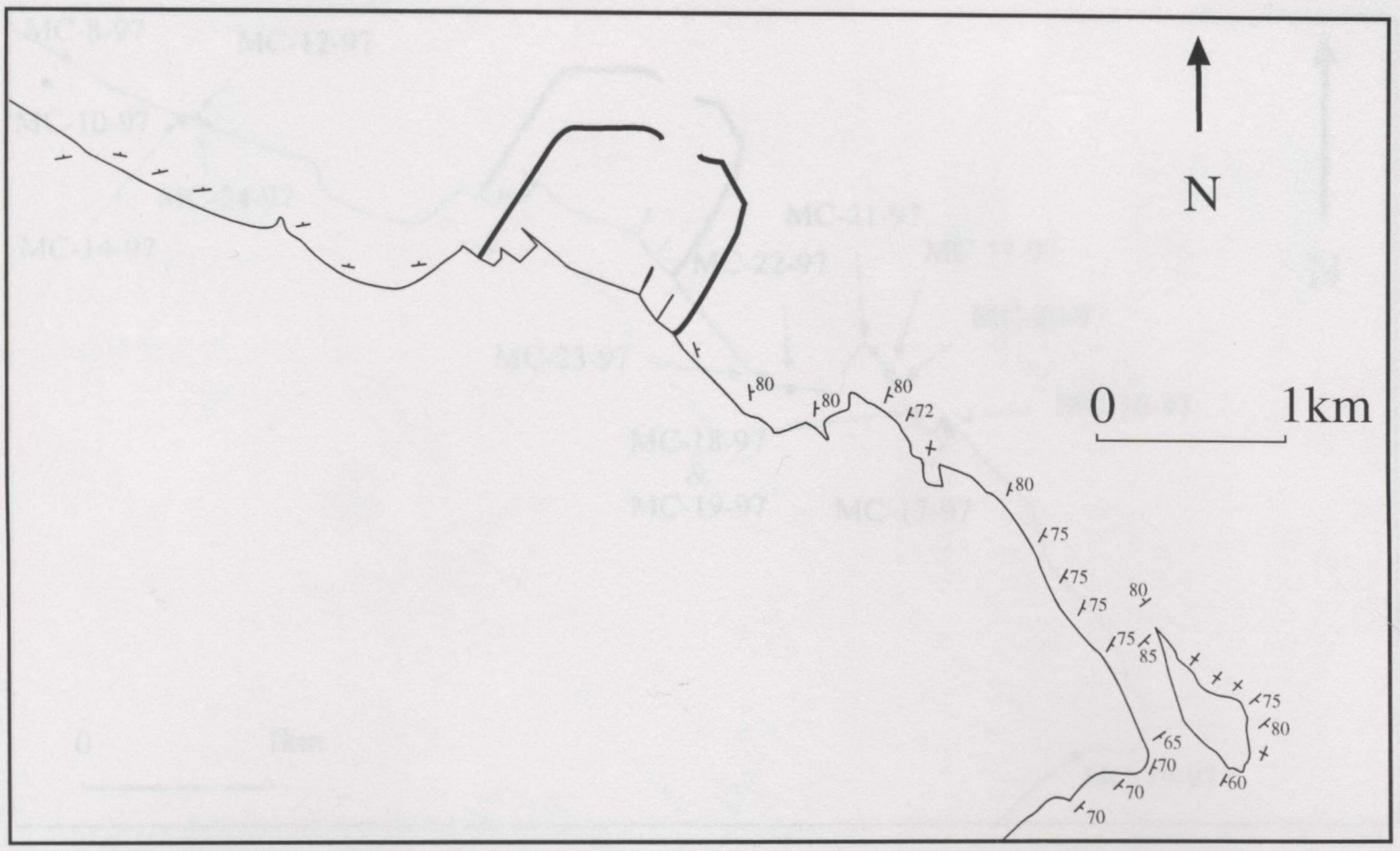

80 Foliation? Foliation vertical

Figure 3.5:- Map of magmatic foliation which is likely to have reactivated during the Tertiary (after GSI map series, 1981).

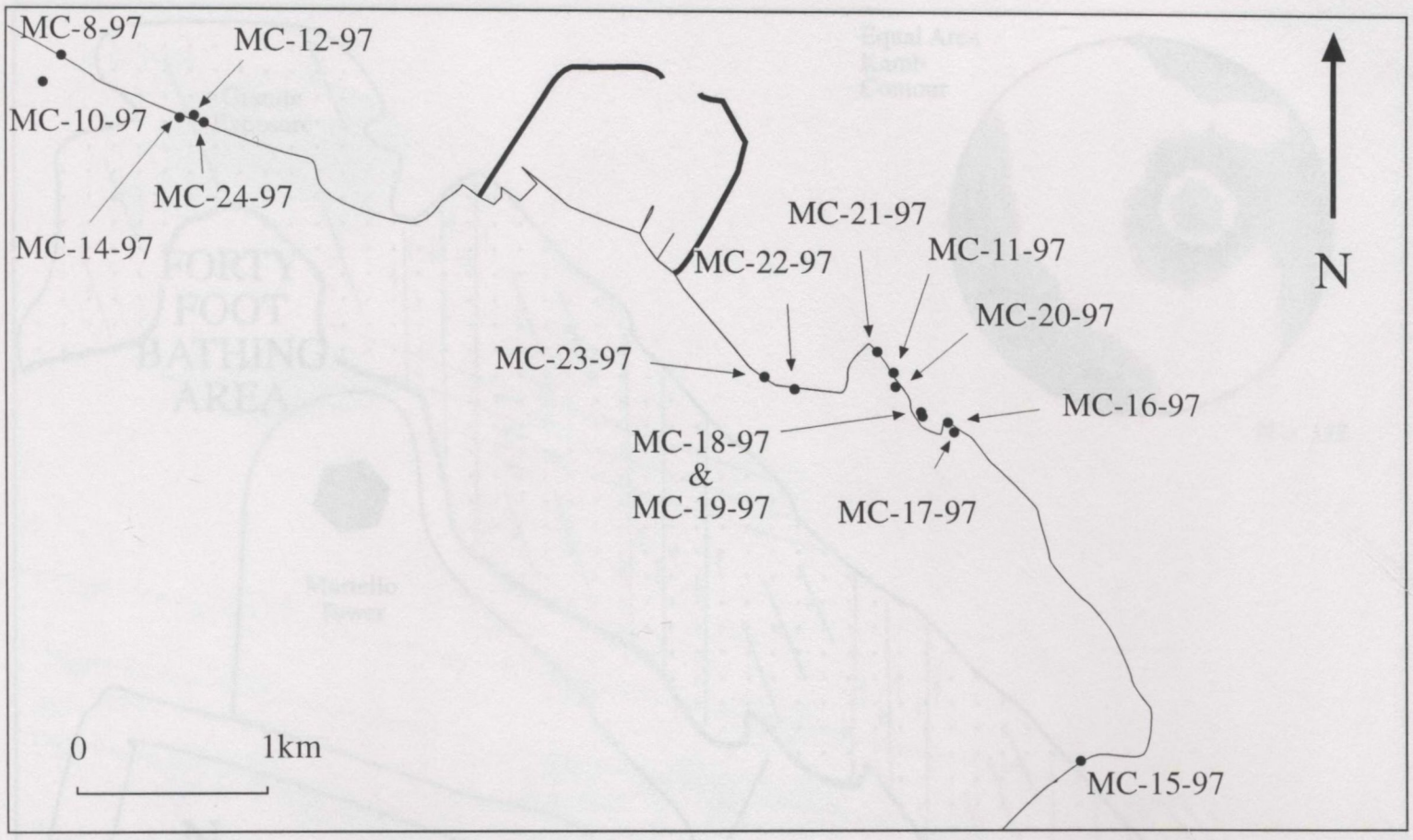

Figure 3.6:- Location map of thin-section studies.

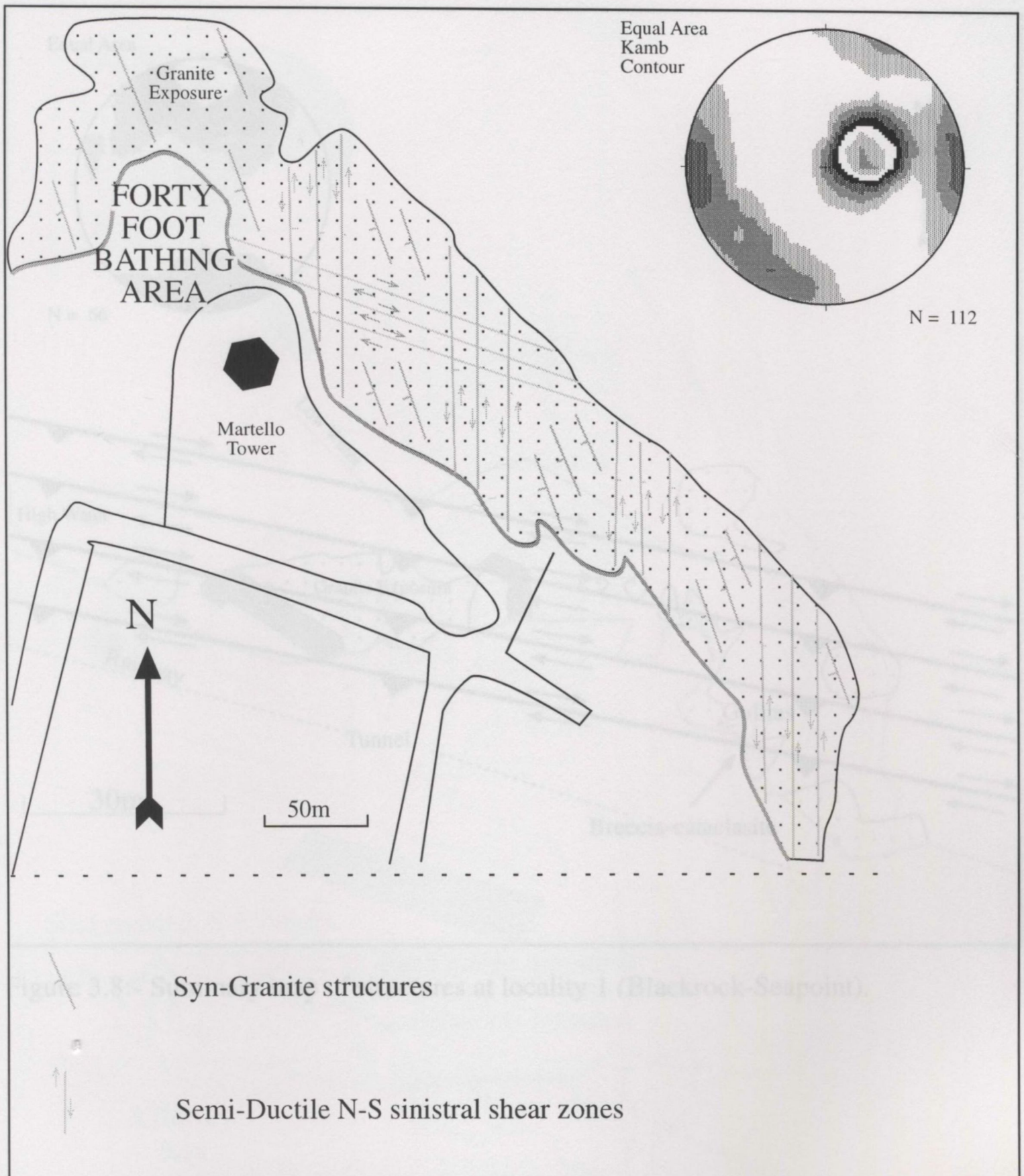

Figure 3.7:- Summary map of structures at locality 2 (Sandycove).

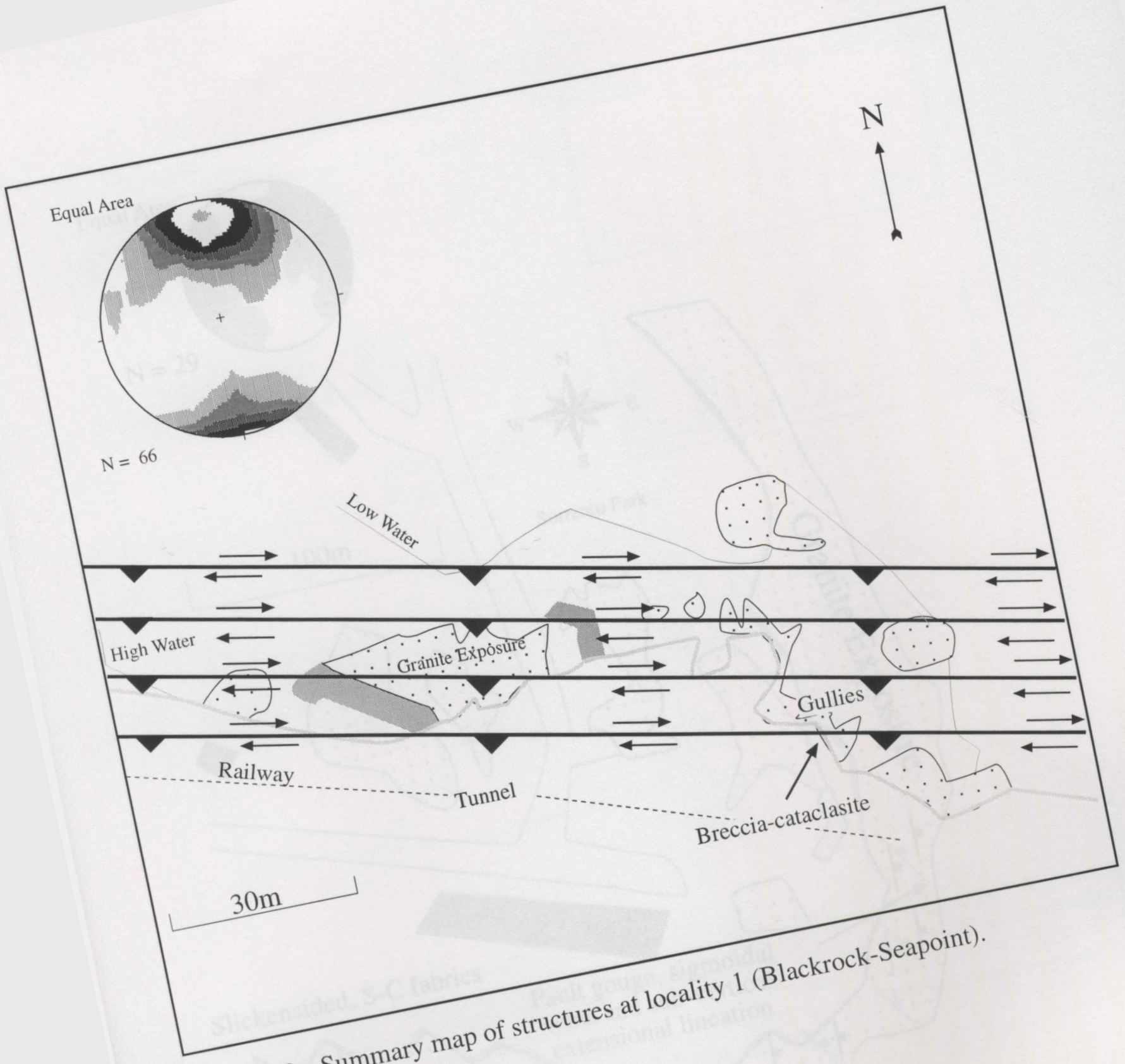

Figure 3.8:- Summary map of structures at locality 1 (Blackrock-Seapoint).

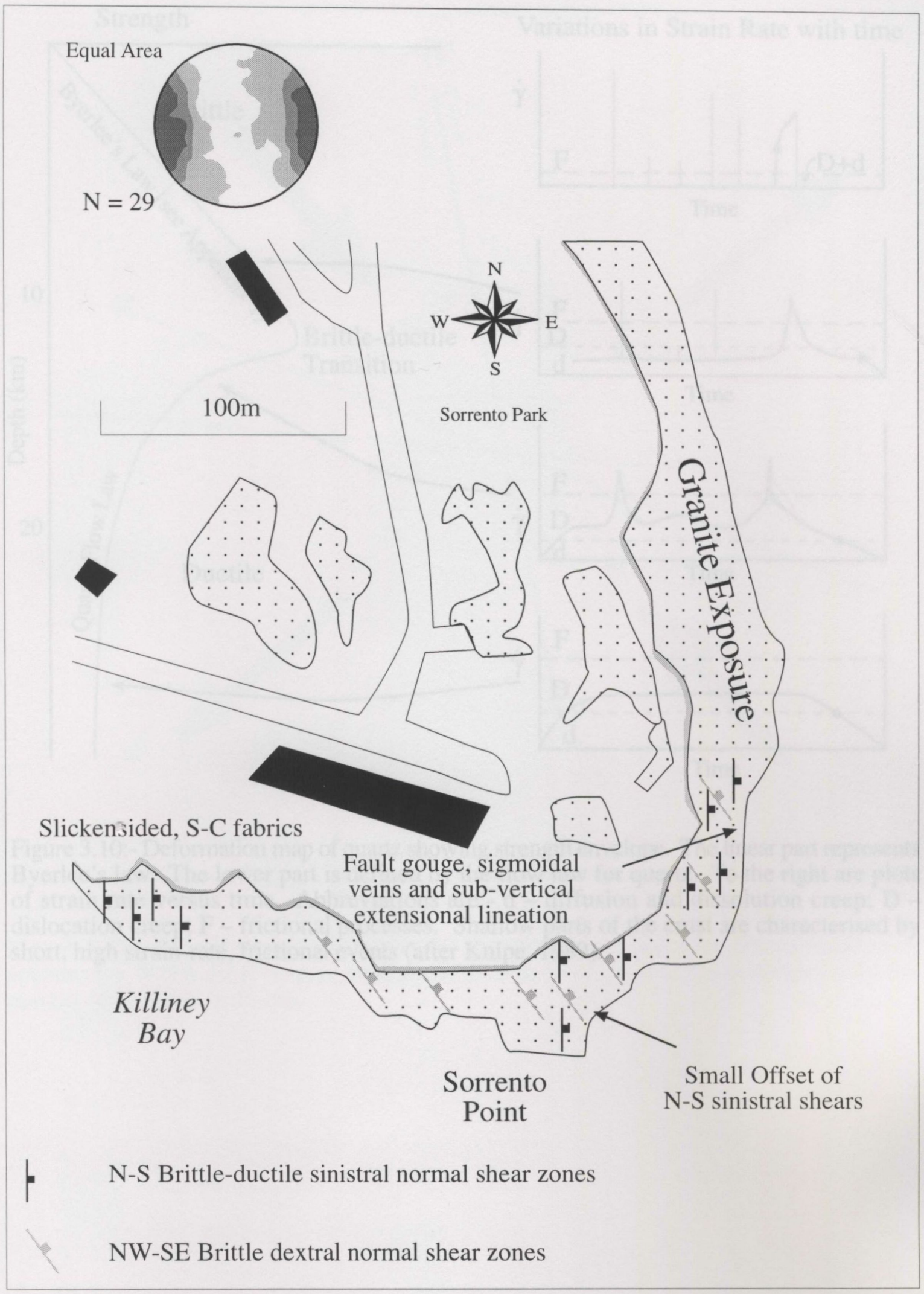

Figure 3.9:- Summary map of structures at locality 3 (Sorrento-Killiney).

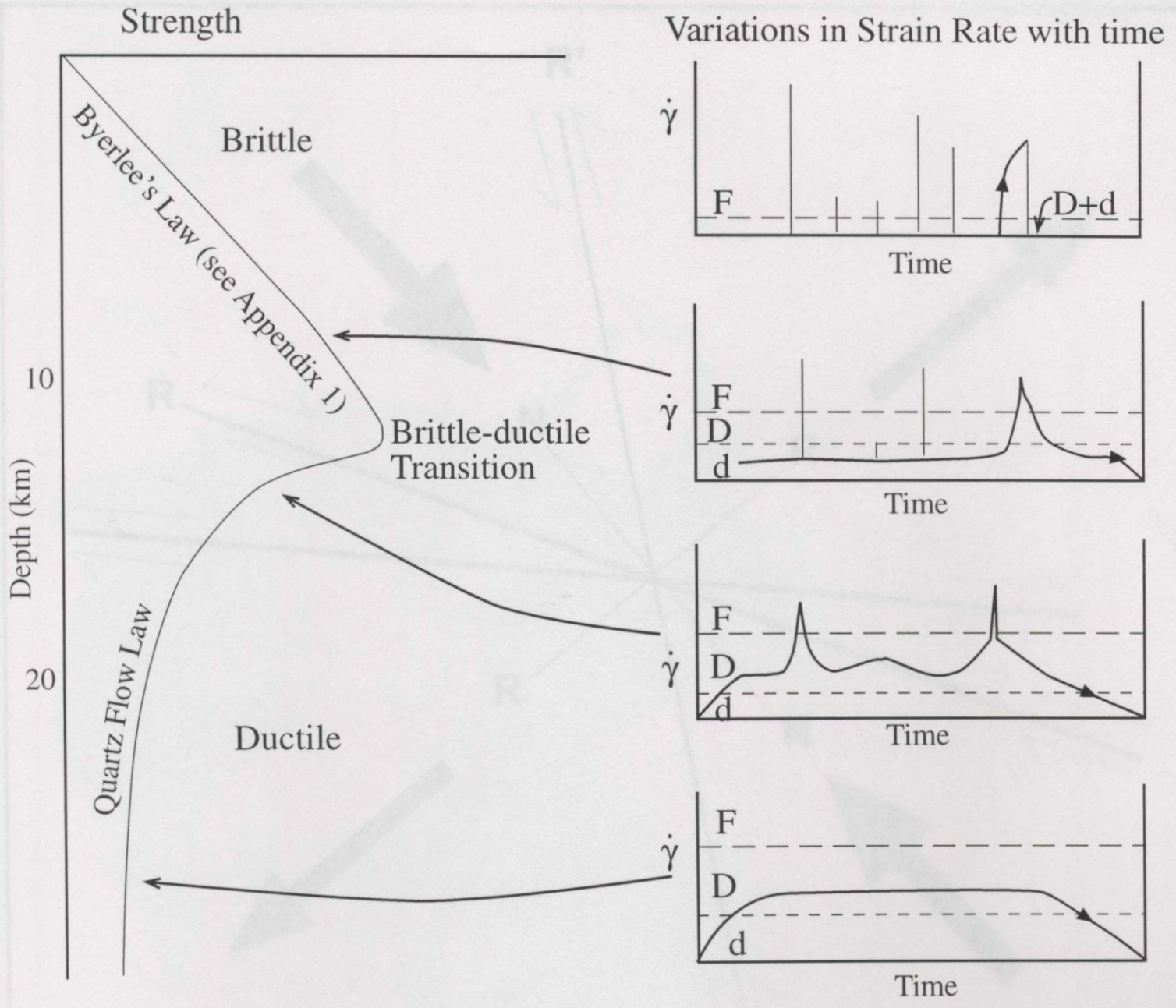

Figure 3.10:- Deformation map of quartz showing strength envelope. The linear part represents Byerlee's law. The lower part is defined by the flow law for quartz. To the right are plots of strain rate versus time. Abbreviations are:- d – diffusion and dissolution creep; D – dislocation creep; F – frictional processes. Shallow parts of the crust are characterised by short, high strain-rate, frictional events (after Knipe, 1989).

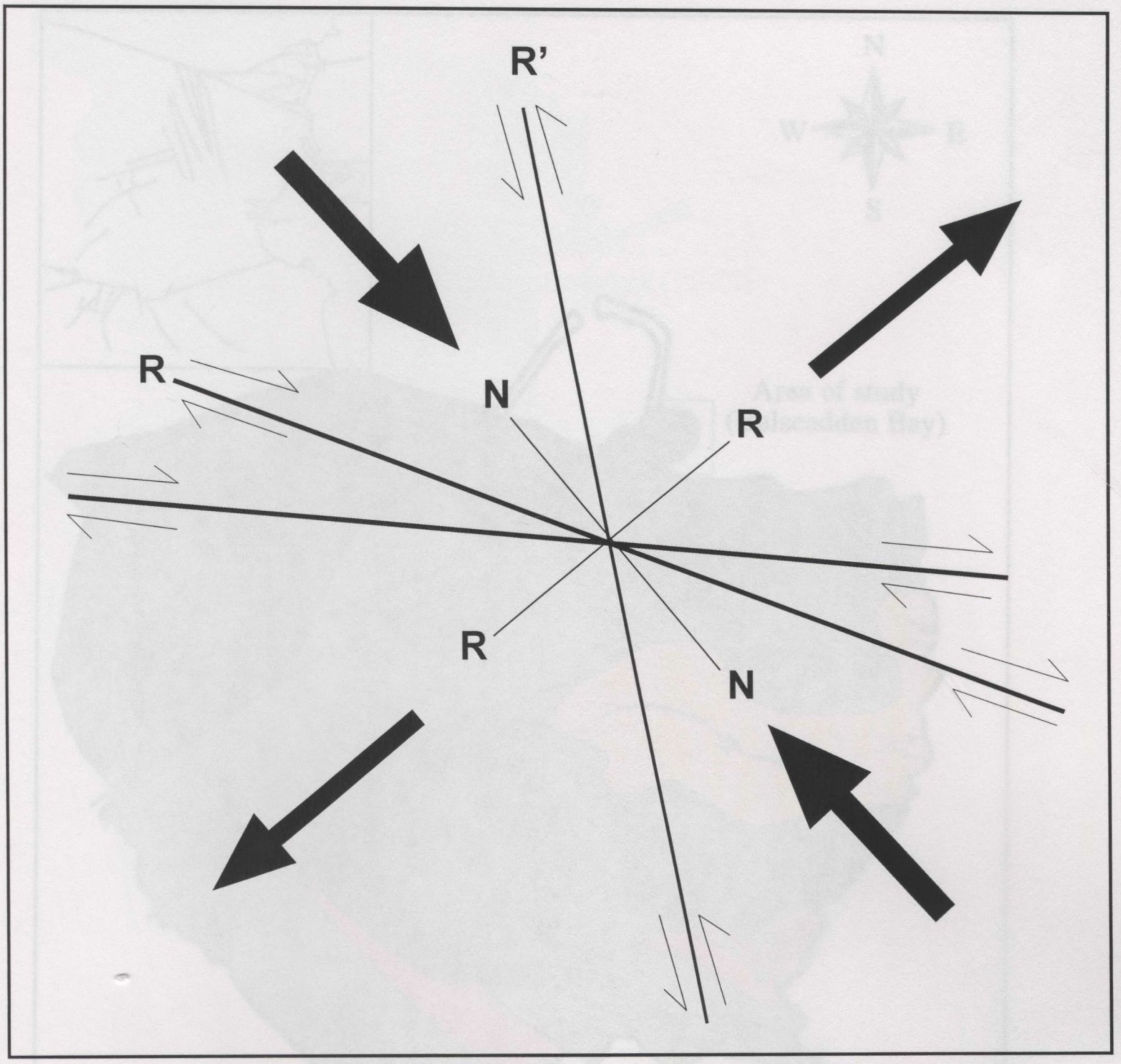

Figure 3.11:- Post-Hercynian (see text for discussion) palaeostress reconstructions to account for WNW-ESE reverse dextral and N-S normal sinistral shear zones - northern margin of Leinster batholith.

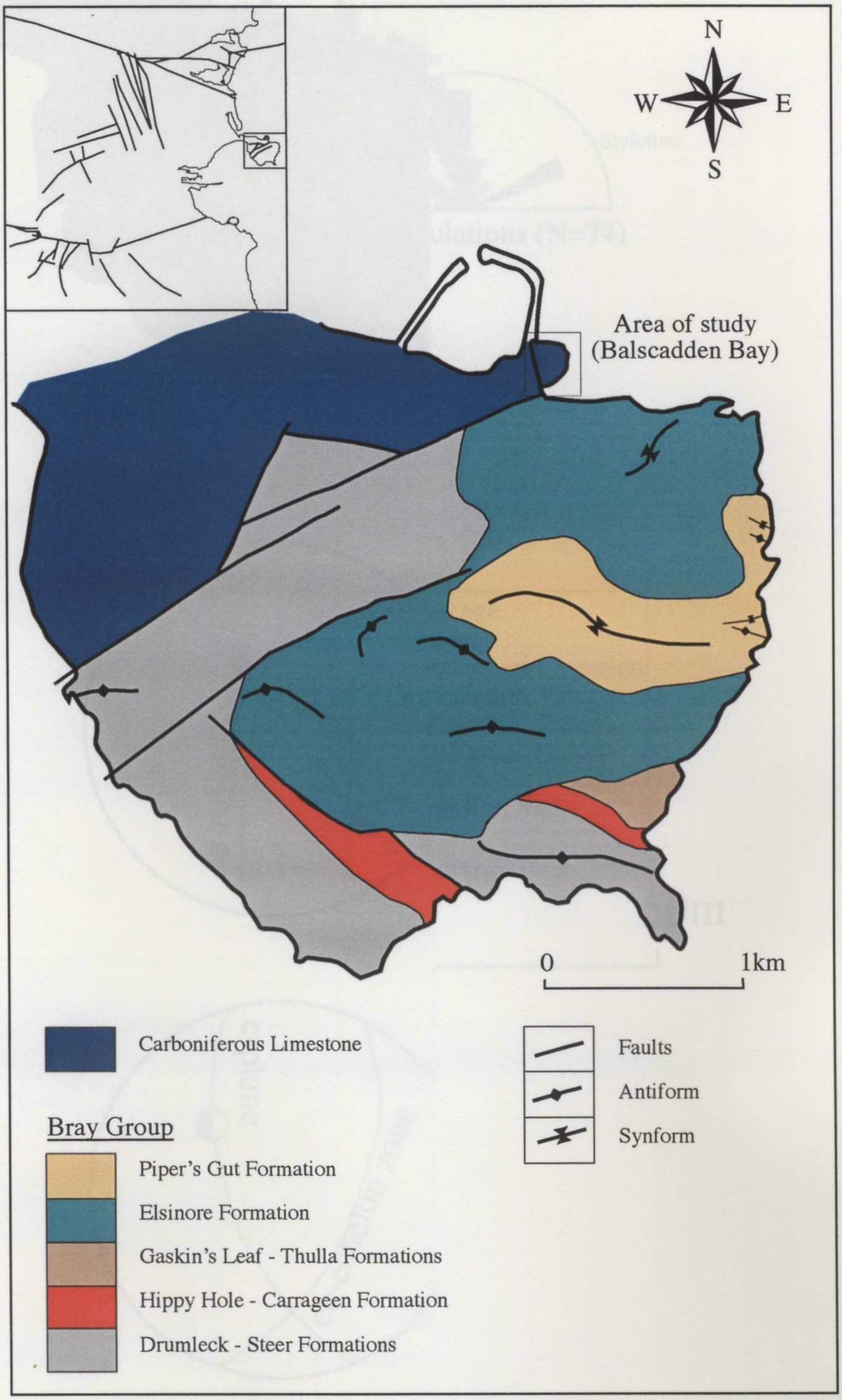

Figure 3.12:- Regional geology of the Howth peninsula, with Cambrian rocks to the east in fault contact with Carboniferous limestones to the west (after Van Lunsan & Max, 1975).

Figure 3.13:- Summary map of structures at Balscadden bay, Howth.

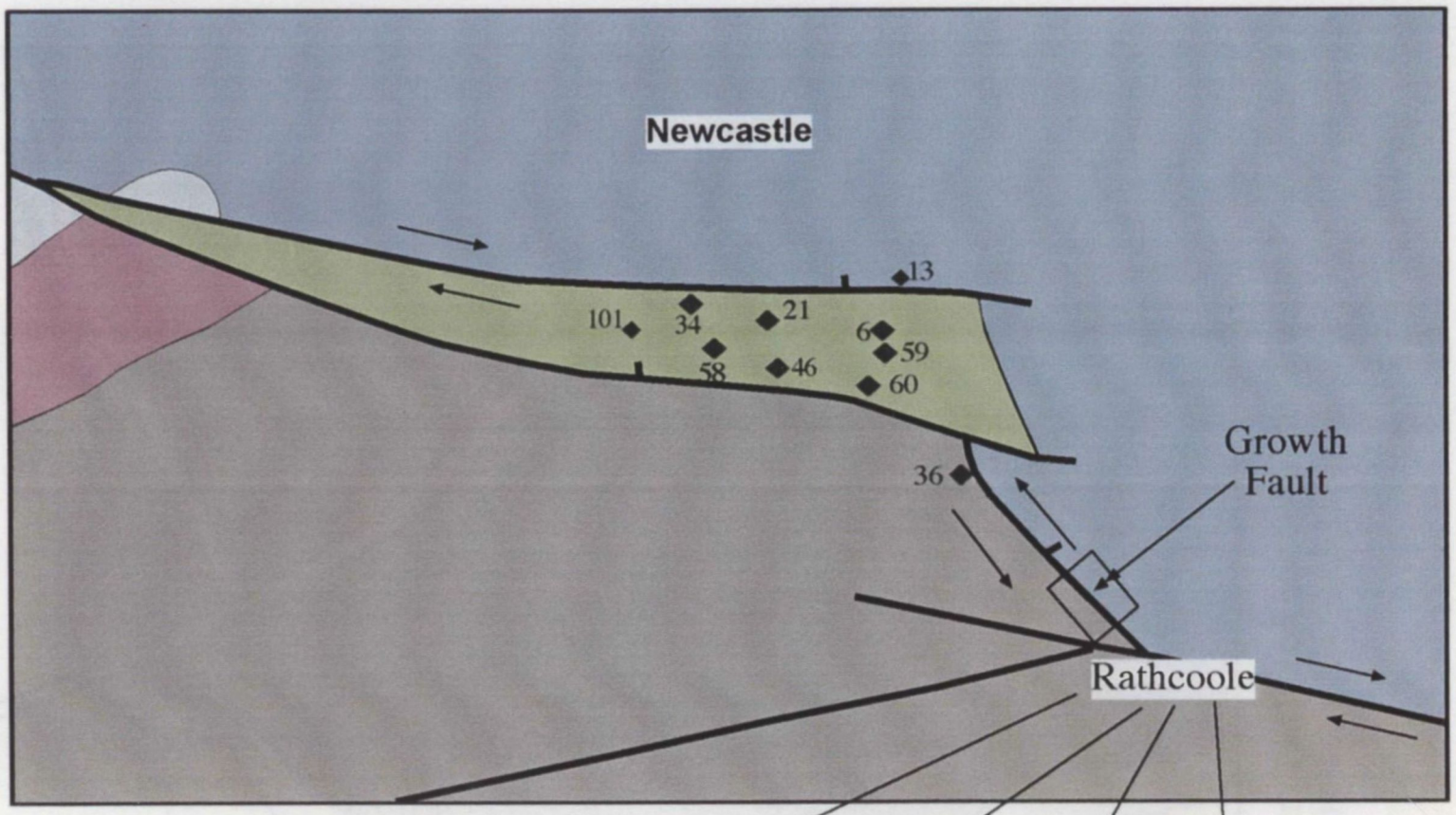

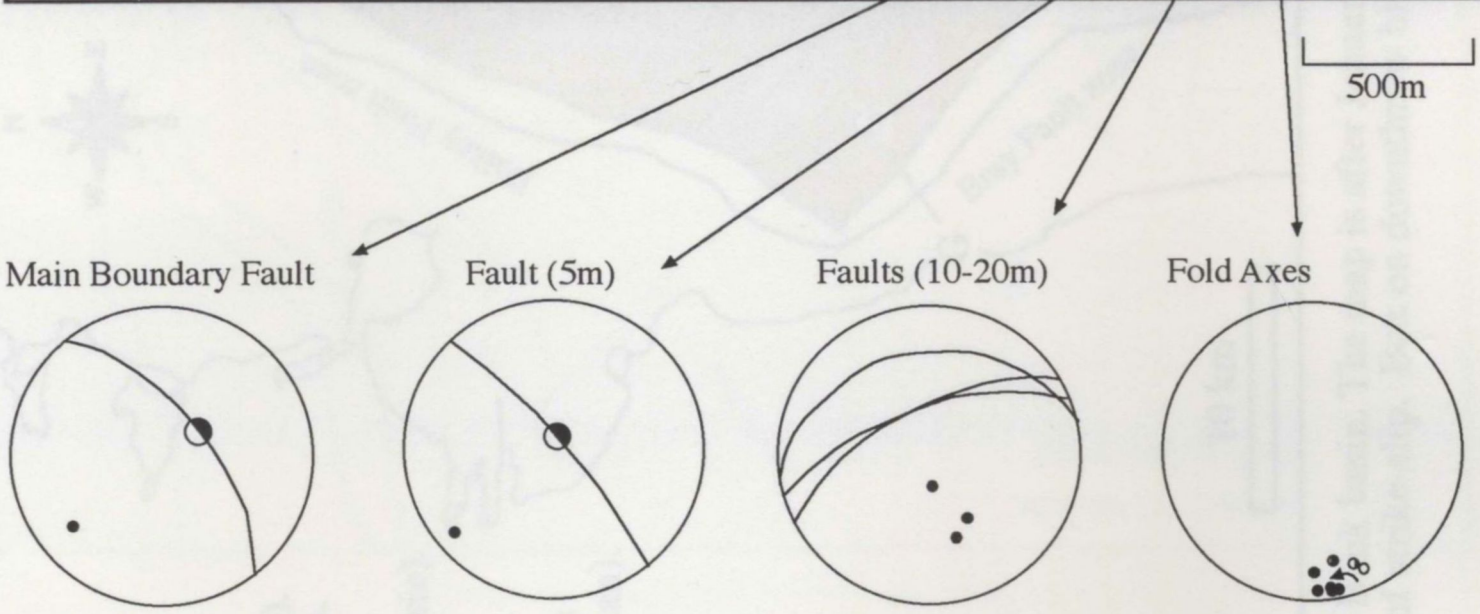

Basinal limestones (Calp). Predominantly dark laminated, argillaceous calcisilitites and calcareous shales with limestone turbidites (Brigantian - Holkerian).

Shallow water limestones (Ballysteen Fm.). Mixture of pale calcarenites with dark grey micrites, olistostromes, and basinal limestones (Holkerian - Chadian).

Basal Carboniferous Transgression Facies (Feighcullen Fm.). Argillaceous Bioclastic Limestones. Medium to dark grey fossiliferous argillaceous calcarenites and subordinate calcareous shales (Courceyan).

Old Red Sandstone. Sandstones, conglomerates and siltstones - alluvial flanglomerates and terrestrial sediments (Devonian to Lower Carboniferous).

Slate, shale and graywacke (Carrighill Fm.). Kilcullen Group (Llandovery - Ludlow).

◆ Borehole - thickness of overburden.

↶ Progressive anticlockwise rotation of fold axes towards the main fault.

Figure 3.14:- Extensional jog on southern boundary fault, between the towns of Rathcoole and Newcastle, Co. Dublin.

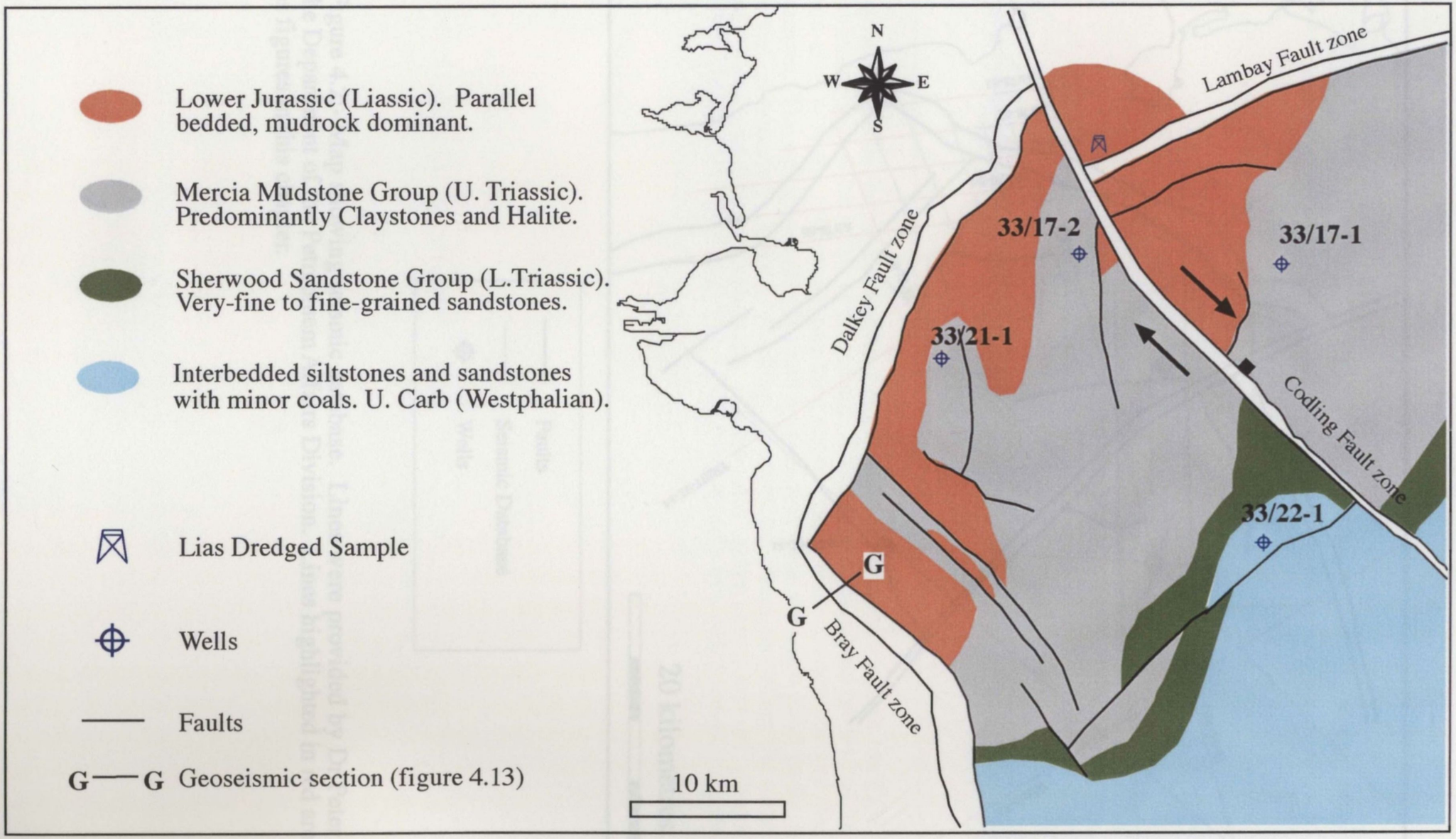

Figure 4.1:- Map of pre-Tertiary geology of the Kish Bank basin. The map is after Jenner (1981) and has been modified by Broughan *et al.*, (1989). Codling Fault zone - arrows show sense of strike-slip. Box on downthrow block.

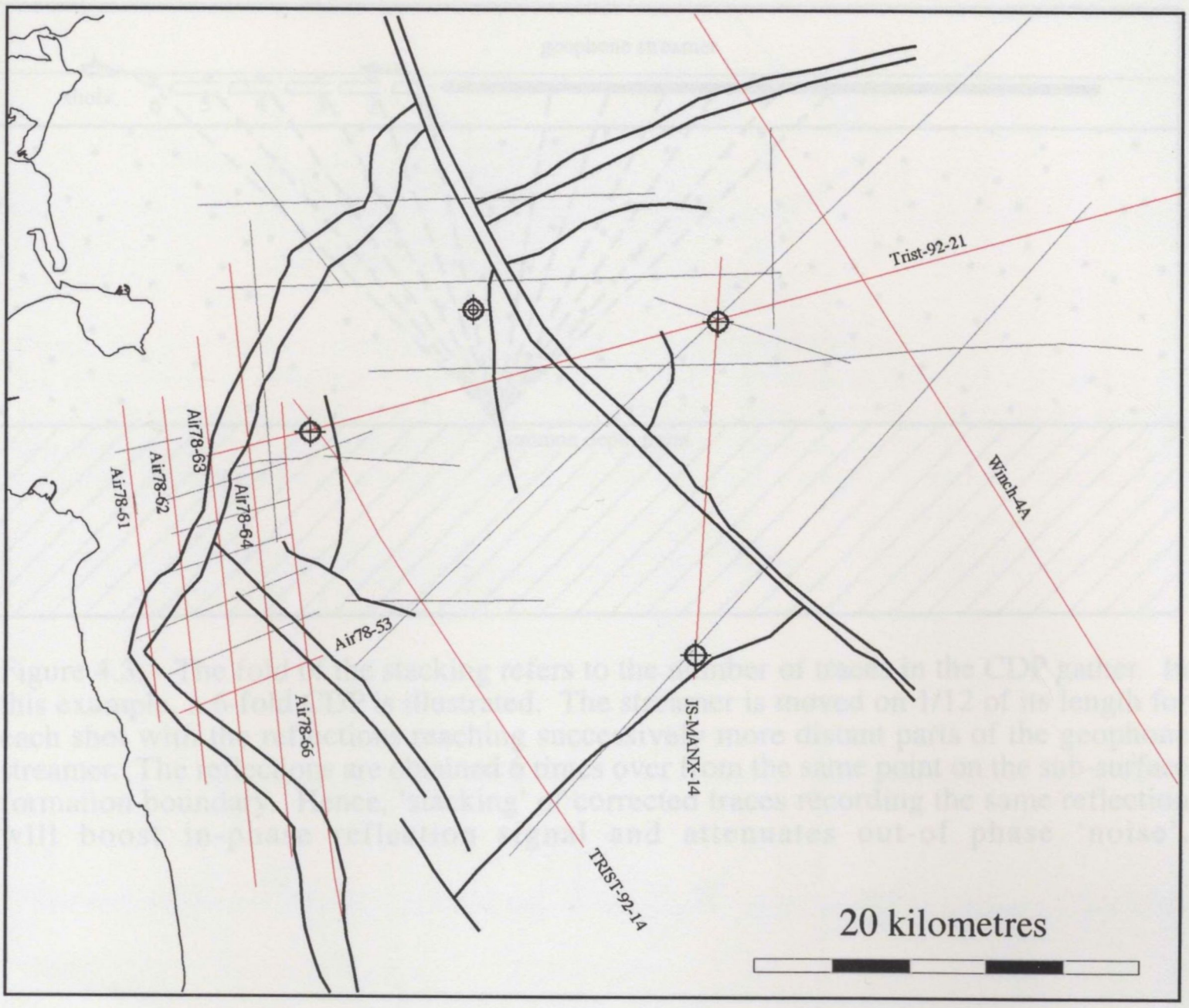

Figure 4.2:- Map showing seismic database. Lines were provided by Dr Peter Croker of the Department of the Petreoluem Affairs Division. Lines highlighted in red are presented as figures in this chapter.

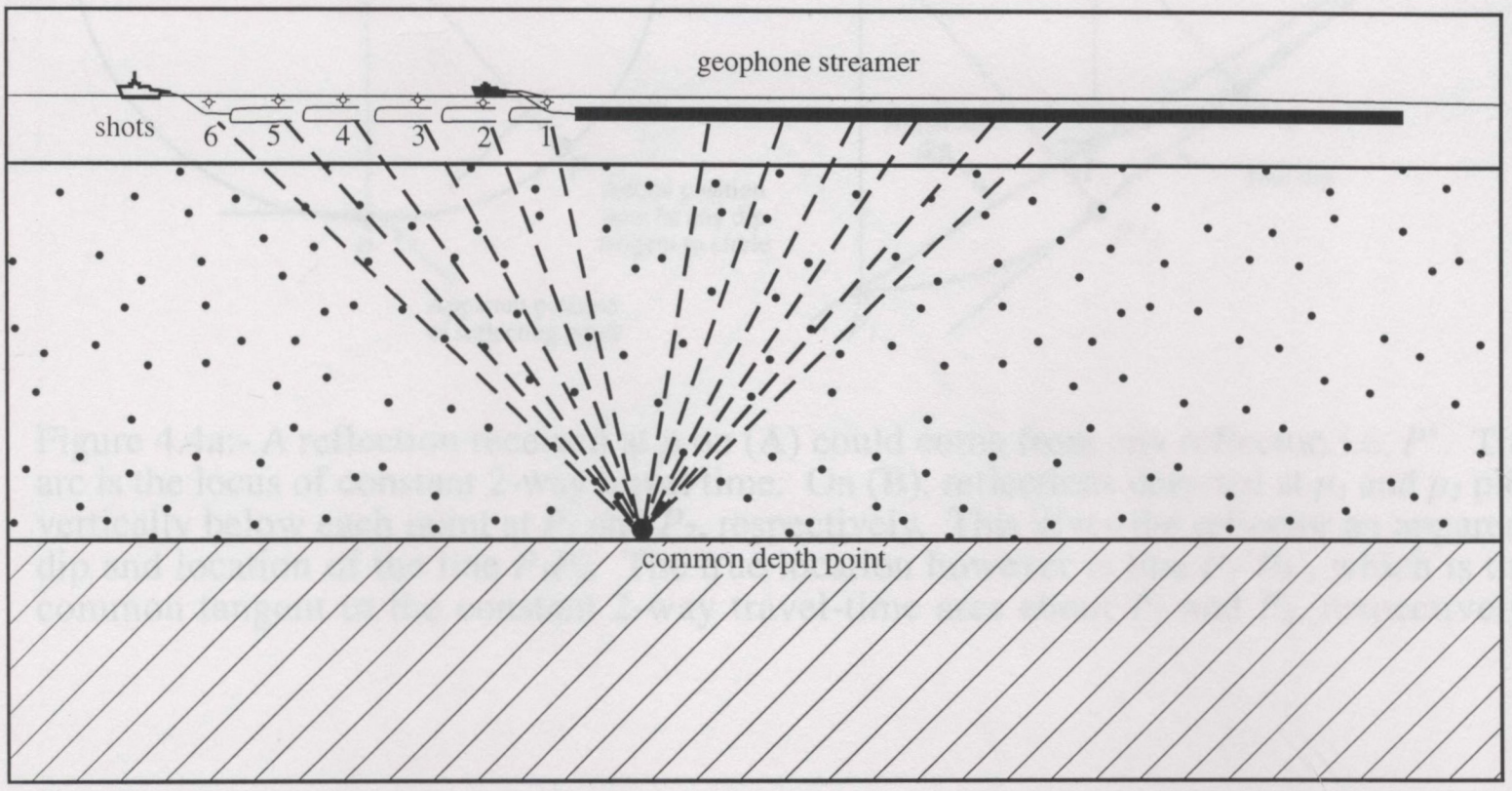

Figure 4.3:- The fold of the stacking refers to the number of traces in the CDP gather. In this example, a 6-fold CDP is illustrated. The streamer is moved on 1/12 of its length for each shot with the reflections reaching successively more distant parts of the geophone streamer. The reflections are obtained 6 times over from the same point on the sub-surface formation boundary. Hence, 'stacking' of corrected traces recording the same reflection will boost in-phase reflection signal and attenuates out-of phase 'noise'.

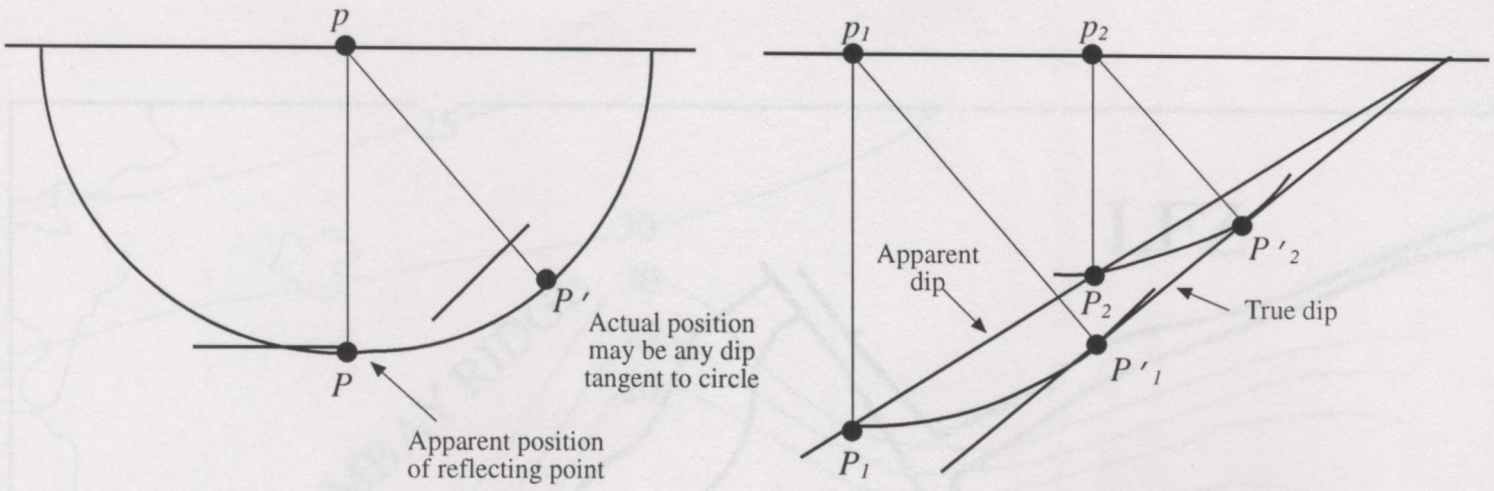

Figure 4.4a:- A reflection received at p on (**A**) could come from any reflector, i.e. P'. The arc is the locus of constant 2-way travel time. On (**B**), reflections detected at p_1 and p_2 plot vertically below each point at P_1 and P_2, respectively. This gives the reflector an apparent dip and location of the line P_1P_2. The true location however is line $P_1'P_2'$, which is the common tangent to the constant 2-way travel-time arcs about P_1 and P_2, respectively.

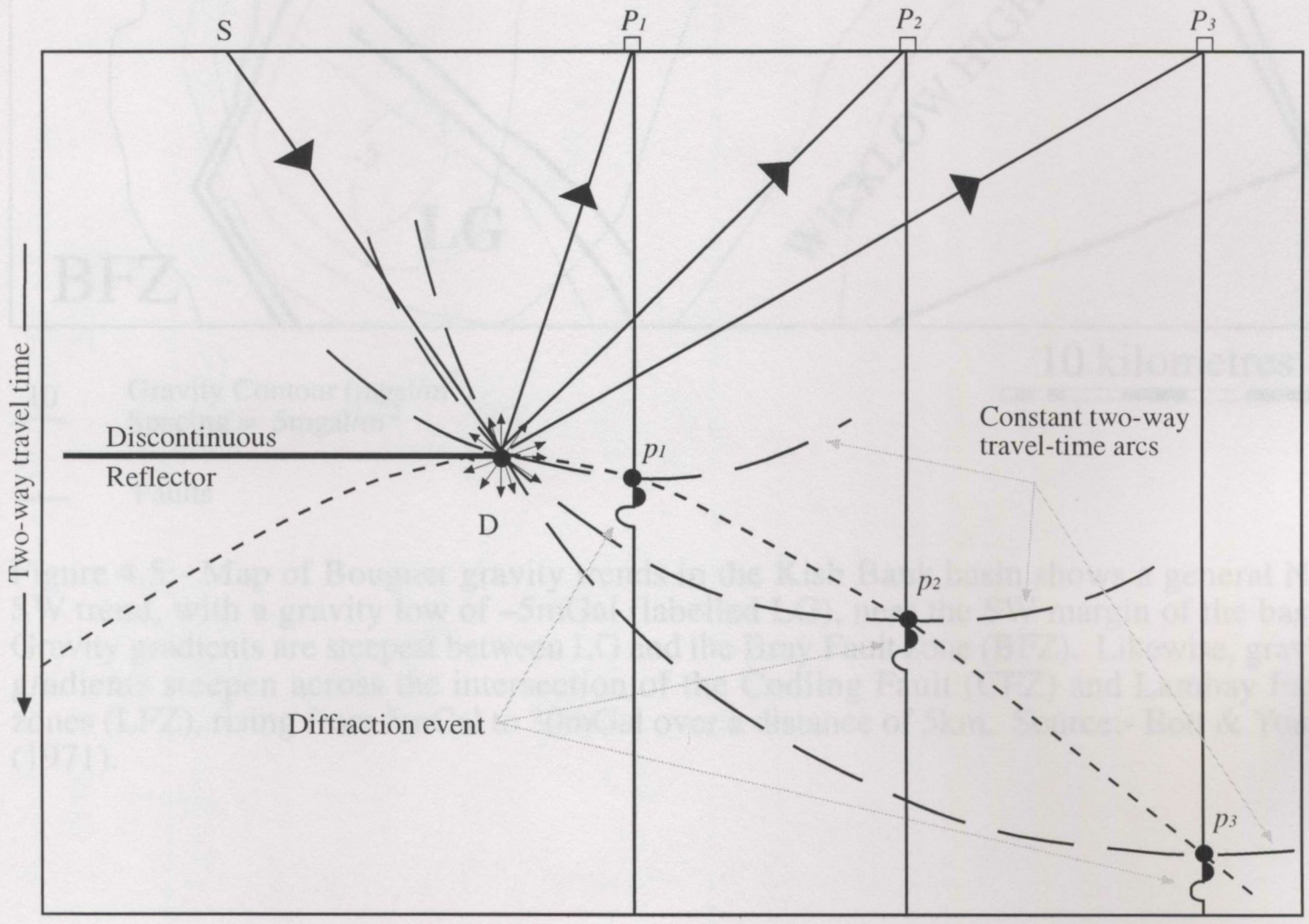

Figure 4.4b:- The end of discontinuous reflectors acts as a diffraction point (**D**) and radiates seismic energy in all directions for any angle of incidence. The greater the distance between the receiver and **D**, the later the diffracted ray arrives. (c) shows that the diffraction energy arrives at receivers P_1, P_2, and P_3 at times that fall along a parabolic arc at p_1, p_2 and p_3 respectively. The constant-travel-time arcs constructed about the 3 receivers with radii p_1P_1, p_2P_2 and p_3P_3, will intersect at the location of the diffraction point.

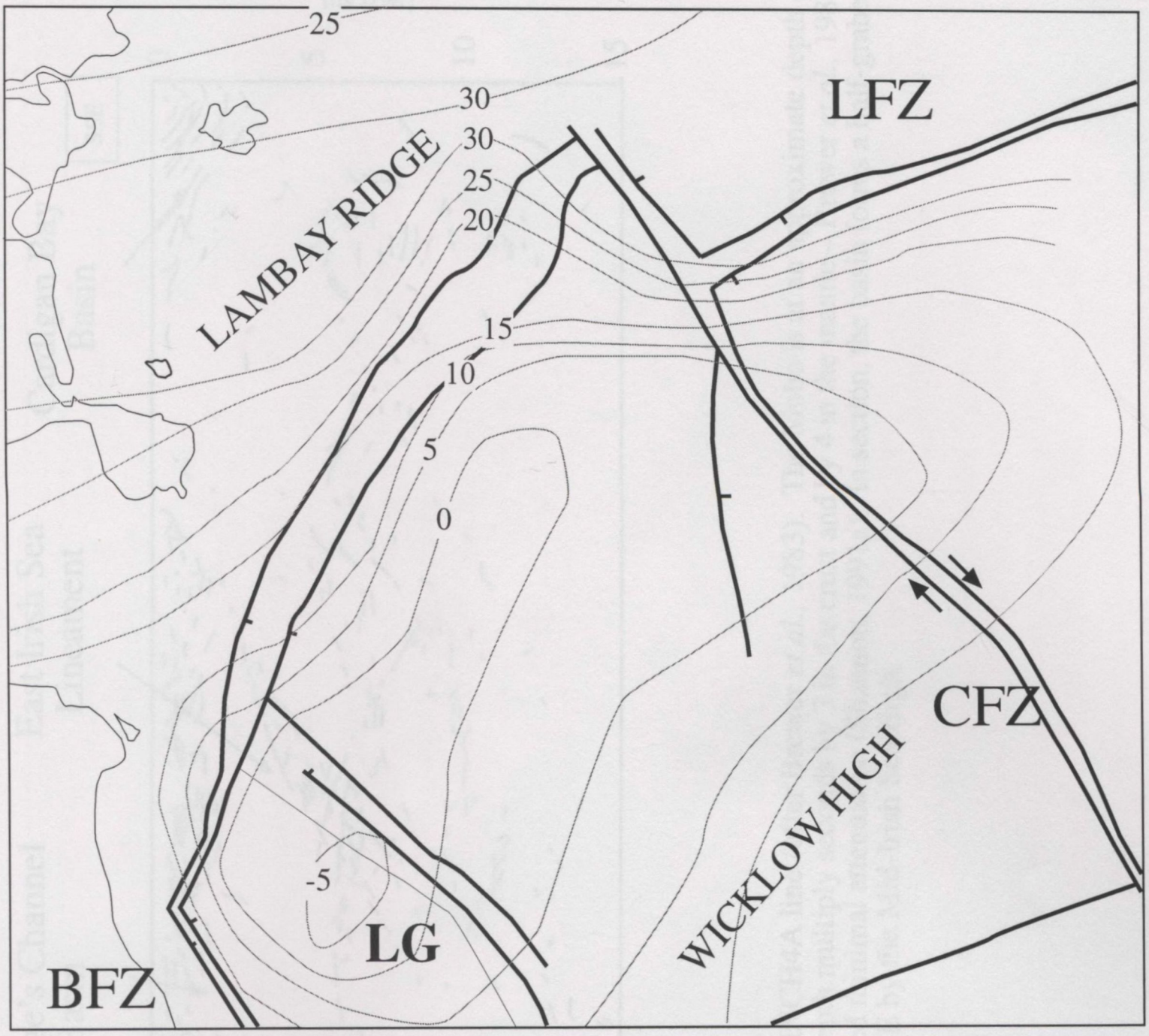

Figure 4.5:- Map of Bouguer gravity trends in the Kish Bank basin shows a general NE-SW trend, with a gravity low of –5mGal (labelled LG), near the SW margin of the basin. Gravity gradients are steepest between LG and the Bray Fault zone (BFZ). Likewise, gravity gradients steepen across the intersection of the Codling Fault (CFZ) and Lambay Fault zones (LFZ), rising from 5mGal to 30mGal over a distance of 5km. Source:- Bott & Young (1971).

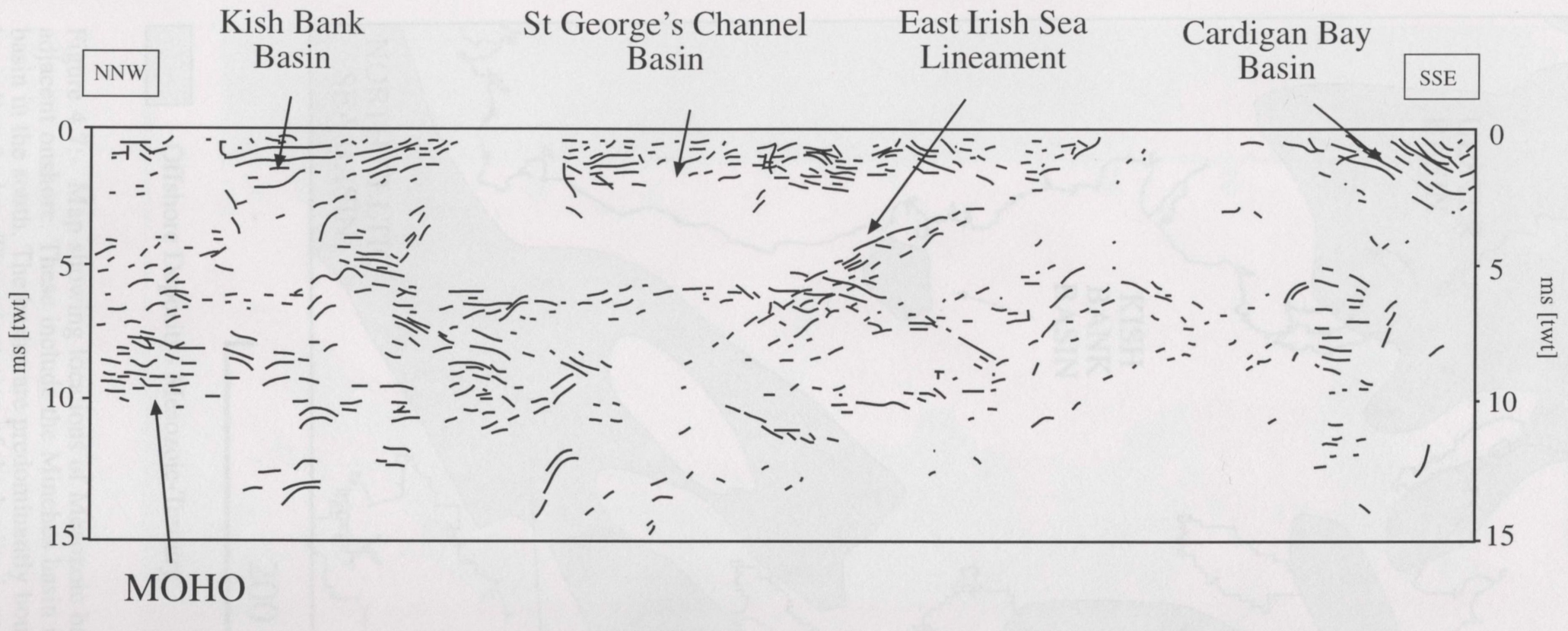

Figure 4.6:- Structural interpretation of unmigrated WINCH4A line (after Brewer *et al.,* 1983). The Moho is at an approximate depth of 10 ms[twt] or ~30km (to convert time to approximate depth multiply seconds by 3 in the crust and by 4 in the mantle – Brewer *et al.,* 1983) beneath the Kish basin. Hence, the crust has experienced minimal attenuation (Shannon, 1991a). In section, the basin forms a half-graben, separated from the St George's Channel basin to the SSE by the Mid-Irish Sea High.

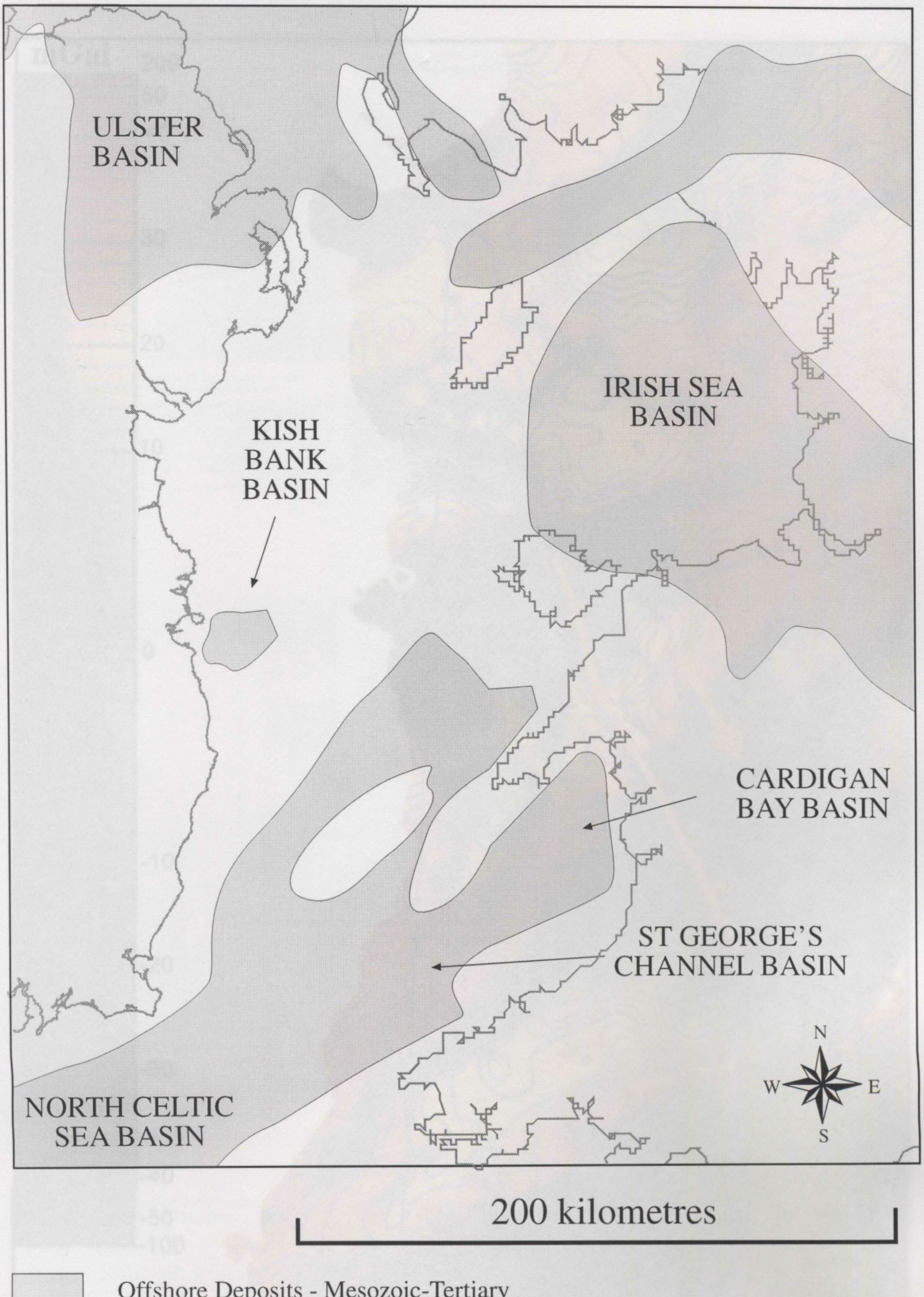

Figure 4.7:- Map showing locations of Mesozoic basins in the Irish Sea region and the adjacent onshore. These include the Minches basin in the north, to the North Celtic Sea basin in the south. The basins are predominantly bounded by NE and NW trending basin bounding faults. The orientation of the basins is mostly NE and NW. Source:- Naylor (1992).

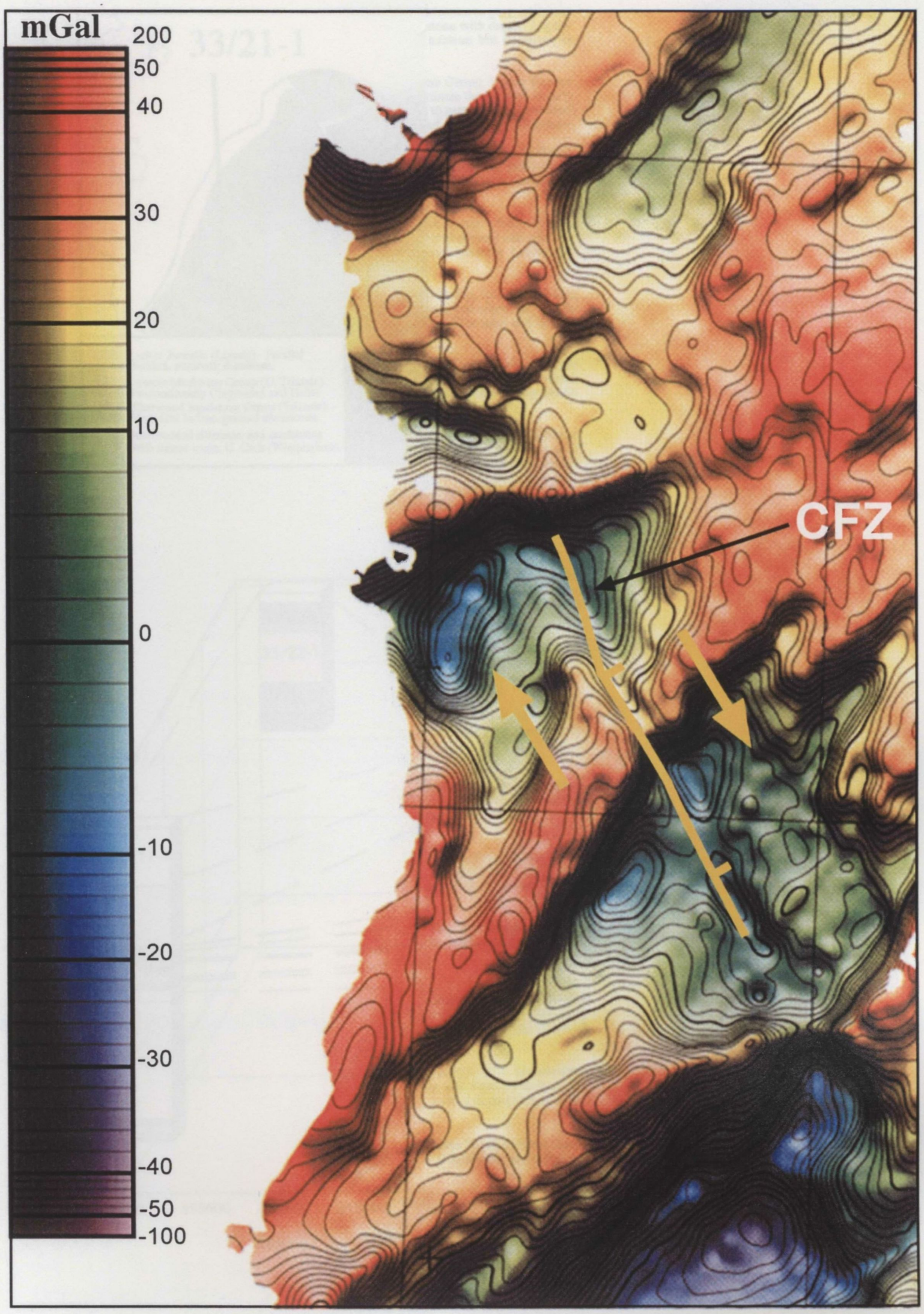

Figure 4.8:- Free-air gravity anomaly map of the Irish Sea region. The Mesozoic basins are associated with relatively low gravity anomalies. The orientation of the basins is mostly NE-SW and NW-SE. Steep gravity gradients delimit the basin boundary faults. Some of the basins are bisected by major strike-slip faults. For example, the NW-SE trending Codling Fault zone bisects the Kish Bank and Central Irish Sea basins. CFZ – Codling Fault zone, with arrows showing sense of shear, and ticks on downthrown block. Source of gravity data:- Smith & Edwards (1997).

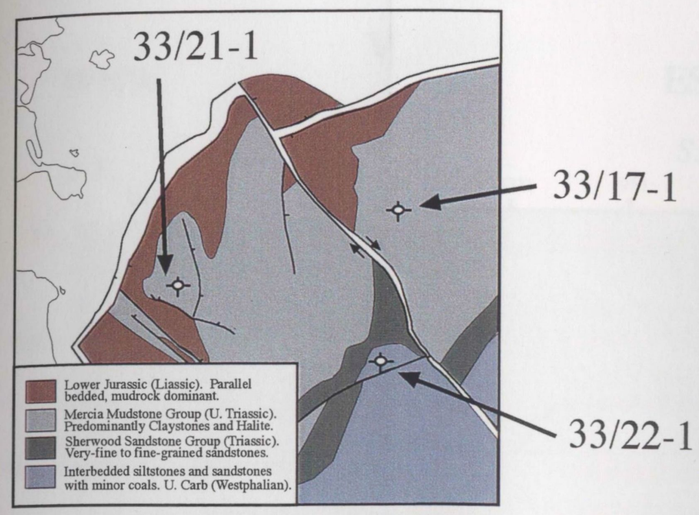

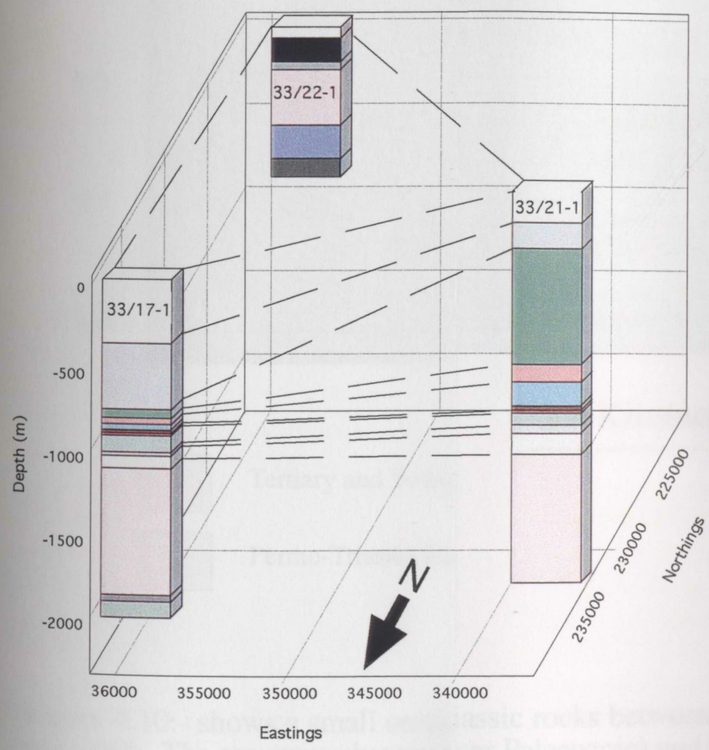

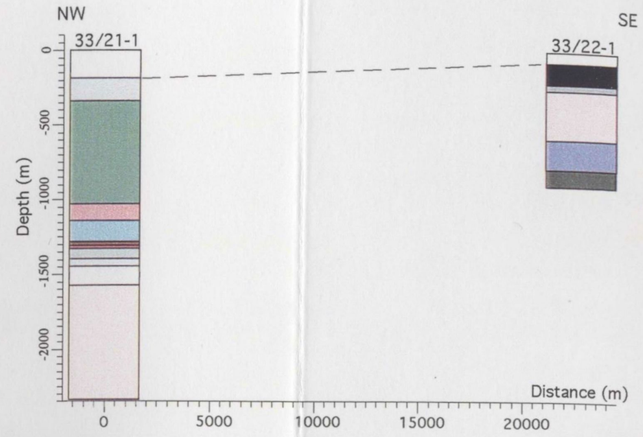

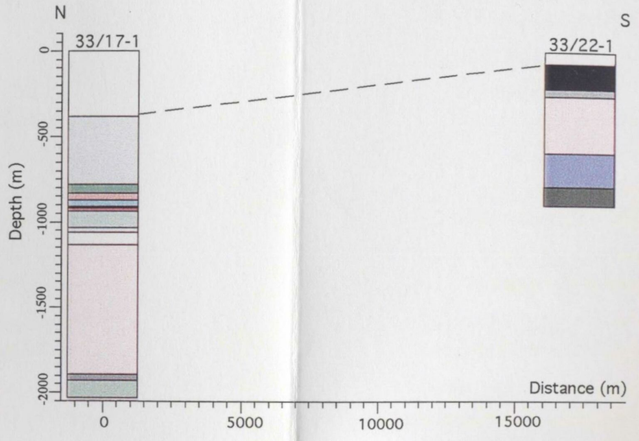

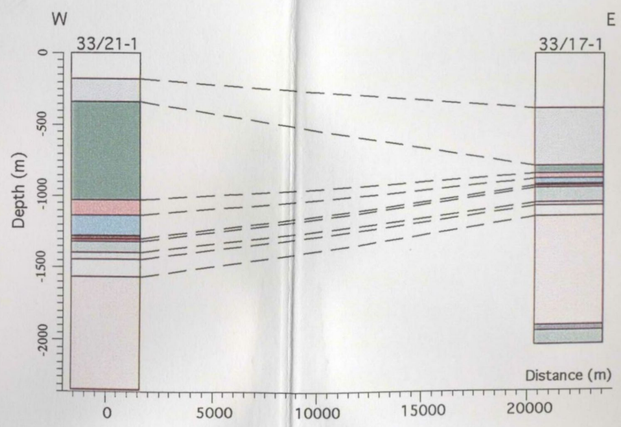

Quaternary-Tertiary. Variable red-brown to grey sandstone with increasing amounts of claystone with depth. Lignite beds typify the upper part of section but decrease in importance downwards.

Upper Triassic. Mercia Mudstone Group, Upper Keuper Marl. Red-brown claystones dominate the interval, locally grading into siltstone, light-brown to green-grey. Occasional intercalations of gypsum and of light-grey sandstone.

Upper Triassic. Mercia Mudstone Group, Upper Saliferous Beds. Equal amounts of halite and silty red-brown, occasionally green-grey, claystones. Minor amounts of intercalated siltstone.

Upper Triassic. Mercia Mudstone Group, Middle Keuper Marl. Red-brown and green-grey claystone and siltstone dominate the interval, with subordinate sandstone.

Upper Triassic. Mercia Mudstone Group, Lower Saliferous Beds. Halite with minor amounts of red claystone. Halite is clear, white or light brown, crystalline hard and blocky.

Upper Triassic. Mercia Mudstone Group, Lower Keuper Marl. Red-brown and grey, soft to firm claystones which are frequently silty or micaceous, and occasionally halitic or anhydritic.

Upper Triassic. Sherwood Sandstone Group, Keuper Waterstones Fm. Dark red-brown claystone and shale with siltstone and white to light-grey, fine-grained sub-rounded sandstone.

Lower Triassic. Sherwood Sandstone Group, Keuper Sst Fm, Member 3. Dominantly red-brown, occasionally grey, fine to medium, rarely coarse, sandstone.

Lower Triassic. Sherwood Sandstone Group, Keuper Sst Fm, Member 2. Dominantly argillaceous fluvial sandstone, light to medium grey, green-grey to red-brown, firm to hard.

Lower Triassic. Sherwood Sandstone Group, Keuper Sst Fm, Member 1. Variegated white to red-brown, very fine to coarse sandstone.

Lower Triassic. Sherwood Sandstone Group, St Bees Sst Fm. Red, very fine- to fine-grained sandstone, moderately well sorted.

Lower Triassic. Manchester Marl. Pink to dark-red or brown claystone, slightly calcareous, with interbeds of red-brown siltstone and fine sandstone.

L Triassic or U Permian (?). Collyhurst Sandstone Fm (St Bees Sandstone). Fine to coarse sandstone, pale to dark red-brown with rounded to well-rounded grains.

Upper Carboniferous (Westphalian 'D'-Stephanian). Grey siltstone with interbeds of reddish shales and greyish brown argillaceous sandstone.

Upper Carboniferous (Westphalian 'D'). No clear division with above. Interbedded grey shales, buff to light grey siltstones, thin tight sandstones and occasional thin coal seams towards base.

Upper Carboniferous (Westphalian 'C'). Interbedded medium to dark grey siltstones and white to dark brown sst with minor shales, claystones and coals (11m of coal).

Upper Carboniferous (Westphalian 'B' ?). A basal sand 10m thick directly overlies the Caledonian unconformity.

Lower Palaeozoic - Bray Group ?. Light green and occasionally light brownish chloritic slates. Correlated with similar Bray Group which outcrop 25km SW at Bray Head.

Figure 4.9:- Stratigraphy of the Kish Bank basin. (a) Well 33/22-1 was drilled in 1977 to test a large, shallow fault-bounded closure. The well encountered a major unconformity between Upper Carboniferous Westphalian, and a thin veneer of Tertiary-Quaternary sediment. (b) Well 33/21-1 was drilled in 1979 to test a four-way closure. The main exploration target was the Lower Triassic Sherwood Sandstone Group, sealed by evaporites of the Keuper Marl and sourced by Carboniferous shales and coals. The test was unsuccessful. VR determinations of the Triassic interval of Rm 1.23-1.67% (Haughey, 1987), puts the base of the interval in the dry-gas window. (c) Well 33/17-1 was drilled in 1986 to test a horst structure. The main exploration target was the Upper Permian-Lower Triassic Collyhurst Sandstone Formation. The NW-SE fault is probably a strand on the eastern periphery of the Codling Fault zone (forming a negative flower structure – see figure 4.15). Many of the faults cut the base Tertiary unconformity. The test was unsuccessful.

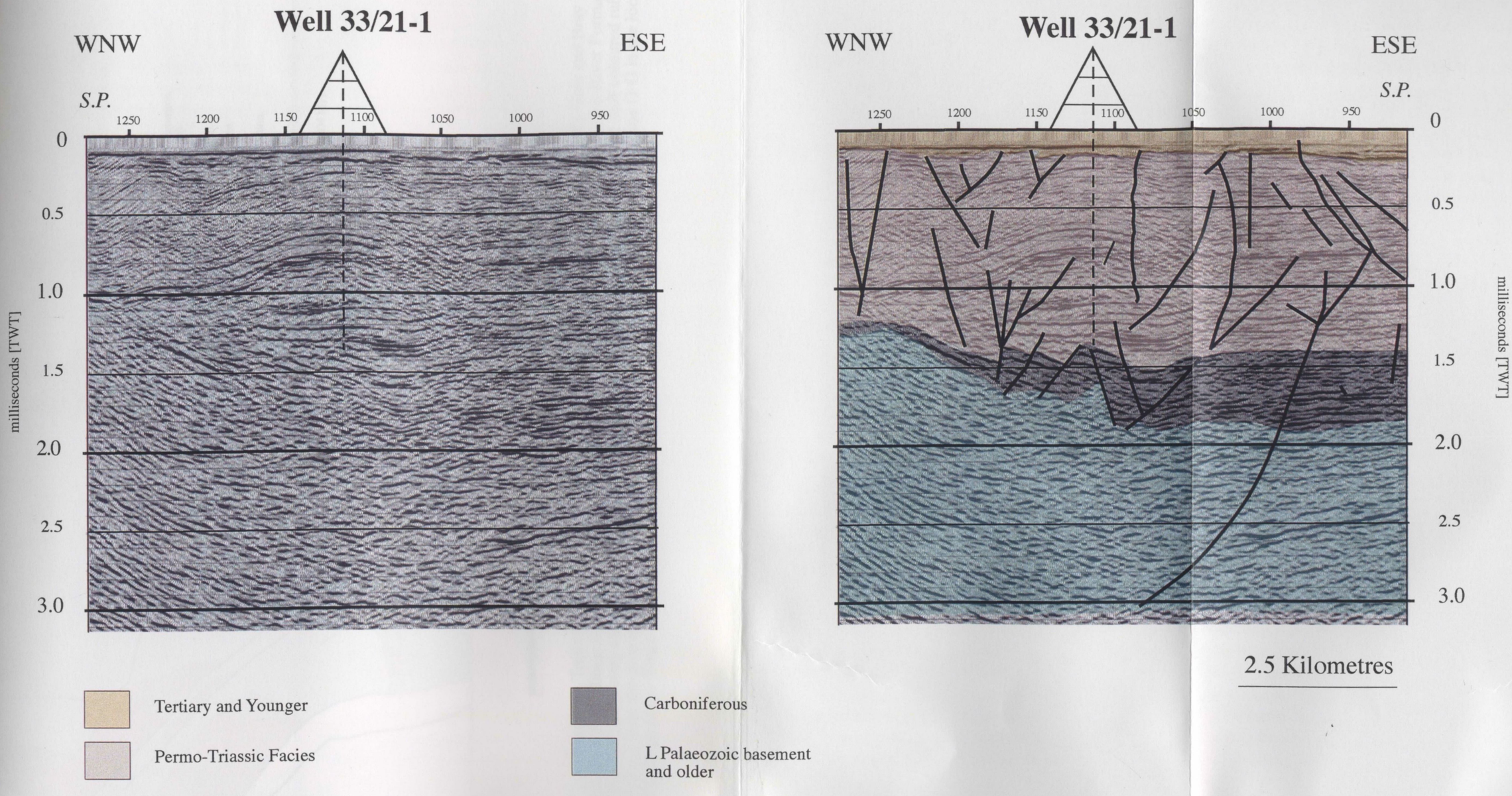

Figure 4.10:- shows a small section of the WNW-ESE trending TRIST-92-14 line. The main feature is the anticlinal structure in the Permo-Triassic rocks between shot-points 1200 and 1050. The structure plunges to the north (not evident here) and is faulted on the southern margin. The boundary between the basement (Lower Palaeozoic) and the Carboniferous is unconformable. The top of the Carboniferous probably includes upper Westphalian coal measures (which were encountered in well 33/22-1), and would provide a potential source for hydrocarbons. The Carboniferous section is highly faulted with block rotation, and the reflectors do not show any change in spacing towards the fault planes. Therefore, these rocks form the pre-rift package of the Kish Bank basin. The Permo-Triassic facies unconformably overlies the Carboniferous with evidence of onlapping and overstepping of the fault blocks. The Permo-Triassic strata is likewise faulted but doesn't exhibit fault block rotation. In addition, the spacing between the reflectors increases in distance with proximity to some but not all the faults, i.e., D labelled above. Onlapping and draping of the antiformal structure is not evident, which means the fold post-dates deposition and is compressional in nature. The age must be post-Liassic and may relate to Early Tertiary uplift, i.e. the unconformity between Maastrichtian chalky limestone and Palaeocene basalts in the Ulster basin (chapter 1).

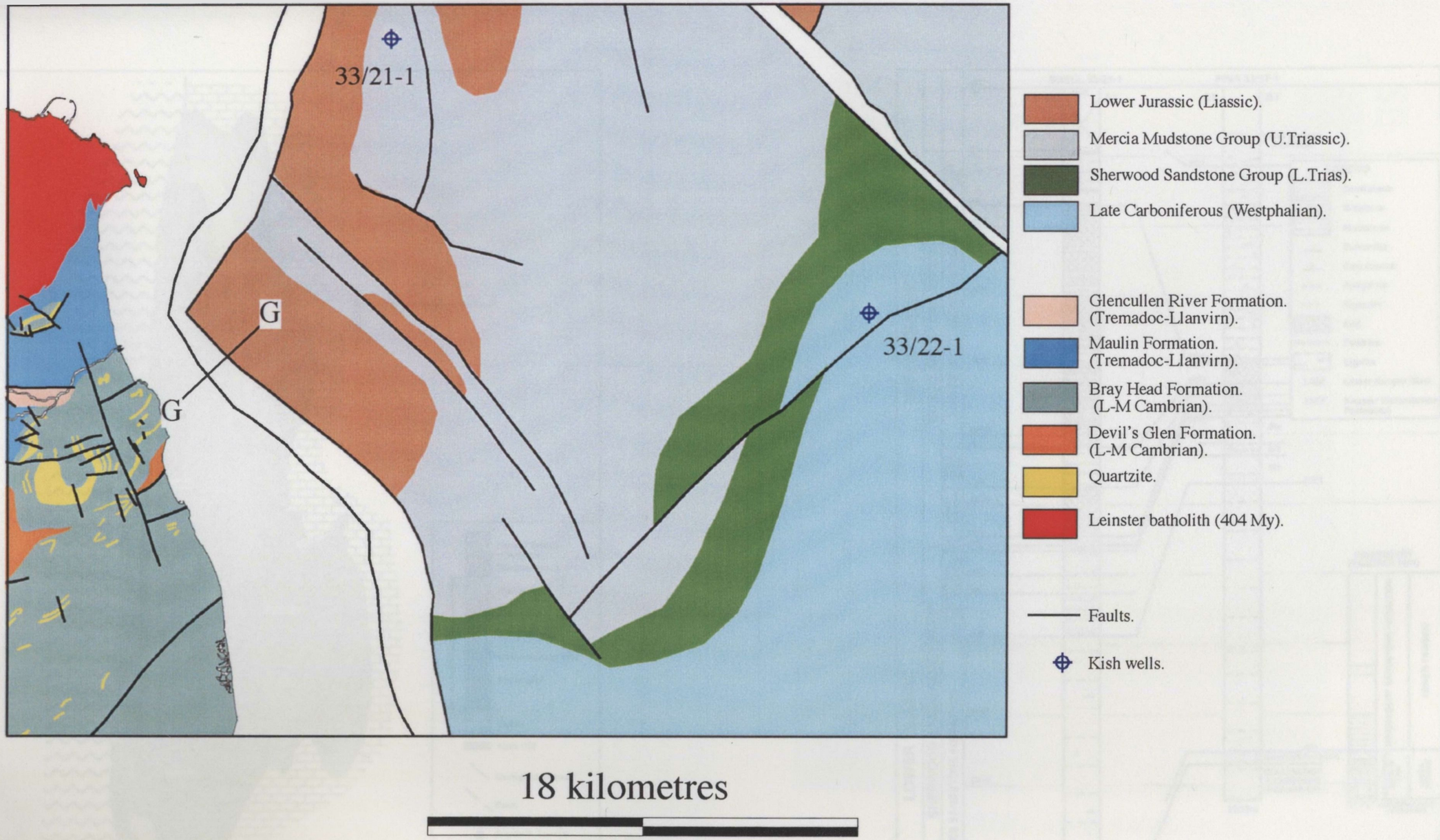

Figure 4.11:- Map showing the offshore pre-Tertiary geology of the Kish Bank basin and the onshore geology. The Devil's Glen and Bray Head Formations belong to the Cambrian Bray Group and consist of greywackes, slate and quartzite. The Maulin and Glencullen River Formations belong to the Lower Ordovician Ribband Group and consist of dark blue-grey slate, phyllite and schist (Maulin Fm.) and buff coloured tuff and greywacke (Glencullin River Fm). Note the proximity of Cambrian quartzites to the offshore Liassic sediments. The line G-G is the location of figure 4.13. Source of onshore geology:- Flegg & O'Connor (1995).

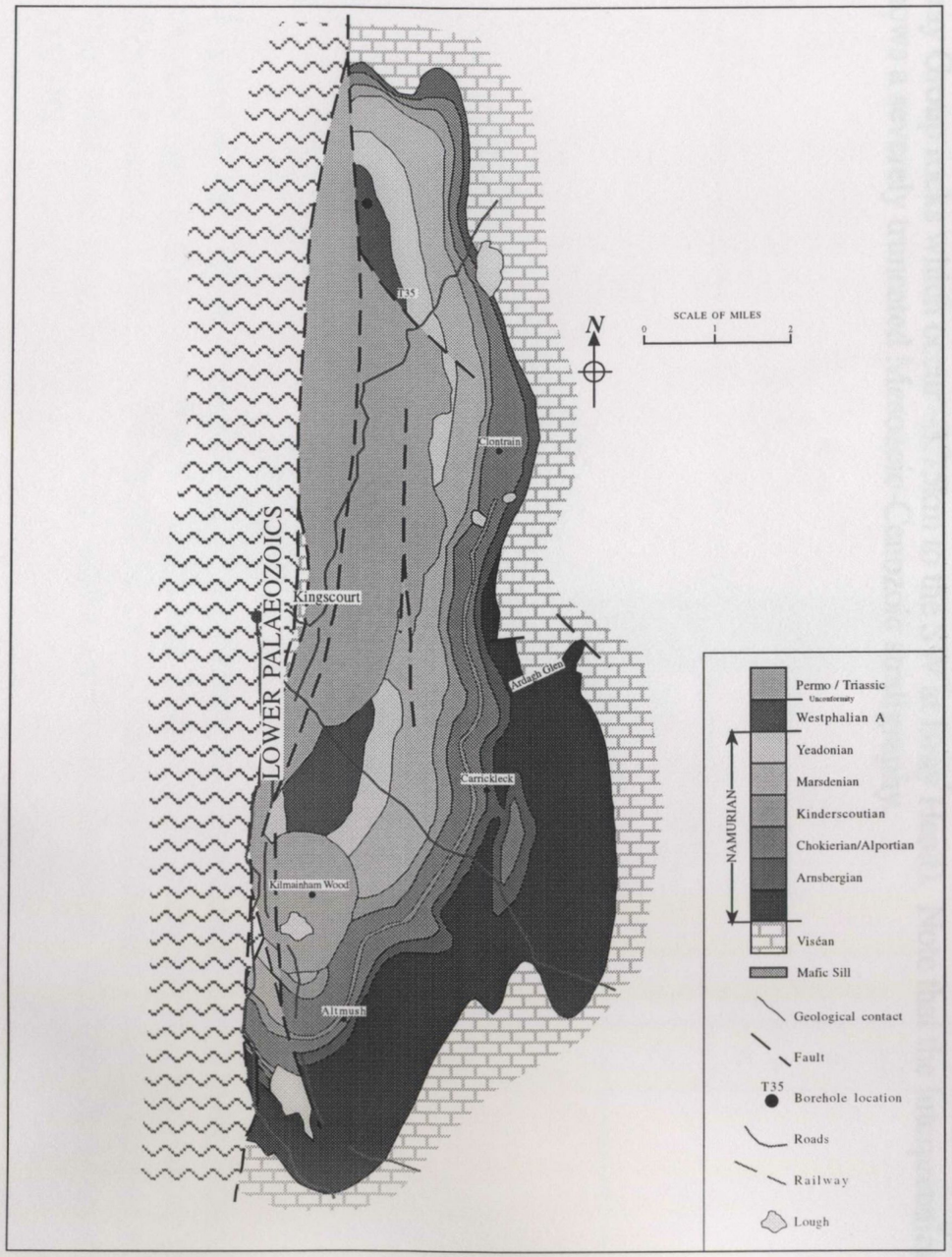

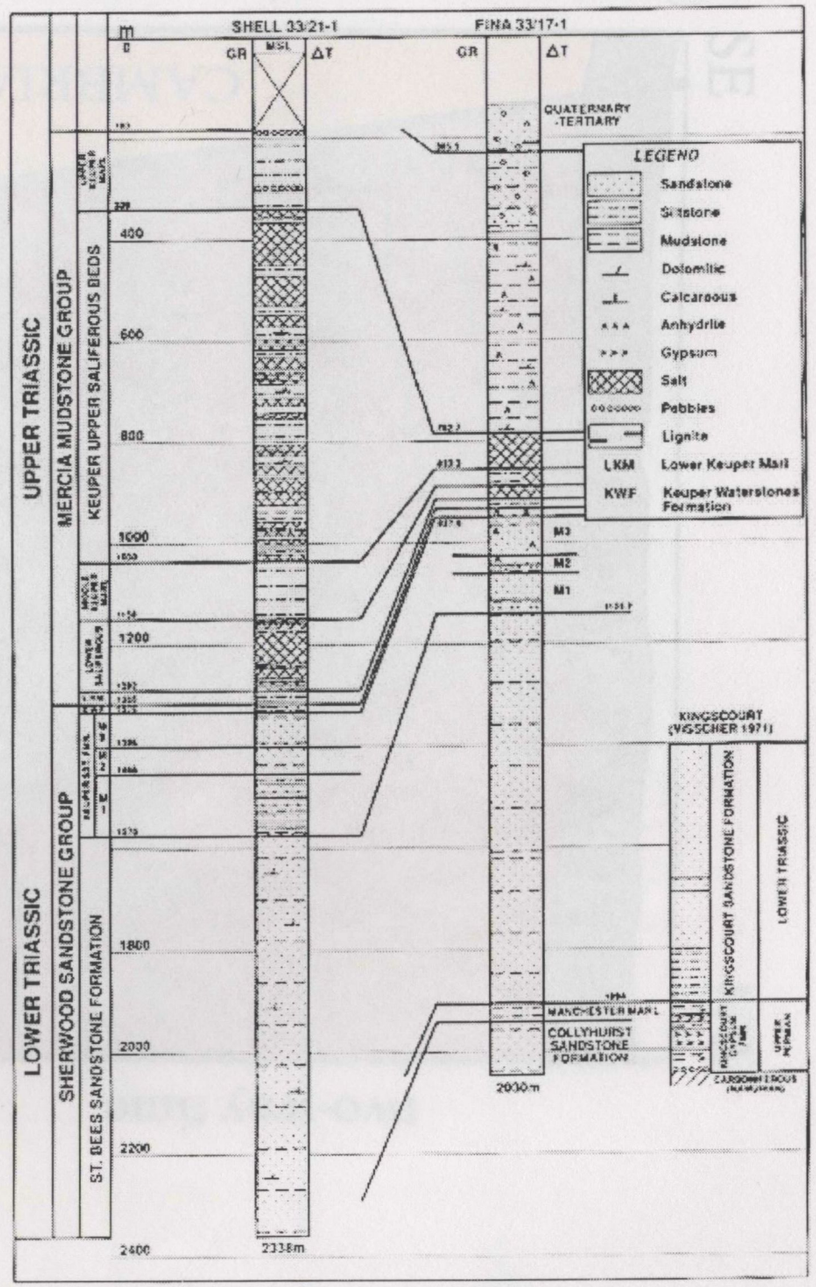

Figure 4.12:- The geology of the Kingscourt area, Co. Louth (after Jackson, 1965). Westphalian 'A' is missing in the Kish basin and Westphalian 'C-D' and Stephanian sequences, which are present in well 33/22-1 are absent at Kingscourt. However, the Permian conglomerate and the 130m thick mudstones and gypsum units are equivalent to the Collyhurst Sandstone and Manchester Marl Formations respectively.

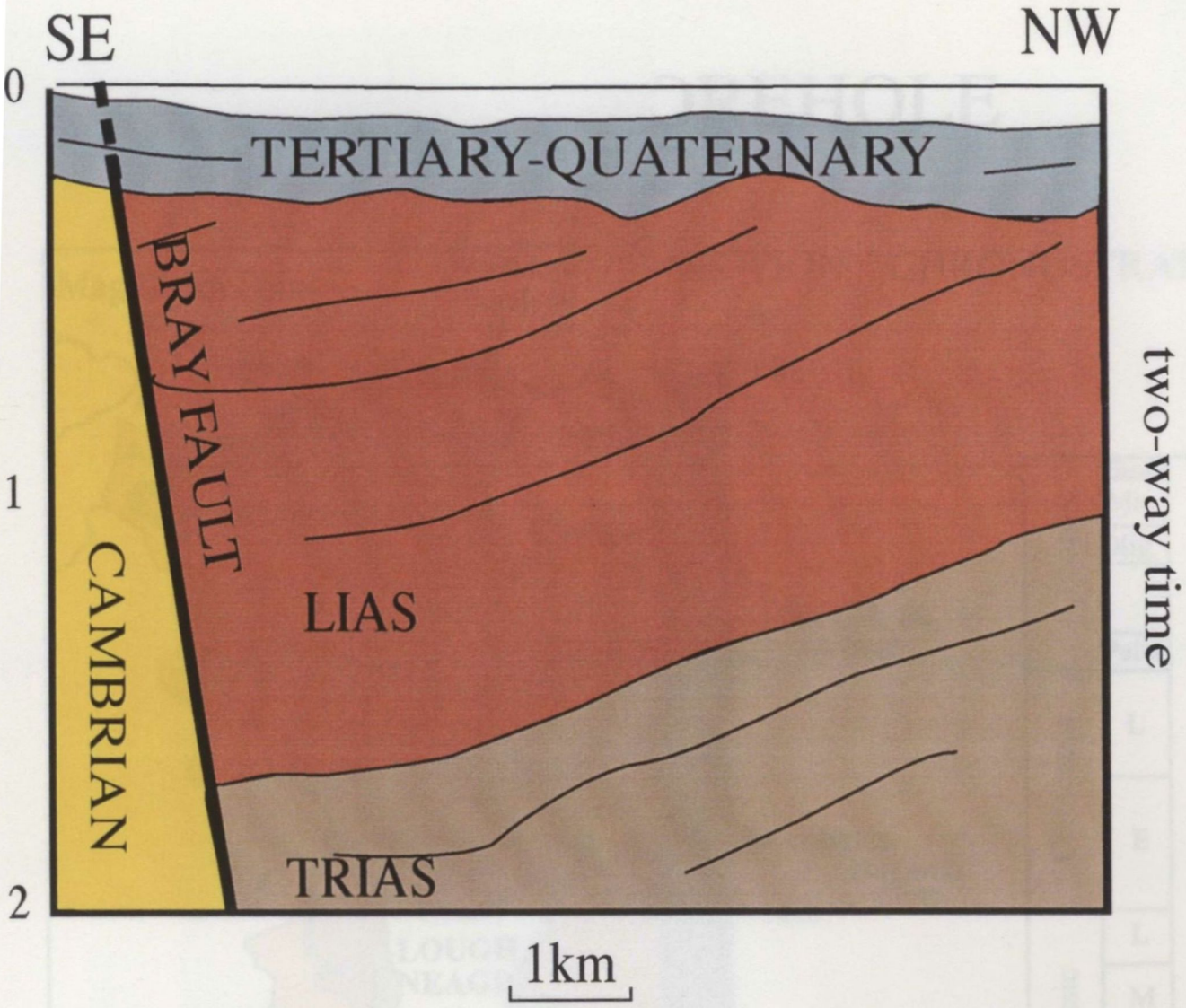

Figure 4.13:- Broughen *et al.*, (1989) postulates ~1.7(ms twt) equivalent to 2,700m of Liassic section, preserved in the hanging-wall of the Bray Fault. The footwall rocks comprise of light green to occasionally light brownish chloritic slates (possibly the Lower-Middle Cambrian aged Bray Group rocks which occur ~3.75km to the SW at Bray Head). Note that the interpretation shows a severely truncated Mesozoic-Cenozoic stratigraphy.

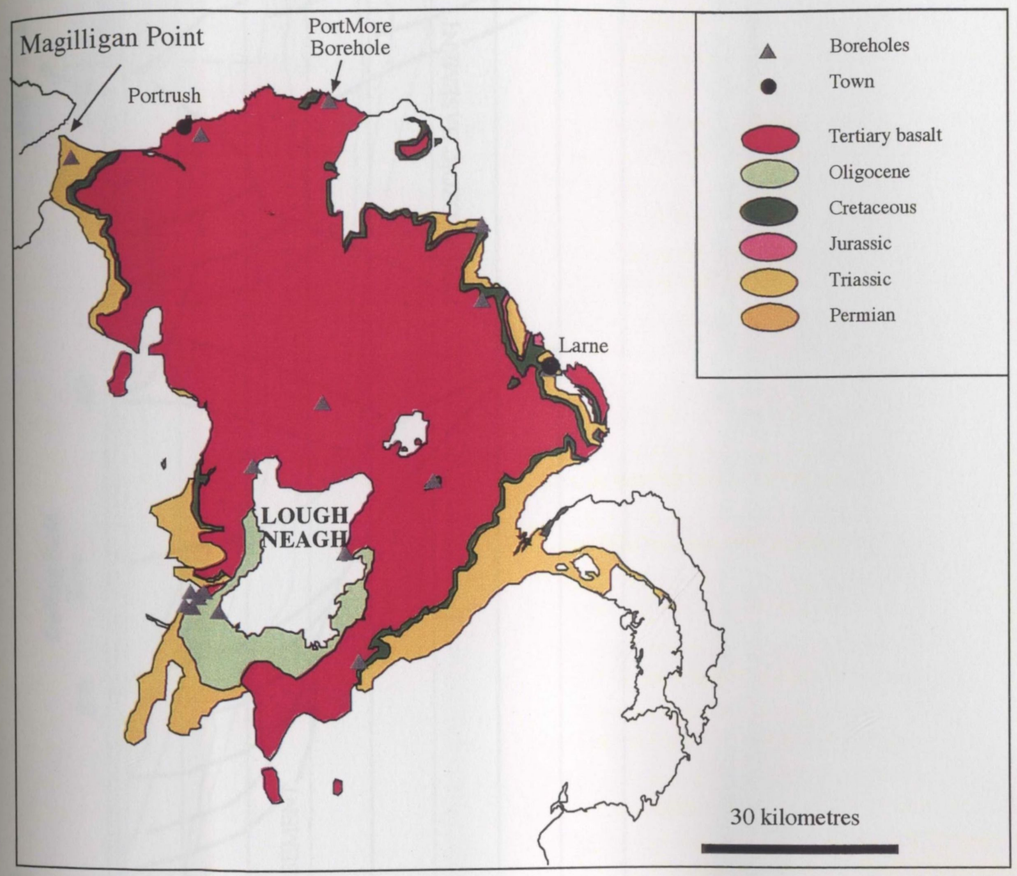

PORTMORE BOREHOLE

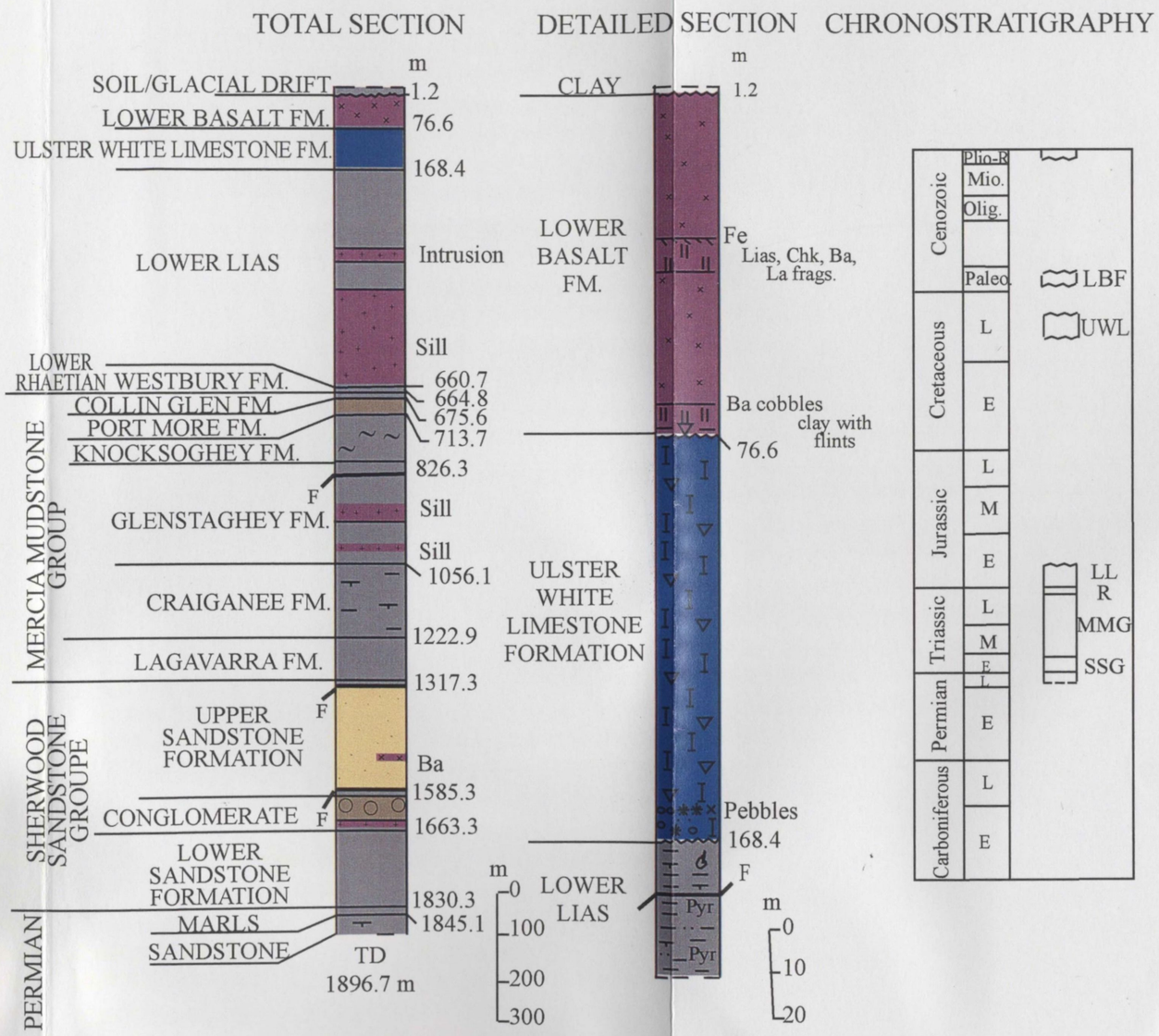

Figure 4.14:- Map showing Mesozoic-Tertiary rocks in the Ulster basin, including the Antrim plateau lavas. Outcrop of Jurassic sequences are restricted in extent. However, outcrop occurs along the coastline at Magilligan Point and Portrush (Co Derry) and, Whitepark Bay and Larne (Co. Antrim). Boreholes confirm that the Jurassic is preserved underneath the flood basalts. Over 250m of Sinemurian to Lower Pliensbachian sediments were present in the PortMore borehole. The rocks comprise "grey calcareous mudstones locally containing thin ribs and interbeds of grey siltstones and grey fossiliferous limestones" (Broughan *et al*. 1989). See Appendix 7 for detailed legend. Source of borehole data: Wilson. & Manning (1978).

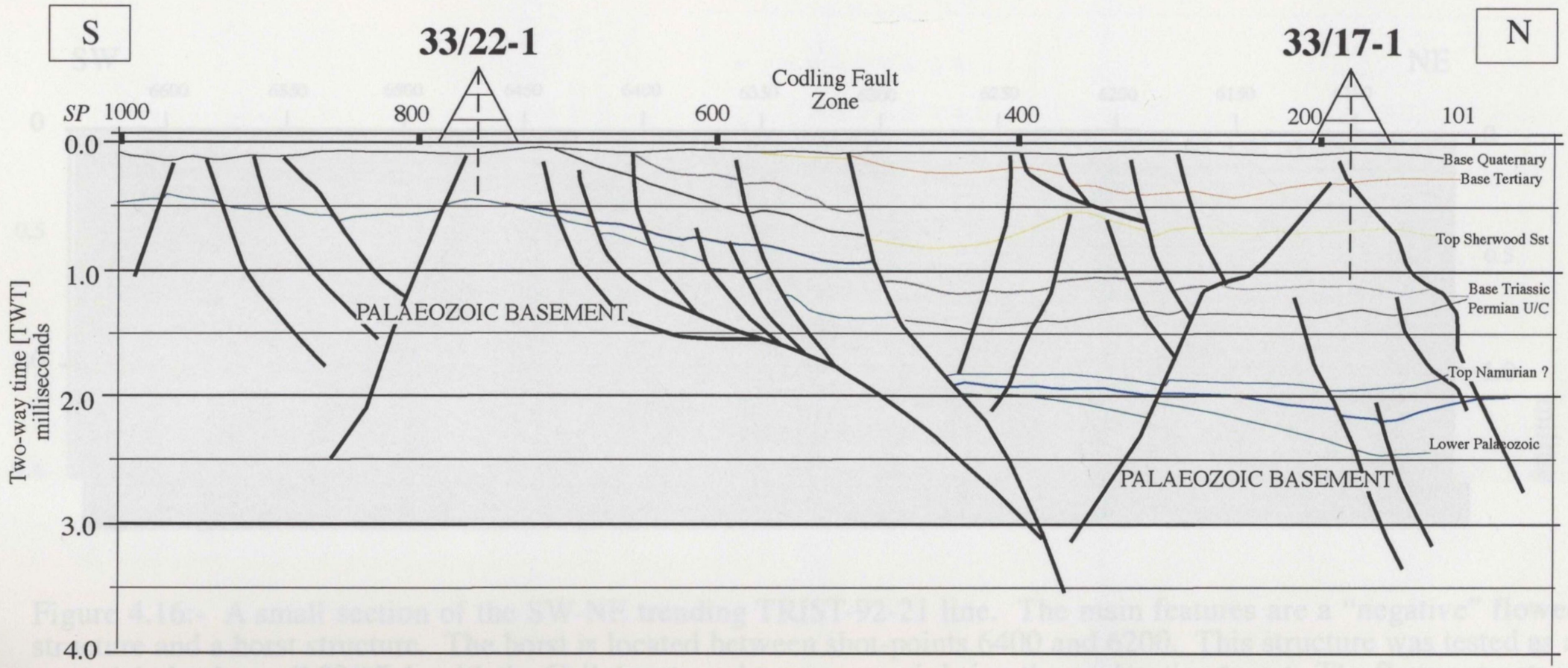

Figure 4.15:- N-S structural and stratigraphical interpretation of a seismic line, traversing the Codling fault zone (JS-MANX-16 interpreted by Corcoran & Clayton (1999)). This line illustrates the Permo-Triassic strata thinning out towards relatively shallow basement to the south. Note the degree of inversion, i.e. block fault rotation.

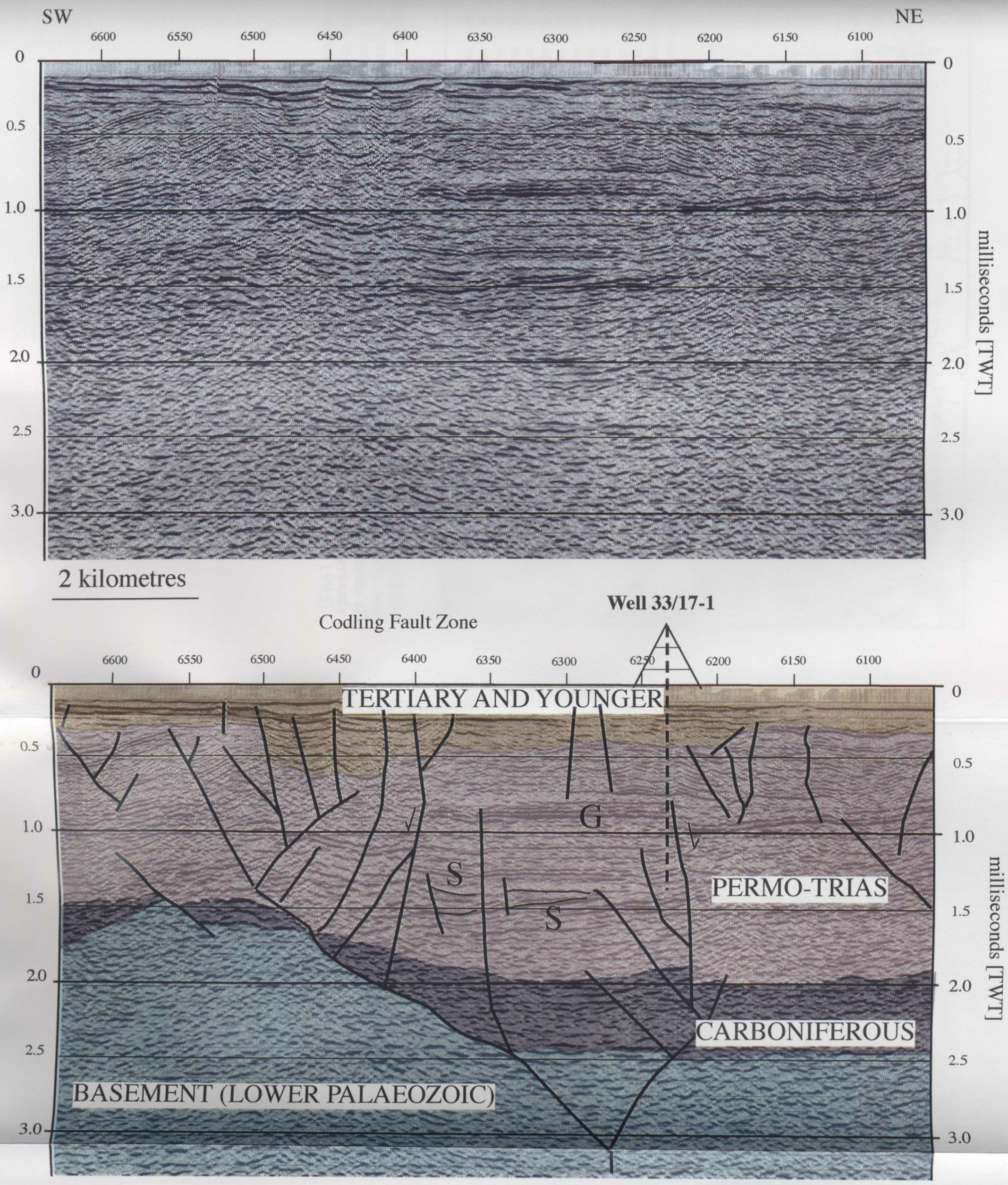

Figure 4.16:- A small section of the SW-NE trending TRIST-92-21 line. The main features are a "negative" flower structure and a horst structure. The horst is located between shot-points 6400 and 6200. This structure was tested as a potential play by well 33/17-1, with the Collyhurst sandstone reservoir being the exploration target. The flower structure has draped basement from ~1.7ms[twt] to ~2.5ms[twt]. Both basement and Carboniferous exhibit a similar structural pattern to line TRIST-92-14, e.g., fault block rotation. Hence, the Carboniferous forms the pre-rift package. The Permo-Triassic shows growth into major faults (labelled S) and drapes the pre-rift geology, and hence, forms the syn-rift stratigraphy. Between shot-points 6500 and 6350, reflectors are truncated and columns of acoustic turbidity are present. This is probably related to the escape of biogenic gas along fault conduits. These faults must have been active (and/or reactivated) in recent times, otherwise, the gas pockets would now be barren. This is supported by the relatively thick Tertiary-Quaternary sequences which unconformably overlies the Permo-Triassic. These sequences reach a maximum thickness of ~0.7ms[twt], with thick fault wedges evident.

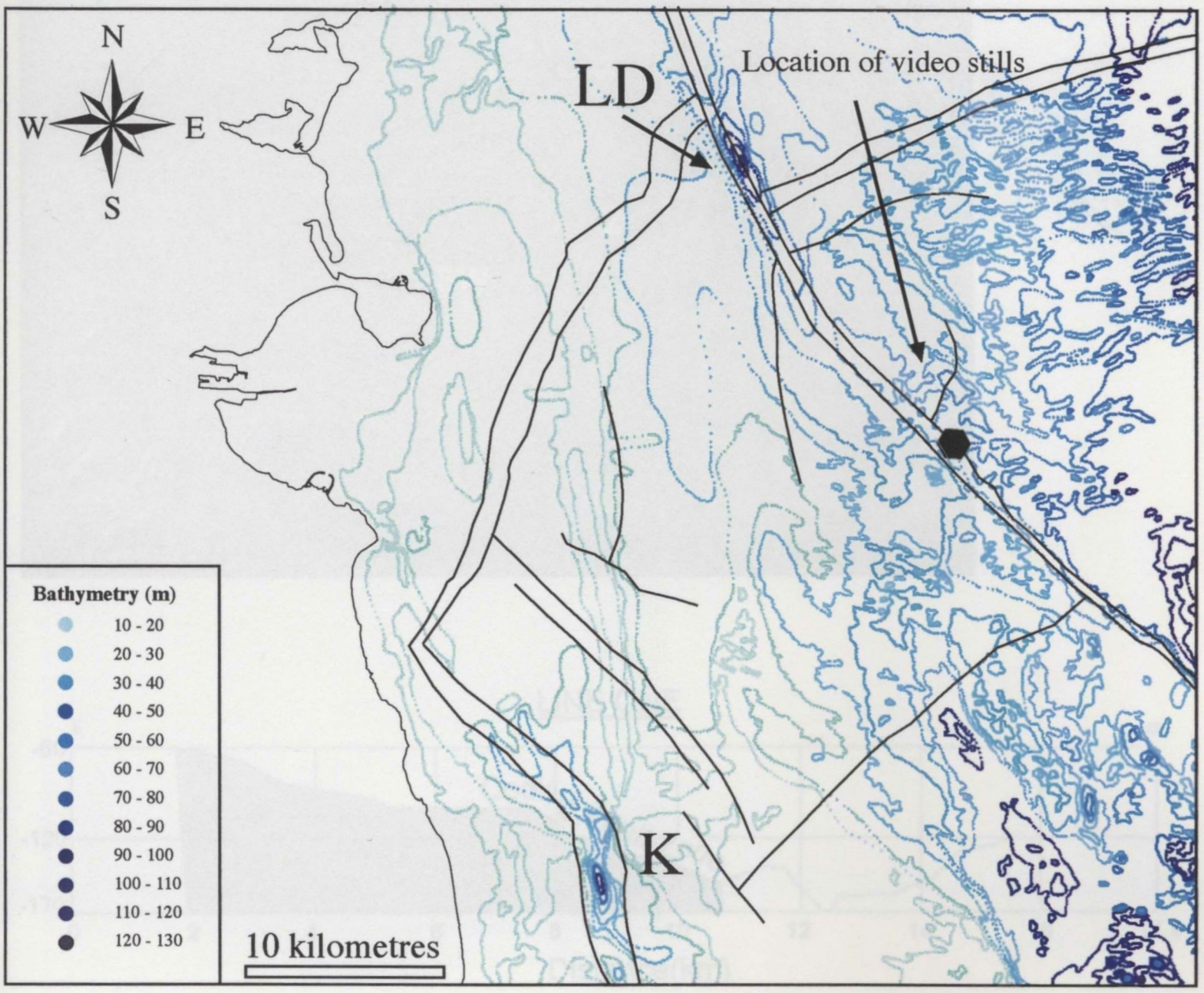

Figure 4.17:- A contoured bathymetry map over the Kish basin. The contour interval is 10m. A bathymetric east facing scarp lies along the trace of the Codling fault. Additionally, two ~N-S elongated holes are lablelled 'K' and 'LD'. Both holes reach maximum depths of ~130m, in comparison with surrounding depths of ~40m. The 'LD' hole has been previously documented as the Lambay Deep (i.e., Jenner, 1981; Croker, 1995).

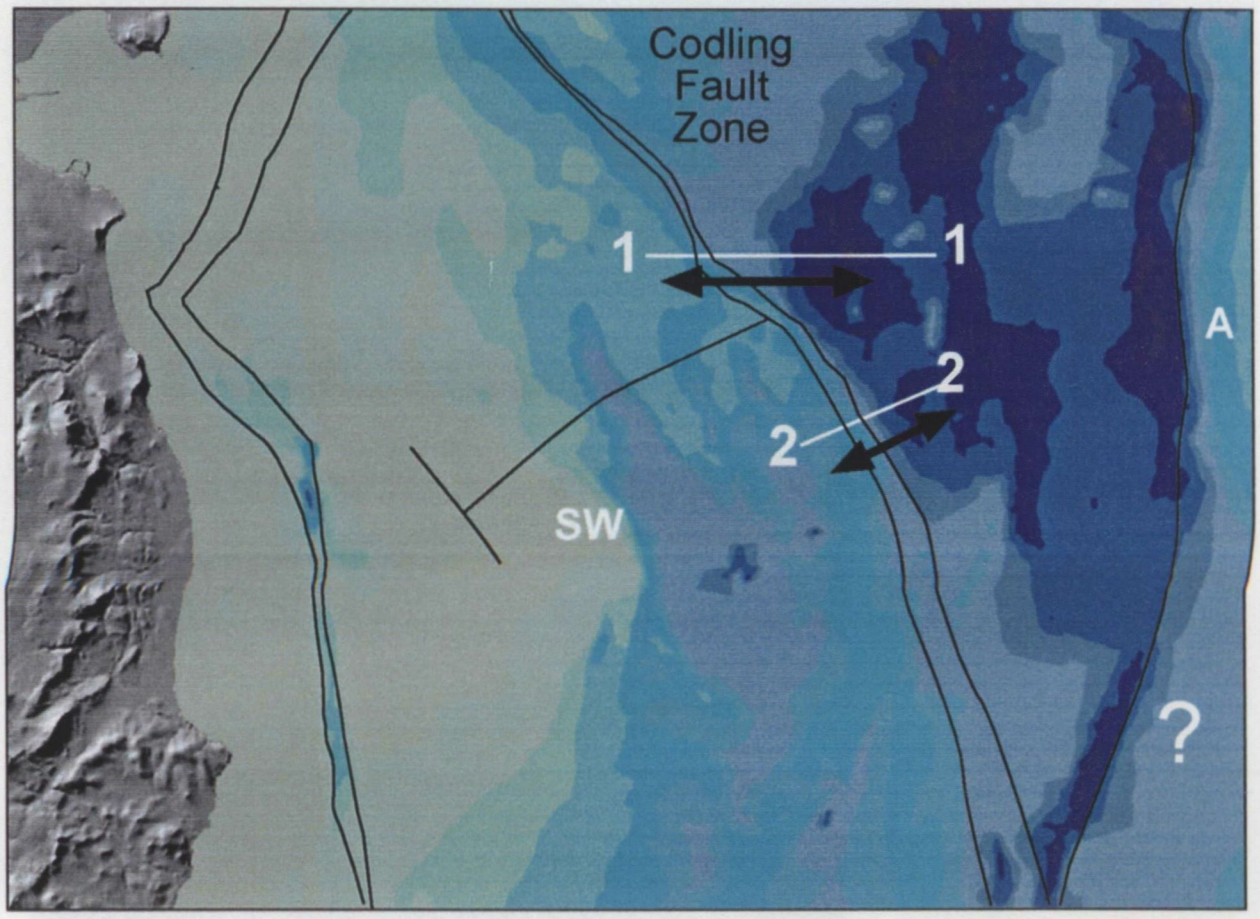

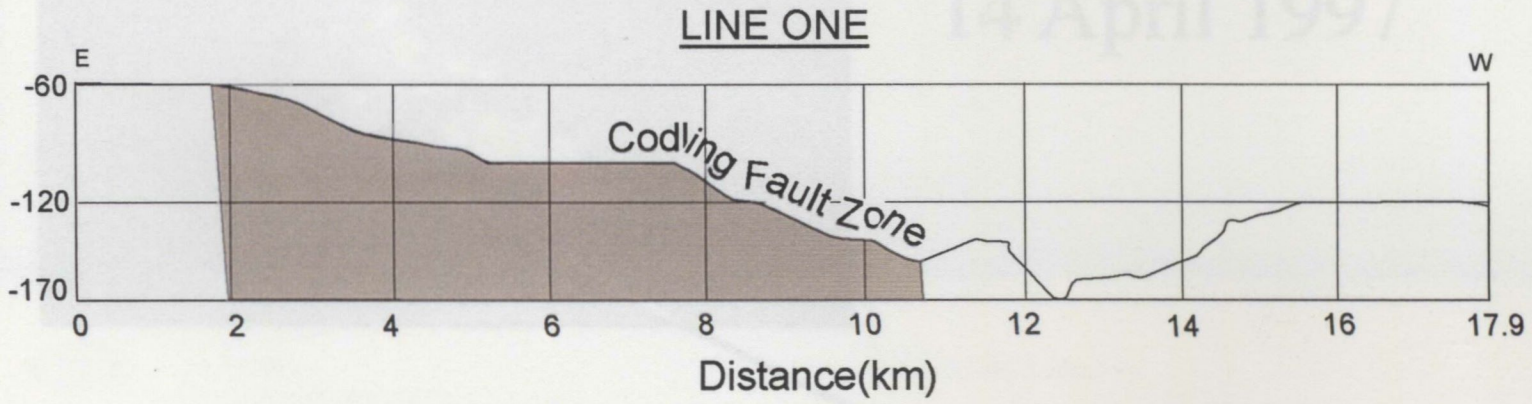

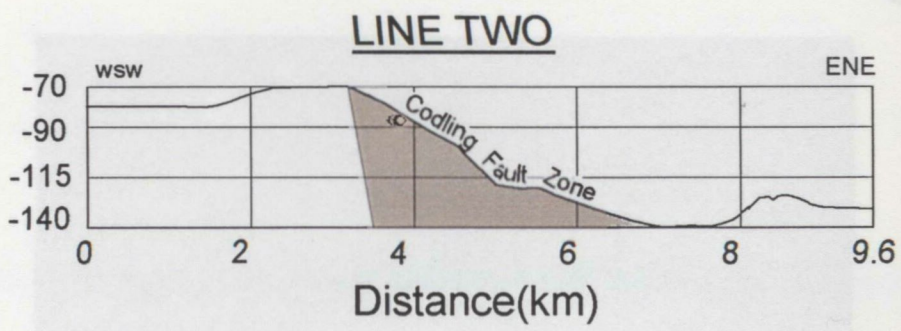

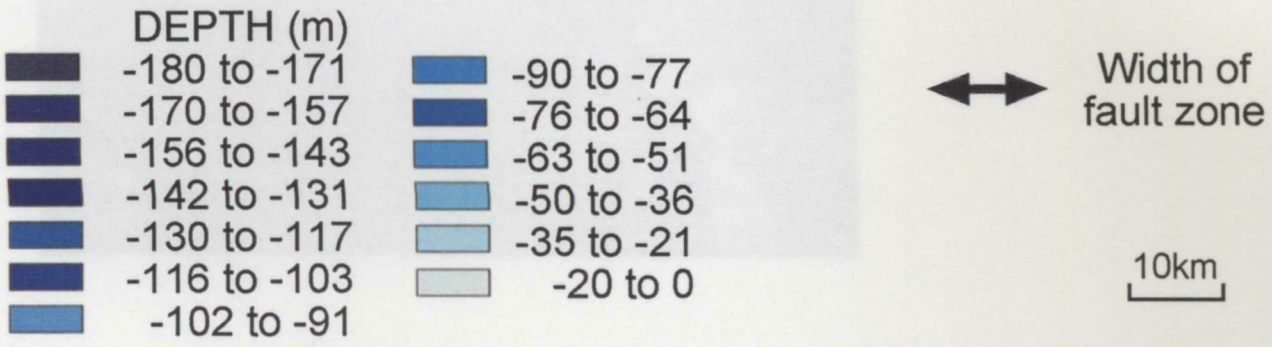

Figure 4.18:- The bathymetry surface derived from the same data-set as above but covers a larger area to give a regional perspective. Two profiles cross the Codling fault to emphasis the relatively steep east facing scarp, i.e. line 1 and 2 increase from depths of ~70m to ~140m, over a short distance of 2-3km. East of the Codling fault, there is another bathemtric scarp, facing westwards. The gradient is even steeper than the Codling scarp, and therefore may represent another potential fault scarp.

14 April 1997

14 April 1997

Edible Crab
for scale

15 April 1997

Figure 4.19:- Three video stills of the Codling fault, taken between the 14 and 15 April 1997. Edible crab gives idea of vertical scale. Drag samples indicate that the scarp is composed of carbonate cemented sandstones (Croker, 1997).

Figure 4.20:- Pre-Tertiary geology map of the Kish Bank basin with seismic lines. Lines labelled are illustrated and discussed in text.

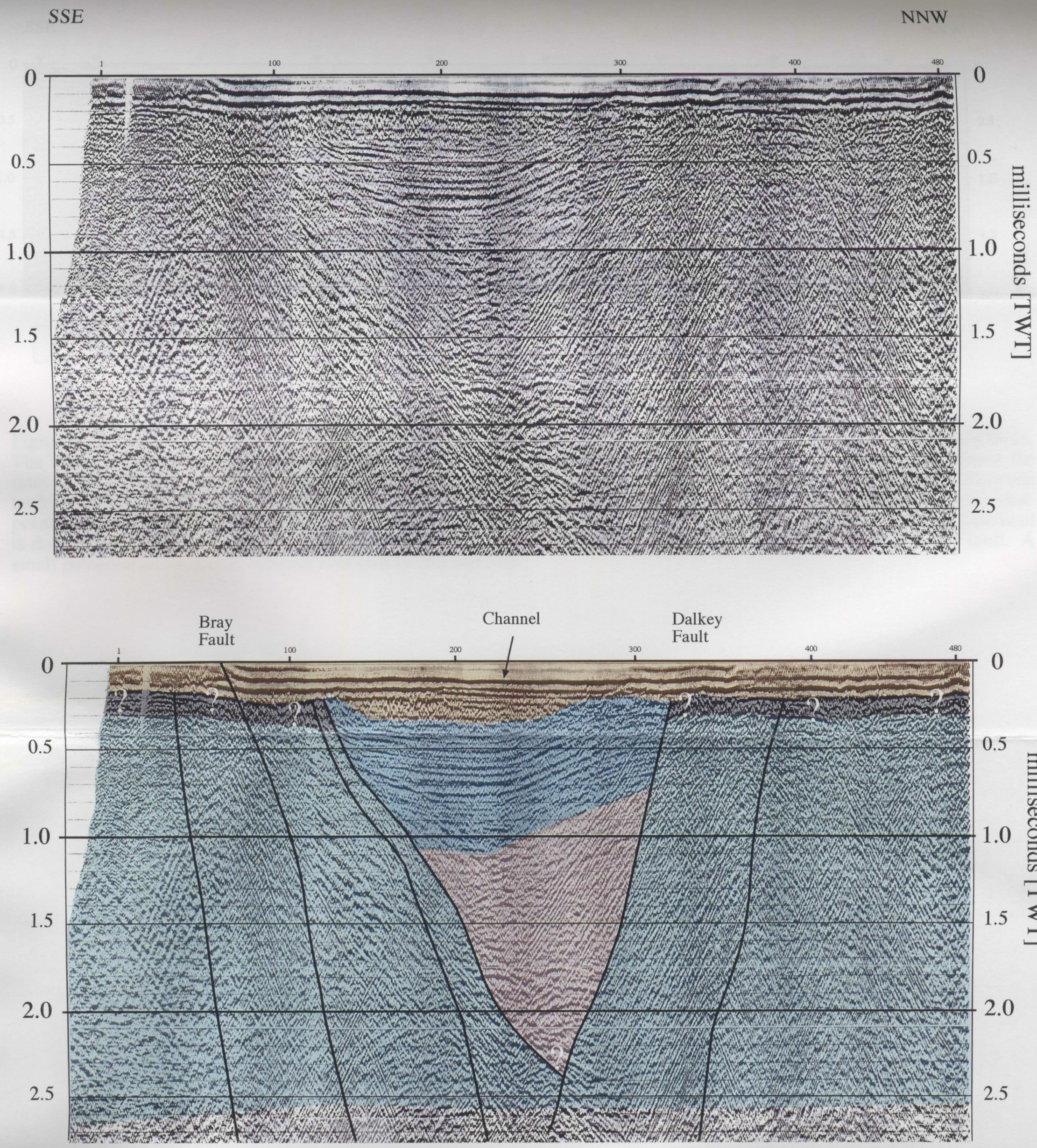

Figure 4.21:- Line AIR 78-61 shows a small triangulated section of Mesozoic strata overlain by a thin veneer (~0.2ms[twt]) of Quaternary-Tertiary sediment. Top Triassic is at a maximum depth of ~1.1ms[twt], rising to ~0.7ms[twt] against the Dalkey fault. The Quaternary-Tertiary unconformity oversteps the Carboniferous and Mesozoic strata, but is offset by the Bray fault, and a small intrabasinal fault (between shot-points 300 and 260). There is onlap and overstep of the Lias section by flat lying reflectors (shot-points 90-320) of Tertiary (?) age, which is conformably overstepped by younger sequences (Quaternary?). This feature probably represents a palaeo-channel.

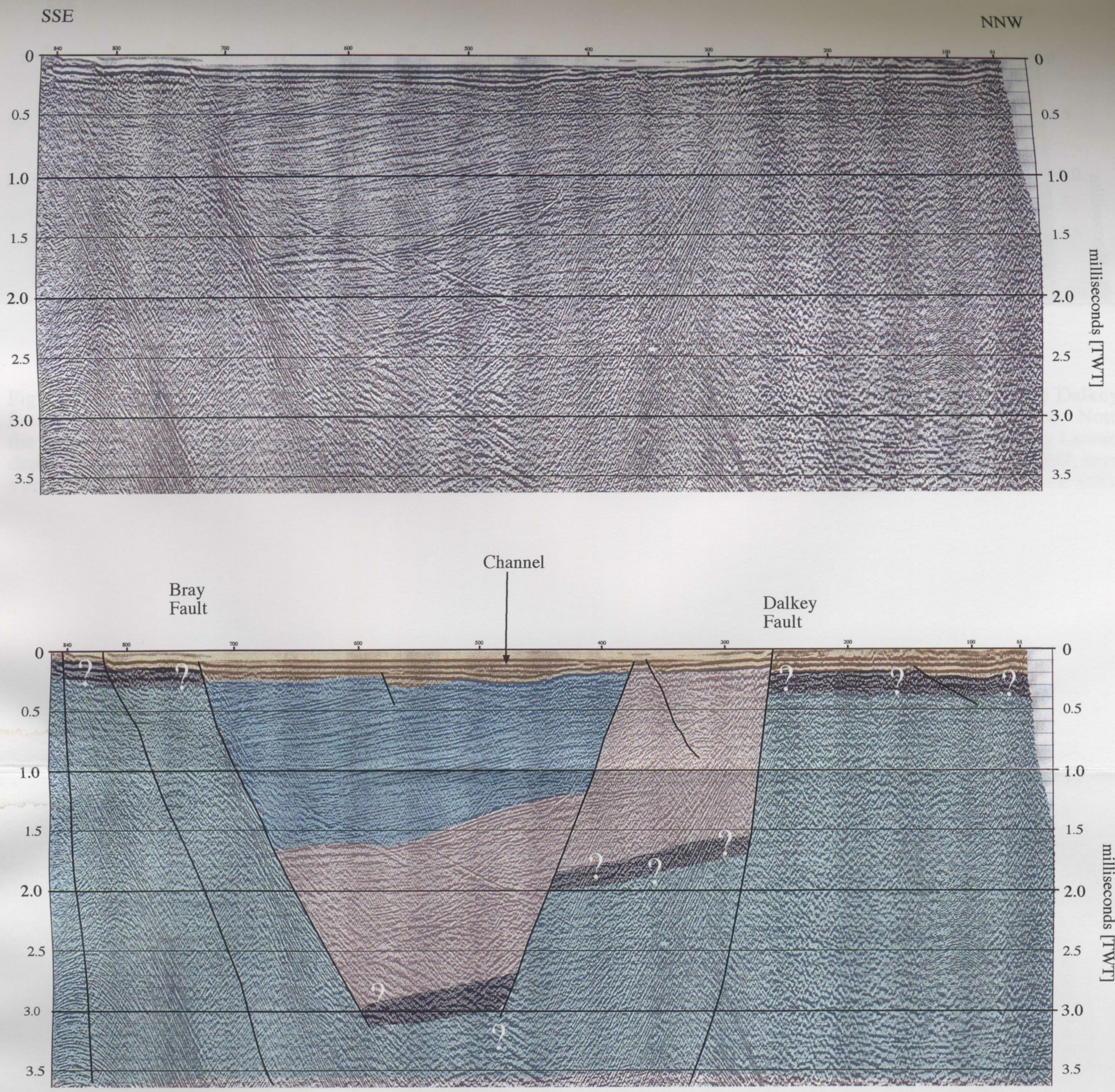

Figure 4.22:- Line AIR 78-62 shows both the Dalkey and Bray faults truncating the Mesozoic sequences of the Kish basin. The Tertiary-Quaternary unconformity is offset by a small fault near shot-point 580, with thickening of sediment against the fault plane. Near shot-point 420, the Lias is truncated against Triassic strata. It appears that the Lias is down-faulted between both the Bray and Dalkey fault but also an intra-basinal structure. Another fault occurs north of the Dalkey fault between shot-points 150 and 100. The fault dips to the north and likewise shows thickening of sediment against the fault plane. Basement is down-faulted from 0.2ms[twt] to 3.2ms[twt] by the Bray fault and from 0.4ms[twt] to 2.5ms[twt] by the Dalkey fault. A small palaeo-channel occurs between shot-points 290 and 380.

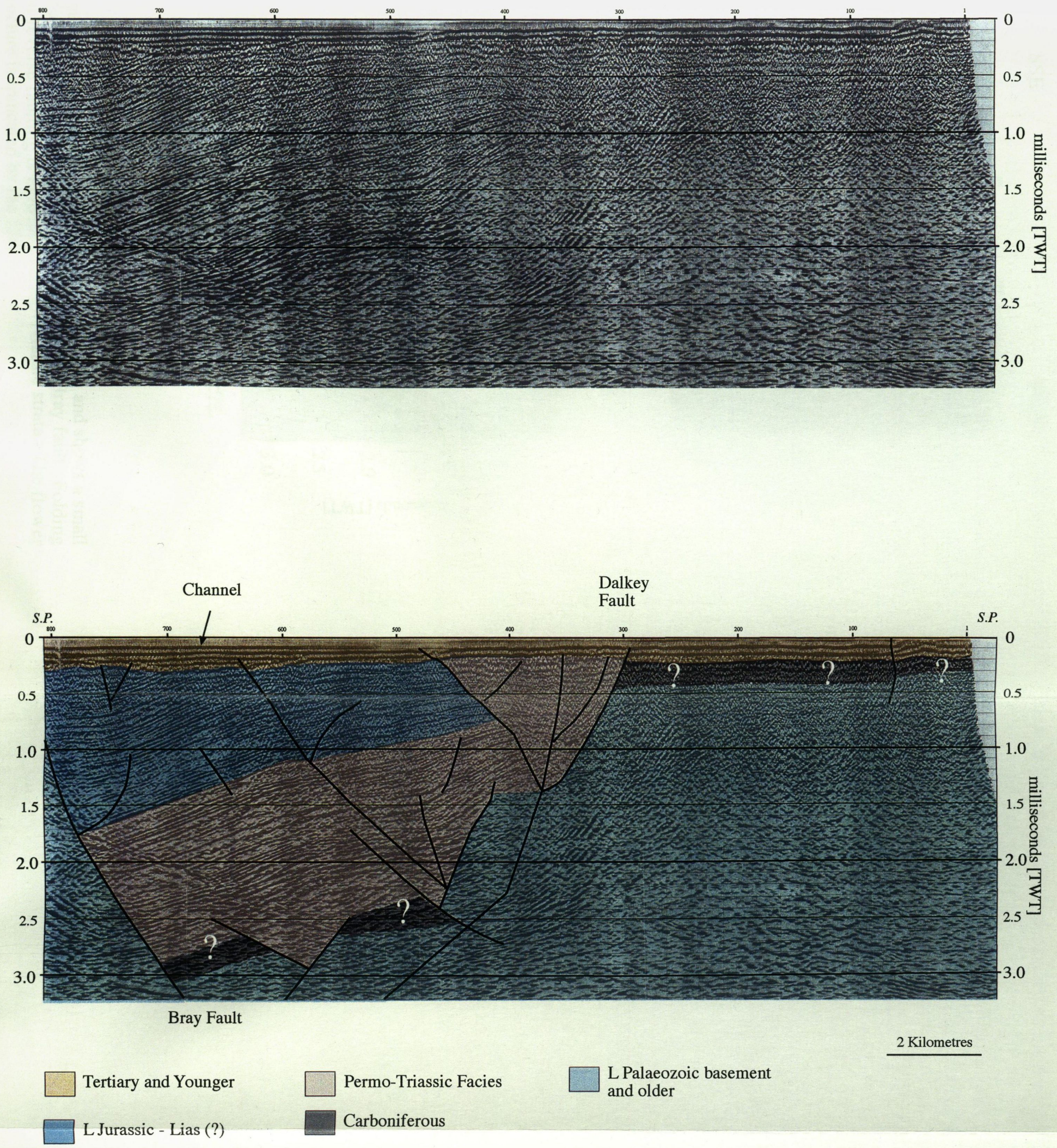

Figure 4.23:- Line AIR 78-63 shows small positive flower structure between shot-points 550 to 300, truncated by the Dalkey fault. The Lias is approximately 2.0ms[twt] thick and a small hanging-wall syncline has developed against the Bray fault. Note the spacing between reflectors stays relatively constant, indicating that the Bray fault appears to have been inactive during Liassic deposition, and has subsequently been reactivated post-Liassic but pre-dates the Tertiary-Quaternary unconformity. A small, near vertical fault occurs near shot-point 80. A small palaeo-channel occurs between shot-points 740 and 600.

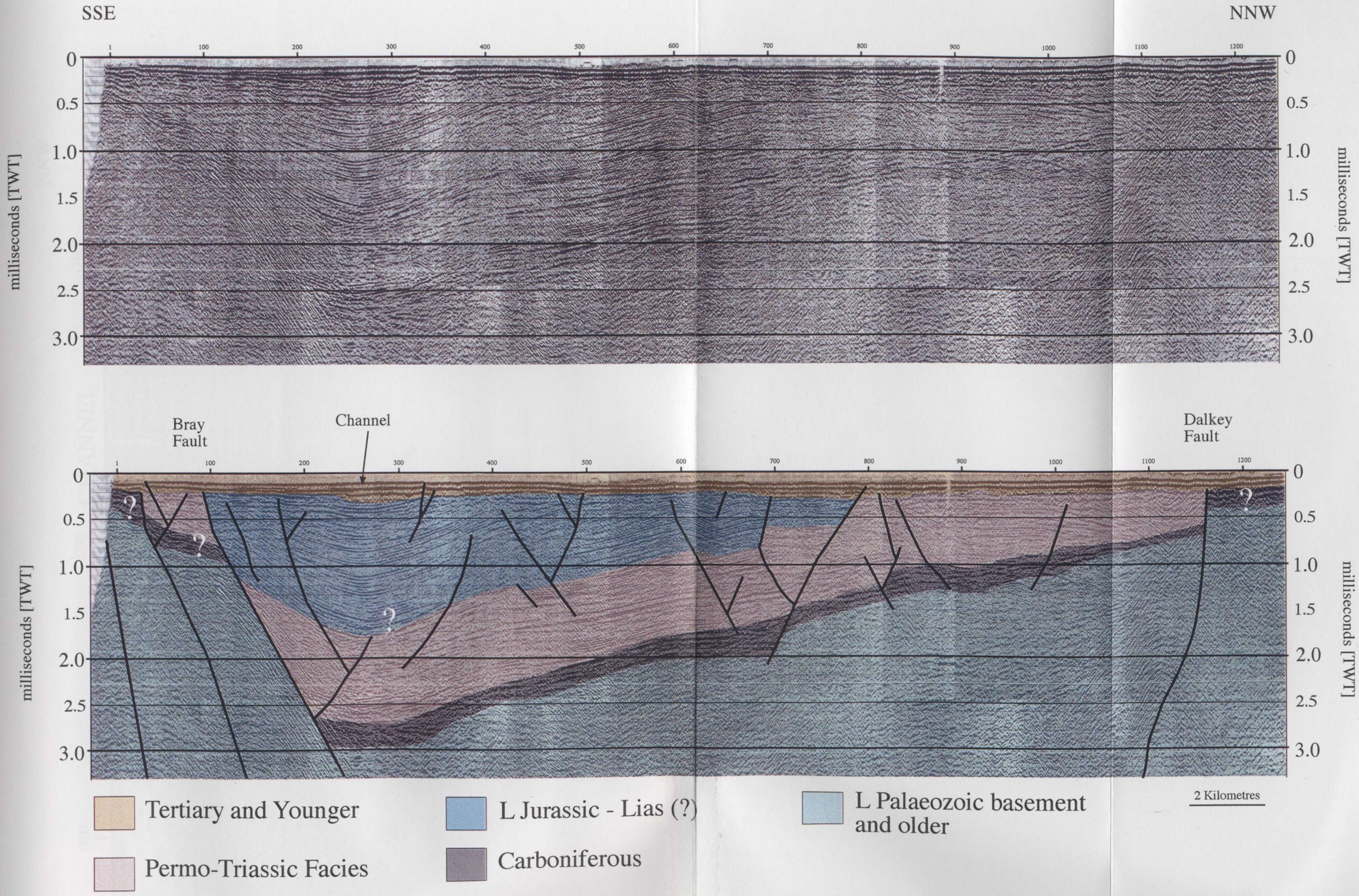

Figure 4.24:- Line AIR 78-64 shows basement offset and down faulted to a maximum depth of 3.0ms[twt]. Basement progressively rises toward the north and shows a small offset against the Dalkey fault, bringing together Carboniferous and Permo-Triassic facies. The Lias section forms a hanging-wall syncline against the Bray fault. Folding and reverse faulting is evident at shot-point 600. A small positive flower structure truncates the thinning Lias sequences and juxtaposes Permo-Triassic strata. The flower structure is truncated by the Dalkey fault. A small palaeo-channel occurs between shot-points 200 and 320.

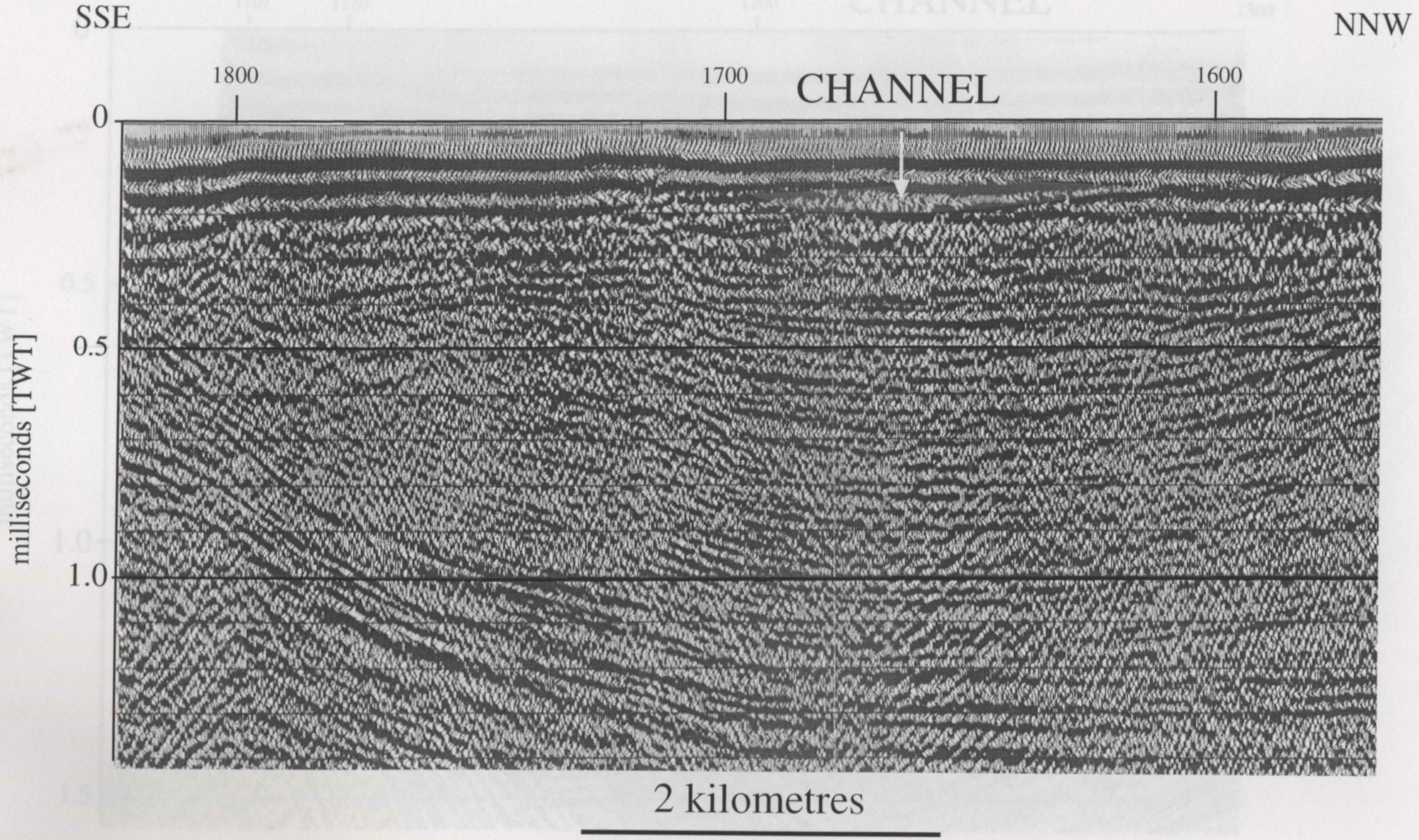

Figure 4.25:- Line AIR 78-66 shows the palaeo-channel is located between shot-points 1610 and 1710.

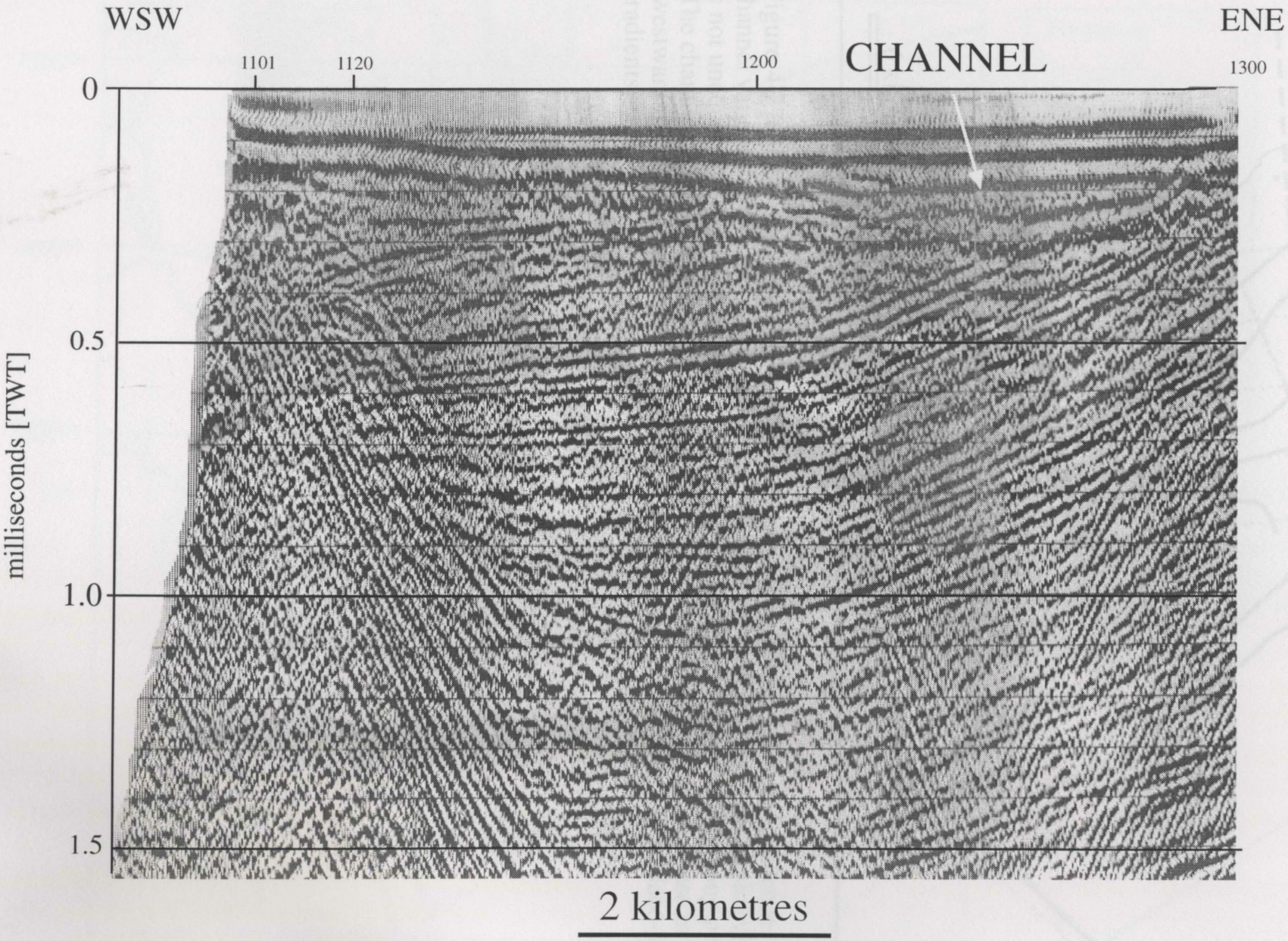

Figure 4.26:- Line AIR 78-53 is almost perpendicular to the lines above. The channel feature is located between shot-points1210 and 1290.

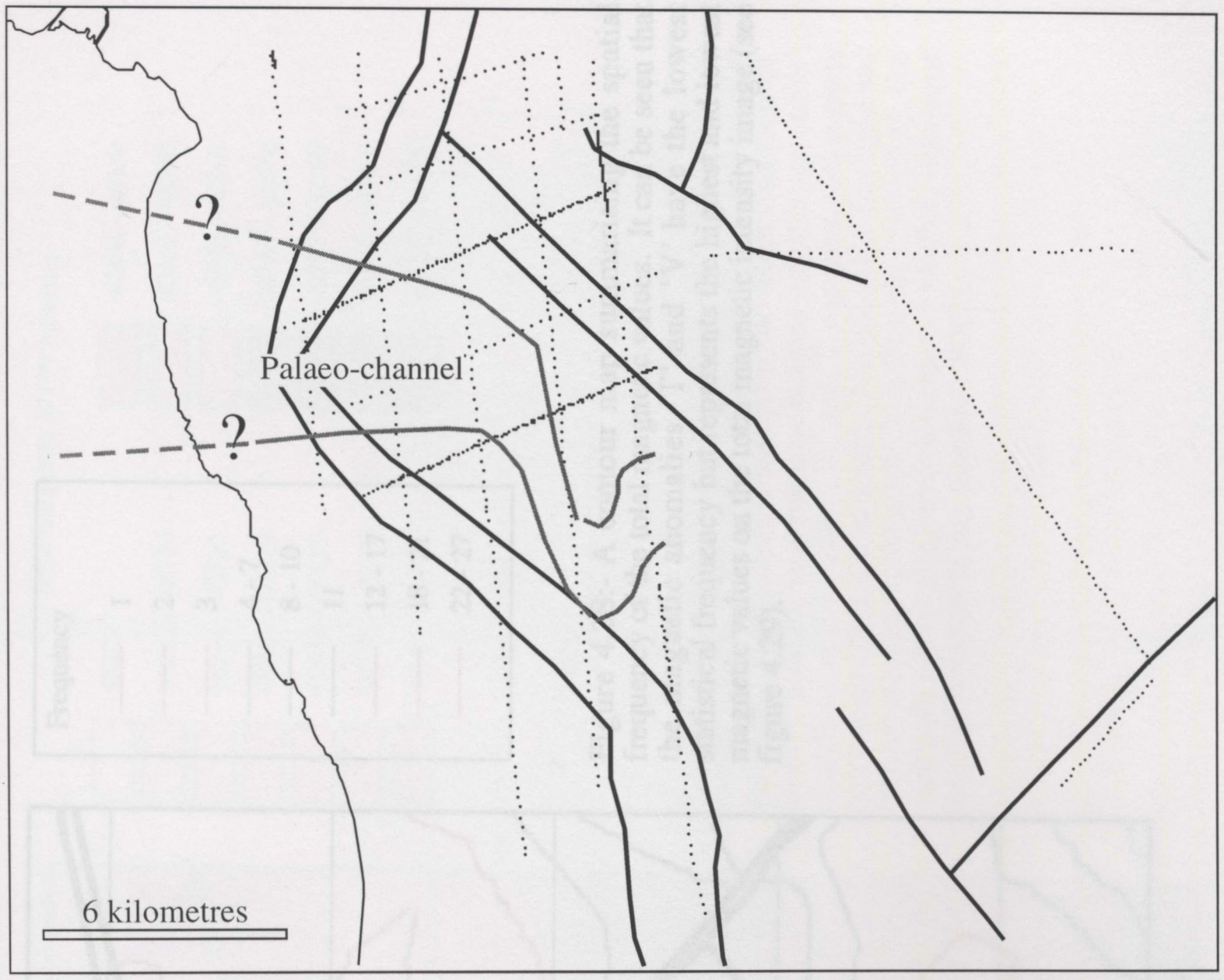

Figure 4.27:- Map showing extent of palaeo-channel, based on seismic evidence. The channel varies in width between 1km and 4km towards the west. Whilst the seismic evidence is not unequivical, there does appear to be a strong case for a palaeo-channel being present. The channel appears to have been flowing from east to west, based on the increase in width (westwards). Although this may be accounted for by changes in lithology and palaeo-stream gradients.

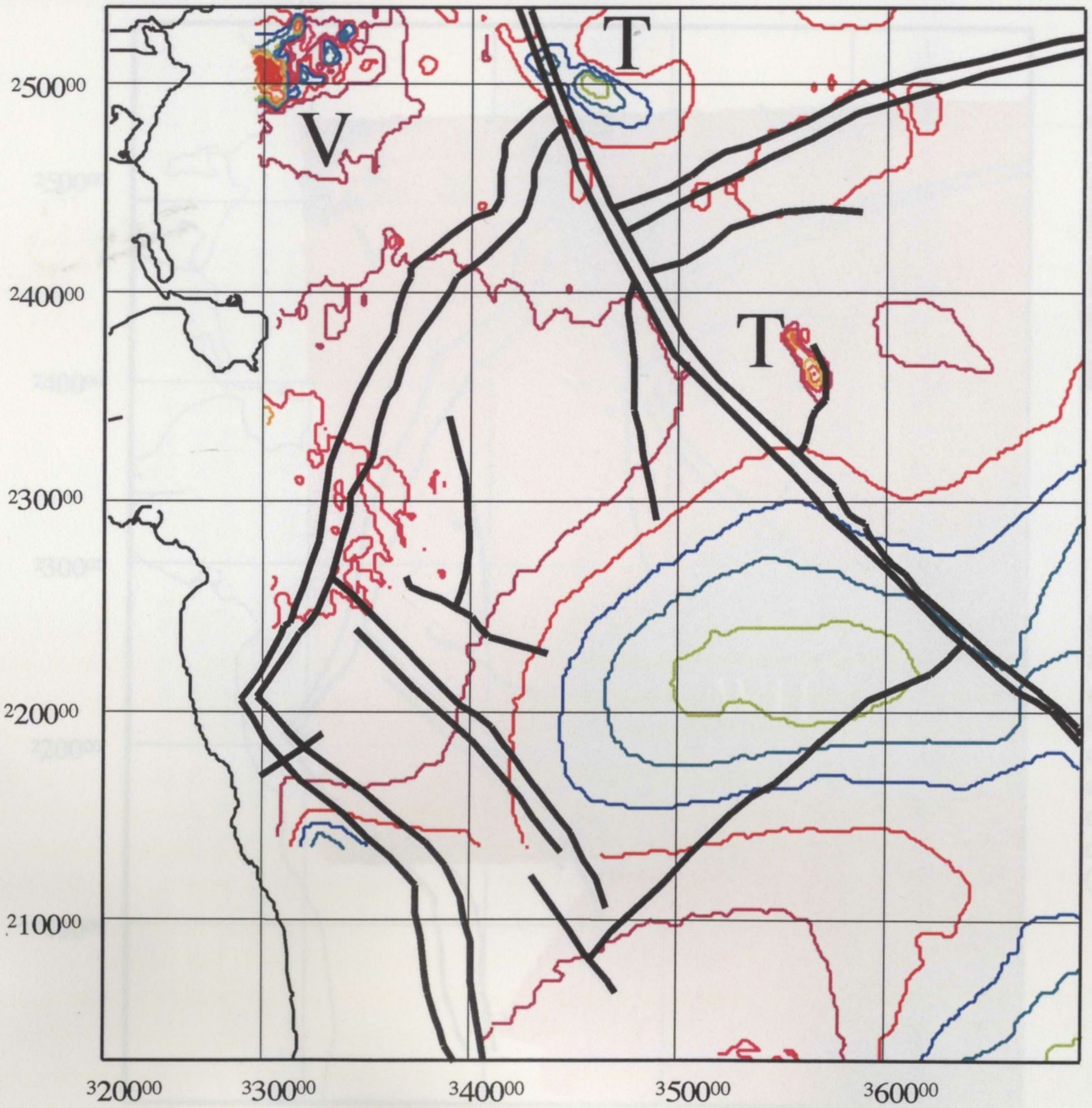

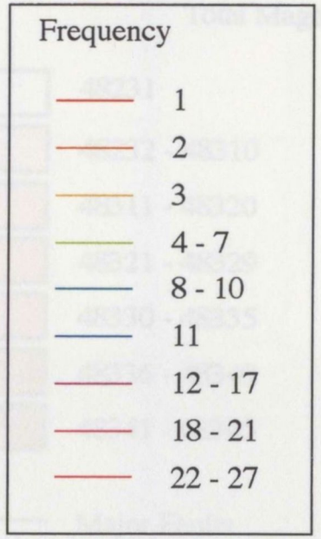

Figure 4.28:- A contour map summarising the spatial frequency of the total magnetic values. It can be seen that the magnetic anomalies 'T' and 'V' have the lowest statistical frequency but represents the highest and lowest magnetic values on the total magnetic intensity image (see figure 4.29).

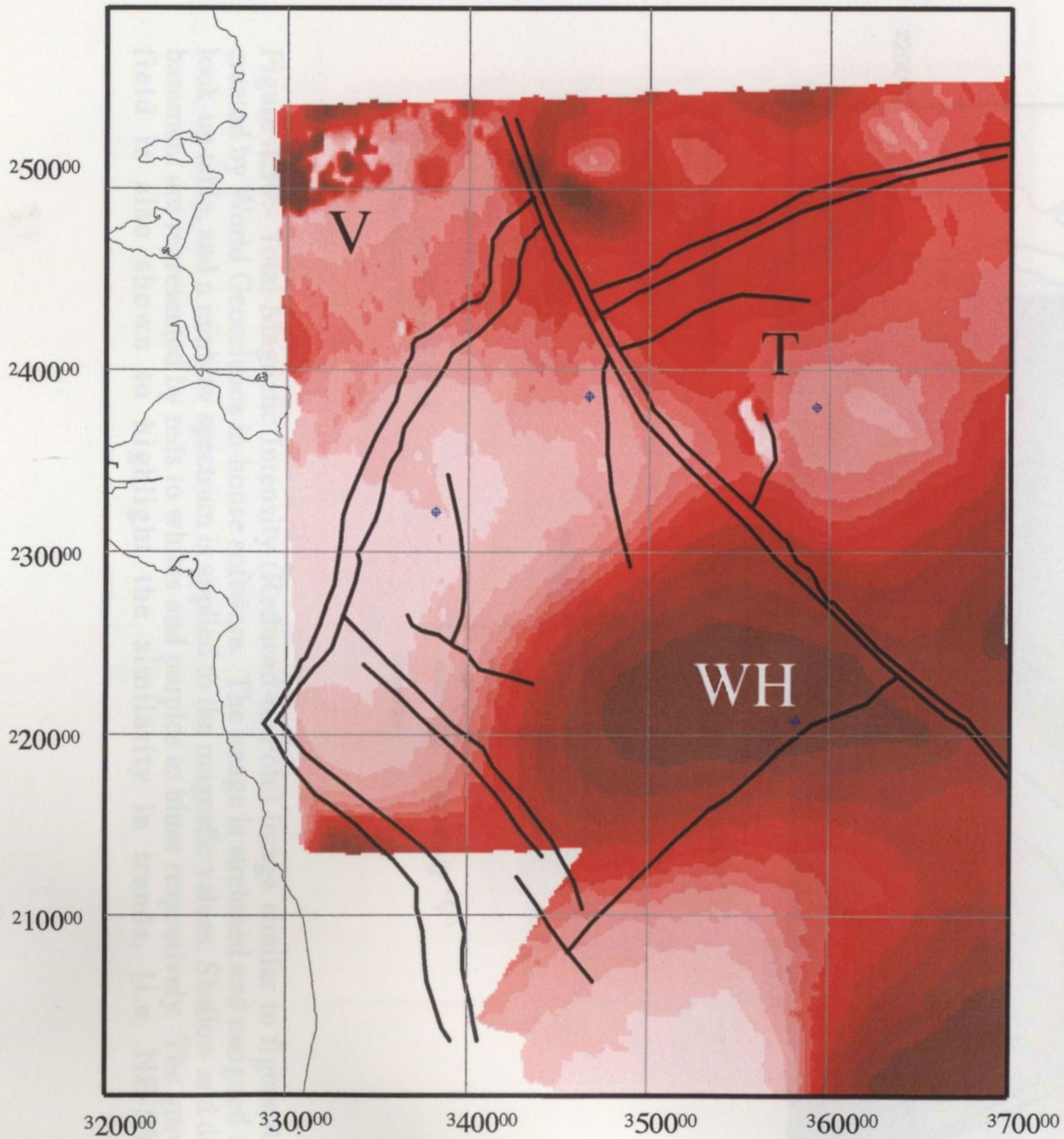

Figure 4.29:- Total Magnetic Intensity (Reduced-to-Pole) image for the Kish Bank basin. Magnetic image was generated from an ascii file (courtesy of World Geoscience). Colour scheme is a red graduation, using a 'quantile' classification (14 classes). 'V' and 'T' represent both highest and lowest magnetic anomalies respectively. The light red colours tend to represent thick sediments, conversely, the dark reds can be attributed to relatively shallow basement (i.e. the Wicklow High, labelled 'WH').

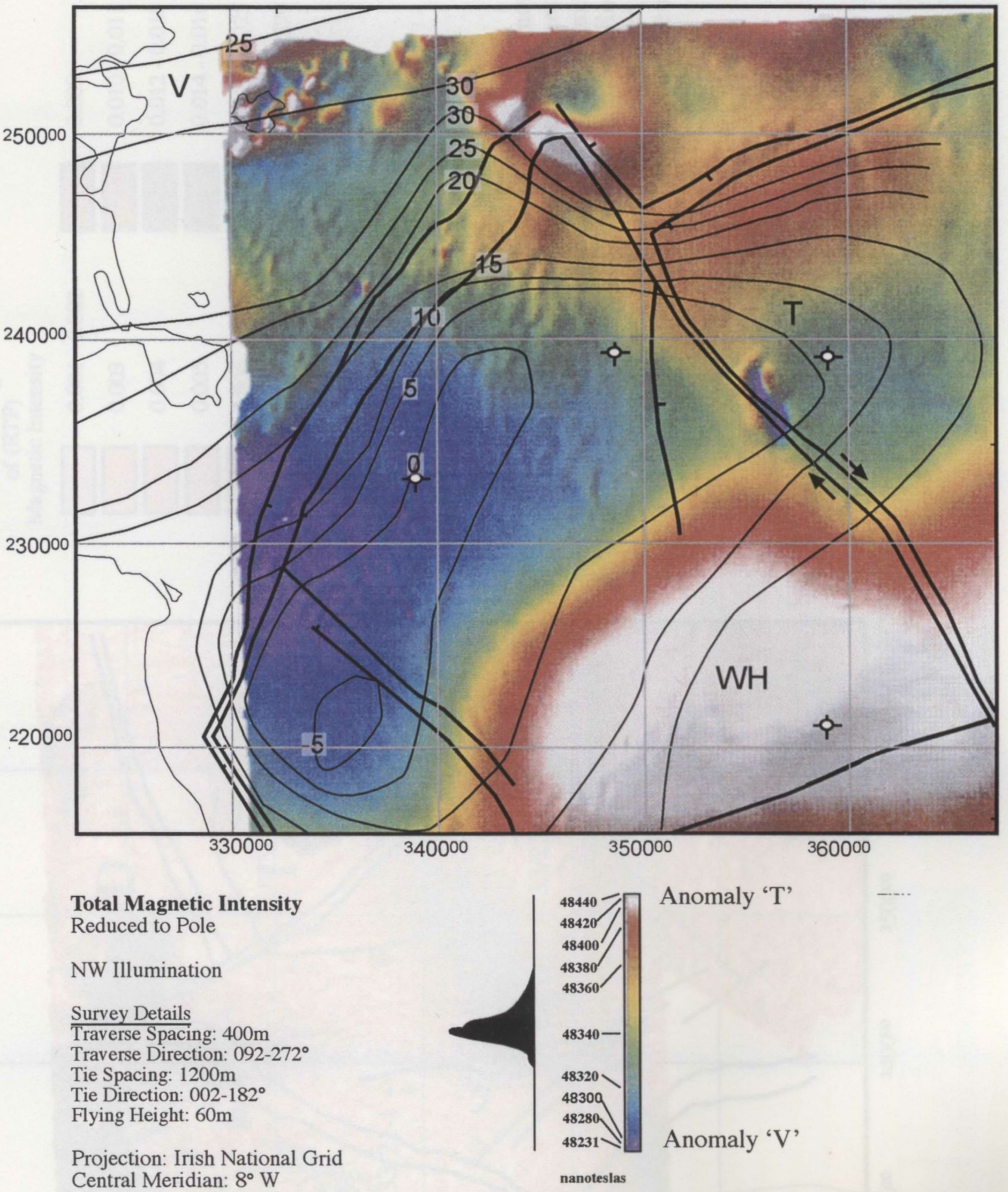

Figure 4.30:- Total Magnetic Intensity (Reduced-to-Pole) image similar to figure 4.29 created by World Geoscience in-house software. The image is stretched and assigned to a look-up table, and a rainbow spectrum is applied to the magnetic values. Shallow and deep basement are represented by reds to whites and purples to blues respectively. The gravity field is also shown to highlight the similarity in trends, (i.e. NE-SW).

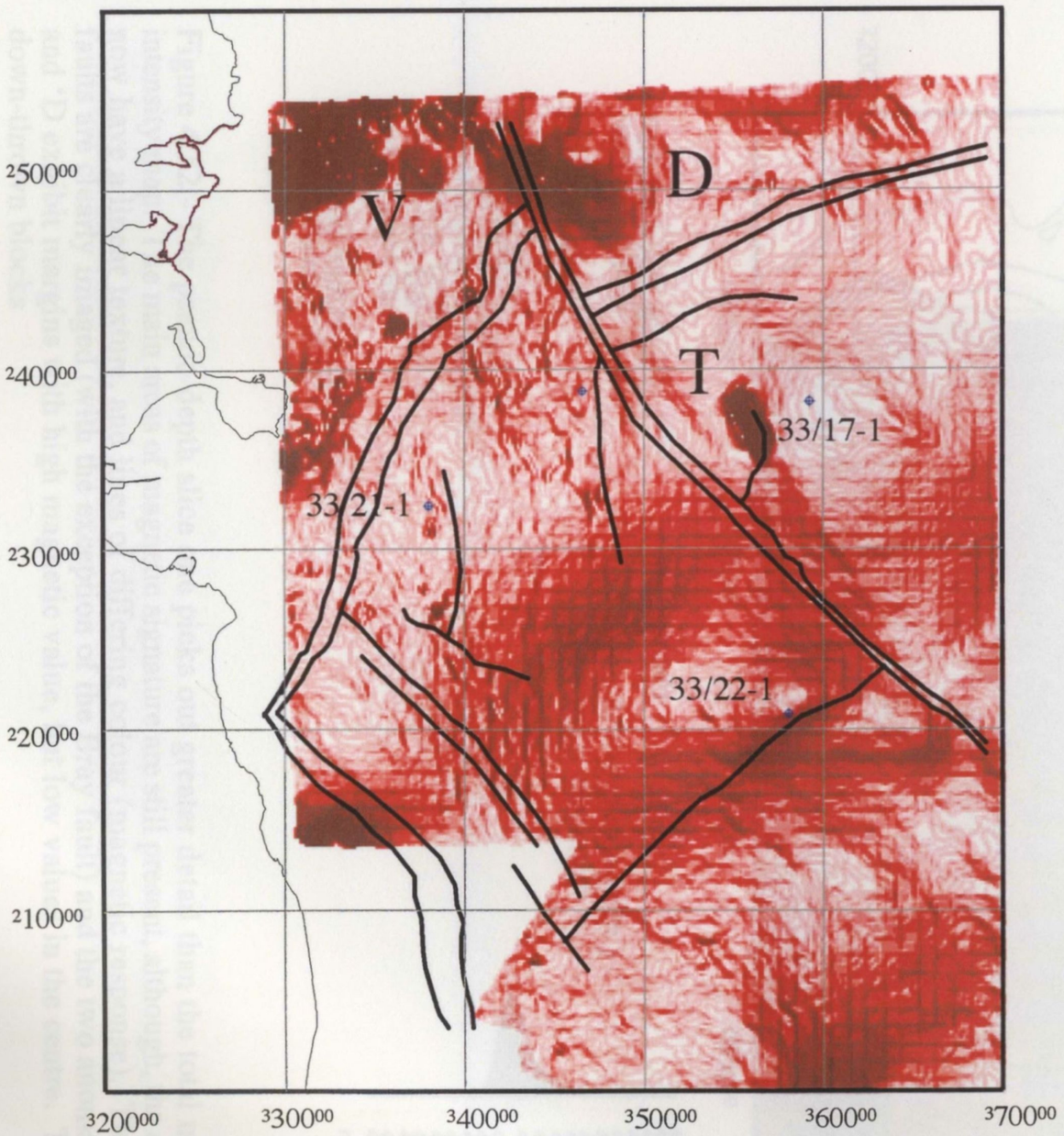

Figure 4.31:- Image of the first horizontal (non-directional) derivative of the total magnetic intensity. The process decreases the signal to noise ratio, but facilitates interpretation of shallow structure and major faults by removing the long-wavelength effects of deep basement.

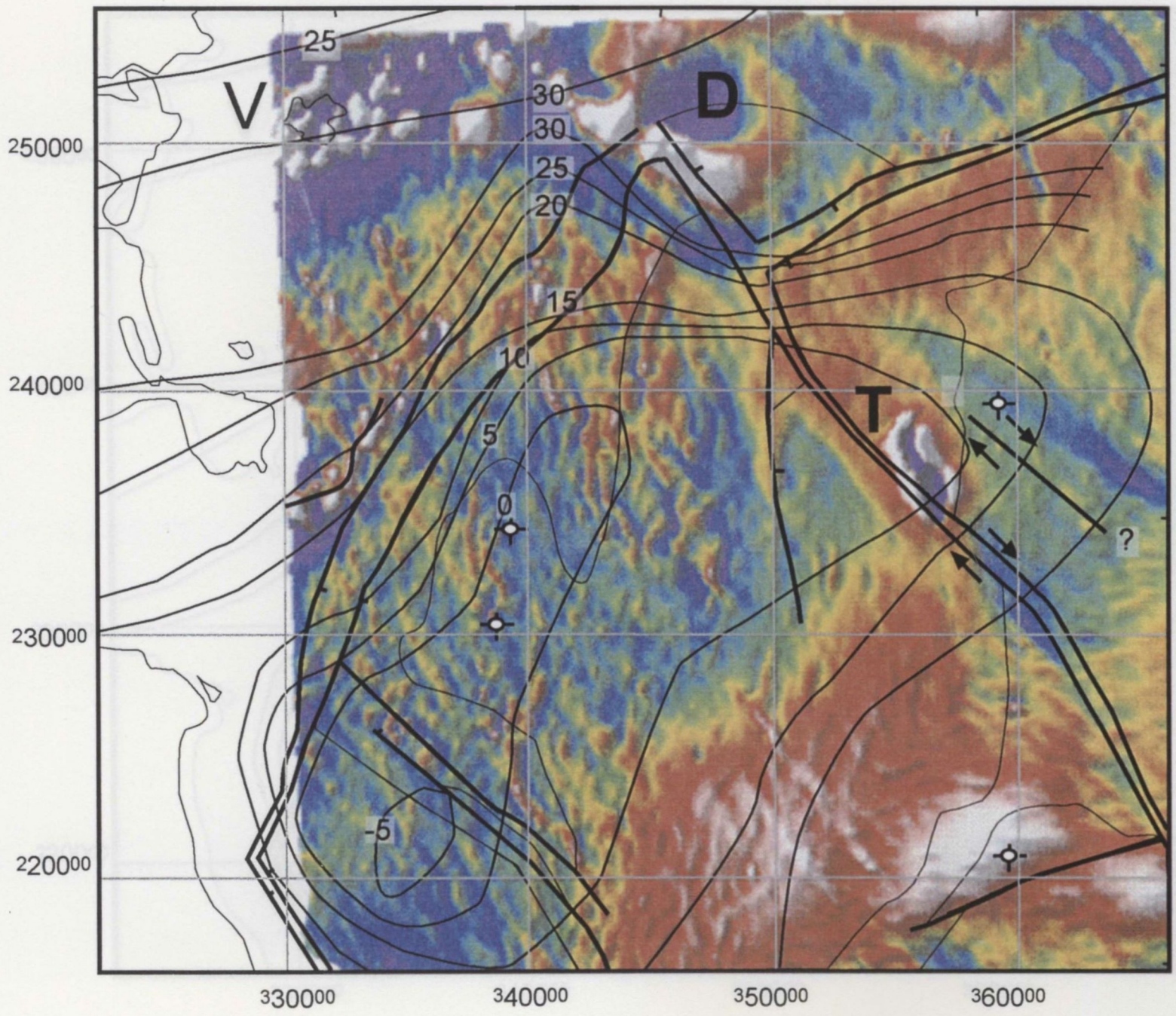

Pseudo Depth Slice 1
Reduced to Pole

NW Illumination

Survey Details
Traverse Spacing: 400m
Traverse Direction: 092-272°
Tie Spacing: 1200m
Tie Direction: 002-182°
Flying Height: 60m

Projection: Irish National Grid
Central Meridian: 8° W

Wells

10 Gravity Contour (mgal/m)
Spacing = 5mgal/m^{-2}

Faults

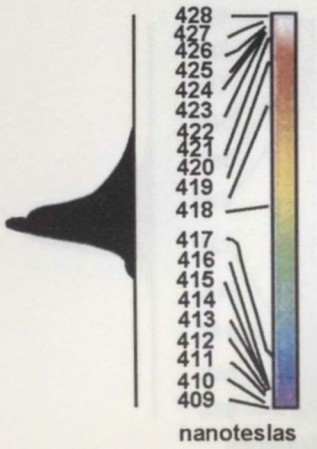

Figure 4.32:- The pseudo-depth slice one picks out greater detail than the total magnetic intensity map. The main areas of magnetic signature are still present, although, the domains now have a linear texture, and lines of differing colour (magnetic response). The major faults are clearly imaged (with the exception of the Bray fault) and the two anomalies 'T' and 'D exhibit margins with high magnetic value, but low values in the centre. Ticks on down-thrown blocks

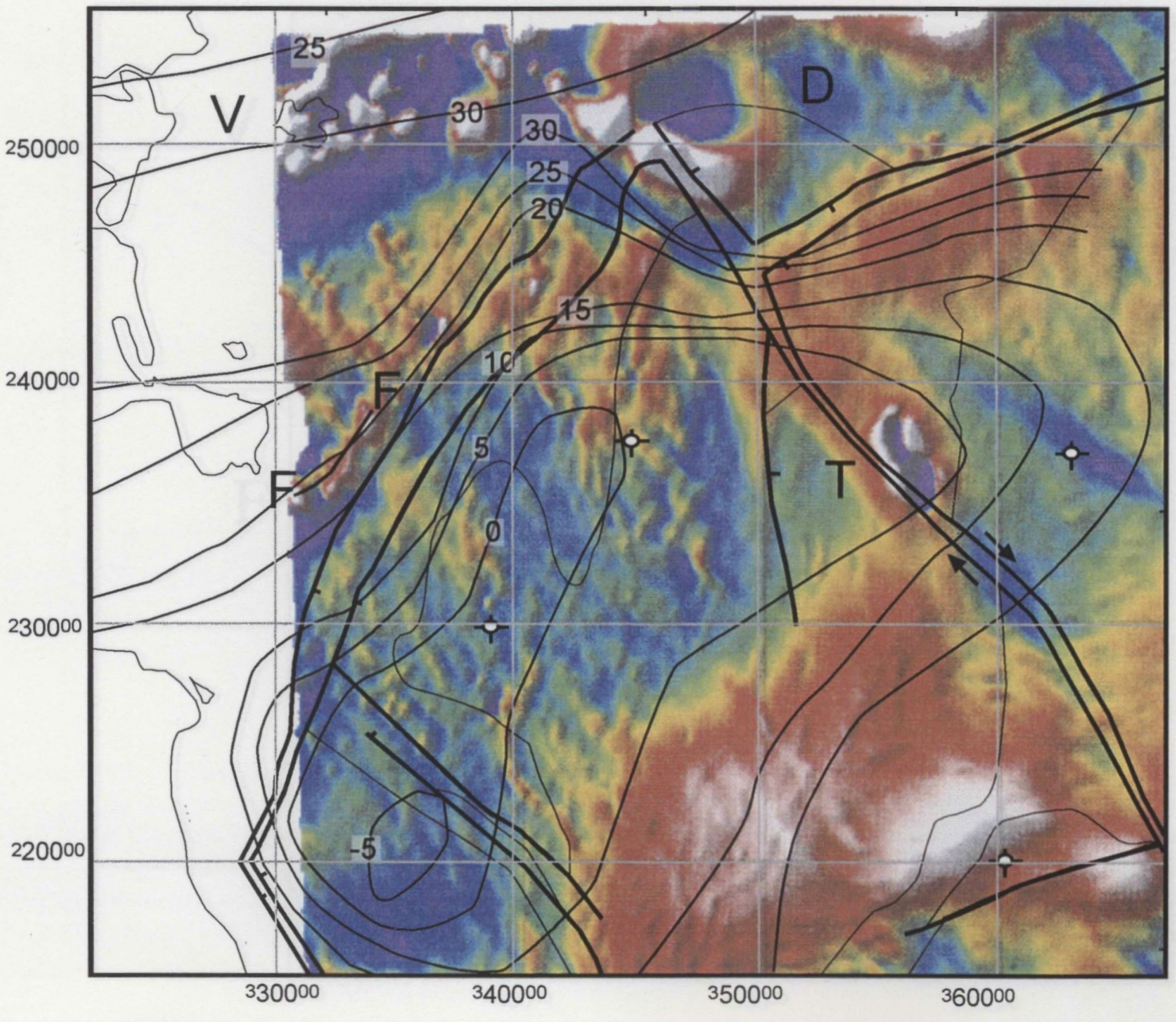

Pseudo Depth Slice 2
Reduced to Pole

NW Illumination

Survey Details
Traverse Spacing: 400m
Traverse Direction: 092-272°
Tie Spacing: 1200m
Tie Direction: 002-182°
Flying Height: 60m

Projection: Irish National Grid
Central Meridian: 8° W

Wells

10 Gravity Contour (mgal/m)
Spacing = 5mgal/m^{-2}

Faults

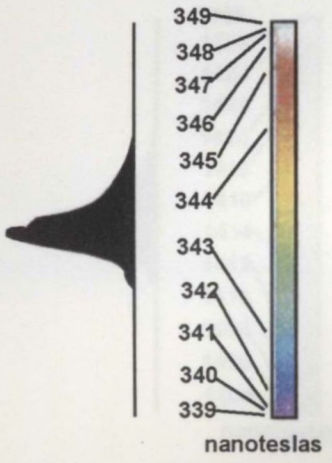

Figure 4.33:- The pseudo-depth slice two shows similar detail as figure 4.32. However, the linear texture is more subdued. The positive margin on anomaly 'T' is no longer imaged on the southeastern margin. The 'F' lineament around the SE side of Howth is more clearly imaged on this depth slice in comparison with the previous.

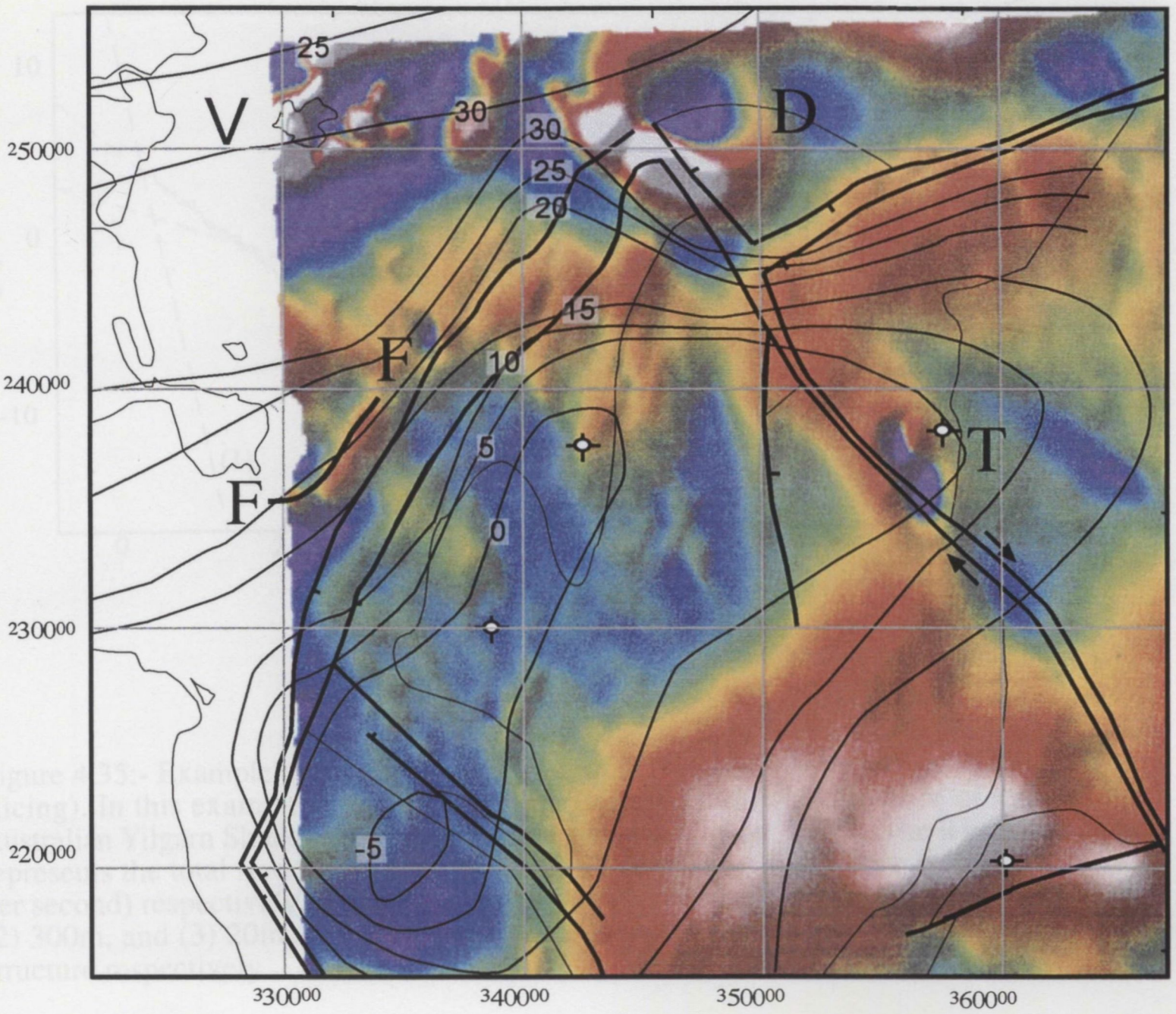

Pseudo Depth Slice 3
Reduced to Pole

NW Illumination

Survey Details
Traverse Spacing: 400m
Traverse Direction: 092-272°
Tie Spacing: 1200m
Tie Direction: 002-182°
Flying Height: 60m

Projection: Irish National Grid
Central Meridian: 8° W

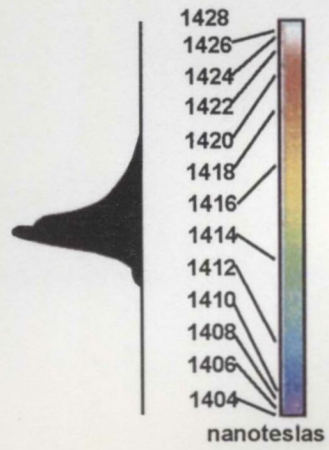

Wells

10 Gravity Contour (mgal/m)
Spacing = 5mgal/m^{-2}

Faults

Figure 4.34:- The pseudo-depth slice three is beginning to filter out the high frequency content from the total magnetic intensity map, and beginning to show a greater influence from deeper, high amplitude structures. The Lambay Ridge and the corresponding dextral offset (bound on the northern margin by the Lambay fault) is quite sharply depicted. The Wicklow High shows a strong gradient on the northern part, probably due to a combination of shallow basement and condensed Permo-Triassic sequences, implying that the area was high during Mesozoic times.

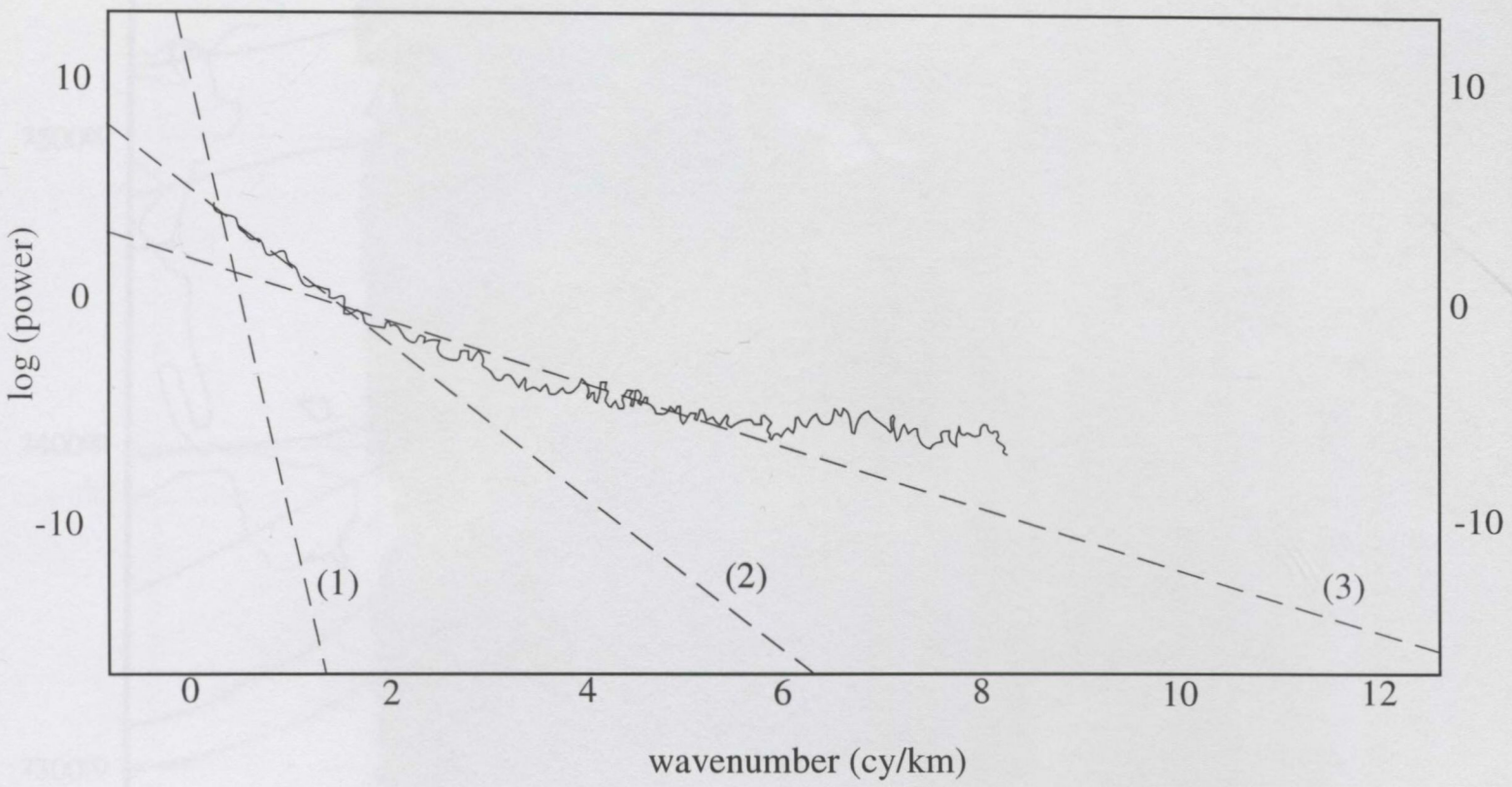

Figure 4.35:- Example of log-power spectrum of a "Total Magnetic Image" (pseudo-depth slicing). In this example, a small part of the Eastern Goldfields Province of the Western Australian Yilgarn Shield is illustrated (after Cowan & Cowan, 1993). The R concave curve represents the total frequency spectrum, from 12 to 0 being high to low-frequency (cycles per second) respectively. The 3 lines correspond to varying average depths of (1) 1500m, (2) 300m, and (3) 20m. The high and low frequency content represent shallow and deep structure respectively.

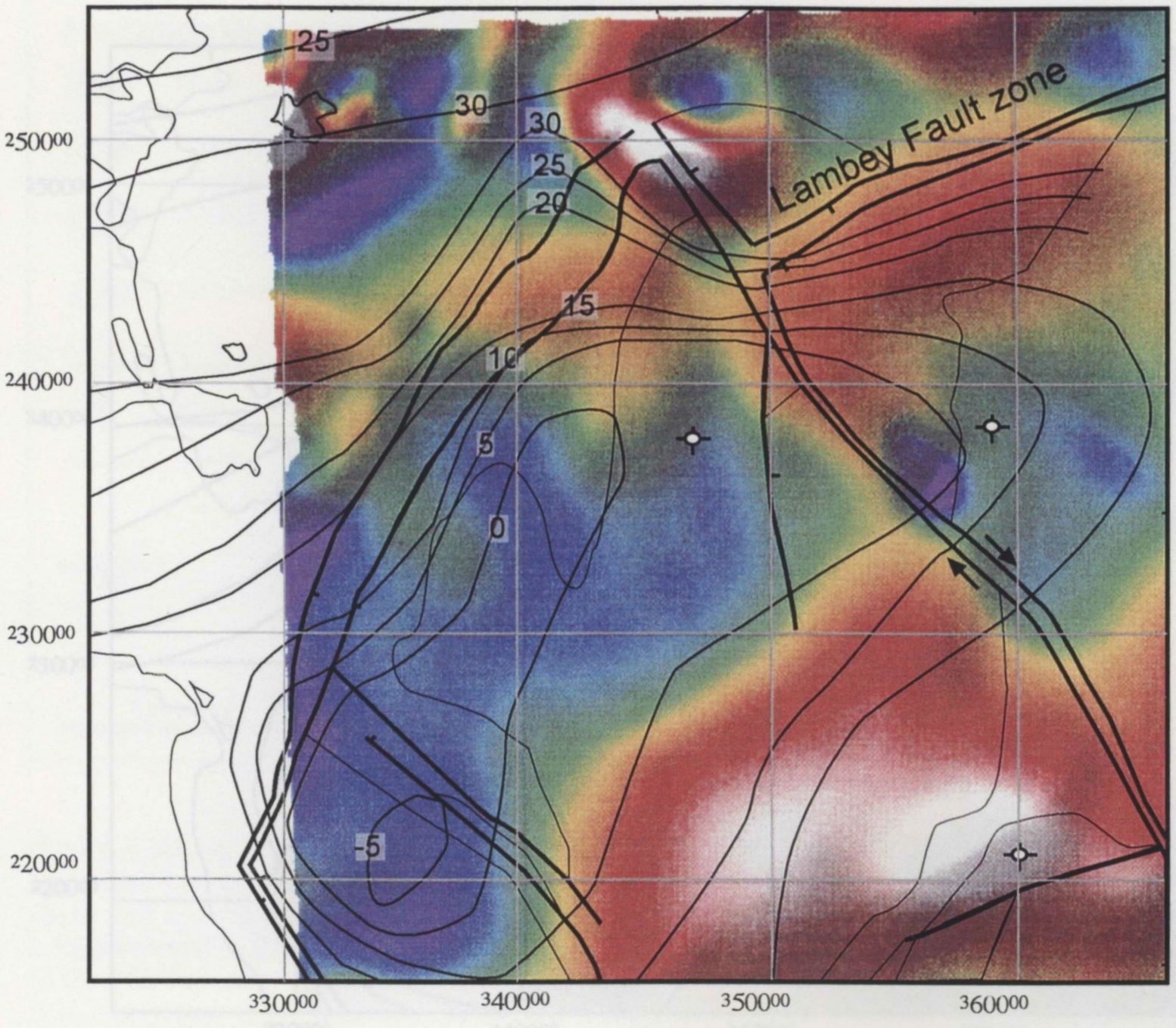

Pseudo Depth Slice 4
Reduced to Pole

NW Illumination

Survey Details
Traverse Spacing: 400m
Traverse Direction: 092-272°
Tie Spacing: 1200m
Tie Direction: 002-182°
Flying Height: 60m

Projection: Irish National Grid
Central Meridian: 8° W

Wells

10 Gravity Contour (mgal/m)
Spacing = 5mgal/m^{-2}

Faults

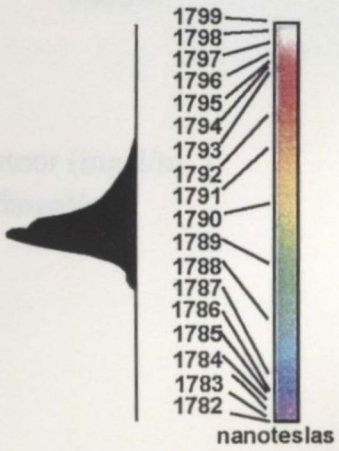

Figure 4.36:- Pseudo-Depth Slice 4 images the effects of deep, low frequency but high amplitude structures (i.e. ~4km depth). The overall trend is Caledonian in style, i.e. NE to NNE and NW to NNW. The gravity contours shows a similar trend (NE). Shallow basement underlying the Lambay fault and the Wicklow High, appear to be connected at depth by a shallow bridge of basement which parallels the Codling fault. This may be related to a small compressional bend on the fault, whereas, anomaly 'T' to the east, would be the product of a jog (extensional bridge).

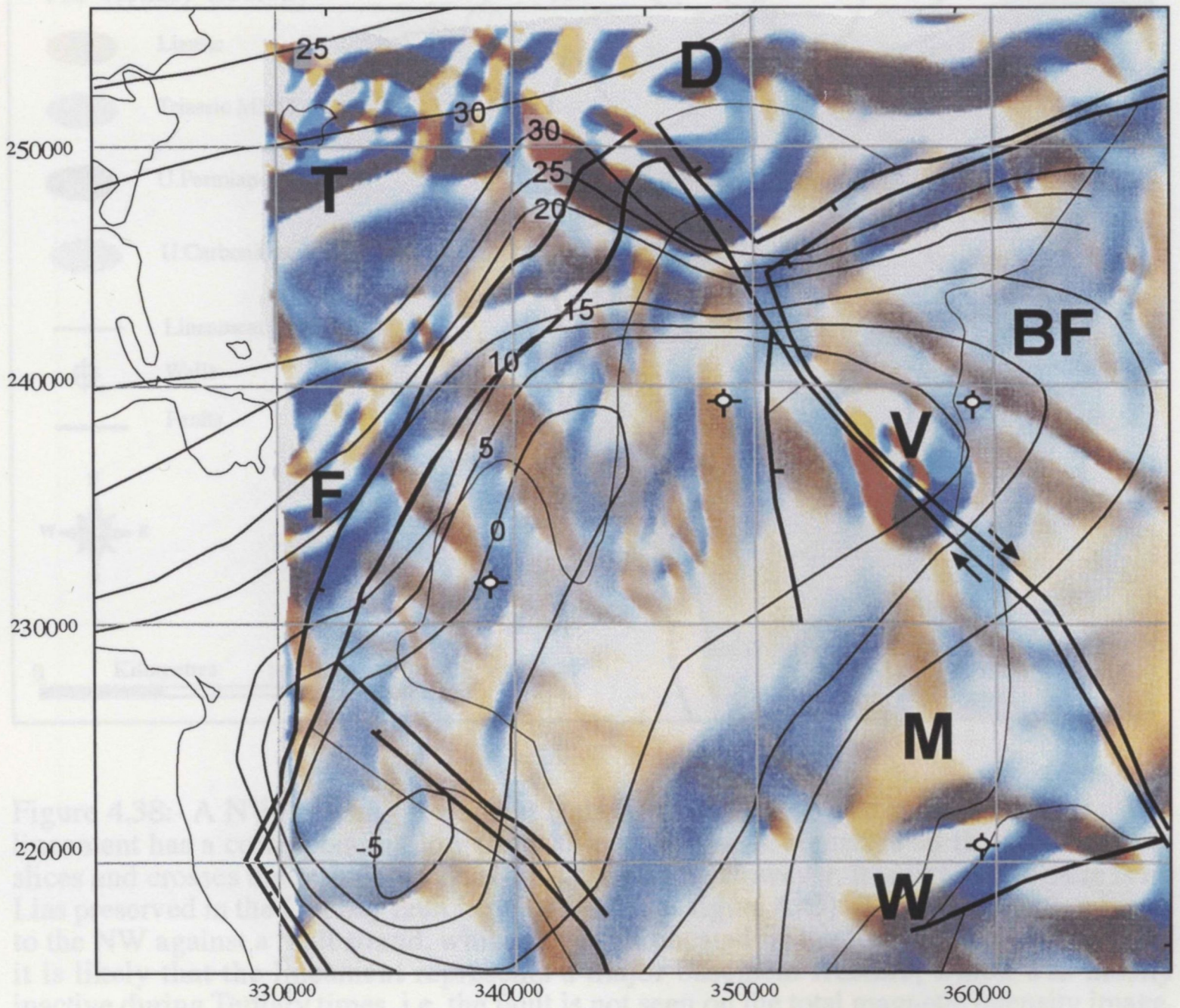

Pseudo Depth Slice 4
Azimuth Map

NW (R), N (G), NE (B) Illumination

Survey Details
Traverse Spacing: 400m
Traverse Direction: 092-272°
Tie Spacing: 1200m
Tie Direction: 002-182°
Flying Height: 60m

Projection: Irish National Grid
Central Meridian: 8° W

Wells

10 Gravity Contour (mgal/m)
Spacing = 5mgal/m^{-2}

Faults

Figure 4.37:- Azimuth 4 is a derivative of pseudo-depth slice 4, which highlights rates of change (edges). The overall picture is a deep NW-SE, NE-SW and E-W structural grain. Of particular interest is the strong ~E-W lineament which well 33/22-1 lies along (labelled 'W'). Azimuth 4 images anomalies 'T', 'D', 'V' and lineament 'F', east of Howth. The northern margin of the Wicklow High, labelled 'M', produces a strong lineament magnetic lineament.

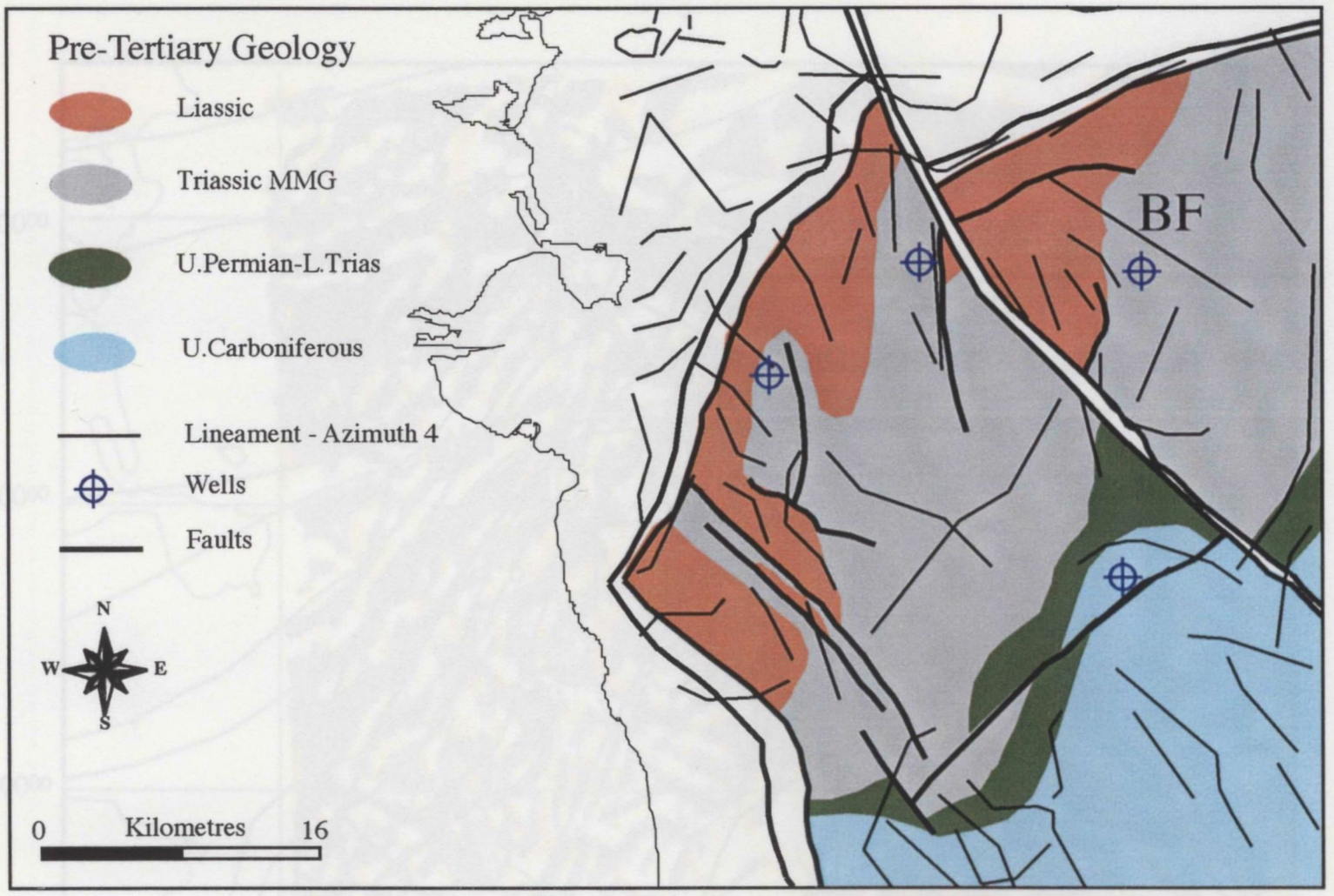

Figure 4.38:- A NW trending lineament (labelled BF) occurs east of well 33/17-1. The lineament has a corresponding low (blue colour) magnetic signature on the pseudo-depth slices and crosses the postulated Trias-Lias boundary. However, it is likely that there is no Lias preserved in the Lambay fault hanging-wall (see figure 4.43). The lineament terminates to the NW against a fault strand, which is itself truncated by the Codling fault. Therefore, it is likely that the lineament represents a major basement fracture, which was mostly inactive during Tertiary times, i.e. the fault is not seen on the total magnetic intensity image, and the Codling fault truncates a fault that appears to offset the lineament.

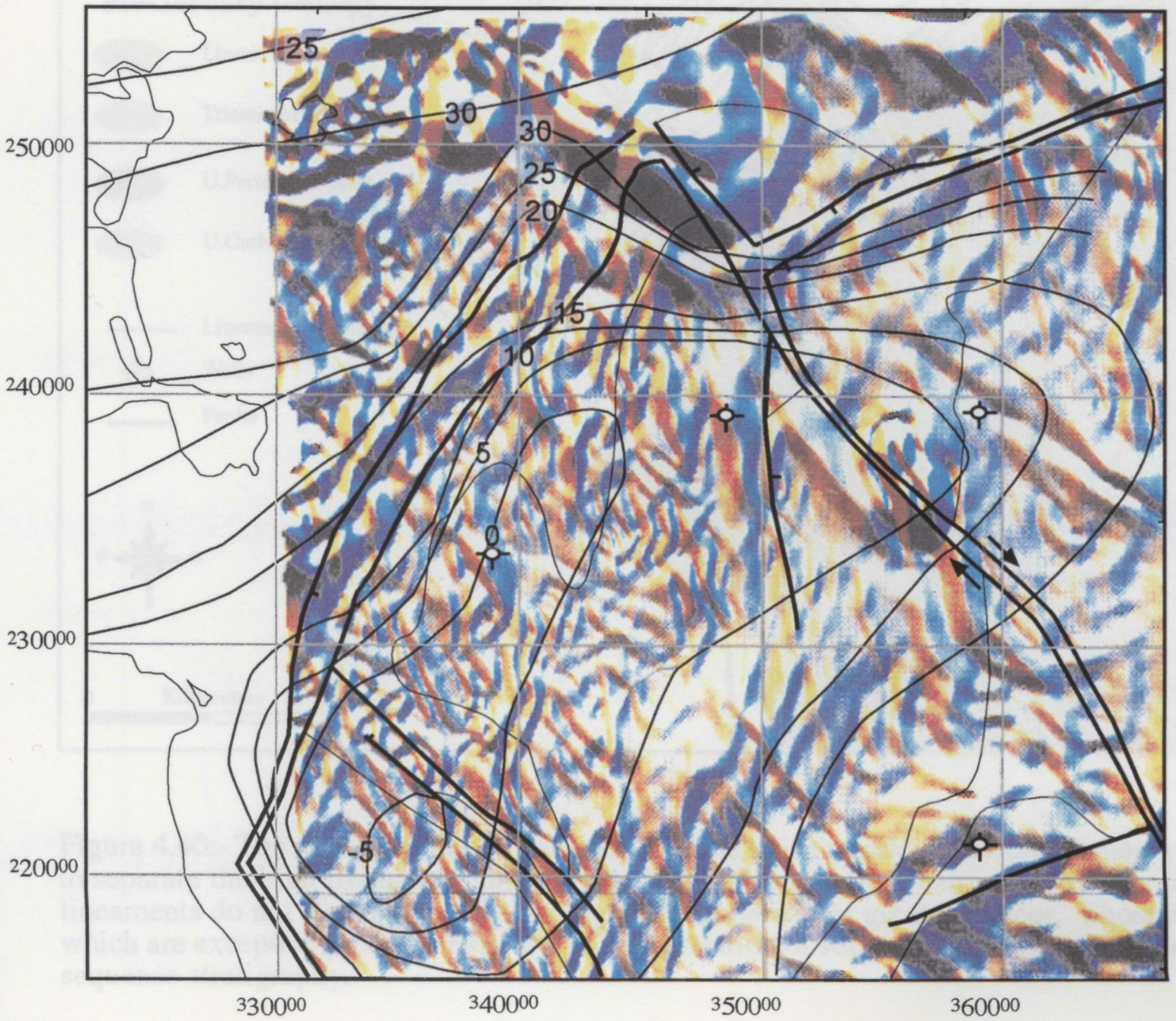

Pseudo Depth Slice 3
Azimuth Map

NW (R), N (G), NE (B) Illumination

Survey Details
Traverse Spacing: 400m
Traverse Direction: 092-272°
Tie Spacing: 1200m
Tie Direction: 002-182°
Flying Height: 60m

Projection: Irish National Grid
Central Meridian: 8° W

Wells

10 Gravity Contour (mgal/m)
Spacing = 5mgal/m^{-2}

Faults

Figure 4.39:- Azimuth 3 highlights shallow magnetic lineament. Linear features are assumed to be associated with rocks of differing magnetite content, i.e. faulted contacts. An important pattern of lineament emerges from first inspection. The lineament pattern in the vicinity of well 33/22-1 is distinctively different to that further north, i.e. WNW in the south to NW, NE and N elsewhere. Strong magnetic lineaments sub-parallel to the Dalkey fault (near the Howth peninsula) are mimicked by the gravity contours, where both the magnetic lineament and gravity contours swing around towards Dublin Bay.

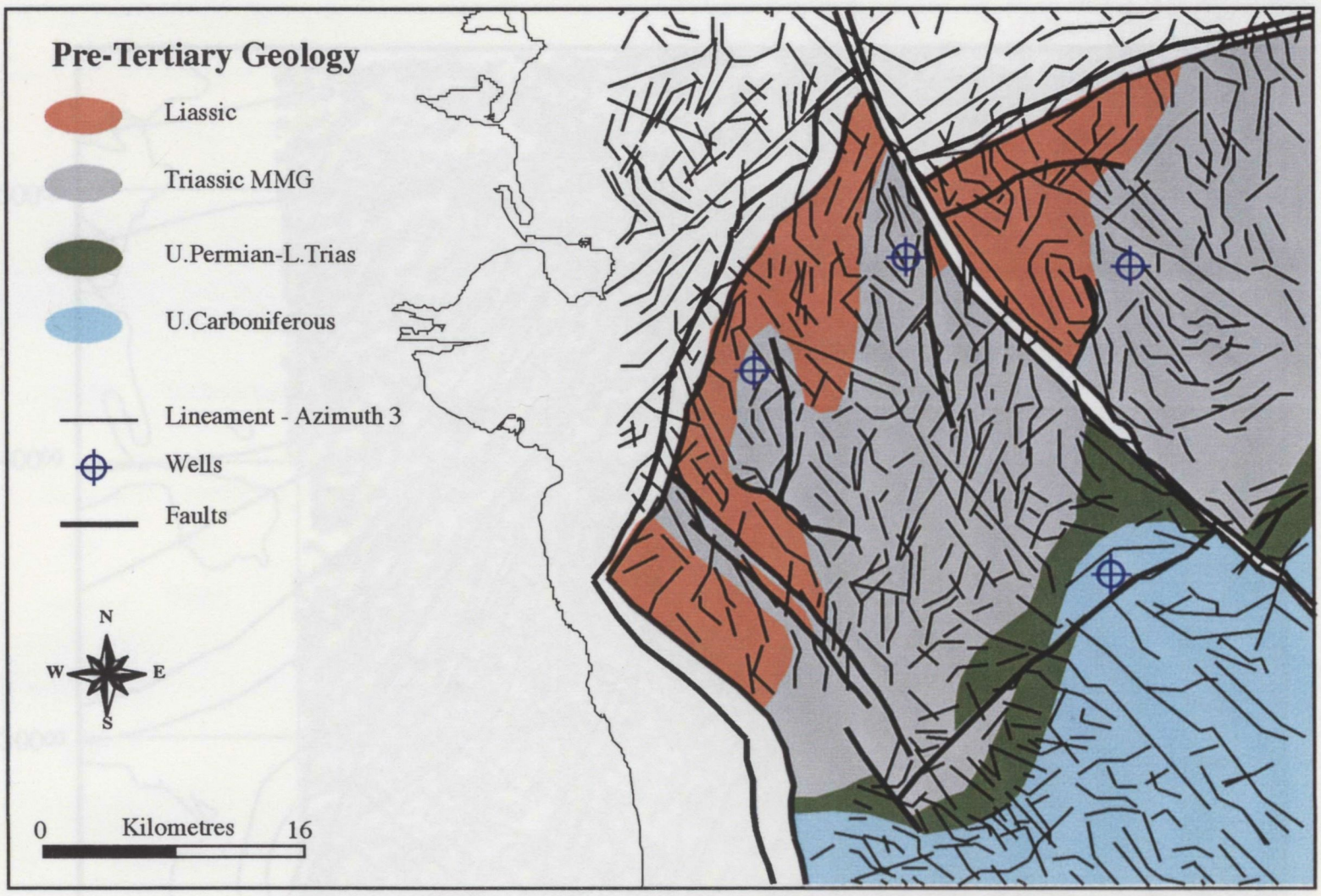

Figure 4.40:- The azimuth 3 image naturally inherits noise which is inevitable when trying to separate the high frequency content from the total magnetic spectrum. However, most lineaments do not frequently cross geological boundaries for great distances. Those areas which are exception probably require a re-interpretation of sub-crop geology, to supplement sequence stratigraphy.

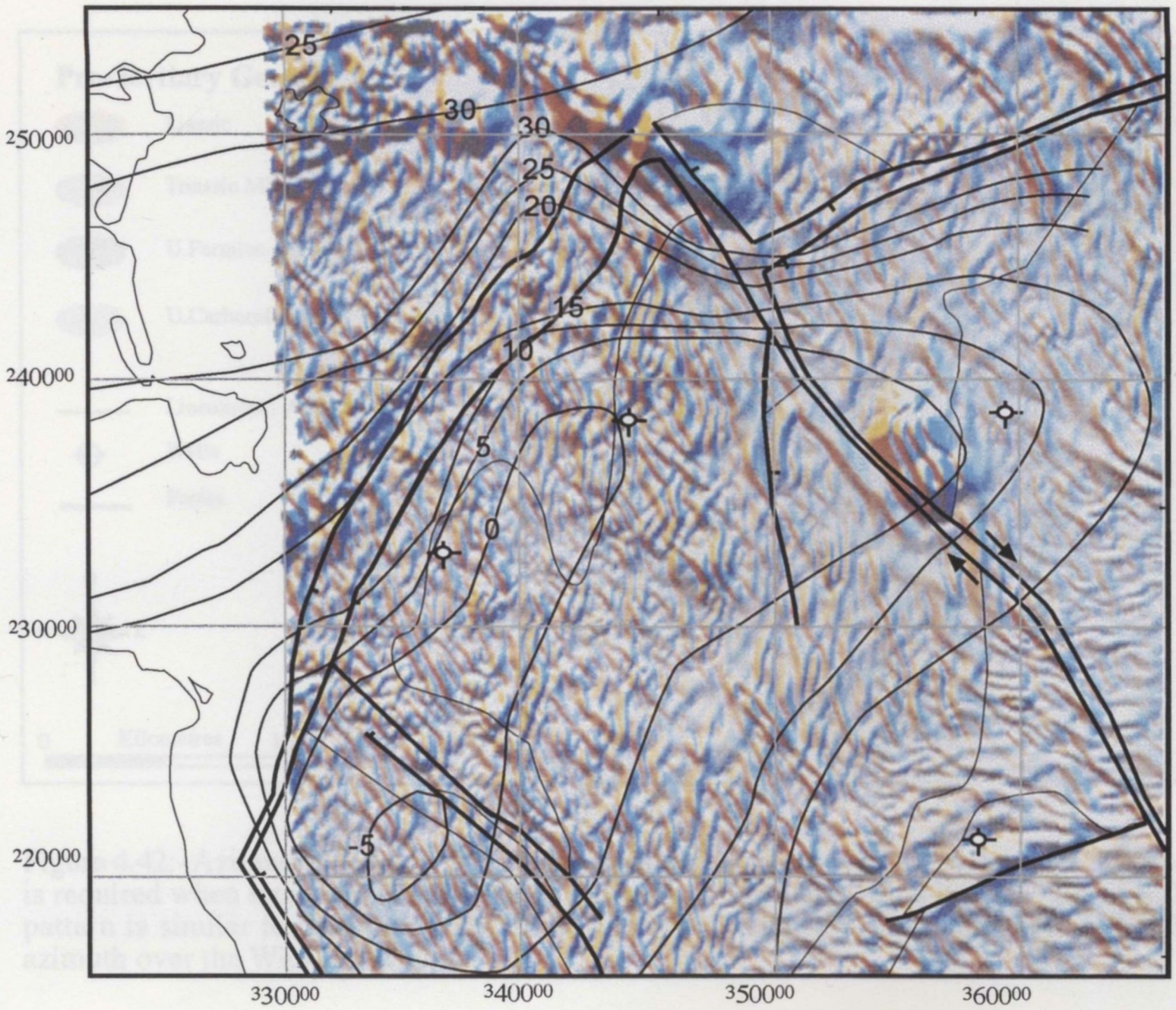

Pseudo Depth Slice 2
Azimuth Map

NW (R), N (G), NE (B) Illumination

Survey Details
Traverse Spacing: 400m
Traverse Direction: 092-272°
Tie Spacing: 1200m
Tie Direction: 002-182°
Flying Height: 60m

Projection: Irish National Grid
Central Meridian: 8° W

Wells

10 Gravity Contour (mgal/m)
Spacing = 5mgal/m^{-2}

Faults

Figure 4.41:- The azimuth 2 image display a similar pattern to figure 4.39. 'MP' denotes the boundary between the two distinctly different magnetic terains. Note that the lineaments show deflection over line 'MP', and display a 'sinistral' sigmoidal geometry.

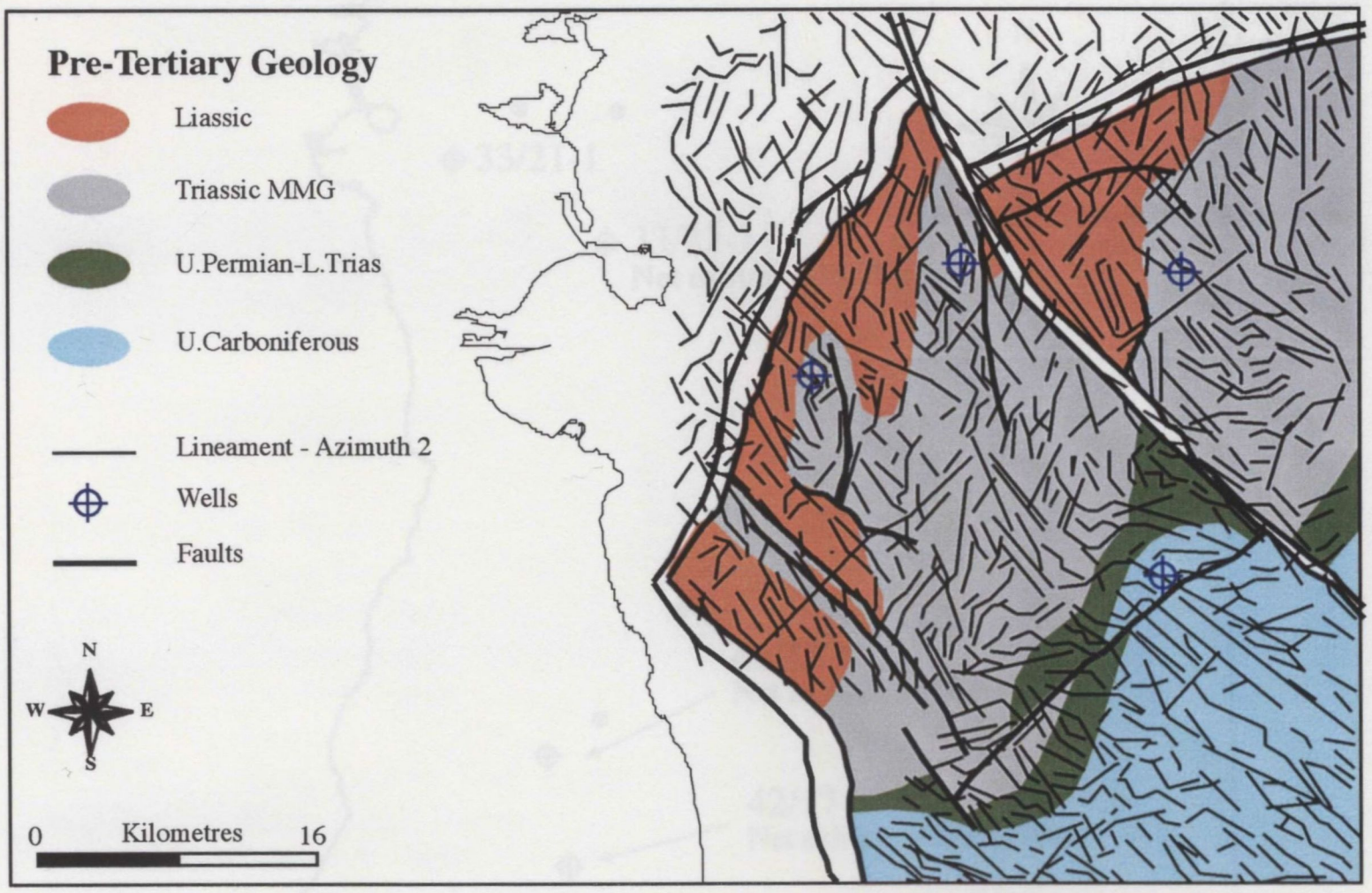

Figure 4.42:- Azimuth 2 lineaments have the smallest signal-to-noise ratio, therefore, caution is required when interpreting what the data means. However, suffice it to say, the overall pattern is similar to the other depth slices, i.e. the lineament trends change to a WNW azimuth over the Wicklow High.

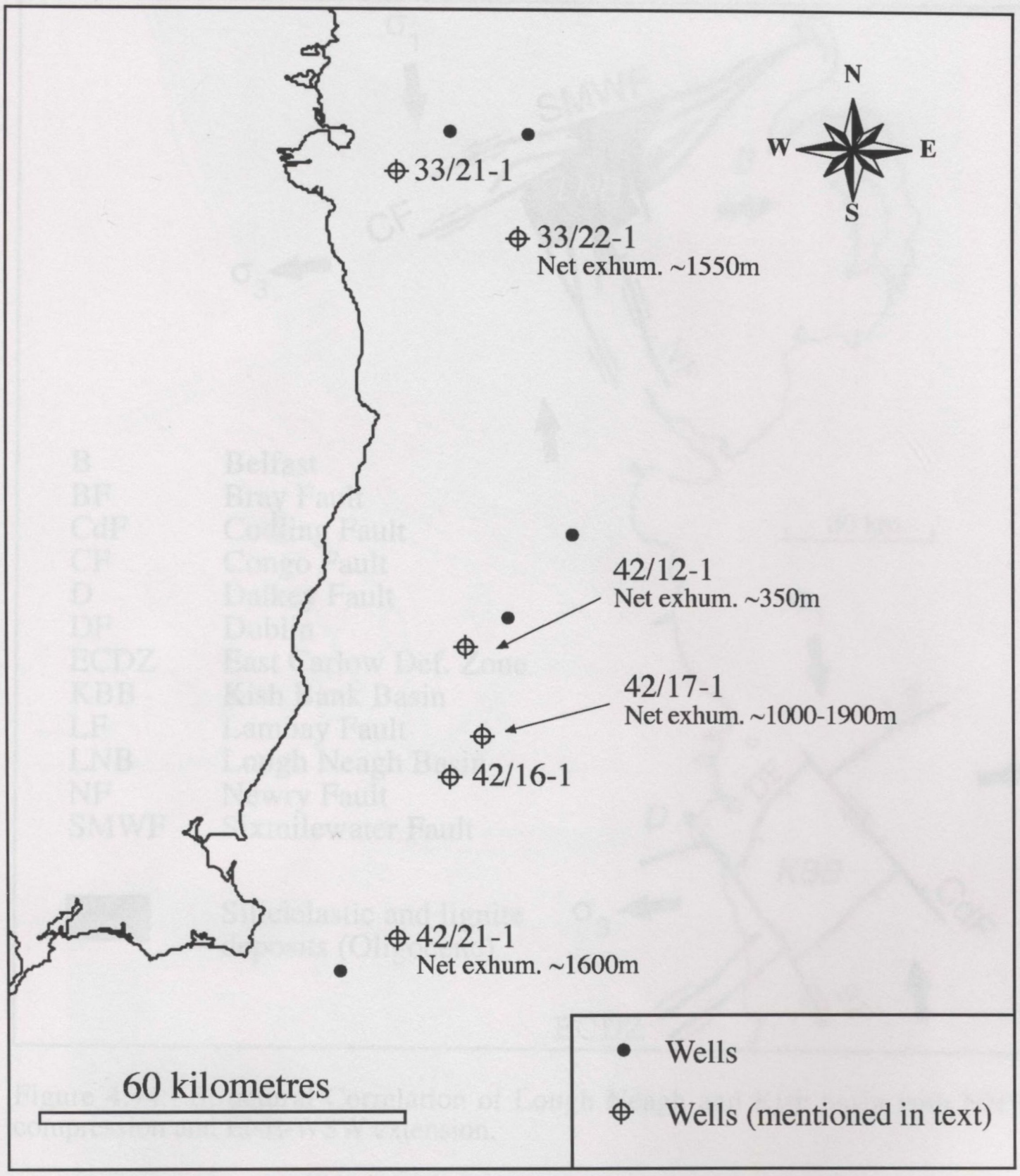

Figure 4.43:- Location Map of wells showing estimates of exhumation from vitrinite (Corcoran & Clayton, 1999).

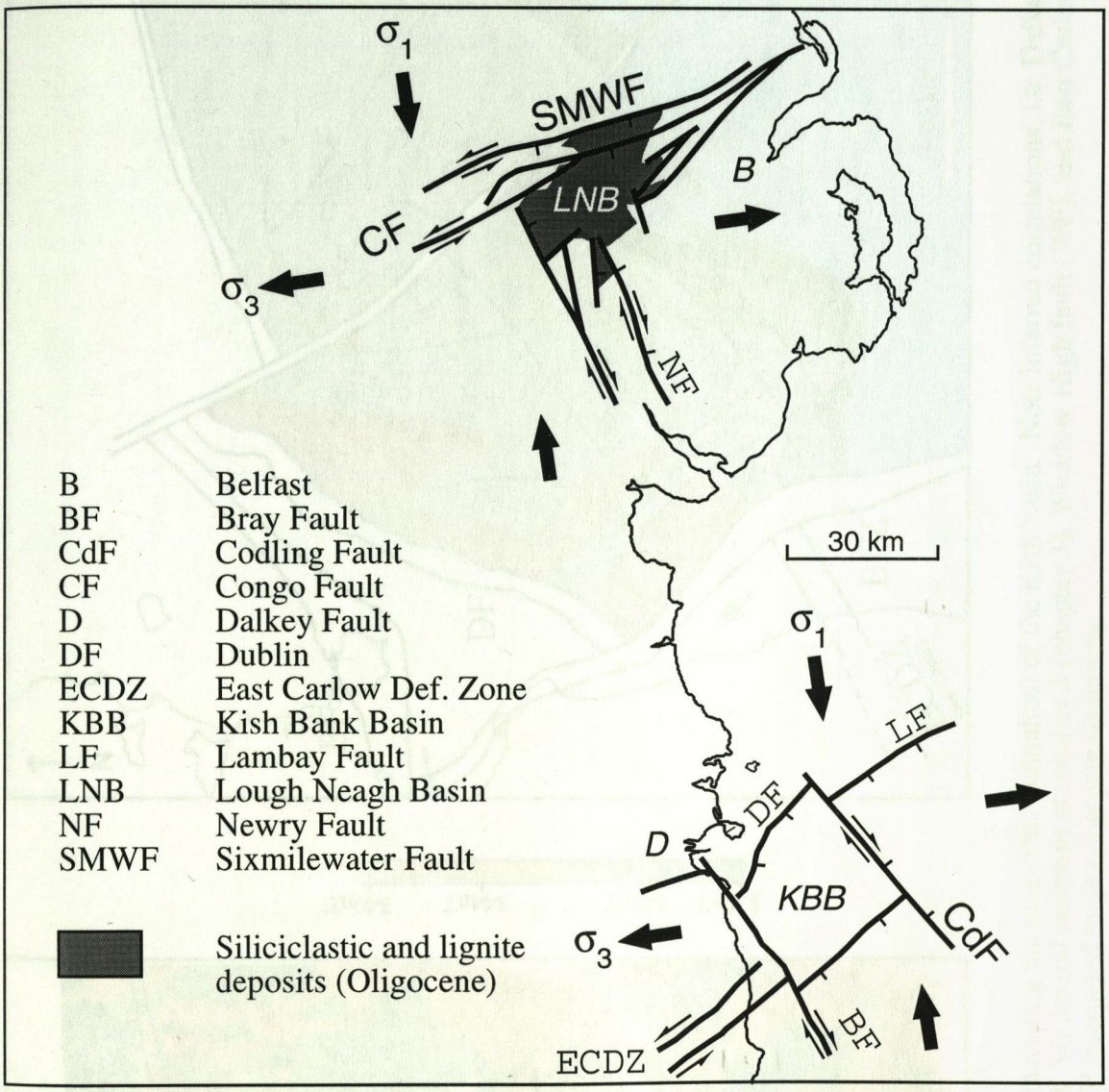

Figure 4.44:- Structural Correlation of Lough Neagh and Kish basin with NNW-SSE compression and ENE-WSW extension.

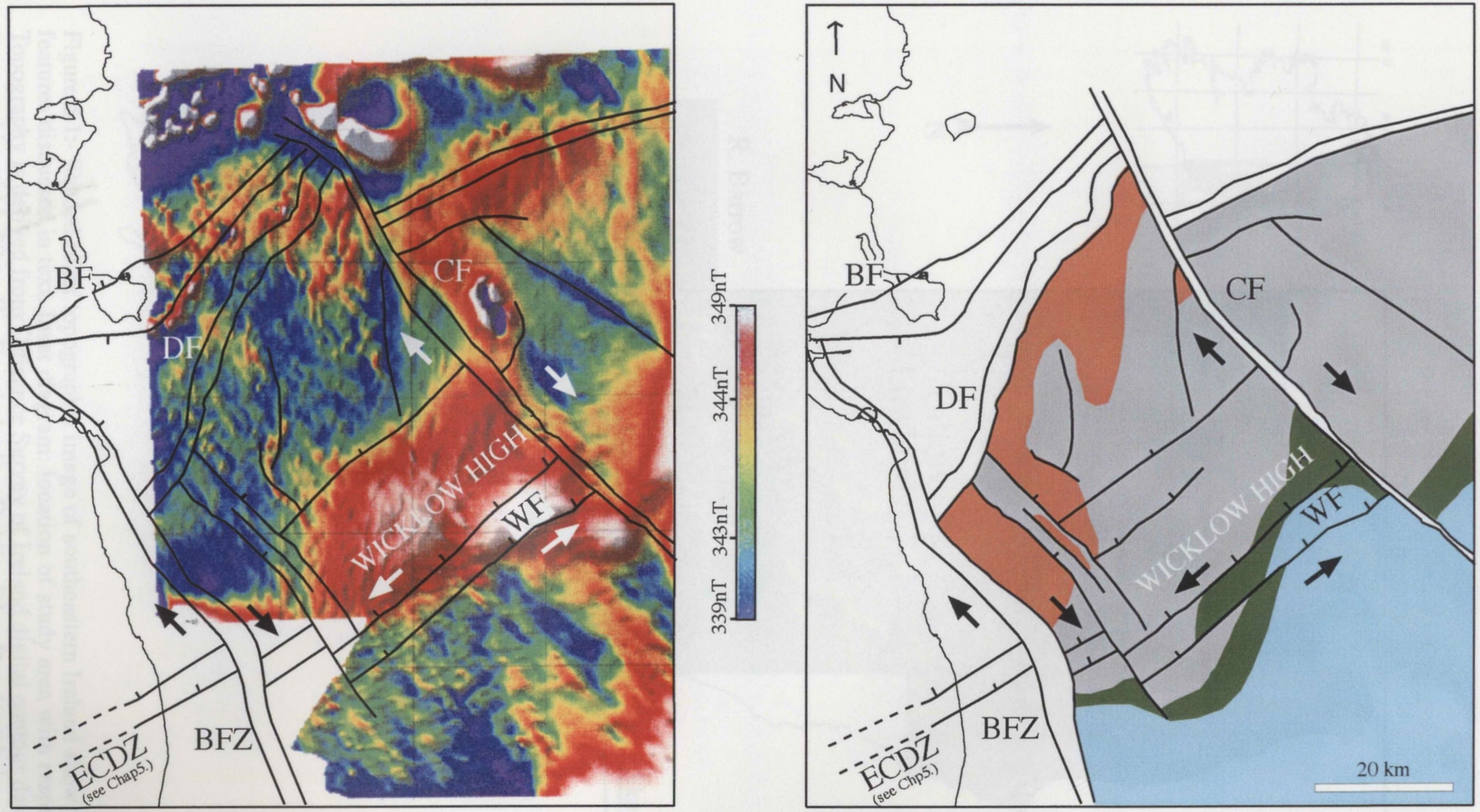

Figure 4.45:- Modified geological and structural maps (including the magnetic anomalies) of the Kish basin. Note inferred correlations, i.e. Dalkey and (DFZ) Balscadden faults (BF), Bray (BFZ) and NW-SE dextral outcrops at locality 3 (chapter 3), Wicklow High fault (WF), and East Carlow Deformation Zone (ECDZ). Codling fault (CF) and WF interpeted to be conjugate structures.

Figure 5.1:- Shaded-relief topographic image of southeastern Ireland showing names and features discussed in text. Inset diagram: location of study area with respect to Ireland. Topography is derived from Ordnance Survey of Ireland digital contour data. Cell size of topographic grid is 50m. B – Bunclody; D – Dublin; DL – Dun Laoghaire; W – Wicklow Town.

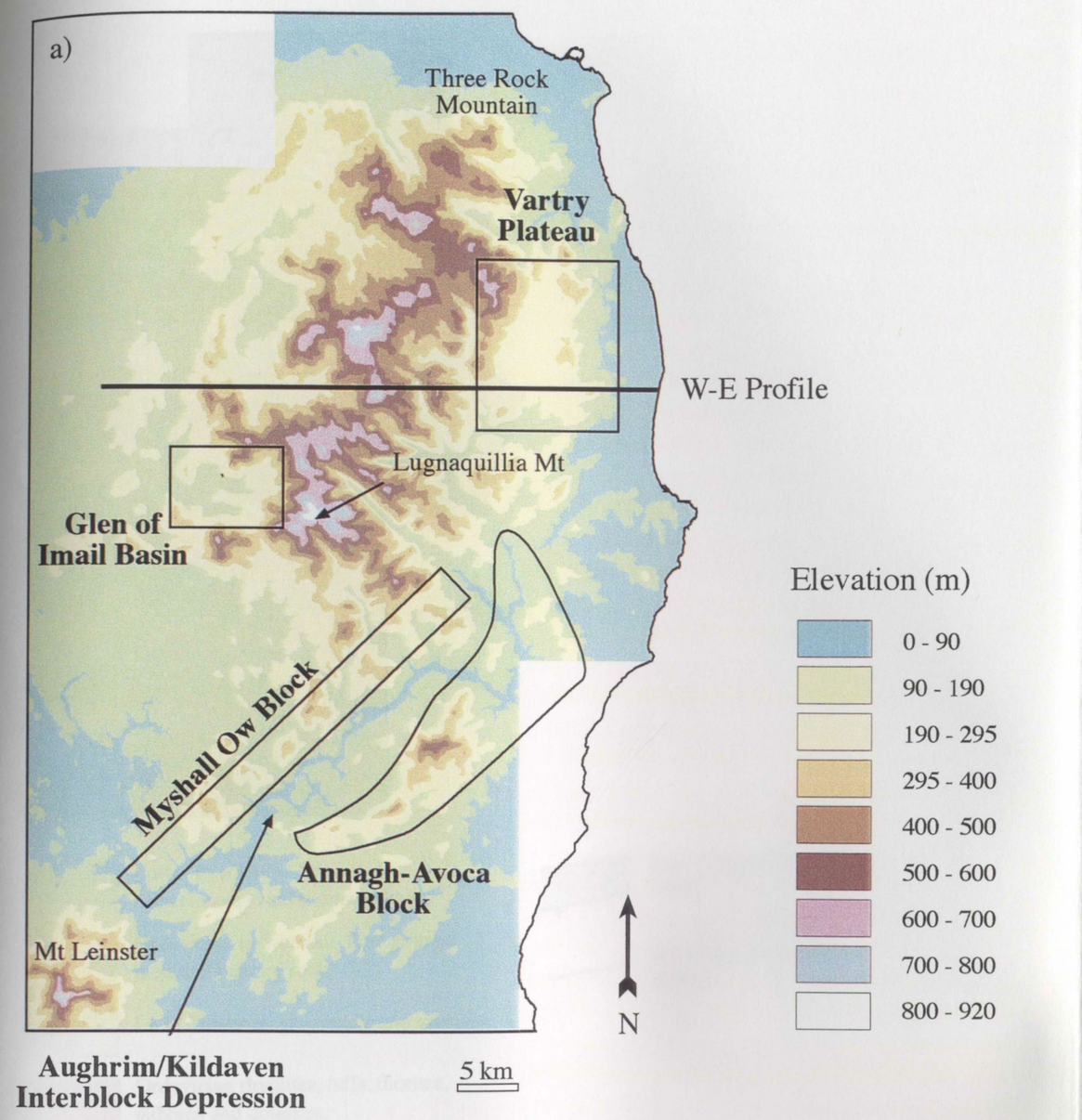

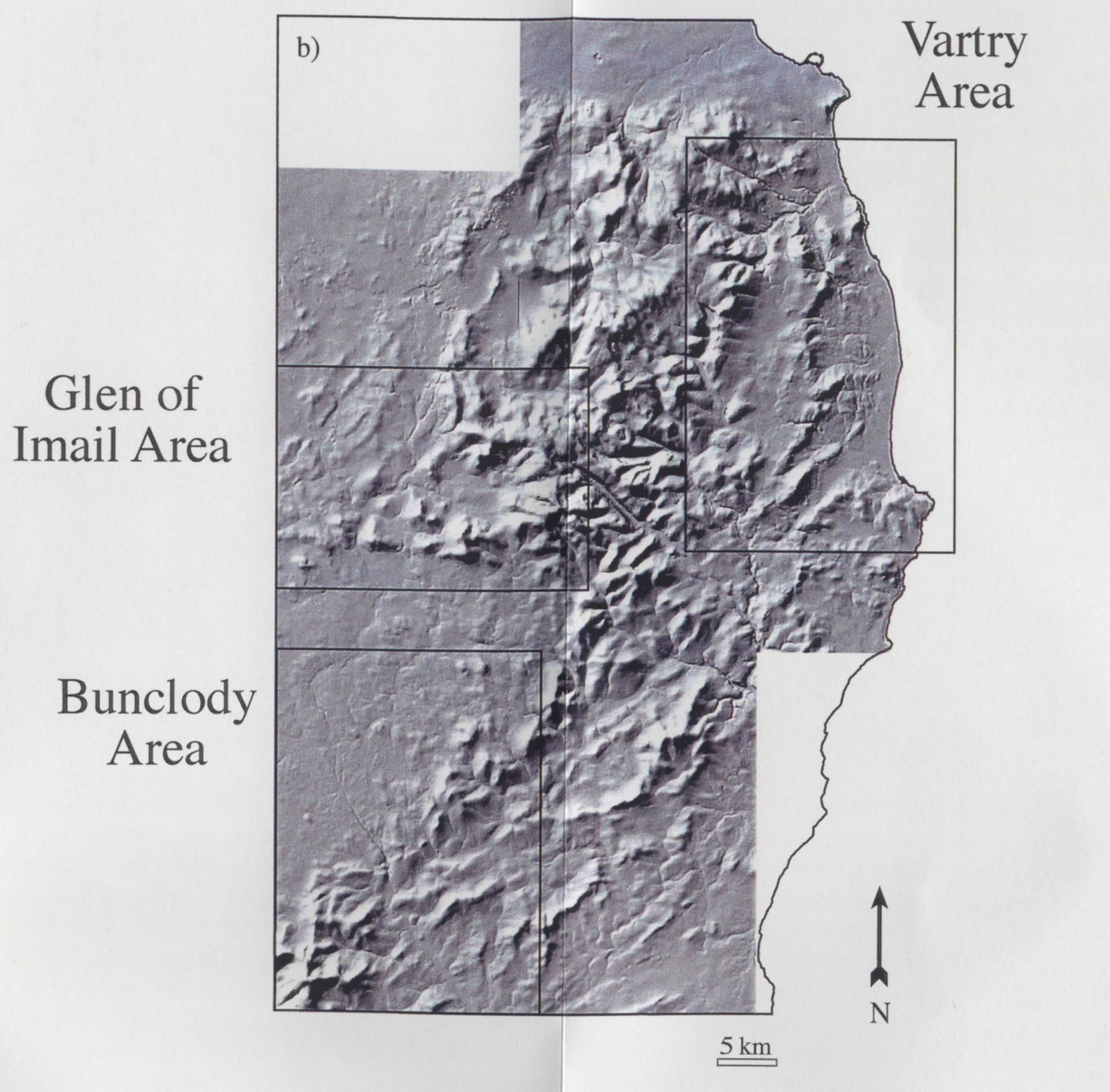

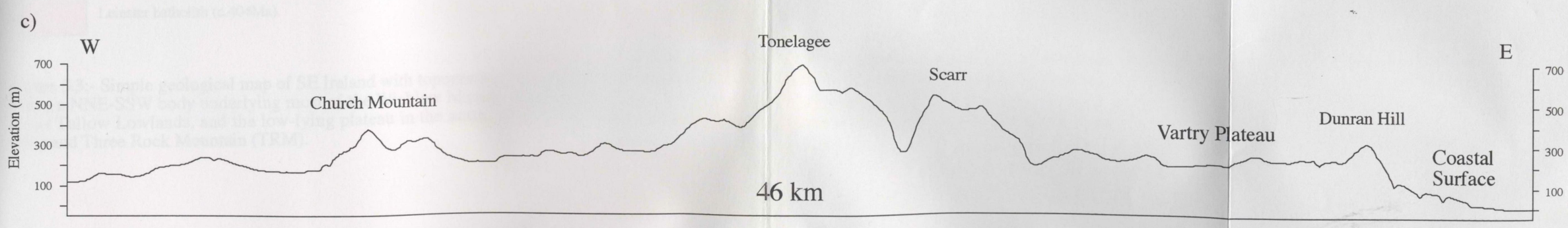

Figure 5.2:- Location of areas of geomorphic and tectonic interest. a) DEM showing areas of geomorphic and potential tectonic interest (after Mitchell, 1985). b) NW illumination of DEM showing areas of study. c) Profile from west to east across the Wicklow Massif showing hillshade and W-E profile across the Wicklow Massif.

Figure 5.3:- Simple geological map of SE Ireland with topography. The Leinster batholith forms a NNE-SSW body underlying most of the Wicklow Massif. Granite also forms the broad Tullow Lowlands, and the low-lying plateau in the north, between Dun Laoghaire (DL) and Three Rock Mountain (TRM).

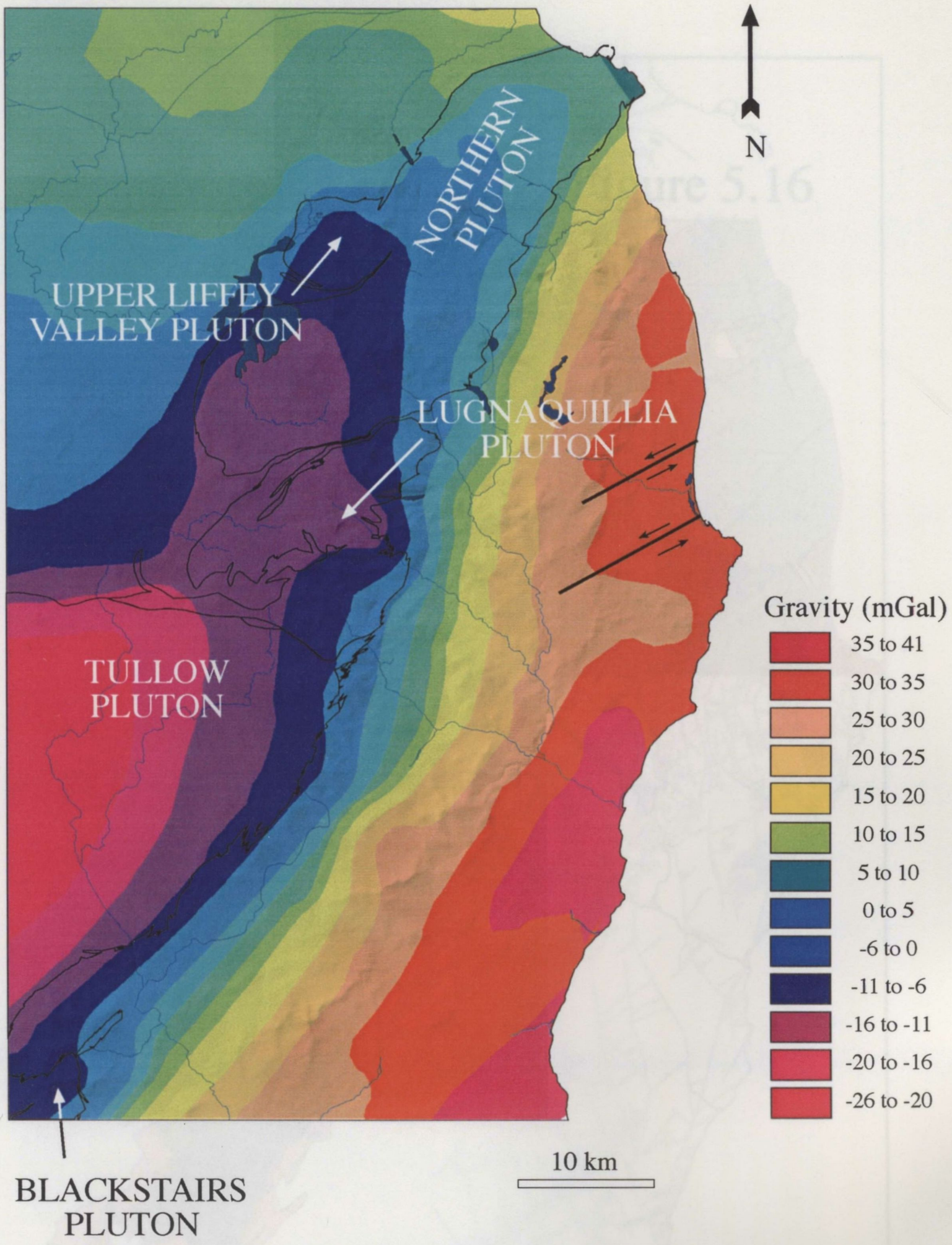

Figure 5.4:- Regional 1-milligal Bouguer gravity anomaly map, obtained from DIAS. Note the large negative anomaly associated with the Tullow pluton.

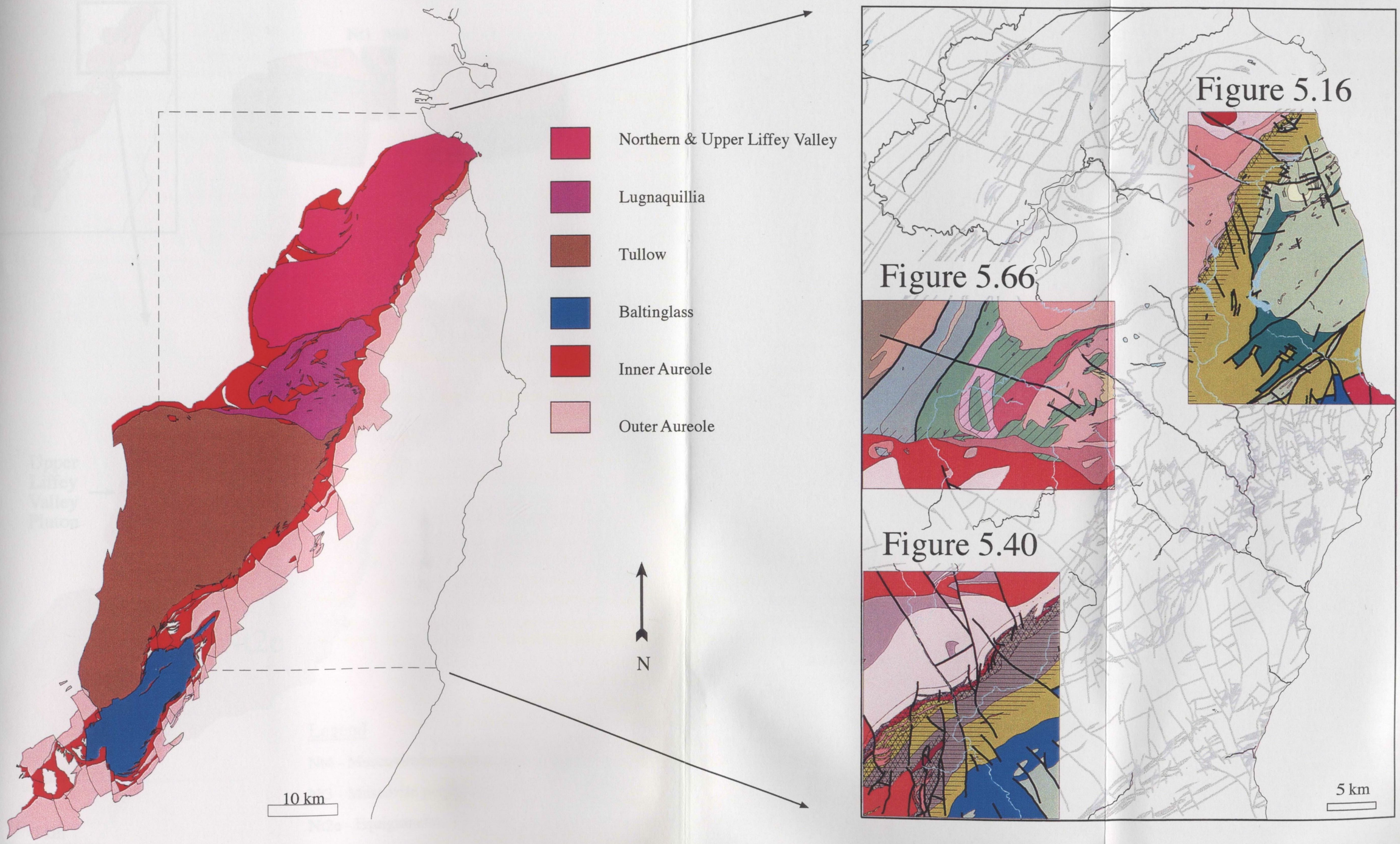

Figure 5.5:- Map showing spatial relationship between areas of study, the various plutons of the Leinster batholith, and the contact aureole. See Figures 5.16, 5.66 & 5.40 for geology of study areas and corresponding legends.

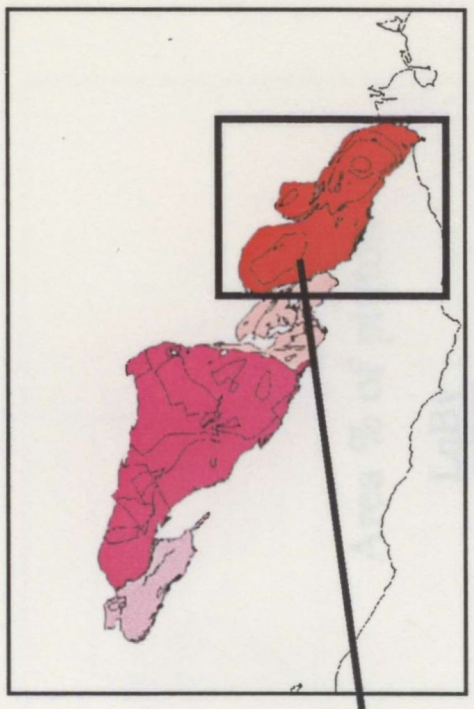

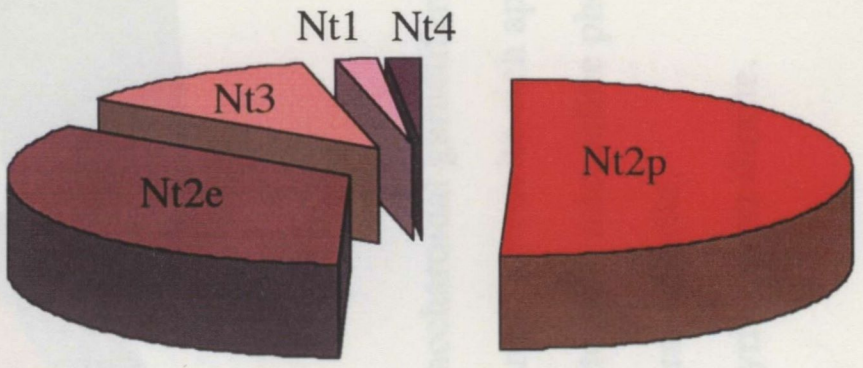

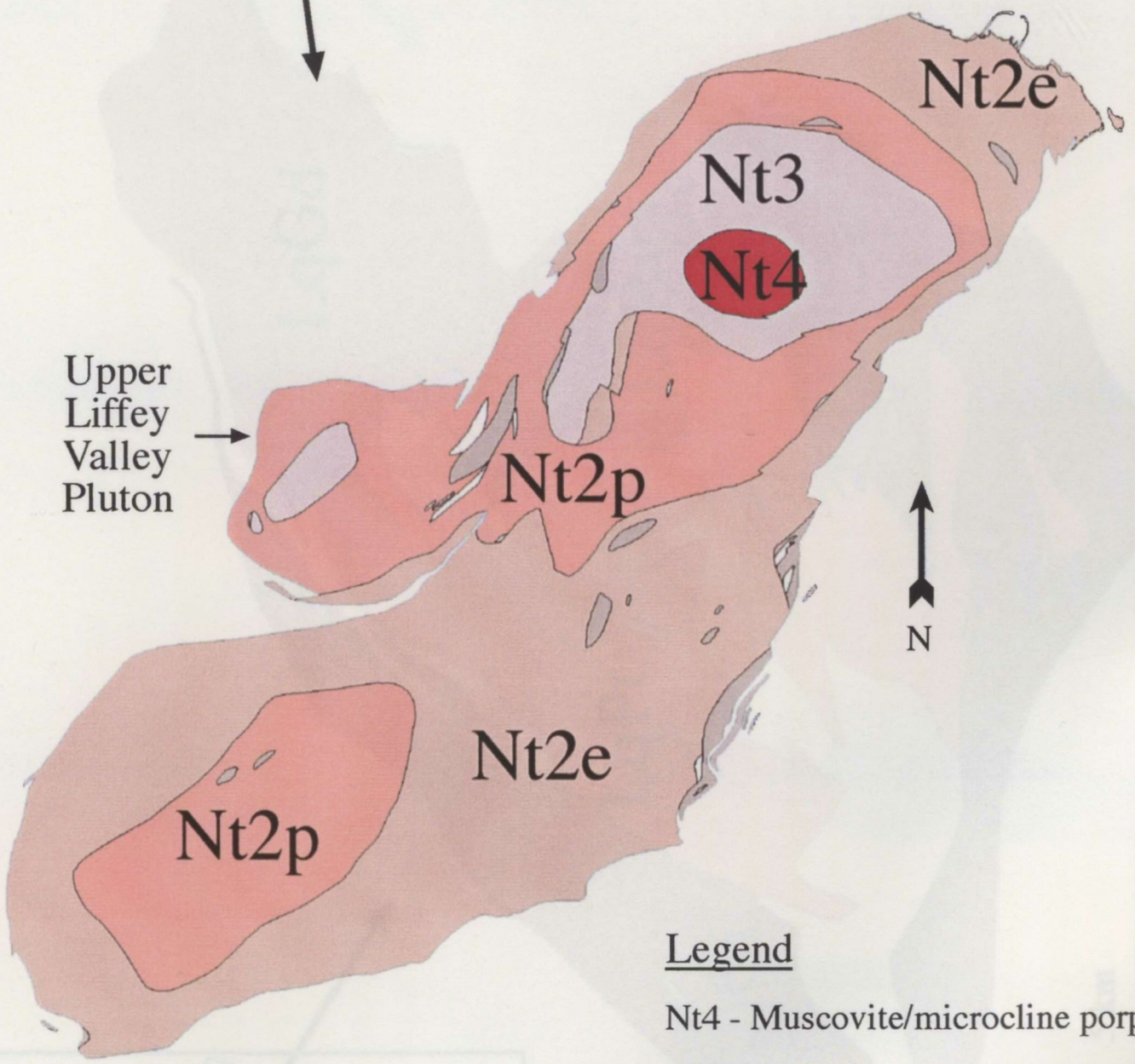

Legend

Nt4 - Muscovite/microcline porphyritic.

Nt3 - Muscovite porphyritic.

Nt2e - Equigranular.

Nt2p - Microcline porphyritic.

Nt1 - Granodiorite.

Figure 5.6:- Geological map of the Northern and Upper Liffey Valley plutons. Inset map: location of pluton within batholith. Pie-chart shows area percentage of the granitic types.

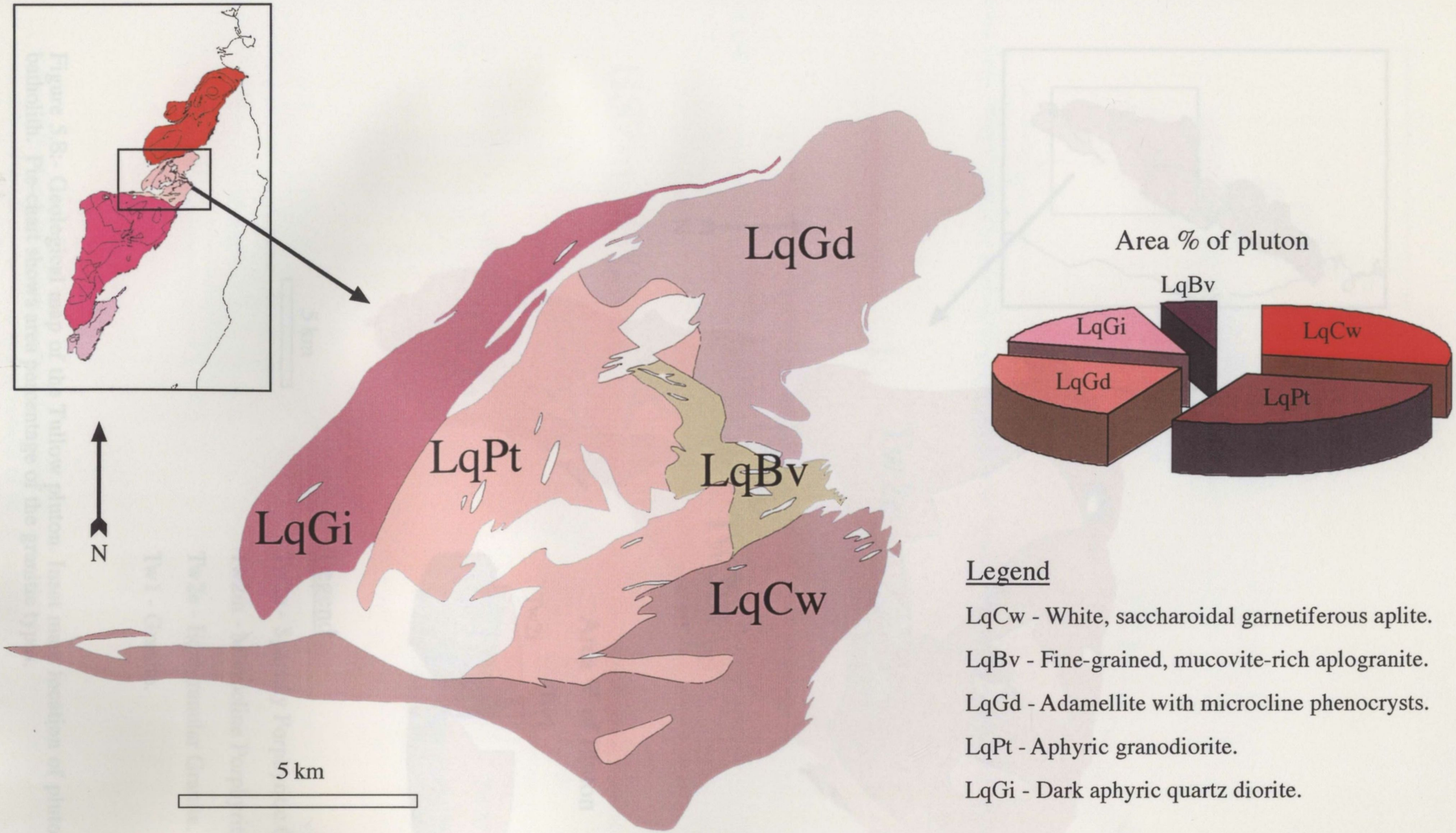

Figure 5.7:- Geological map of the Lugnaquillia pluton. Inset map: location of pluton within batholith. Pie-chart shows area percentage of the granitic types.

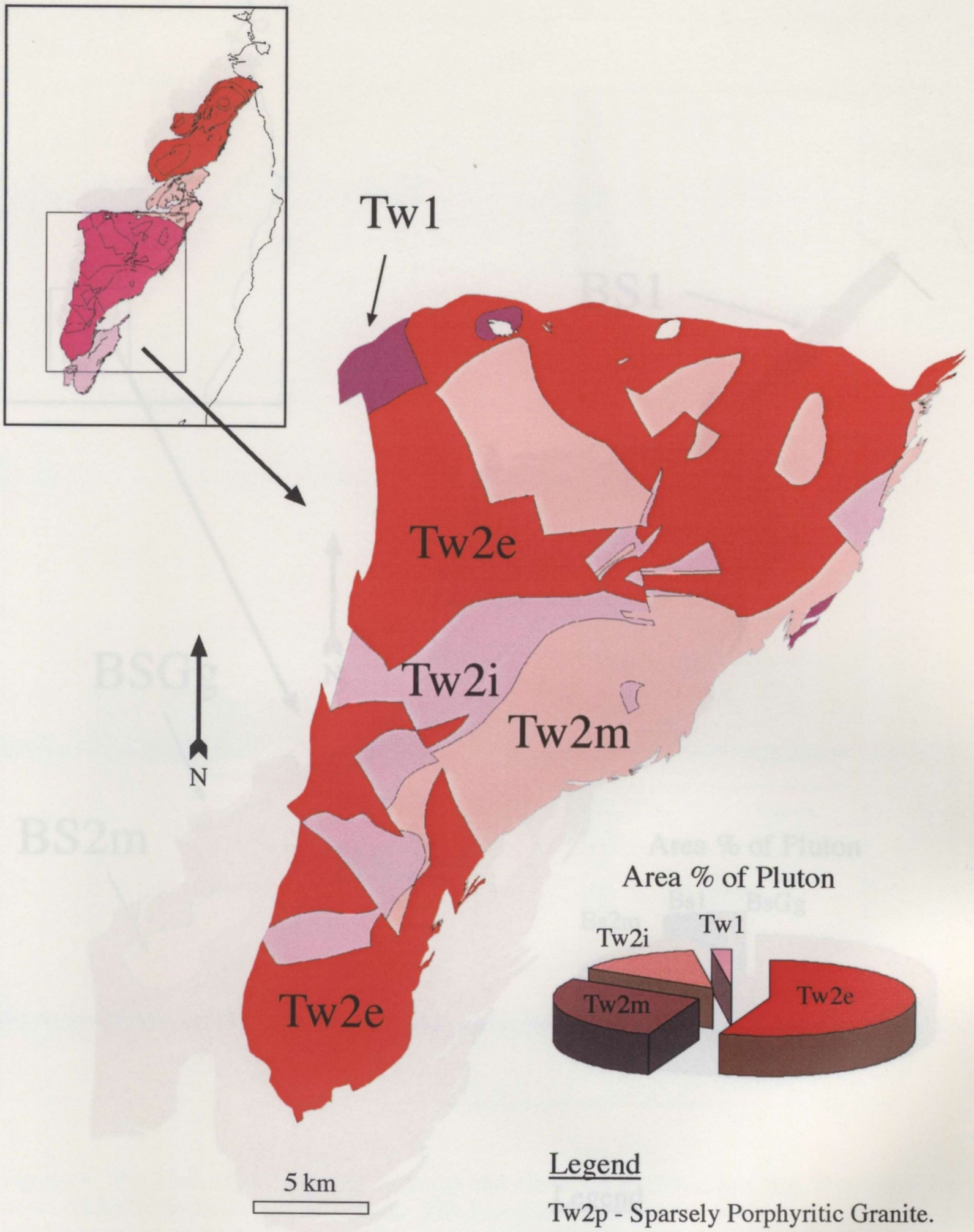

Figure 5.8:- Geological map of the Tullow pluton. Inset map: location of pluton within batholith. Pie-chart shows area percentage of the granitic types.

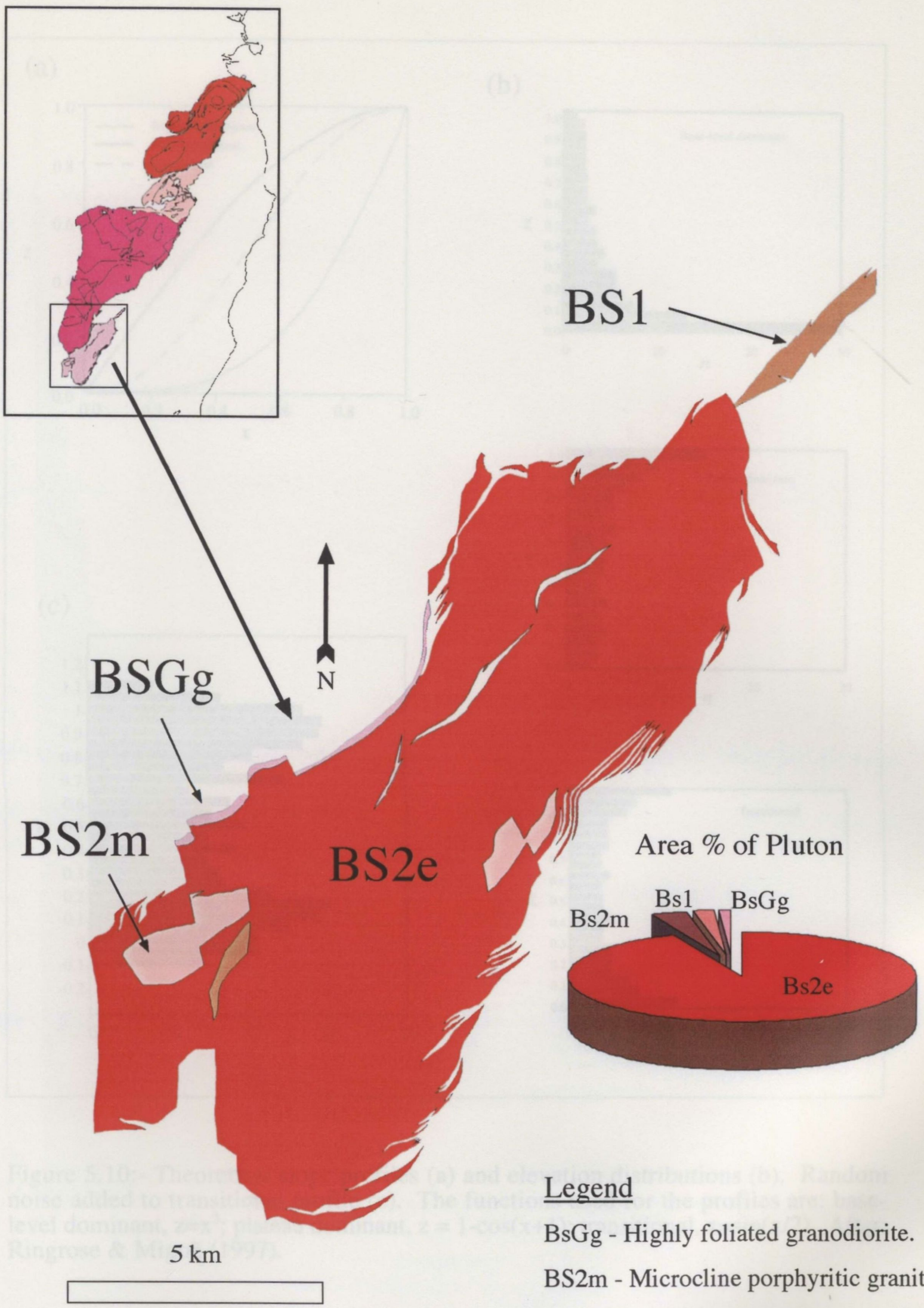

Figure 5.9:- Geological map of the Blackstairs pluton. Inset map: location of pluton within batholith. Pie-chart shows area percentage of the granitic types.

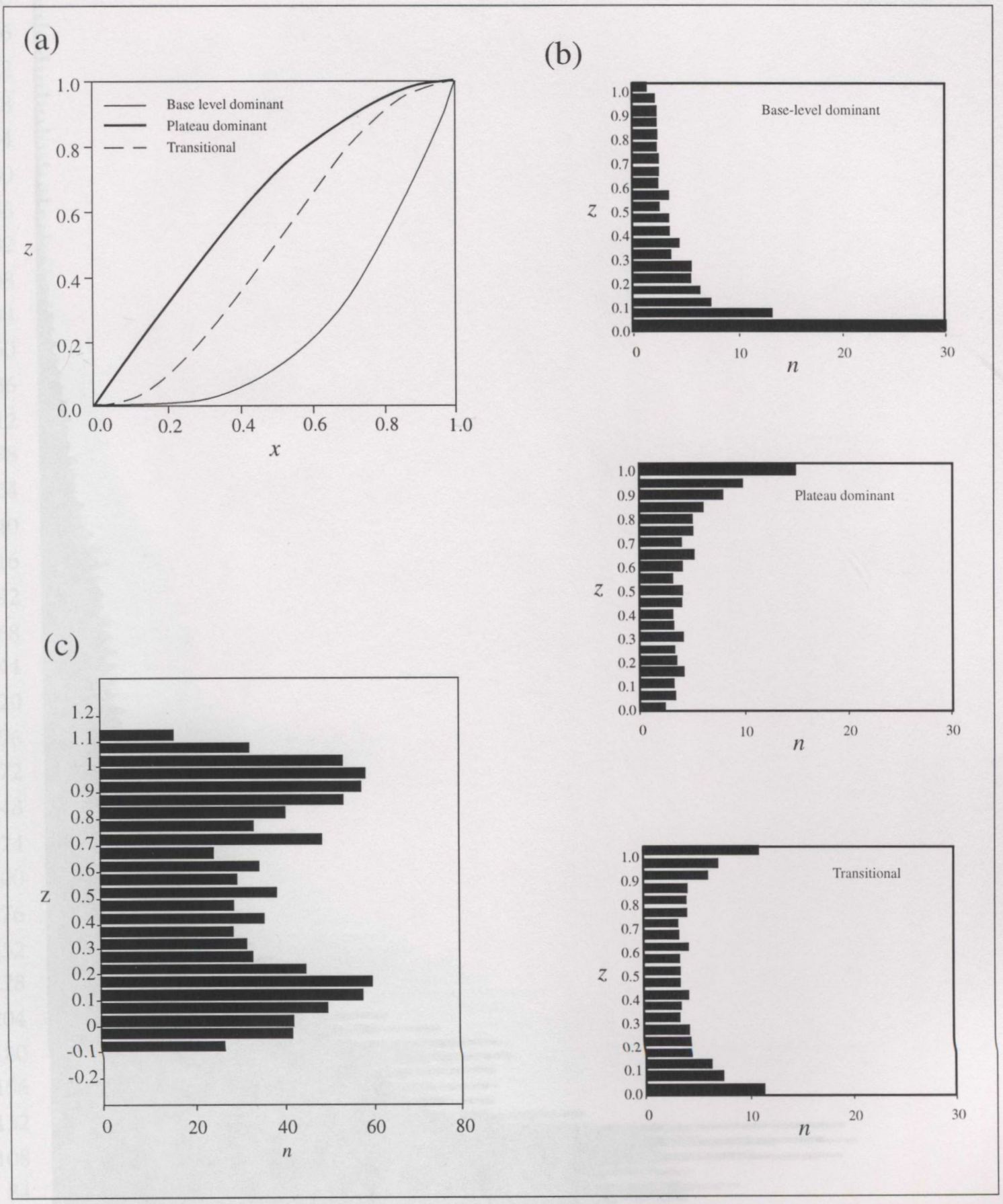

Figure 5.10:- Theoretical slope profiles (a) and elevation distributions (b). Random noise added to transitional profile (c). The functions used for the profiles are: base-level dominant, $z=x^3$; plateau dominant, z = 1-cos(x+1); transitional, z=sin(x/2). After: Ringrose & Migoñ (1997).

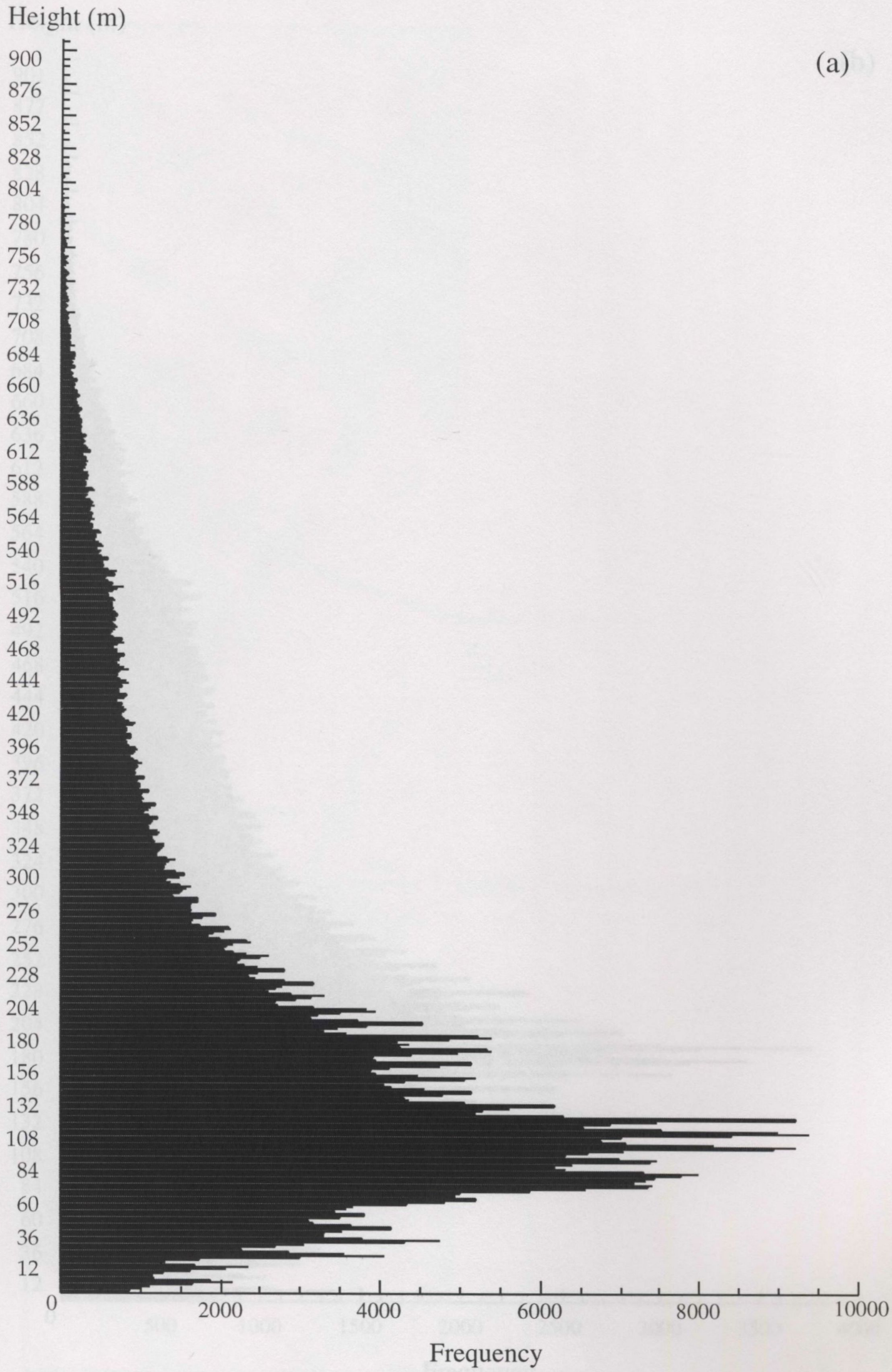

Figure 5.11a:- Elevation histogram for the Leinster Mountain chain and Tullow Lowlands area. See discussion in text.

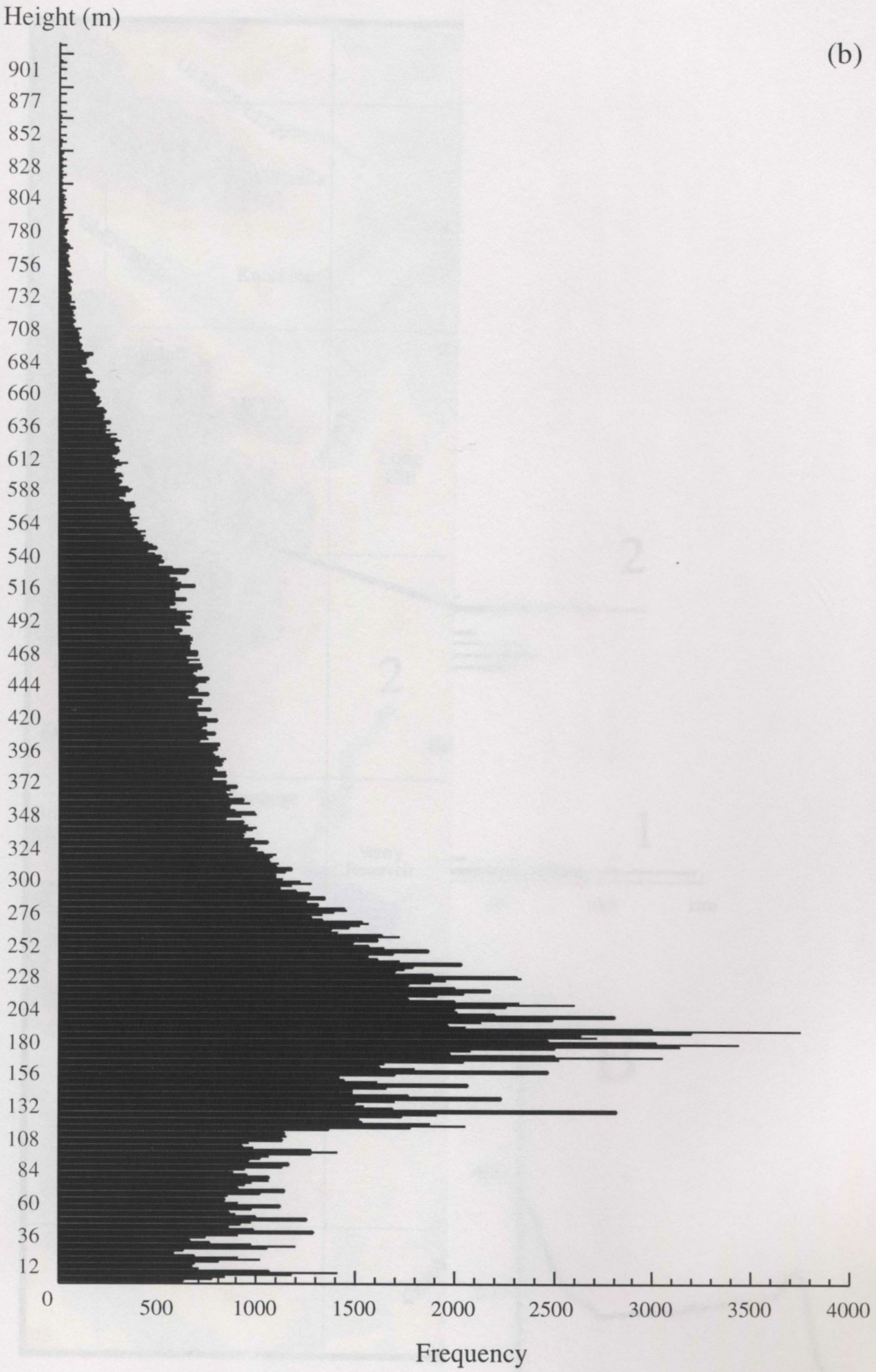

Figure 5.11b:- Elevation histogram of Wicklow Massif only. Note that the histogram shows that the area is transitional with several elevation peaks indicating where plateau processes dominate.

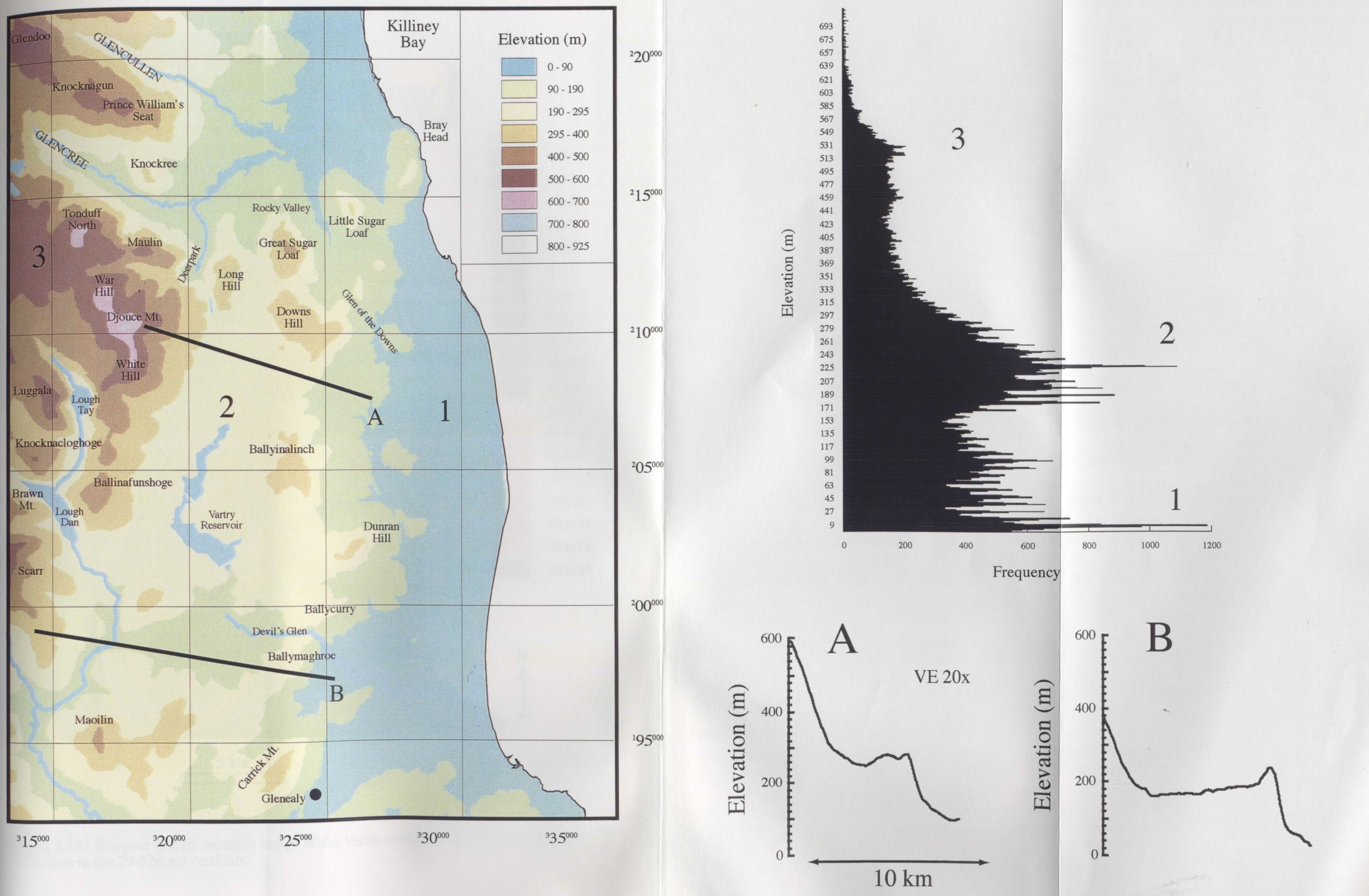

Figure 5.12:- Digital elevation model and elevation histogram for the Vartry area of study. Profiles A & B show that considerable relief occurs over the escarpments which bound the three identified surfaces (i.e. the 1 - Coastal, 2 - Vartry and 3 - Djouce).

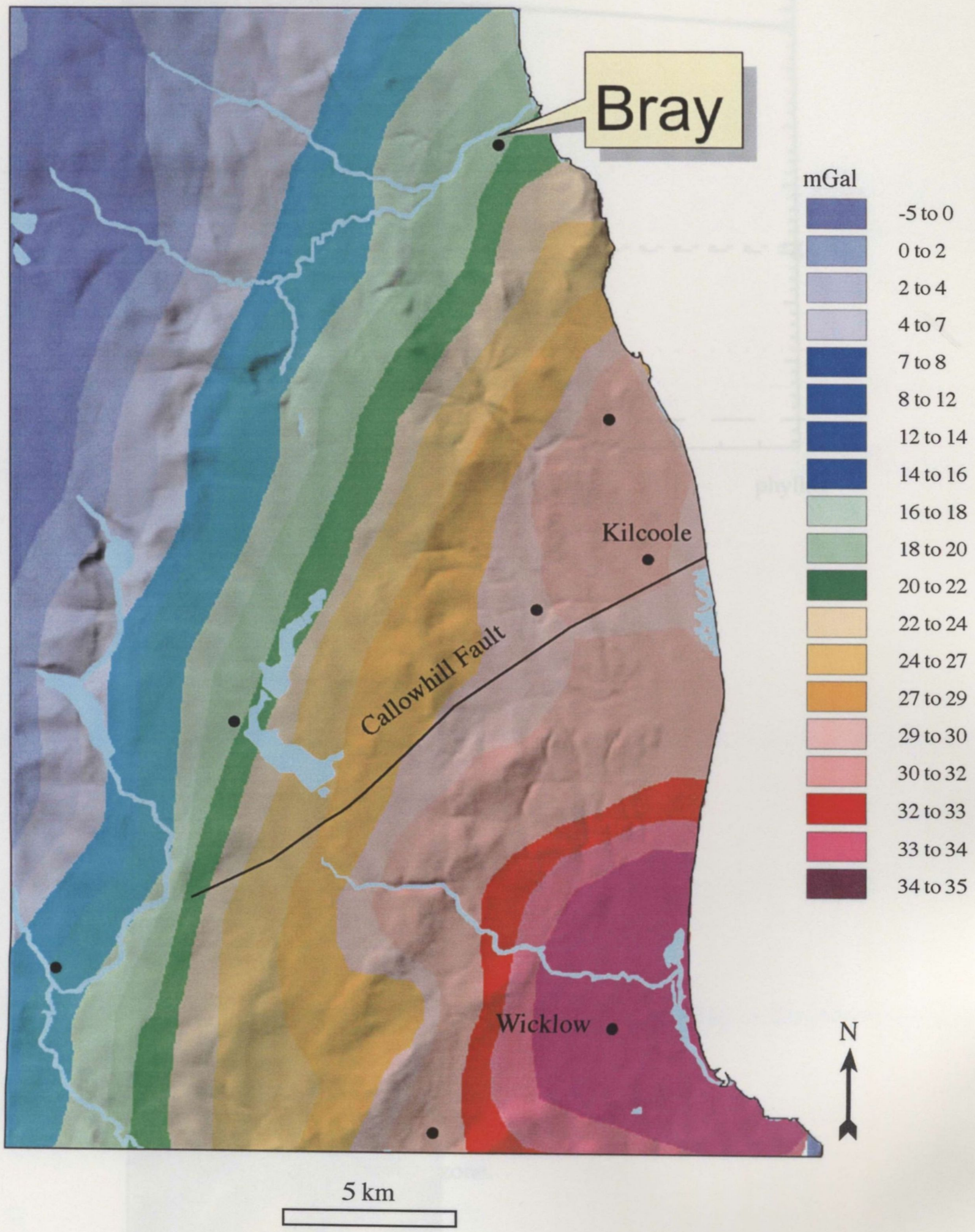

Figure 5.13:- Bouguer gravity anomaly image of the Vartry area of study. Note the sinistral deflection in the 29-32mgal contours.

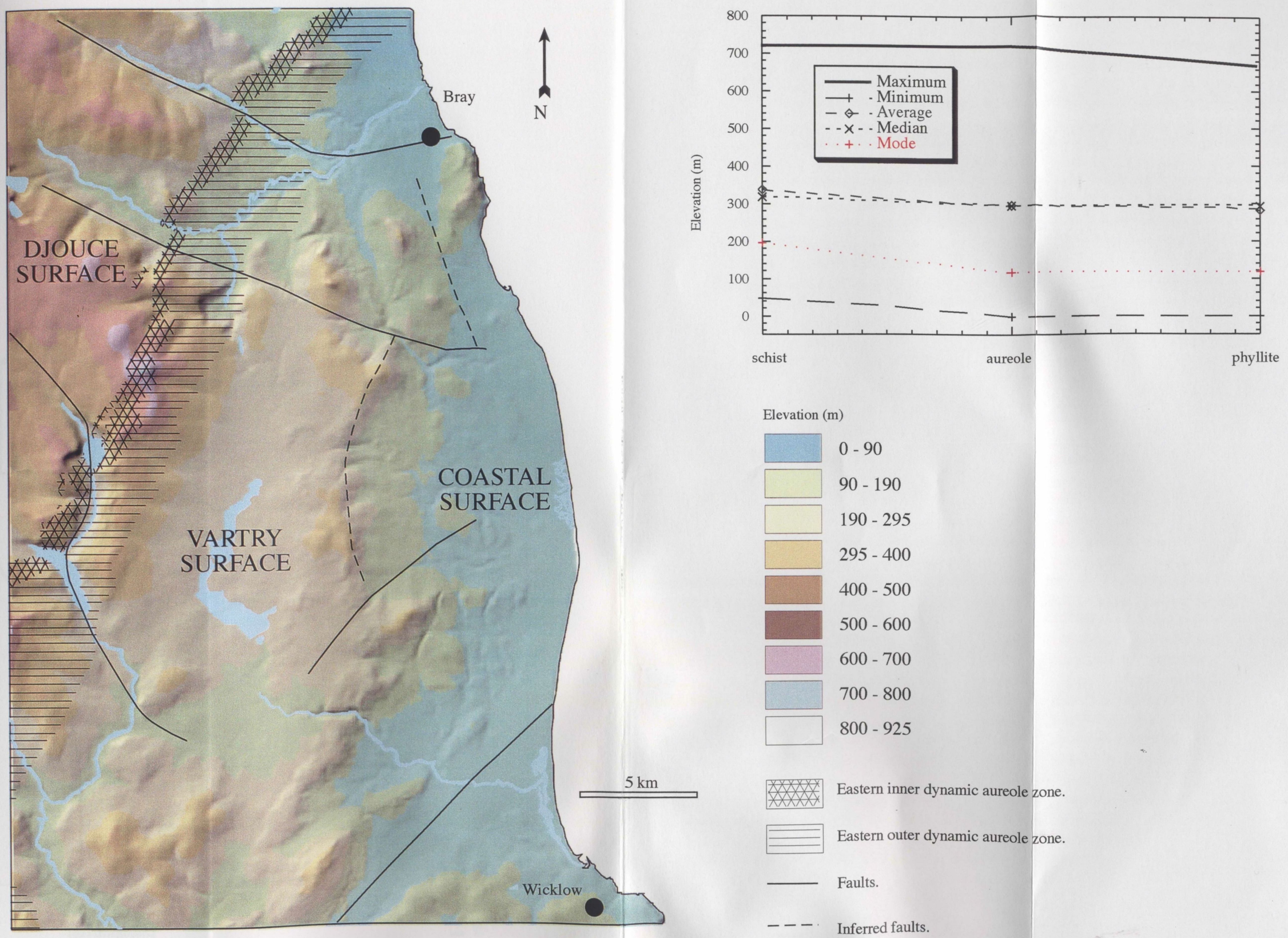

Figure 5.14:- Shaded relief topographic image of the Vartry study area showing the 3 surfaces. The extent of the inner aureole schists and the outer aureole phyllites obliquely separates the Djouce and Vartry surfaces. Inset graph shows that there is very little difference between the elevation of the inner and outer aureole rocks.

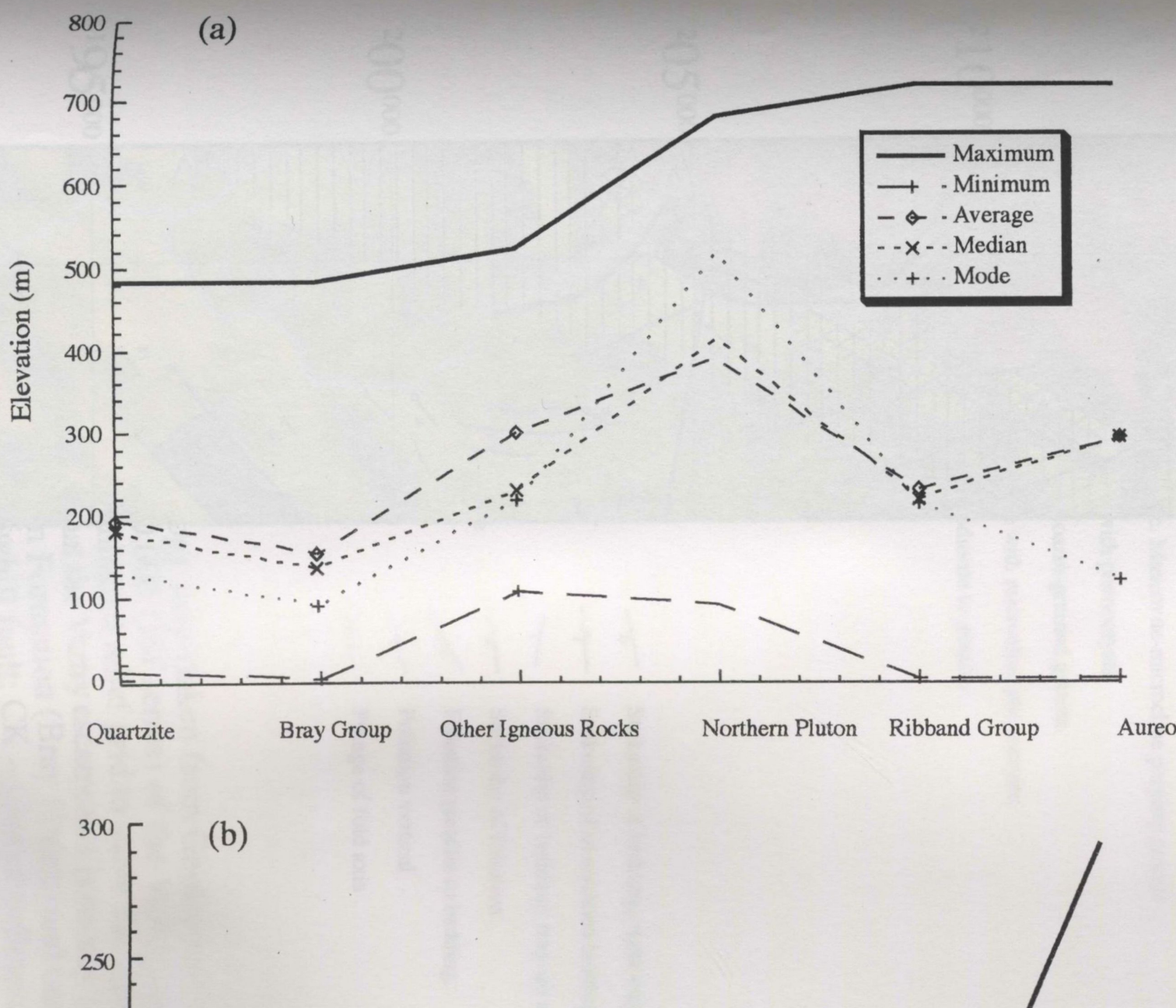

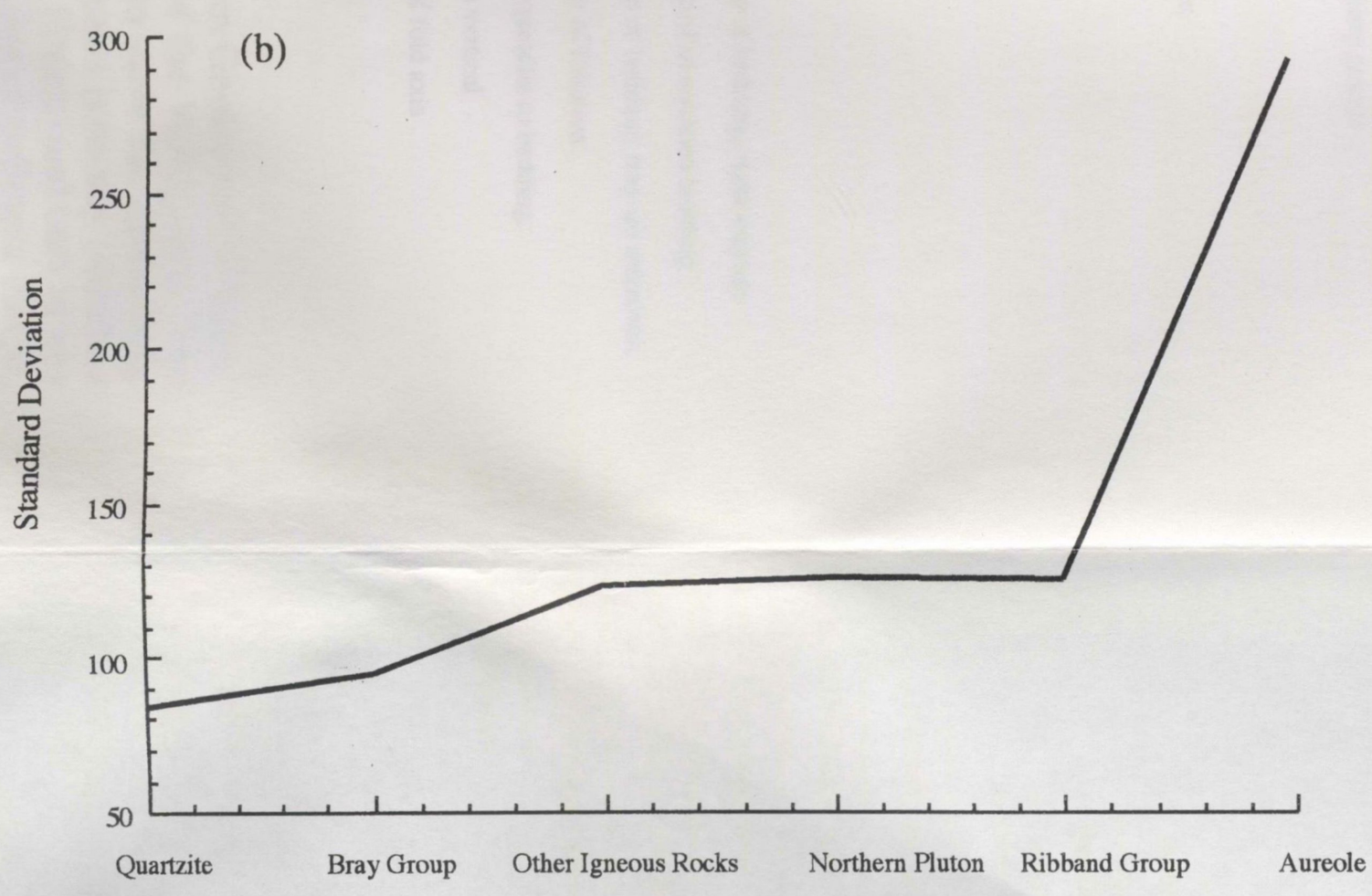

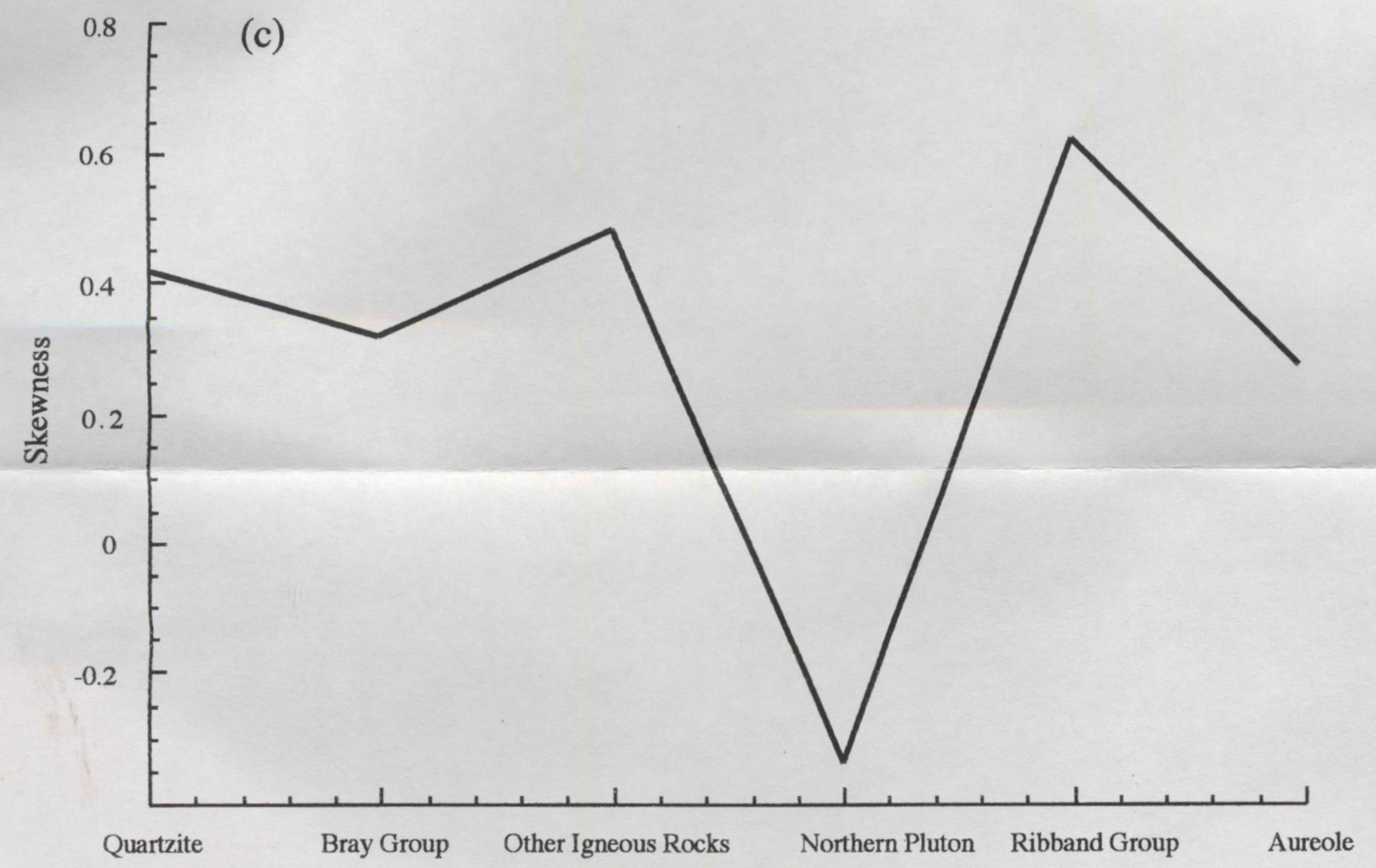

Figure 5.15a,b,c:- Statistical graphs showing the relationship between elevation and the various rock types of the Vartry area (as discussed in text).

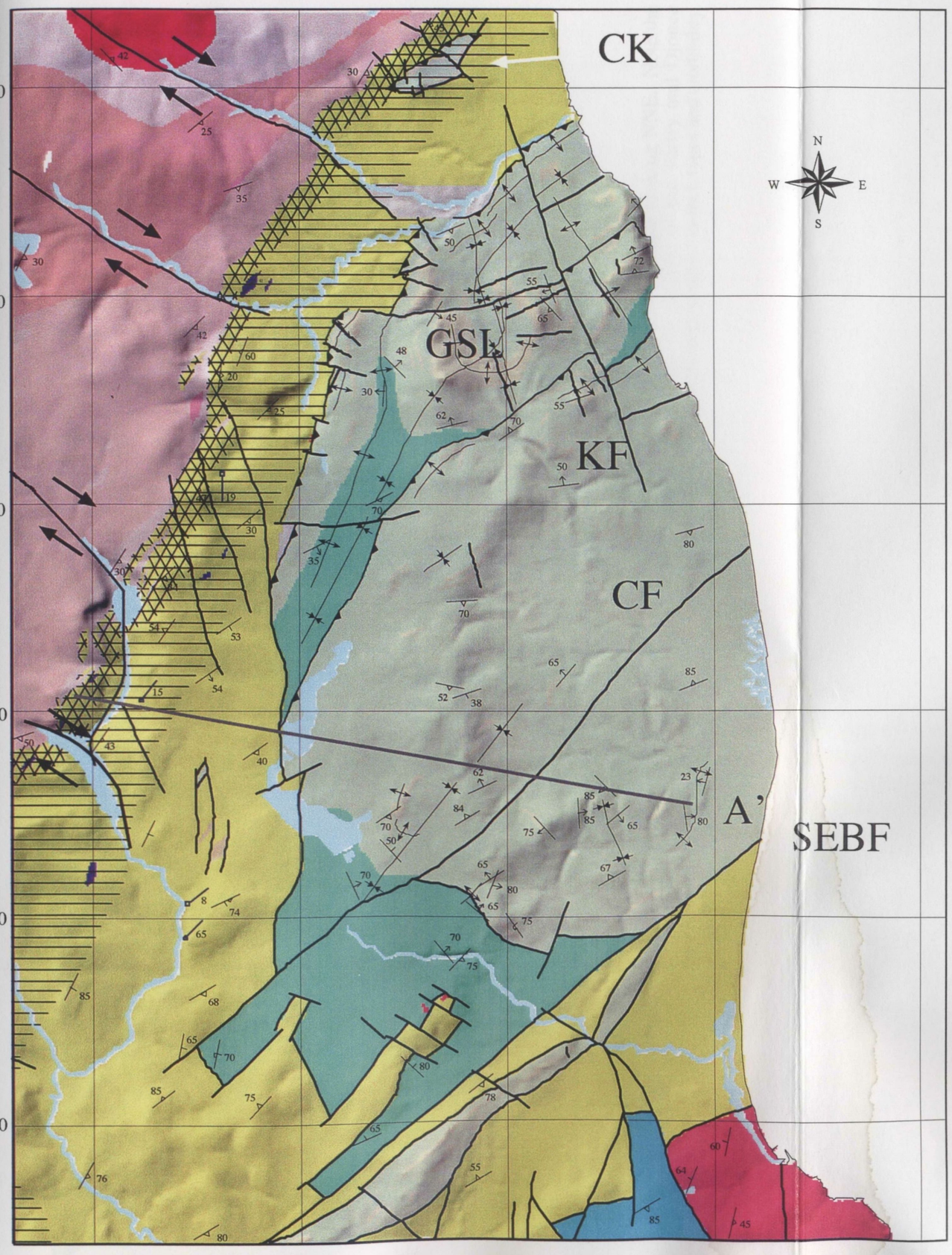

Ribband Group. Cambrian (Tremadoc-Llanvirn)

- Ballylane Formation. Green and grey slate with thin siltstone.
- Glencullen River Formation. Tuffs, phyllites and siltstones.
- Maulin Formation. Dark to grey siltstones and shales with coticule horizons.
  Roundwood Member. Often porphyritic andesitic amphibolites.
  Knockree Member. Quartzite.
- Wicklow Head Formation. Silver-grey mica schist.

Bray Group. Lr-M Cambrian

- Bray Head Formation. Greywackes and quartzite.
- Devil Glen's Formation. Greywackes and shale.

Northern Pluton

- Type 4 muscovite/microcline porphyritic. Muscovite-microcline porphry granite.
- Type 3 muscovite porphyritic. Granite with phenocrysts.
- Type2e equigranular. Pale grey fine to coarse-grained granite.
- Type 2p microcline porphyritic. Granite with microcline phenocrysts.
- Type 1 granodiorite. Fine-grained granodiorite to granite.

Other Rocks

- Aplite.
- Microgranite.
- Mafic volcanics.

- Eastern inner dynamic aureole zone.
- Eastern outer dynamic aureole zone.
- Fault.
- Thurst fault, barbs on hangingwall side.
- Anticline.
- Syncline.
- A — A′ Line of Section (figure 5.36)

- Strike/dip of bedding, right way-up.
- Strike/dip of overturned bedding.
- Strike/dip of bedding, way-up unknown.
- Strike/dip of foliation.
- Foliation parallel to bedding.
- Foliation vertical
- Plunge of fold axis

Figure 5.16:- Solid bedrock geology map (taken from Geology of Kildare-Wicklow (1995), Sheet 16, 1:100,000 GSI series) of the Vartry area. The geology is draped over a NW illuminated relief grid to show the relationship of geology and topography. Note that the Vartry escarpment is mostly underlain by greywackes of the Devil's Glen Formation (Bray Group) and cuts across the Caledonian strike. CF – Callowhill fault; CK – Carrickgollogan klippe; GSL – Great Sugar Loaf Mountain; KF – Kilruddery fault; SEBF – South-Eastern Boundary fault.

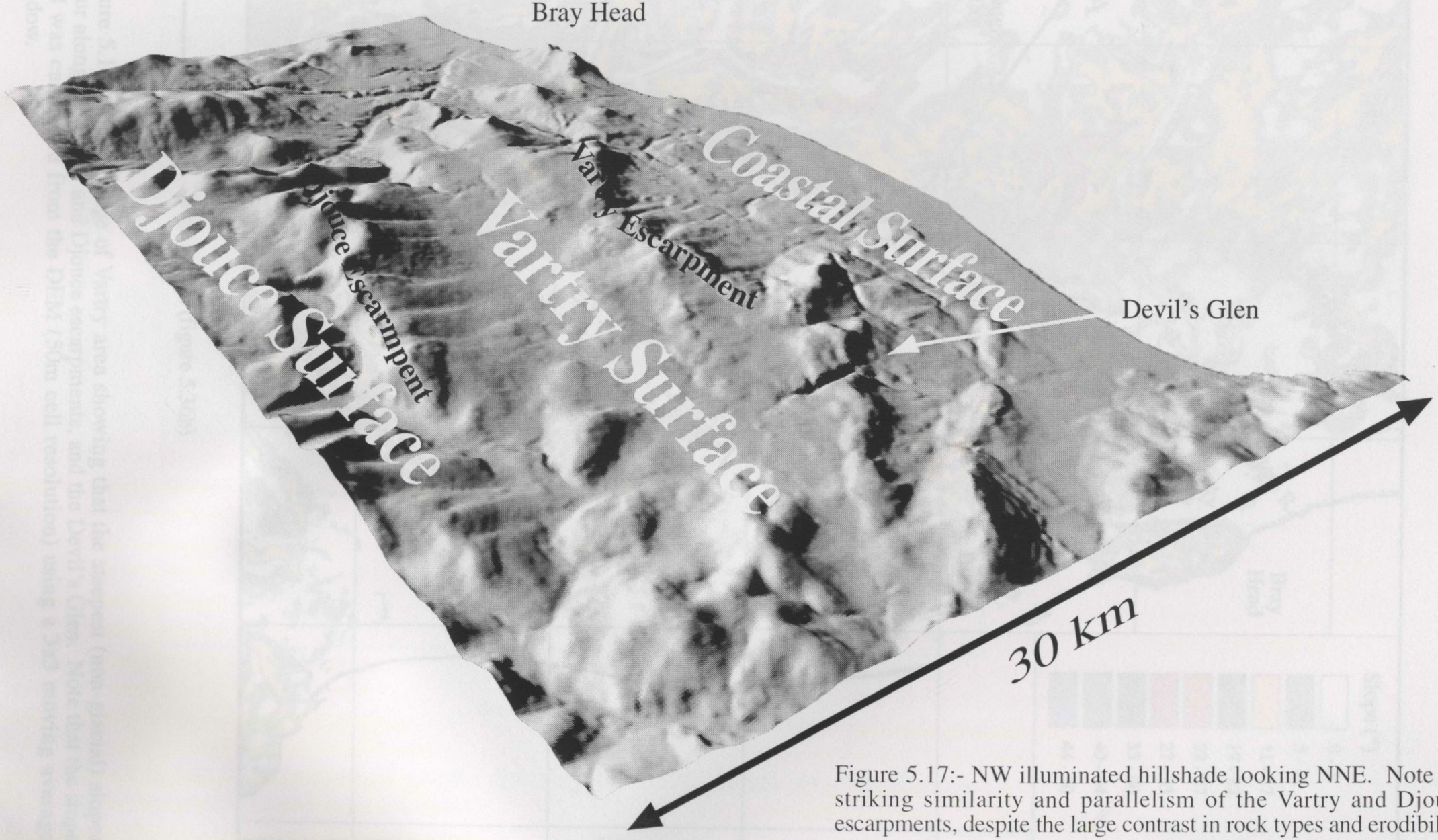

Figure 5.17:- NW illuminated hillshade looking NNE. Note the striking similarity and parallelism of the Vartry and Djouce escarpments, despite the large contrast in rock types and erodibility.

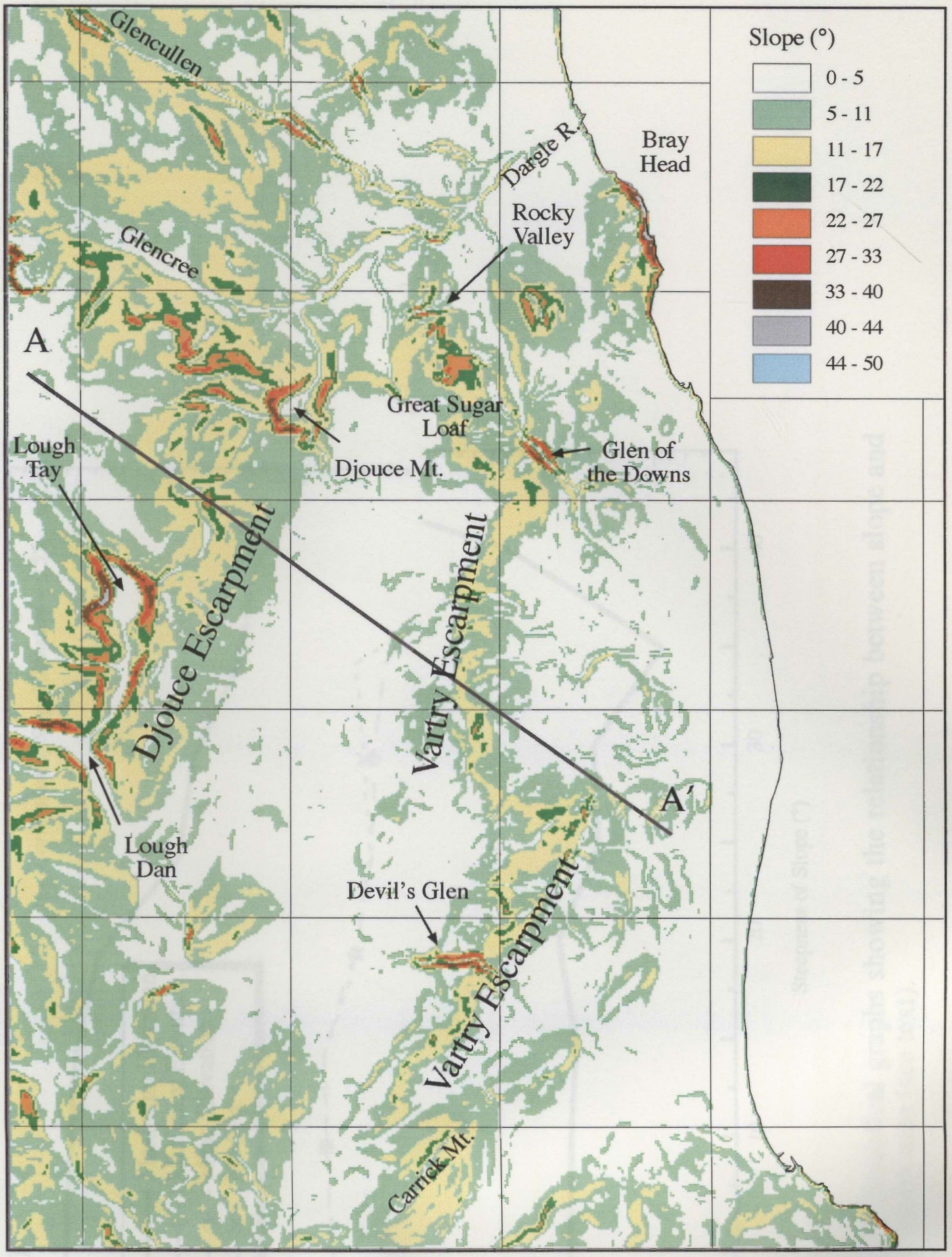

A _____ A′ Slope profile (figure 5.36b)

Figure 5.18:- Slope image of Vartry area showing that the steepest (non-glacial) slopes occur along the Vartry and Djouce escarpments, and the Devil's Glen. Note that the slope grid was calculated from the DEM (50m cell resolution) using a 3x3 moving average window.

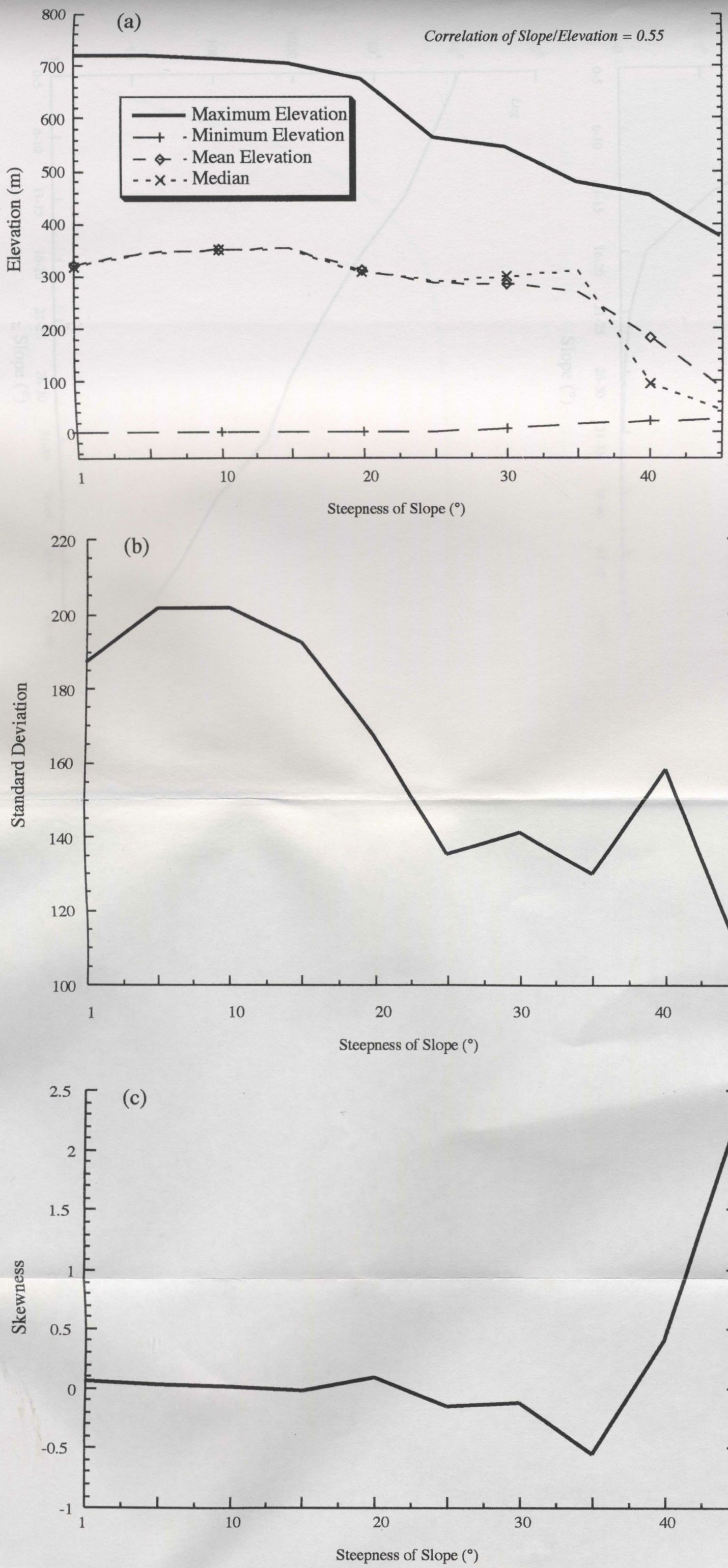

Figure 5.19a,b,c:- Statistical graphs showing the relationship between slope and elevation in the Vartry area (see text).

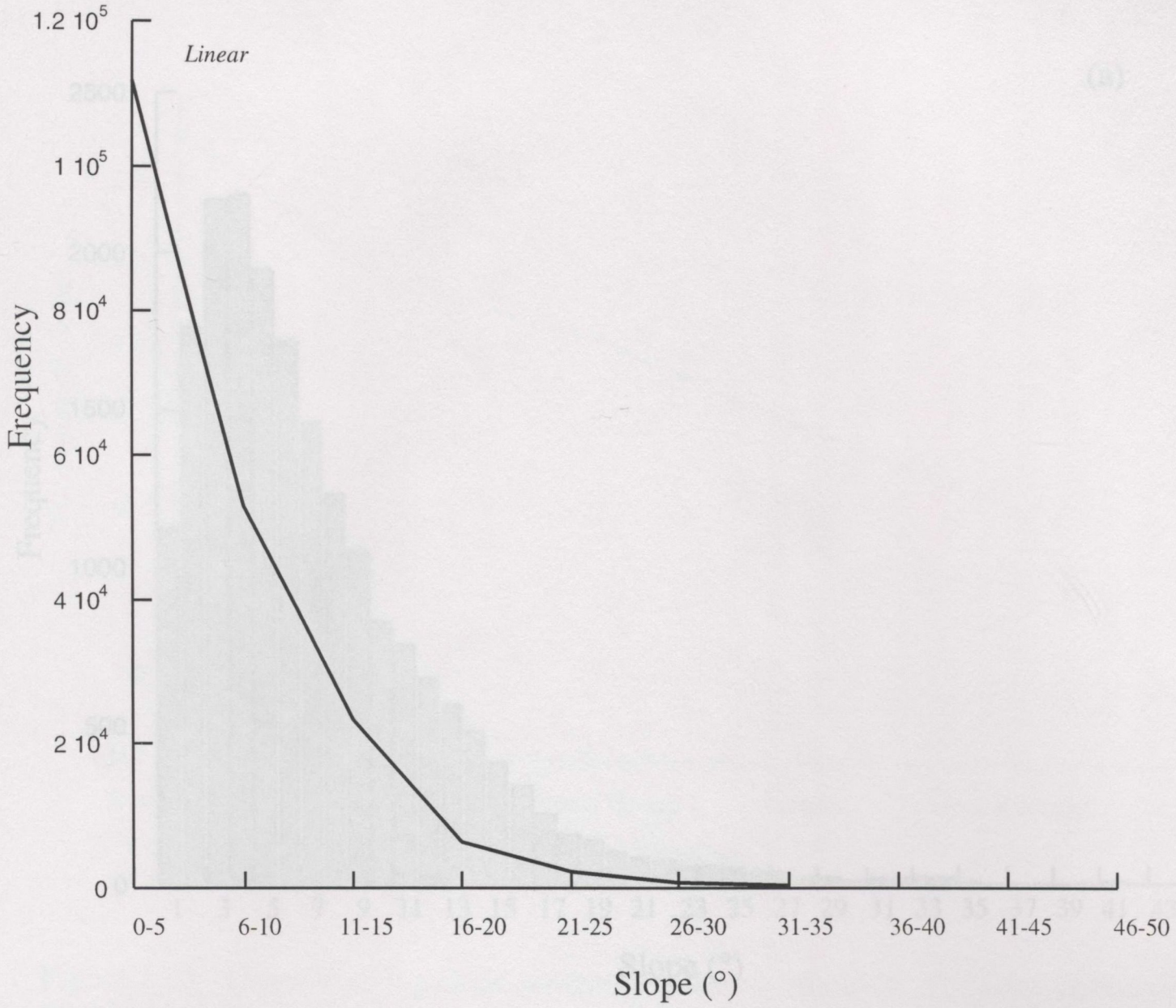

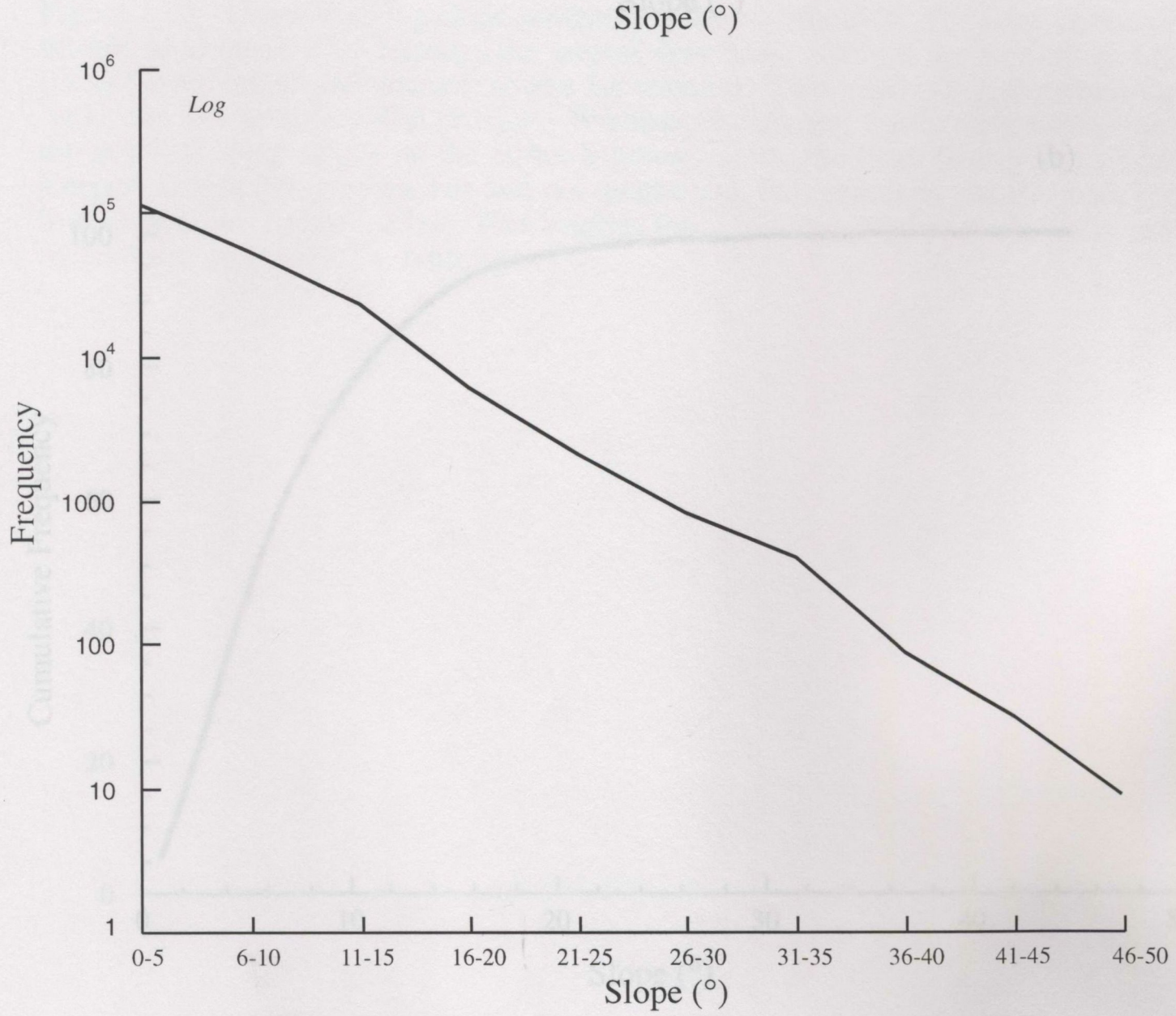

Figure 5.20:- Graph showing the frequency of slopes in the area.

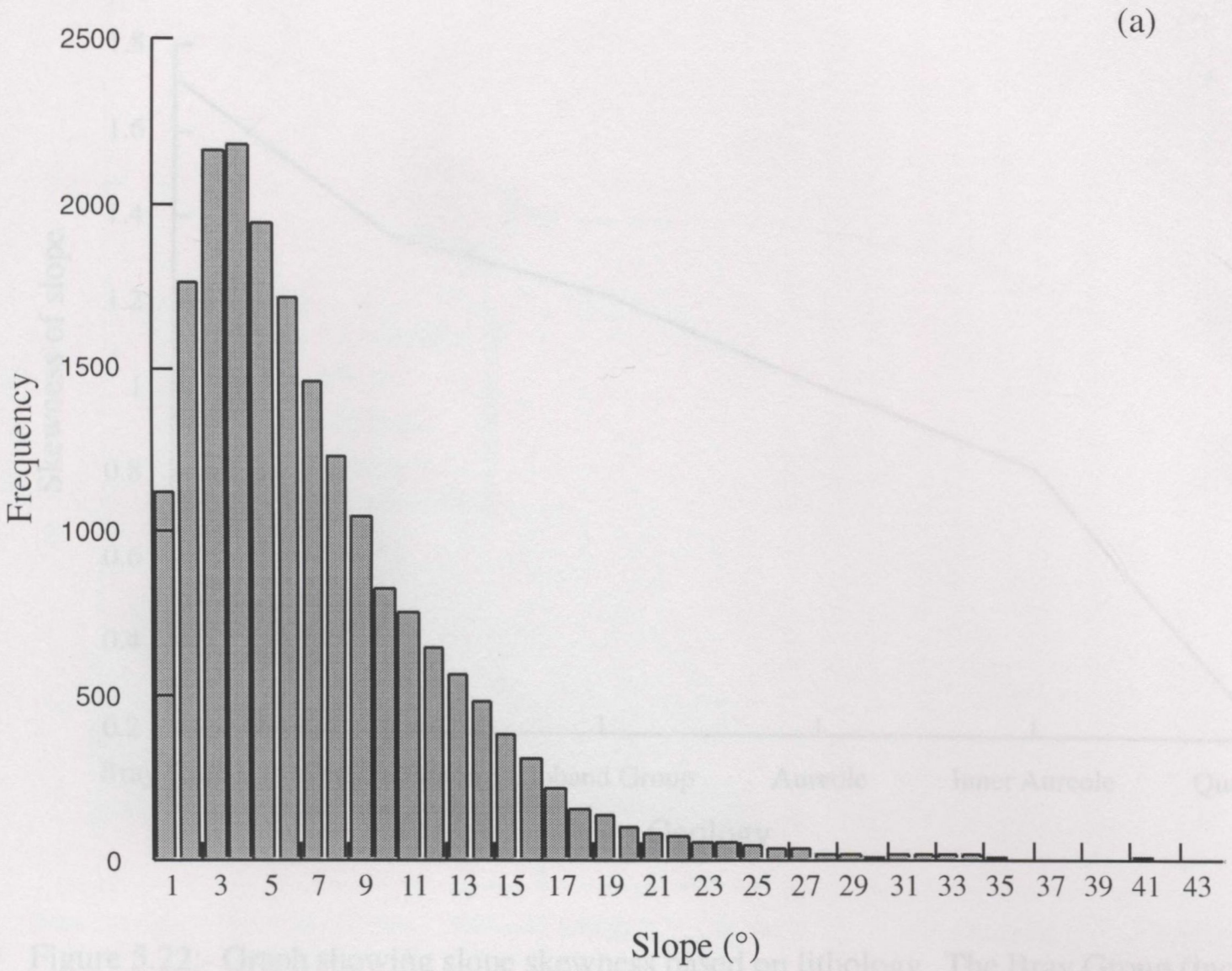

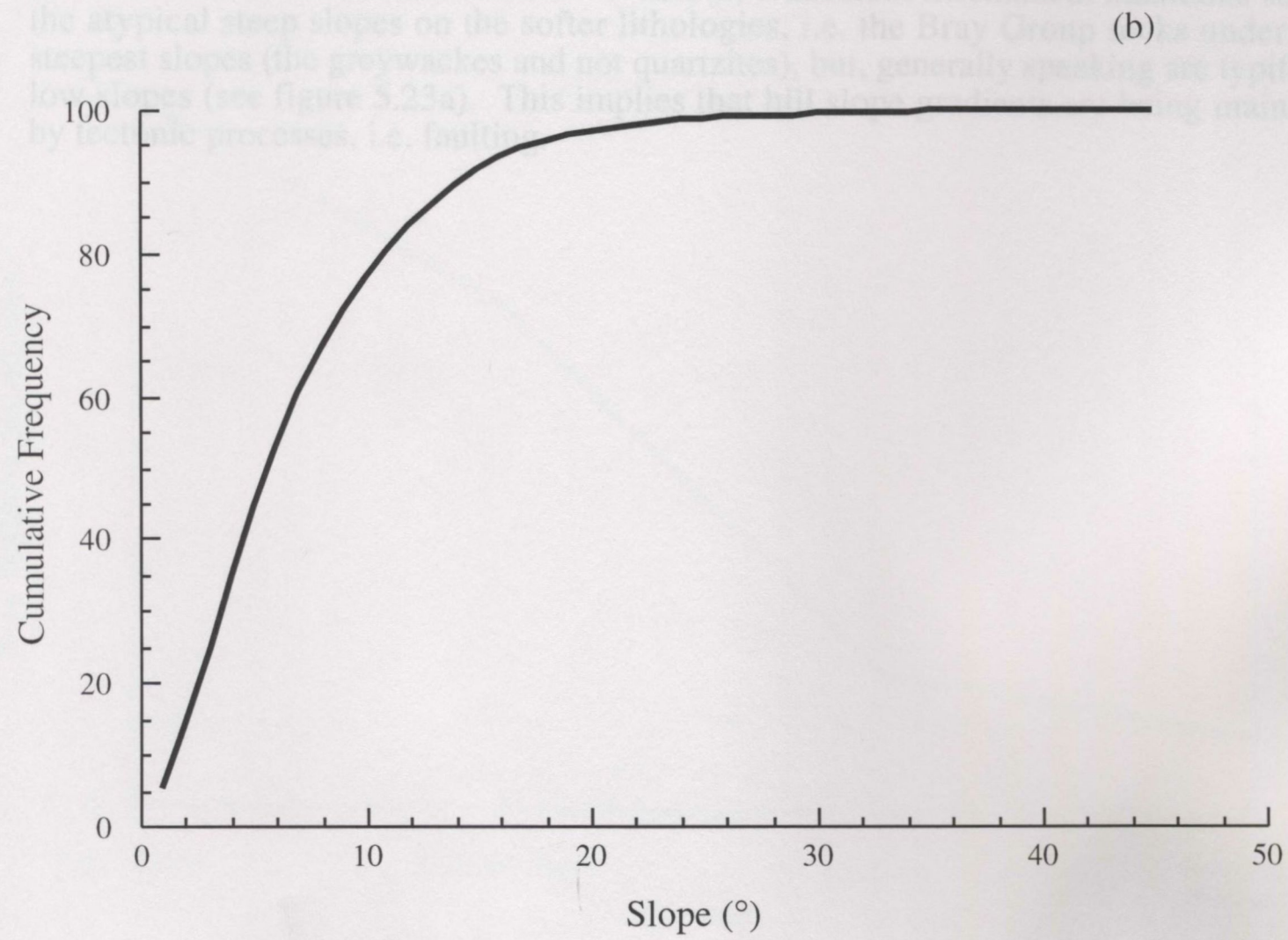

Figure 5.21a,b:- a) Histogram of slopes that occur on the Bray Group rocks. b) The cumulative frequency shows that the Bray Group rocks are typified mostly by gentle slopes. The steepest slopes occurring on quartzites.

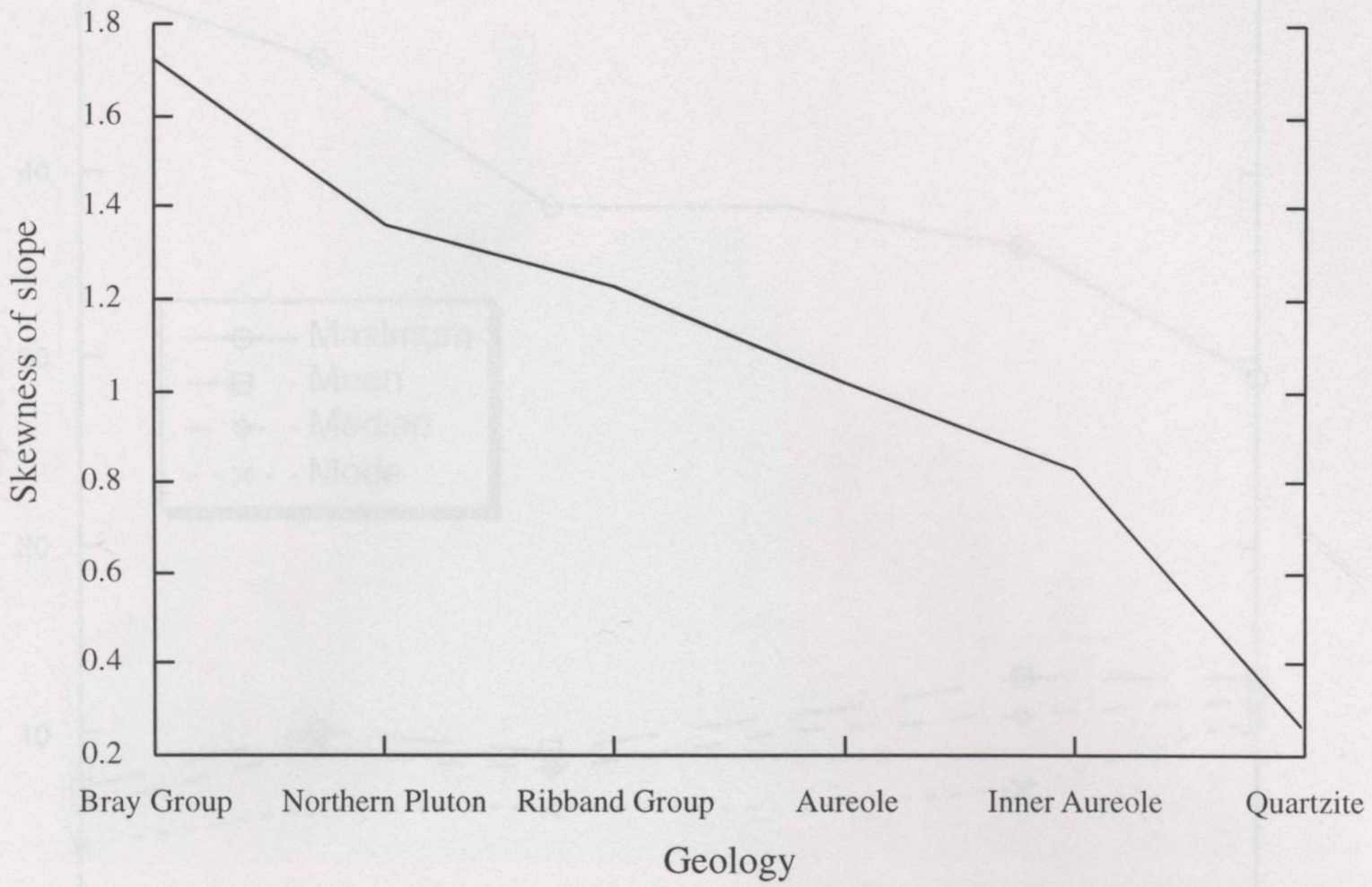

Figure 5.22:- Graph showing slope skewness based on lithology. The Bray Group (including interbedded quartzites) displays the largest skewness, whereas the aureole and quartzites (Bray Group minus greywackes) shows the smallest. This implies that slopes on the hardest rocks are due to differential erosion. Whereas, a different mechanism maintains some of the atypical steep slopes on the softer lithologies, i.e. the Bray Group rocks underlie the steepest slopes (the greywackes and not quartzites), but, generally speaking are typified by low slopes (see figure 5.23a). This implies that hill slope gradients are being maintained by tectonic processes, i.e. faulting.

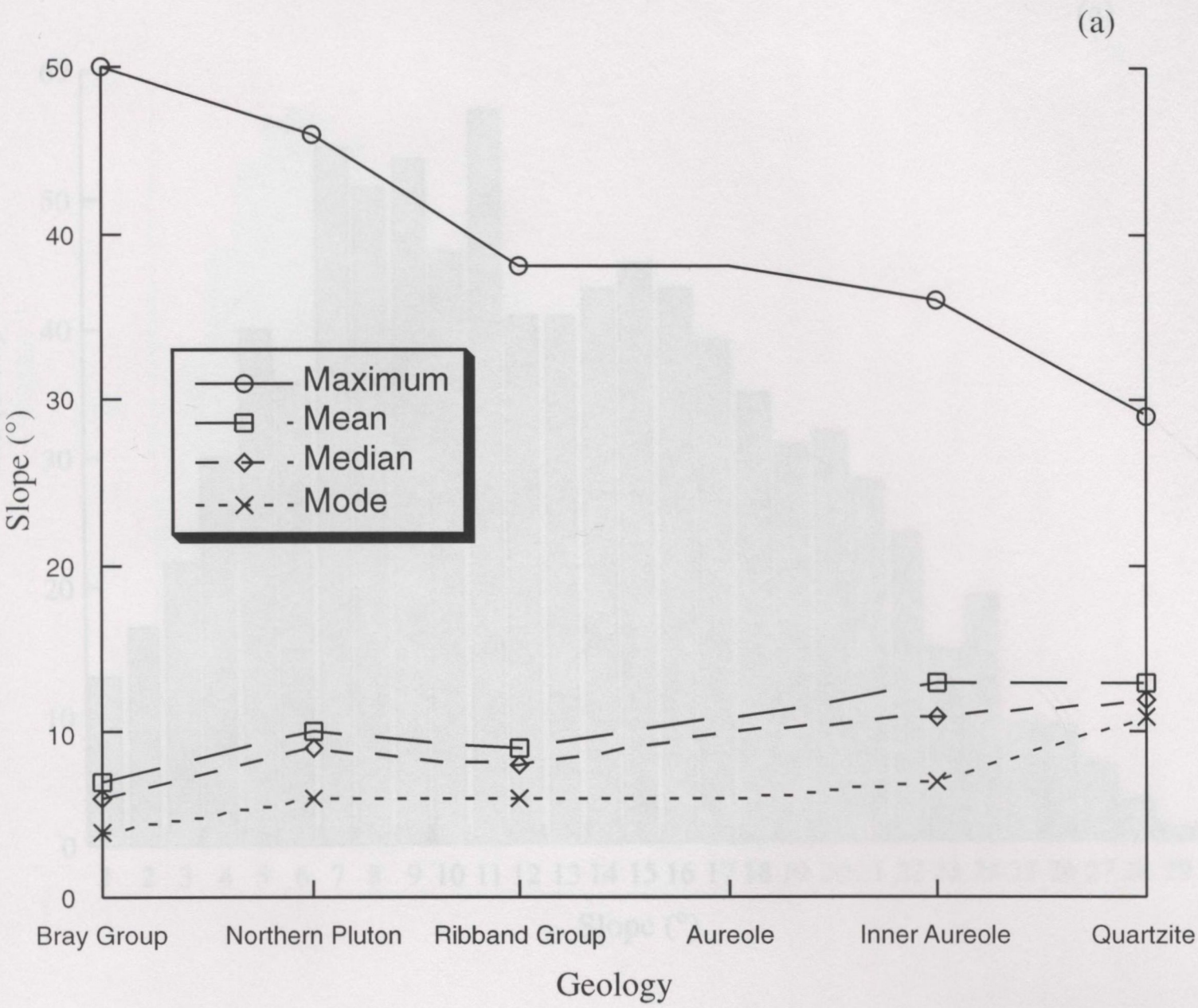

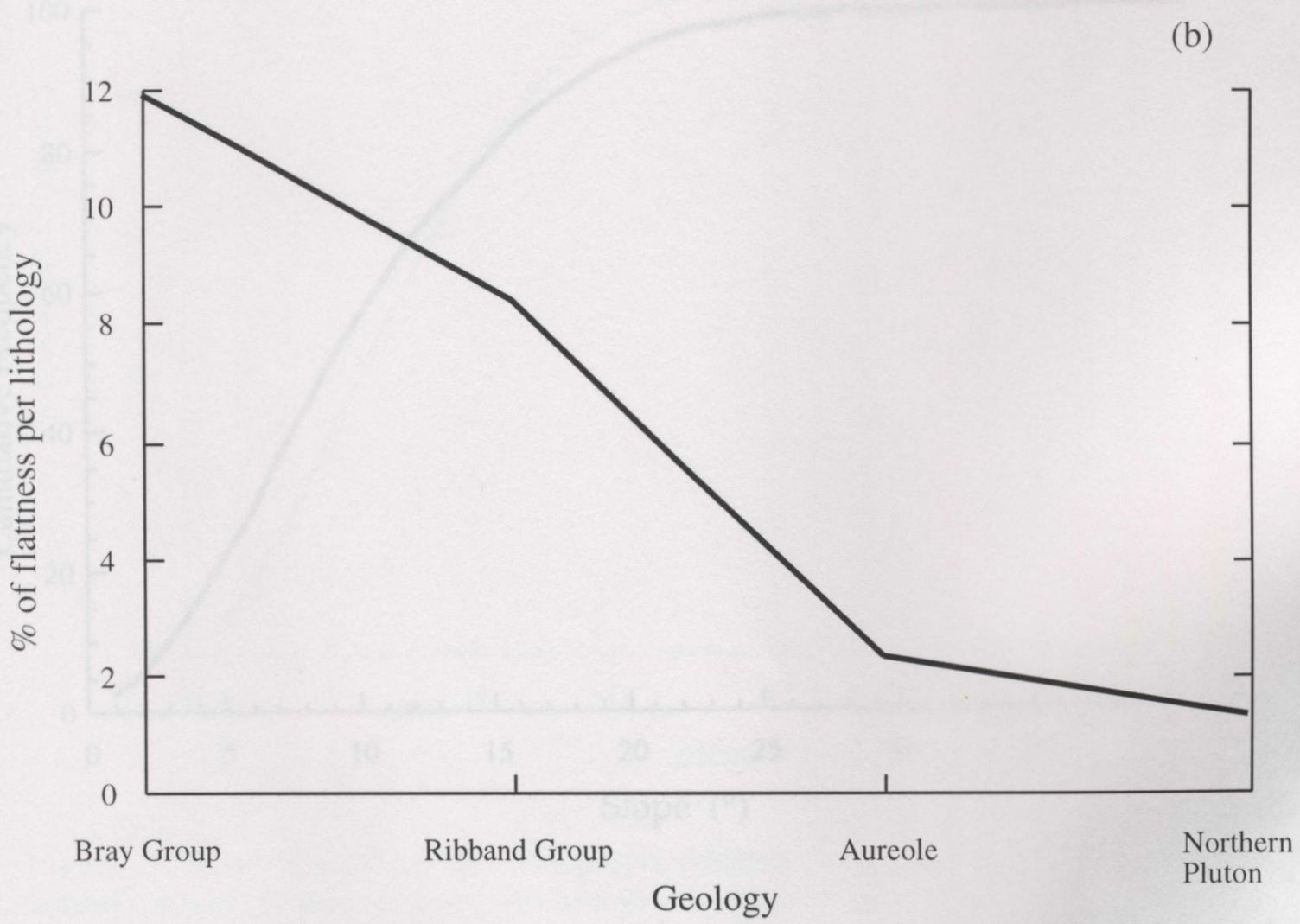

Figure 5.23a,b:- Graph showing slope characteristics of the main lithological types of the Vartry area. The Bray Group rocks form the maximum slopes (a) but also produce, the lowest average hill slope gradients (b).

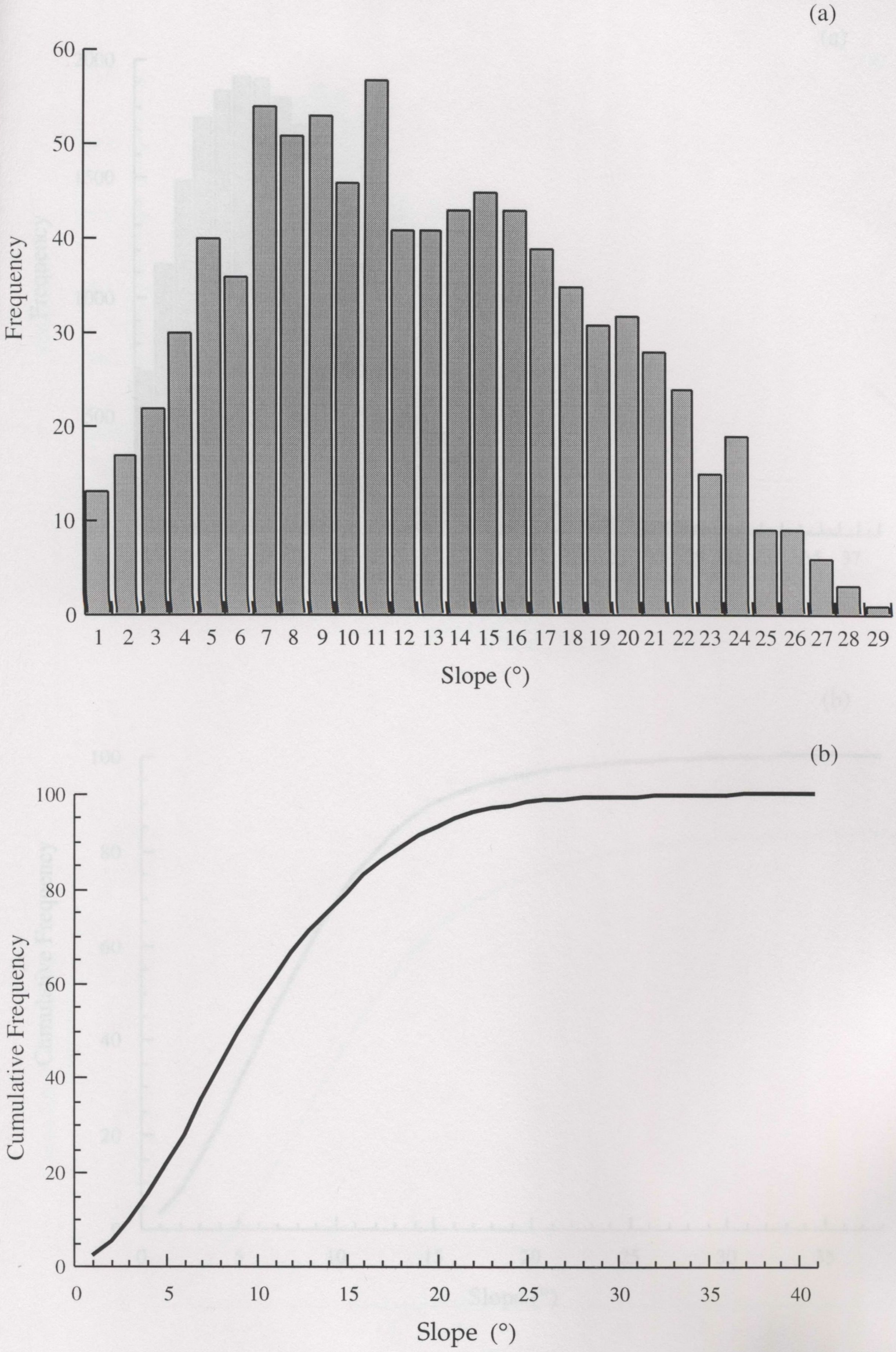

Figure 5.24a,b:- Histogram of slope type on quartzites. These form moderate to high slopes and are mostly due to differential weathering, with possible faulting (see figure 5.37).

(a)

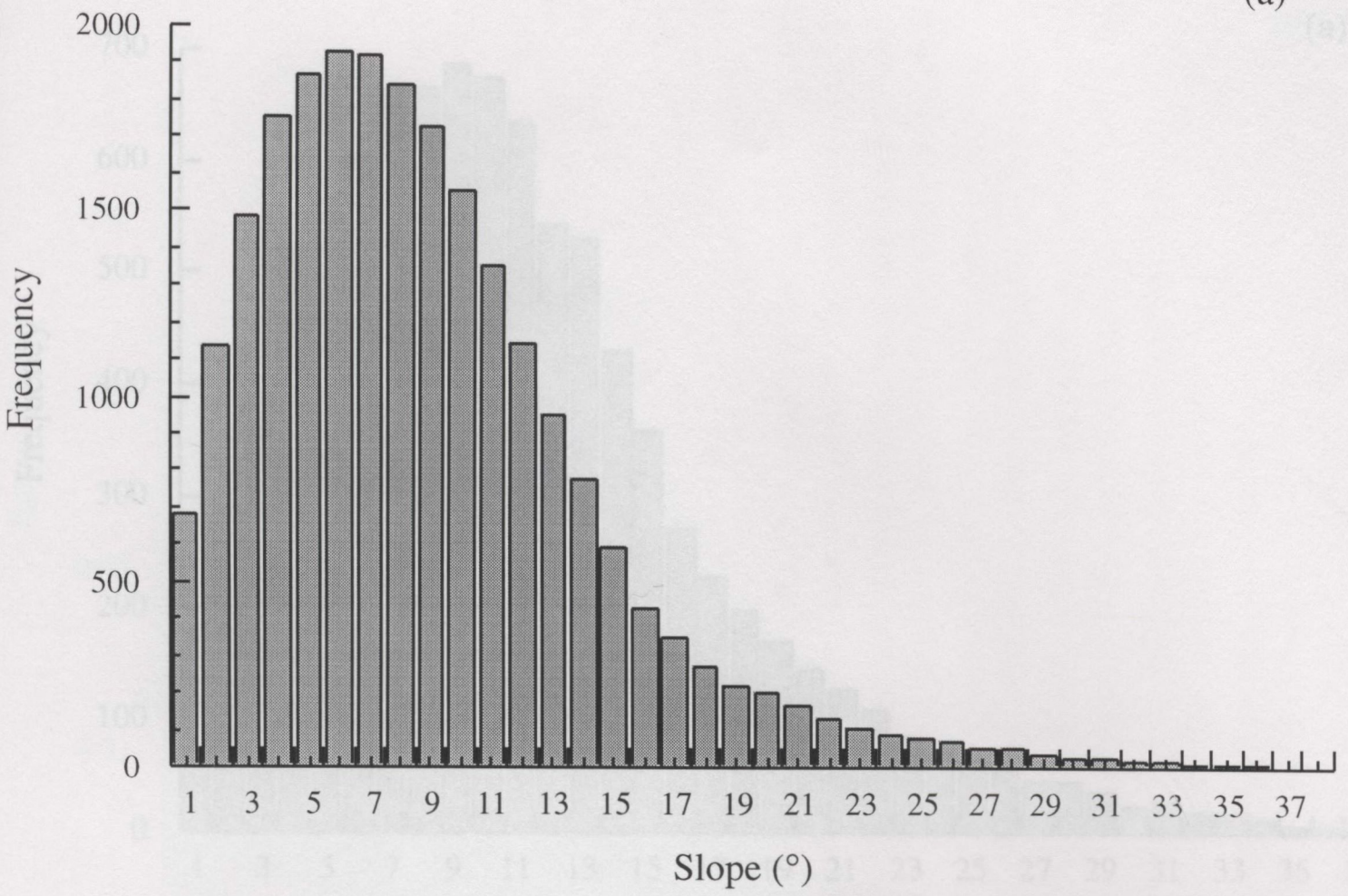

(b)

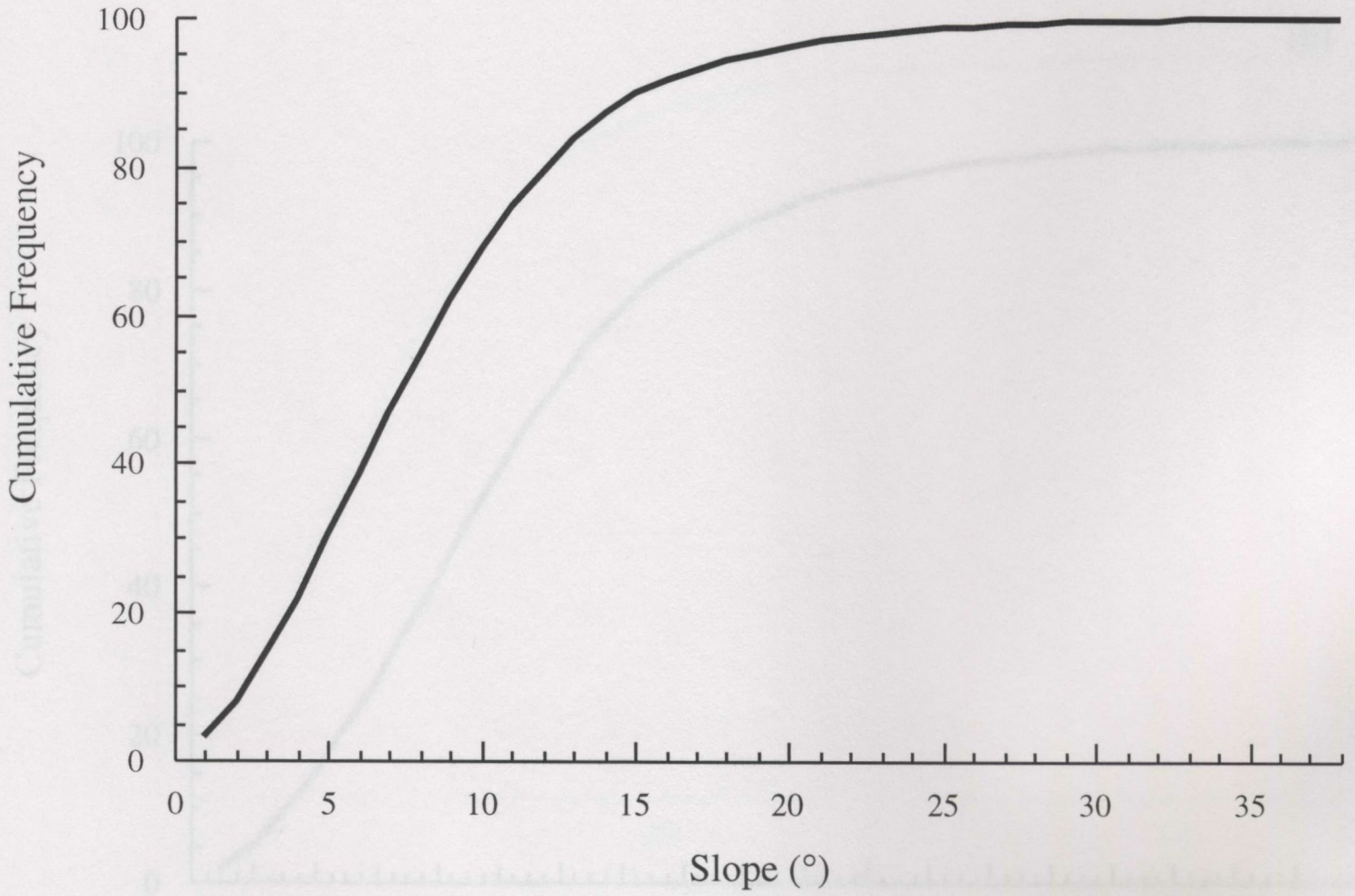

Figure 5.25a,b:- Histogram and cumulative frequency of slope type on Ribband Group (+ aureole) rocks. These tend to form low to moderate slope.

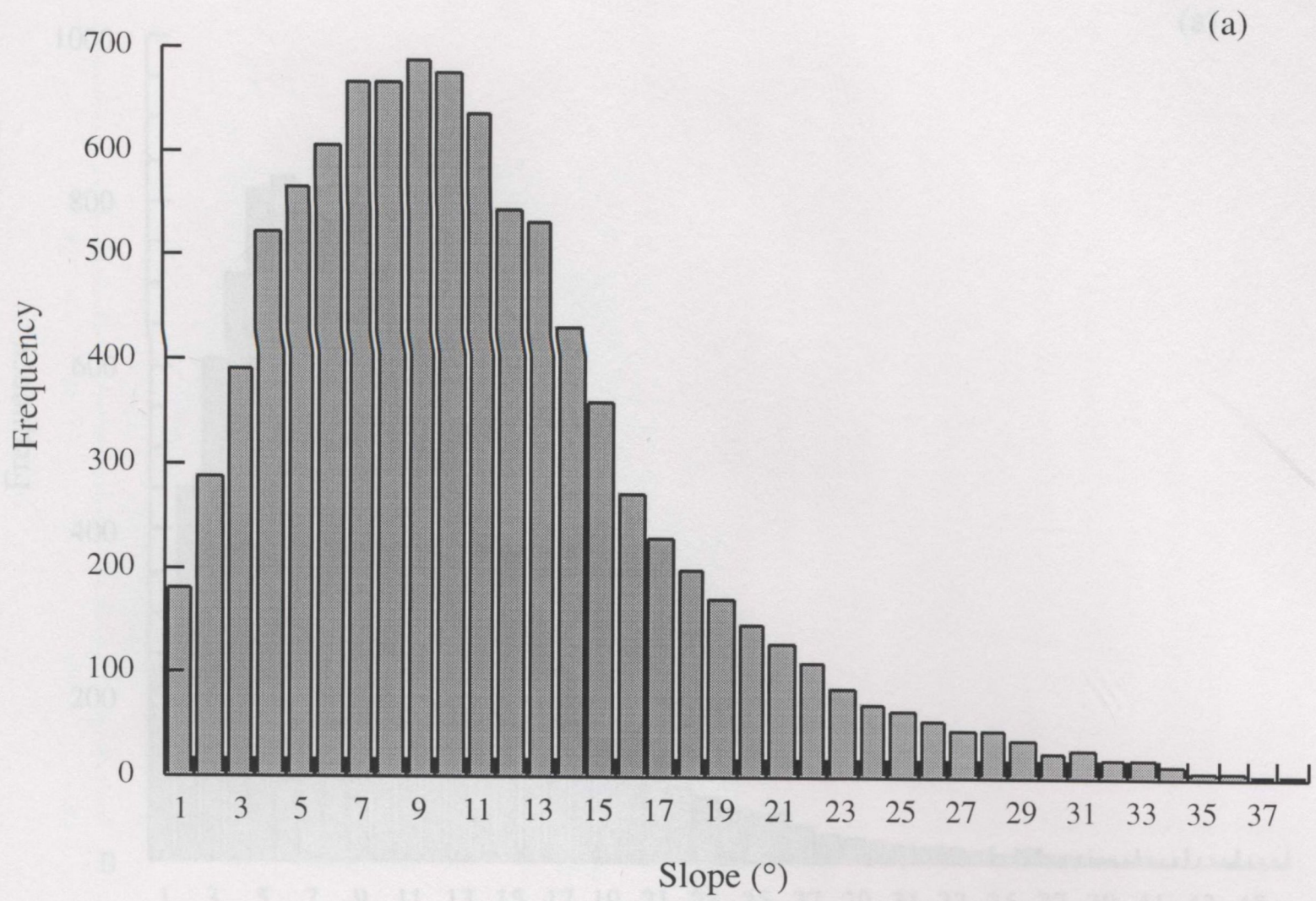

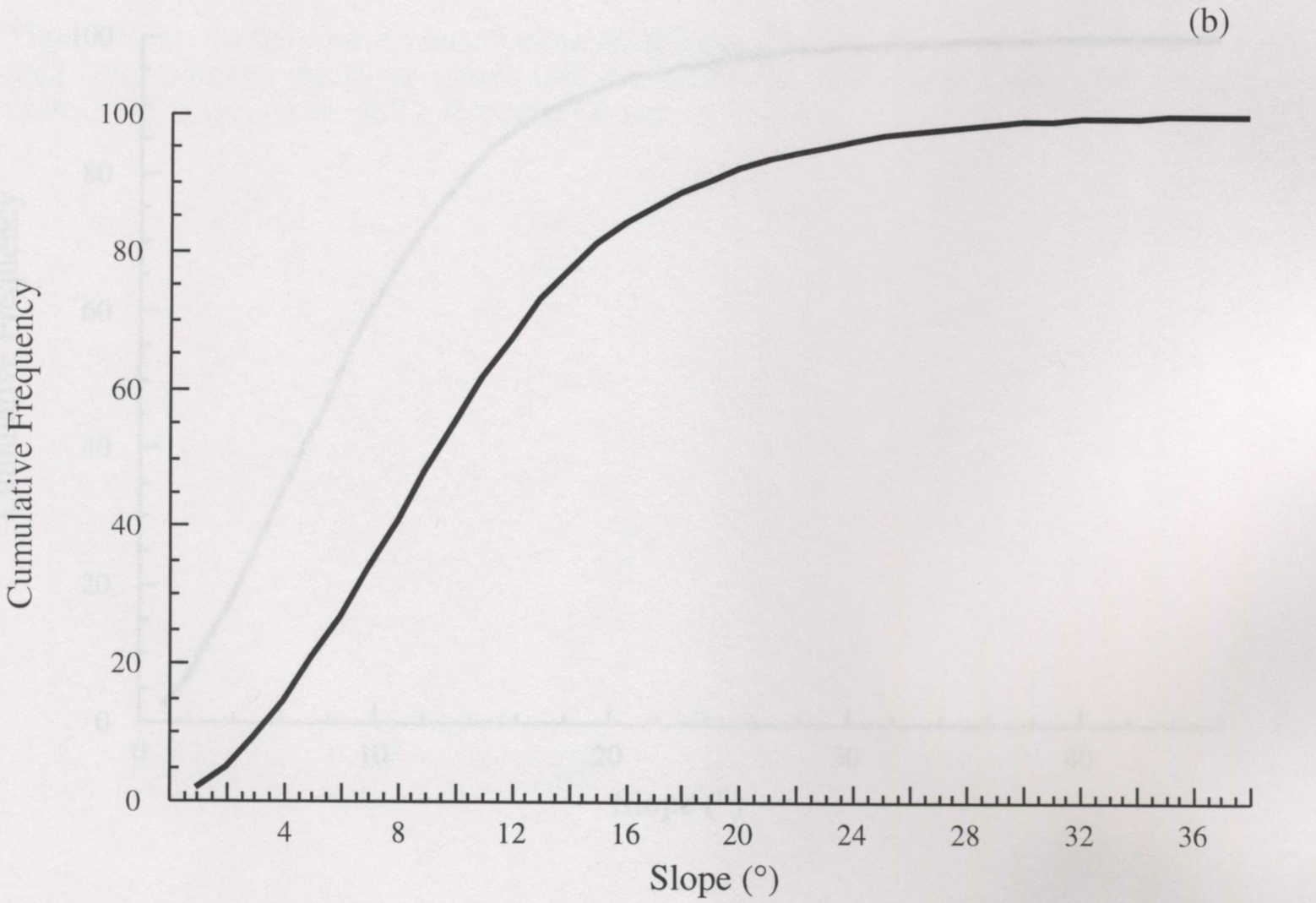

Figure 5.26a,b:- Histogram and cumulative frequency of slope type on aureole rocks. These rocks form mostly moderate slope and is in part due to incision of Tertiary glacial valleys.

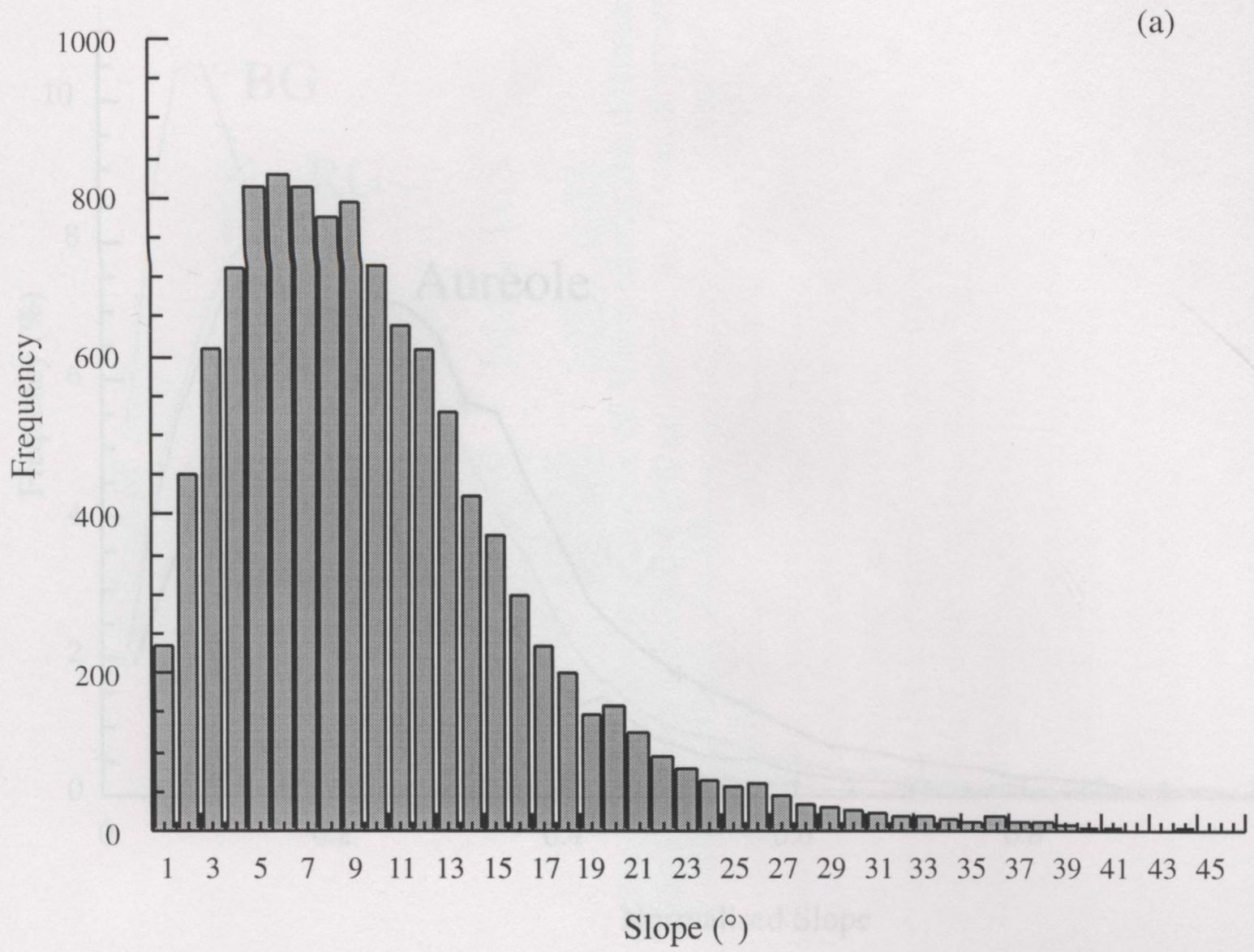

Figure 5.27a,b:- Histogram and cumulative frequency of slope type on rocks of the Northern pluton. Again, hills slope gradients on these rocks is low to moderate, and generally less than the Ribband Group rocks. This is probably due to Quaternary glaciers moving from the granitic areas with maximum erosion from bedrock fragments reaching the base of the glacier and further enhanced as ice is forced through aureole rocks (e.g. Farrington, 1934).

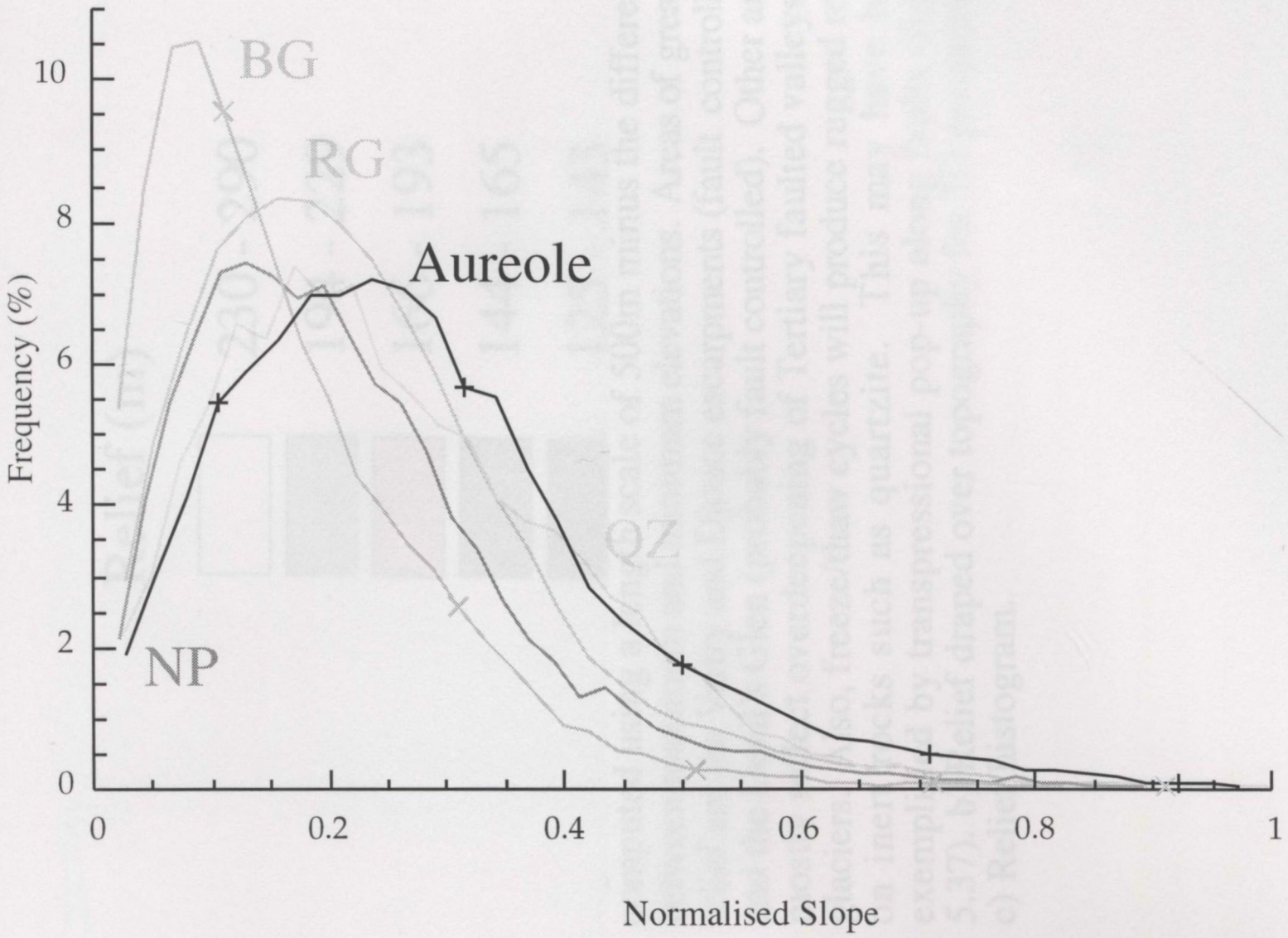

Figure 5.28:- Graph of normalised slope distribution for the main lithologies in the Vartry area. Normalising the slope values aids interpretation. BG – Bray Group, NP – Northern pluton; QZ – Quartzite; RG – Ribband Group.

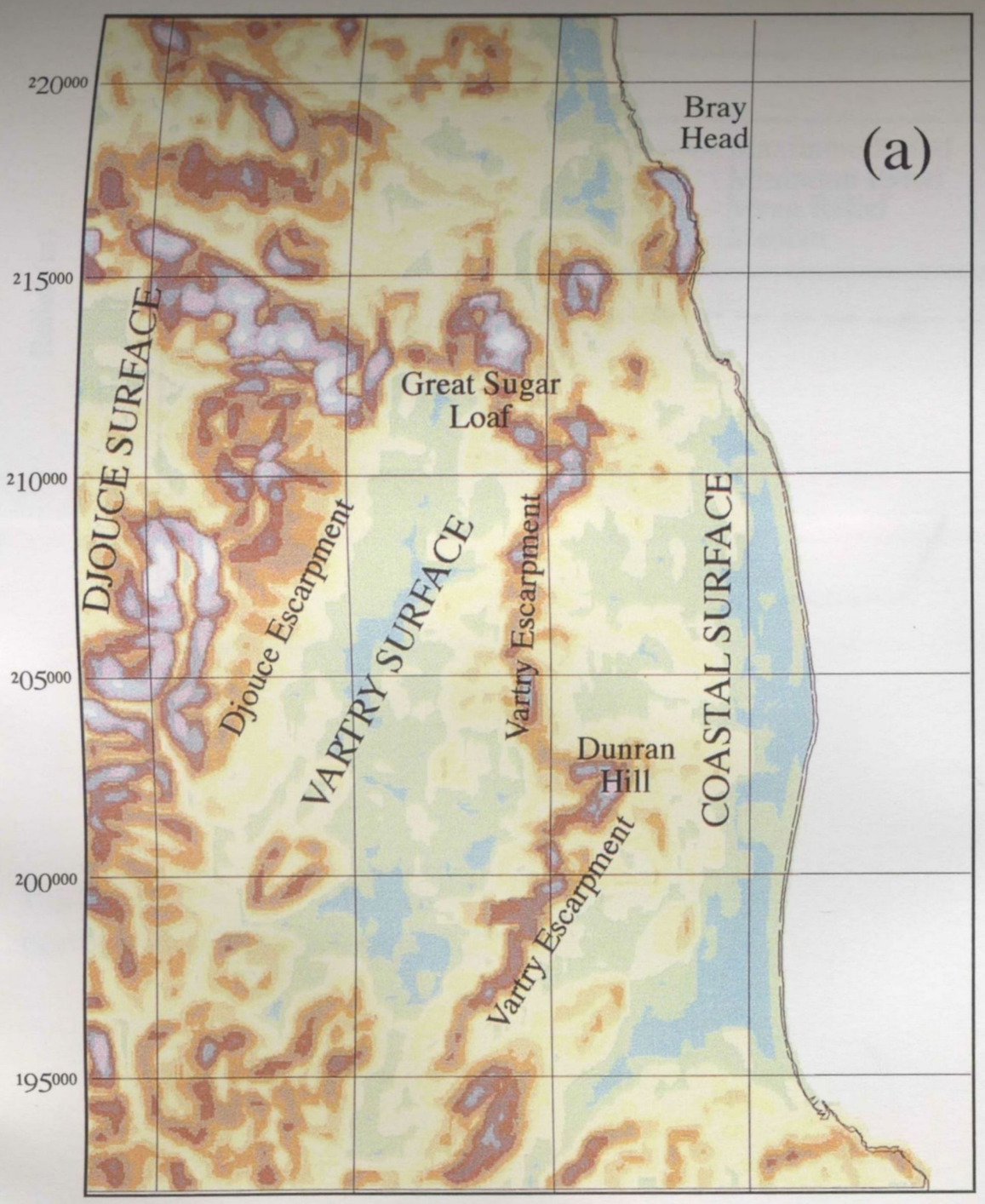

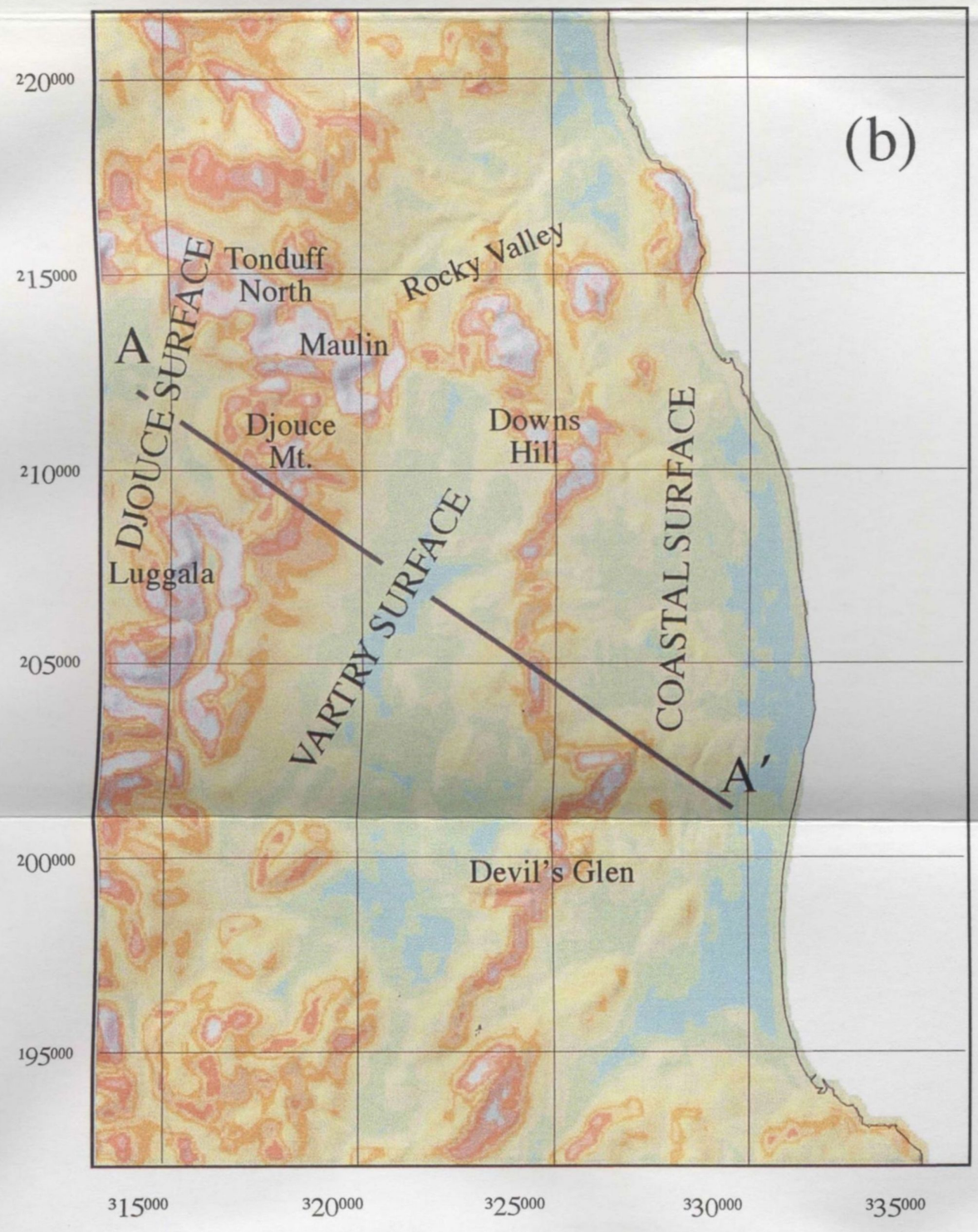

A ____ A′ Relief profile (see Fig5.36c)

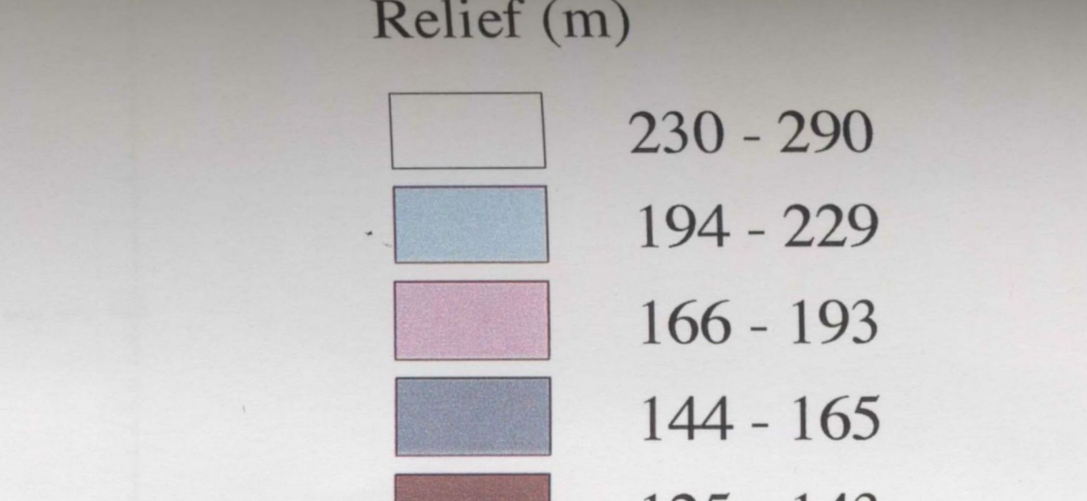

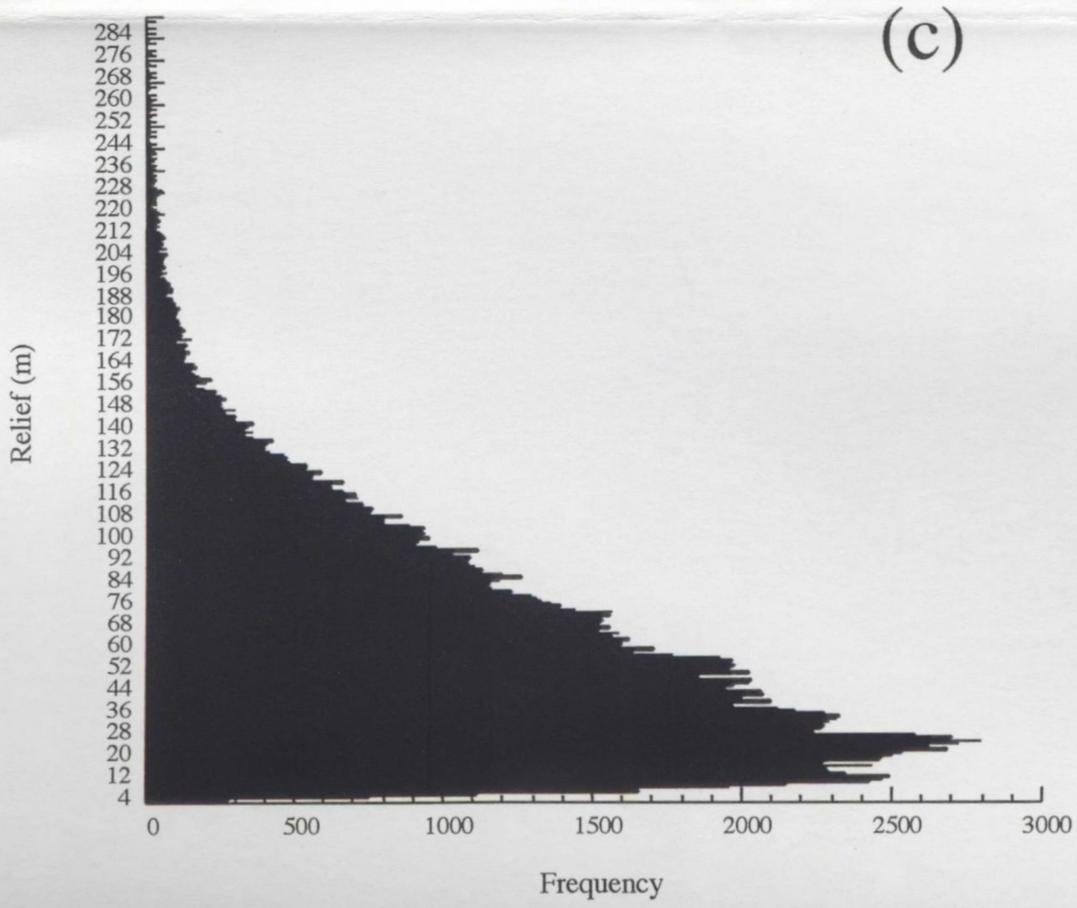

Figure 5.29a,b:- Relief images of the Vartry area. Relief is computed using a length scale of 500m minus the difference between maximum and minimum elevations. Areas of greatest relief are the Vartry and Djouce escarpments (fault controlled) and the Devil's Glen (probably fault controlled). Other areas mostly reflect overdeepening of Tertiary faulted valleys by glaciers. Also, freeze/thaw cycles will produce rugged relief on inert rocks such as quartzite. This may have been exemplified by transpressional pop-up along faults (figure 5.37). b) Relief draped over topography for 3D perspective. c) Relief histogram.

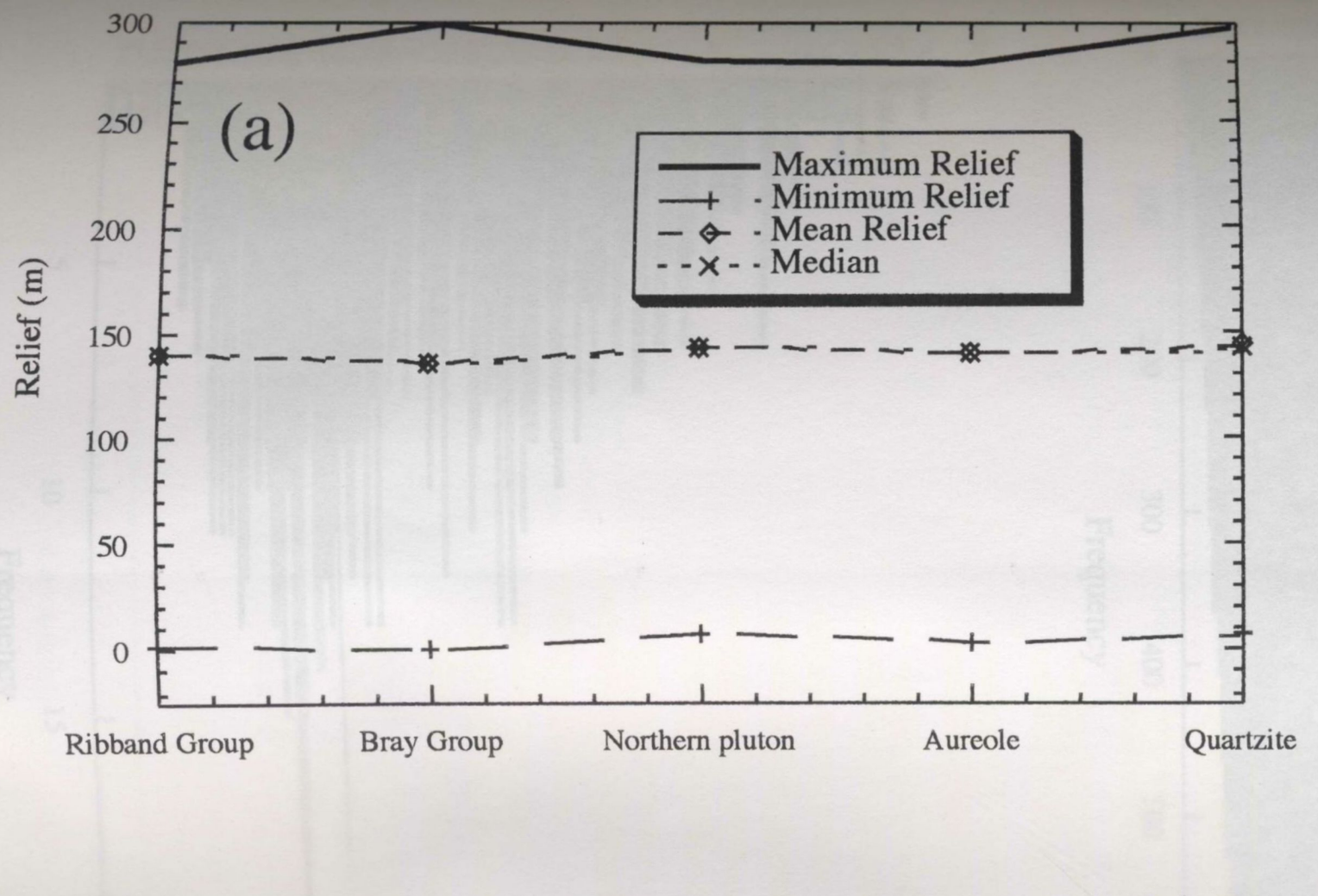

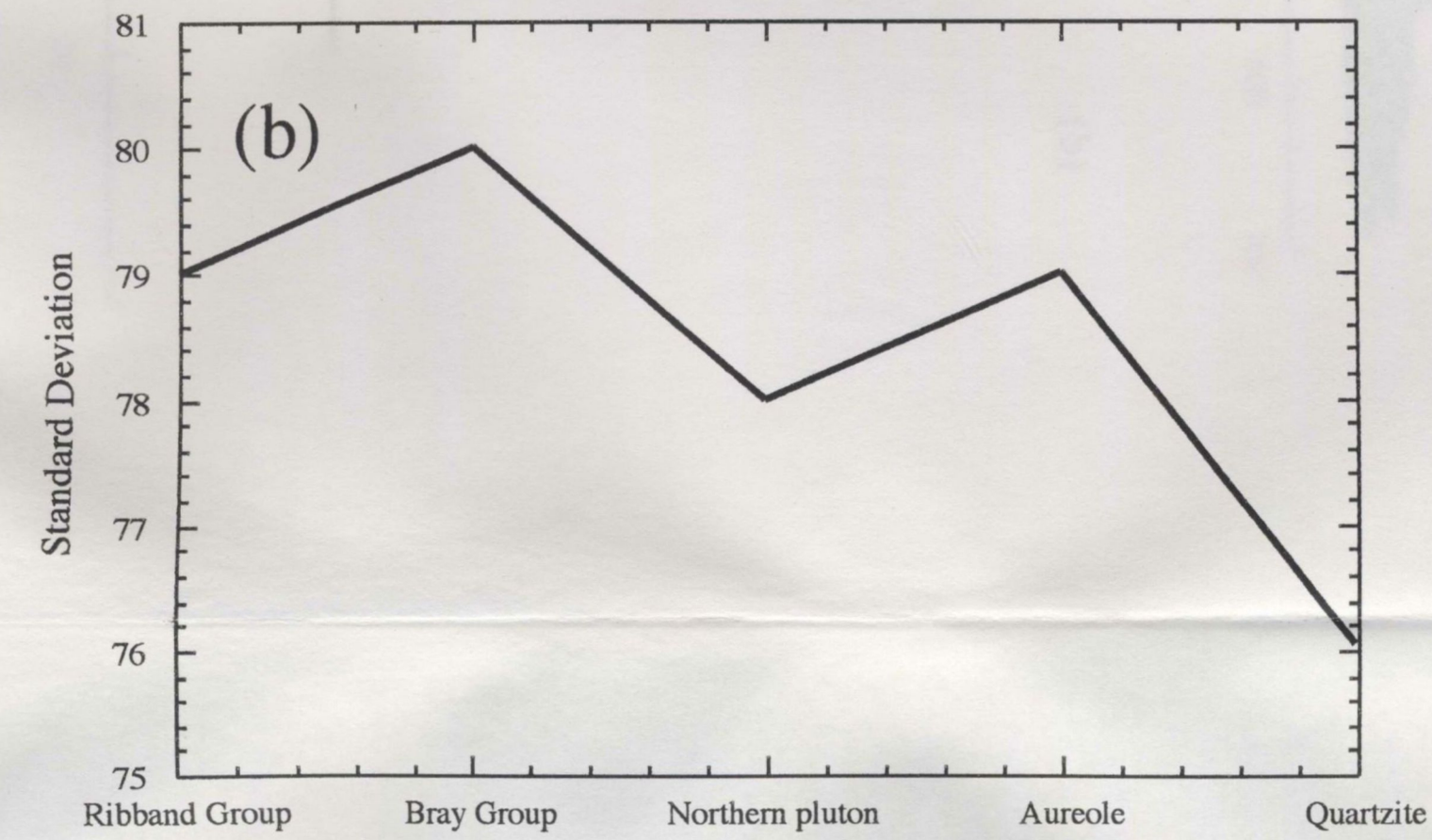

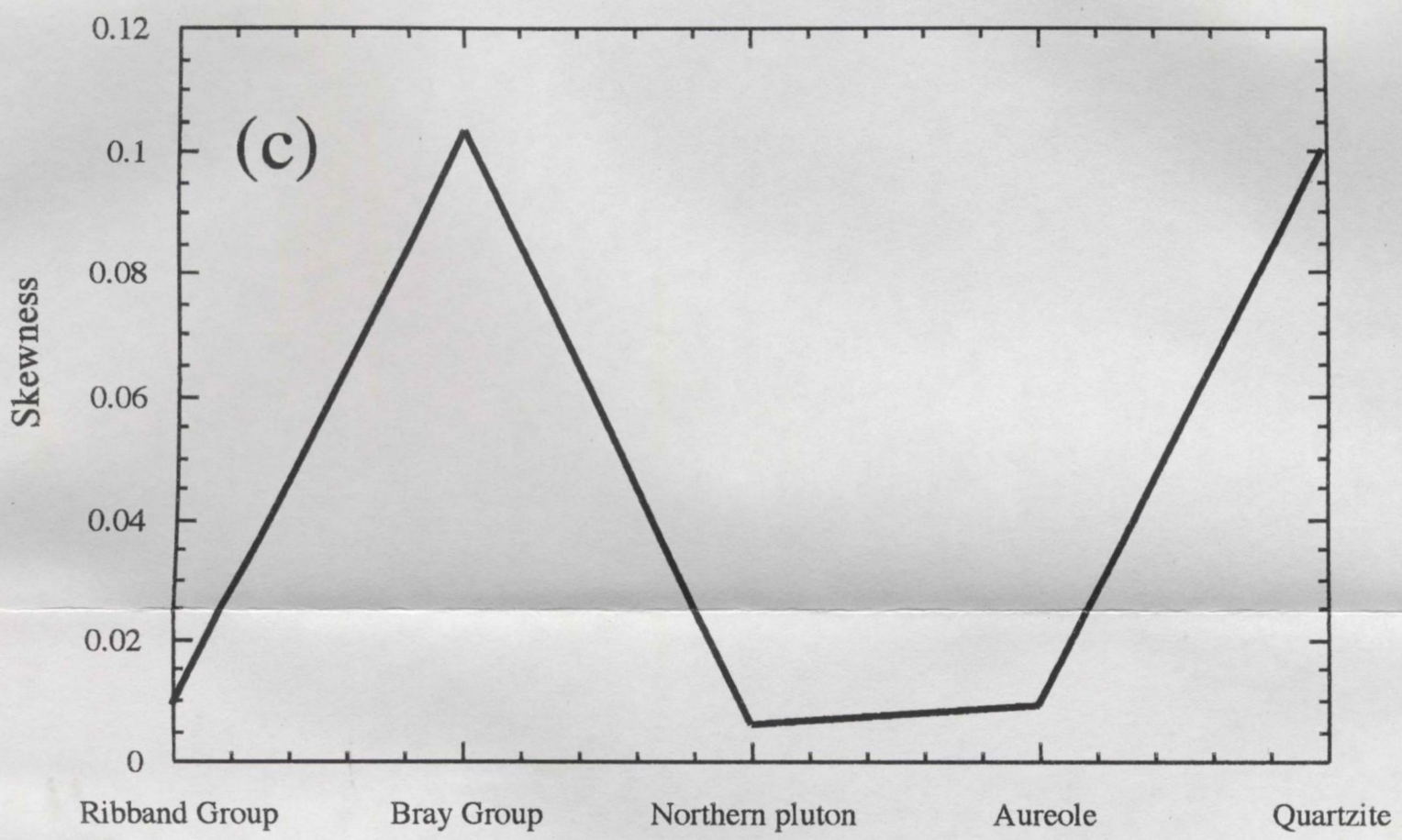

Figure 5.30a,b,c:- Descriptive statistical graphs showing the relationship between various rock type and relief in the Vartry area.

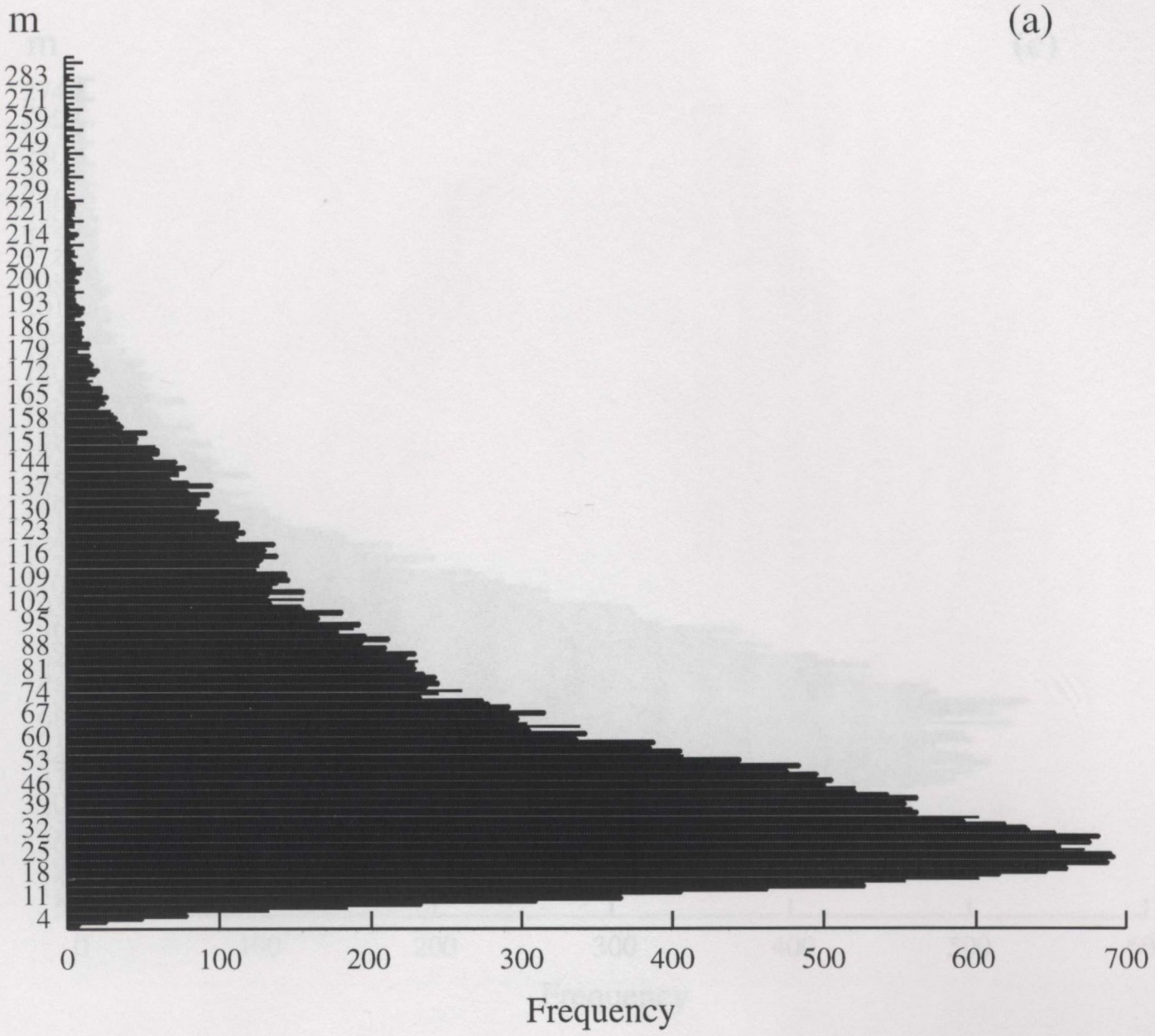

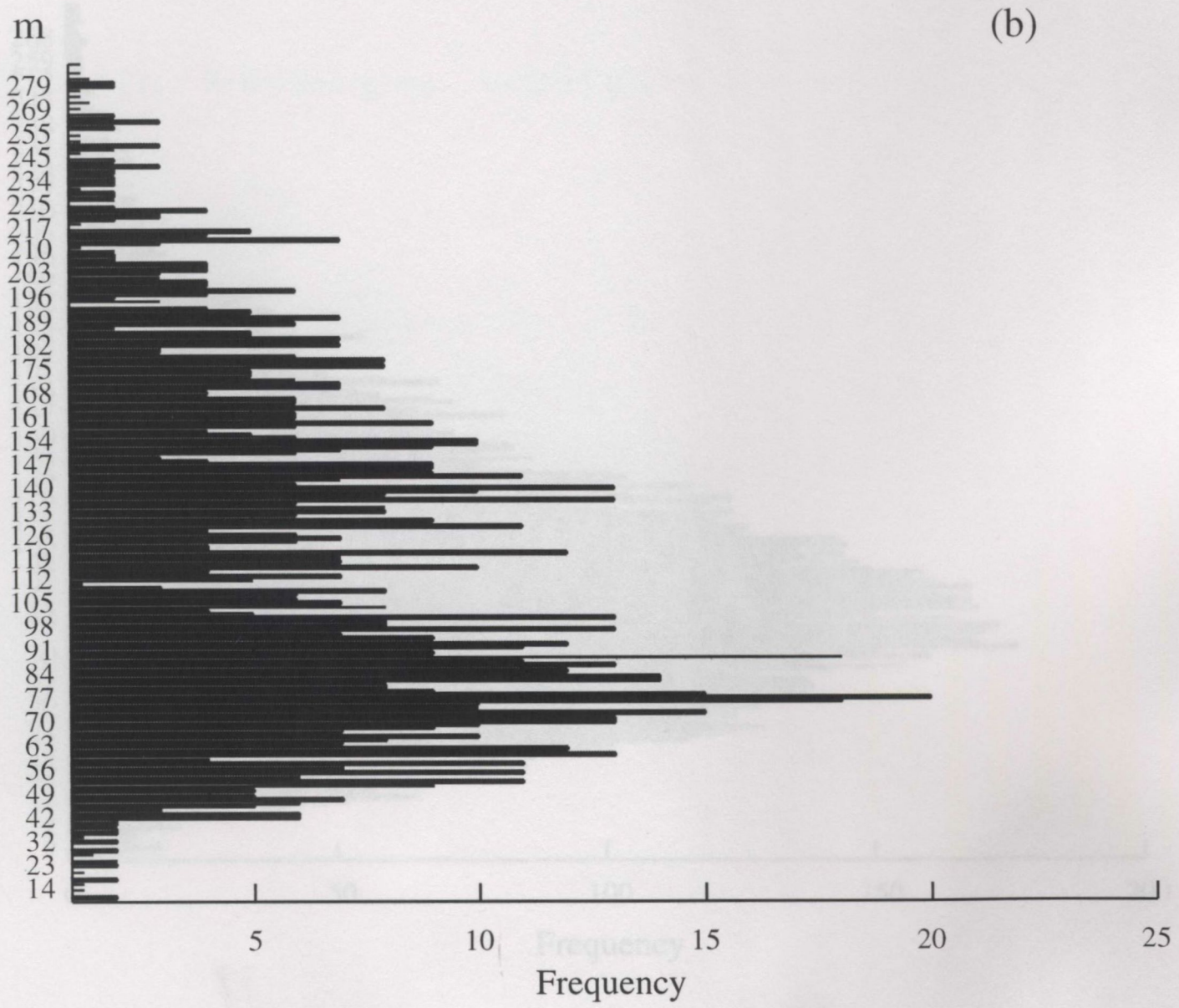

Figure 5.31a,b:- Relief histograms; a) Bray Group, b) Quartzites.

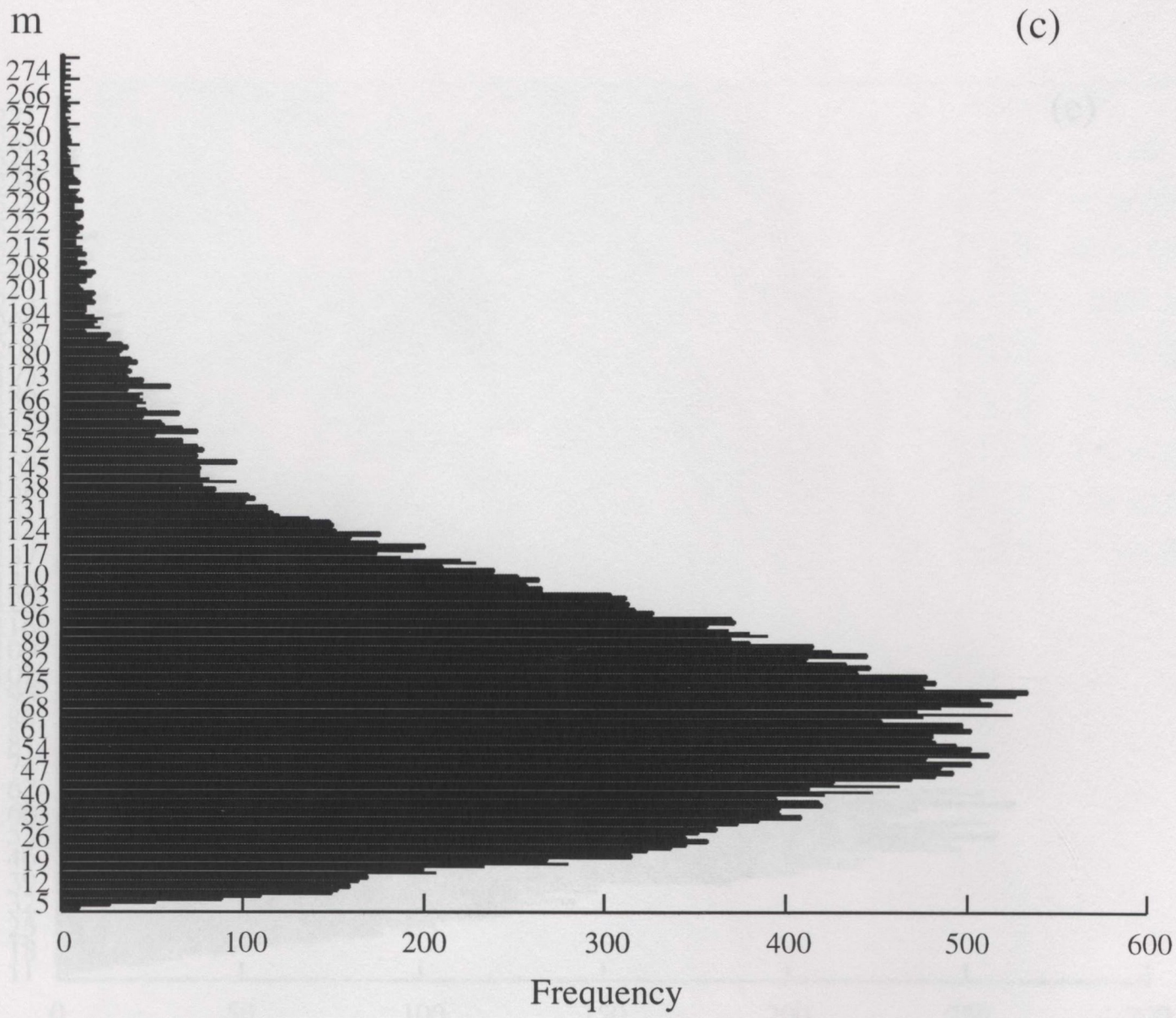

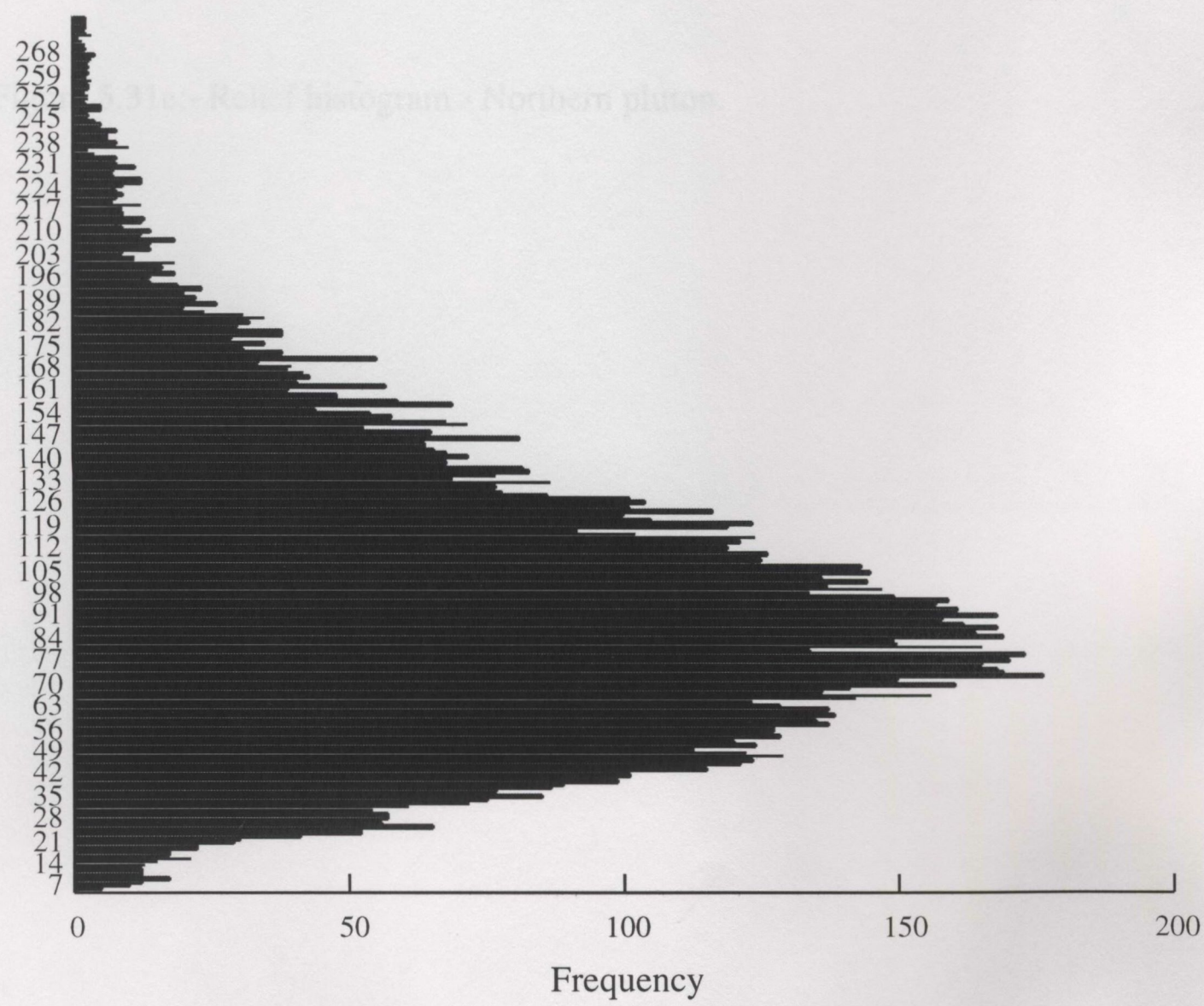

Figure 5.31c,d:- Relief histograms; c) Ribband Group (+ aureole), d) Aureole.

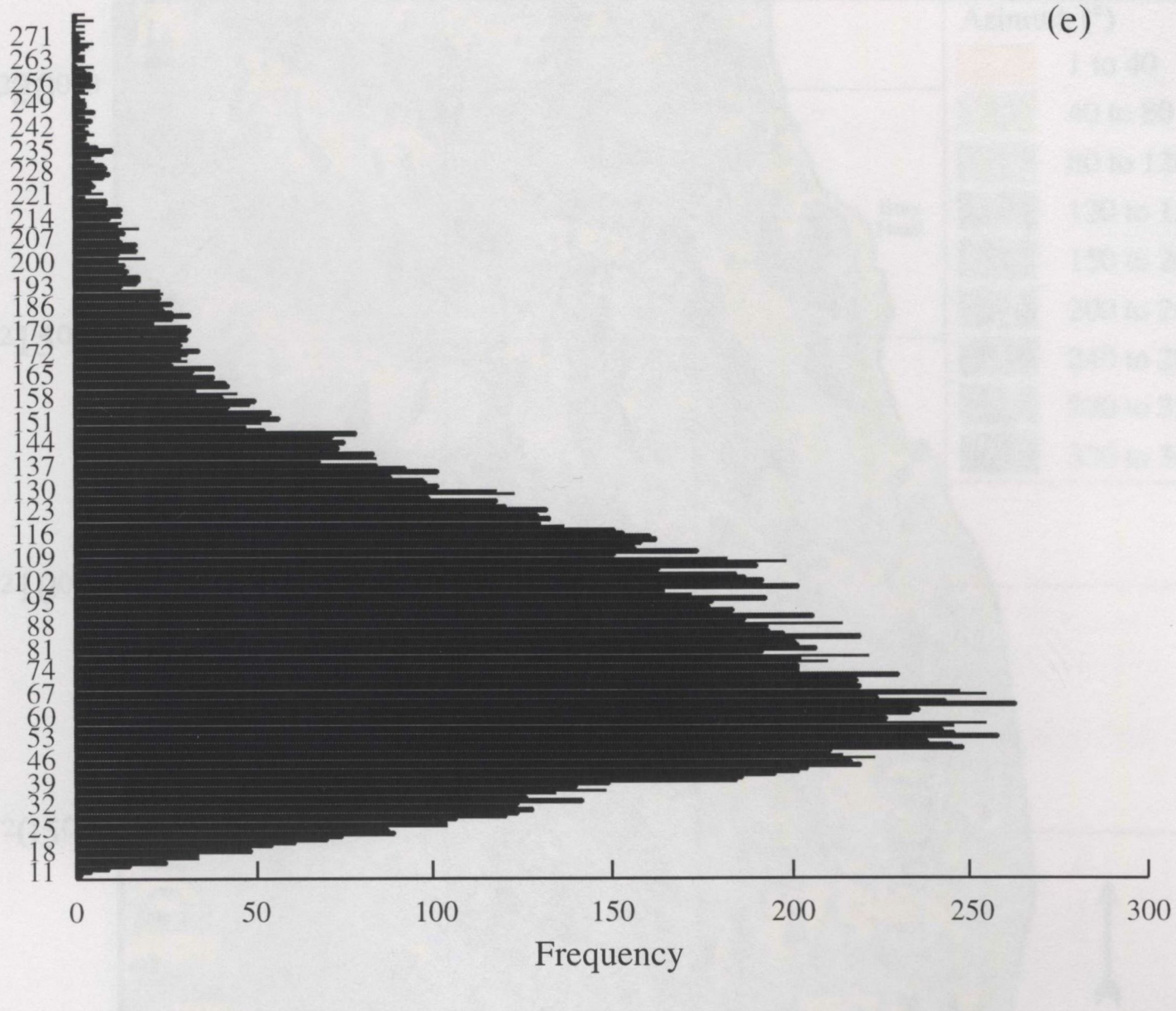

Figure 5.31e:- Relief histogram - Northern pluton.

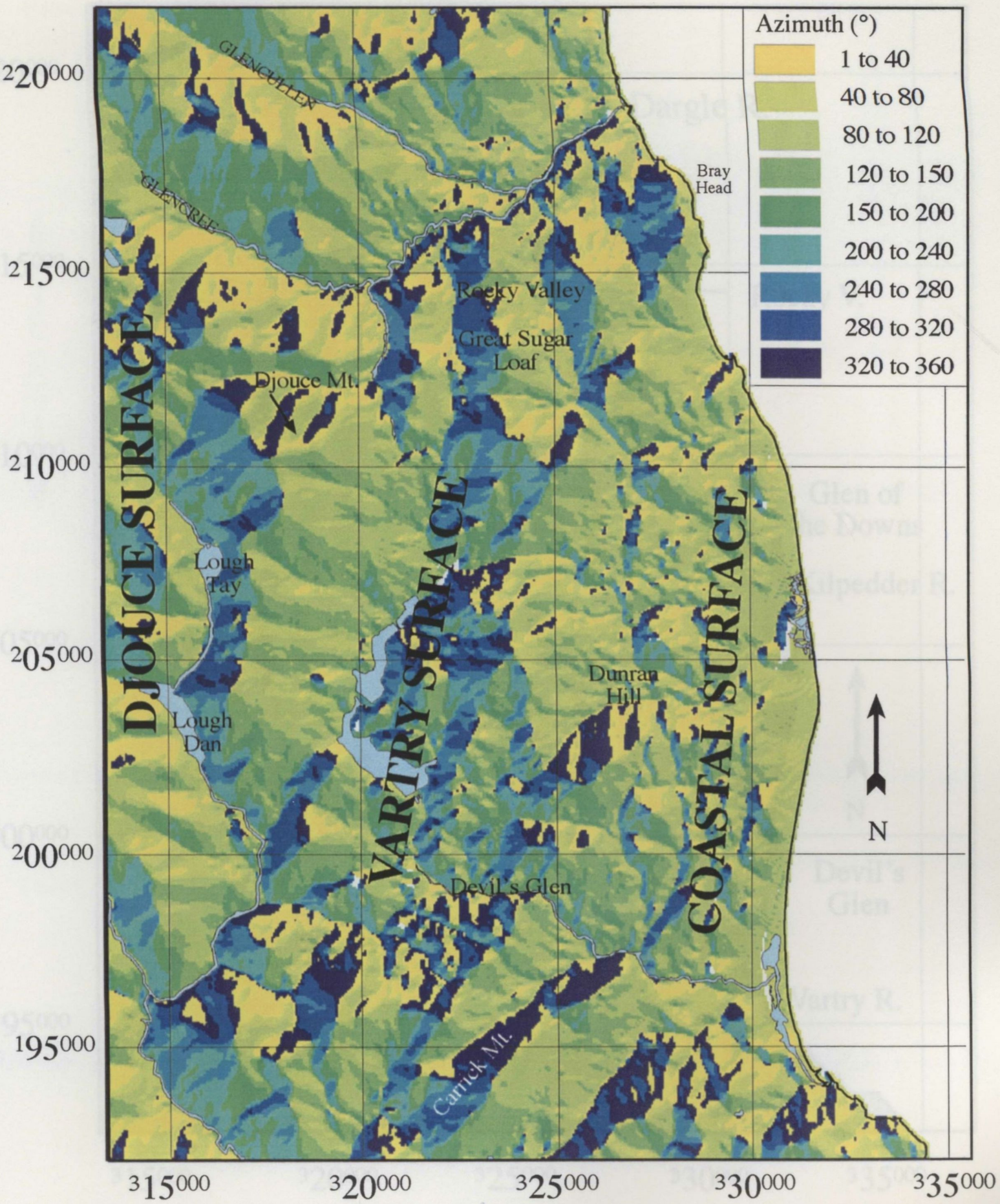

Figure 5.32:- Image showing aspect of the Vartry area. Note that the Vartry surface dips to the west at ~3° (e.g. see figure 5.18).

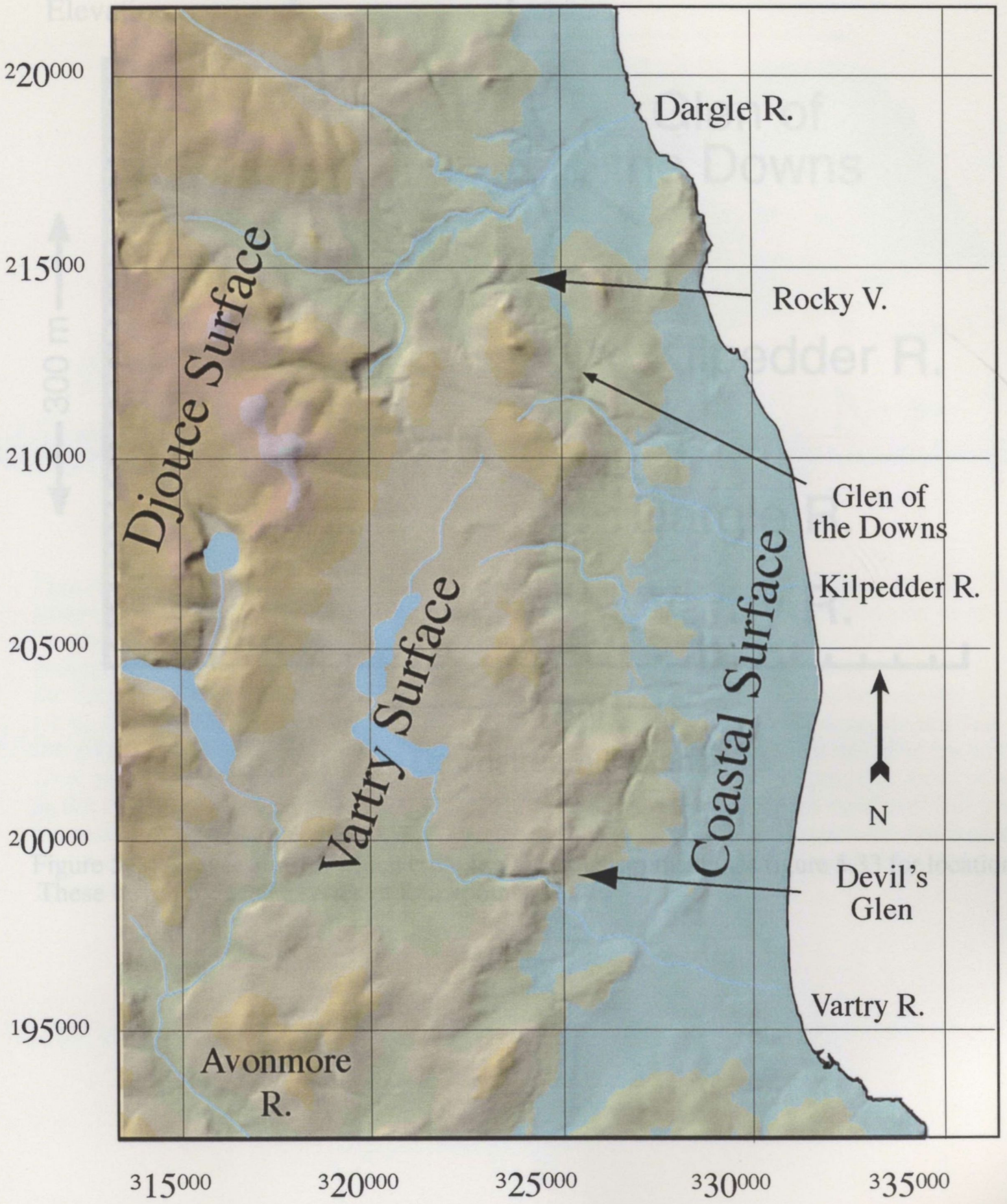

Figure 5.33:- Shaded relief topographic image of the Vartry area showing the main rivers that cross the area. A number of small rivers cross the Vartry escarpment (see figure 5.34 below).

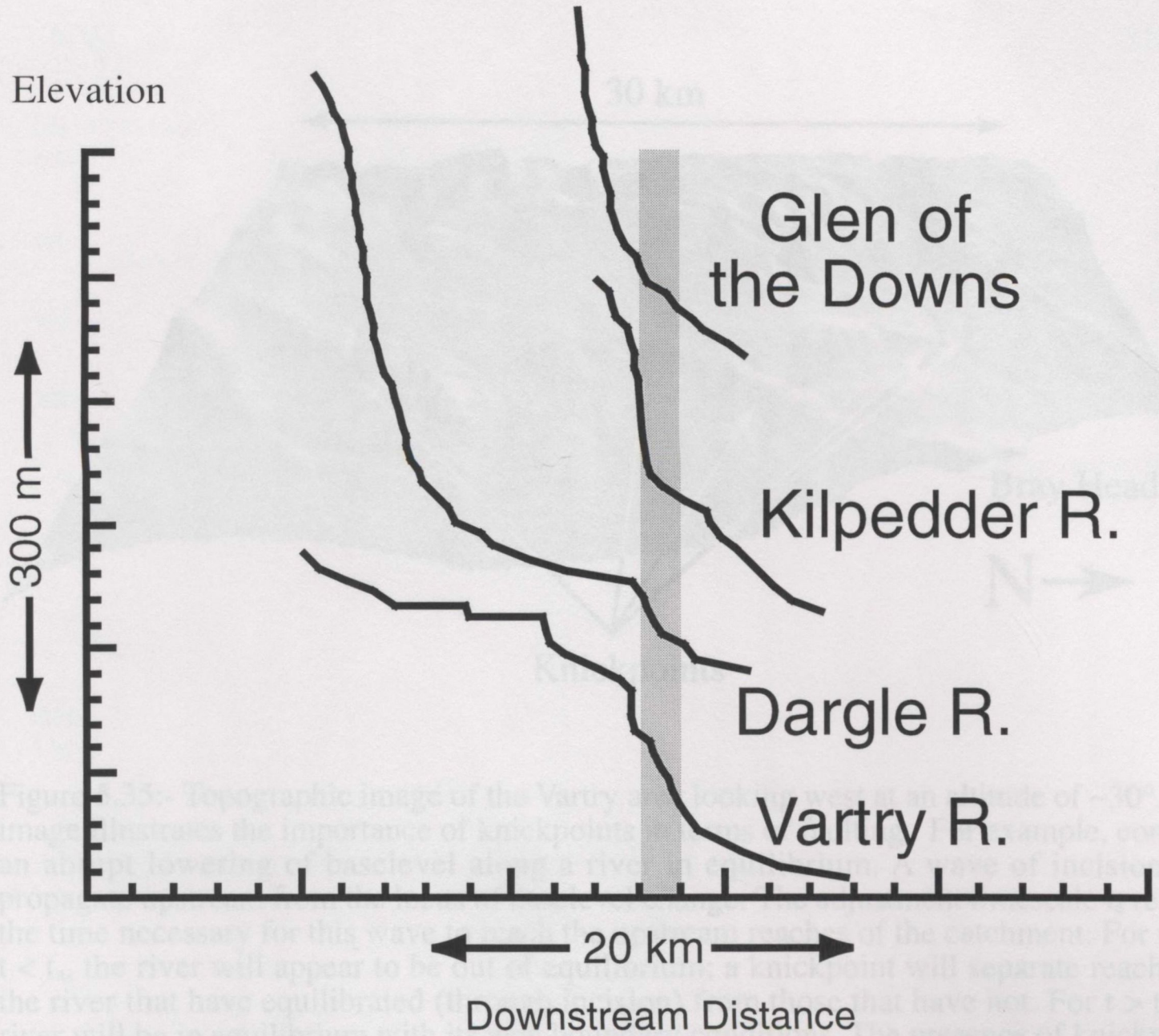

Figure 5.34:- River profiles which cross the Vartry escarpment (see figure 5.33 for location). These have produced a series of knickpoints.

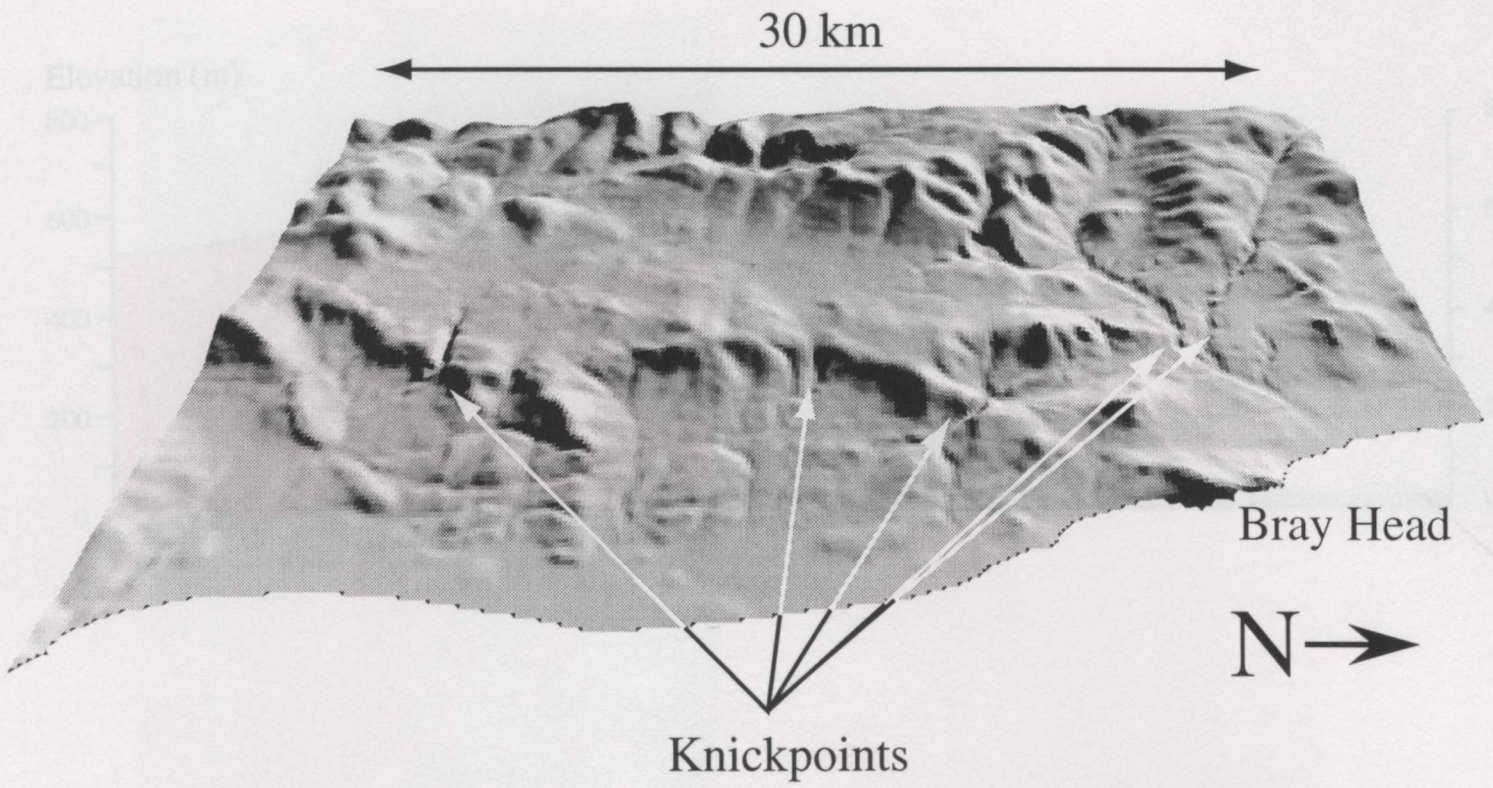

Figure 5.35:- Topographic image of the Vartry area looking west at an altitude of ~30°. This image illustrates the importance of knickpoints in terms of faulting. For example, consider an abrupt lowering of baselevel along a river in equilibrium. A wave of incision will propagate upstream from the locus of baselevel change. The adjustment timescale t_a reflects the time necessary for this wave to reach the upstream reaches of the catchment. For times $t < t_a$, the river will appear to be out of equilibrium; a knickpoint will separate reaches of the river that have equilibrated (through incision) from those that have not. For $t > t_a$, the river will be in equilibrium with its new boundary conditions. The presence of knickpoints in the catchments draining the Vartry surface argues that the most recent baselevel fall must have occurred less than t_a years ago, and the spatial correspondence between the knickpoints and the escarpment implies that the knickpoints have not yet migrated significant distances upstream (Cunningham *et al.,* in prep).

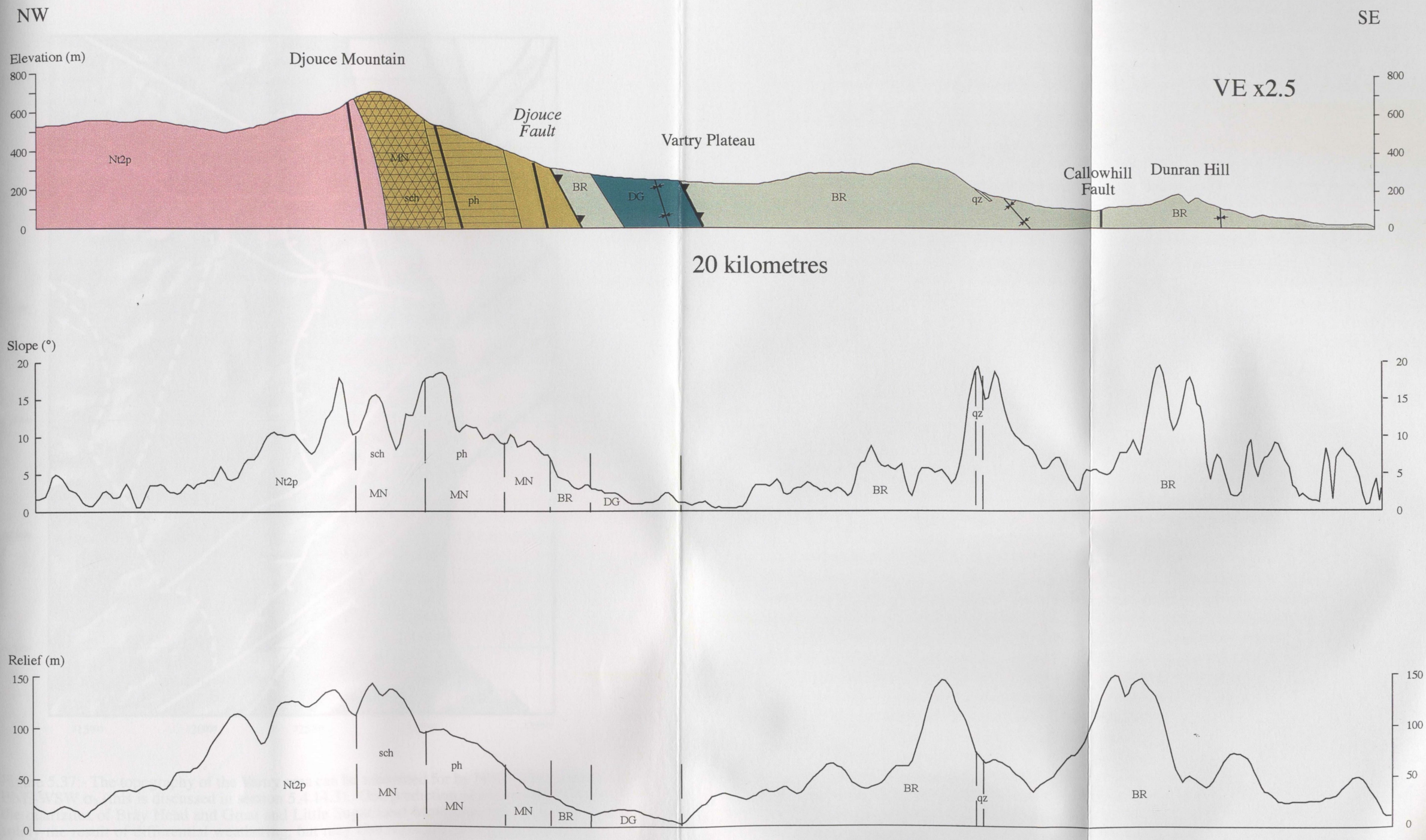

Figure 5.36a,b,c:- NW-SE geological, slope and relief profiles of the Vartry area. Abrupt changes in slope do not have a strong association with variations in rock type. Hence, the controlling factors is faulting.

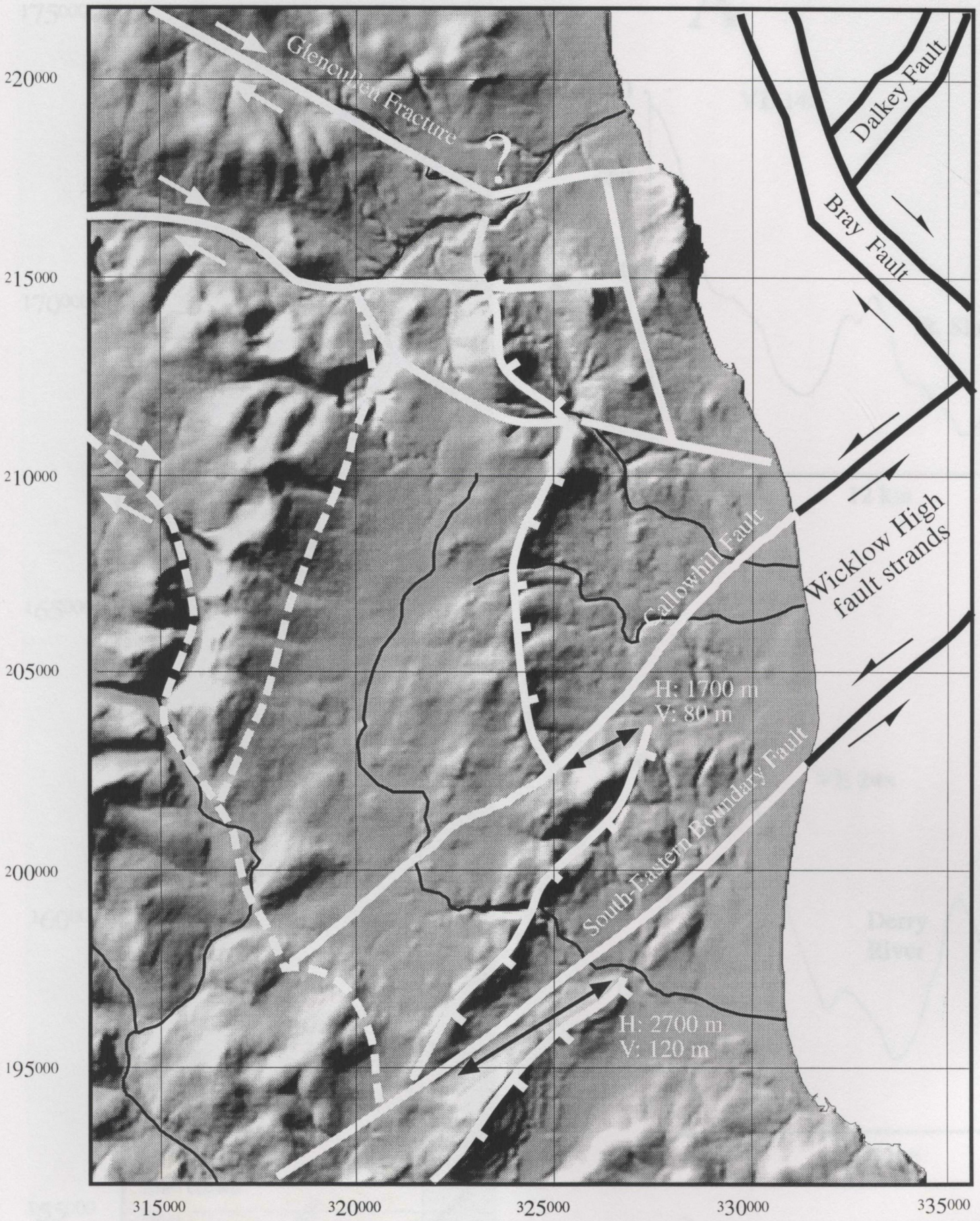

Figure 5.37:- The topography of the Vartry area can be accounted for by NNW-SSE σ_1 and ENE-WSW σ_3 (this is discussed in section 5.4.14.3). One prediction of this model is that the quartzites of Bray Head and Great and Little Sugar Loaf Mountains may not just be solely the result of differential weathering, but may also represent pop-up structures on restraining bends between NW-SE trending dextral faults.

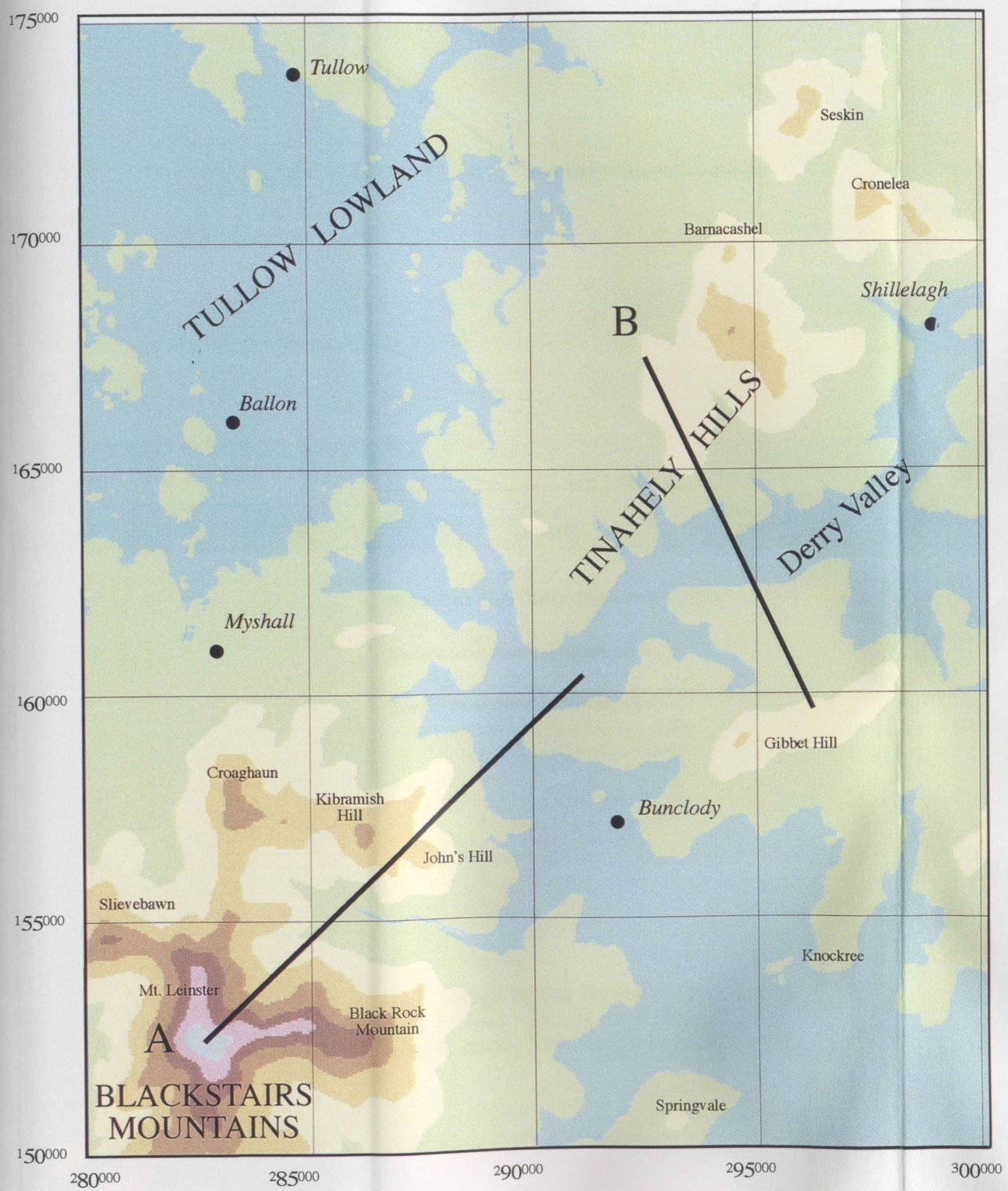

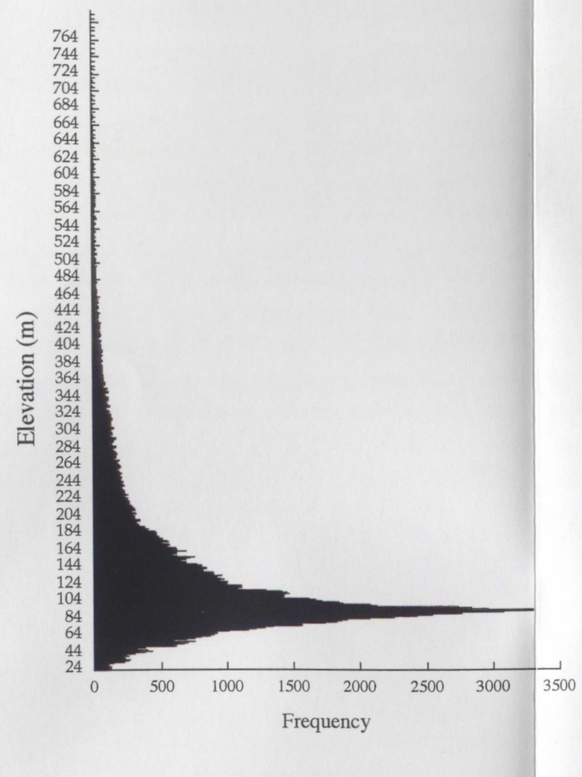

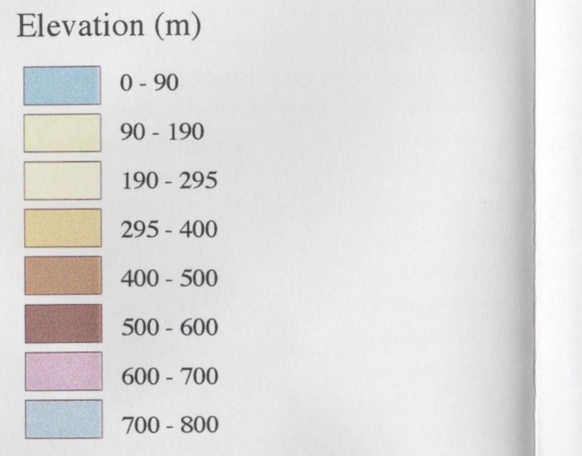

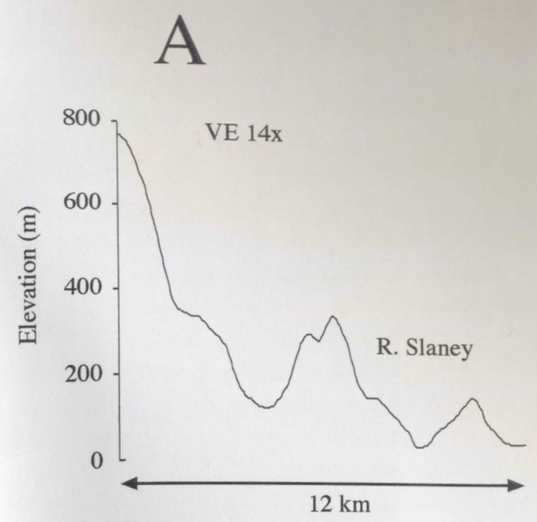

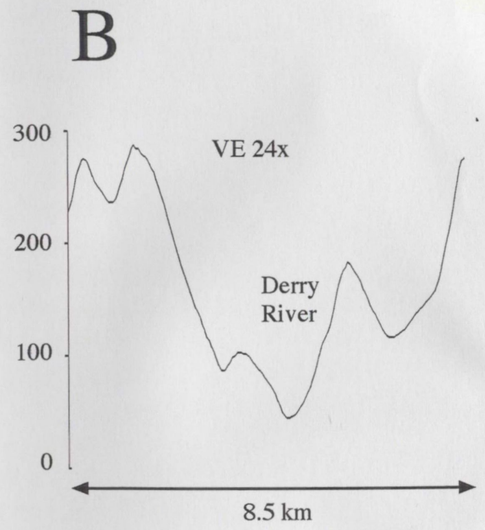

Figure 5.38:- DEM and elevation histogram for the Bunclody area of study. The area is dominated by transitional to base-level processes, with the exception of Mt Leinster, and the area occupied by a major Caledonian shear zone (East Carlow Deformation Zone - ECDZ).

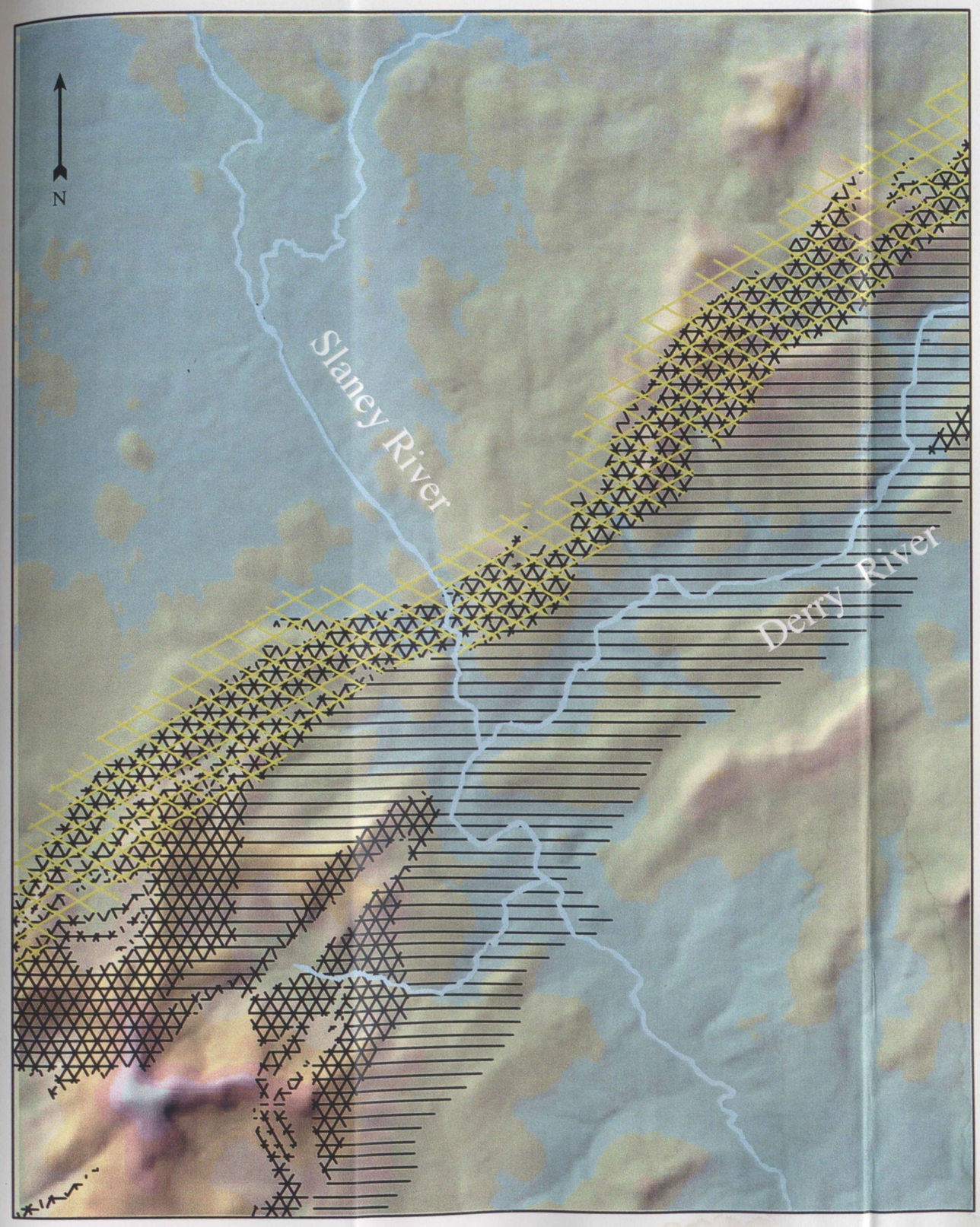

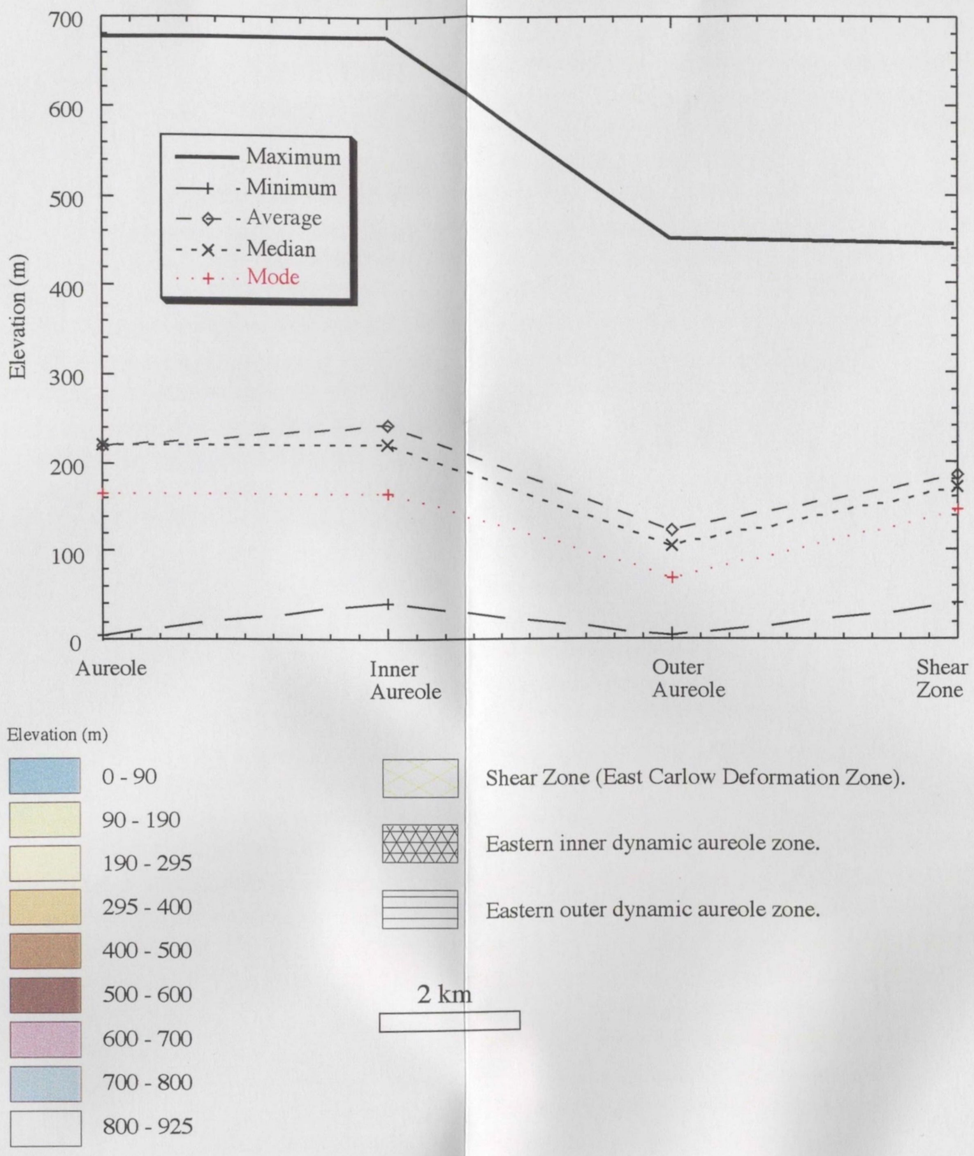

Figure 5.39:- Shaded relief topographic image of the Bunclody study area showing the extent of the inner and outer aureole rocks of the Ribband Group. The ECDZ partially overlaps with aureole rocks. The margins mostly occur within rocks of the Tullow pluton.

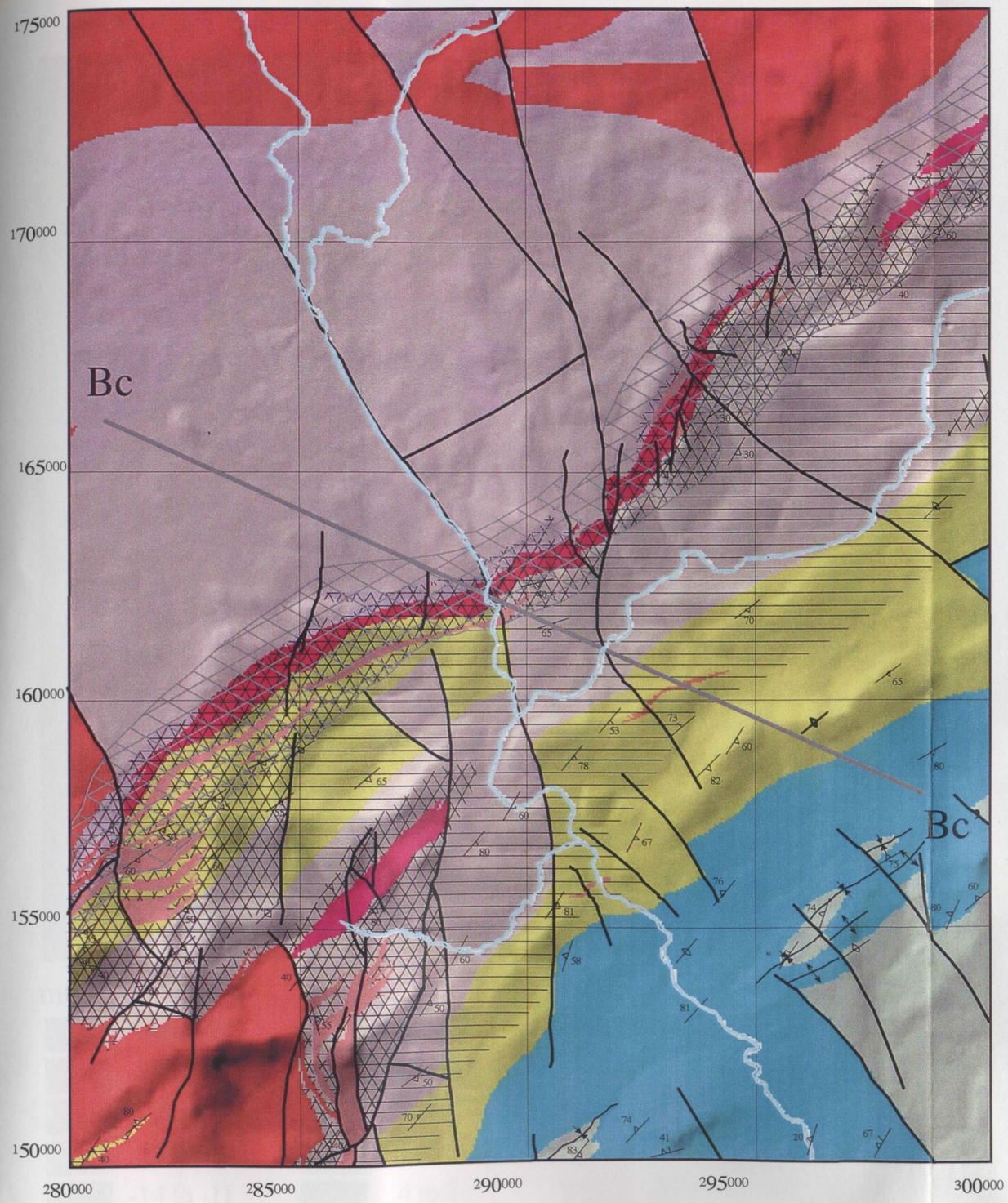
175000
170000
165000
160000
155000
150000
280000
285000
290000
295000
300000
Bc
Bc
Bc

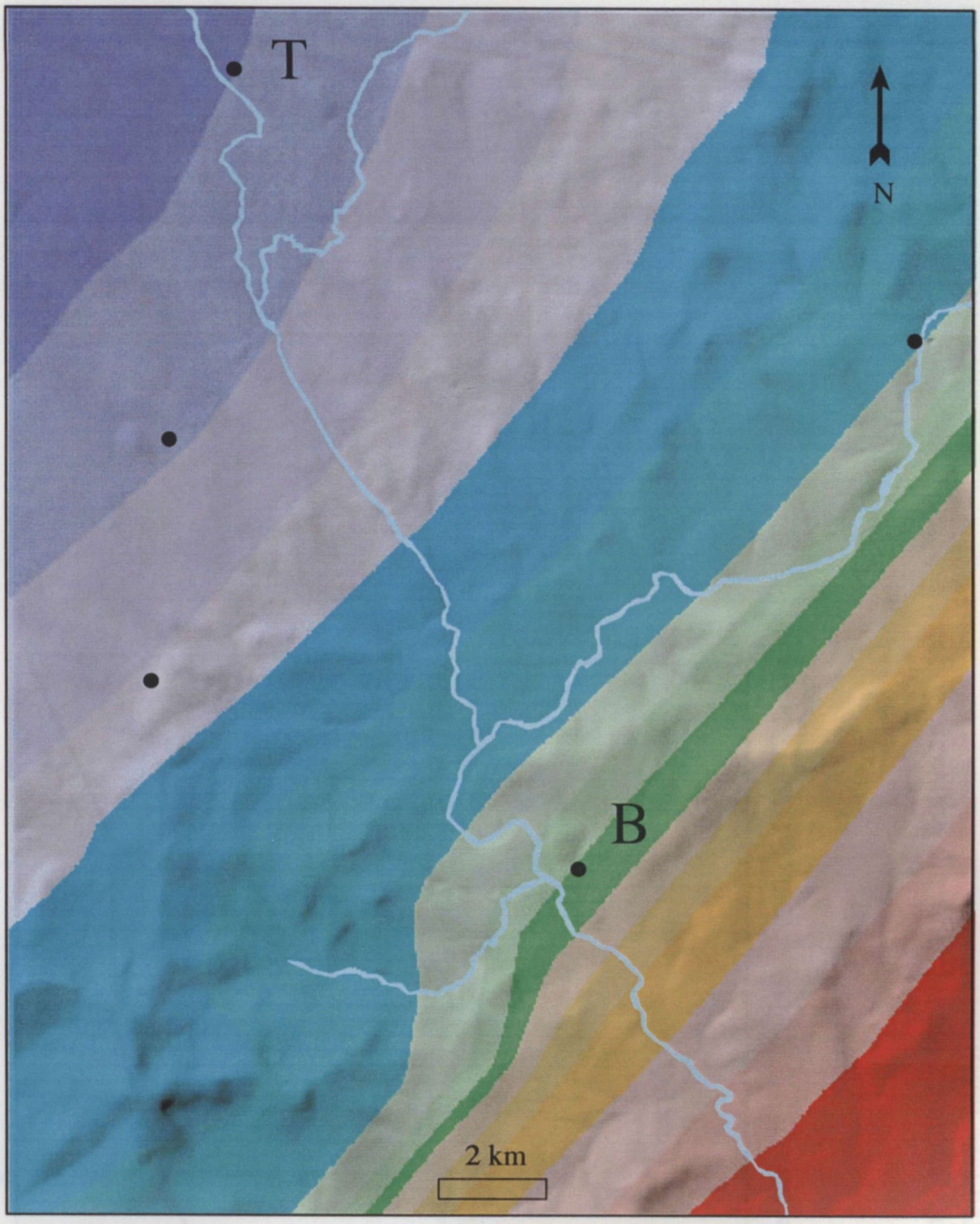

mGal

-26 to -22	-8 to -5	10 to 13
-22 to -19	-5 to -2	13 to 16
-19 to -17	-2 to 1	16 to 19
-17 to -14	1 to 4	19 to 22
-14 to -11	4 to 7	22 to 25
-11 to -8	7 to 10	25 to 29

Figure 5.41:- Bouguer gravity anomaly image of the Bunclody area showing NE-SW trends. Towns: B = Bunclody; T = Tullow.

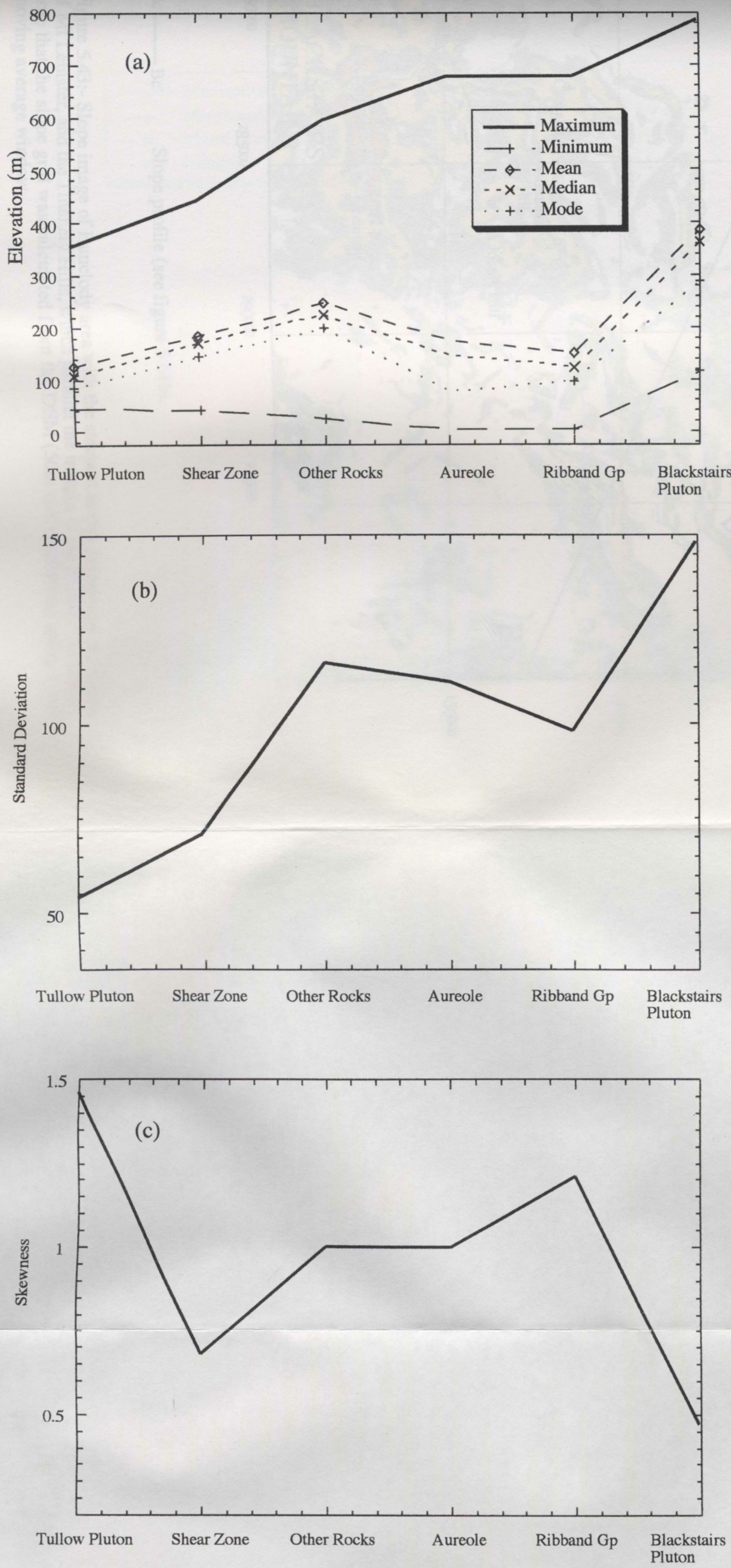

Figure 5.42a,b,c:- Statistical graphs showing the relationship between slope and elevation in the Bunclody area (see text).

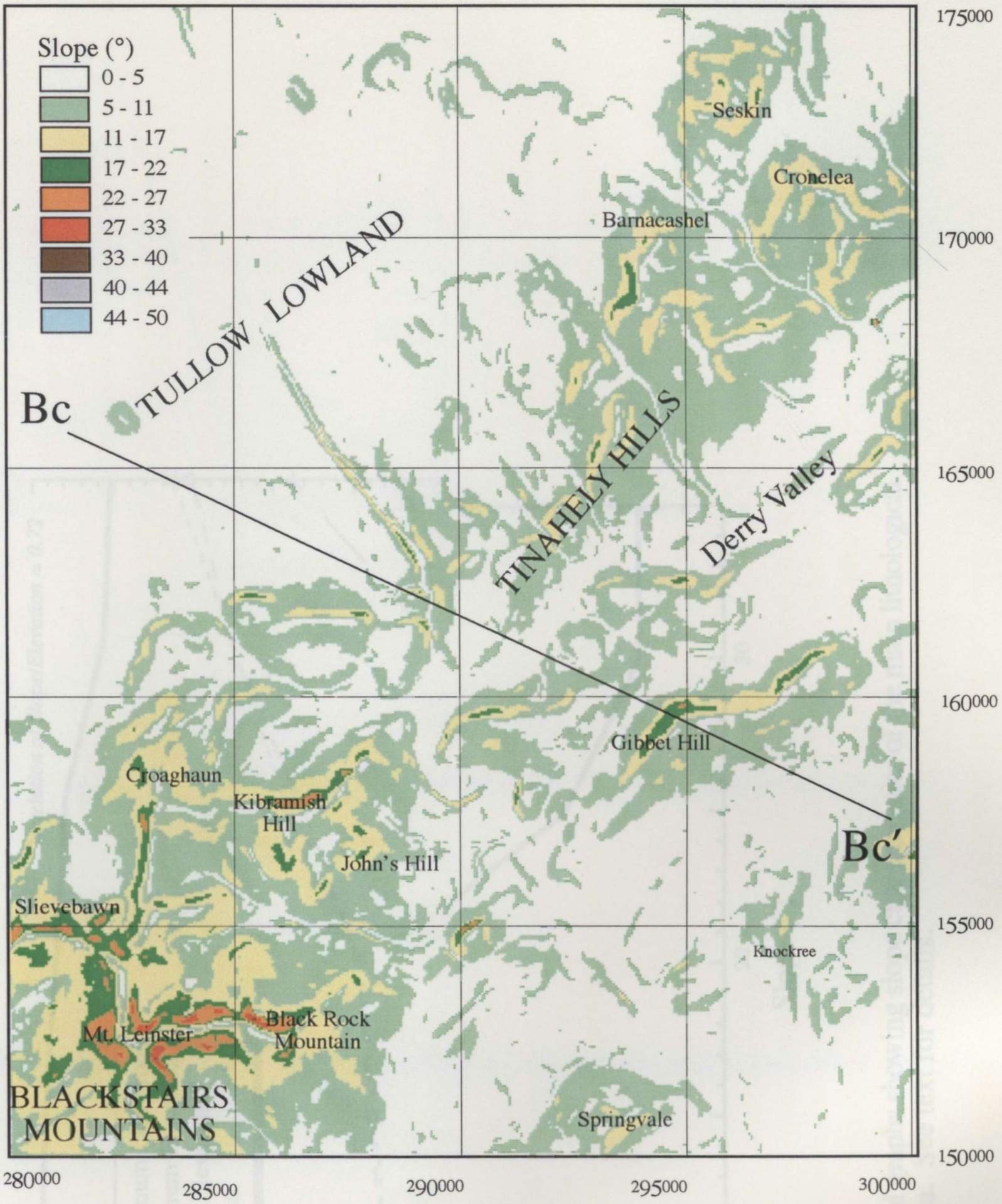

Bc ——— Bc′ Slope profile (see figure 5.61b).

Figure 5.43:- Slope image of Bunclody area with the steepest slopes occupying the flanks of Mt Leinster, and the Tinahely Hills, which parallel the margin of the ECDZ. As before, note that the slope grid was calculated from the DEM (50m cell resolution) using a 3x3 moving average window.

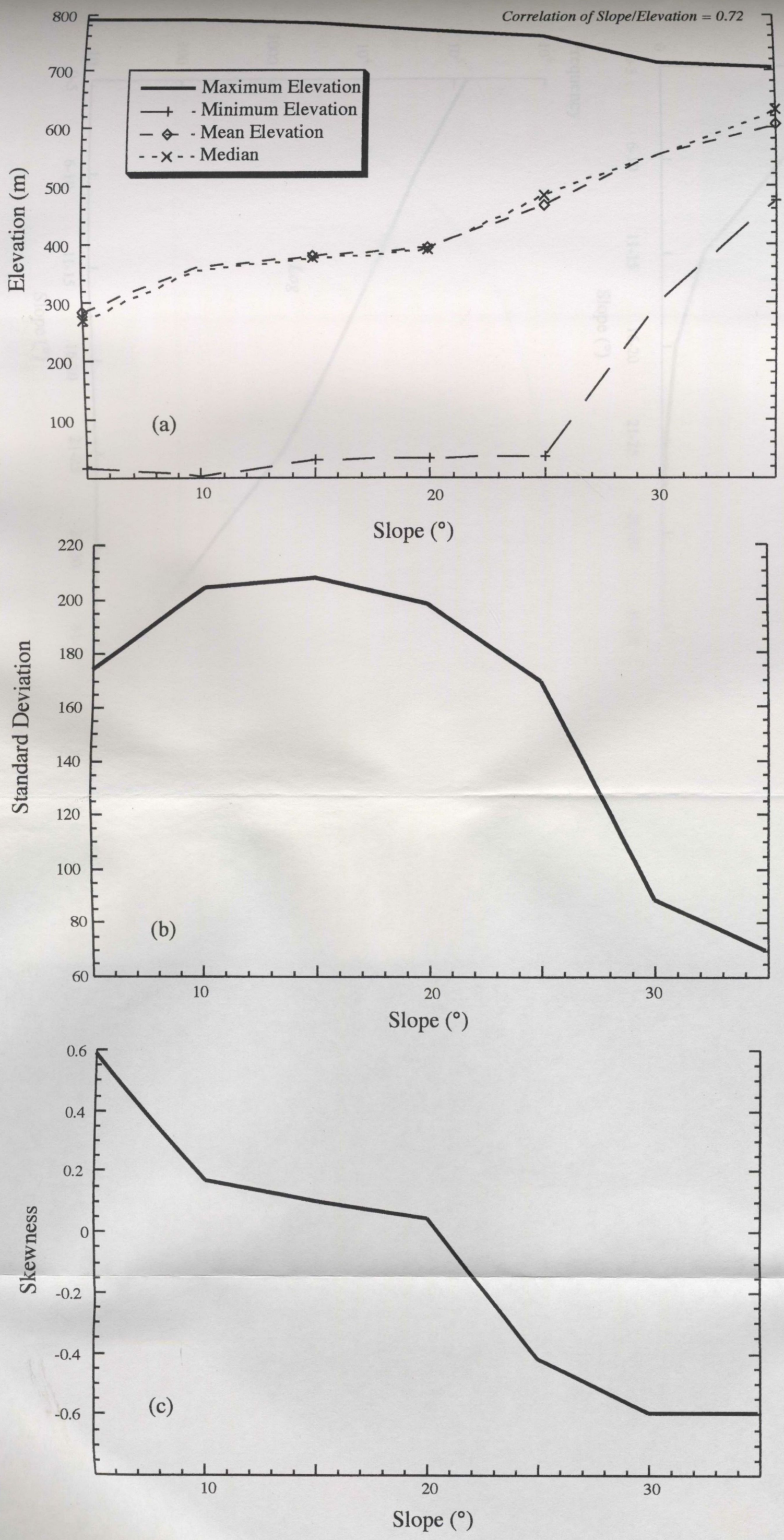

Figure 5.44a,b,c:- Statistical graphs showing slope characteristics of the main lithological types of the Bunclody area. See text for details.

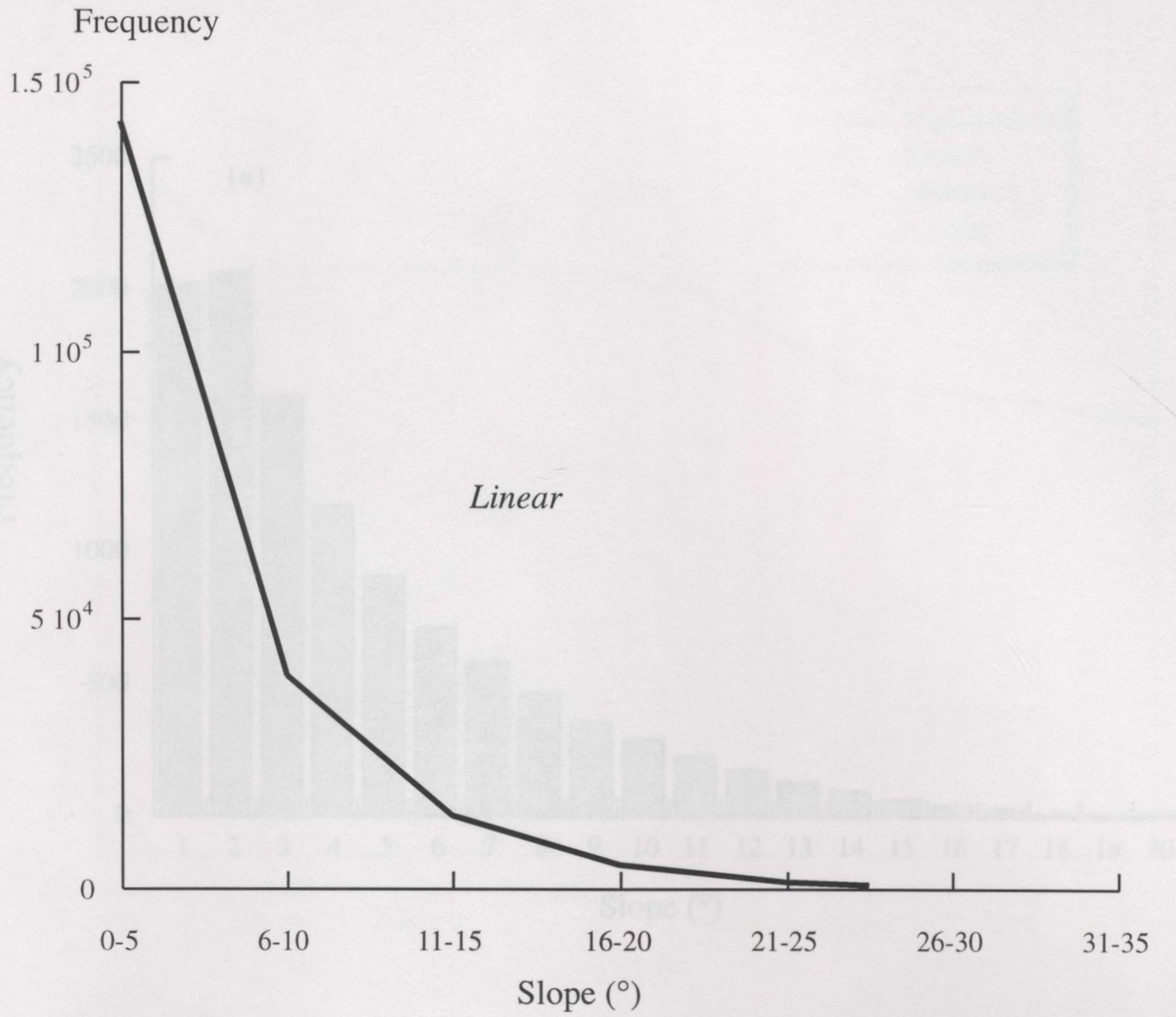

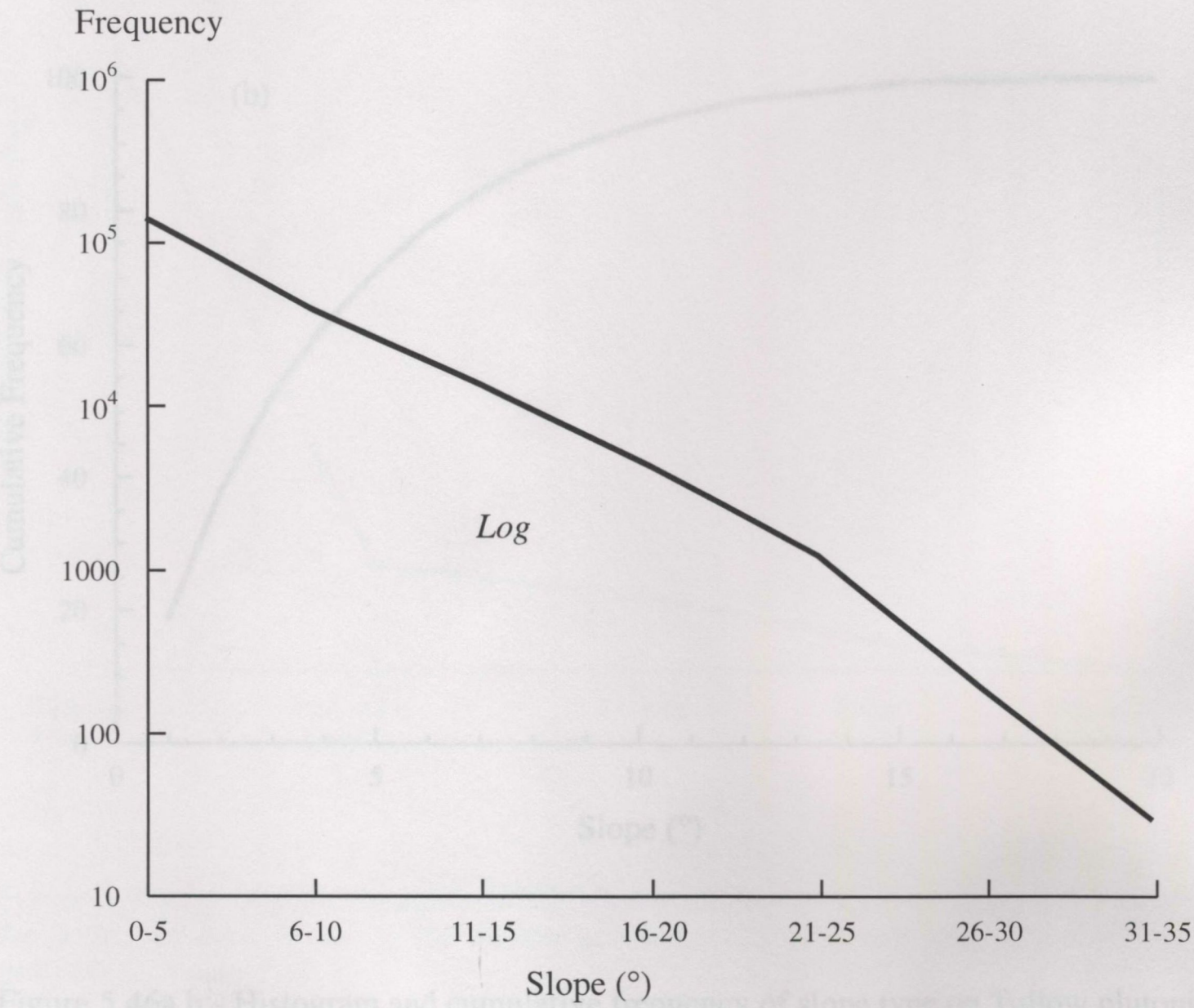

Figure 5.45:- Graph showing the frequency of slopes in the area.

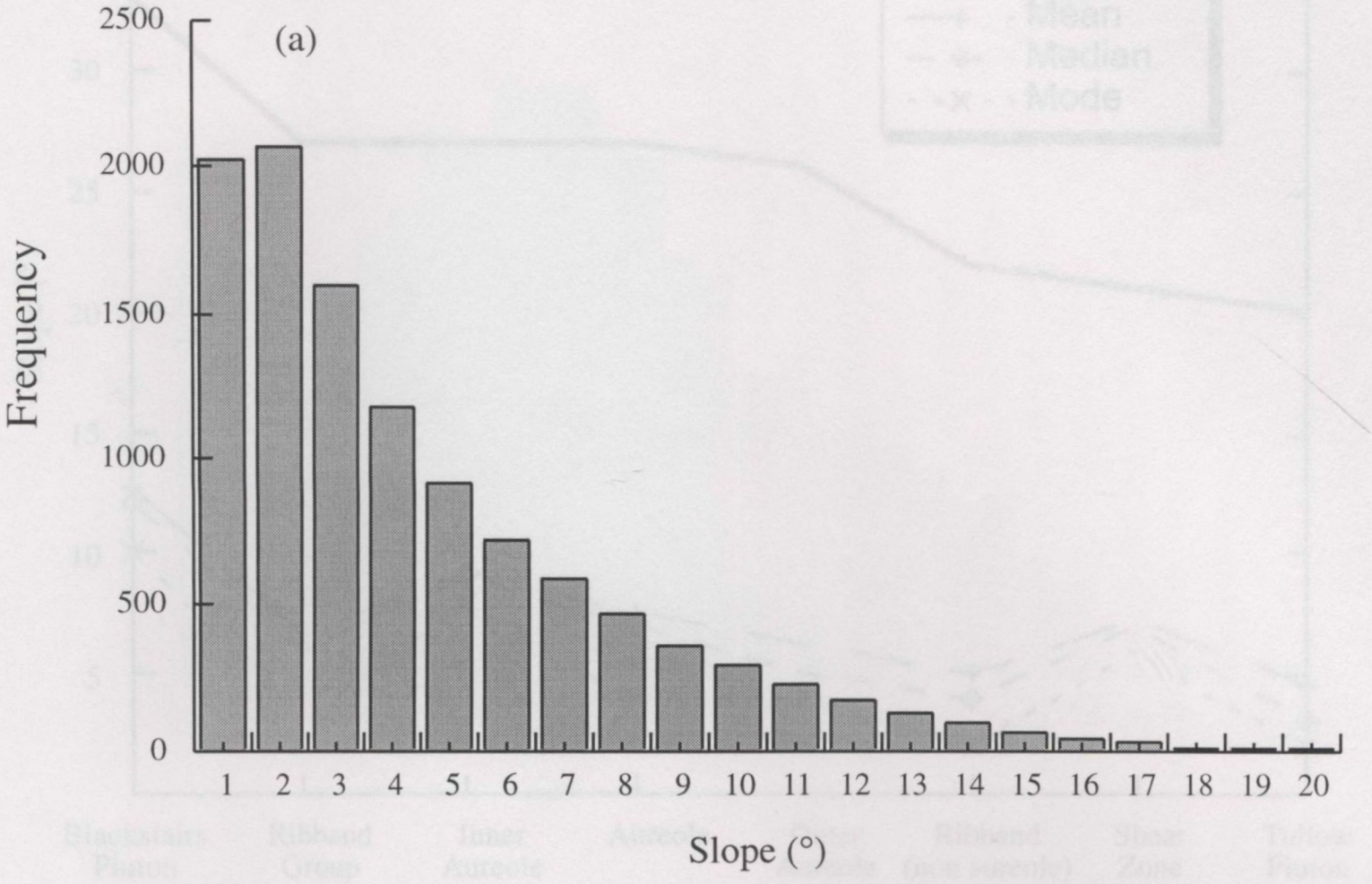

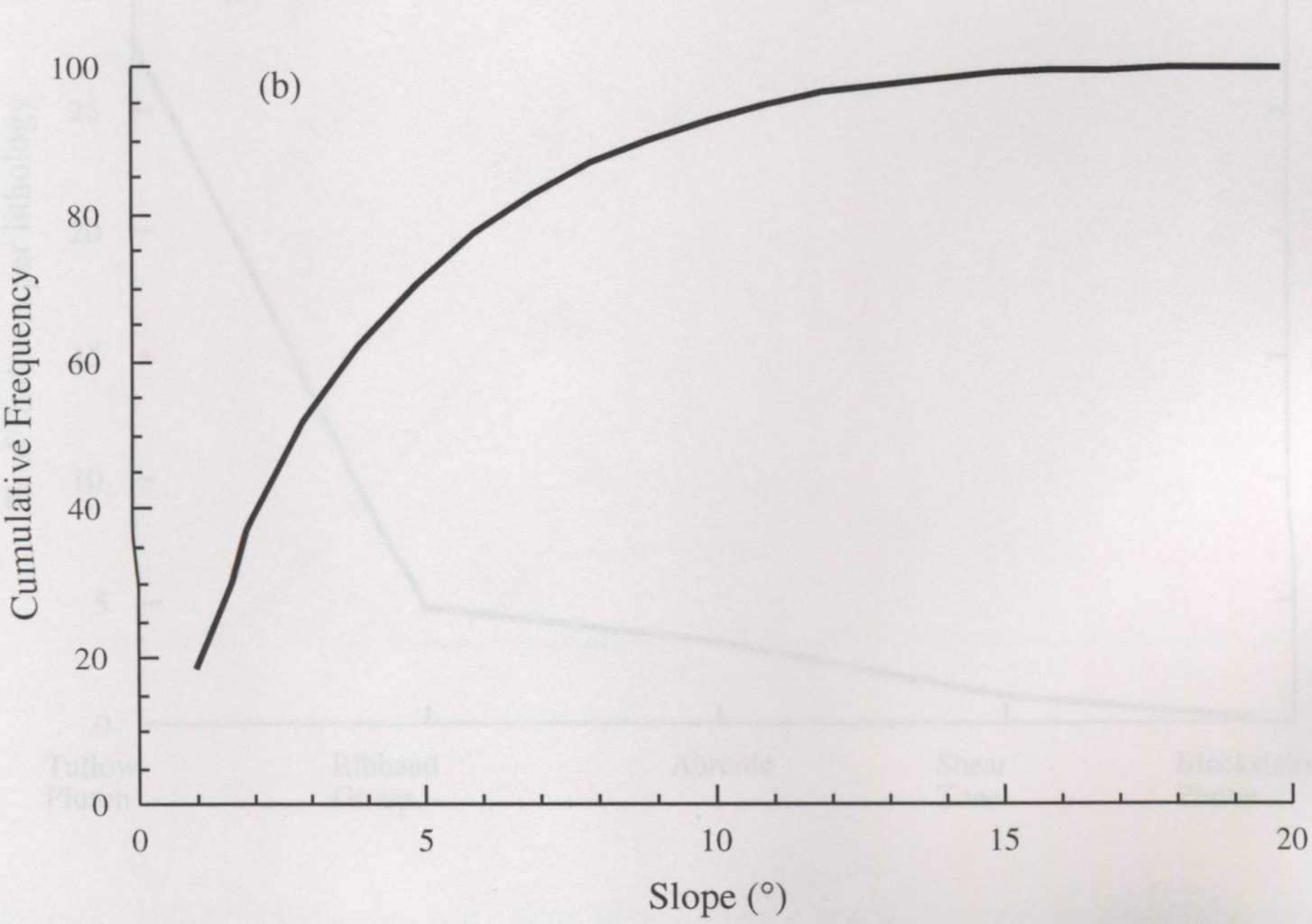

Figure 5.46a,b:- Histogram and cumulative frequency of slope type on Tullow plutonic rocks. These rocks generally form low hill slopes.

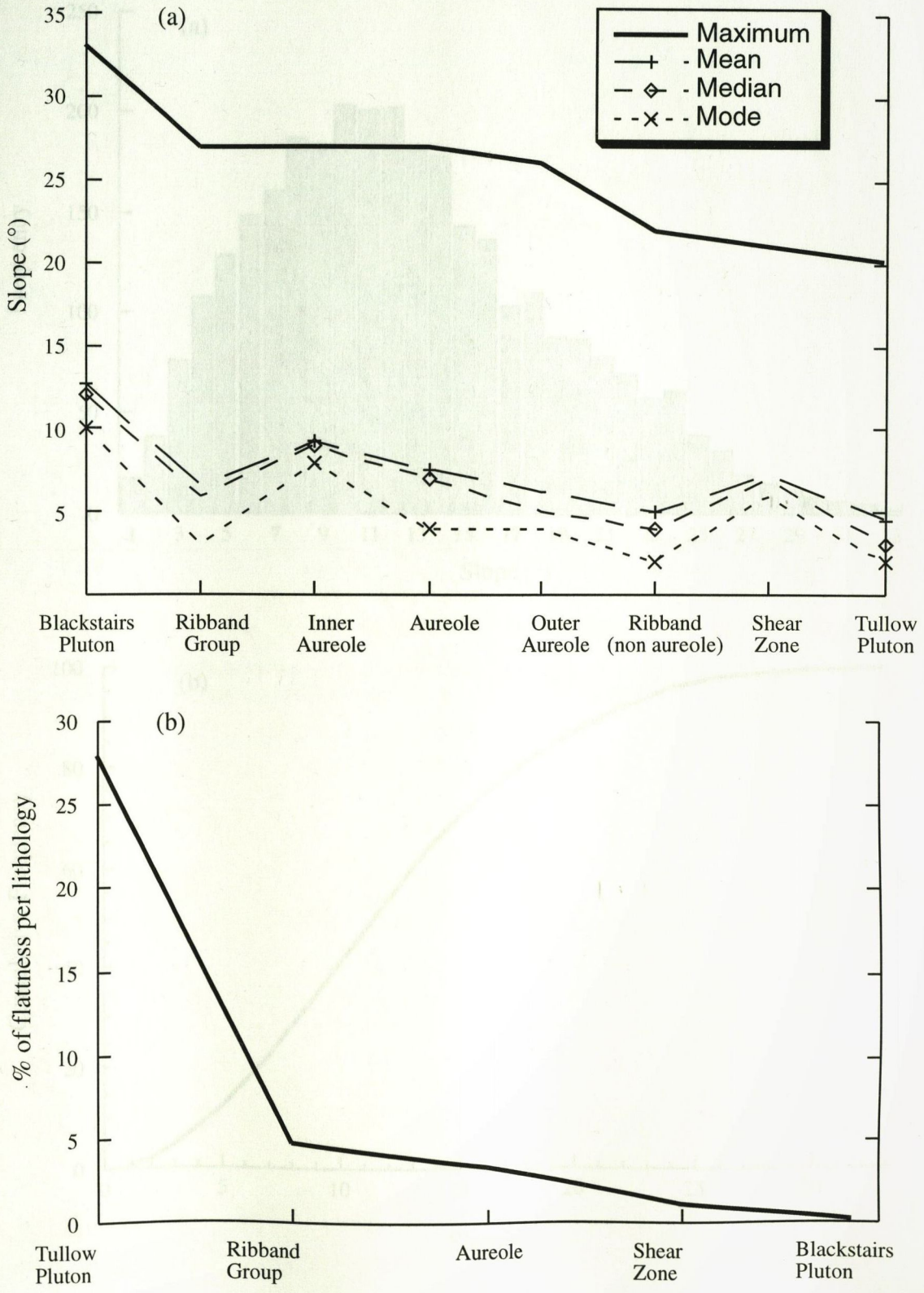

Figure 5.47a,b:- Statistical graphs showing the relationship between slope and lithology in the Bunclody area. Rocks of the Tullow pluton occupy relatively large areas of flat-lying ground.

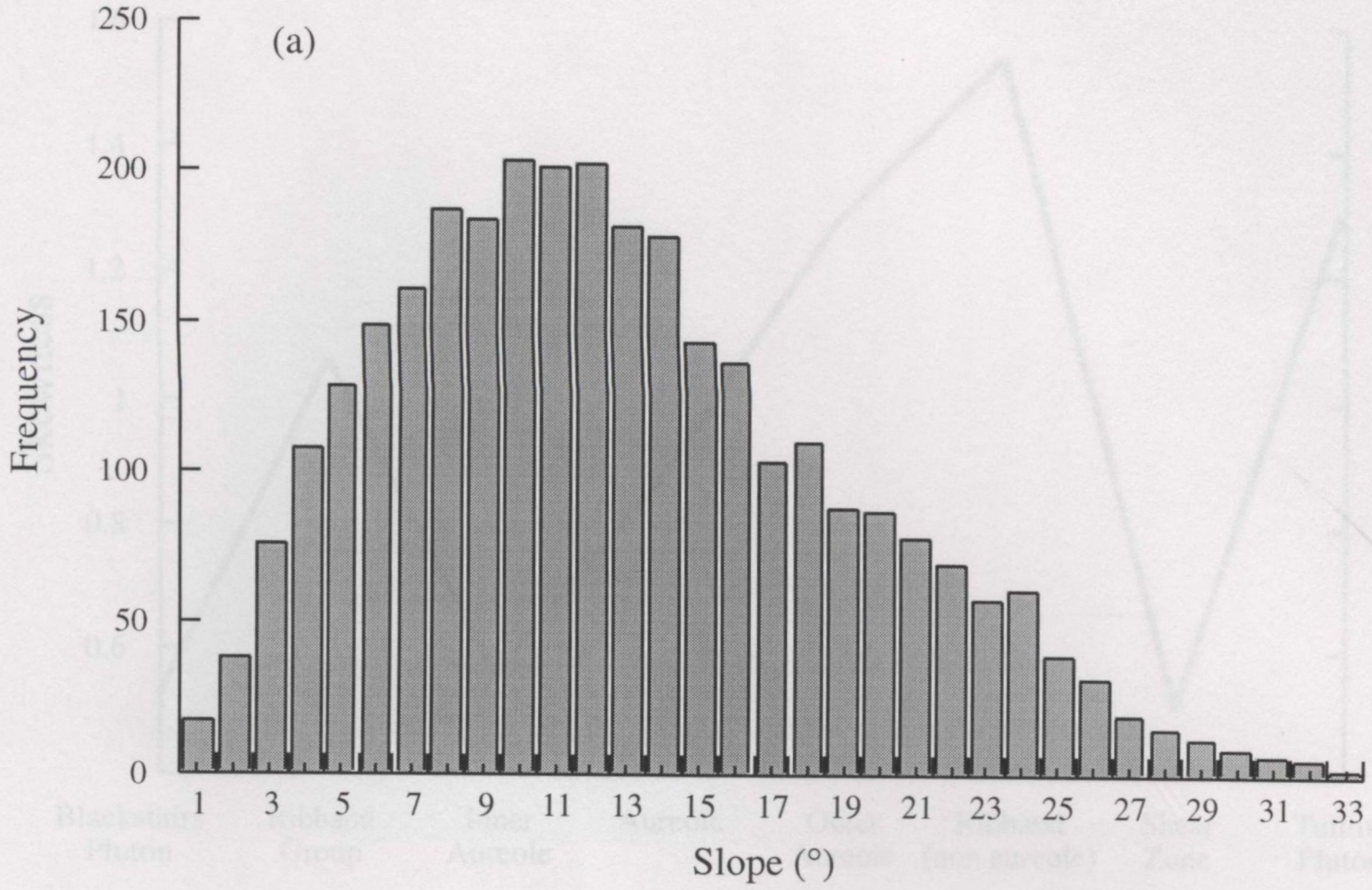

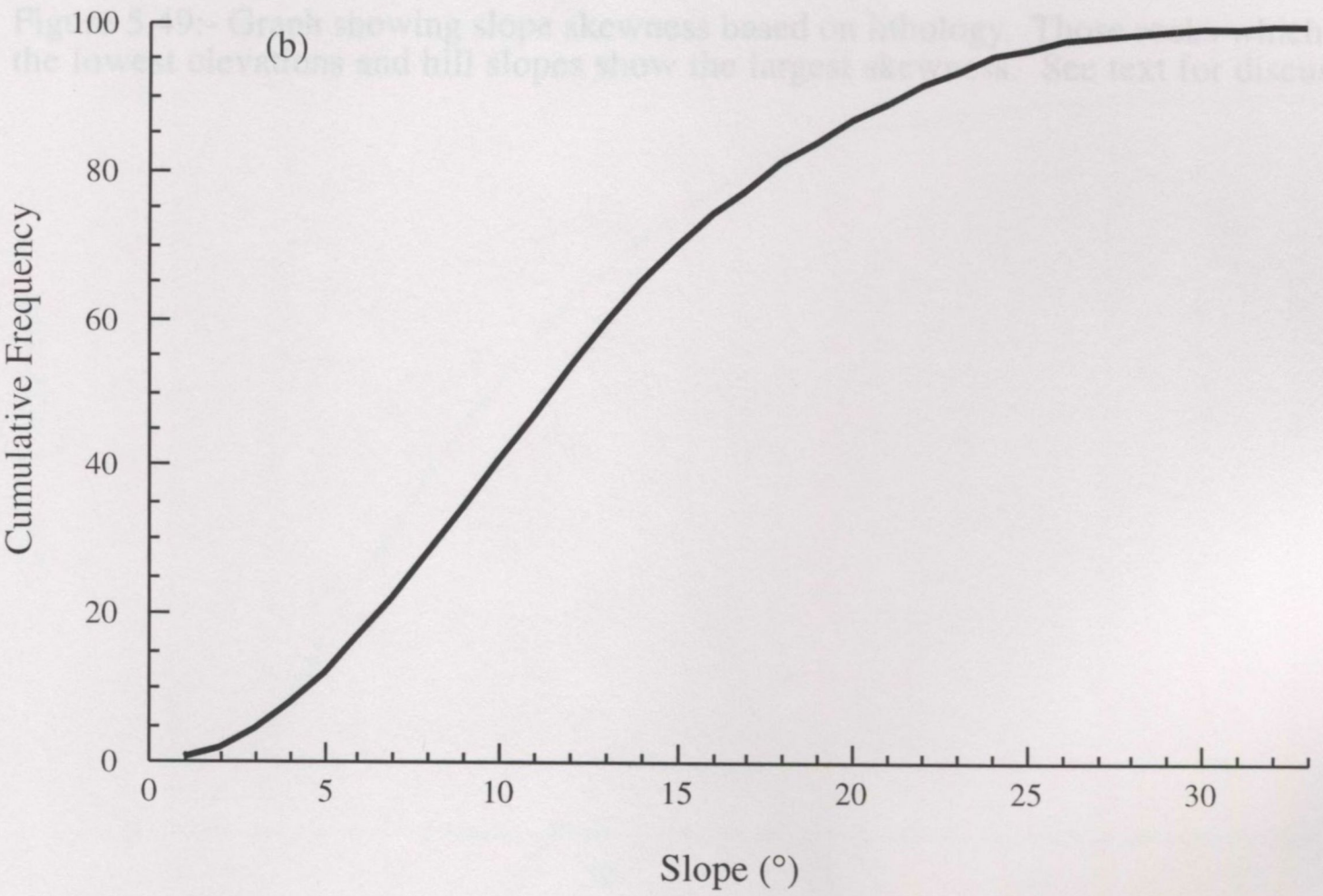

Figure 5.48a,b:- Histogram and cumulative frequency of slope type for Blackstairs plutonic rock. These rocks are typified by moderate to high slope type. This may be due to recent uplift (see text for discussion).

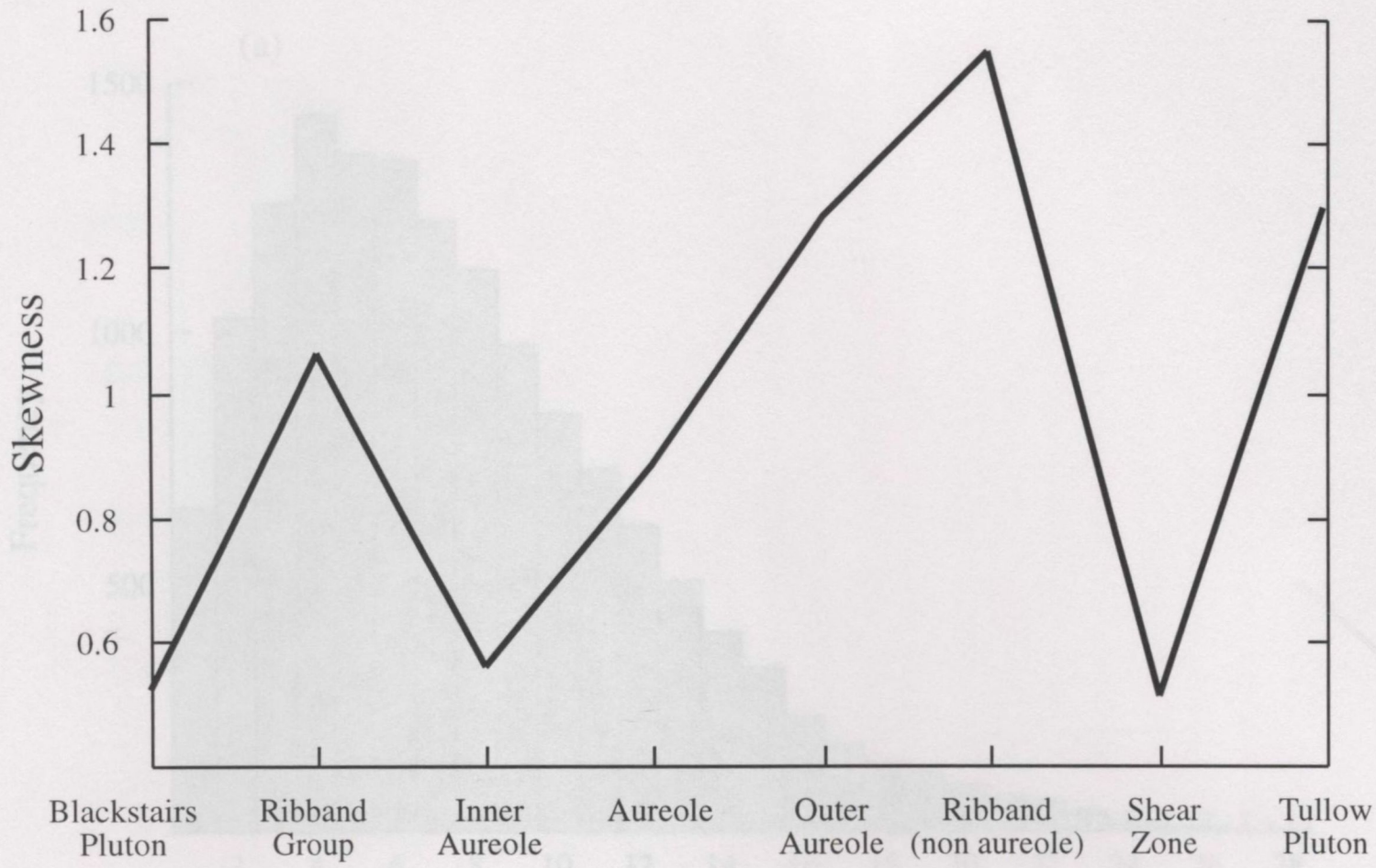

Figure 5.49:- Graph showing slope skewness based on lithology. Those rocks which form the lowest elevations and hill slopes show the largest skewness. See text for discussion.

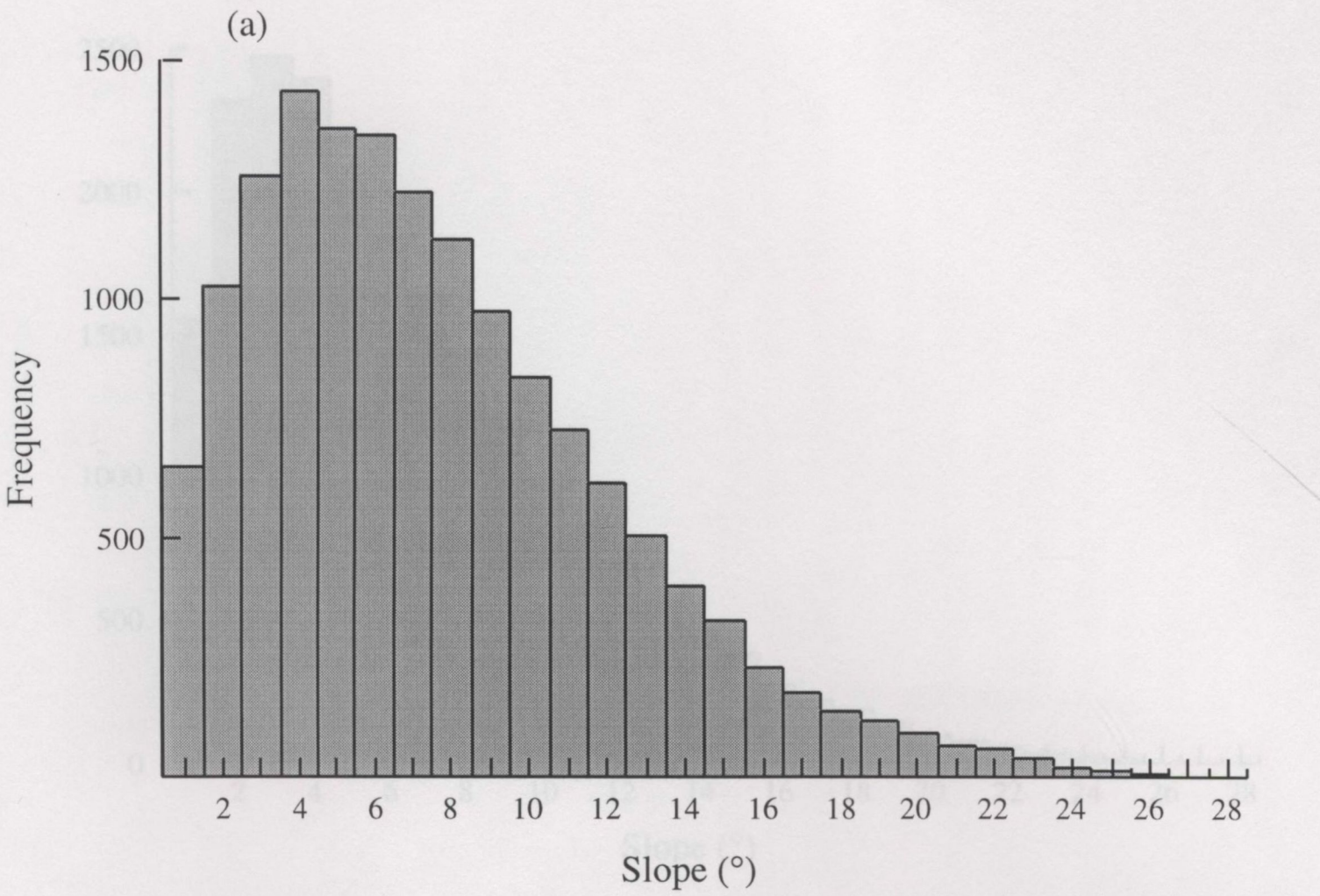

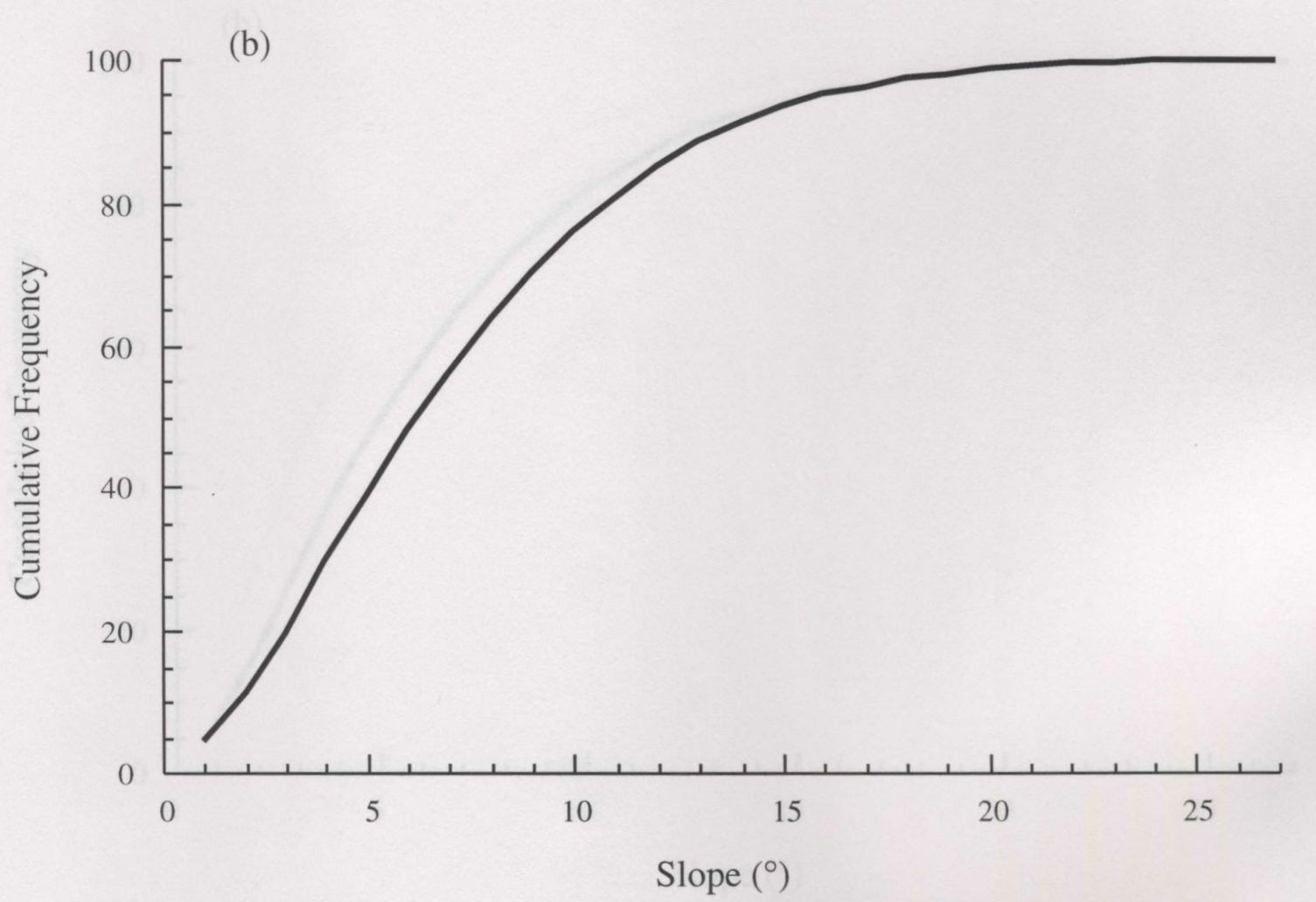

Figure 5.50a,b:- Histogram and cumulative frequency of slope type for aureole rocks in the Bunclody area.

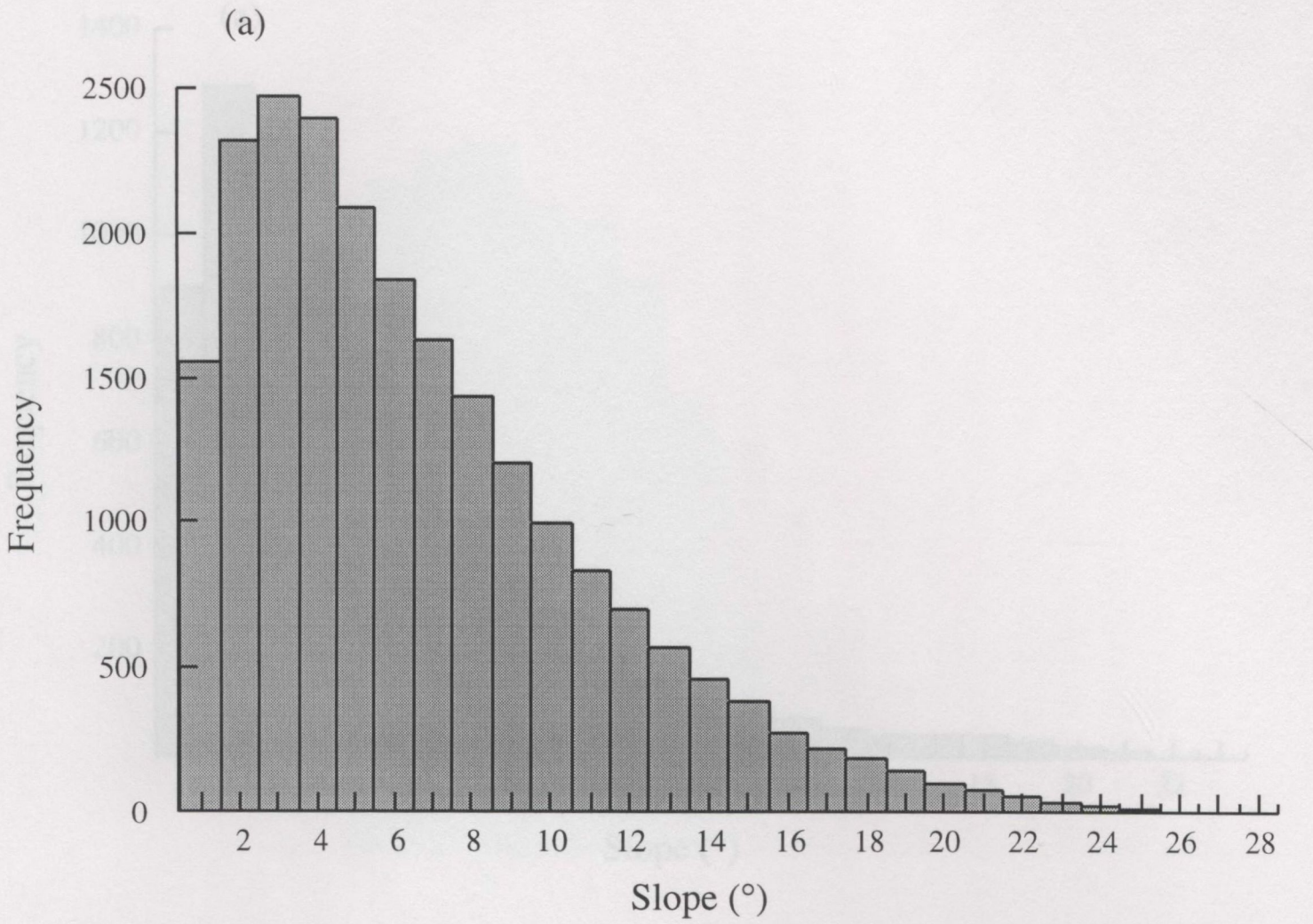

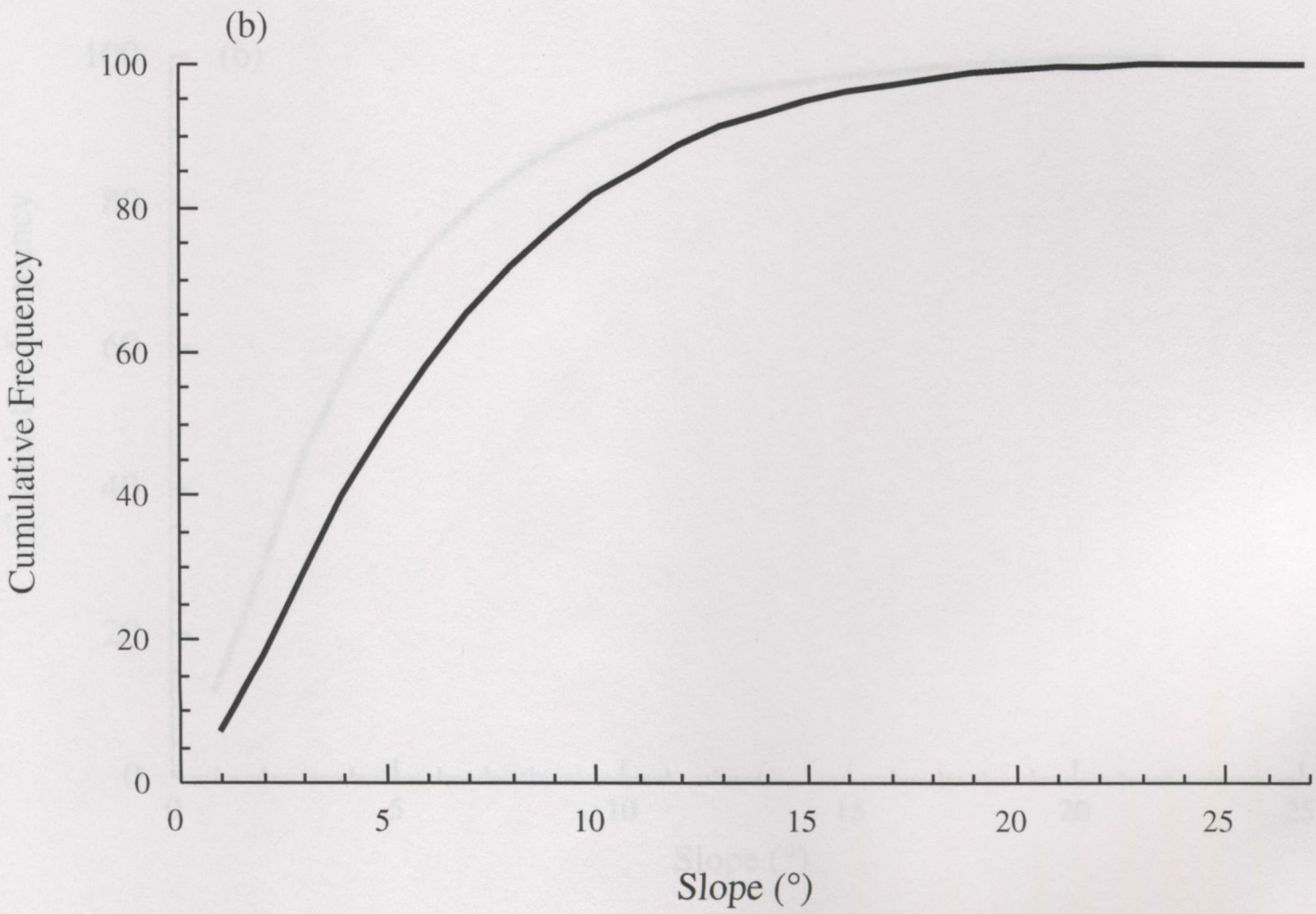

Figure 5.51a,b:- Histogram and cumulative frequency of slope type for rocks of the Ribband Group (inc. aureole rocks) in the Bunclody area of study.

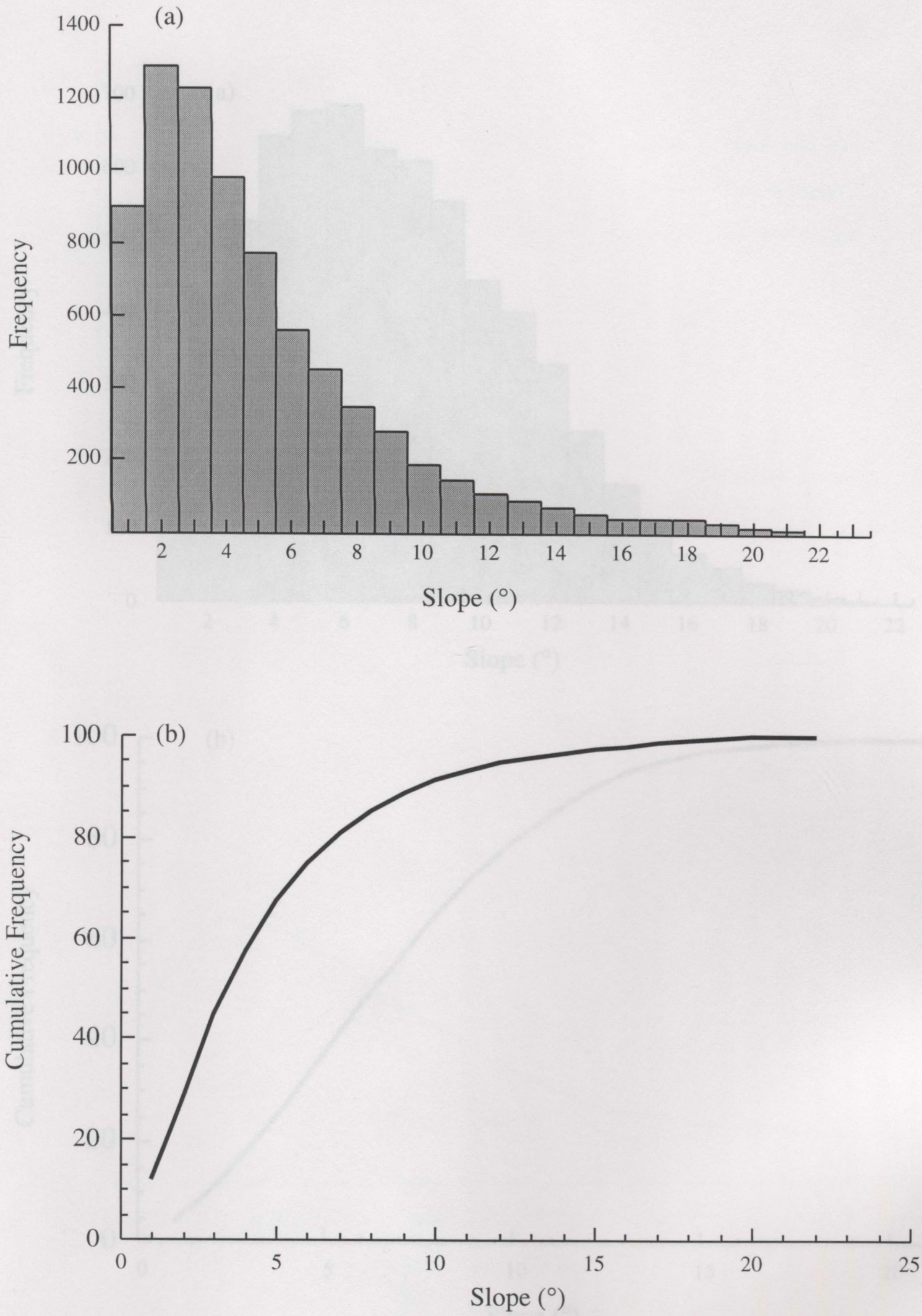

Figure 5.52a,b:- Histogram and cumulative frequency of slope type for rocks of the Ribband Group minus aureole rocks. This shows that slopes on the Ribband Group are primarily dependent on rock erodibility, i.e. aureole rocks being relatively more resistant to weathering.

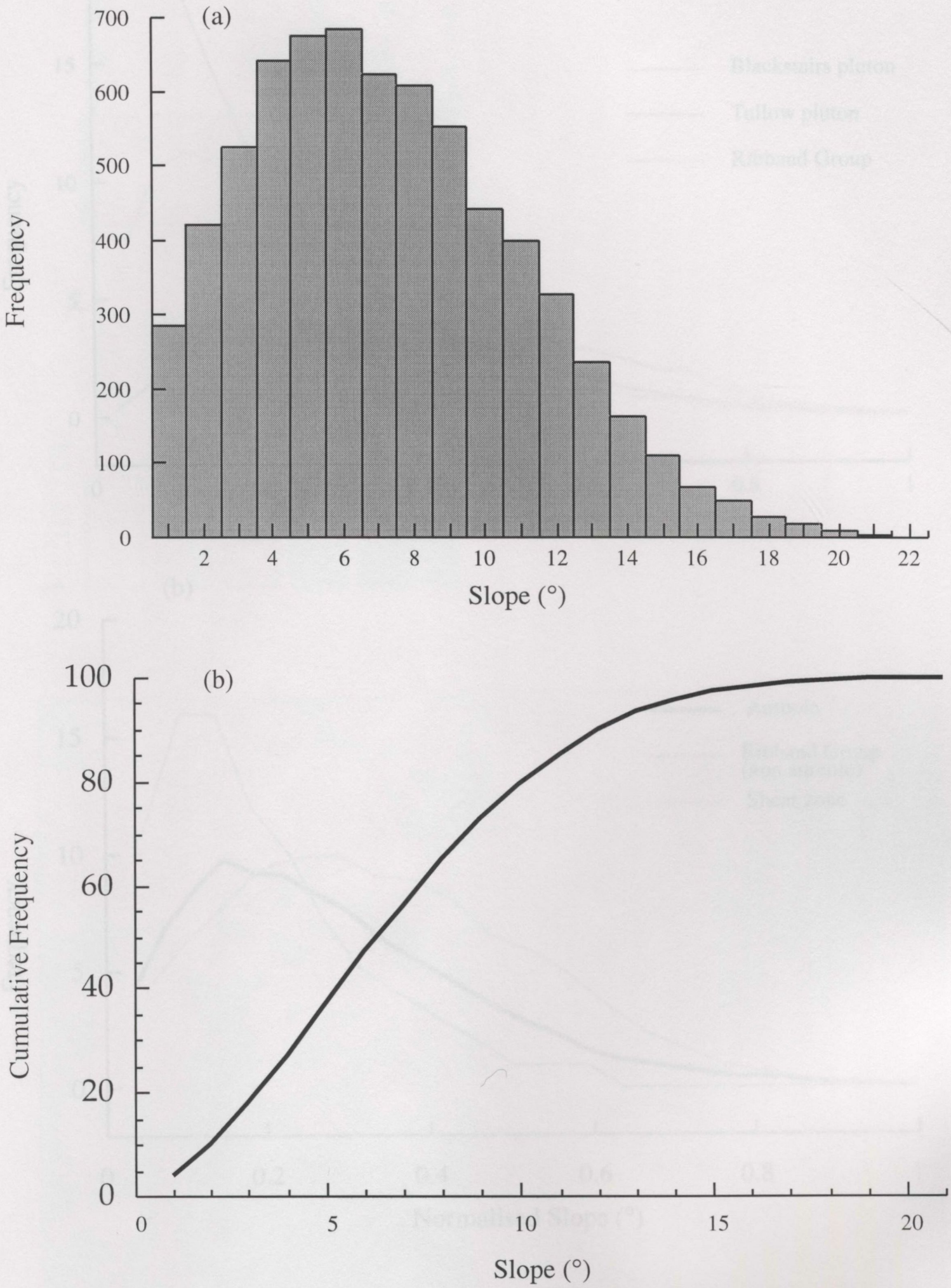

Figure 5.53a,b:- Histogram and cumulative frequency of slope type for rocks that occur within the ECDZ, and includes, the Maulin Formation (Ribband Group), rocks of the Tullow pluton, and subordinate amounts of Blackstairs plutonic rocks. In general, slopes within the shear-zone are low to moderate to high, comparable to which occur on rocks of the Blackstairs pluton.

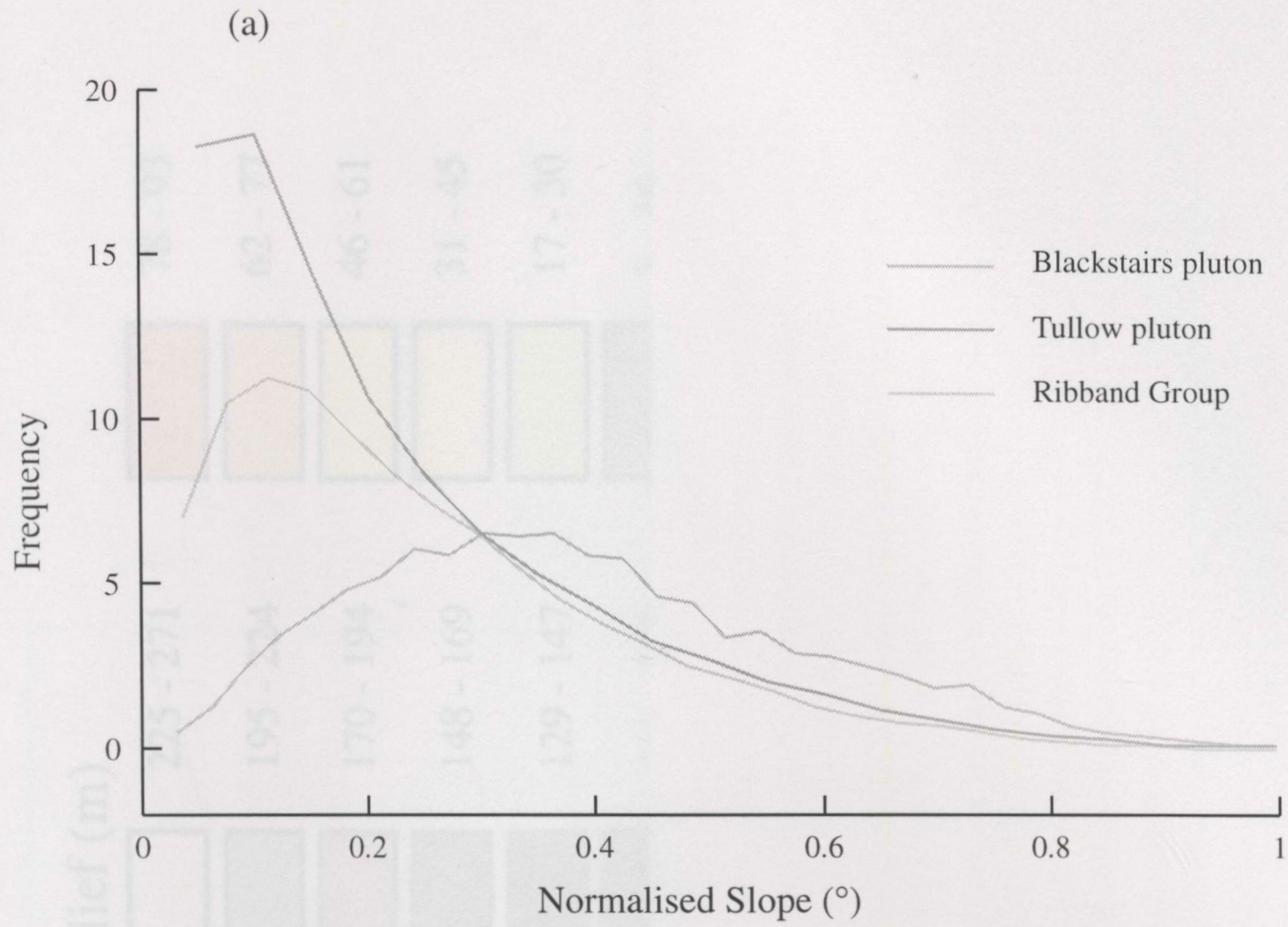

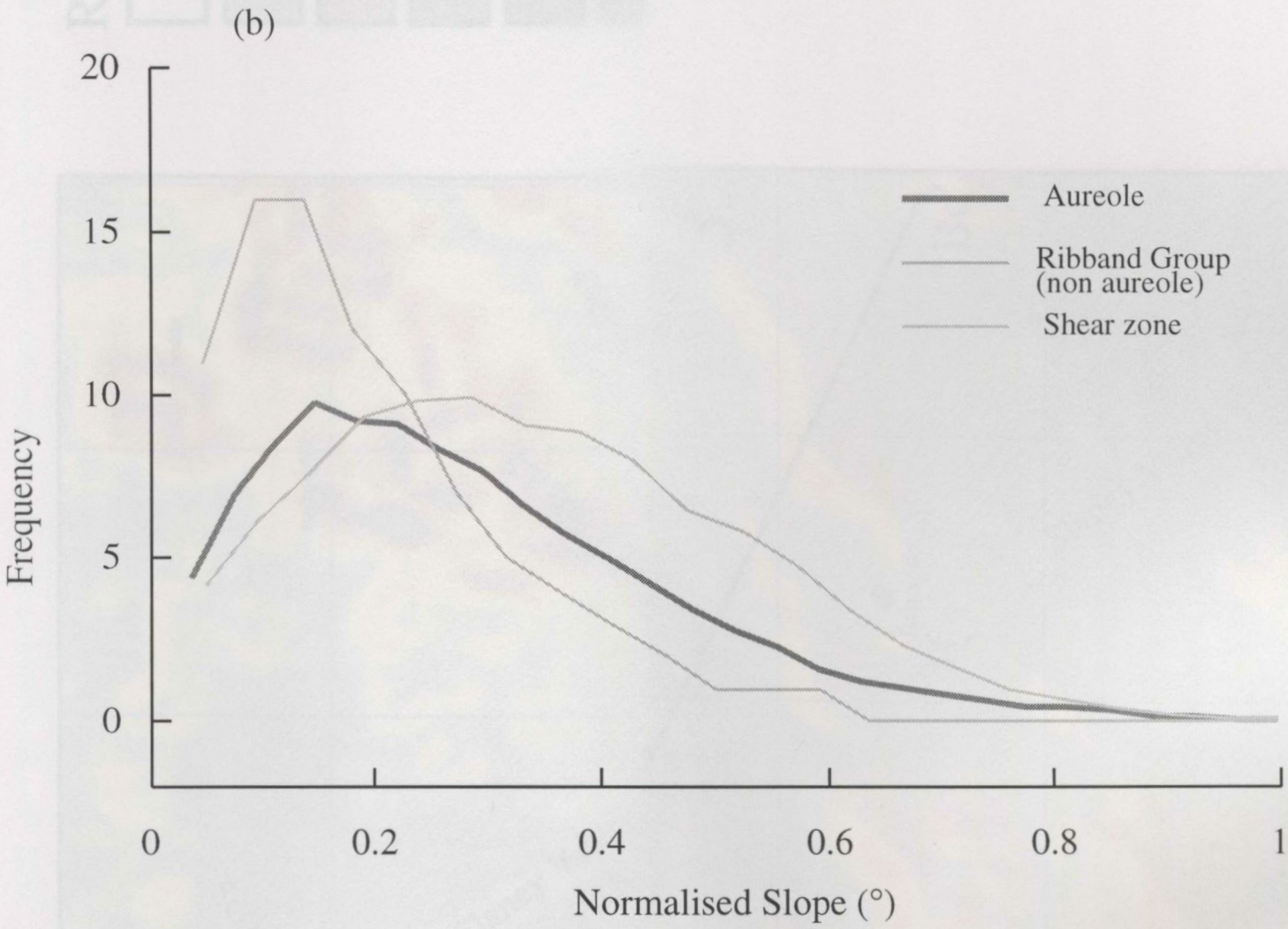

Figure 5.54a,b:- Graph of normalised slope distribution for the main lithologies in the Bunclody area (see text for discussion).

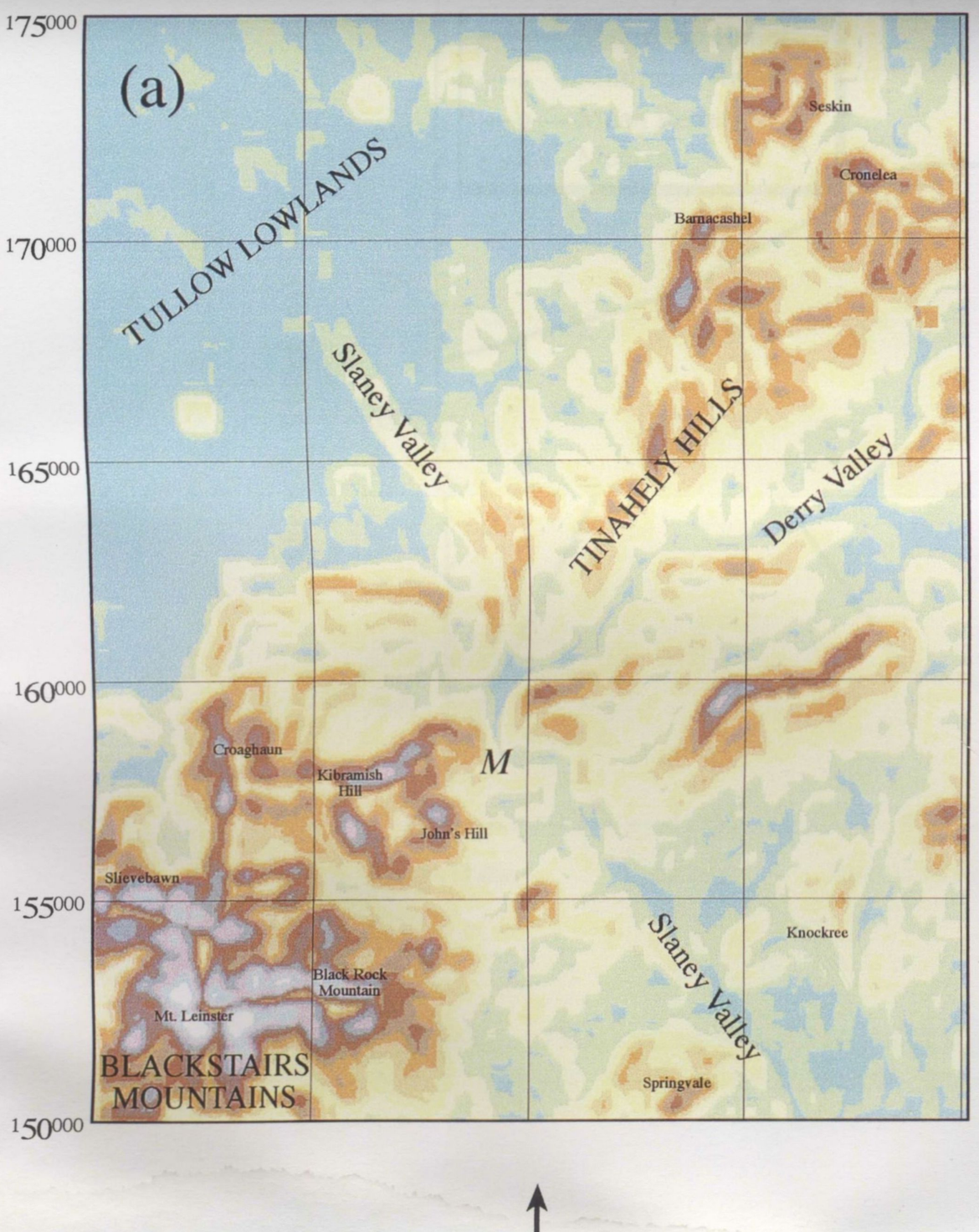

Relief (m)

225 - 271	78 - 93
195 - 224	62 - 77
170 - 194	46 - 61
148 - 169	31 - 45
129 - 147	17 - 30
111 - 128	1 - 16
94 - 110	

Bc _____ Bc′ Relief profile (see figure 5.61c)

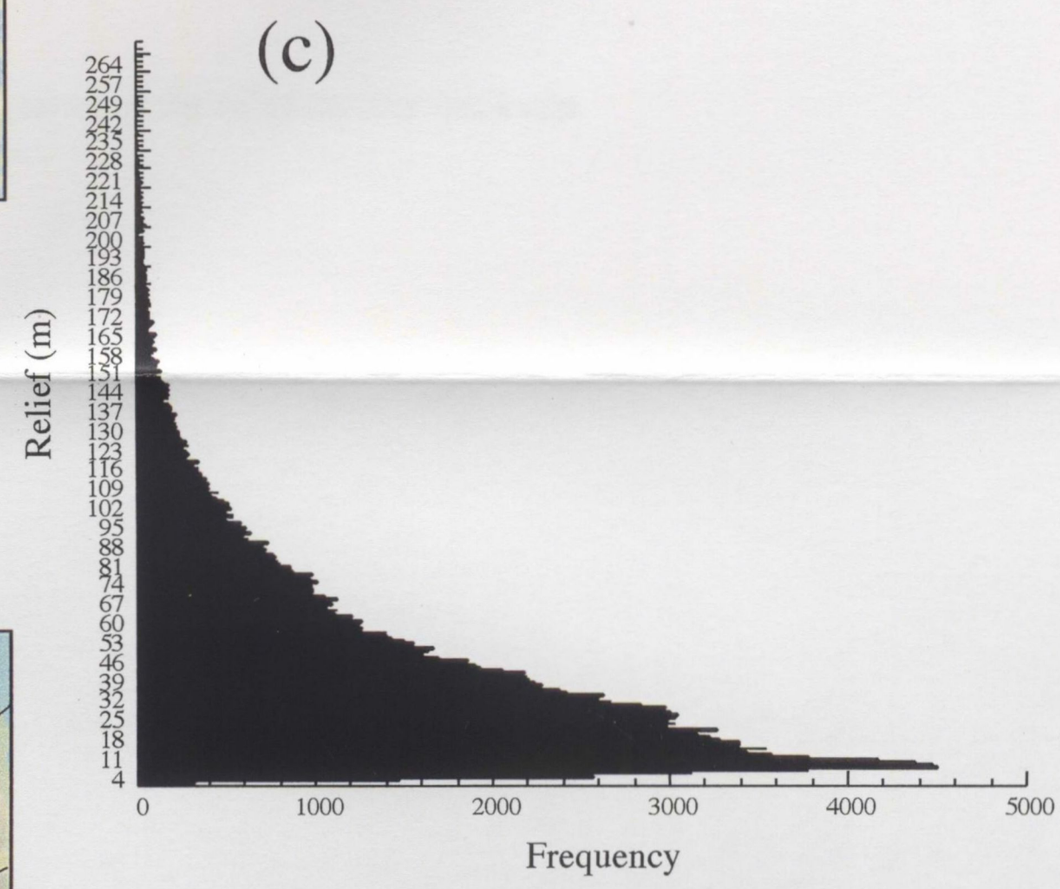

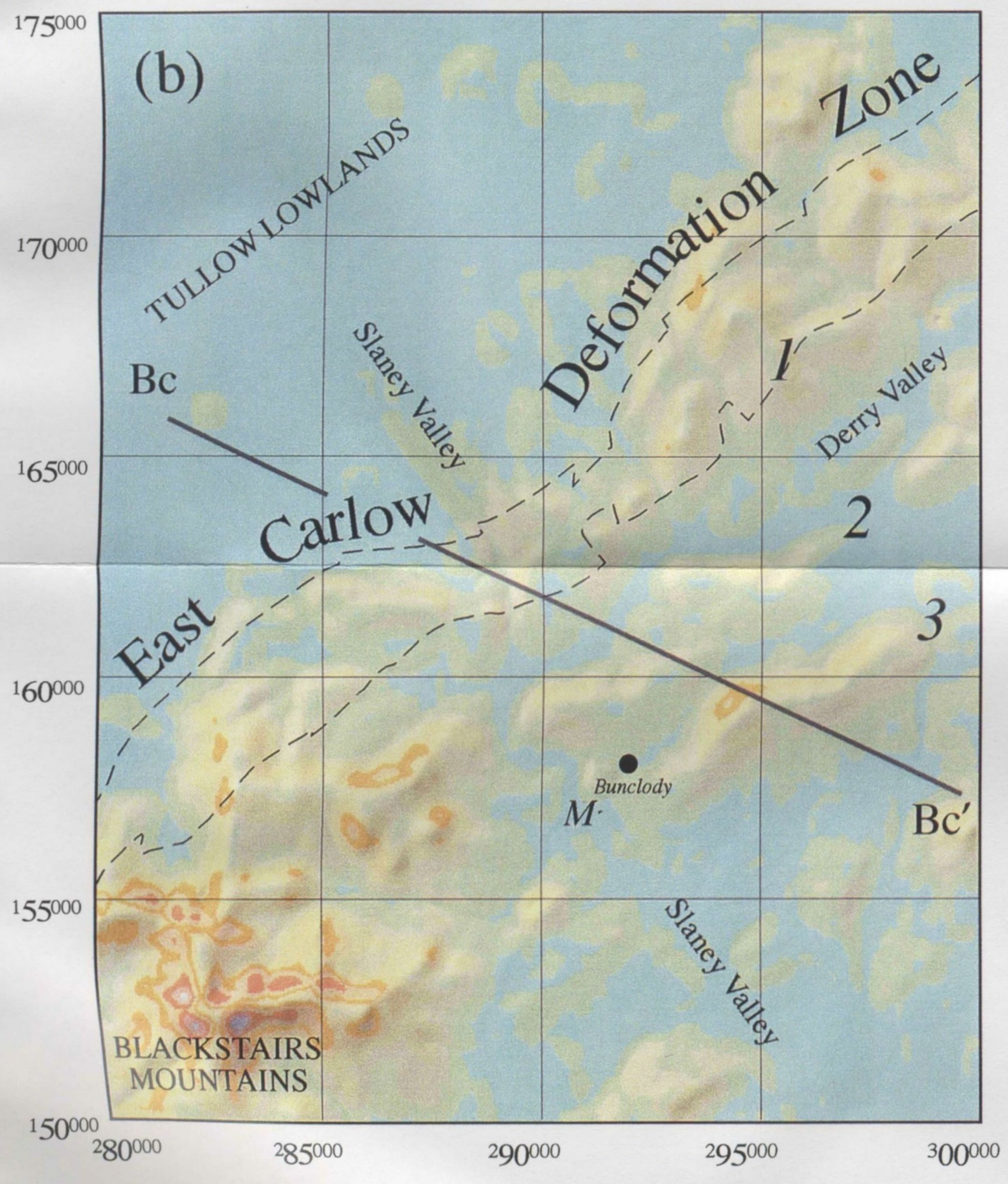

Figure 5.55a,b,c:- Relief images of the Bunclody area. See text for discussion.

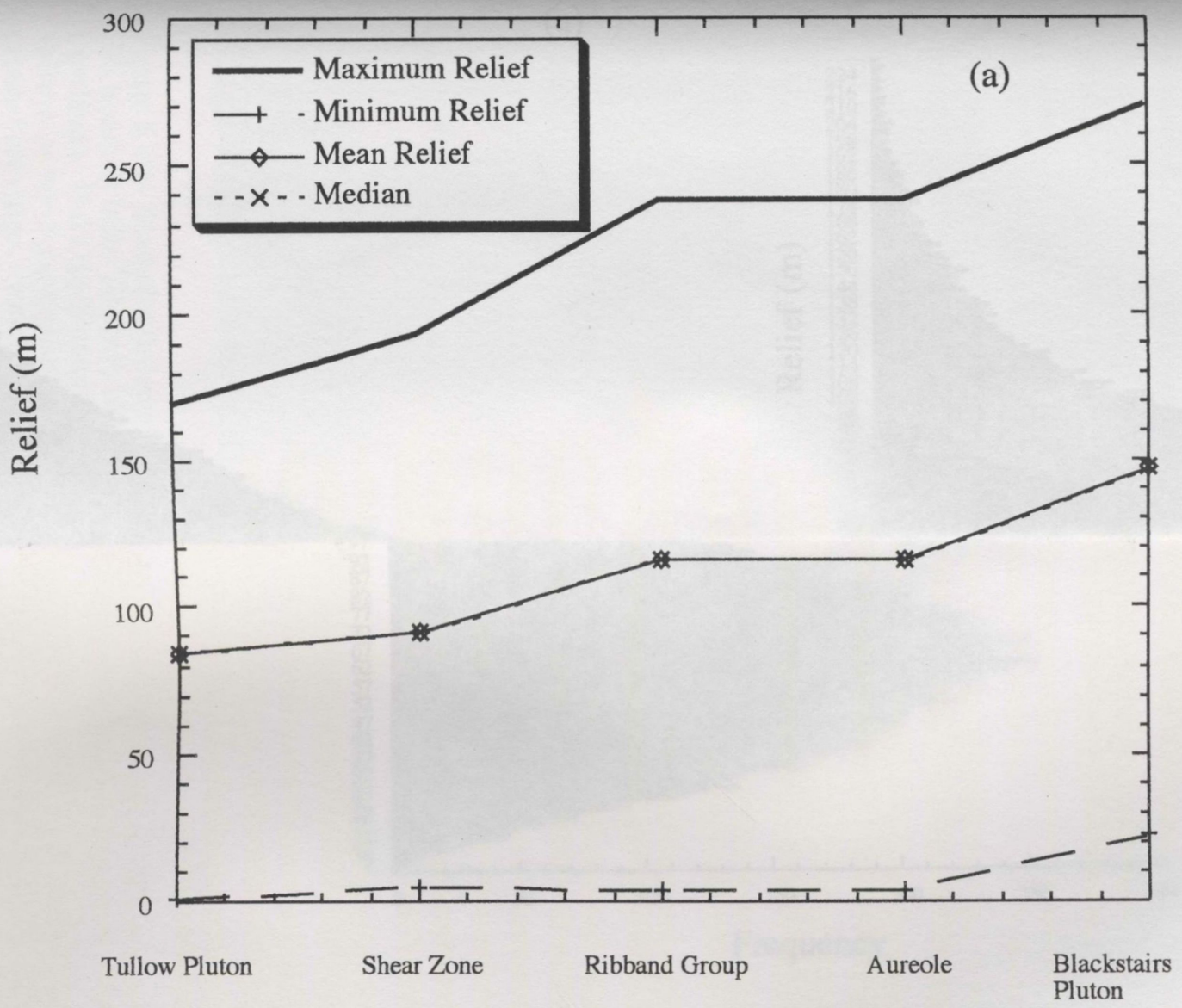

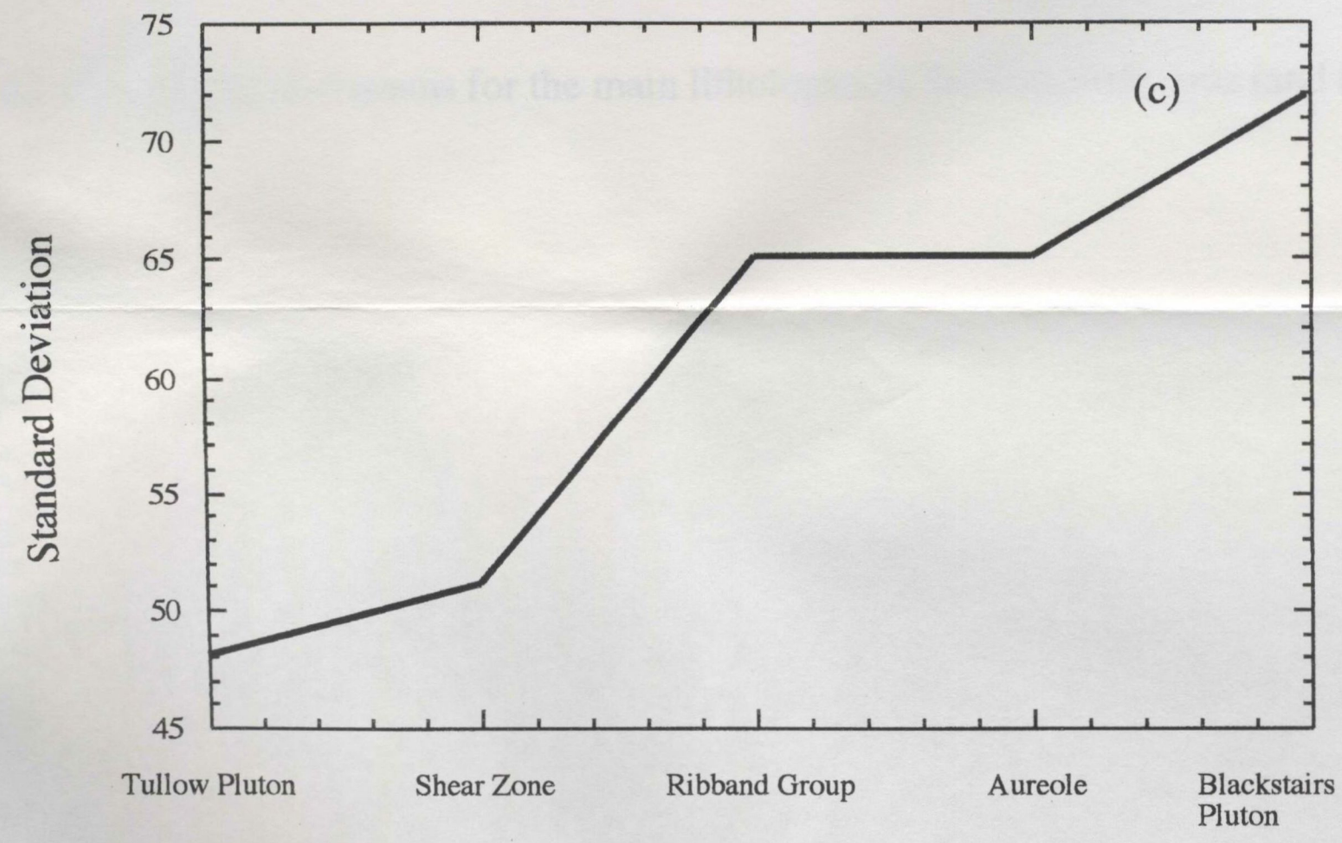

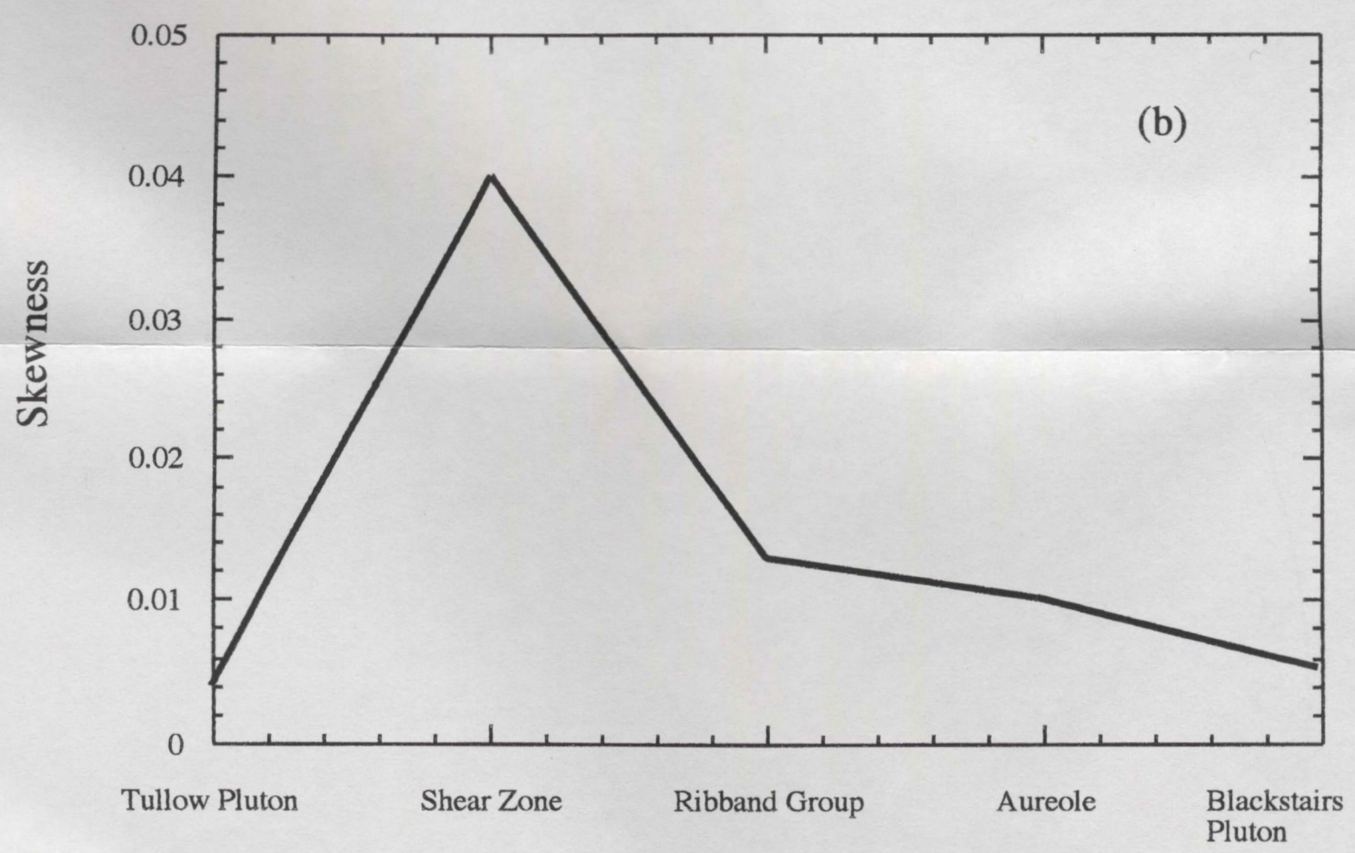

Figure 5.56a,b,c:- Descriptive statistical graphs showing the relationship between various rock type and relief in the Bunclody area.

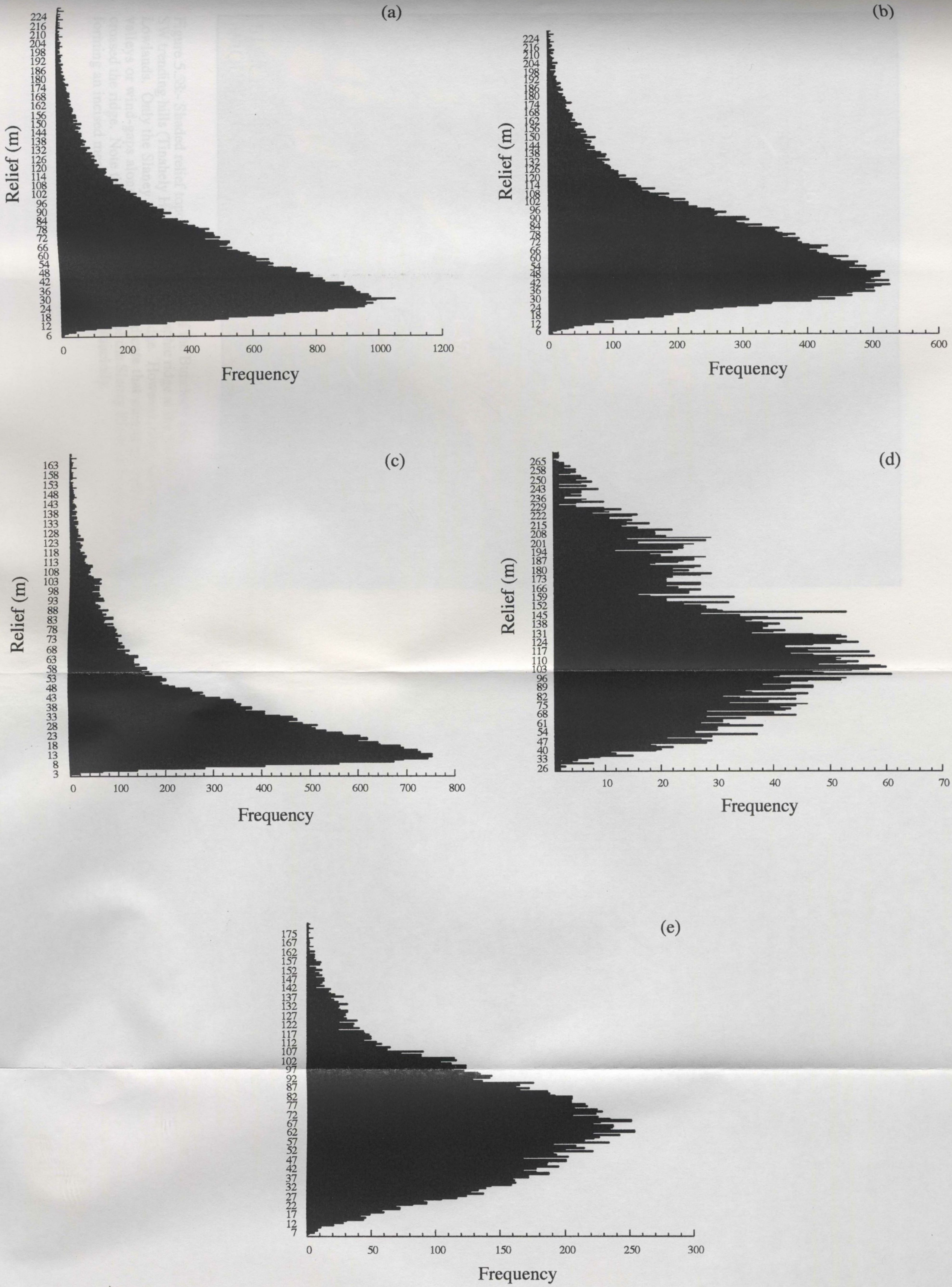

Figure 5.57a,b,c,d,e:- Relief histograms for the main lithologies in the Bunclody area (and are discussed in text).

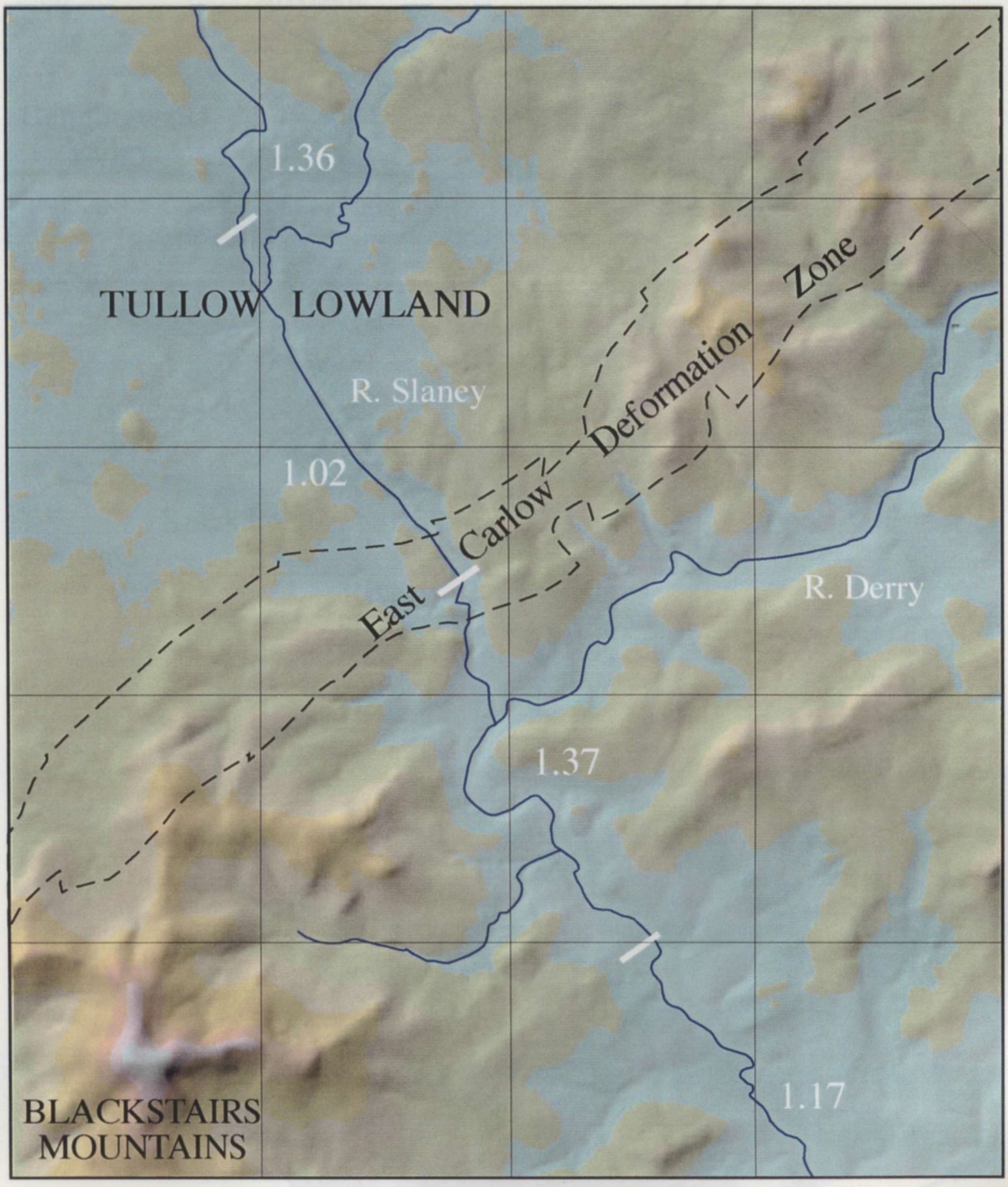

Figure 5.58:- Shaded relief topographic image of the Bunclody area. A broad zone of NE-SW trending hills (Tinahely Hills) form a topographic ridge at the SE margin of the Tullow Lowlands. Only the Slaney River crosses the ridge. However, there are a number of dry valleys or wind-gaps along the ridge, which indicate that numerous other streams once crossed the ridge. Note the change in sinuosity of the Slaney River as it crosses the ridge, forming an incised meander around the town of Bunclody.

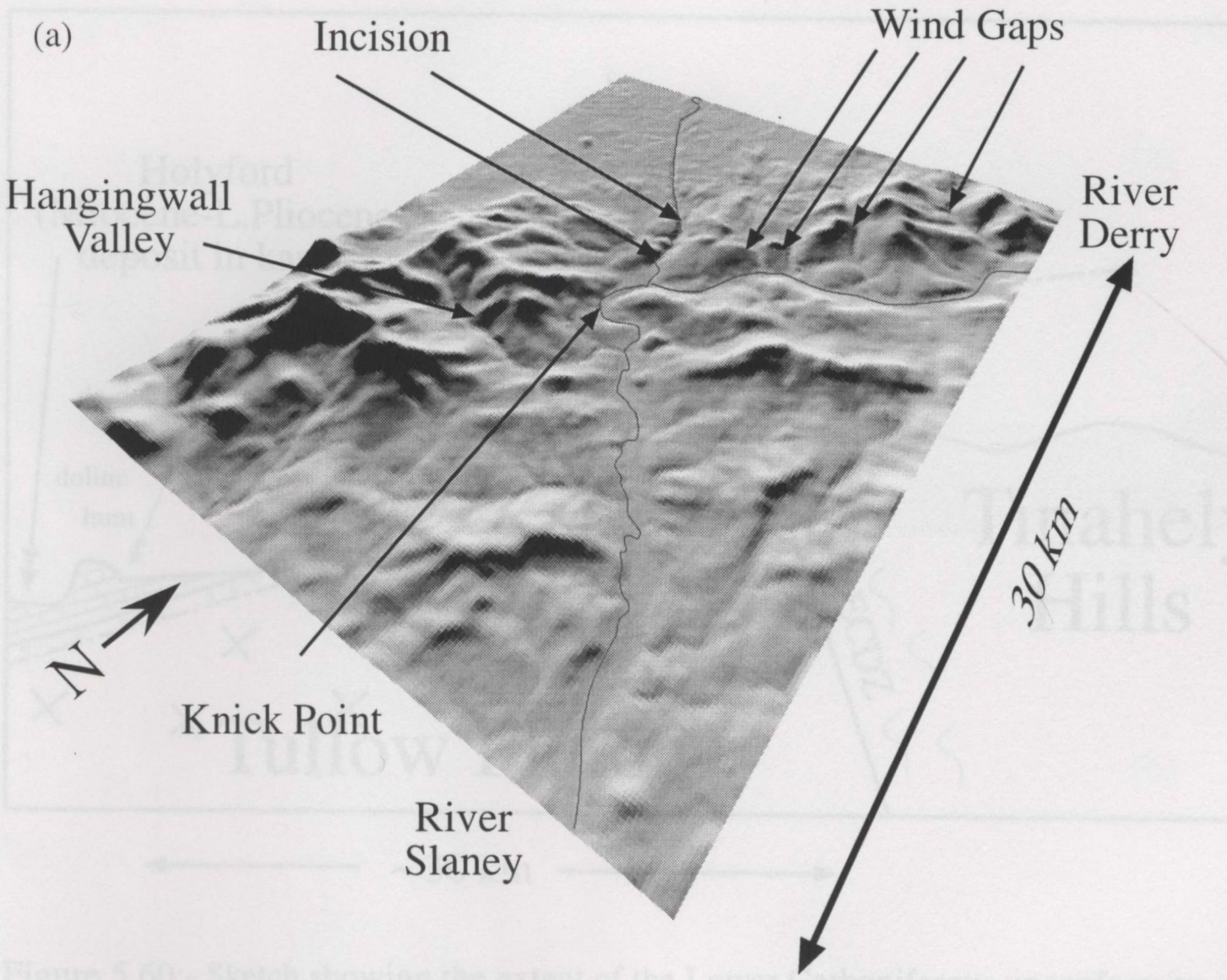

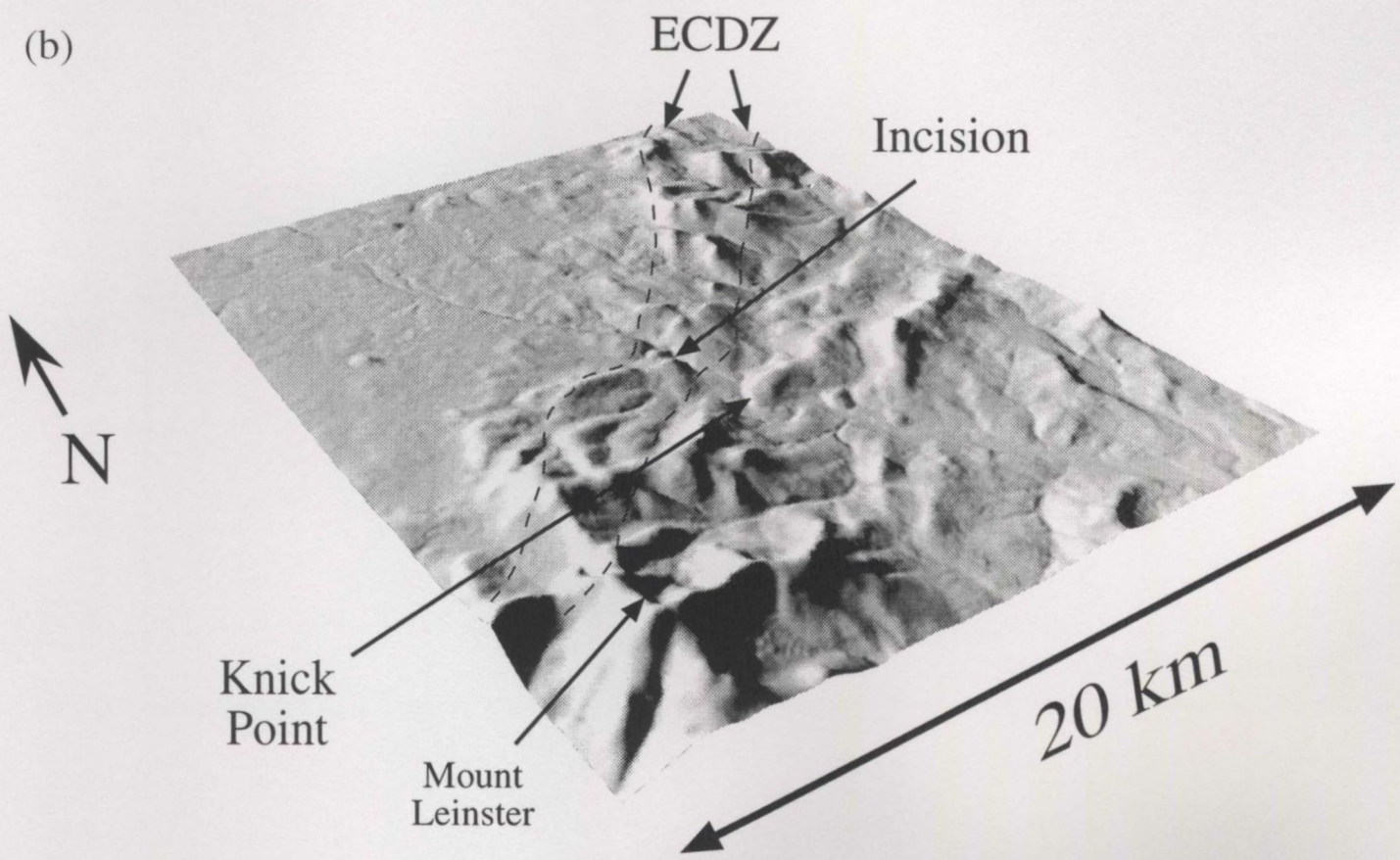

Figure 5.59a,b:- Two topographic relief images of the Bunclody area. a) image is viewed NE along strike of the ECDZ, and b) image viewed NNW along trend of Slaney River to illustrate the abrupt changes in sinuosity as it crosses the topographic ridge, which roughly coincides with the mapped width of the ECDZ. See text for discussion.

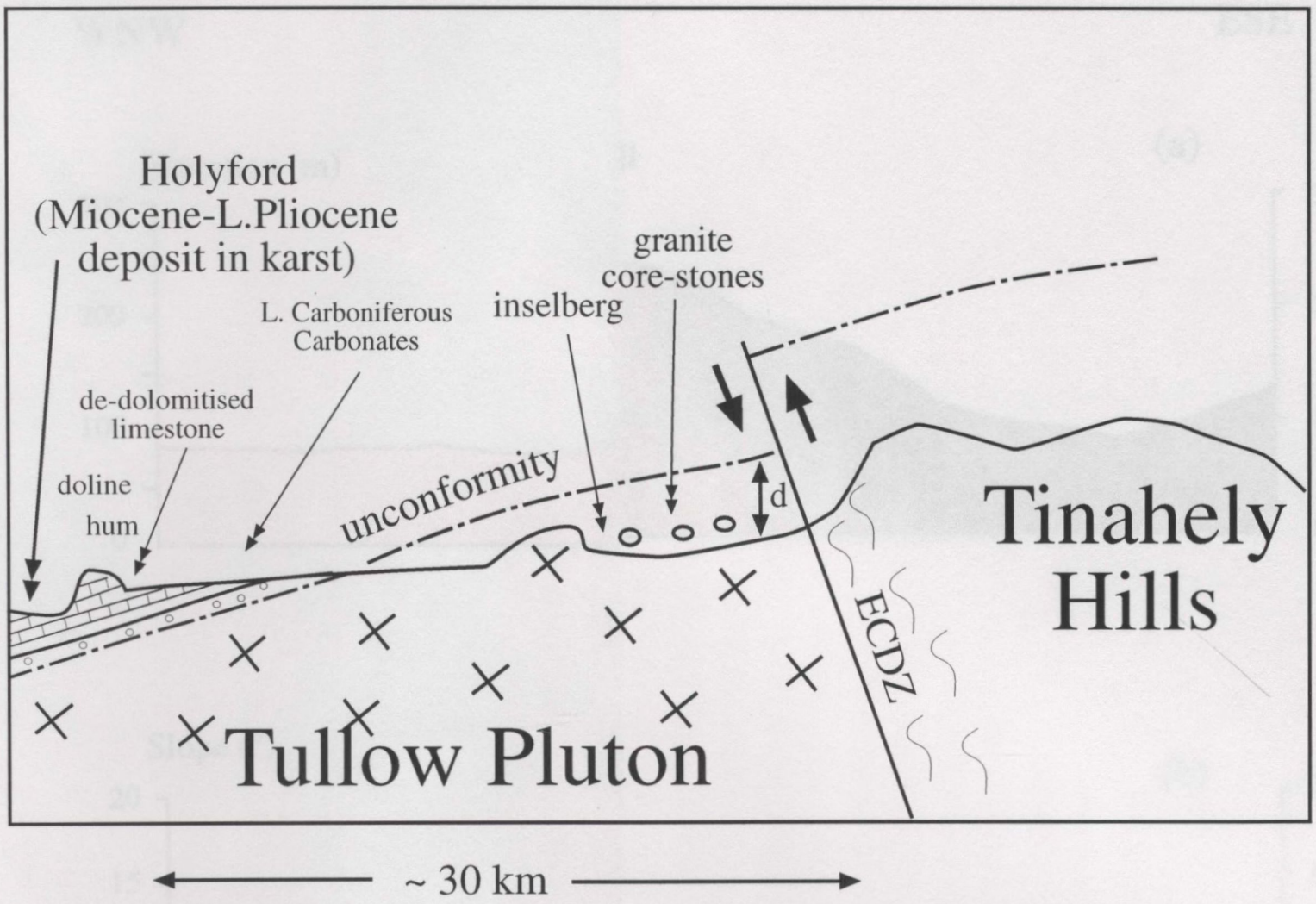

Figure 5.60:- Sketch showing the extent of the Lower Carboniferous unconformity which shows that the Tullow pluton has suffered only minor denudation in the Upper Palaeozoic. Conceptually shows Tertiary weathering features such as doline and hum, core-stones, inselbergs and de-dolomitised limestones. ECDZ – East Carlow Deformation Zone. Maximum post-Carboniferous erosion (d) is c.100-200m.

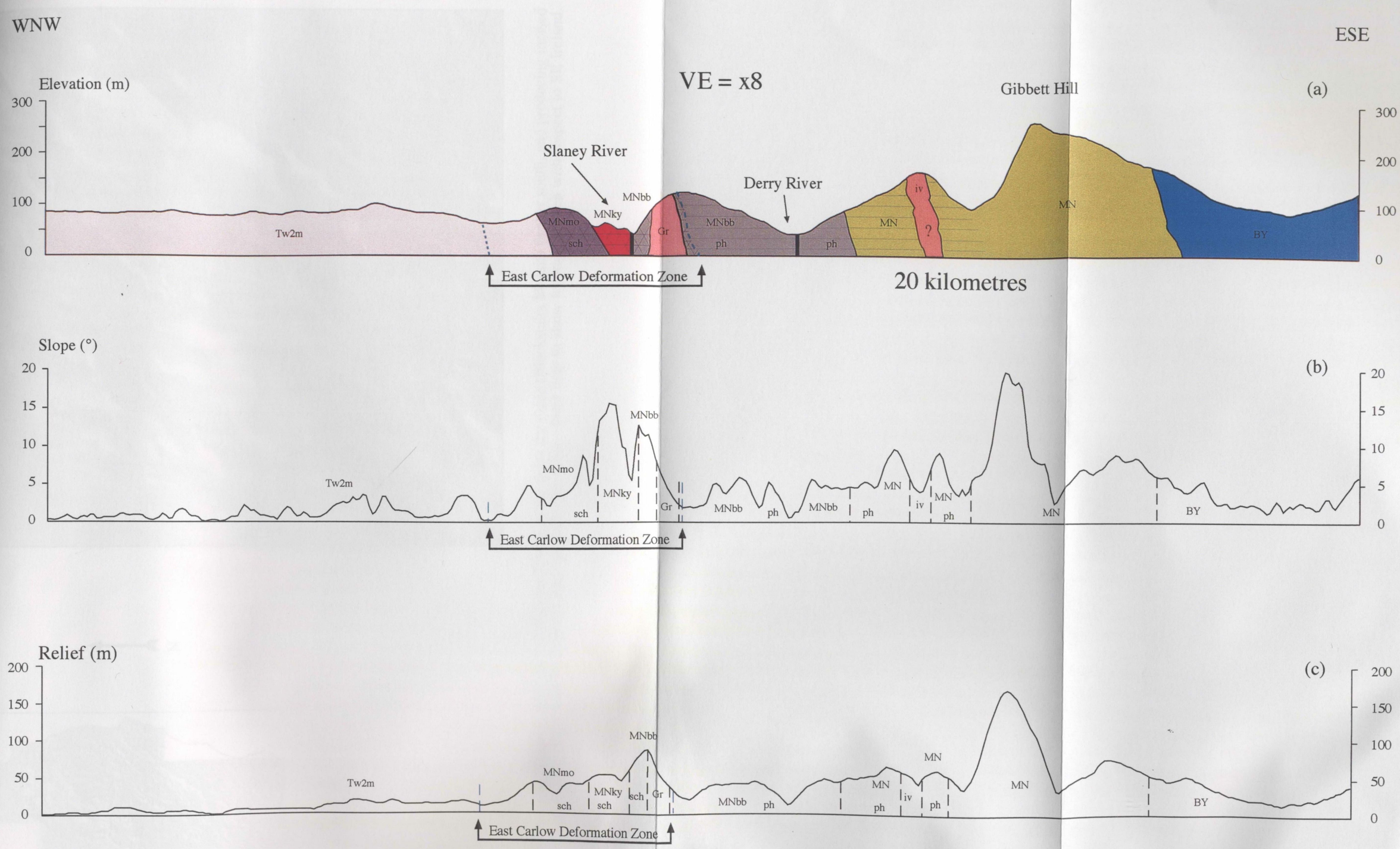

Figure 5.61a,b,c:- WNW-ESE geological, slope and relief profiles of the Bunclody area. Abrupt changes in slope and relief are influenced more by the ECDZ and less by differential weathering at lithological contacts.

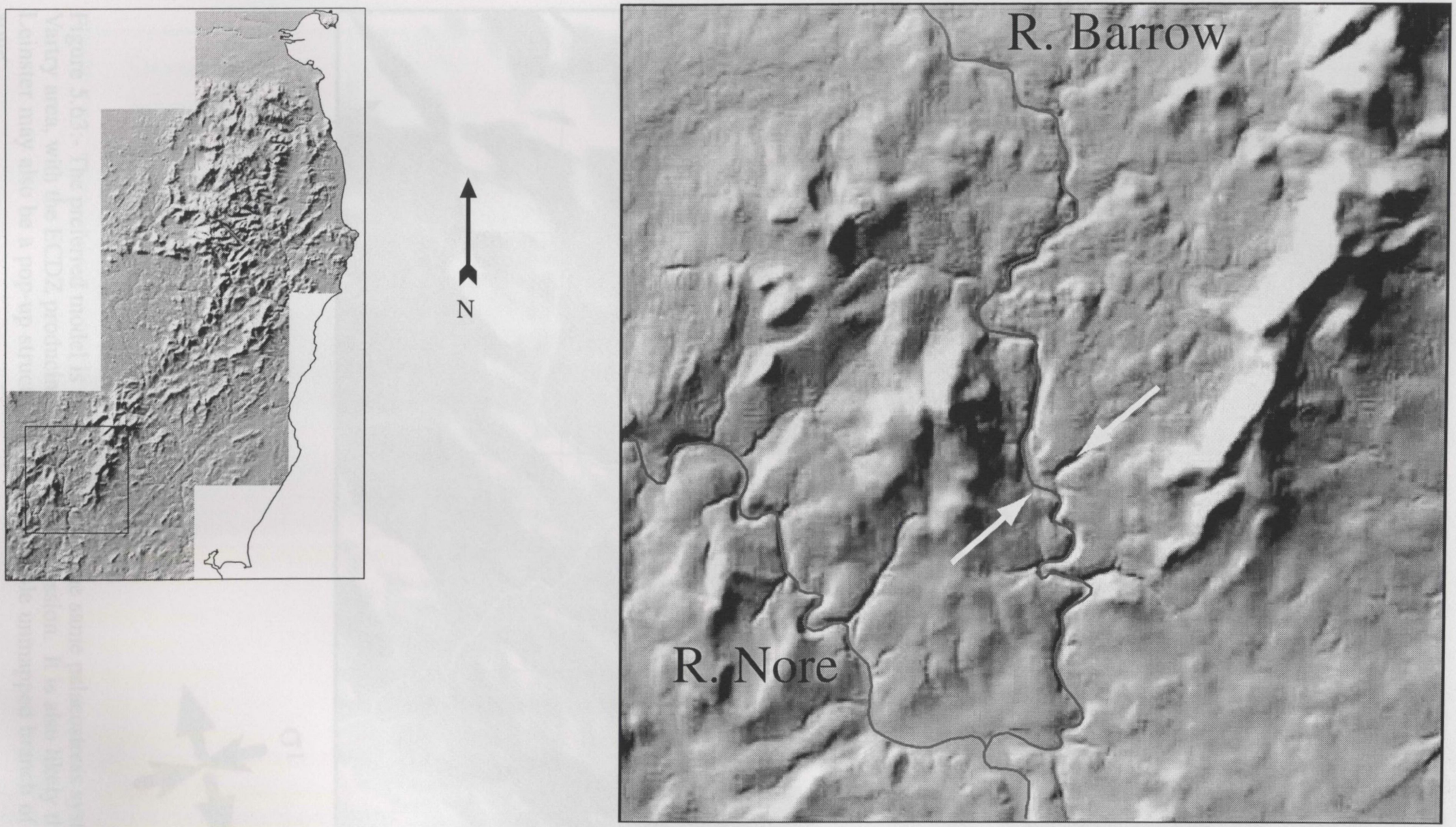

Figure 5.62:- Hillshaded image of the Nore and Barrow Rivers as the cross the ridge (Blackstairs Massif) further south, and producing incised gorges and meanders. The rivers (and the Slaney) must pre-date the ridge. Inset map to show location of area with respect to SE Ireland.

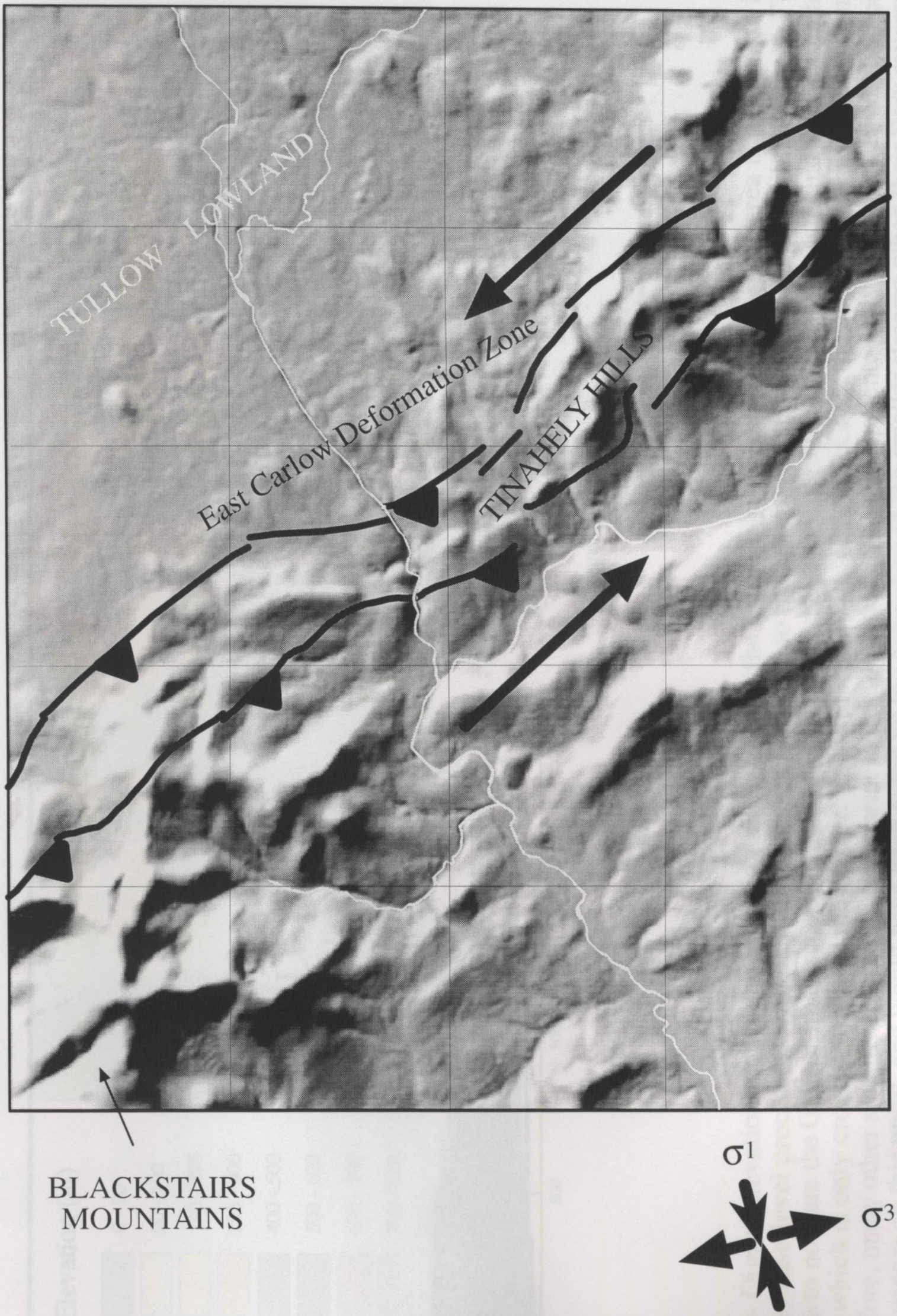

Figure 5.63:- The preferred model is in harmony with the same palaeostress system of the Vartry area, with the ECDZ producing sinistral transpression. It is also likely that Mount Leinster may also be a pop-up structure along a possible unmapped branch of the shear zone.

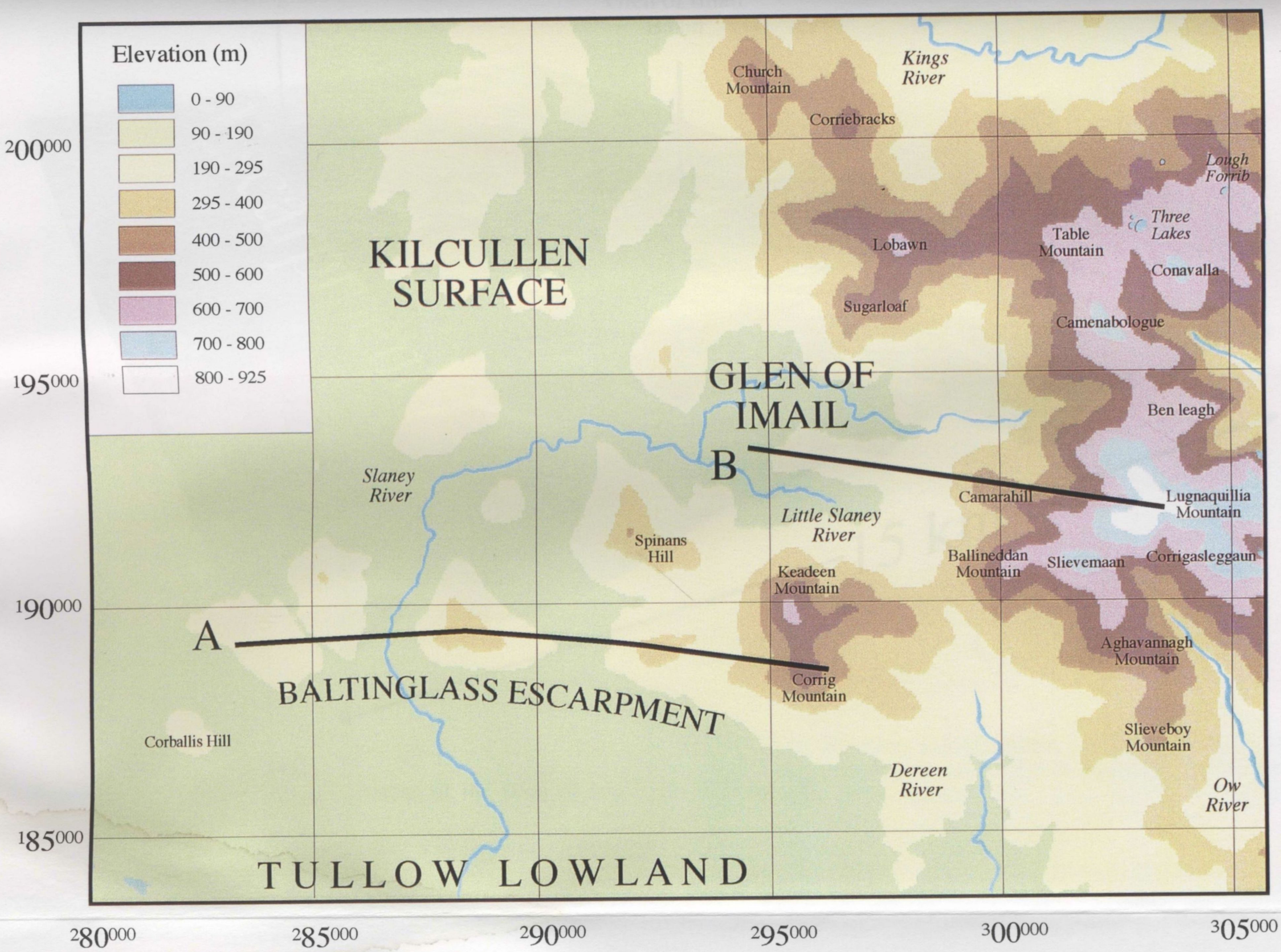

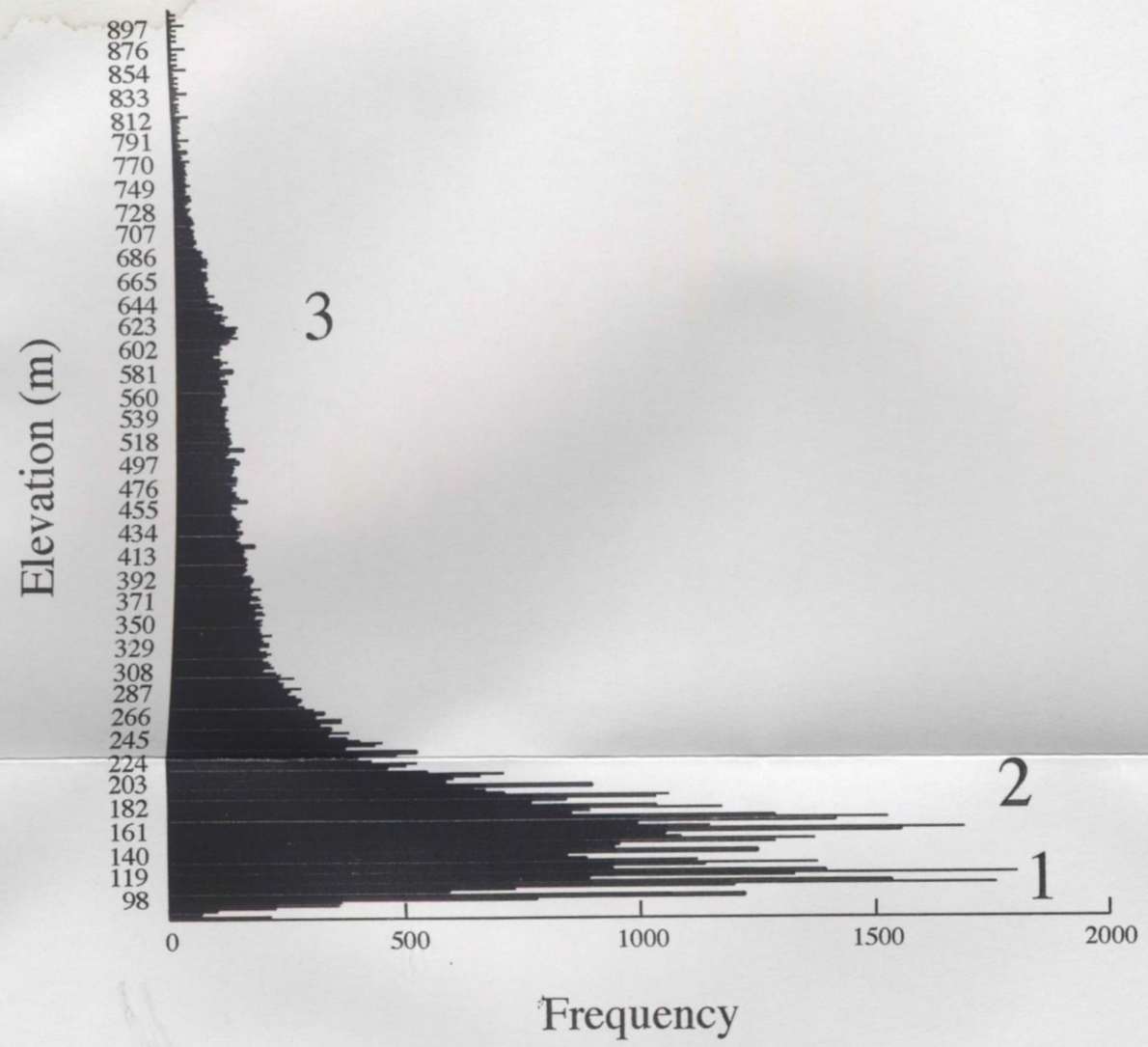

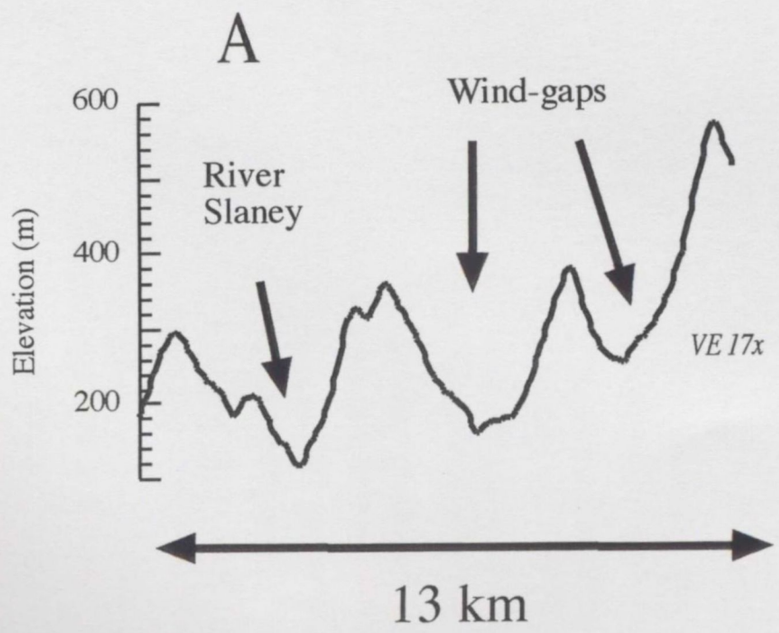

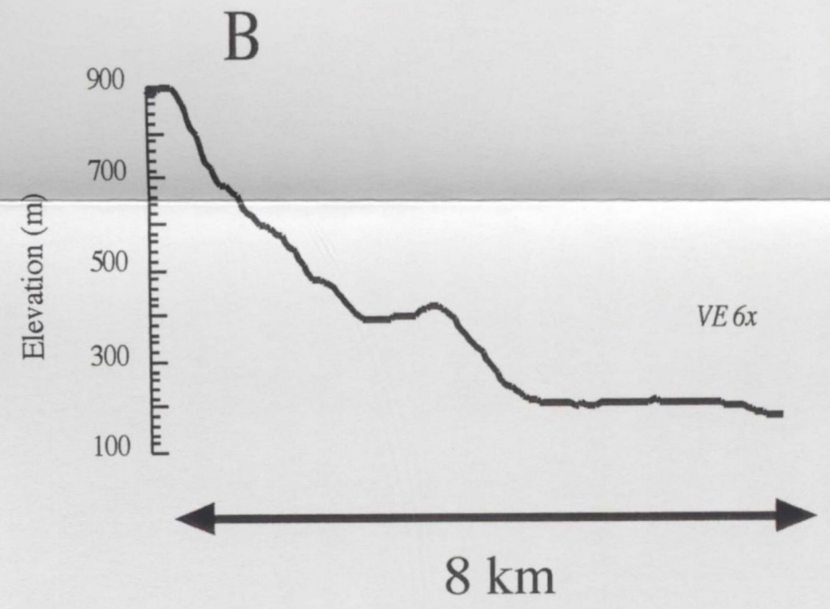

Figure 5.64:- Digital elevation model and elevation histogram for the Glen of Imail area of study. The area is dominated by transitional to base-level processes, with plateau processes restricted to the east of the area, i.e. the Lugnaquillia surface. The main features to note are the Glen of Imail scoop shaped basin, on the western flanks of the Wicklow Massif, and the Baltinglass escarpment, which is only crossed by the Slaney River. In similar fashion with the ECDZ, the escarpment has several wind-gaps. Therefore, many other streams crossed this area prior to the formation of the escarpment. Only the Slaney River has been able to keep pace with this uplift, and would have been aided by the beheading of the smaller streams when their flow reversed back towards the Glen of Imail area.

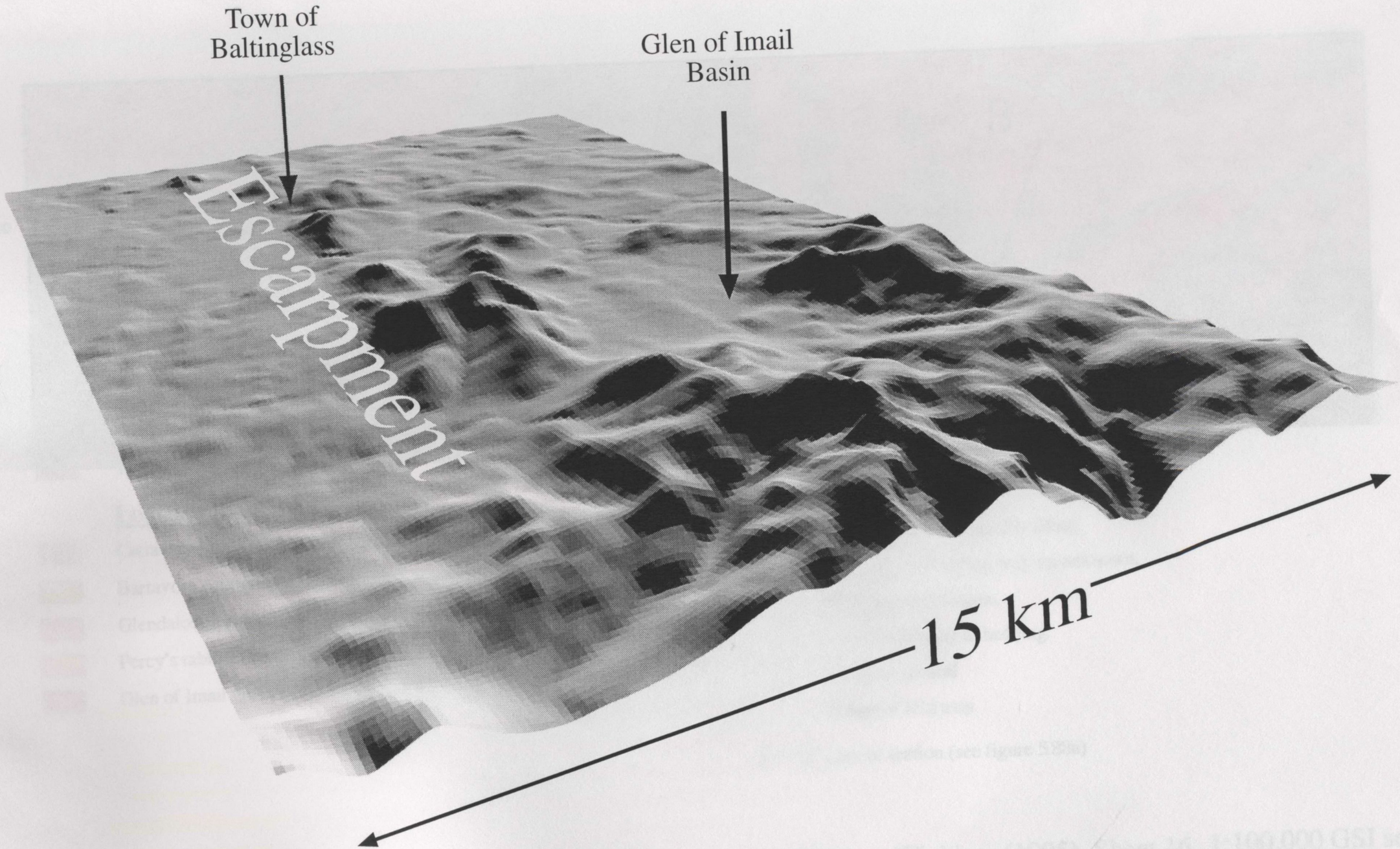

Figure 5.65:- Topographic relief image of the Glen of Imail area looking ~W.

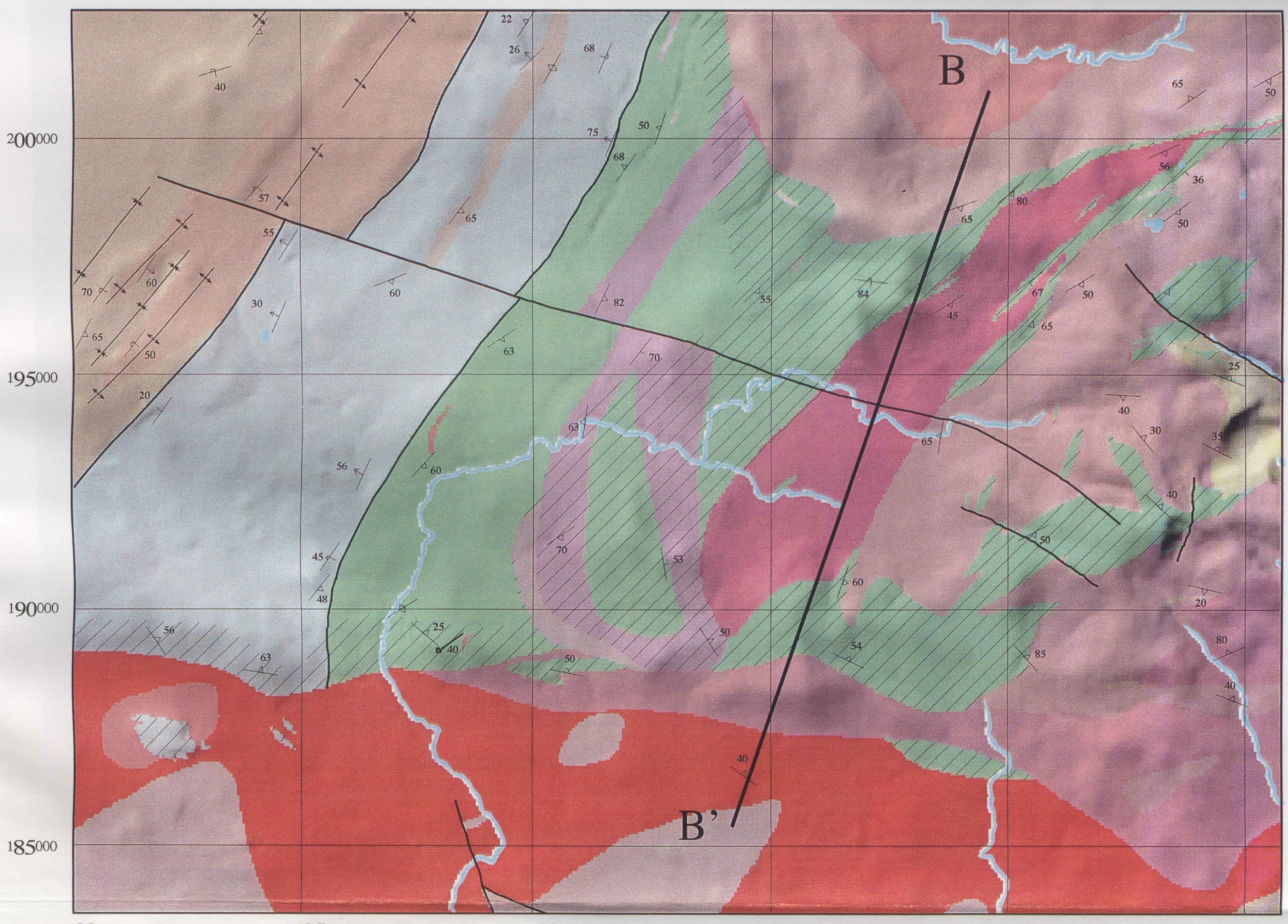

Kilcullen Group. Llandovery (-Ludlow)

Carrighill Formation. Calcareous, greywackes, siltstone and shale.

Tipperkevin Formation. Greywacke and shale.

Glen Ding Formation. Chloritic, feldspathic greywackes.

Slate Quarries Formation. Slate and greywackes.

Pollaphuca Formation. Coarse, greywacke and shale.

Ribband Group. Cambrian (Tremadoc-Llanvirn)

Maulin Formation. Dark grey semi-pelitic, psammitic schist.

Butter Mountain Formation. Dark slate-schist, quartzite & coticule.
Donard Andesite Member. Andesite & andesitic tuff.

Northern Pluton

Type2e equigranular. Pale grey fine to coarse-grained granite.

Type 2p microcline porphyritic. Granite with microcline phenocrysts.

Type 1 granodiorite. Fine-grained granodiorite to granite.

Lugnaquillia Pluton

Carrawaystick Aplite. White, saccharoidal garnetiferous aplite.

Barravore Aplogranite. Fine-grained, mucovite-rich aplogranite.

Glendalough Adamellite. Adamellite with microcline phenocrysts.

Percy's table Granodiorite. Aphyric granodiorite.

Glen of Imail Quartz-Diorite. Dark aphyric quartz diorite.

Tullow Pluton

Type 2 Microcline Porphyritic Granite. Granite with microcline phenocrysts.

Type 2 Equigranular. Pale, fine to coarse-grained granite.

Type 1 Granite. Fine-grained granodiorite to granite.

Other Rocks

Granite (undifferentiated).

Aplite.

Appanite.

Dolerite.

Western dynamic aureole zone.

Fault.

Thurst fault, barbs on hangingwall side.

Anticline.

Syncline.

Strike/dip of bedding, right way-up.

Strike/dip of overturned bedding.

Strike/dip of bedding, way-up unknown.

Strike/dip of foliation.

Foliation parallel to bedding.

Foliation vertical

Plunge of fold axis

B—B' Line of section (see figure 5.88a)

Figure 5.66:- Solid bedrock geology map (taken from Geology of Kildare-Wicklow (1995), Sheet 16, 1:100,000 GSI series) of the Glen of Imail area. The geology is draped over a NW illuminated topographic relief grid to show the relationship of geology with topography. Note that lack of outcrop in the glen makes the map quite speculative.

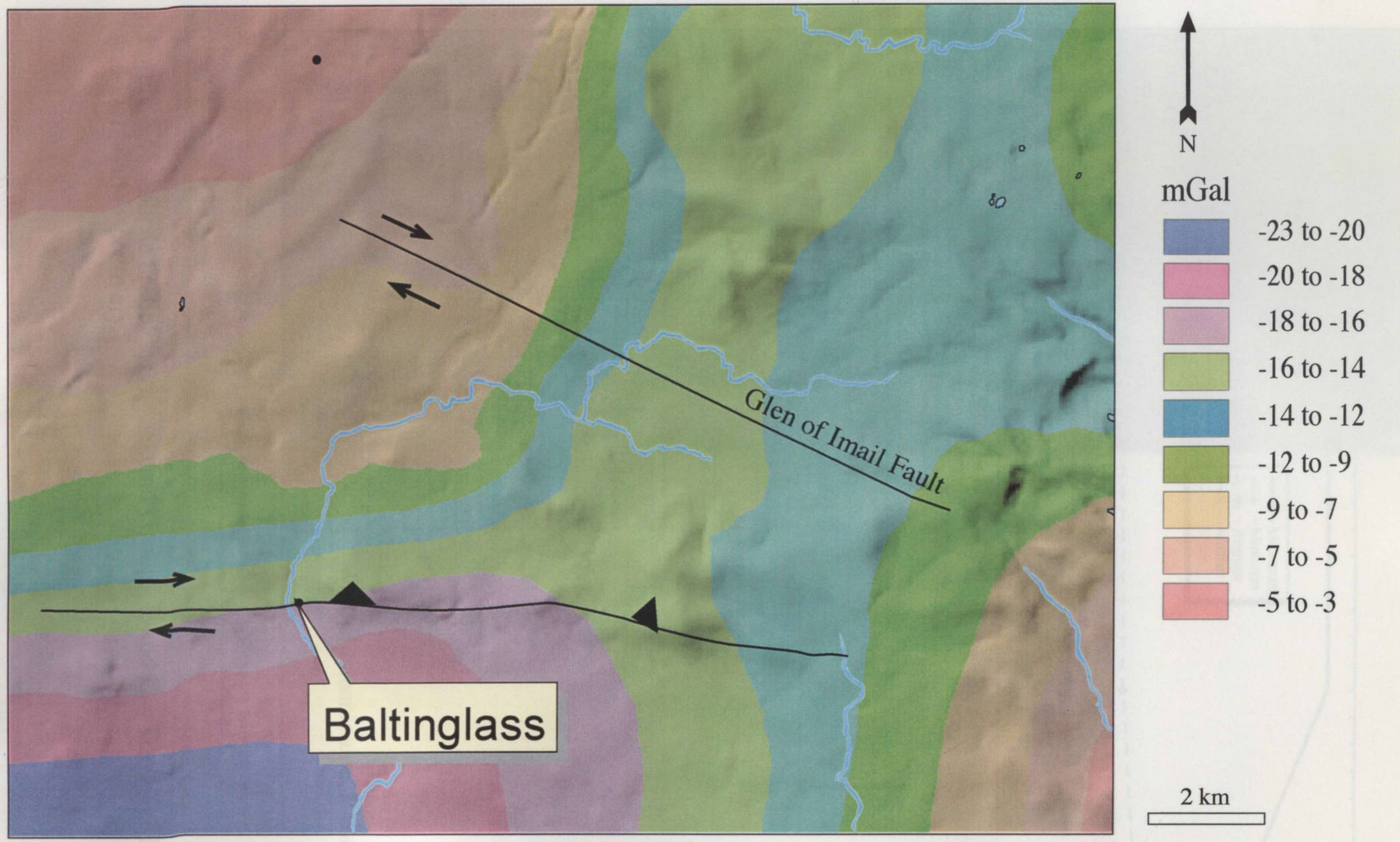

Figure 5.67:- Bouguer gravity anomaly image of the Glen of Imail area. Note the dextral offset of the gravity contours by the dextral Glen of Imail fault.

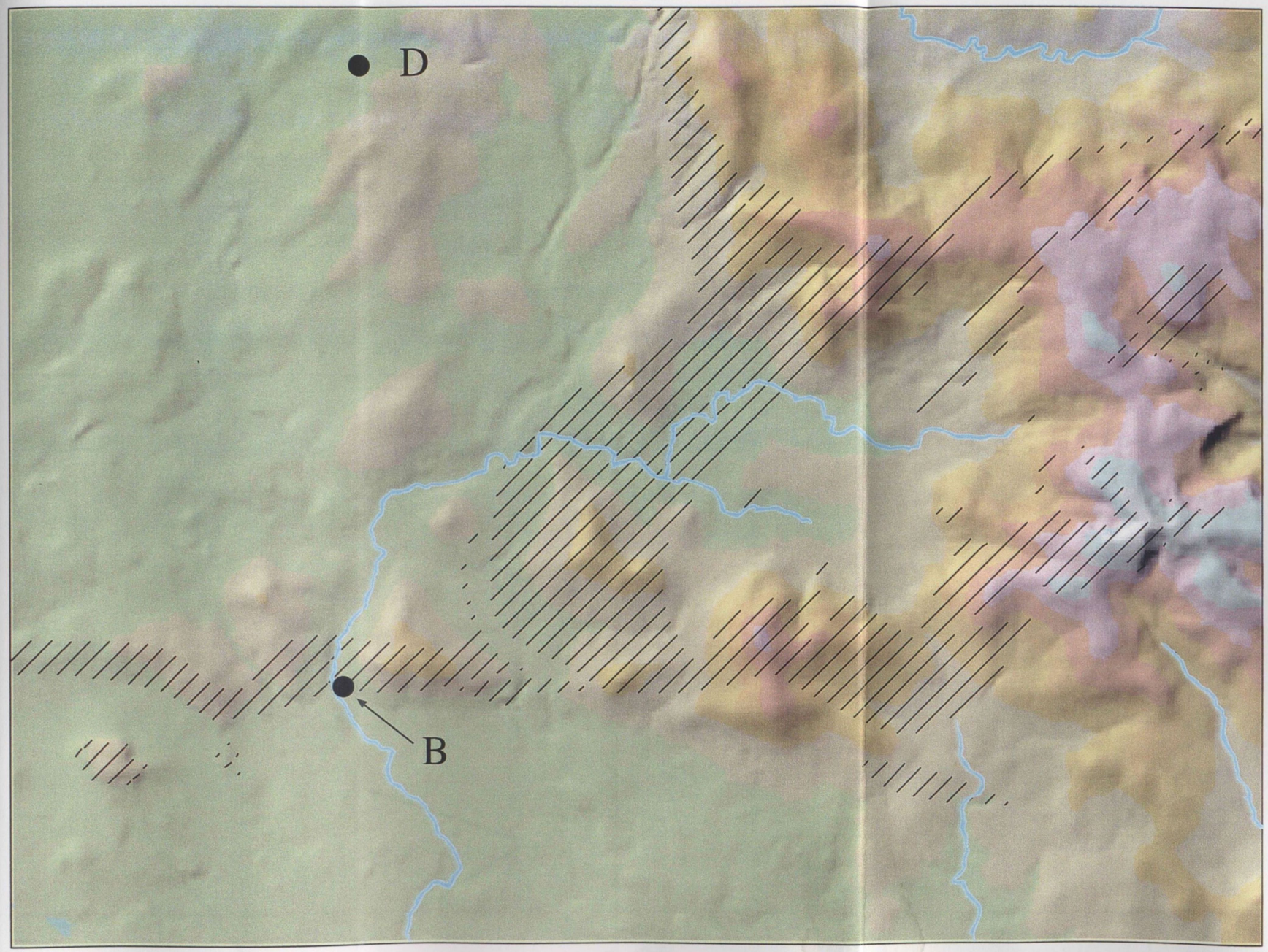

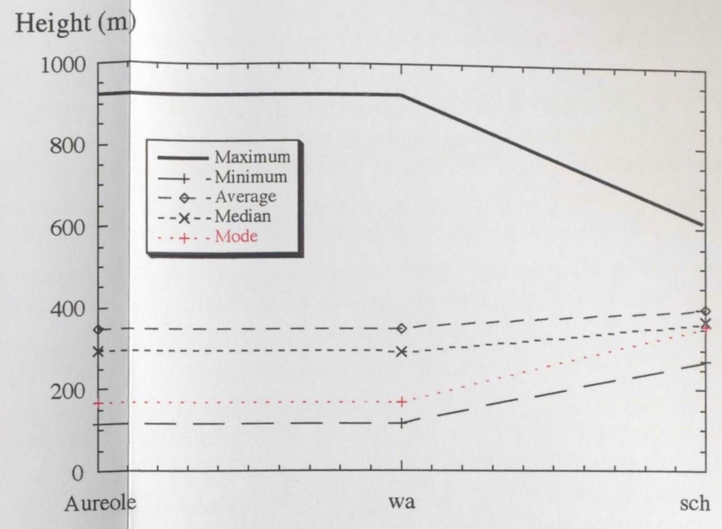

Elevation (m)

- 0 - 90
- 90 - 190
- 190 - 295
- 295 - 400
- 400 - 500
- 500 - 600
- 600 - 700
- 700 - 800
- 800 - 925

N

Western dynamic aureole zone.

5 kilometres

Figure 5.68:- Shaded relief topographic image of the Glen of Imail study area showing the extent of the inner and outer aureole rocks of the Ribband Group. B and D = Towns of Baltinglass and Dunlavin respectively.

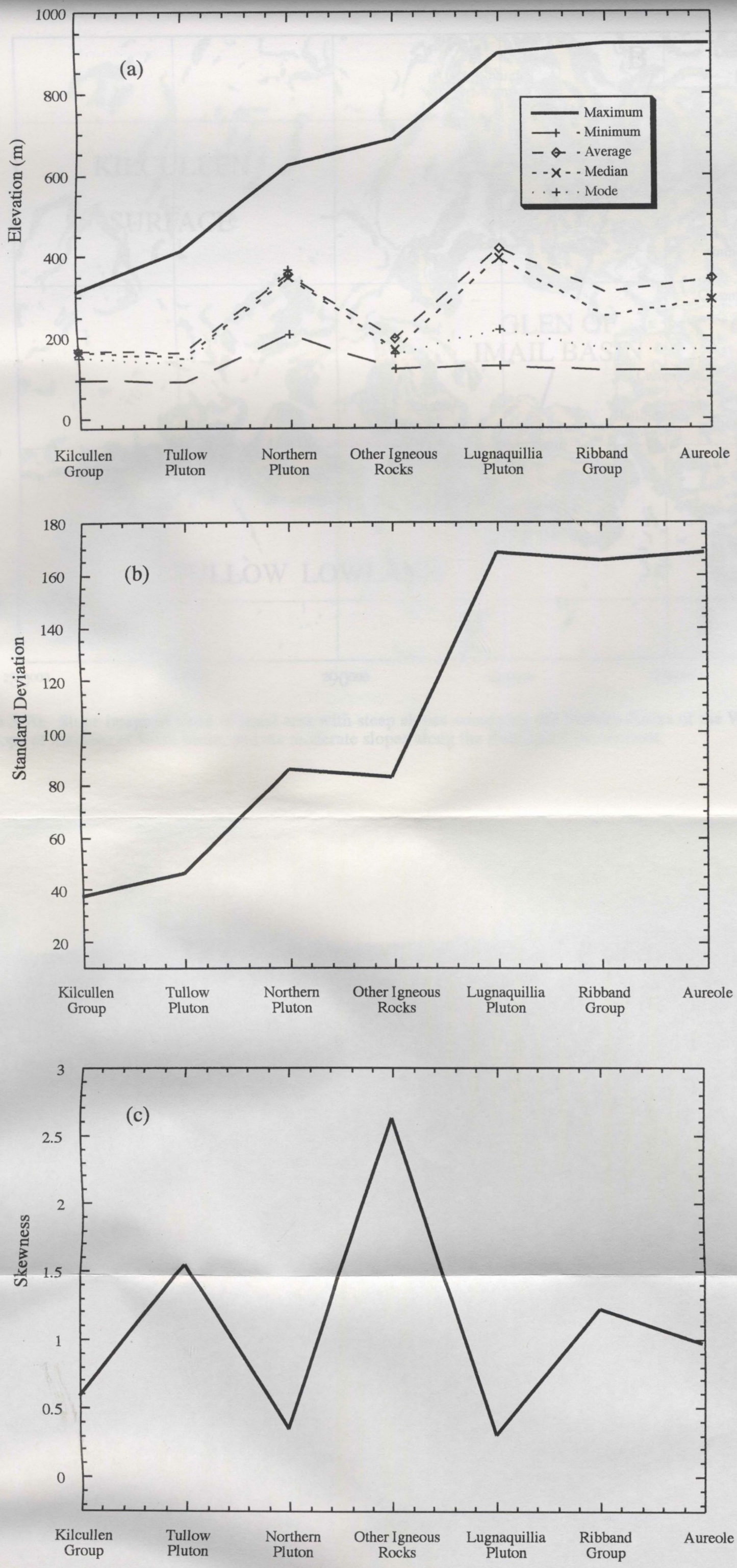

Figure 5.69a,b,c:- Statistical graphs showing the relationship between lithology and elevation in the Glen of Imail area. See text for details.

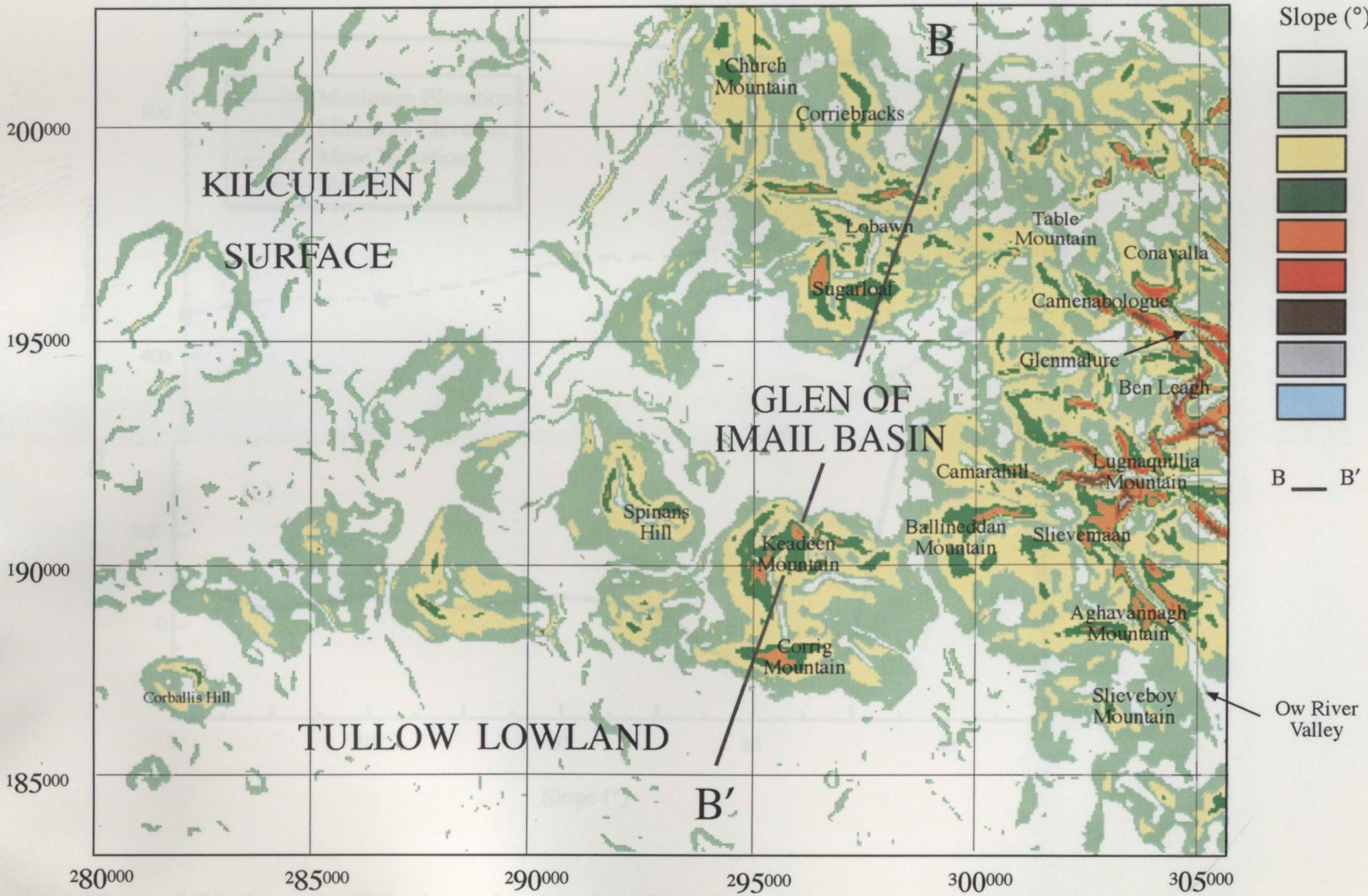

Figure 5.70:- Slope image of Glen of Imail area with steep slopes occupying the western flanks of the Wicklow Massif (in east of study area). Note the low slope of the Glen of Imail basin, and the moderate slopes along the Baltinglass escarpment.

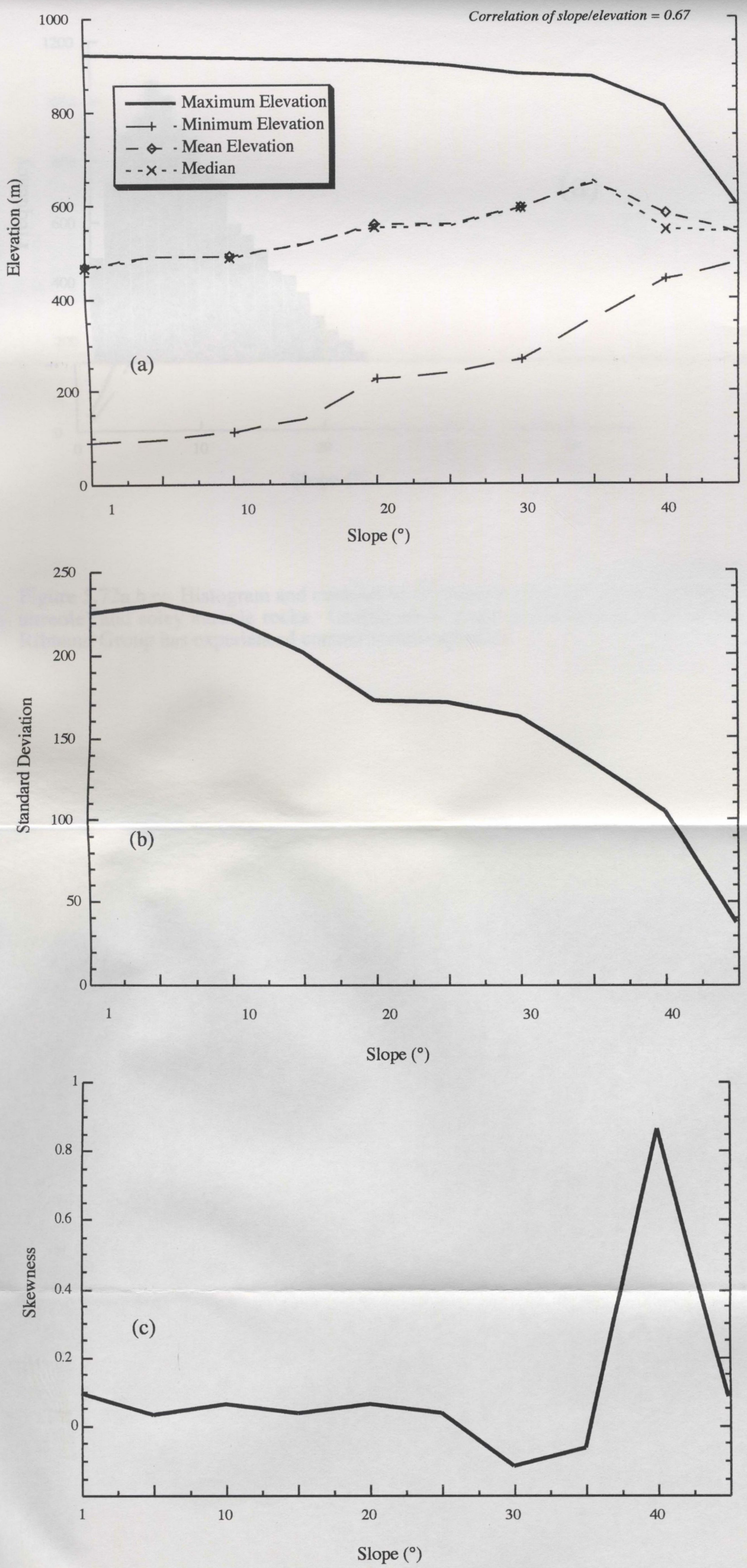

Figure 5.71a,b,c:- Statistical graphs showing the relationship between slope and elevation in the Glen of Imail area (see text).

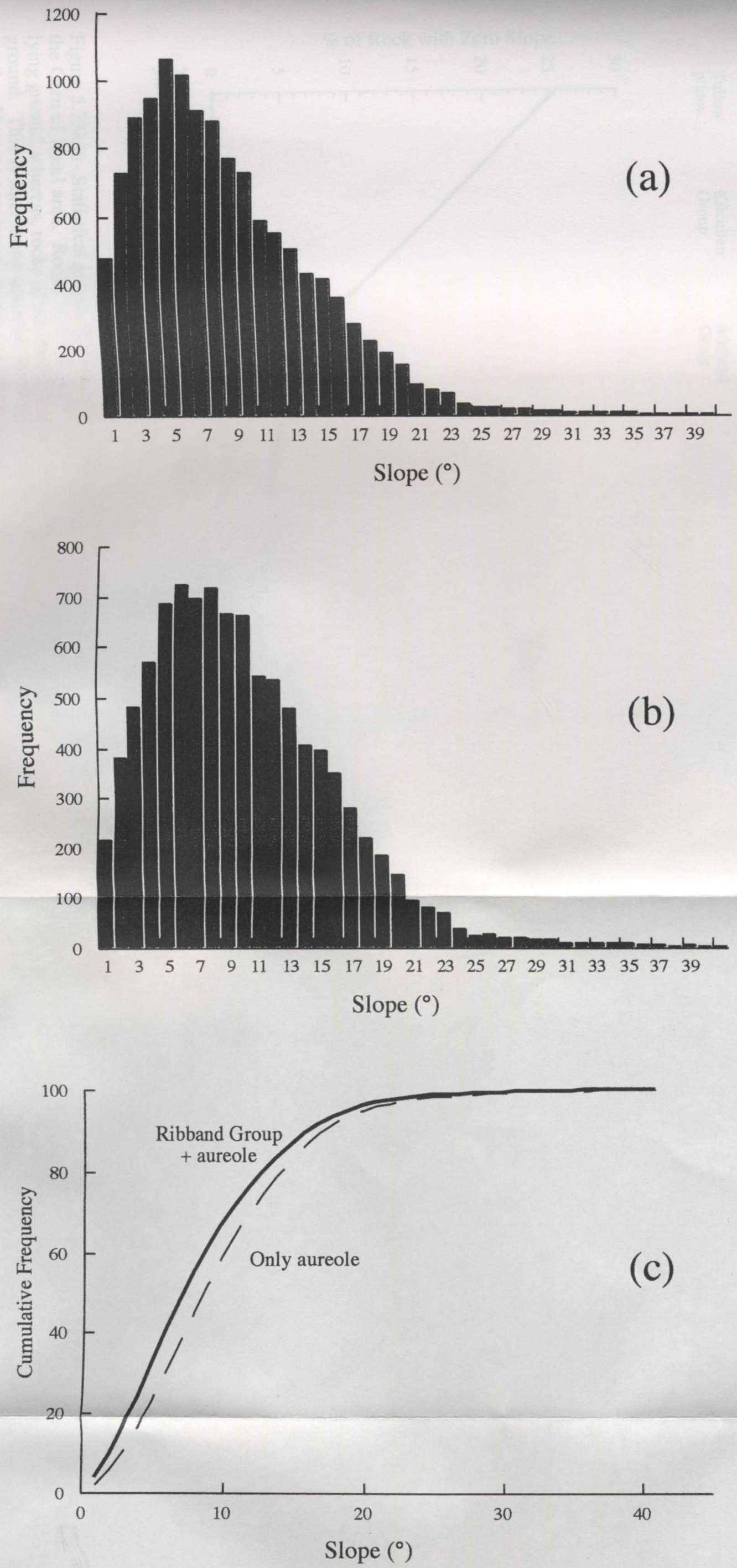

Figure 5.72a,b,c:- Histogram and cumulative frequencies of the Ribband Group (+ aureole) and soley aureole rocks. Graphs show close similarities as most of the Ribband Group has experienced contact metamorphisms.

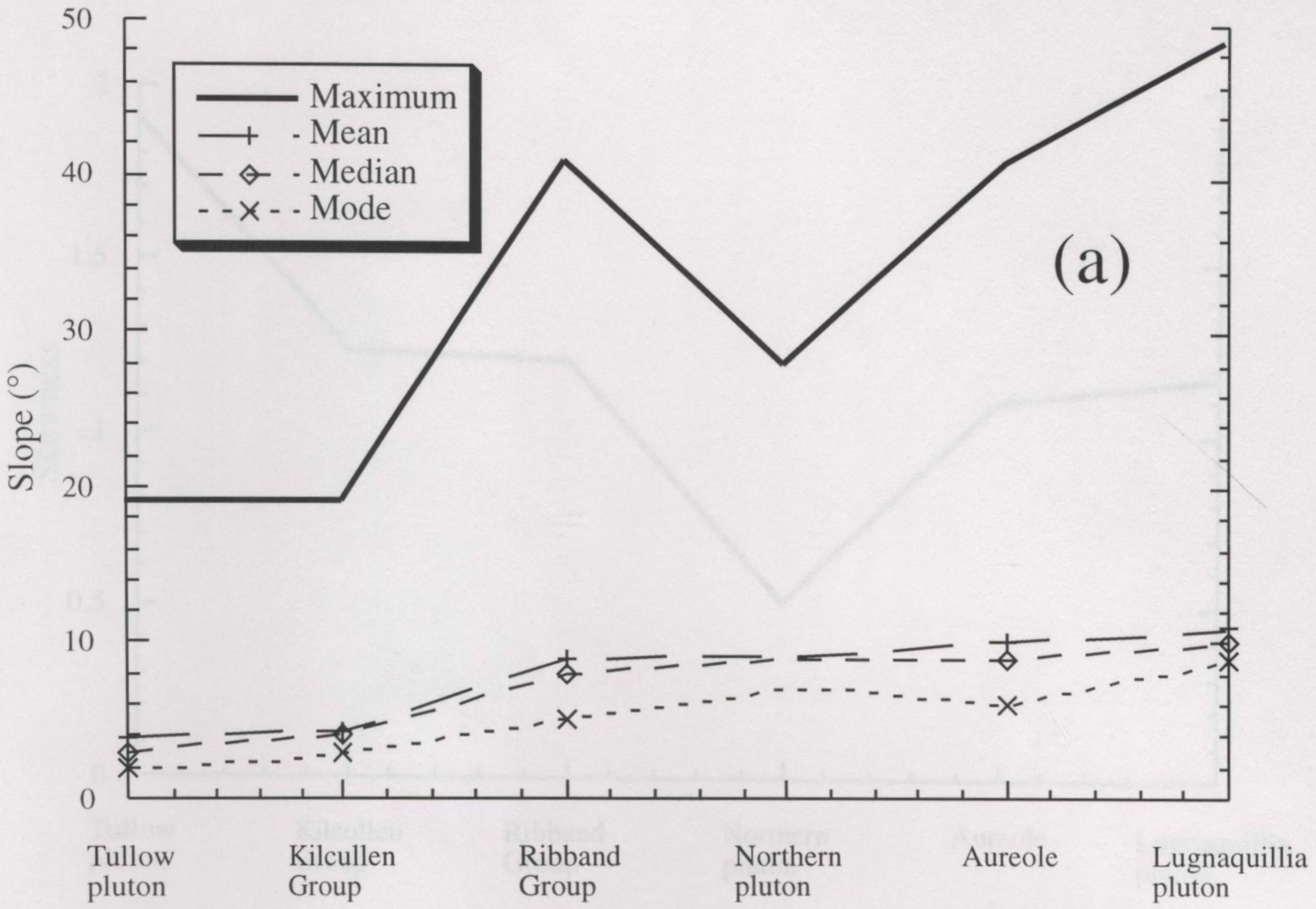

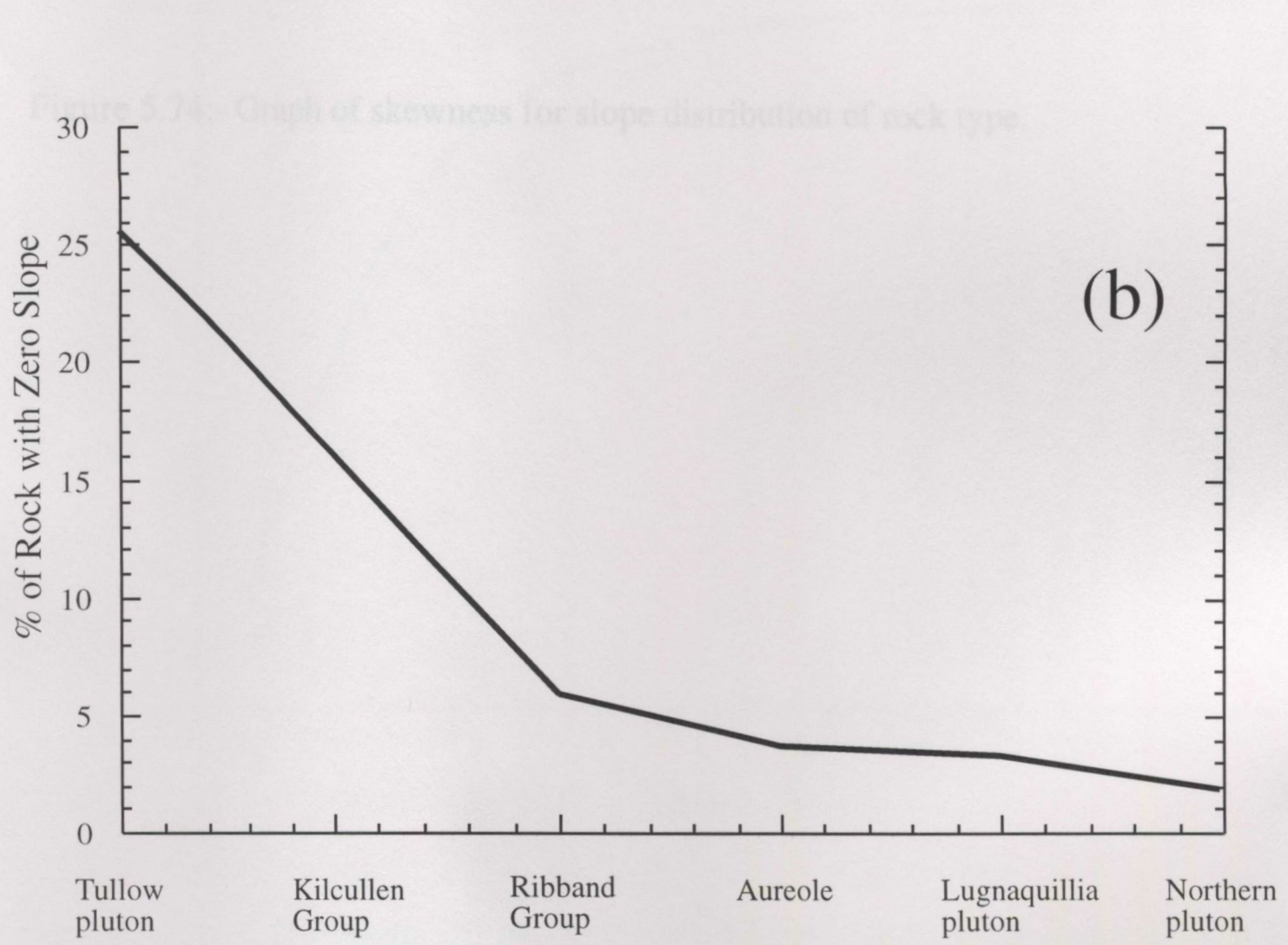

Figure 5.73a,b:- Statistical graphs showing the relationship between slope and lithology in the Glen of Imail area. Rocks of the Tullow pluton occupy relatively large areas of flat-lying ground, whereas, rocks of the Northern pluton produced the smallest area of flat-lying ground. This is interesting because, on chemistry and texture, the two plutons are very similar. Hence, tectonic activity needs to be invoked to explain these differences (see section 5.6.17).

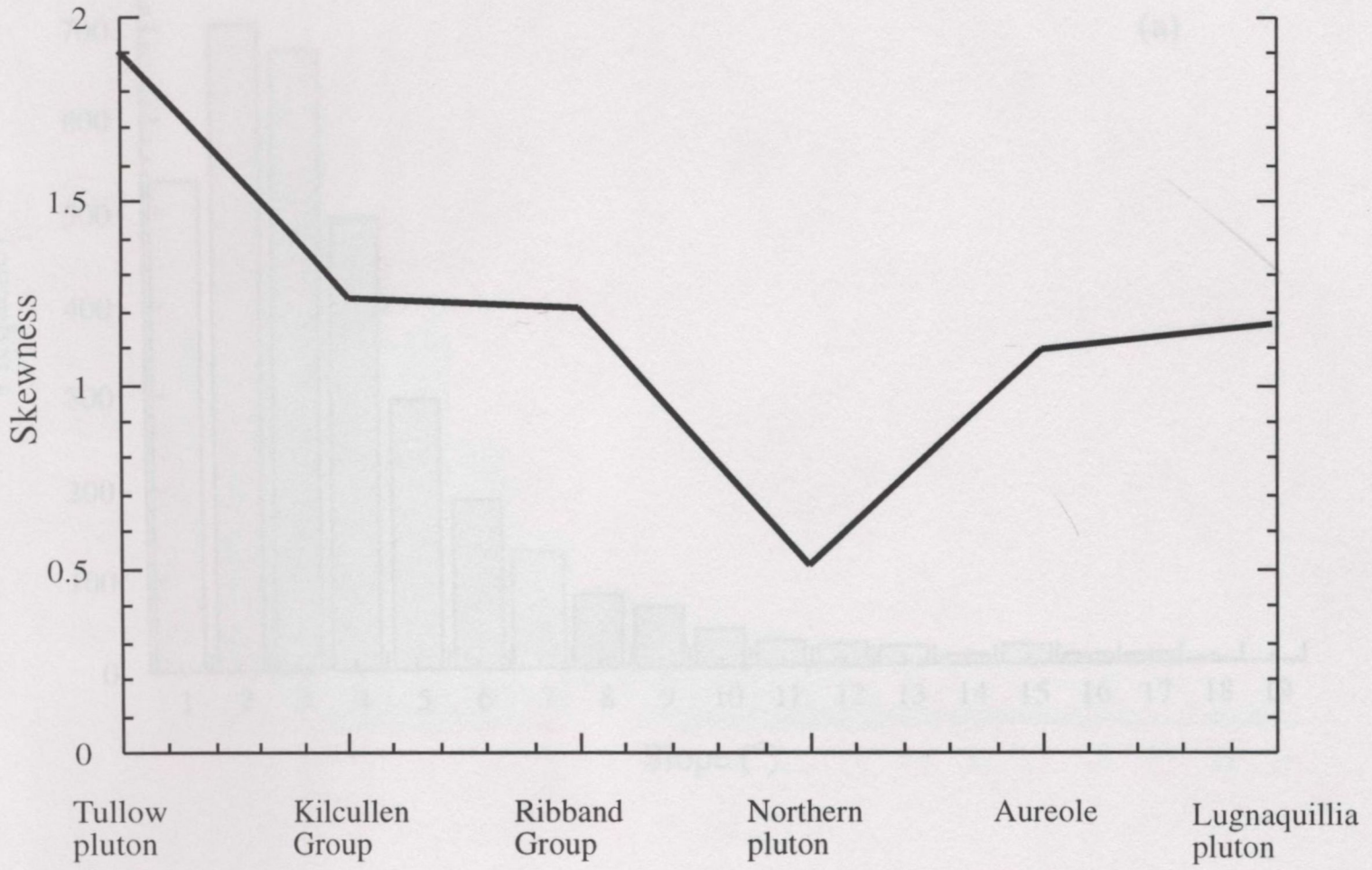

Figure 5.74:- Graph of skewness for slope distribution of rock type.

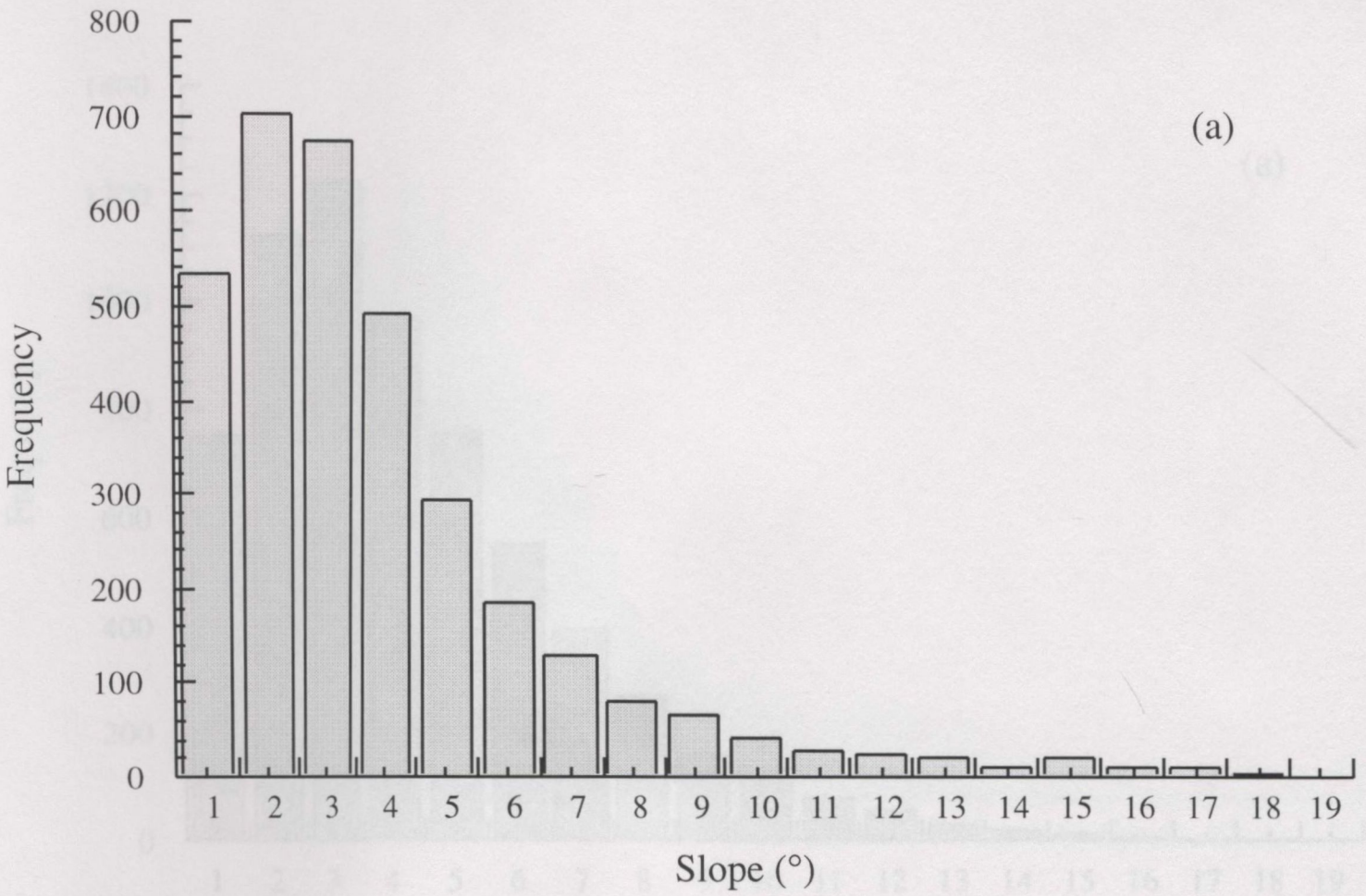

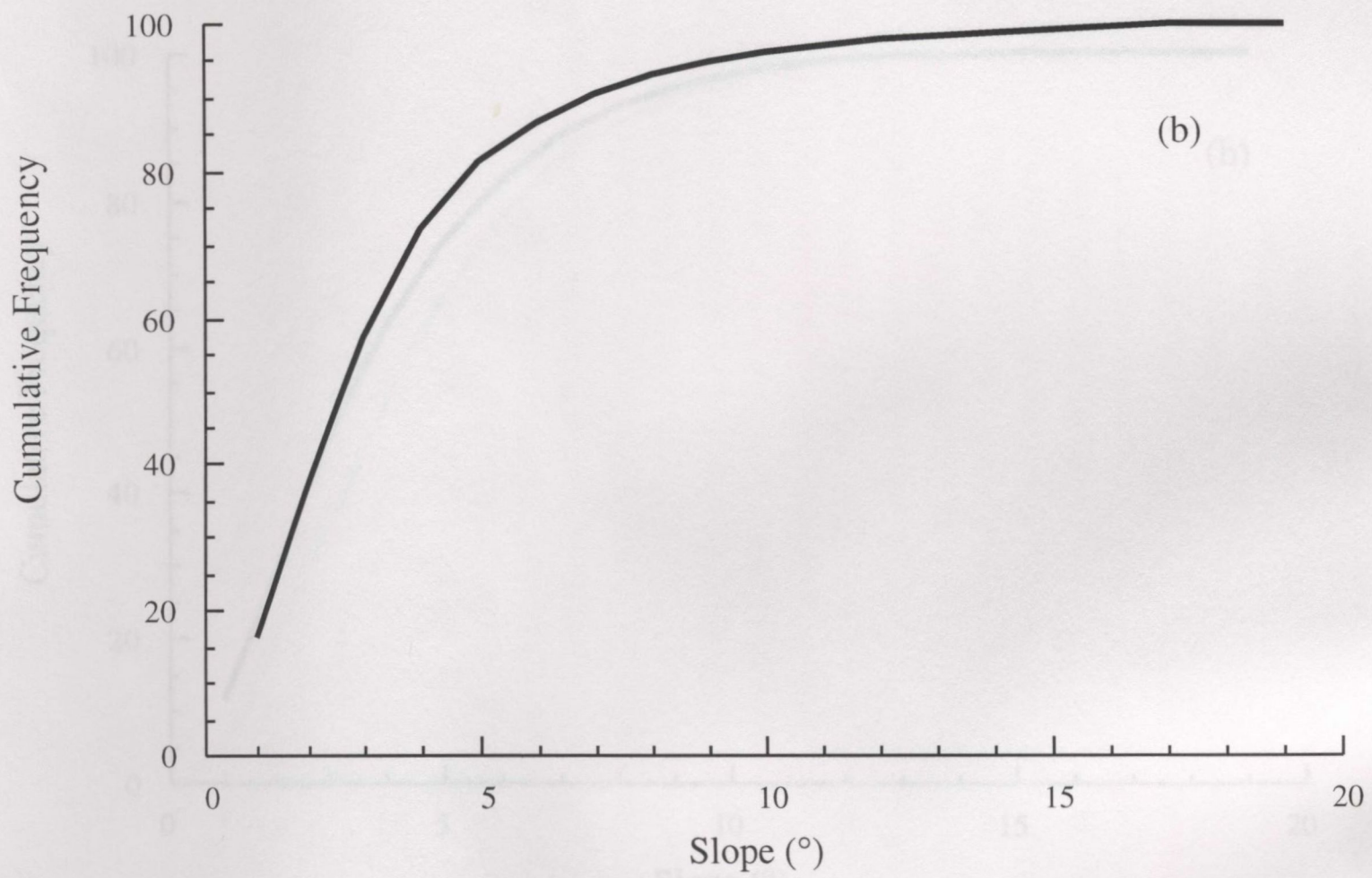

Figure 5.75a,b:- Histogram (a) and cumulative frequencies (b) for rocks of the Tullow pluton. These rocks are typified with relatively low slopes.

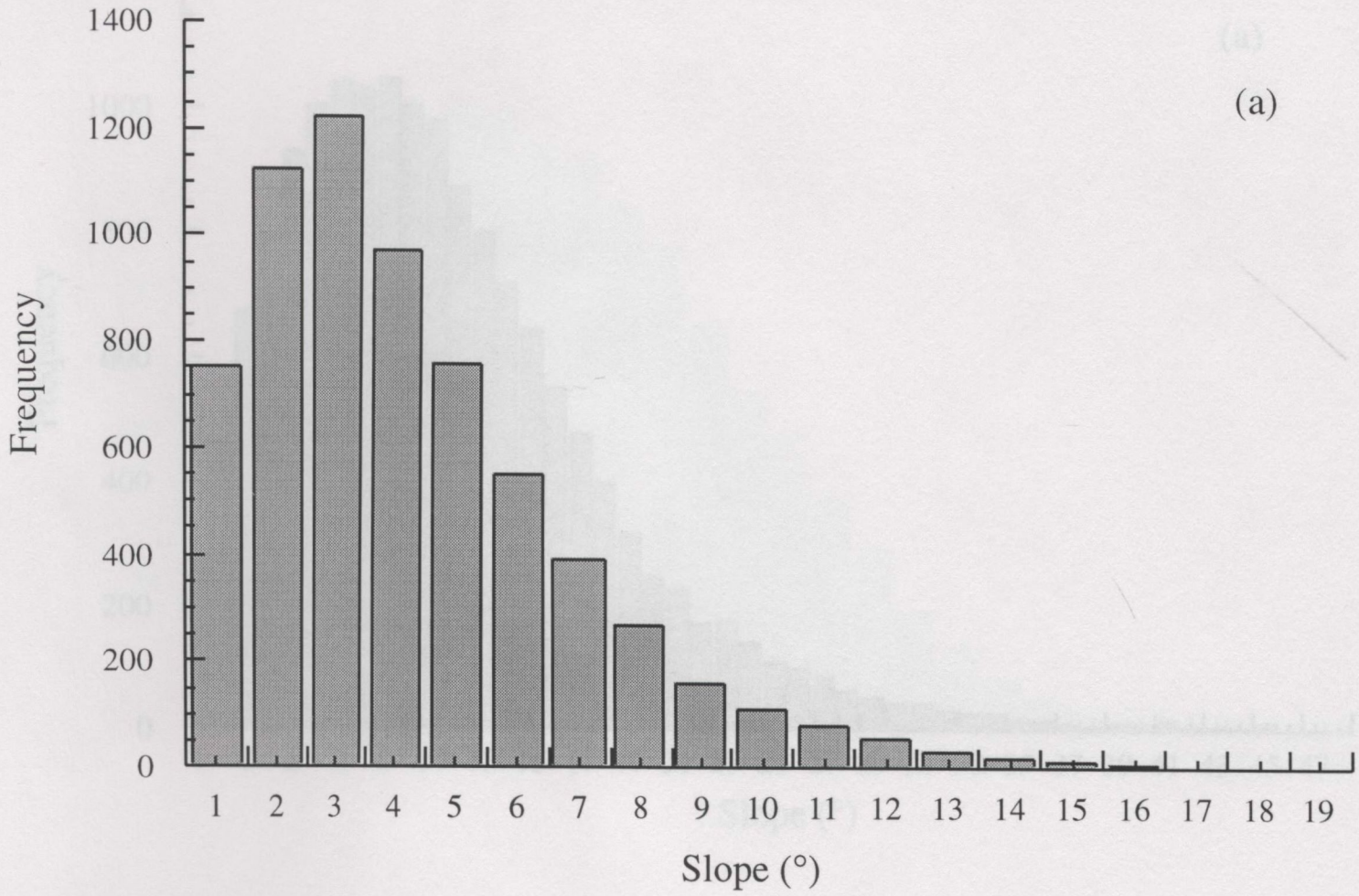

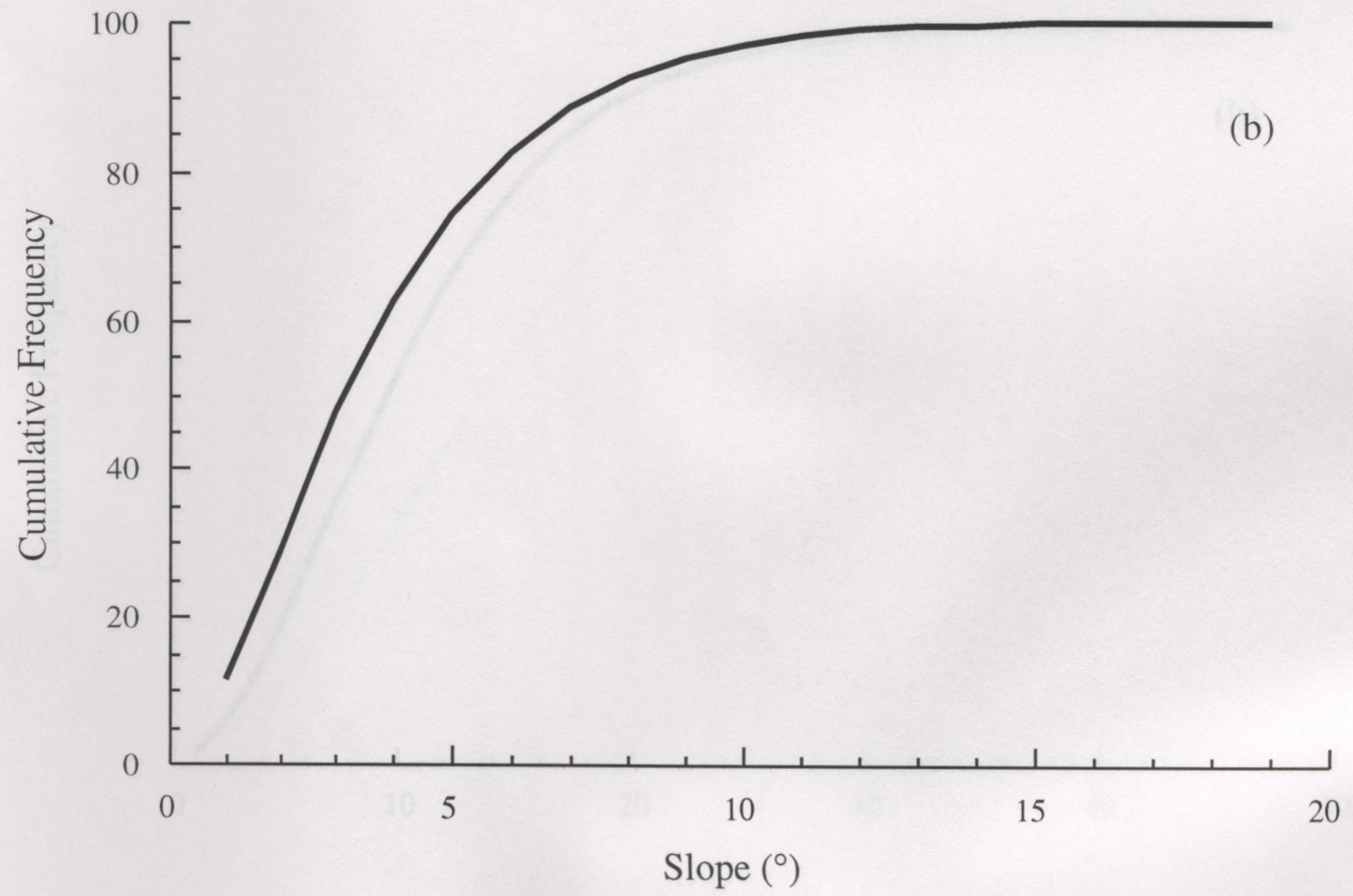

Figure 5.76a,b:- Histogram (a) and cumulative frequencies (b) of rocks of the Kilcullen Group likewise form relatively flat-lying land to the west of the Wicklow Massif.

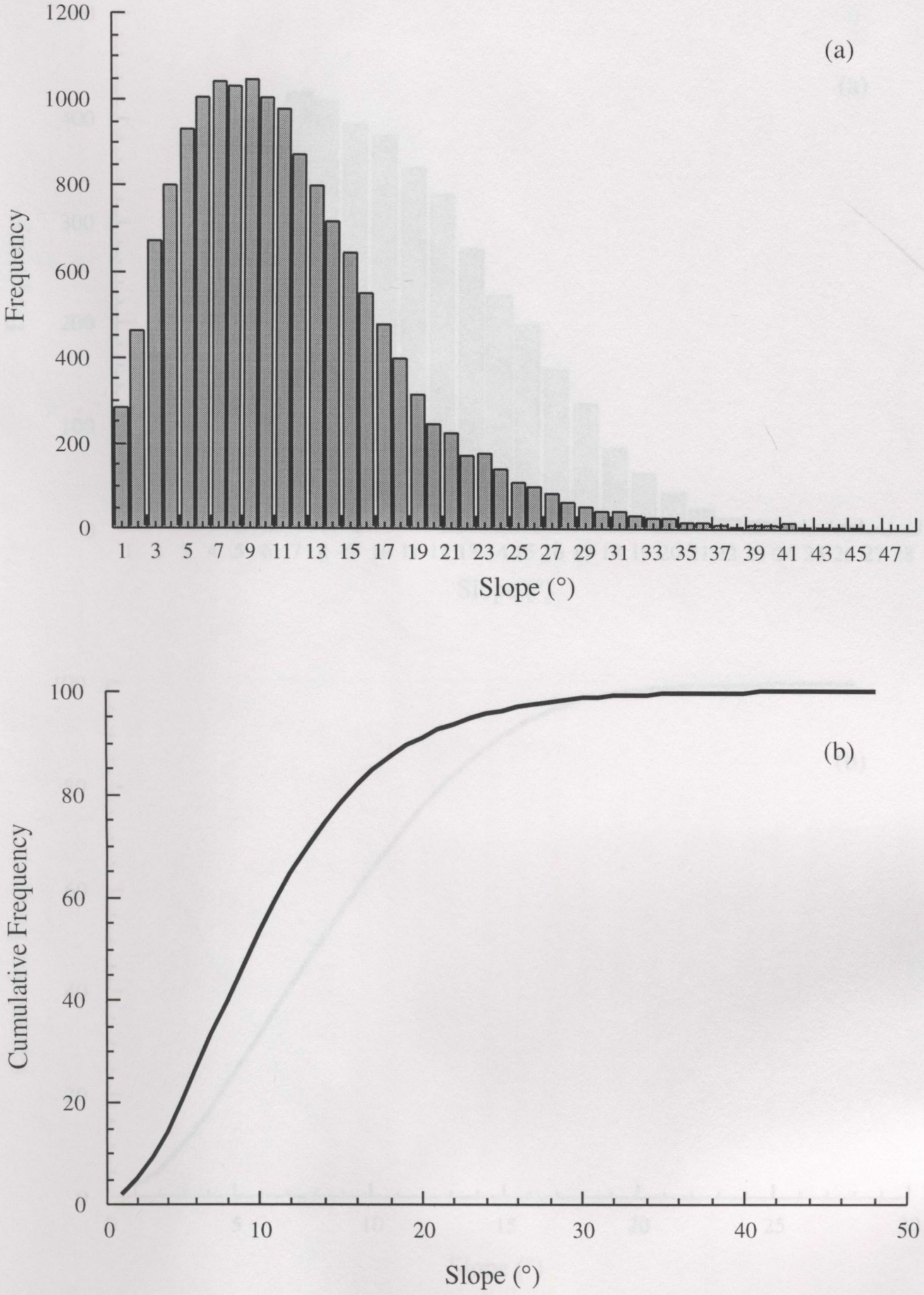

Figure 5.77a,b:- Histogram (a) and cumulative frequencies (b) of the Lugnaquillia plutonic rocks is moderate to high (see text for discussion).

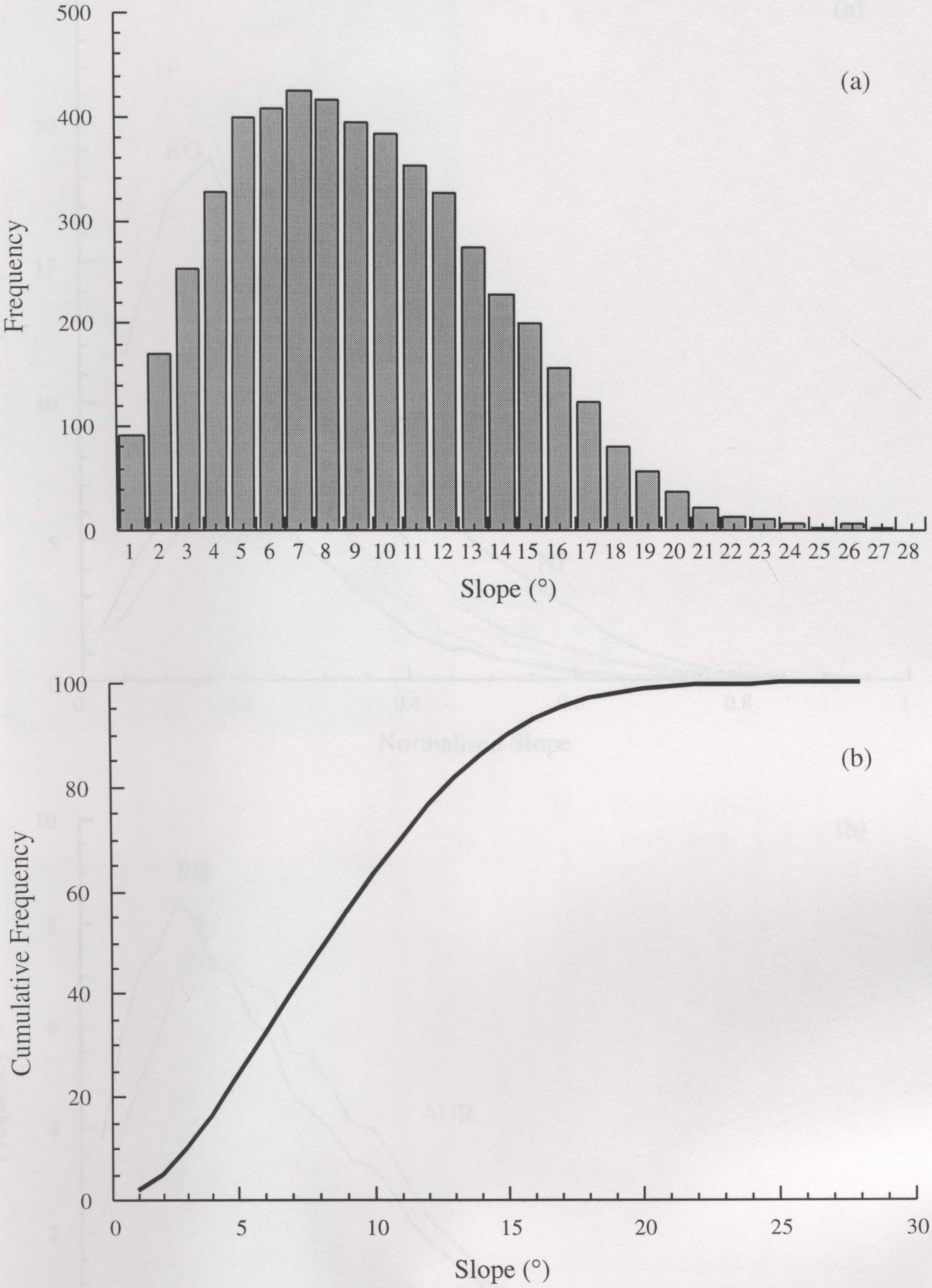

Figure 5.78a,b:- Histogram (a) and cumulative frequencies (b) of the Northern pluton which shows moderate slopes.

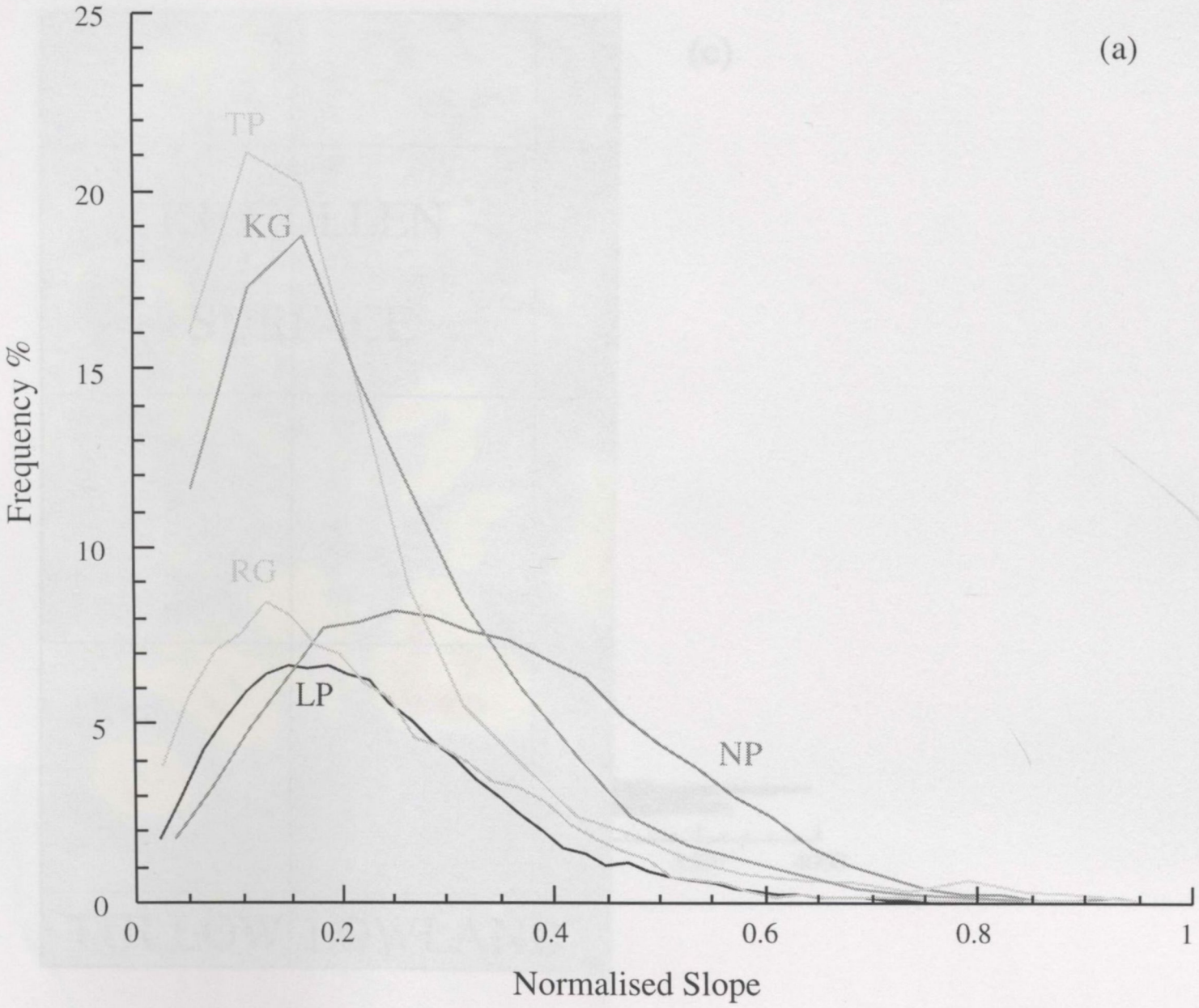

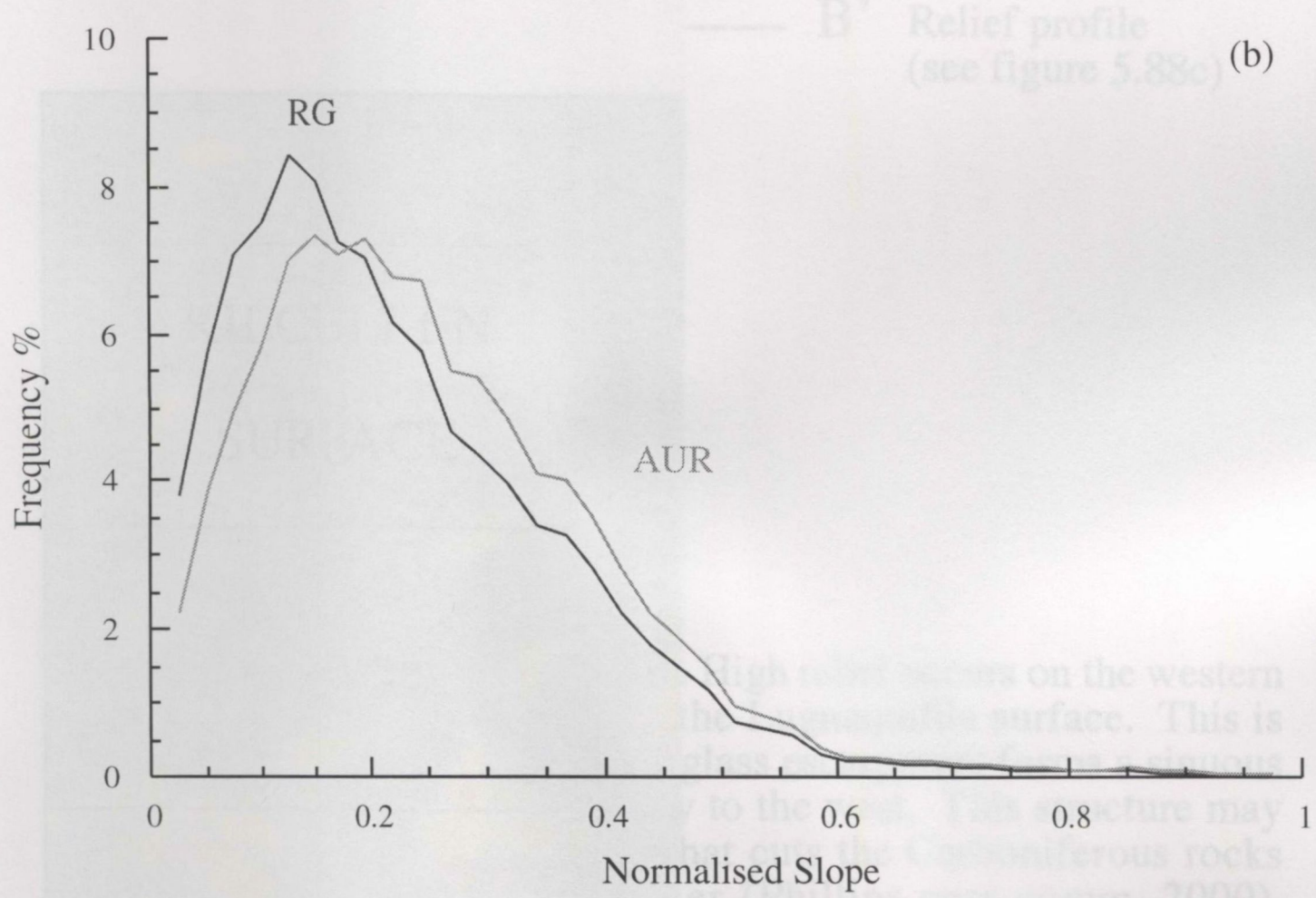

Figure 5.79a,b:- Graph of normalised slope distribution for the main lithologies in the Glen of Imail area. See text. AUR – Aureole; KG – Kilcullen Group; LP – Lugnaquillia pluton; NP – Northern pluton; RG – Ribband Group; TP – Tullow pluton.

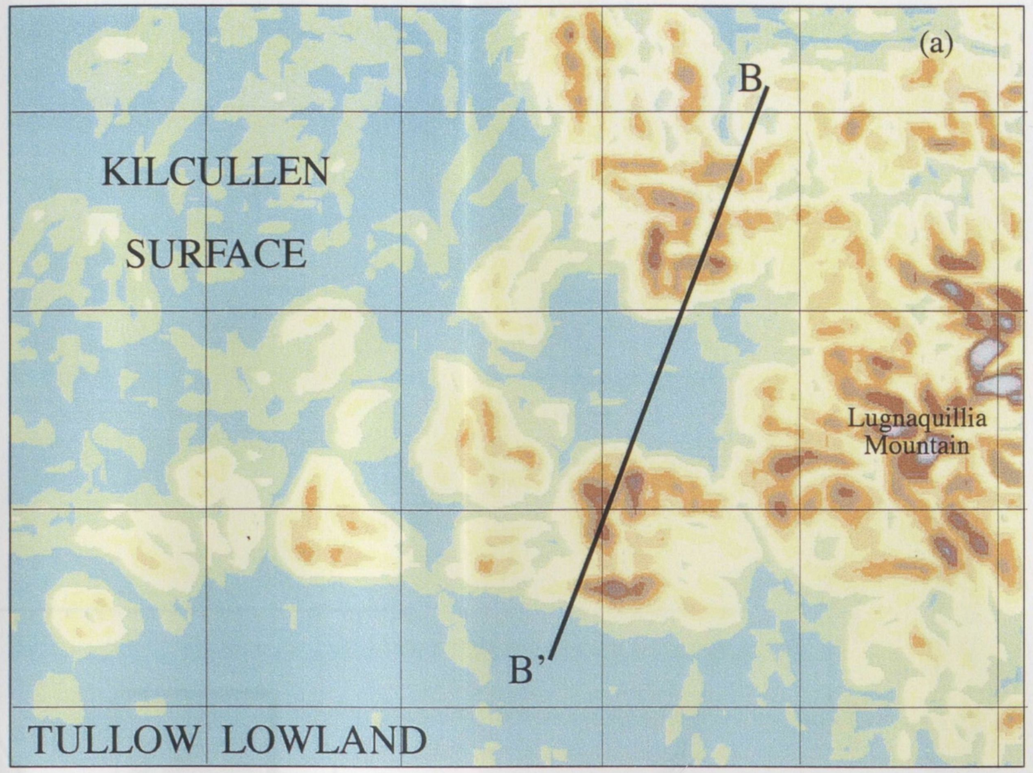

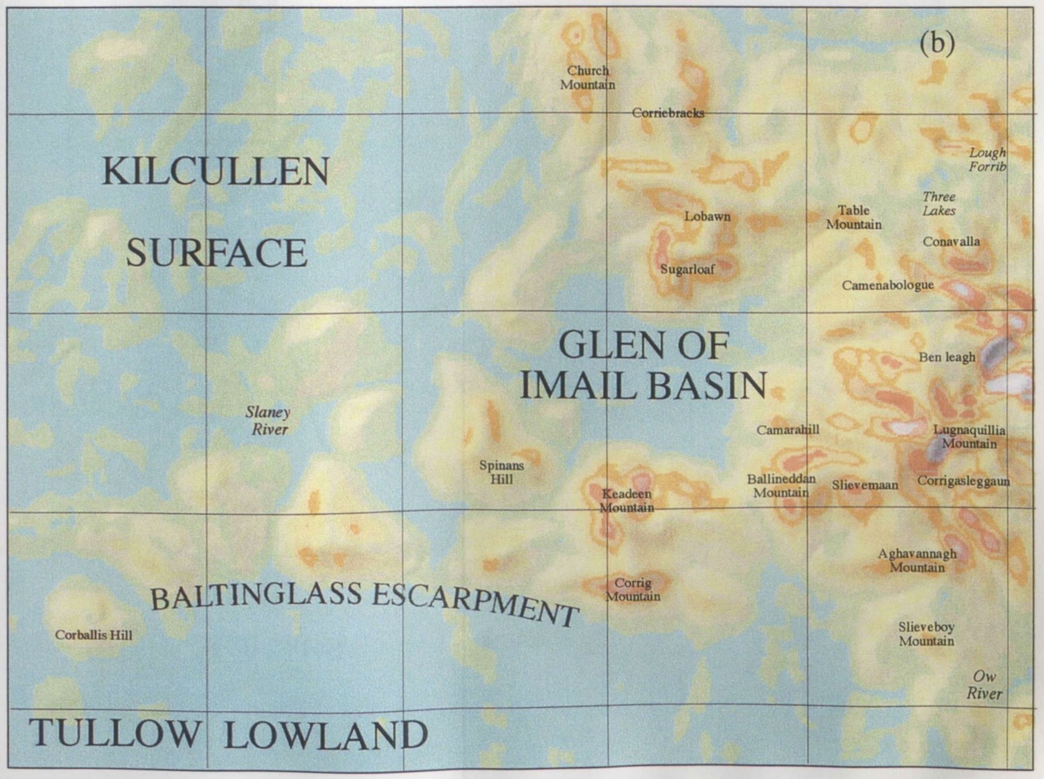

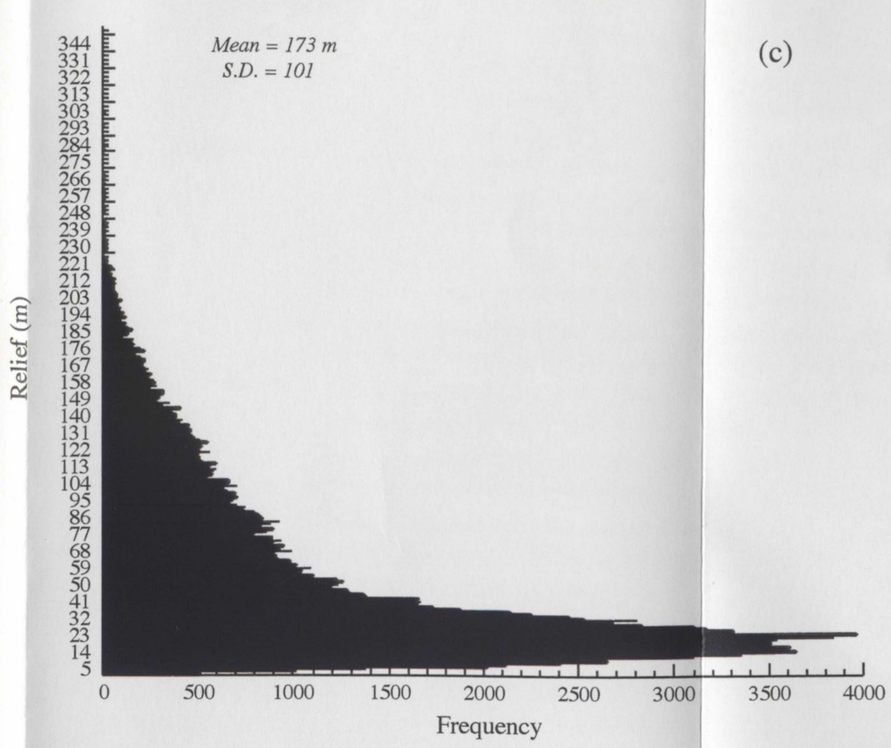

Relief (m)

325 - 365	135 - 162
297 - 325	108 - 135
270 - 297	82 - 108
244 - 270	54 - 82
216 - 244	27 - 54
189 - 216	1 - 27
162 - 189	

B —— B' Relief profile (see figure 5.88c)

Figure 5.80a,b:- Relief images of the Glen of Imail area. High relief occurs on the western flanks of the Wicklow Massif, which is moderate on the Lugnaquillia surface. This is low in the floor of the Glen of Imail basin. The Baltinglass escarpment forms a sinuous ridge of moderate relief, which diminishes in intensity to the west. This structure may correlate with a large E-W to ENE-WSW structure that cuts the Carboniferous rocks further west and cuts across the Slieve Bloom inlier (Phillips pers comm. 2000).

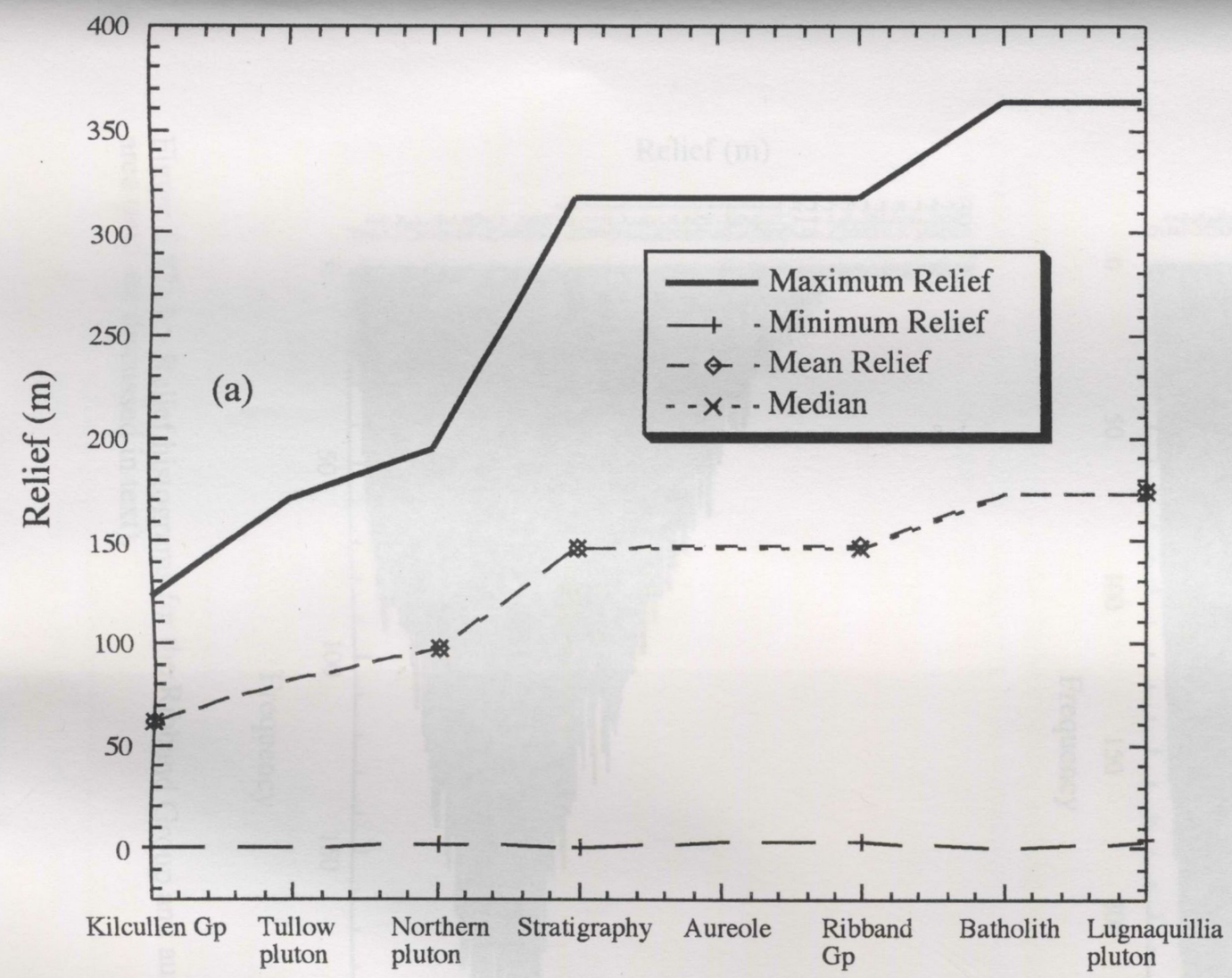

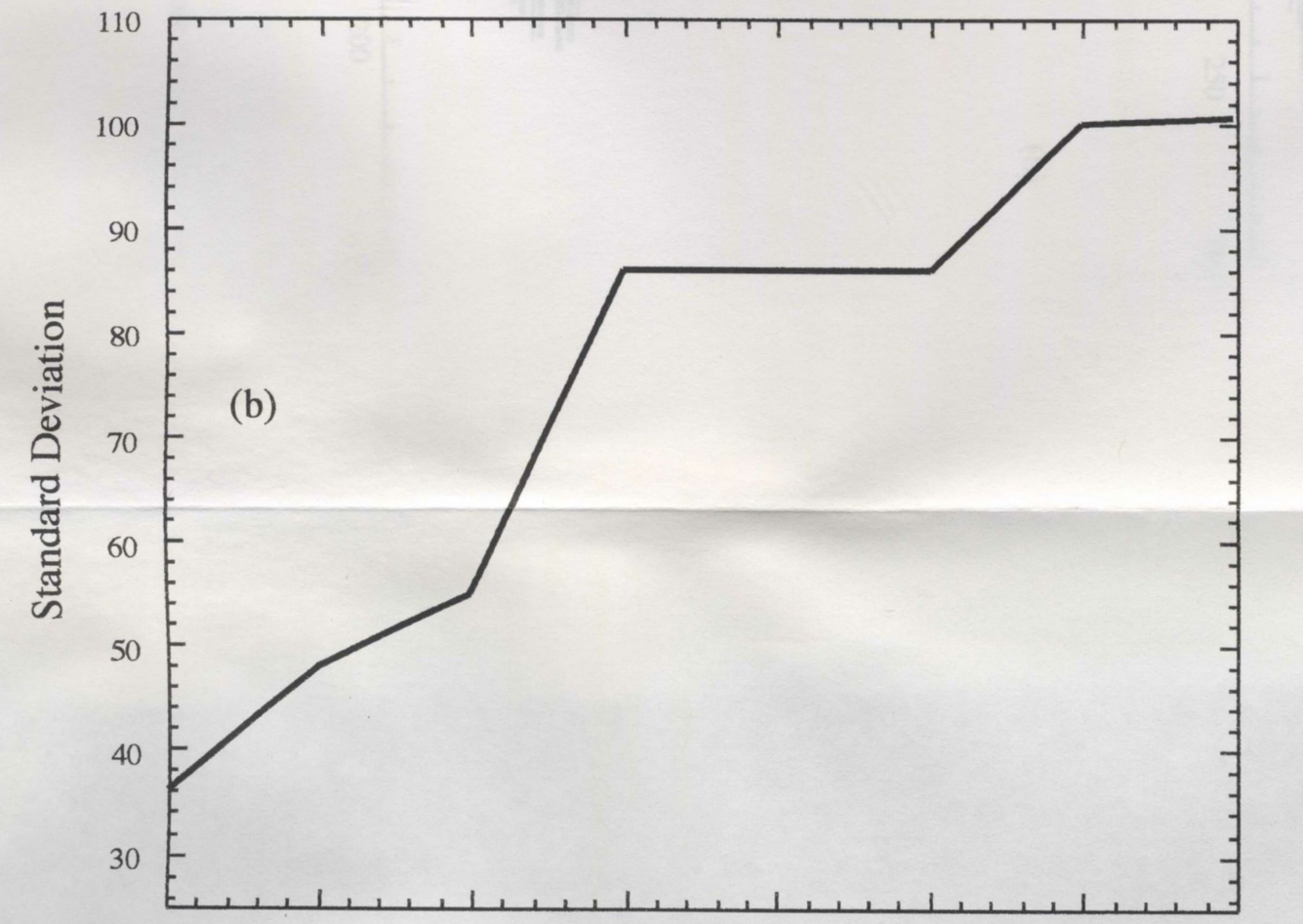

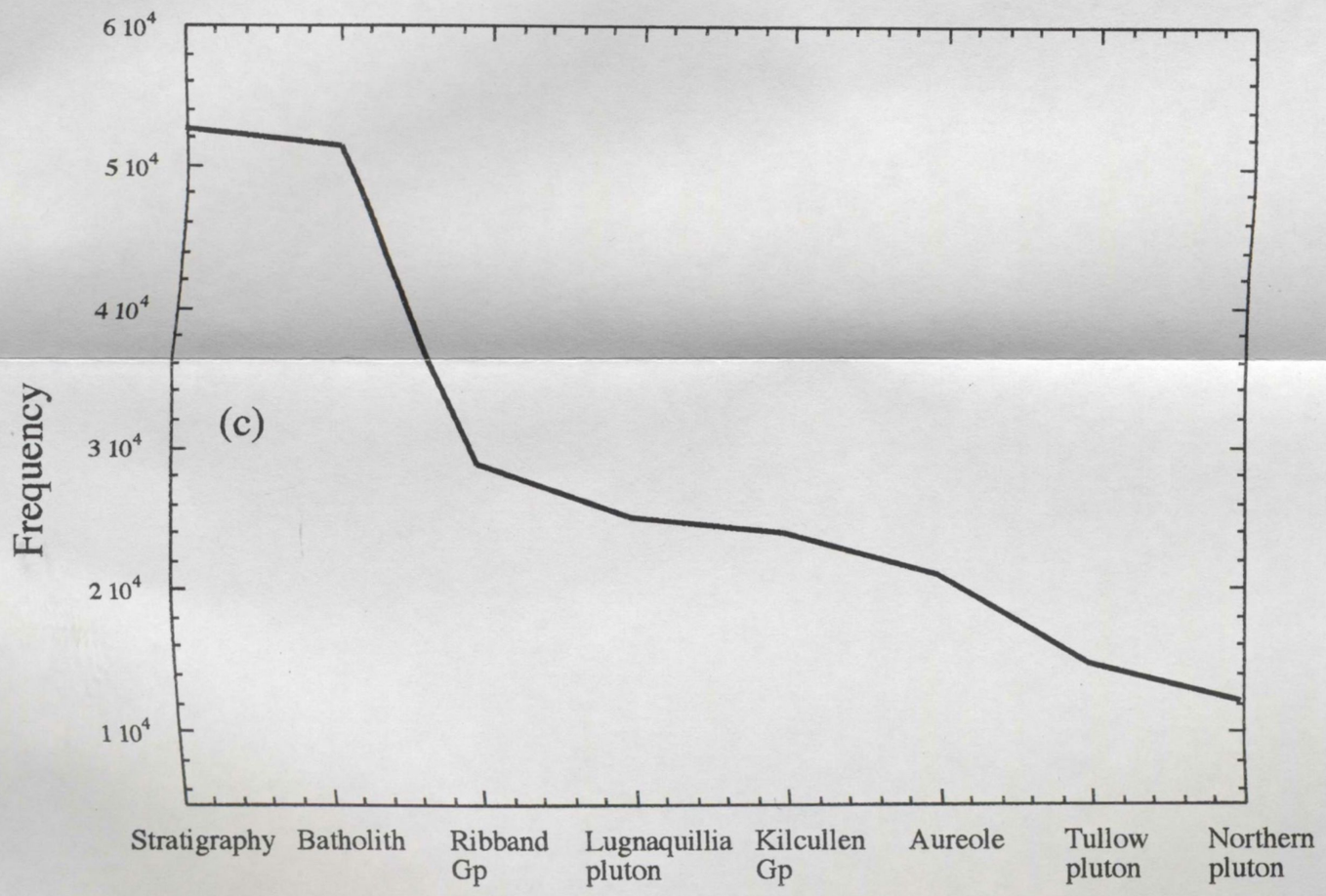

Figure 5.81a,b,c:- Descriptive statistical graphs showing the relationship between various rock type and relief in the Glen of Imail area. Batholith = all plutons; stratigraphy = Ribband & Kilcullen Groups.

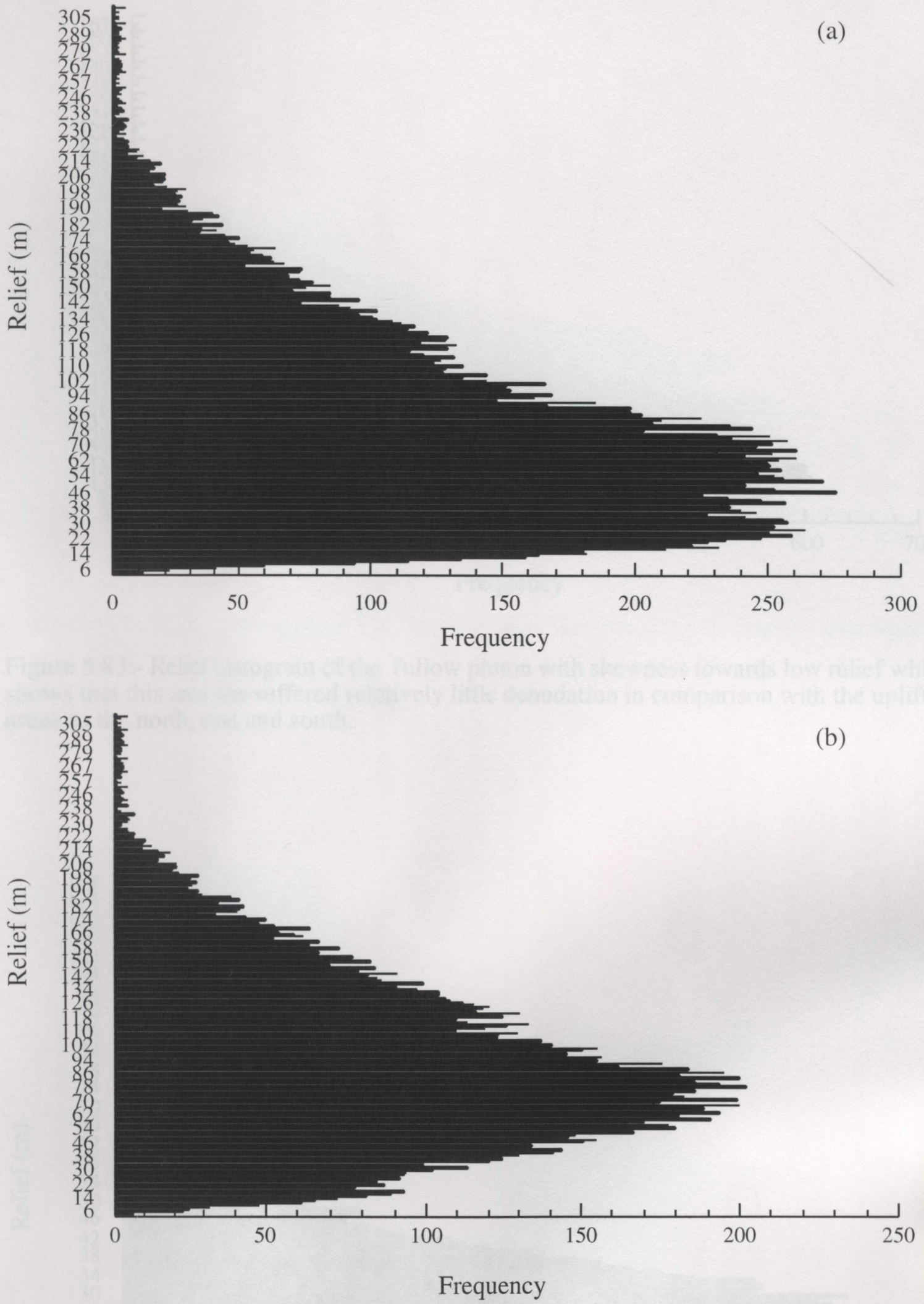

Figure 5.82a,b:- Relief histograms for the Ribband Group and aureole in the Glen of Imail area (and are discussed in text).

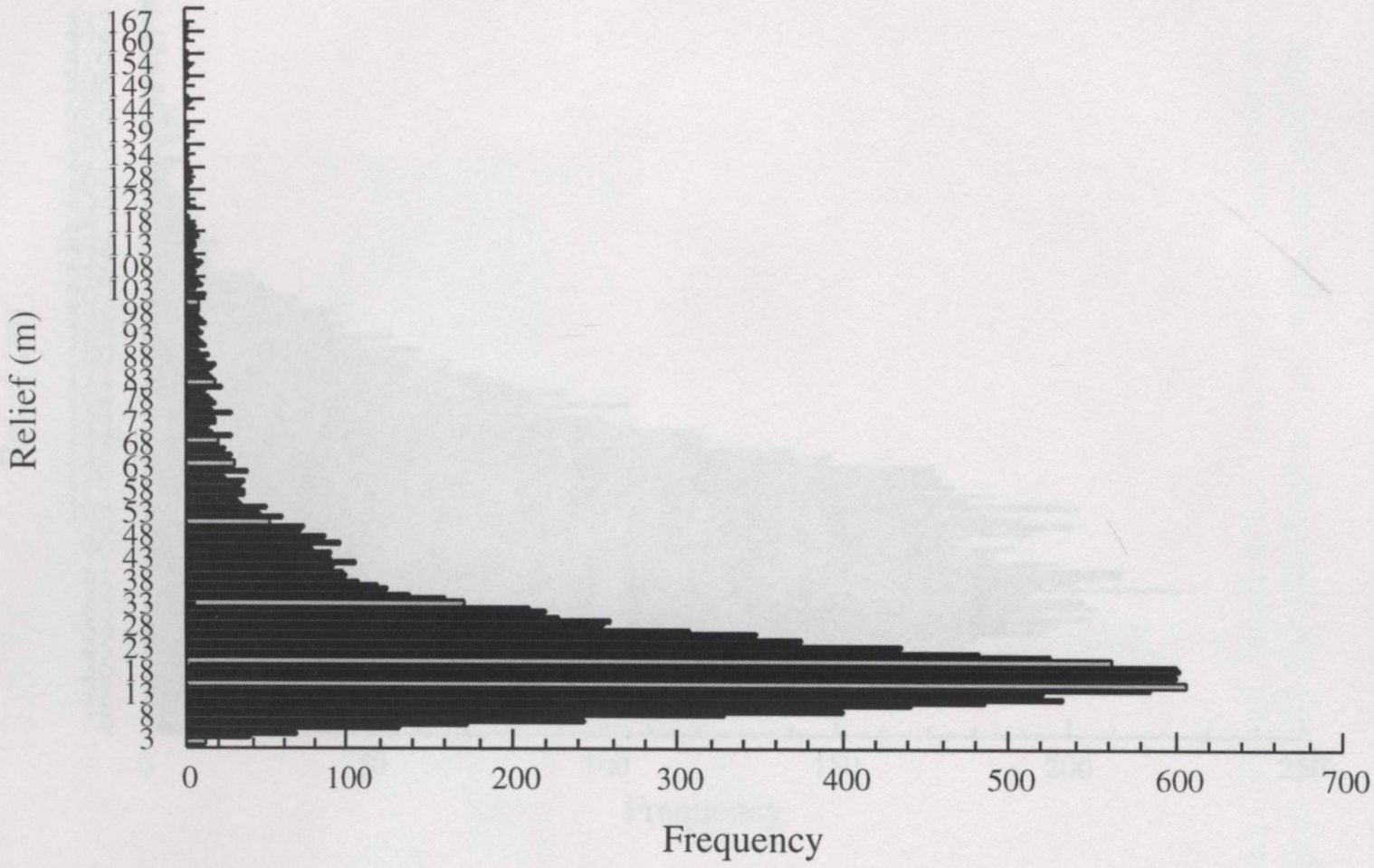

Figure 5.83:- Relief histogram of the Tullow pluton with skewness towards low relief which shows that this area has suffered relatively little denudation in comparison with the uplifted areas to the north, east and south.

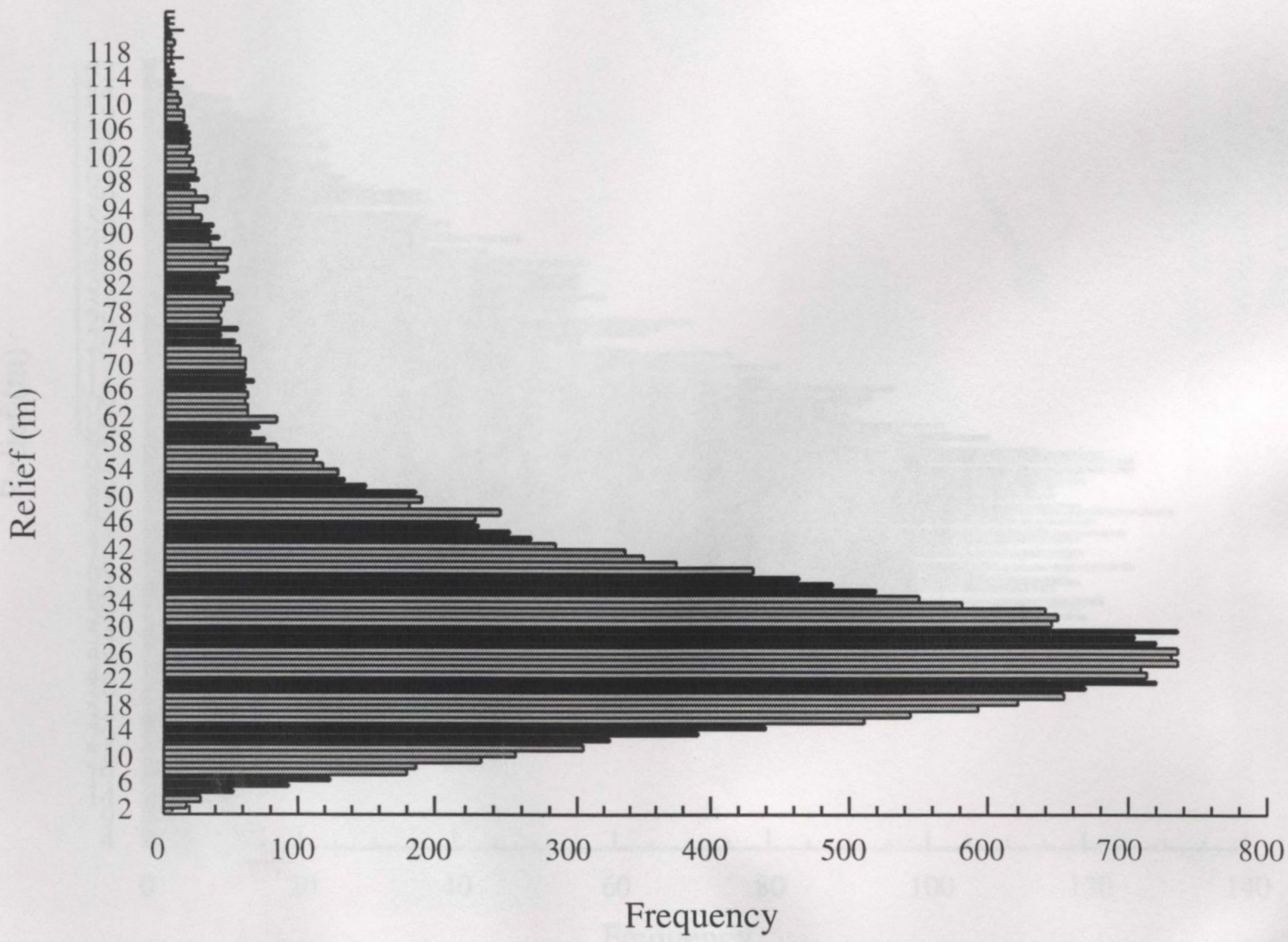

Figure 5.84:- Relief histograms for the Kilcullen Group.

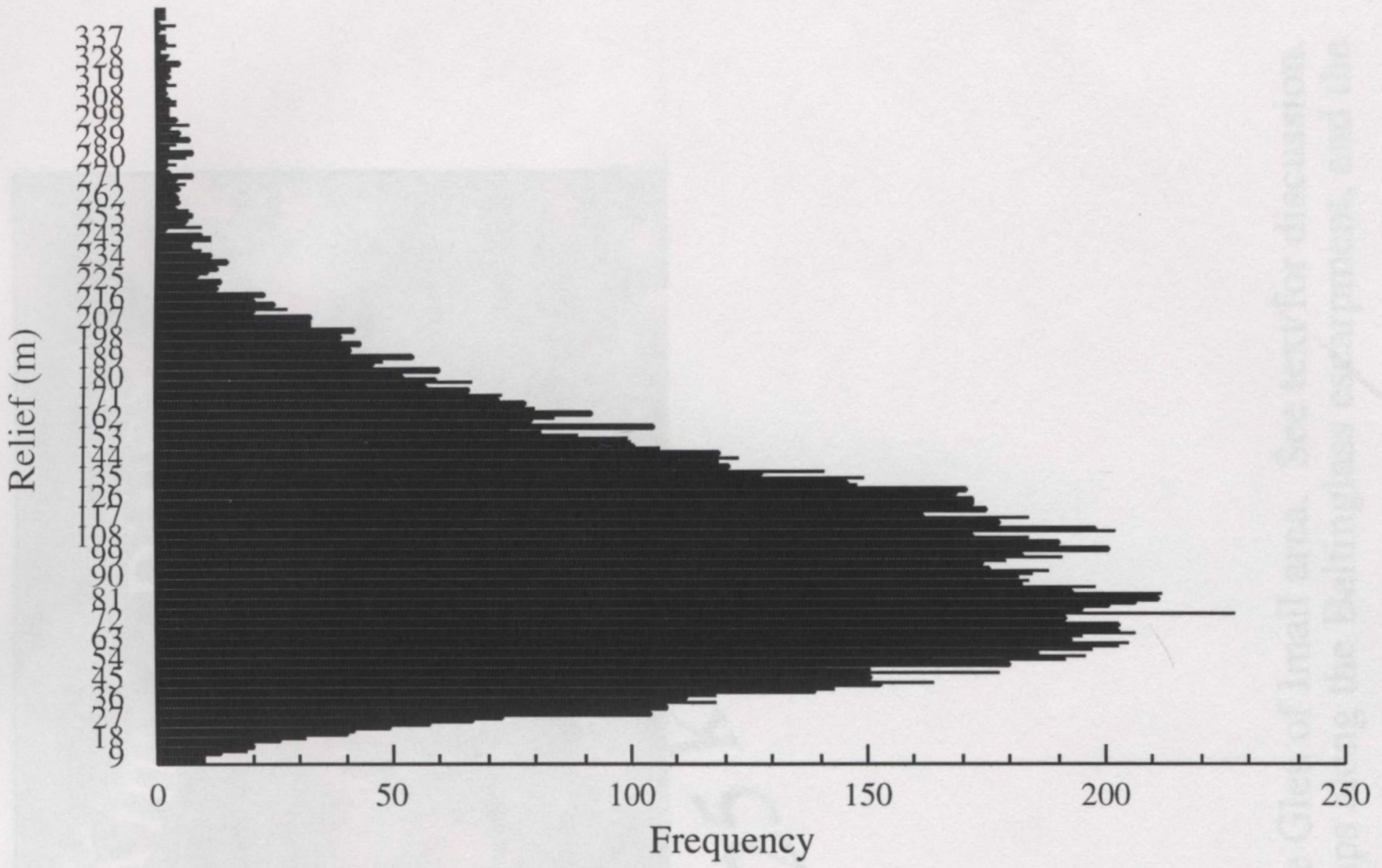

Figure 5.85:- Relief histograms for the Lugnaquillia pluton. See text for discussion.

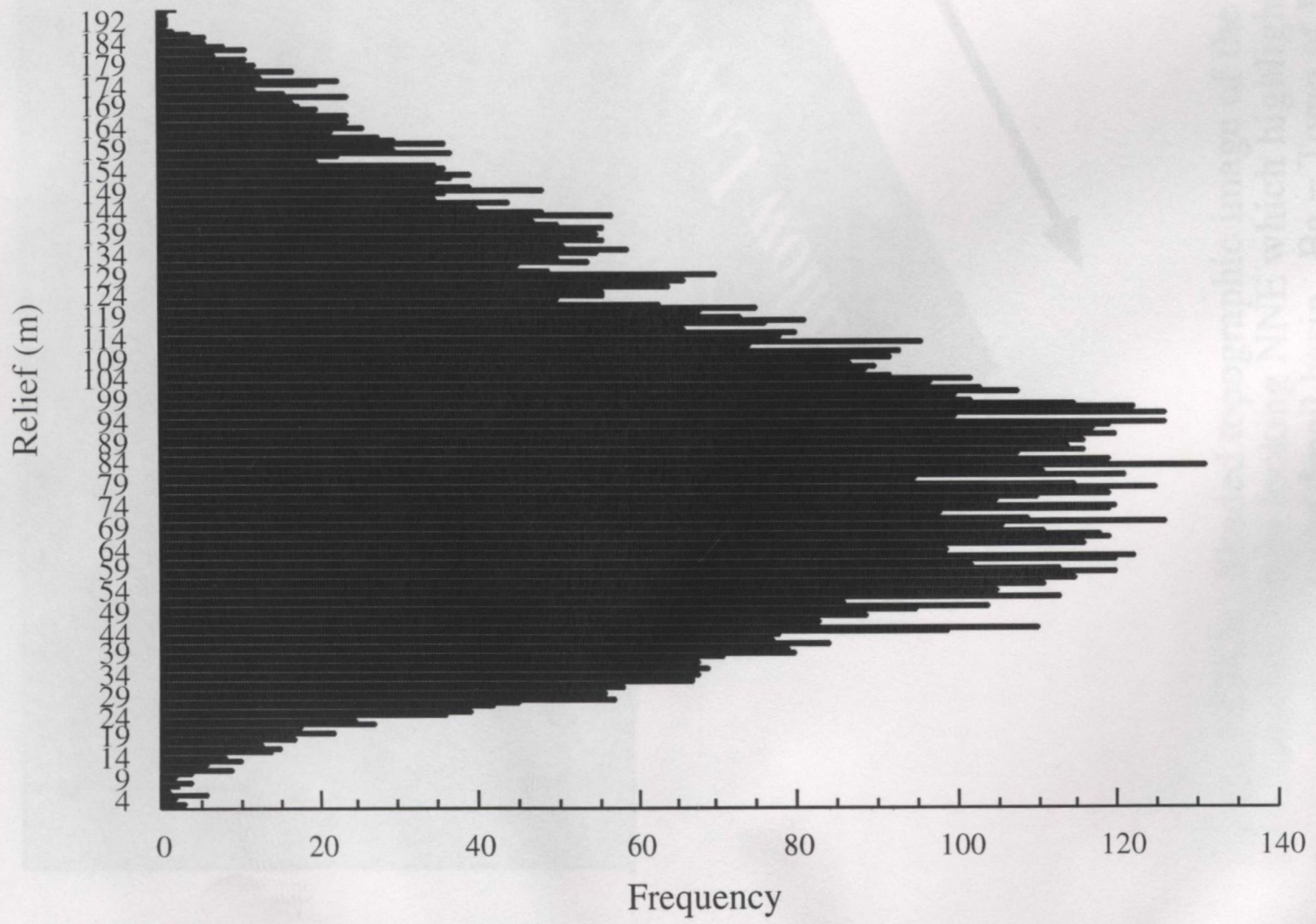

Figure 5.86:- Relief histograms for the Northern pluton. See text for discussion.

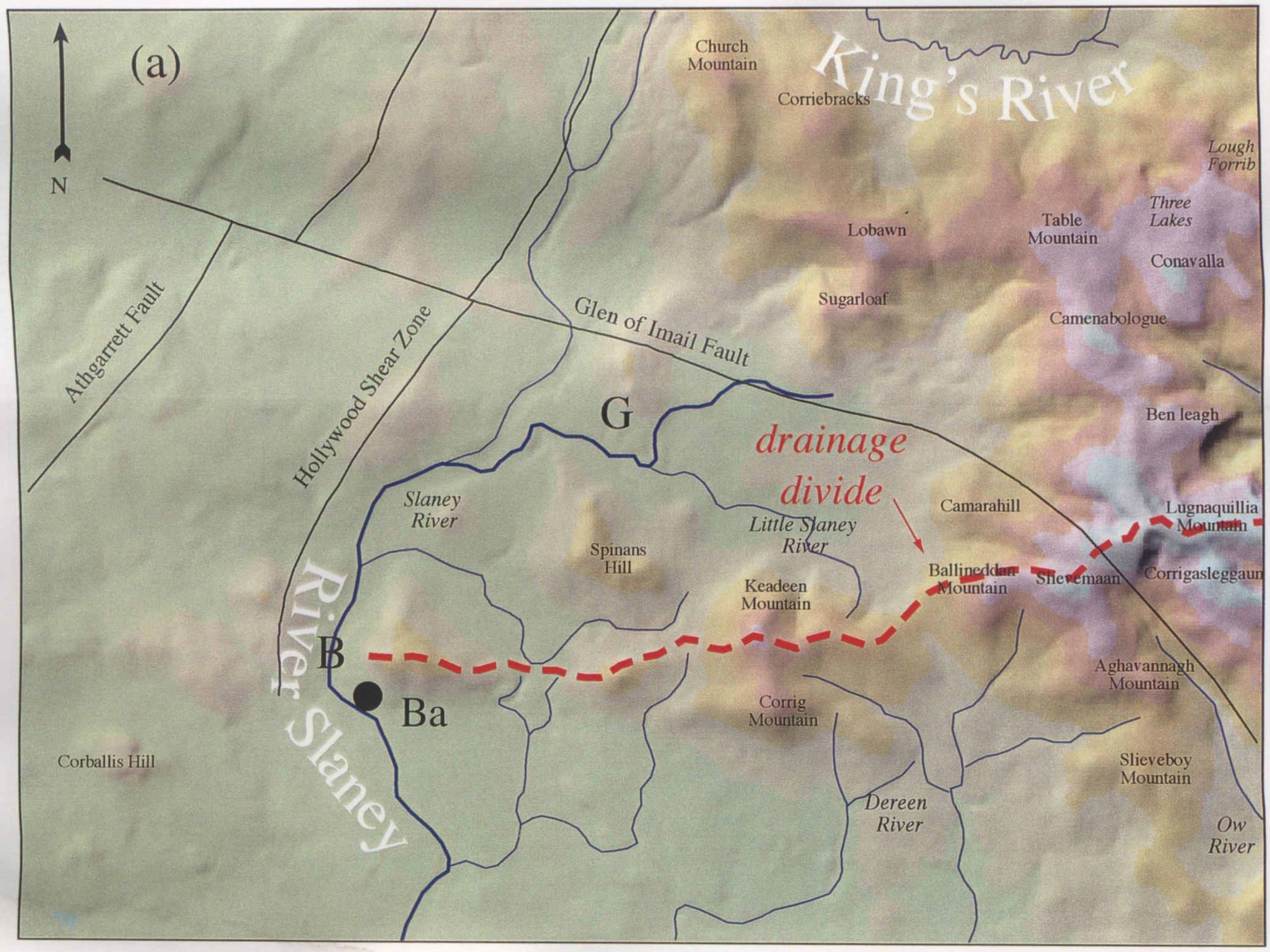

Figure 5.87a,b:- Shaded topographic image of the a) geomorphology of the Glen of Imail area. See text for discussion. B) hillshaded image looking NNE which highlights the numerous wind-gaps along the Baltinglass escarpment, and the scoop shaped Glen of Imail basin. Ba = Town of Baltinglass.

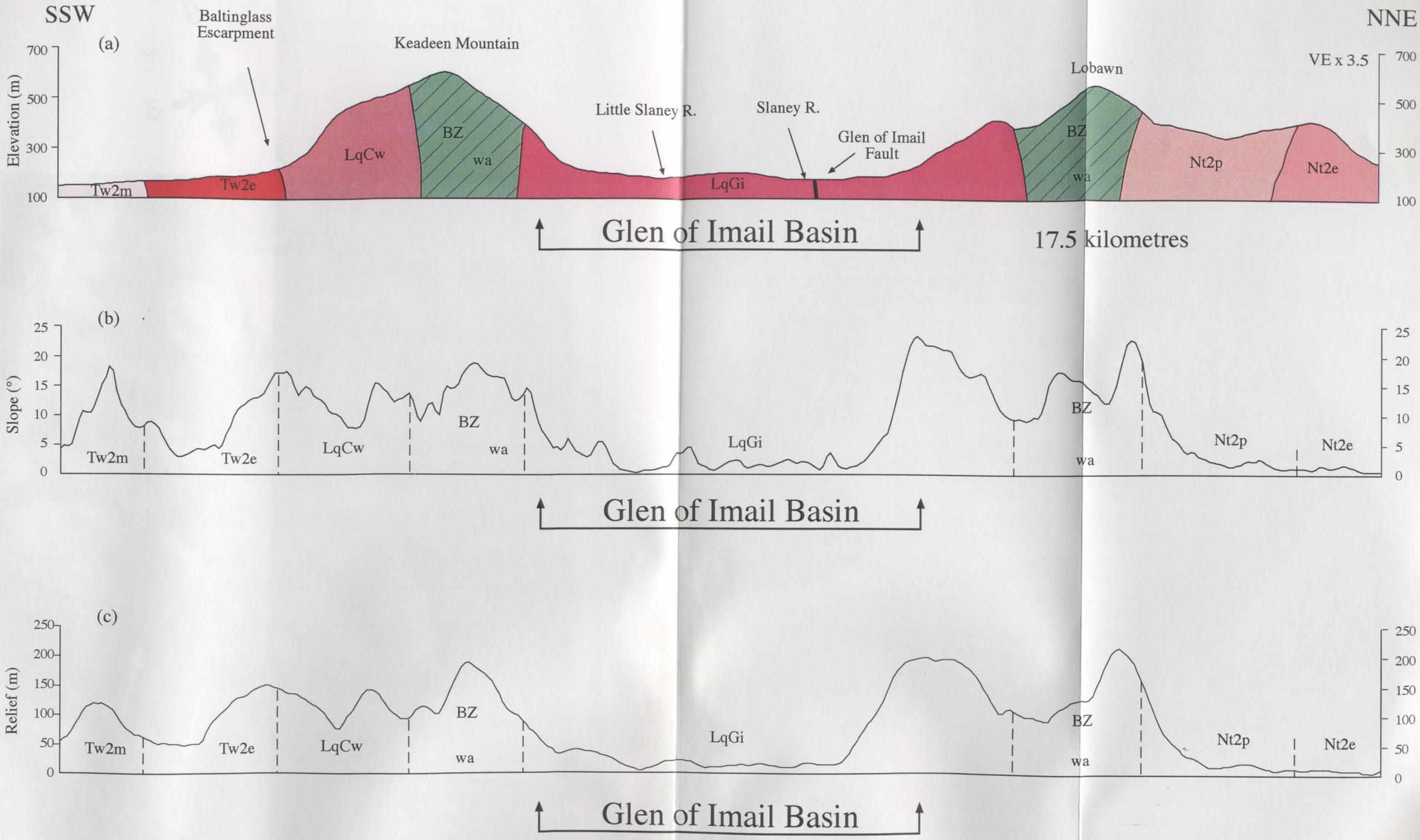

Figure 5.88a,b,c:- NNE-SSW geological (a), slope (b) and relief (c) profiles of the Glen of Imail area. The section crosses from the relatively high ground on the Northern pluton, to the floor of the Glen of Imail basin and over the Baltinglass escarpment. The lack of evidence to suggest that these changes in slope and relief are lithologically controlled strengthens the fault premise. The only exception to this is the apparent lithological control forming the Glen of Imail basin, i.e. Glen of Imail quartz-diorite forming the low slopes and relief, whereas the aureole schists form relatively high slope and relief. However, as noted in appendix 3, there is no outcrop in this area, and the contacts have thus been inferred from the occurrence of a few glacial erratics and break in slope (see Brück & Reeves, 1983).

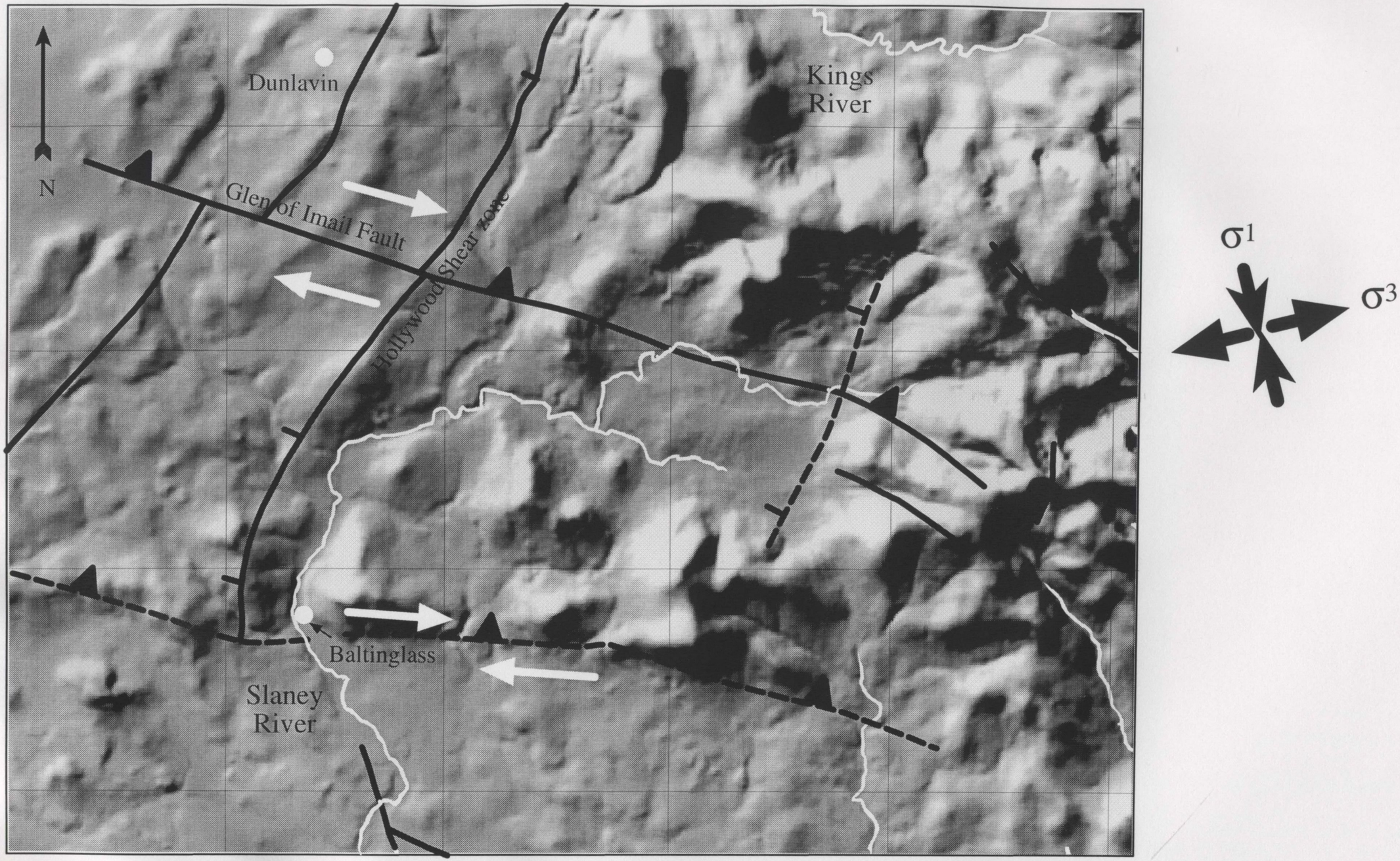

Figure 5.89:- The preferred model is in harmony with the same palaeostress system of the Vartry and Bunclody areas, but with evidence of an earlier Tertiary NW-SE σ_1 and NE-SW σ_3 (see text for discussion).